RESEARCH & DEVELOPMENT

Investigation of Primary Causes of Fatigue Cracking in Asphalt Pavement in North Carolina

Y. Richard Kim, Ph.D., P.E., F. ASCE

Hong Joon Park, Ph.D.

Dept. of Civil, Construction, & Environmental Engineering

North Carolina State University

NCDOT Project 2010-01

FHWA/NC/2010-01

March 2015

Investigation of Primary Causes of Fatigue Cracking in Asphalt Pavement in North Carolina

Research Project No. HWY-2010-01

Submitted to:
North Carolina Department of Transportation
Office of Research

Submitted by

Y. Richard Kim, Ph.D., P.E., F.ASCE
Distinguished University Professor
Campus Box 7908
Department of Civil, Construction & Environmental Engineering
North Carolina State University
Raleigh, NC 27695-7908
Tel: 919-515-7758, Fax: 919-515-7908
kim@ncsu.edu

Hong Joon Park
Transportation Project Specialist Senior
Division of Materials and Tests
Tennessee Department of Transportation
6601 Centennial Blvd.
Nashville, TN 37243
E-mail: hong.park@TN.Gov

Department of Civil, Construction & Environmental Engineering
North Carolina State University
Raleigh, NC

March 2015

Technical Report Documentation Page

1. Report No. FHWA/NC/2010-01	2. Government Accession No.	3. Recipient's Catalog No.
4. Title and Subtitle Investigation of Primary Causes of Fatigue Cracking in Asphalt Pavement in North Carolina		5. Report Date March 2015
		6. Performing Organization Code
7. Author(s) Y. Richard Kim and Hong Joon Park		8. Performing Organization Report No.
9. Performing Organization Name and Address Campus Box 7908, Dept. of Civil, Construction, & Environmental Engrg. NCSU, Raleigh, NC 27695-7908		10. Work Unit No. (TRAIS)
		11. Contract or Grant No. HWY-2010-01
12. Sponsoring Agency Name and Address NC Department of Transportation Research and Analysis Group 1 South Wilmington Street Raleigh, NC 27601		13. Type of Report and Period Covered Final Report Aug. 2009 – Dec. 2012
		14. Sponsoring Agency Code 2010-01
15. Supplementary Notes		

16. Abstract

This report presents causes of cracking in asphalt concrete pavement in North Carolina through field investigation and laboratory experiments with field extracted material. Specific objectives of this research were to: (1) investigate whether systematic bias exists in the NCDOT's volumetric mix design that pertains to such factors as dry asphalt concrete mixtures, aggregate structures, etc.; (2) investigate the strength and uniformity of the pavement substructure; and (3) identify dominant causes of premature crack propagation patterns, such as top-down cracking, bottom-up cracking, and bidirectional cracking. A total of 34 pavement sites were selected for this study that constitute 6 old and well performing pavements and 24 young and poor performing pavements. The research team visited these 34 pavement sites and conducted the following investigations: (1) visual condition survey, (2) falling weight deflectometer testing, (3) full depth coring and visual observation of cracking patterns, and (4) dynamic cone penetrometer testing. In order to assess condition of existing pavement, alligator cracking index (ACI) was developed by combining the amounts of alligator cracking and longitudinal cracking on the wheel path. Deduct values for low, moderate, and high severity cracking were subtracted from 100 to determine the ACI value. Therefore, higher ACI values indicate a better condition than lower ACI values. In addition to the *in-situ* testing, laboratory tests were performed on the cores, including: (1) dynamic modulus and fatigue testing, (2) ignition oven testing, and (3) frequency sweep and linear amplitude sweep testing of extracted and recovered binder. Finally, pavement performance simulations were done using the Pavement ME program and the Layered ViscoElastic pavement analysis for Critical Distresses (LVECD) program.

It was found that the asphalt content in the top layer that exhibits top-down cracking or bottom-up cracking has a proportional relationship to ACI values. The air void content in a bottom layer that exhibits top-down cracking or bottom-up cracking shows an inverse proportional relationship to ACI values. These observations reflect reasonable results. A comparison between ACI and asphalt film thickness values does not produce noteworthy findings, but somewhat reasonable results are evident once the range of comparison is narrowed down. Thicker film thicknesses show higher ACI values. From field core visual observations, road widening is identified as a major cause of longitudinal cracking. Regions with observed layer interface separation (debonding) tend to have low ACI values. Through tensile strain simulation based on actual field conditions, it is observed that sites with observed bottom-up cracking have higher tensile strain levels at the bottom of the asphalt layer than sites with observed top-down cracking. Extracted binder fatigue test results indicate that the performance difference between *good* and *poor* sections of a given site is not the result of differences in the binder properties. Hence, other mixture design factors are at work in controlling the site variability in terms of fatigue resistance.

17. Key Words Fatigue cracking, top down cracking, bottom up cracking, debonding, forensic, mix design, Pavement ME, S-VECD, LVECD	18. Distribution Statement		
19. Security Classif. (of this report)	20. Security Classif. (of this page)	21. No. of Pages 329	22. Price

Form DOT F 1700.7 (8-72) **Reproduction of completed page authorized**

DISCLAIMER

The contents of this report reflect the views of the authors and are not necessarily the views of North Carolina State University. The authors are responsible for the facts and the accuracy of the data presented herein. The contents do not necessarily reflect the official views or policies of the North Carolina Department of Transportation at the time of publication. This report does not constitute a standard, specification, or regulation.

ACKNOWLEDGMENTS

This research was sponsored by the North Carolina Department of Transportation. The Steering and Implementation Committee consisted of: Judith Corley-Lay, Ph.D., P.E. (Chair); Jack Cowsert, P.E.; Wiley W. Jones III, P.E.; Clark Morrison, Ph.D., P.E.; James Phillips, P.E.; Todd Whittington, P.E. The Friends of the Committee include: Moy Biswas, Ph.D., P.E.; Joseph Geigle; Ron Hancock, P.E.; Chris Peoples, P.E.; Mustan Kadibhai, P.E. Special thanks to Josh Holland and Vladmir Mitchev from *Pavement Management Unit* and James Budday from *Material and Test Unit* of NCDOT for helping field work even in increment weather.

EXECUTIVE SUMMARY

The most common failures observed in asphalt pavements in North Carolina are due to fatigue cracking. This situation may have worsened in recent years due to the fact that the Superpave mix design, as a national effort, focused on mitigating permanent deformation. Because mixes that are resistant to permanent deformation are also, in general, prone to fatigue, these efforts may have inadvertently led to the use of mixtures that are more prone to cracking. In addition to any changes made in the mix design due to this national driving force to eliminate permanent deformation, a pavement with observed fatigue cracking may represent failure in the structural design or failure related to construction.

This report summarizes the findings from a research project funded by the North Carolina Department of Transportation (NCDOT). The goal of the project was to identify the primary causes of fatigue cracking in North Carolina asphalt pavements. Specific objectives of this research were to:

- Investigate whether systematic bias exists in the NCDOT's volumetric mix design that pertains to such factors as dry asphalt concrete mixtures, aggregate structures, etc.
- Investigate the strength and uniformity of the pavement substructure.
- Identify dominant causes of premature crack propagation patterns, such as top-down cracking (TDC), bottom-up cracking (BUC), and bidirectional cracking (BDC).

In order to accomplish these objectives, this study examined material properties through laboratory experiments using field-extracted materials and investigated *in situ* pavements and pavement structures. An initial review of the NCDOT Pavement Management Unit database resulted in the selection of 525 sites as candidates for this study. Further screening of pavement sections yielded six 'old' and well performing pavements and 28 'young' and poor performing pavements. The research team visited these 34 pavement sites and conducted forensic investigation of fatigue cracking in these pavements. The investigative efforts included:

- Visual condition surveys, including detailed crack mapping
- Falling weight deflectometer (FWD) testing
- Full depth coring and visual observation of cracking patterns
- Dynamic cone penetrometer testing

- Dynamic modulus and fatigue testing of small cores obtained by coring from the side of field cores
- Ignition oven testing of field cores to determine aggregate gradations and asphalt contents
- Extraction and recovery of asphalt binder
- Frequency sweep and linear amplitude sweep testing of recovered binders using a dynamic shear rheometer
- Pavement performance simulations using the Pavement ME program and the newly developed Layered ViscoElastic pavement analysis for Critical Distresses (LVECD) program

The cracking conditions of the pavements were represented by the alligator cracking index (ACI), which combines the amount and severity of alligator cracking and longitudinal cracking that is found in the wheel path. Higher ACI values indicate a better condition than lower ACI values. Comparisons between the ACI values and forensic results from *in situ* and laboratory testing resulted in the following specific conclusions:

- In general, correlations between the mix design factors and ACI values are weak at best. The interaction of the various mix design factors made it difficult to identify clear relationships. The following observations summarize the trends that were relatively clear:
  - The asphalt content in a top layer that exhibited TDC or BDC showed a proportional relationship to the ACI values.
  - The air void content in a bottom layer that exhibited BUC or BDC showed an inverse proportional relationship to the ACI values.
  - For quality analysis, the given data were partitioned into different categories: different nominal maximum aggregate size (NMAS) and aggregate gradation types. In the case of a top layer exhibiting TDC or BDC, the same conclusions could be drawn as for the comparison of the ACI values and asphalt content regardless of the NMAS and aggregate gradation type. However, for the case of a bottom layer exhibiting BUC or BDC, reasonable correlations were observed in specific categories: 9.5 mm NMAS and penetrating aggregate gradation for BUC or BDC, and fine aggregate gradation for BUC-only in the bottom layer.
  - A comparison between the ACI and film thickness values did not produce noteworthy findings, but somewhat reasonable results were evident once the range of comparison

was narrowed down. Thicker film thicknesses showed higher ACI values, which means better cracking performance.

- The field core visual observations identified road widening as a major cause of longitudinal cracking.
- Regions with observed layer interface separation (debonding) tended to have low ACI values.
- Debonding was observed in 29 out of 56 condition regions, which is more than 51 percent. This finding indicates that layer interface separation is a major cause of cracking, but can be relatively easily resolved by quality control/quality assurance protocols.
- Overall, sites with observed BUC showed higher tensile strain levels at the bottom of the asphalt layer than sites with observed TDC.
- The *AREA* parameter versus pavement thickness relationship differentiates the TDC sections from pavements with full-depth cracking that is caused by the BUC mechanism. Therefore, the FWD-based *in situ* method will allow pavement engineers to identify the existence and likelihood of TDC. This simplified method will not only reduce the time and cost involved for engineers to verify the structural soundness of a pavement, but will also lead to selecting the optimal maintenance treatment and rehabilitation designs.
- The binder fatigue test results indicate that the binder properties between *good* and *poor* sections at a given site are not the result of differences in the binder properties. Hence, other mixture design factors are at work in controlling the site variability in terms of fatigue resistance.
- The fact that the predicted cracking propensity and locations obtained from the LVECD simulations are in good agreement with the condition survey results and with the visual observations from the cores suggests that the LVECD analysis program can be an effective tool in determining the TDC propensity of asphalt pavements, if the mechanical properties of the individual layers are available. The LVECD program prediction results can be calibrated against the field performance data to develop a powerful and accurate pavement cracking performance prediction system that allows the prediction of cracking intensity as well as the cracking initiation location.
- The ability to identify TDC and BUC based on surface cracks is one of the most important starting points for creating cost-effective rehabilitation strategies for project-

level pavement management systems. Therefore, the LVECD program and the *AREA* parameter method can be effective tools for building a cost-effective pavement management system.

- The Pavement ME cannot effectively capture the direction of cracking using Level 3 simulation inputs.
- A direct comparison of the capability of the Pavement ME and the LVECD program is difficult, but it appears that the LVECD program tends to capture cracking propensity better than the Pavement ME, based on field observations. Thus, the LVECD-based mechanistic approach also can be used as a performance prediction model for pavement design.

Recommendations for future research regarding field-extracted materials are summarized as follows.

- Integrated materials and pavement condition database development. A significant challenge for this project was the lack of job mix formulae (JMFs) and material data, which made it difficult to find systematic flaws in the mix design. If the JMF for each material had been available to the research team, an enormous amount of information, such as construction quality, material quality, aggregate blending, density records during onsite compaction, etc., could have been obtained for the field-extracted materials. Also, if local or Division engineers had accurate records of the need for past rehabilitation efforts, a more effective analysis approach could have been taken for this research. Furthermore, the process of finding valid field sites was lengthy for this research project. The depth of this research could have been more extensive if the NCDOT had test tracks or test roads and a full construction and materials database. Therefore, future research is needed for the development of an integrated materials and pavement condition database.
- Road widening. A sand mix layer was observed in many of the road-widening locations. According to a Division engineer, sand mixes typically are used for elevation purposes. A higher quality mix needs to be developed for these purposes, and the effect of the poor quality patching mix on the pavement's service life needs to be evaluated.
- *AREA* parameter. In order to predict the TDC potential and to determine the direction of cracking in new pavements, the applicability of *AREA* parameter needs to be further studied.

- Pavement ME. The simulation results obtained from Level 3 inputs could not capture field-observed deterioration in terms of crack location. The usefulness of low-level inputs for simulations needs to be investigated, and an approach to mediate this problem needs to be studied.
- Pavement ME. The pass and fail results of long-term simulations could not effectively capture the crack propagation observed from the field cores, even though a strong correlation was found from the comparison between the maximum BUC percentage and the ACI values obtained from BUC-observed sites. This problem needs to be investigated to develop and implement an effective design and evaluation tool.
- Implementation and calibration of the LVECD program and associated material test methods. The LVECD program and associated material tests have shown potential to be used as a reliable performance prediction approach for the State of North Carolina. This approach serves as the basis for the FHWA's newly developed Performance-Related Specifications for asphalt concrete and is now being verified using field performance results obtained for various pavements in the United States and other countries. The specifications for the direct tension fatigue test method used in this study have been accepted as a provisional standard (TP 107) by the AASHTO Subcommittee on Materials. The LVECD program has been released to a group of about 50 experts for alpha testing and later will be released to the public for routine use for pavement design and analysis.

TABLE OF CONTENTS

Chapter 1 Introduction 1
1.1 Background 1
1.2 Research Objectives 2
1.3 Outline of Research Presented 2
Chapter 2 Forensic Study 3
2.1 Finding Valid Field Sites 3
2.1.1 Pavement Age 3
2.1.2 Pavement Traffic 5
2.1.3 Fatigue Performance 8
2.1.4 Valid Field Sites 11
2.2 Field Investigation 22
2.2.1 Selecting Pavement Sites for Investigation 22
2.2.2 Field Investigation Protocols 22
2.3 Investigated Data Elements 24
Chapter 3 Experimental Approaches 25
3.1 Determination of Mix Design Parameters with Field-Extracted Materials 25
3.1.1 Introduction 25
3.1.2 Material Collection Strategy from In-Service Pavement 25
3.1.3 Experiment Sample Preparation 26
3.1.4 Determination of Mix Design Parameters 27
3.2 Mechanical Experiment 30
3.2.1 Test Setup 30
3.2.2 Theoretical Background 31
3.2.3 Dynamic Modulus Testing 33
3.2.4 Controlled Crosshead Cyclic Tension Testing with S-VECD Program 34

3.3 Small Geometry Specimens 34
3.3.1 Introduction 34
3.3.2 38 mm Diameter Cylindrical Specimens 35
3.3.3 Prismatic Specimens 35
3.3.4 Ancillary Devices for Small Geometries 36
3.3.5 Verification of Small Geometry Specimens 38
3.4 Rheological Properties of Asphalt Binder 45
3.4.1 Introduction 45
3.4.2 Sample Extraction and Recovery 45
3.4.3 Specimen Preparation 47
3.4.4 Frequency Sweep Test 48
3.4.5 Linear Amplitude Sweep (LAS) Test 48
Chapter 4 Causes of Cracking 49
4.1 Introduction 49
4.2 Master Database 54
4.3 Pavement Condition Index 54
4.4 Mix Deign 58
4.4.1 Introduction 58
4.4.2 Analysis Results 58
4.4.3 Summary 71
4.5 Structural Uniformity 71
4.5.1 Pavement Substructure Analysis 71
4.5.2 Roadway Widening 77
4.6 Layer Interface Separation 80
4.6.1 Introduction 80
4.6.2 Field Observations of Debonding 80
4.6.3 Summary 82

4.7 Top-Down Cracking Identification 85
4.7.1 *AREA* Parameter Method 85
4.8 Bottom-Up Cracking Identification 87
4.9 Rheological Properties 92
4.9.1 Analysis Results 92
4.9.2 Summary 95
Chapter 5 Long-Term Performance Simulations 96
5.1 Introduction 96
5.2 Layered Viscoelastic Continuum Damage Program 96
5.2.1 LVECD Inputs 96
5.2.2 LVECD Simulation Results 97
5.3 DARWin-ME Pavement ME Design 120
5.3.1 Required Inputs 120
5.3.2 DARWin-ME Analysis Results 124
5.4 Summary 131
Chapter 6 Conclusions and Recommendations 132
6.1 Conclusions 132
6.2 Recommendations for Future Research 134
REFERENCES 136
APPENDICES 144
Appendix A: Master Database for the Research 145
Appendix B: Field Observation and Record 154
Appendix C: Field Extracted Material Test Results 260

LIST OF FIGURES

Figure 2.1 Distribution of pavement ages within the performance database. 4
Figure 2.2 Cumulative distribution of pavement ages within the performance database. 4
Figure 2.3 Distribution of traffic levels within the pavement performance database: (a) by region and (b) compiled for all regions. 6
Figure 2.4 Cumulative distribution of traffic volumes and 31th and 64th percentiles: (a) by region and (b) compiled for all regions. 7
Figure 2.5 Distribution of pavement performance: (a) normalized alligator cracking index and (b) fatigue composite index. 10
Figure 2.6 Cumulative distribution of fatigue performance and 50th and 80th percentiles. 11
Figure 2.7 Test site distribution on North Carolina map. 21
Figure 2.8 Photographs of field investigation procedure: (a) FWD testing, (b) coring spot marking, (c) coring machine mounted on truck, and (d) DCP testing. 23
Figure 3.1 Schematic diagram of field cores used (US 70). 26
Figure 3.2 Use of field samples for mechanical tests: (a) cored sample from in-service pavement (b) cutting layers of hockey pucks, (c) side coring and cutting for mechanical tests, and (d) dimensions of test samples. 27
Figure 3.3 (a): CoreDry, (b), Corelock, and (c) Gilson water tank. 28
Figure 3.4 (a) Test-ready separated sample and (b) vacuum assembly with metal bowl. 29
Figure 3.5 (a) Material before ignition and after ignition, and (b) Troxler NTO ignition chamber. 30
Figure 3.6 Core-holding vise for horizontal coring: (a) initial design for one coring per layer and (b) developed vise for 2 corings per layer. 37
Figure 3.7 End platens gluing jig with alignment adjuster: (a) 38 mm diameter cylindrical specimen and (b) prismatic specimen. 37
Figure 3.8 Multi-use target gluing jig: (a) 38 mm diameter cylindrical specimen and (b) prismatic specimen. 38
Figure 3.9 Mechanical test-ready samples and new design of end platens for prismatic and small geometric specimens: (a) new LVDT bracket attached to test-ready samples, (b) end platens for prismatic geometry specimens, and (c) end platens for small geometry samples. 38
Figure 3.10 Top view of gyratory specimen for cutting and coring small geometries. 39
Figure 3.11 Mixture gradation chart. 40
Figure 3.12 Comparison of material properties measured from standard, 38 mm, and prismatic geometry specimens: (a) dynamic modulus in semi-log space, (b) dynamic modulus in log-log space, (c) phase angle, and (d) damage characteristic curve. 41
Figure 3.13 Photograph of vertical coring for 38 mm specimen. 43
Figure 3.14 Photographs of test-ready prismatic specimens: (a) from vertical direction and (b) horizontal direction. 43
Figure 3.15 Photpgraphs of aggregate orientation perpendicular to compaction direction: (a) from vertical direction and (b) horizontal direction 43

Figure 3.16 Comparison of material properties measured from vertical and side coring of 38 mm and prismatic geometry specimens: (a) dynamic modulus in semi-log space, (b) dynamic modulus in log-log space, (c) phase angle, and (d) damage characteristic curve. 44
Figure 3.17 (a) Extraction unit bowl and (b) rotary evaporator and recovery system. 47
Figure 3.18 (a) AR-G2 rheometer and (b) 8 mm silicon mold with asphalt binder. 48
Figure 4.1 Comparison of alligator cracking index to air void and asphalt content: (a) and (b) from TDC or BDC observed condition regions, (c) and (d) TDC observed condition regions, (e) and (f) BUC or BDC observed condition regions, and (g) and (h) BUC observed condition regions. 60
Figure 4.2 Comparison of alligator cracking index to air void content and asphalt content: (a) and (b) divided NMSAs for TDC or BDC observed condition regions, (c) and (d) divided aggregate gradations for TDC or BDC observed condition regions, (e) and (f) divided NMSAs for TDC only observed condition regions, and (g) and (h) divided aggregate gradations for TDC only observed condition regions. 62
Figure 4.3 Comparison of alligator cracking index to air void content and asphalt content for the BUC or BDC observed condition regions: (a) and (b) divided NMSA for BUC or BDC observed condition regions, (c) and (d) divided aggregate gradation for BUC or BDC observed condition regions, and (e) and (f) divided aggregate gradation for BUC only observed condition regions. 64
Figure 4.4 Example of 0.45 power aggregate gradation chart used NCDOT 65
Figure 4.5 Comparison of alligator cracking index to aggregate gradation from top layer: (a) data with TDC only or BDC (b) data with BUC only or BDC. 67
Figure 4.6 Comparison of alligator cracking index to aggregate gradation from bottom layer: (a) data with TDC only or BDC (b) data with BUC only or BDC. 68
Figure 4.7 Comparison of alligator cracking index to asphalt film thickness of top layer: (a) data from all top layers with TC and (b) data from different NMSA values. 70
Figure 4.8 Schematic of DCP device (ASTM D6951/D6951M). 73
Figure 4.9 Penetration ratio vs. penetration depth for four US 601 pavement regions: (a) DCP data from A1 condition region, (b) 1st DCP data from B1 condition region, (c) 2nd DCP data from B1 condition region, and (d) DCP data from B2 condition region. 74
Figure 4.10 Plots of penetration depth vs. number of blows for four US 601 pavement regions: (a) raw data and (b) modified data for base and subgrade layers. 75
Figure 4.11 Modified DCP data for base and subgrade layers showing PR values and coefficients of determination for four US 601 pavement regions: (a) DCP data from A1 condition region, (b) 1st DCP data from B1 condition region, (c) 2nd DCP data from B1 condition region, and (d) DCP data from B2 condition region. 75
Figure 4.12 Field core with pavement substructure as evidence of road widening. 78
Figure 4.13 Illustration of pavement structure shown in Figure 4.12 (US 220, Montgomery County). 78
Figure 4.14 Field cores with marking paint as evidence of road widening. 79

Figure 4.15 Pavement condition survey from NC87 and field cores: (a) condition survey and (b) to (e) cores presented in the condition survey map..... 79
Figure 4.16 Percentage of debonding frequency for different construction histories of all condition regions..... 81
Figure 4.17 Debonding (layer interface separation) in core-extracted hole (NC-24)..... 82
Figure 4.18 Photographs of smooth debonding (layer interface separation) surfaces in field cores. 82
Figure 4.19 Alligator cracking index values from the condition regions with or without debonding..... 83
Figure 4.20 Percentage of area with light alligator cracking in condition regions with or without debonding..... 83
Figure 4.21 Percentage of area with moderate alligator cracking in condition regions with or without debonding. 84
Figure 4.22 Percentage of area with severe alligator cracking in condition regions with or without debonding. 84
Figure 4.23 Comparison of *AREA* values for TDC and BUC sections..... 87
Figure 4.24 Simulation flow chart 90
Figure 4.25 Tensile strain result for the investigation of bottom-up cracking: (a) tensile strain kernel at the bottom of asphalt layer and (b) maximum tensile strain at the bottom of asphalt layer..... 91
Figure 4.26 Comparison of number of cycles to failure of asphalt binder and mixture. 92
Figure 4.27 Comparison of number of cycles to failure of asphalt binder and mixtures from different information categories: (a) young and poor condition regions and (b) old and good condition regions..... 93
Figure 4.28 Comparison of number of cycles to failure of asphalt binder from different condition regions..... 94
Figure 4.29 Comparison of number of cycles to failure of (a) asphalt binder and (b) mixtures from different condition regions. 94
Figure 4.30 Comparison of number of cycles to failure of asphalt binder from different condition regions in different categories..... 95
Figure 5.1 Damage contours for the B1 region in NC 24 pavement: (a) 1 year, (b) 5 years, (c) 10 years, and (d) 20 years. 100
Figure 5.2 Damage contours for the A1 region in NC 24 pavement: (a) 1 year, (b) 5 years, (c) 10 years, and (d) 20 years. 101
Figure 5.3 Damage contours for the B2 region in I 540 pavement: (a) 1 year, (b) 5 years, (c) 10 years, and (d) 20 years. 102
Figure 5.4 Damage contours for the A1 region in I 540 pavement: (a) 1 year, (b) 5 years, (c) 10 years, and (d) 20 years. 103
Figure 5.5 Damage contours for the A2 region in I 540 pavement: (a) 1 year, (b) 5 years, (c) 10 years, and (d) 20 years. 104

Figure 5.6 Damage contours for the B1 region in US 601 pavement: (a) 1 year, (b) 5 years, (c) 10 years, and (d) 20 years. 105
Figure 5.7 Damage contours for the B2 region in US 601 pavement: (a) 1 year, (b) 5 years, (c) 10 years, and (d) 20 years. 106
Figure 5.8 Damage contours for the A1 region in US 601 pavement: (a) 1 year, (b) 5 years, (c) 10 years, and (d) 20 years. 107
Figure 5.9 Damage contours for the B2 region in NC 17 pavement: (a) 1 year, (b) 5 years, (c) 10 years, and (d) 20 years. 108
Figure 5.10 Damage contours for the A2 region in NC 17 pavement: (a) 1 year, (b) 5 years, (c) 10 years, and (d) 20 years. 109
Figure 5.11 Damage contours for the B1 region in NC 209 pavement: (a) 1 year, (b) 5 years, (c) 10 years, and (d) 20 years. 110
Figure 5.12 Damage contours for the A1 region in NC 209 pavement: (a) 1 year, (b) 5 years, (c) 10 years, and (d) 20 years. 111
Figure 5.13 Damage contours for the B2 region in US 70 pavement: (a) 1 year, (b) 5 years, (c) 10 years, and (d) 20 years. 112
Figure 5.14 Damage contours for the A2 region in US 70 pavement: (a) 1 year, (b) 5 years, (c) 10 years, and (d) 20 years. 113
Figure 5.15 Damage contours for the B1 region in US 74 pavement: (a) 1 year, (b) 5 years, (c) 10 years, and (d) 20 years. 114
Figure 5.16 Damage contours for the A1 region in US 74 pavement: (a) 1 year, (b) 5 years, (c) 10 years, and (d) 20 years. 115
Figure 5.17 Damage contours for the B1 region in US 76 pavement: (a) 1 year, (b) 5 years, (c) 10 years, and (d) 20 years. 116
Figure 5.18 Damage contours for the A1 region in US 76 pavement: (a) 1 year, (b) 5 years, (c) 10 years, and (d) 20 years. 117
Figure 5.19 Damage contours for the B1 region in US 87 pavement: (a) 1 year, (b) 5 years, (c) 10 years, and (d) 20 years. 118
Figure 5.20 Damage contours for the A1 region in US 87 pavement: (a) 1 year, (b) 5 years, (c) 10 years, and (d) 20 years. 119
Figure 5.21 Comparison between ACI values and 20-year simulation results from DARWin-ME with Level 1 input: (a) maximum BUC% and (b) length of maximum TDC at surface. 127
Figure 5.22 Comparison between ACI values and 20-year simulation results from DARWin-ME with Level 3 input: (a) maximum BUC% and (b) length of maximum TDC at surface. 127
Figure 5.23 Comparison between ACI values and 20-year simulation results of maximum BUC% and maximum length of TDC at surface from DARWin-ME with higher-level inputs: (a) and (b) from TDC observed sites, (c) and (d) from TDC or BDC observed sites, (e) and (f) BUC observed sites, (g) and (h) from TDC or BDC observed sites. 129
Figure 5.24 Comparison between ACI values and 20-year simulation results of maximum BUC% and maximum length of TDC at surface from DARWin-ME with lower-level inputs: (a) and (b)

from BUC observed sites, (c) and (d) from BUC or BDC observed sites, (e) and (f) TDC observed sites, (g) and (h) from TDC or BDC observed sites. 130

LIST OF TABLES

Table 2.1 Number of sites categorized for a given pavement condition 12
Table 2.2 Distribution of test sites for the research 13
Table 2.3 List of 81 selected sites for the research 14
Table 2.4 Supplemental information for 81 selected sites given in Table 2.3 16
Table 2.5 Distribution of number of valid candidate test sites after NCDOT review 18
Table 2.6 List of test sites from 2010 condition survey database with layer information 20
Table 2.7 List of field-investigated pavement sites 21
Table 2.8 Investigated data elements corresponding to each cracking observed 24
Table 3.1 Mass requirement for the theoretical maximum specific gravity measurement 28
Table 3.2 Mass requirement for determining the asphalt content by the ignition method 29
Table 3.3 Required minimum mass of sample for extraction 47
Table 4.1 Summary of research into top-down cracking (NCHRP 2004c) 53
Table 4.2 Alligator cracking index and transverse cracking index with numerical values of distress obtained from condition survey data 57
Table 4.3 Substructure properties of selected field sites from *in situ* DCP test results 76
Table 4.4 Frequency of debonding and no debonding under different construction scenarios 81
Table 4.5 Summary of pavement information for the selected sites 86
Table 4.6 List of regions selected for simulation 89
Table 5.1 Cracking Severity and Propagation Direction Observed from Field Cores and Their Agreement with LVECD Prediction Results 99
Table 5.2 Required traffic inputs 121
Table 5.3 Required climatic inputs 122
Table 5.4 Required base layer inputs 123
Table 5.5 Required subgrade inputs 124
Table 5.6 Crack Propagation Propensity Observed from Field Cores and 20-year Simulation Results of DARWin-ME for Input Levels 1 and 3 126

Chapter 1 Introduction

1.1 Background

The Strategic Highway Research Program (SHRP) has identified permanent deformation, fatigue cracking, and low-temperature cracking as the three major distresses in asphalt pavements. According to the national survey conducted during NCHRP project 9-19, *Superpave Support and Performance Models Management*, permanent deformation was identified as the distress that causes the most problems in highways and runways in the United States. As a result, much more funding and research efforts have been focused on permanent deformation than other distress types.

Unlike the concern over permanent deformation distress at the national level, the most common failures in North Carolina are due to fatigue cracking. This situation may have worsened in recent years due to the fact that the Superpave mix design, as a national effort, focused on permanent deformation. Because mixes that are resistant to permanent deformation are also, in general, prone to fatigue, these efforts may have inadvertently led to the use of mixtures that are more prone to fatigue. In addition to this national driving force to eliminate permanent deformation, another issue is the fact that a pavement with observed fatigue cracking may represent a failure in the mix design or structural design, or failure related to construction; however, a pavement with observed asphalt concrete permanent deformation failure usually reflects failure only in the mix design or construction.

Currently, North Carolina is experiencing higher than anticipated rates of fatigue cracking. These higher than expected rates could be reflective of the national trends in mix design practice or could be caused by structural pavement failures. The problems associated with premature cracking in North Carolina pavements point to the need to evaluate the North Carolina Department of Transportation (NCDOT) mixes, processes, and measures to ensure that these factors properly balance the goals of preventing cracking and minimizing permanent deformation.

1.2 Research Objectives

The objectives of this research are to:

- Investigate whether systematic bias exists in the NCDOT's volumetric mix design, such as for dry asphalt concrete mixtures, aggregate structures, etc.
- Investigate strength and uniformity of the pavement substructure.
- Identify dominant causes of premature crack propagation patterns, such as top-down cracking (TDC), bottom-up cracking (BUC), and bidirectional cracking (BDC).

Without solid data from in-service pavements, any conclusions regarding the causes of these failures might be pure conjecture. Accordingly, in order to accomplish these objectives, this study examines material properties through laboratory experiments using field-extracted materials and investigates *in situ* pavements and pavement structure.

1.3 Outline of Research Presented

Chapter 2 describes the process of finding optimal field sites and the progress of the site investigative work. Chapter 3 presents the fundamental laboratory test procedures, mechanical test procedures, and binder tests used for this research. Also, the need for small geometries and their applications for this research are presented in Chapter 3. Chapter 4 describes the comprehensive literature review of the causes of cracking and the findings from field investigations and laboratory experiments. Chapter 5 describes the long-term performance of the investigated sites using two different simulation tools. Chapter 6 summarizes the findings of this research and suggests future research. Appendix A contains the master database built as a result of all of the experiments and field observations. Appendix B contains field material observation and records and the field condition survey map. Appendix C contains results from the laboratory tests, mechanical experiments, and rheological experiments.

Chapter 2 Forensic Study

2.1 Finding Valid Field Sites

The first step in performing this forensic study was to identify potential test sites. In order to find field sites that could be used to meet the study objectives, the 2010 version of the NCDOT's pavement condition survey database was obtained from the NCDOT Pavement Management Unit (PMU). This database is divided into regions (Coast, Piedmont and Mountains) and includes basic information, such as site identifications, route descriptions and mile postings, construction dates, ages, average annual daily traffic (AADT) data, overall pavement ratings, and the approximate extent of low, moderate, and severe cracking. The database was processed in order to set the study limits for the experiments. Specifically, the research team wanted to set quantifiable limits for factors such as age (new, typical, and old), traffic (low, medium, and high), and performance (good, typical, and poor). Because construction and material data generally are lacking for secondary roads, only primary roads were selected for setting the quantifiable limits. The total number of sites for the analysis is 525. Details of the database analysis are described in the following paragraphs.

2.1.1 Pavement Age

The statistical probability function for the pavement age within each region is shown in Figure 2.1. This figure shows that in the database the results are skewed towards a high concentration of *young* pavements. From the database it is found that the Coast region has a high frequency of *old* sites, but the Piedmont and Mountain regions have high frequencies of *young* pavements. This trend can be seen in Figure 2.2. To balance the frequency and reduce the effect of outliers in the Piedmont and Mountain regions, it was decided to use 8 years and 14 years to establish the lower and upper test limits. Percentiles corresponding to the lower and upper limits are the 44^{th} and 85^{th} percentiles, respectively. Using combined data from each region, the limit for *young* pavements is found to be 8 years, and the limit for *old* pavements is 14 years.

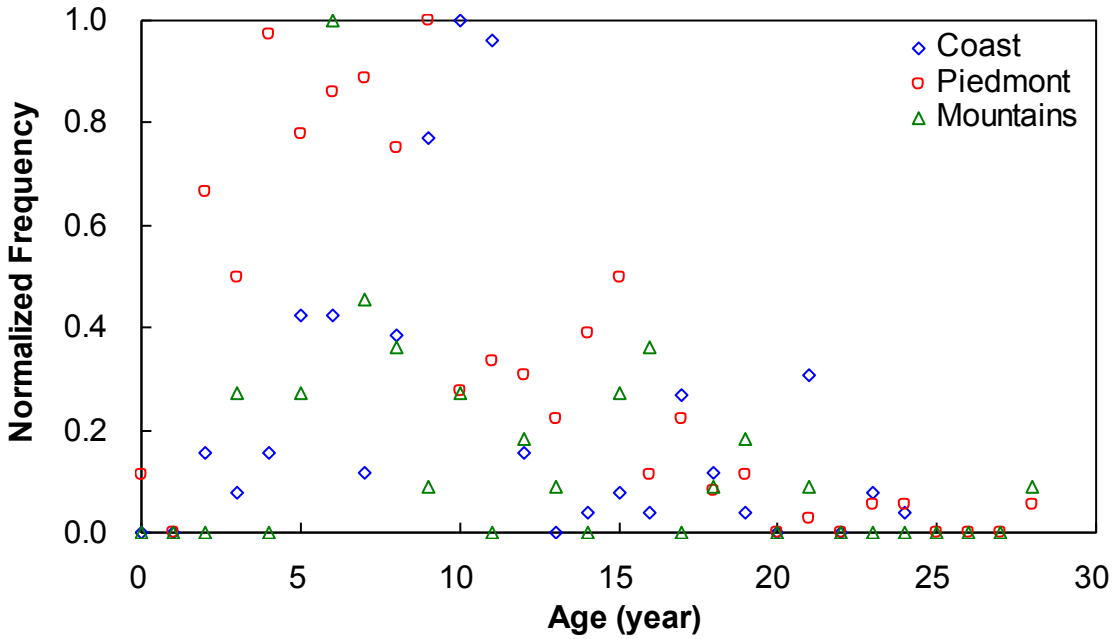

Figure 2.1 Distribution of pavement ages within the performance database.

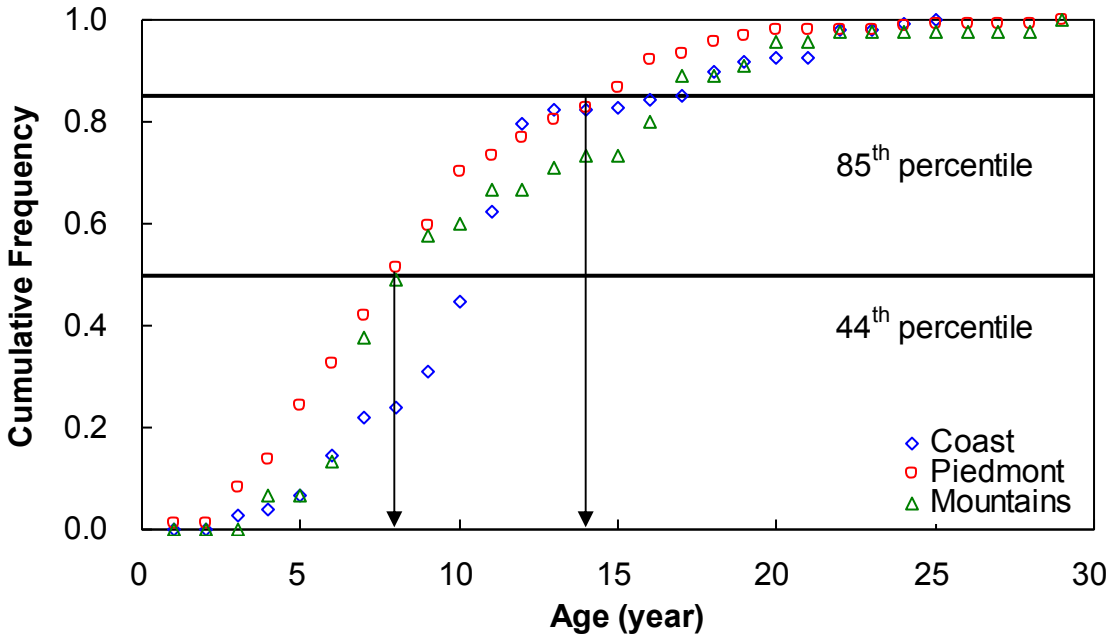

Figure 2.2 Cumulative distribution of pavement ages within the performance database.

2.1.2 Pavement Traffic

The AADT data are used to categorize the traffic levels for the available sites. This index has been compiled for all of the pavement sites in the database, and the results are summarized by region in Figure 2.3 (a) and cumulatively in Figure 2.3 (b). The majority of the pavements in the database contain relatively light traffic. Because this distribution is skewed to *low* traffic volumes, and because it is important in this research to obtain results from pavements that have been subjected to *high* traffic volumes, the research team decided to use the 31st and 64th percentiles to establish the upper and lower test limits. Figure 2.4 shows these limits along with the cumulative distributions. The figure shows also that the proposed upper limit for a *low* traffic level is an AADT of 4,000, and the proposed upper limit for the *moderate* traffic level is an AADT of 10,000.

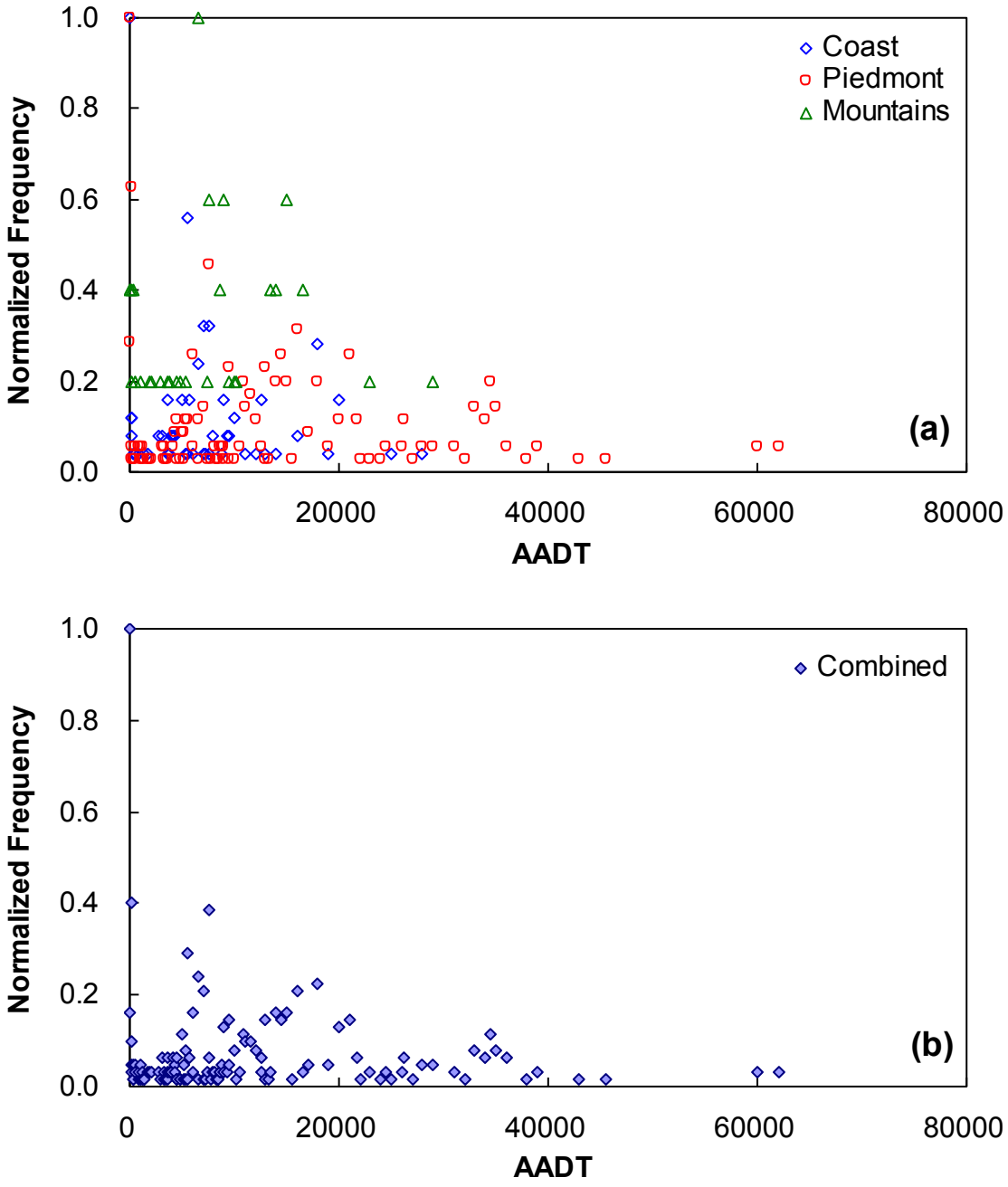

Figure 2.3 Distribution of traffic levels within the pavement performance database: (a) by region and (b) compiled for all regions.

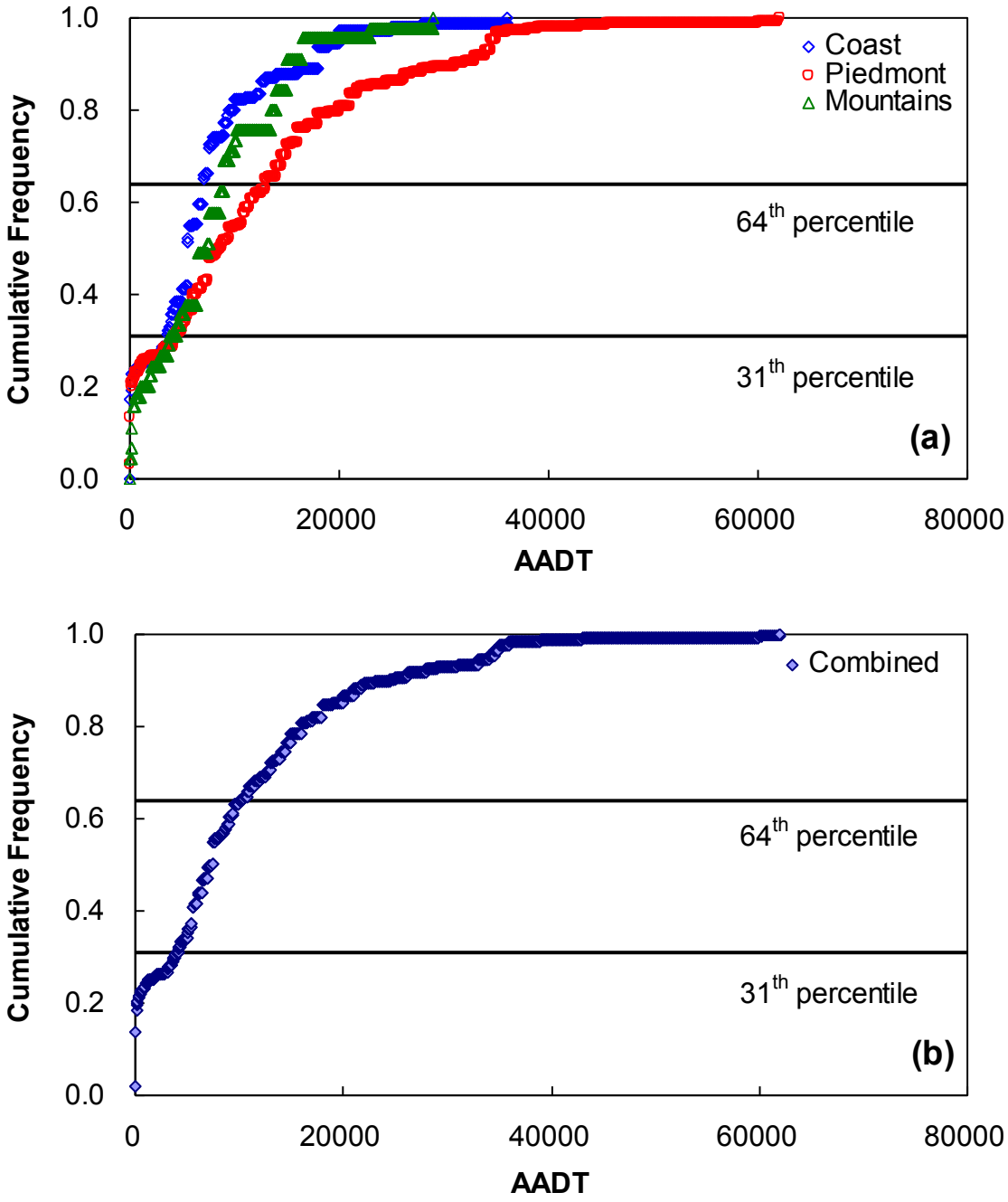

Figure 2.4 Cumulative distribution of traffic volumes and 31th and 64th percentiles: (a) by region and (b) compiled for all regions.

2.1.3 Fatigue Performance

As noted above, the pavement performance database provided by the NCDOT lists the percentage of each pavement site in terms of low, moderate, and severe alligator cracking. To analyze these data two different indices were utilized. The first index was developed by Corley-Lay et al. (2010) as a means to process the NCDOT network level performance quantities for Mechanistic-Empirical Pavement Design Guide (MEPDG) calibrations. The model that these researchers developed can be used to predict the total amount of alligator cracking in a pavement site from the network level measures of low, moderate, and severe alligator cracking. For the purposes of this research, the relationships established by Corley-Lay et al. (2010) have been normalized according to site length to yield the area of alligator cracking per distance of the travel lane, as shown in Equation (1), which is referred to here as *normalized alligator cracking* (NAC). The second fatigue index is a weighted average of the different cracking severity levels. This index was applied, based on input from the NCDOT, by Underwood and Kim (2009) to examine cracking along a 90-mile site of North Carolina roadway. The simple index function is given in Equation (2), and is referred to here as the *fatigue composite index*.

$$NAC = \frac{5.9(0.46 \times Low) + 1.7(0.61 \times Moderate) + 13.9(0.76 \times Severe)}{Sectional\ length(m)}, \quad (1)$$

where

$NAC = normalized\ alligator\ cracking$

$Low = amount\ of\ low\ alligator\ cracking$ (%)

$Moderate = amount\ of\ \text{mod}erate\ alligator\ cracking$ (%)

$Severe = amount\ of\ severe\ alligator\ cracking$ (%); *and*

$0.46,\ 0.61,\ and\ 0.76 = assumed\ width\ of\ cracking\ for\ each\ severity\ level,\ respectively.$

$$Fatigue\ Composite\ Index = 1\left(\frac{Low}{10}\right) + 2\left(\frac{Moderate}{10}\right) + 3\left(\frac{Severe}{10}\right) \quad (2)$$

Like the traffic trends, most of the pavements in the performance database have relatively low index values. This trend is not unexpected because *poor* performing pavements are likely to have been rehabilitated and, thus, would be excluded from the current study. Based on the same reasoning used to define the limits for traffic levels, it is proposed that the 50th and 80th percentiles be used to define the low and high limits for fatigue performance. Because both the

NAC and the fatigue composite indices show similar trends, and because the NAC index yields a quantifiable value for cracking (m^2/m), the NAC values are used for this analysis. These data are summarized in Figure 2.5 for both the NAC index, Equation (1), and the fatigue composite index, Equation (2). The cumulative distribution of the NAC values is shown along with the 50^{th} and 80^{th} percentile lines in Figure 2.6. Based on these percentiles and the distribution of performance levels, the division between *good* and *moderate* fatigue performance levels is found to be 0.01 m^2/m, and the division between *moderate* and *poor* fatigue performance levels is found to be 0.06 m^2/m.

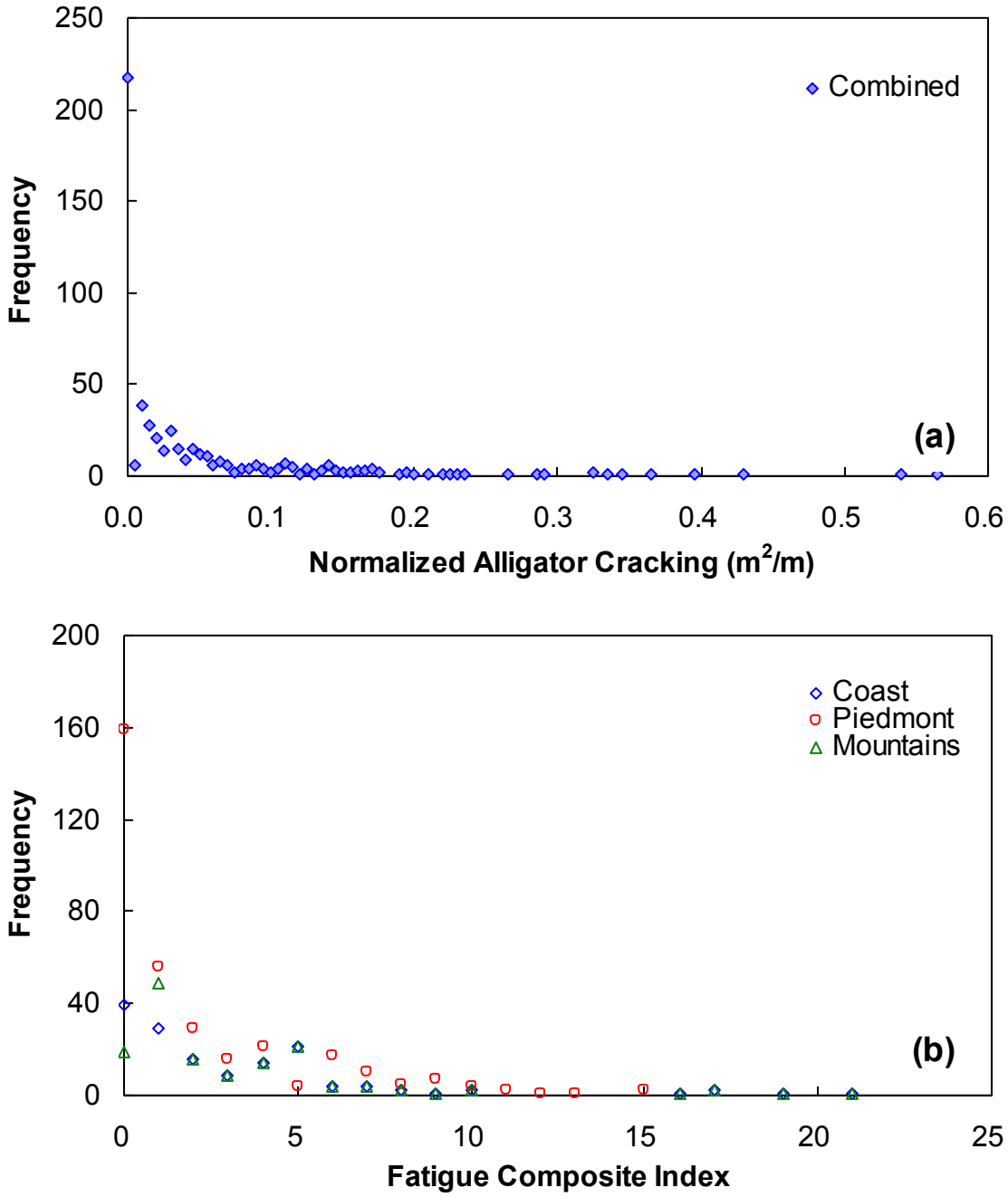

Figure 2.5 Distribution of pavement performance: (a) normalized alligator cracking index and (b) fatigue composite index.

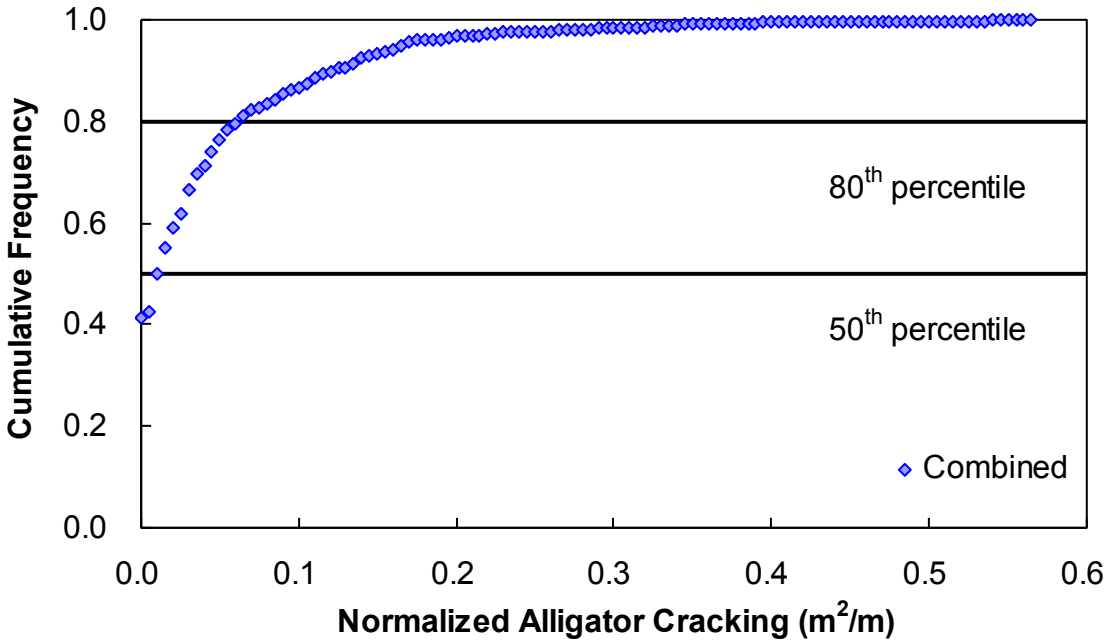

Figure 2.6 Cumulative distribution of fatigue performance and 50th and 80th percentiles.

2.1.4 Valid Field Sites

A naming convention for the pavement groupings has been adopted for this project. The identification reference format for the A-BCD (i.e., A = region, B= age, C = alligator cracking, D = AADT) case conditions is as follows. The first letter stands for the region in which the pavement site is located: **M**ountain, **P**iedmont, or **C**oast. The second letter stands for the age of the pavement site: **Y**oung or **O**ld. The third letter stands for the alligator cracking condition for a given site: **G**ood, **M**oderate, or **P**oor. The fourth letter stands for the AADT of the pavement site: **L**ow, **M**edium, or **H**igh. For example, **M-YPH** indicates that the pavement site is in the *Mountain* region**,** is in the *young* age group, exhibits *poor* alligator cracking, and has a *high* volume of AADT.

With the proposed limits in place, a query of the NCDOT database was performed to identify the number of potential sections that could be extracted for each combination of performance, traffic, age and region. The results are shown in Table 2.1. It was found that some cases (C-YGH, C-YPH, P-OPL) have no chosen test sites. These situations occurred because no

sites with these criteria were available in the database. Also, the low number of sites in the Mountain region, which is only 45 out of a potential 525 sites in the entire database, contributes to such situations.

Table 2.1 Number of sites categorized for a given pavement condition

Alligator Cracking	ADT	Young Age (X ≤ 8)			Middle Age (8 < X ≤ 14)			Old Age (X > 14)		
		Coast	Piedmont	Mountains	Coast	Piedmont	Mountains	Coast	Piedmont	Mountains
Good (X ≤ 0.01 m^2/m)	Low (X ≤ 4,000)	8	51	3	18	9	1	0	0	2
	Medium (4,000 < X ≤ 10,000)	9	21	6	10	25	1	3	4	3
	High (X > 10,000)	0	30	5	8	17	0	3	17	0
Moderate (0.01 m^2/m < X ≤ 0.06m^2/m)	Low (X ≤4,000)	4	10	2	5	7	0	2	0	0
	Medium (4,000 < X≤ 10,000)	3	10	2	18	7	3	8	7	3
	High (X > 10,000)	0	18	0	4	21	4	3	14	1
Poor (X > 0.06m^2/m)	Low (X ≤ 4,000)	3	9	4	11	2	2	1	0	0
	Medium (4,000 < X≤ 10,000)	8	6	0	6	2	0	3	5	1
	High (X > 10,000)	0	10	0	5	13	0	3	11	2

In order to attain the primary objectives of the research, major attention was given to four extreme cases, i.e., *young* pavements with *good* performance, *young* pavements with *poor* performance, *old* pavements with *good* performance, and *old* pavements with *poor* performance. The number of pavement sites in the four extreme cases is 231 in Table 2.1. Out of the 231 sites, 81 sites were selected as field investigation candidate sites, as shown in Table 2.2. Detailed information about the 81 sites is presented in Table 2.3 and Table 2.4. After selecting these 81 sites, the research team inquired about the possibility of obtaining construction data regarding the candidate sites listed in these tables. The research team felt that these records could provide possible clues as to the cause of fatigue cracking. As a result of this request, the NCDOT reviewed the list of sites presented in Table 2.3 and Table 2.4 and contacted Division/County engineers for the requested information. The NCDOT received responses for 68 sites out of 81 sites, and it was found that 22 sites out of these 68 sites had been rehabilitated since their original

construction. Thus, only 46 of the original 81 sites could be confirmed as valid sites for the purposes of this project. Furthermore, the NCDOT agreed that the sites with highest priority and of significant interest to this project include those sites that are old and show little fatigue cracking and those that are new and show relatively high fatigue cracking. As shown in Table 2.5, there are 6 and 28 sites available in these two categories, respectively.

Table 2.2 Distribution of test sites for the research

Alligator Cracking	ADT	Young Age (X ≤ 8)			Middle Age (8 < X ≤ 14)			Old Age (X > 14)		
		Coast	Piedmont	Mountains	Coast	Piedmont	Mountains	Coast	Piedmont	Mountains
Good (X ≤ 0.01 m^2/m)	Low (X ≤ 4,000)	2	1	1	-	-	-	0	0	2
	Medium (4,000 < X ≤ 10,000)	2	1	1	-	-	-	3	4	3
	High (X > 10,000)	0	1	1	-	-	-	3	15	0
Moderate (0.01 m^2/m < X ≤ 0.06m^2/m)	Low (X ≤4,000)	-	-	-	-	-	-	-	-	-
	Medium (4,000 < X≤ 10,000)	-	-	-	-	-	-	-	-	-
	High (X > 10,000)	-	-	-	-	-	-	-	-	-
Poor (X > 0.06m^2/m)	Low (X ≤ 4,000)	3	6	4	-	-	-	1	0	0
	Medium (4,000 < X≤ 10,000)	7	6	0	-	-	-	2	2	1
	High (X > 10,000)	0	4	0	-	-	-	1	2	2

Table 2.3 List of 81 selected sites for the research

Site ID	SURF. MATL.	SERVICE NUMBERS		COUNTY		ROUTE	YEAR FOR ACTION			AGE	RAT ING	AADT	ALGTR_PCT				%_OV RLP	NAC
		CONTRA CT	TIP	NAME	#		SUR VEY	REH AB	CON STR.				NONE	LOW	MDRT	HIGH		
CYGL-1	S12.5C	C200178	R-2719BA	LENOIR	54	40402010	2010	2003	2003	7	100	2800	10	0	0	0	65.2	0.00
CYGM-1	S9.5B	C200432	U-3449	PASQUOTANK	70	30000344	2010	2004	2004	6	100	10000	10	0	0	0	52.5	0.00
CYGM-2	S9.5B	C200479	R-2548E	TYRRELL	89	20600064	2010	2005	2005	5	100	5000	10	0	0	0	51.2	0.00
CYGM-3	S9.5B	C200479	R-2548E	TYRRELL	89	20600064	2010	2005	2005	5	100	5000	10	0	0	0	48.8	0.00
PYGL-1	S9.5B	C105166	R-2120AA	YADKIN	99	40001444	2010	2002	2002	8	100	40	10	0	0	0	96.9	0.00
PYGM-1	S9.5B	C200675	U-3110A	ALAMANCE	1	40401311	2010	2005	2005	5	100	5000	10	0	0	0	100	0.00
PYGH-1	S9.5C	C200312	U-2307AD	CATAWBA	18	40401005	2010	2005	2005	5	100	22000	10	0	0	0	100	0.00
MYGL-1	S9.5B	C200180	B-3071	WILKES	97	30000016	2010	2004	2004	6	100	3700	10	0	0	0	100	0.00
MYGM-1	S12.5C	C105429	R-2239C	WILKES	97	20400421	2010	2003	2003	7	100	6500	10	0	0	0	63.1	0.00
MYGH-1	OGAFC	C105227	I-0907B	MCDOWELL	59	10000040	2010	2003	2003	7	100	13500	10	0	0	0	96.9	0.00
COGM-1	BCSC			GREENE	40	20000264	2010	1988	1988	22	96.7	7500	9	1	0	0	54.9	0.01
COGM-2	BCSC			GREENE	40	20600264	2010	1988	1988	22	96.7	7500	9	1	0	0	45.6	0.01
COGM-3	BCSC			GREENE	40	20600264	2010	1988	1988	22	96.7	7500	9	1	0	0	54.4	0.01
COGH-1	HDS			BRUNSWICK	10	20000017	2010	1991	1991	19	86.7	13000	9	1	0	0	100	0.01
COGH-2	BCSC			JOHNSTON	51	20000070	2010	1991	1991	19	96.7	12500	9	1	0	0	44.2	0.01
COGH-3	BCSC			NEW HANOVER	65	30000132	2010	1994	1994	16	88.4	19000	8	2	0	0	43.4	0.01
POGM-1	OGAFC			CUMBERLAND	26	30000087	2010	1981	1981	29	96.7	9500	9	1	0	0	68.1	0.01
POGM-2	BCSC			SURRY	86	30000103	2010	1993	1993	17	100	6500	10	0	0	0	94	0.00
POGM-3	BCSC			SURRY	86	30000103	2010	1993	1993	17	100	6500	10	0	0	0	100	0.00
POGM-4	BCSC			SURRY	86	30000103	2010	1993	1993	17	100	6500	10	0	0	0	43.6	0.00
POGH-1	HDS			CATAWBA	18	20000321	2010	1995	1995	15	100	14500	10	0	0	0	54	0.00
POGH-2	HDS			CATAWBA	18	20000321	2010	1995	1995	15	100	14500	10	0	0	0	46	0.00
POGH-3	HDS			CATAWBA	18	20400321	2010	1995	1995	15	96.7	14500	9	1	0	0	46.2	0.01
POGH-4	HDS			CATAWBA	18	20400321	2010	1995	1995	15	96.7	14500	9	1	0	0	53.8	0.01
POGH-5	HDS			LINCOLN	55	20400321	2010	1995	1995	15	100	14500	10	0	0	0	100	0.00
POGH-6	BCSC			LINCOLN	55	20400321	2010	1993	1993	17	100	14500	10	0	0	0	62.5	0.00
POGH-7	BCSC			LINCOLN	55	20400321	2010	1994	1994	16	100	14500	10	0	0	0	60.9	0.00
POGH-8	I-1			LINCOLN	55	20400321	2010	1990	1990	20	100	14500	10	0	0	0	100	0.00
POGH-9	HDS			MECKLENBURG	60	10000085	2010	1994	1994	16	100	60000	10	0	0	0	40.8	0.00
POGH-10	HDS			MECKLENBURG	60	10400085	2010	1994	1994	16	100	60000	10	0	0	0	40.6	0.00
POGH-11	BCSC			PERSON	73	20400501	2010	1986	1986	24	96.7	10500	9	1	0	0	64.7	0.01
POGH-12	BCSC			PERSON	73	20400501	2010	1985	1985	25	96.7	16000	9	1	0	0	68.3	0.01
POGH-13	HDS			SCOTLAND	83	20000015	2010	1994	1994	16	95	15000	10	0	0	0	100	0.00
POGH-14	BCSC			YADKIN	99	20400421	2010	1995	1995	15	91.7	18000	9	1	0	0	56.7	0.01
POGH-15	BCSC			YADKIN	99	20400421	2010	1995	1995	15	91.7	18000	9	1	0	0	43.3	0.01
MOGL-1	BCSC			BURKE	12	30000126	2010	1981	1981	29	100	490	10	0	0	0	95.6	0.00
MOGL-2	I-1			HAYWOOD	44	30000209	2010	1994	1994	16	100	1900	10	0	0	0	40.8	0.00
MOGM-1	I-1			HAYWOOD	44	30000209	2010	1994	1994	16	95	5300	10	0	0	0	59.2	0.00
MOGM-2	HMA			SWAIN	87	20000441	2010	1988	1988	22	92.5	7400	9	0	1	0	100	0.01
MOGM-3	HDS			WILKES	97	20400421	2010	1993	1993	17	91.7	9500	9	1	0	0	40.4	0.00

Table 2.3 List of 81 selected sites for the research (continued)

Site ID	SURF. MATL.	SERVICE NUMBERS		COUNTY		ROUTE	YEAR FOR ACTION			AGE	RATING	AADT	ALGTR_PCT				%_OVRLP	NAC
		CONTRACT	TIP	NAME	#		SURVEY	REHAB	CONSTR.				NONE	LOW	MDRT	HIGH		
CYPL-1	SF9.5A	C200805	B-3482	JOHNSTON	51	40002320	2010	2004	2004	6	80.1	200	7	3	0	0	100	0.17
CYPL-2	HDS	C105196	R-1023AB	WILSON	98	20000264	2010	2002	2002	8	88.4	3100	8	2	0	0	100	0.07
CYPL-3	HDS	C105196	R-1023AB	WILSON	98	20600264	2010	2002	2002	8	76.8	3100	6	4	0	0	100	0.14
CYPM-1	S12.5C			MARTIN	58	20000013	2010	2003	2003	7	67.6	5650	6	3	1	0	100	0.11
CYPM-2	S12.5C			MARTIN	58	20000013	2010	2003	2003	7	67.6	5650	6	3	1	0	100	0.06
CYPM-3	S12.5C			MARTIN	58	20400013	2010	2003	2003	7	55	5650	1	2	6	1	100	0.23
CYPM-4	S12.5C			MARTIN	58	20400013	2010	2003	2003	7	55	5650	1	2	6	1	100	0.12
CYPM-5	S9.5B	C200156	R-0218B	PITT	74	20000013	2010	2004	2004	6	88.4	5500	8	2	0	0	100	0.11
CYPM-6	S12.5C	8T340302	R-1023B	WILSON	98	20000264	2010	2004	2004	6	71.8	7000	6	4	0	0	100	0.13
CYPM-7	S12.5C	8T340302	R-1023B	WILSON	98	20600264	2010	2004	2004	6	69.3	7000	5	4	1	0	100	0.14
PYPL-1	S9.5A	C200733	B-3401	ALAMANCE	1	40001921	2010	2004	2004	6	73.4	900	6	2	2	0	50	0.14
PYPL-2	S9.5A	C200733	B-3401	ALAMANCE	1	40001921	2010	2004	2004	6	73.4	900	6	2	2	0	50	0.14
PYPL-3	S9.5B	C200765	B-3601	ALAMANCE	1	40002158	2010	2005	2005	5	73.4	1900	6	2	2	0	100	0.12
PYPL-4	S9.5B			CHATHAM	19	40001349	2010	2006	2006	4	51.9	40	3	7	0	0	45.8	0.14
PYPL-5	S9.5B	C105501	R-2568A	DAVIDSON	29	40002144	2010	2003	2003	7	93.4	90	8	2	0	0	100	0.10
PYPL-6	HDS	C104952	I-2511BB	ROWAN	80	40002539	2010	2004	2004	6	93.4	3200	8	2	0	0	100	0.10
PYPM-1	S9.5B	C105520	B-2802	ALAMANCE	1	40001530	2010	2003	2003	7	48	6500	5	2	2	1	100	0.36
PYPM-2	HDS	C105414	R-2562AA	CUMBERLAND	26	30400087	2010	2003	2003	7	85.1	7500	7	3	0	0	100	0.09
PYPM-3	S12.5B	C104780	U-2581A	GUILFORD	41	20000070	2010	2002	2002	8	88.4	9400	8	2	0	0	100	0.11
PYPM-4	S12.5B	C105450	U-3307B	MECKLENBURG	60	40003632	2010	2002	2002	8	86.8	5400	6	4	0	0	68.6	0.19
PYPM-5	S12.5B	C105450	U-3307B	MECKLENBURG	60	40003632	2010	2002	2002	8	75.2	5400	4	6	0	0	100	0.06
PYPM-6	HDS	C104717	R-2000D	WAKE	92	40001005	2010	2003	2003	7	88.4	8100	8	2	0	0	100	0.11
PYPH-1	S9.5C	C201365	B-4009	ANSON	4	20600074	2010	2007	2007	3	70.1	16000	7	3	0	0	100	0.14
PYPH-2	S12.5B	C105417	U-2421	IREDELL	49	20000070	2010	2002	2002	8	79.3	28000	5	4	1	0	100	0.17
PYPH-3	S12.5B	C105417	U-2421	IREDELL	49	20000070	2010	2002	2002	8	79.3	28000	5	4	1	0	100	0.14
PYPH-4	S12.5D	C105254	R-2000EA	WAKE	92	10000540	2010	2002	2002	8	84.2	34500	8	1	1	0	100	0.07
MYPL-1	S9.5A	C200906	B-3310	BUNCOMBE	11	40002173	2010	2006	2006	4	83.4	2100	8	2	0	0	67.5	0.08
MYPL-2	S9.5B	C105200	R-2239B	WILKES	97	40002325	2010	2002	2002	8	88.4	260	8	2	0	0	44.1	0.06
MYPL-3	S9.5B	C105200	R-2239B	WILKES	97	40002325	2010	2002	2002	8	83.4	260	8	2	0	0	55.9	0.06
MYPL-4	S9.5B	C105200	R-2239B	WILKES	97	40002576	2010	2002	2002	8	72.6	1000	6	3	1	0	100	0.15
COPL-1	BCSC			DUPLIN	31	20000117	2010	1990	1990	20	45	3700	0	1	7	2	100	0.19
COPM-1	HDS			BRUNSWICK	10	20400017	2010	1992	1992	18	57.5	9000	2	6	2	0	100	0.07
COPM-2	BCSC			BRUNSWICK	10	30000904	2010	1986	1986	24	45	9300	7	0	2	1	100	0.07
COPH-1	BCSC			PITT	74	40001467	2010	1985	1985	25	75.9	28000	7	2	1	0	100	0.13
POPM-1	HDS			CASWELL	17	30000086	2010	1994	1994	16	47.6	5100	5	3	1	1	72.2	0.06
POPM-2	HDS			CUMBERLAND	26	30400087	2010	1990	1990	20	76.9	9500	3	7	0	0	100	0.11
POPH-1	HDS			CABARRUS	13	30600024	2010	1995	1995	15	31	12000	2	3	3	2	100	0.12
POPH-2	HDS			MONTGOMERY	62	30600024	2010	1991	1991	19	54	16000	2	4	3	1	100	0.08
MOPM-1	BCSC			HENDERSON	45	30000280	2010	1990	1990	20	67.7	9000	3	6	1	0	100	0.33
MOPH-1	HDS			WILKES	97	30000018	2010	1993	1993	17	88.4	14000	8	2	0	0	56.7	0.11
MOPH-2	HDS			WILKES	97	30000018	2010	1993	1993	17	75.9	14000	7	2	1	0	100	0.12

Table 2.4 Supplemental information for 81 selected sites given in Table 2.3

Site ID	ROUTE	CONDITION DESCRIPTION				AGE	RATING	PROJECT DESCRIPTION				AADT	%_OVRLP	NAC
		BMP	FROM	EMP	TO_DESC			BMP	EMP	BEG._DESC.	END._DESC.			
CYGL-1	40402010	0.730	SR 1575	2.100	SR 1572	7	100	0.000	2.100	US 258	SR 1572	2800	65.2	0.00
CYGM-1	30000344	18.875	SR 1479	20.715	END DIV HW	6	100	17.484	20.415	US 17	NC 344 WEST	10000	52.5	0.00
CYGM-2	20600064	17.190	MM 564	19.190	MM 562	5	100	17.190	21.100	US 64	SR 1116 + 0.22 MI	5000	51.2	0.00
CYGM-3	20600064	19.190	MM 562	21.190	MM 560	5	100	17.190	21.100	US 64	SR 1116 + 0.22 MI	5000	48.8	0.00
PYGL-1	40001444	0.420	PVMT CHG	0.730	SR 1150	8	100	0.410	0.730	EOM + 0.41 MI	SR 1150	40	96.9	0.00
PYGM-1	40401311	0.956	SR 1309	1.679	US 70	5	100	0.956	1.679	SR 1309	US 70	5000	100	0.00
PYGH-1	40401005	1.823	SR 1692	3.102	I-40	5	100	1.823	3.102	SR 1007 + 0.224 MI	I-40	22000	100	0.00
MYGL-1	30000016	18.515	SR 1559	20.355	BRIDGE	6	100	19.245	19.555	SR 1560 + 0.36 MI	SR 1560 + 0.67 MI	3700	100	0.00
MYGM-1	20400421	32.350	SR 2309	34.584	SR 2314	7	100	32.920	35.557	SR 2309 + .57 MI	YADKIN CO LINE	6500	63.1	0.00
MYGH-1	10000040	24.158	MM 91	26.218	BURKE CO	7	100	24.091	26.218	SR 1760 + 0.51 MI	BURKE CO	13500	96.9	0.00
COGM-1	20000264	0.000	WILSON CO	1.303	SR 1308	22	96.7	0.000	2.373	WILSON CO LINE	NC 91 + 0.20 MI	7500	54.9	0.01
COGM-2	20600264	1.093	SR 1311	2.860	SR 1308	22	96.7	1.780	4.150	NC 121 + 0.50 MI	WILSON CO LINE	7500	45.6	0.01
COGM-3	20600264	2.860	SR 1308	4.152	WILSON CO	22	96.7	1.780	4.150	NC 121 + 0.50 MI	WILSON CO LINE	7500	54.4	0.01
COGH-1	20000017	21.585	NC 211	23.645	US 17 BUS	19	86.7	21.585	23.645	NC211	US 17 BUS	13000	100	0.01
COGH-2	20000070	14.277	SR 1929	16.177	US 70 BYP	19	96.7	15.227	17.377	SR 1915	US 70 BUS	12500	44.2	0.01
COGH-3	30000132	2.390	ECL WILMIN	4.220	US 117	16	88.4	0.000	4.220	US 421	US 117	19000	43.4	0.01
POGM-1	30000087	9.683	I-95 SBL	12.023	SR 1007	29	96.7	8.773	11.623	NC 87 SOUTH	SR 2283	9500	68.1	0.01
POGM-2	30000103	0.510	SR 1760	1.210	QUARRY RD	17	100	0.740	1.240	NC 89	SR 1748	6500	94	0.00
POGM-3	30000103	1.210	QUARRY RD	2.940	SR 1846	17	100	1.240	2.630	NC 89	SR 1748	6500	100	0.00
POGM-4	30000103	2.940	SR 1846	3.690	SR 1748	17	100	2.630	4.350	NC 89	SR 1748	6500	43.6	0.00
POGH-1	20000321	0.000	LINCOLN CO	1.490	MP 1.49	15	100	0.000	2.760	LINCOLN CO LINE	SR 1005	14500	54	0.00
POGH-2	20000321	1.490	MP 1.49	2.760	SR 1005	15	100	0.000	2.760	LINCOLN CO LINE	SR 1005	14500	46	0.00
POGH-3	20400321	13.638	SR 1005	14.898	MP 14.898	15	96.7	13.638	16.368	SR 1005	LINCOLN CO LINE	14500	46.2	0.01
POGH-4	20400321	14.898	MP 14.898	16.368	LINCOLN CO	15	96.7	13.638	16.368	SR 1005	LINCOLN CO LINE	14500	53.8	0.01
POGH-5	20400321	0.000	CATAWBA CO	2.470	US 321 BUS	15	100	0.000	2.470	CATAWBA CO LINE	US 321 BUS	14500	100	0.00
POGH-6	20400321	2.470	US 321 BUS	4.070	SR 1282	17	100	2.470	5.030	US 321 BUS	SR 1267	14500	62.5	0.00
POGH-7	20400321	5.440	MP 5.44	6.079	NC 150	16	100	5.030	6.079	SR 1267	NC 27	14500	60.9	0.00
POGH-8	20400321	10.742	US 321 BUS	11.092	GASTON CO	20	100	10.742	11.092	US 321 BUS	GASTON CO LINE	14500	100	0.00
POGH-9	10000085	0.749	MM 28.4	2.082	MM 29.8	16	100	0.760	4.000	SR 1601	I-485 + 1.26 MI	60000	40.8	0.00
POGH-10	10400085	19.074	MM 29.8	20.415	MM 28.37	16	100	17.148	20.388	SR 1641 + .48 MI	SR 1601	60000	40.6	0.00
POGH-11	20400501	18.133	SR 1770	19.819	SR 1131	24	96.7	17.506	19.282	SR 1708 + 0.05 MI	SR 1218 + 0.22 MI	10500	64.7	0.01
POGH-12	20400501	21.249	END C&G	22.495	BRIDGE	25	96.7	21.255	23.071	SR 1742 + 0.07 MI	SR 1202 + 0.82 MI	16000	68.3	0.01
POGH-13	20000015	5.370	BEG DIV HW	6.950	US 74 BUS	16	95	5.370	5.730	US 15 SOUTH	SR 1108	15000	100	0.00
POGH-14	20400421	12.500	US 601	13.640	SR 1765	15	91.7	12.500	14.510	US 601	SR 1710 + 2.18 MI	18000	56.7	0.01
POGH-15	20400421	13.640	SR 1765	15.130	MP 15.13	15	91.7	12.500	14.510	US 601	SR 1710 + 2.18 MI	18000	43.3	0.01
MOGL-1	30000126	0.000	MCDOWEL CO	0.960	END 24'PVT	29	100	0.100	1.000	MCDOW.CO LINE+.1MI	SR 1310 + 0.30 MI	490	95.6	0.00
MOGL-2	30000209	7.784	SR 1501	8.804	PVMT CHG	16	100	6.624	8.584	SR 1355	SR 1501 + 0.80 MI	1900	40.8	0.00
MOGM-1	30000209	6.624	SR 1355	7.784	SR 1501	16	95	6.624	8.584	SR 1355	SR 1501 + 0.80 MI	5300	59.2	0.00
MOGM-2	20000441	0.000	JACKSON CO	0.760	US 19	22	92.5	0.000	0.760	JACKSON CO LINE	US 19	7400	100	0.01
MOGM-3	20400421	20.790	SR 2461	22.200	NC 115	17	91.7	20.390	23.880	SR 1001 + 0.67 MI	NC 115 + 1.68 MI	9500	40.4	0.00

Table 2.4 Supplemental information for 81 selected sites given in Table 2.3 (continued)

Site ID	ROUTE	CONDITION DESCRIPTION				AGE	RATING	PROJECT DESCRIPTION				AADT	%_OVRLP	NAC
		BMP	FROM	EMP	TO_DESC			BMP	EMP	BEG._DESC.	END._DESC.			
CYPL-1	40002320	3.953	SR 2141	5.783	SR 2342	6	80.1	4.713	5.013	SR 2362 + .38 MI	SR 2362 + .68 MI	200	100	0.17
CYPL-2	20000264	9.840	US 301	10.960	SR 1612	8	88.4	9.850	10.330	US 117	US 301 + .51 MI	3100	100	0.07
CYPL-3	20600264	13.290	SR 1612	14.390	US 301	8	76.8	13.920	14.390	SR 1612 + .59 MI	US 117	3100	100	0.14
CYPM-1	20000013	16.830	US 17	18.540	US 64 ALT	7	67.6	16.830	17.330	SR 1001 + .65 MI	US 64	5650	100	0.11
CYPM-2	20000013	16.830	US 17	18.540	US 64 ALT	7	67.6	17.330	18.240	SR 1001 + .65 MI	US 64	5650	100	0.06
CYPM-3	20400013	1.510	US 64 ALT	3.220	US 17 BRG	7	55	1.510	2.100	US 64	US 17 + .32 MI	5650	100	0.23
CYPM-4	20400013	1.510	US 64 ALT	3.220	US 17 BRG	7	55	2.100	3.220	US 64	US 17 + .32 MI	5650	100	0.12
CYPM-5	20000013	24.657	NC 30	26.222	US 64 ALT	6	88.4	24.667	24.977	SR 1509 + .39 MI	US 13 BUS	5500	100	0.11
CYPM-6	20000264	15.360	NC 58	16.760	MP 16.76	6	71.8	15.360	15.890	US 117 + .48 MI	NC 58 + .53 MI	7000	100	0.13
CYPM-7	20600264	7.460	MP 7.46	8.910	NC 58	6	69.3	8.370	8.910	US 264 ALT + 2.86 MI	SR 1612 + .63 MI	7000	100	0.14
PYPL-1	40001921	0.900	SR 1916	1.850	BRIDGE	6	73.4	1.680	2.020	SR 1916 + 0.78 MI	SR 1916 + 1.12 MI	900	50	0.14
PYPL-2	40001921	1.850	BRIDGE	2.990	SR 1948	6	73.4	1.680	2.020	SR 1916 + 0.78 MI	SR 1916 + 1.12 MI	900	50	0.14
PYPL-3	40002158	5.700	SR 2163	6.812	SR 2116	5	73.4	6.435	6.812	SR 2156	SR 2116	1900	100	0.12
PYPL-4	40001349	0.000	ALAM CO	0.380	SR 1350	4	51.9	0.000	0.830	ALAM. CO LINE	SR 1337	40	45.8	0.14
PYPL-5	40002144	0.000	NC 109	0.660	END MAINT	7	93.4	0.000	0.340	NC 109	NC 109 + .34 MI	90	100	0.10
PYPL-6	40002539	1.110	I-85	2.090	SR 1002	6	93.4	1.110	1.430	SR 2544 + .41 MI	SR 2582 + .19 MI	3200	100	0.10
PYPM-1	40001530	2.590	SR 1686	3.671	SR 1515	7	48	2.870	3.180	SR 1660 + 0.07 MI	SR 1658	6500	100	0.36
PYPM-2	30400087	23.406	SR 2238	24.896	SR 2245	7	85.1	23.446	24.016	SR 2238 + 0.04 MI	SR 2238 + 0.61 MI	7500	100	0.09
PYPM-3	20000070	24.124	CL GBORO	24.667	SR 3045	8	88.4	24.158	24.458	SR 2848 + .11 MI	SR 2848 + 1.53 MI	9400	100	0.11
PYPM-4	40003632	1.980	SR 5722	2.260	TOLLAND	8	86.8	1.870	2.220	SR 3630 + 0.81 MI	SR 5722 + 0.24 MI	5400	68.6	0.19
PYPM-5	40003632	2.920	SR 3628	4.570	NC 16	8	75.2	2.920	4.570	SR 5722 + 0.83 MI	NC 16	5400	100	0.06
PYPM-6	40001005	5.124	SR 3575	6.124	SR 1830	7	88.4	5.194	5.504	SR 3575 + 0.07 MI	SR 1830 + 0.12 MI	8100	100	0.11
PYPH-1	20600074	18.230	ECL POLKTN	19.130	PVMT CHG	3	70.1	18.659	19.029	SR 1420 + 1.25 MI	SR 1249 + 0.45 MI	16000	100	0.14
PYPH-2	20000070	13.929	SR 2352	15.059	SR 2354	8	79.3	14.489	14.919	SR 2735	SR 2318 + 0.08 MI	28000	100	0.17
PYPH-3	20000070	13.929	SR 2352	15.059	SR 2354	8	79.3	13.979	14.489	SR 2735	SR 2318 + 0.08 MI	28000	100	0.14
PYPH-4	10000540	12.418	MM 13	14.474	MM 15	8	84.2	12.650	12.970	SR 2005 +0.21 MI	SR 2013 + 0.11 MI	34500	100	0.07
MYPL-1	40002173	1.335	BRIDGE	2.165	SR 2175	4	83.4	1.200	1.615	SR 2231 + 1.19 MI	SR 2174 + 0.02 MI	2100	67.5	0.08
MYPL-2	40002325	2.740	SR 2576	3.100	BEG 36'PVT	8	88.4	2.863	3.400	SR 2438 + .38 MI	SR 2324 + .15 MI	260	44.1	0.06
MYPL-3	40002325	3.100	BEG 36'PVT	3.400	SR 2324	8	83.4	2.863	3.400	SR 2438 + .38 MI	SR 2324 + .15 MI	260	55.9	0.06
MYPL-4	40002576	6.880	BEG 36'PVT	7.350	DEAD END	8	72.6	6.970	7.350	SR 2325 + .31 MI	SR 2325 + .69 MI	1000	100	0.15
COPL-1	20000117	33.130	NCL CALYP	34.210	WAYNE CO	20	45	33.210	34.210	SR 1006 + 0.64 MI	WAYNE CO. LINE	3700	100	0.19
COPM-1	20400017	16.609	US 17 BUS	18.579	SR 1401	18	57.5	16.759	18.379	US 17 BUS	US 17 BUS	9000	100	0.07
COPM-2	30000904	17.240	NC 179	18.420	SR 1144	24	45	17.240	18.420	NC 179	SR 1144	9300	100	0.07
COPH-1	40001467	0.860	END HIV HW	2.500	US 13	25	75.9	1.260	1.560	SR 1200 + 0.22 MI	SR 1203 + 0.60 MI	28000	100	0.13
POPM-1	30000086	0.140	NC 49	1.930	SR 1719	16	47.6	0.500	2.480	NC 49	SR 1774	5100	72.2	0.06
POPM-2	30400087	15.806	US 301	17.476	SR 1007	20	76.9	16.446	17.476	SR 1007	SR 2283	9500	100	0.11
POPH-1	30600024	0.000	STANLY CO	1.730	END DIV HW	15	31	0.000	1.730	STANLEY CO LINE	NC 24	12000	100	0.12
POPH-2	30600024	5.210	BEG DIV HW	7.030	END DIV HW	19	54	5.210	7.030	NC 24	NC 24	16000	100	0.08
MOPM-1	30000280	8.770	SR 1354	9.630	BUNCOMB CO	20	67.7	9.310	9.630	NC 191	BUN. COLINE	9000	100	0.33
MOPH-1	30000018	16.040	SR 2510	16.210	BRIDGE	17	88.4	16.040	16.340	SR 1001	NC 18 SOUTH	14000	56.7	0.11
MOPH-2	30000018	16.650	CBD LOOP	16.990	6TH ST	17	75.9	16.650	16.980	NC 18 SOUTH	SR 2366	14000	100	0.12

Table 2.5 Distribution of number of valid candidate test sites after NCDOT review

Alligator Cracking	ADT	Young Age (X ≤ 8)			Middle Age (8 < X ≤ 14)			Old Age (X > 14)		
		Coast	Piedmont	Mountains	Coast	Piedmont	Mountains	Coast	Piedmont	Mountains
Good (X ≤ 0.01 m^2/m)	Low (X ≤ 4,000)	-	-	-	-	-	-	0	0	1
	Medium (4,000 < X ≤ 10,000)	-	-	-	-	-	-	0	0	1
	High (X > 10,000)	-	-	-	-	-	-	2	2	0
Moderate (0.01 m^2/m < X ≤ 0.06m^2/m)	Low (X ≤4,000)	-	-	-	-	-	-	-	-	-
	Medium (4,000 < X≤ 10,000)	-	-	-	-	-	-	-	-	-
	High (X > 10,000)	-	-	-	-	-	-	-	-	-
Poor (X > 0.06m^2/m)	Low (X ≤ 4,000)	3	6	4	-	-	-	-	-	-
	Medium (4,000 < X≤ 10,000)	7	6	0	-	-	-	-	-	-
	High (X > 10,000)	0	2	0	-	-	-	-	-	-

In spite of the time and effort spent in finding valid field sites through database analysis, the actual pavement conditions did not match the records in the database or the responses of Division engineers. For example, when records in the database indicated moderate to severe fatigue cracking at a site, no fatigue cracking was found at the actual site. In one extreme case, concrete pavement was found at a site, even though the database records indicated an asphalt pavement construction and profile. Accordingly, all of the sites listed in Table 2.5 were visited by the research team to verify whether the field conditions matched the records. It was found that only 6 out of 32 sites matched the records in the database. Therefore, 6 sites from the 2010 condition survey database were selected for field investigation. Also, the research team directly contacted 14 Divisions in North Carolina to obtain the 2011 scheduled resurfacing list. Eight Divisions out of 14 Divisions responded to the request, and those eight Divisions provided the locations of 120 sites. Those 120 sites were divided into different condition groups for the analysis process.

Scheduling field work also was a challenge for this research, because it was necessary to consider the schedules of NCDOT personnel, weather on the test date, the traffic maintenance

contractor's schedule and so forth. For these reasons, it was not possible to conduct field investigations for all of the field site candidates before the scheduled resurfacing of the selected sites. Accordingly, the 2012 scheduled resurfacing list was obtained through the NCDOT PMU and analyzed using the same process as for the 2011 list, and then onsite investigations were conducted. Finally, 9 sites were investigated for test Level 1, and 10 sites were investigated for test Level 2. Table 2.7 shows the final list of pavement sites tested for both Level 1 and Level 2. Figure 2.7 shows the distribution of the tested sites on a map of North Carolina. The numbers shown on the map in Figure 2.7 are the site numbers listed in Table 2.7.

Table 2.6 List of test sites from 2010 condition survey database with layer information

Site ID	Layer 1			Layer 2			Layer 3			Layer 4		
	MC	Thickness	Year	MC	Thickness	Year	MC	Thickness	Year	MC	Thickness	Year
COGH-1	HDS	2.5	1991	HDB	2	1991	ABC	8	1991			
COGH-2	BCSC	1.75	1994	BCBC	5	1994						
CYPL-1	SF9.5A	2.5	2004	B25.0B	3.5	2004						
CYPL-2	HDS	2.5	2002	HDB	3.5	2002	ABC	10	2002	STAB	8	2002
CYPL-3	HDS	2.5	2002	HDB	3.5	2002	ABC	10	2002	STAB	8	2002
CYPM-1	S12.5C	3	2003	I19.0C	2.5	2003	ABC	10	2003			
CYPM-2	S12.5C	3	2003	I19.0C	2.5	2003	ABC	10	2003			
CYPM-3	S12.5C	3	2003	I19.0C	2.5	2003	ABC	10	2003			
CYPM-4	S12.5C	3	2003	I19.0C	2.5	2003	ABC	10	2003			
CYPM-5	S9.5B	2.5	2004	I19.0B	3	2004	ABC	8	2004			
CYPM-6	S12.5C	2	2004	I19.0C	3.5	2004	ABC	8	2004	STAB	8	2004
CYPM-7	S12.5C	2	2004	I19.0C	3.5	2004	ABC	8	2004	STAB	8	2004
MOGL-2	I-1	2	1994	H	2	1994	ABC	8	1994			
MOGM-1	I-1	2	1994	H	2	1994	ABC	8	1994			
MYPL-1	S9.5A	2.5	2006	I19.0B	2.5	2006	B25.0B	3	2006			
MYPL-2	S9.5B	2	2002	I19.0B	3	2002	ABC	10	2002			
MYPL-3	S9.5B	2	2002	I19.0B	3	2002	ABC	10	2002			
MYPL-4	S9.5B	2	2002	I19.0B	2.5	2002	B25.0B	3	2002	ABC	8	2002
POGH-10	HDS	2.5	1994	HDB	3.5	1994	HB	11	1994			
POGH-9	HDS	2.5	1994	HDB	3.5	1994	HB	11	1994			
PYPH-1	S9.5C	3	2007	I19.0C	3	2007	B25.0C	10	2007			
PYPL-1	S9.5A	2.5	2004	I19.0B	2.5	2004	ABC	6	2004			
PYPL-2	S9.5A	2.5	2004	I19.0B	2.5	2004	ABC	6	2004			
PYPL-3	S9.5B	2.5	2005	I19.0B	3.5	2005	ABC	8	2005			
PYPL-5	S9.5B	2.5	2003	I19.0B	4.5	2003	ABC	6	2003			
PYPL-6	HDS	2.5	2004	HDB	2	2004	HB	4.5	2004			
PYPM-1	S9.5B	2.5	2003	I19.0B	3	2003	B25.0B	5.5	2003			
PYPM-2	HDS	2.5	2003	HDB	3.5	2003	HB	5	2003			
PYPM-3	S12.5B	2.5	2002	I19.0B	4.5	2002	B25.0B	4.5	2002			
PYPM-4	S12.5B	3	2002	I19.0B	3	2002	ABC	6	2002	STAB	8	2002
PYPM-4	S12.5B	3	2002	I19.0B	3	2002	ABC	6	2002	STAB	8	2002
PYPM-6	HDS	2.5	2003	HDB	3.5	2003	HB	8	2003			

Table 2.7 List of field-investigated pavement sites

No	Test Level	County	Route	Age	Region	Condition	List from
1	1	Wake	I 540	9	Piedmont	Young and Poor	2010 condition survey database
2		Mecklenburg	NC 24	6	Piedmont	Young and Poor	2011 resurfacing scheduled list
3		Johnston	US 70	3	Coast	Young and Poor	2010 condition survey database
4		Brunswick	US 17	20	Coast	Old and Good	2010 condition survey database
5		Union	US 601	10	Piedmont	Young and Poor	2011 resurfacing scheduled list
6		New Hanover	US 76	11	Coast	Young and Poor	2012 resurfacing scheduled list
7		Cumberland	NC 87	8	Piedmont	Young and Poor	2010 condition survey database
8		Swain	US 74	9	Mountains	Young and Poor	2011 resurfacing scheduled list
9		Haywood	NC 209	17	Mountains	Old and Good	2010 condition survey database
10	2	Martin	US 13	7	Coast	Young and Poor	2010 condition survey database
11		Richmond	NC 177	7	Piedmont	Young and Poor	2011 resurfacing scheduled list
12		Montgomery	US 220	7	Piedmont	Young and Poor	2011 resurfacing scheduled list
13		Davidson	NC 47	9	Piedmont	Young and Poor	2011 resurfacing scheduled list
14		Cumberland	NC 82	6	Piedmont	Young and Poor	2012 resurfacing scheduled list
15		Cumberland	US 401	10	Piedmont	Young and Poor	2012 resurfacing scheduled list
16		Harnett	NC 55	11	Piedmont	Young and Poor	2012 resurfacing scheduled list
17		Brunswick	NC 179	3	Coast	Young and Poor	2012 resurfacing scheduled list
18		Avery	NC 194	10	Mountains	Young and Poor	2011 resurfacing scheduled list
19		Alamance	SR 1530	7	Piedmont	Young and Poor	NCDOT invitation

Figure 2.7 Test site distribution on North Carolina map.

2.2 Field Investigation

On-site pavement conditions, test protocols and the visual investigation of field-extracted cores are described in the following subsections. Detailed analysis of each pavement site is discussed in Appendix B.

2.2.1 Selecting Pavement Sites for Investigation

All candidate sites for investigation were selected based on the condition survey results. Because the condition survey was conducted based on visual surveys of the pavement surface, the length of the surveyed pavement segment did not necessarily match the construction history of the pavement and the profile for underneath the surface course. In order to obtain quality information from consistent construction histories and profiles, all of the candidate sites were verified in the NCDOT database in terms of construction history, profile, or other possible variations.

2.2.2 Field Investigation Protocols

When selecting a test section at a site for field investigation, several factors were considered, including the drivers' clear vision of the lane closure, consistent traffic that may be changed by connecting roads, and the exit and safety of field workers. Thus, all of the finally selected sites were visited prior to the test date in order to define optimal sections within a single site.

On the test date, the outer lane of each selected section was closed by traffic control crews from the local or Division office of the NCDOT. Material extraction (coring) locations were selected by the research team. Coring locations were selected in the wheel path, between wheel paths, on top of a cracked surface, and from a non-cracked surface near a cracked surface. A basic assumption that is made of field-extracted materials to be used for lab experiments is that they should come from between wheel paths and that no cracking should be evident at the coring location such that the site condition is considered to be undamaged. Therefore, materials extracted from between the wheel paths were used to investigate the material properties for this research. In addition, materials extracted from surface cracked areas and near cracked areas were used for the visual investigation of cracking propensity and propagation. The coring locations

were defined roughly and marked on the side of the pavement section prior to the onsite testing date, and the exact locations of the coring spots were identified on the test date.

Falling weight deflectometer (FWD) testing at regular distances, depending on the length of the entire site, at 100 ft or 200 ft intervals was conducted by PMU personnel while the research team marked the locations of material extraction (coring). After marking the coring locations, FWD testing was conducted on top of the coring spot or close to the coring spot. After FWD testing at these coring locations, materials were extracted using a 6-inch diameter drill bit. The positioning of the coring device mounted on a truck and the actual coring times depended on the lane width, pavement shoulder width and asphalt layer depth (coring depth), but it usually took 10 to 20 minutes for a single coring process to be completed.

Dynamic cone penetrometer (DCP) testing was conducted at the cored location in order to investigate the strength of the pavement substructure. In a single condition region within the test site, DCP testing was conducted at least two times. Because lane closures should begin immediately after morning commuting time and finish before afternoon commuting time, all of the cored spots needed to be filled with rock asphalt before the roadway could be opened again to traffic. Therefore, a limited number of DCP tests were conducted for the onsite investigation.

Figure 2.8 Photographs of field investigation procedure: (a) FWD testing, (b) coring spot marking, (c) coring machine mounted on truck, and (d) DCP testing.

2.3 Investigated Data Elements

In Table 2.8, investigated data elements that correspond to each cracking type observed through this research are presented. Data elements are grouped into three different levels: pavement level, material level, and evaluation tool. How to investigate and evaluate cracking types observed are marked under different data items. Except for those gray highlighted data elements in Table 2.8, all elements are considered to both test level 1 and 2, and those gray highlighted data elements apply to test level 1 that is higher ranked investigation. In order to define layer interface separation, the research team visually investigated extracted cores and cored holes.

Table 2.8 Investigated data elements corresponding to each cracking observed

Observation	Pavement Level									
	Field Observation		Structural Design						Exposure Factor	
	Core Observation	Crack Survey	FWD	DCP	Layer Thickness	Bottom Strain	Top Strain	Subgrade Modulus	Temp.	Traffic
Widening	√	√								
Top-Down	√	√	√	√	√		√	√	√	√
Bottom-Up	√	√	√	√	√	√		√	√	√
Bi-Directional	√	√	√	√	√	√	√	√	√	√
Transversal	√	√							√	

Observation	Material Level				Evaluation Tool					
	Mixture Design				Mixture		Binder		Pavement Simulation	
	% Asphalt Content	% Air Void	agg. Gradation	Film Thickness	|E*|	C vs.S	|G*|	C vs.S	LVECD	DARWin ME
Widening										
Top-Down	√	√	√	√	√	√	√	√	√	√
Bottom-Up	√	√	√	√	√	√	√	√	√	√
Bi-Directional	√	√	√	√	√	√	√	√	√	√
Transversal	√			√						

Chapter 3 Experimental Approaches

3.1 Determination of Mix Design Parameters with Field-Extracted Materials

3.1.1 Introduction

As stated in the research objectives, the major materials handled in this study are field-extracted materials. Materials from in-service pavements are extremely valuable due to their limited amounts and the difficulties associated with acquiring them. For these reasons, the limited amounts of field-extracted materials must be used efficiently, which is one of the keys to the success of this project. Accordingly, all of the field-extracted cores were named and labeled immediately after their extraction from the pavement, and the core identifications were recorded on both surfaces of the cores and on their storage containers. Also, these core identifications were marked on the on-site pavement condition survey map for future reference. Once the cores were brought to the laboratory, they were air-dried in an open space for two days to allow the evaporation of any surface moisture. In order to build a quality database, as much information about the cores as possible was recorded; this information includes surface condition, layer thickness, cracking condition and cracking propensity, and so on. After recording all of the possible information, the asphalt layer was identified by comparing one core's mixture pattern on its side to that of another core and/or comparing the actual core to records from the NCDOT database (described in Chapter 2). Usually, a solid tack coat line was evident on the side of the core, which indicated a gap in the construction between one layer to another layer. This clue, as well as the mixture patterns and/or color of the layer, were used to define the boundary lines of the different materials used for each layer.

3.1.2 Material Collection Strategy from In-Service Pavement

As stated in Chapter 2, selected pavement sites were divided into two to four different condition regions, i.e., relatively *good* condition regions and relatively *poor* condition regions. Materials were extracted from both the wheel path and between the wheel paths. For the laboratory tests, cores were extracted from between the wheel paths and from locations where no cracking was observed, because these areas were less likely to have experienced damage from traffic loading than heavily trafficked areas of the roadway. For the mechanical tests, cores were

extracted as far away as possible from the other extraction locations, because material characterization by mechanical testing requires quality materials that can represent the undisturbed pavement. A schematic diagram of the field cores is presented in Figure 3.1, which presents the pavement condition survey for US 70.

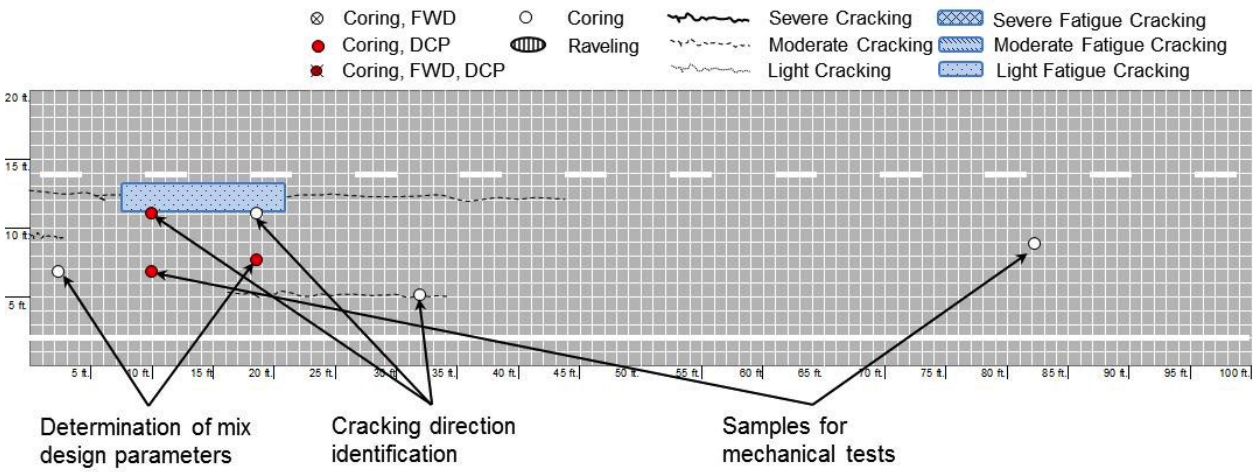

Figure 3.1 Schematic diagram of field cores used (US 70).

3.1.3 Experiment Sample Preparation

Figure 3.2 shows the procedure for fabricating specimens from field cores for the mechanical tests. Once the boundary lines of each layer were determined, as shown in Figure 3.2 (a) and Figure 3.2 (b), field samples were cut from each layer. These cut layers are sometimes referred to as *hockey pucks* based on their disk-like shape. Then, either side coring was conducted on the hockey pucks to create cylindrical specimens, or additional cutting was undertaken for the prismatic specimens to fabricate samples for the mechanical testing, as shown in Figure 3.2 (c). Figure 3.2 (d) shows the dimensions of the mechanical test samples for both the cylindrical and prismatic specimens. These prepared hockey pucks were used for binder extraction and fundamental laboratory experiments to determine air void content, maximum specific gravity, asphalt content, and aggregate gradation.

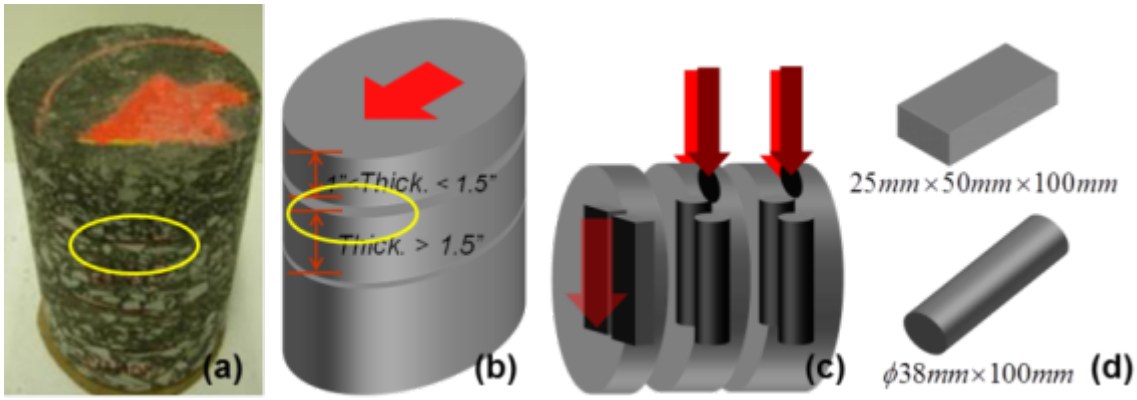

Figure 3.2 Use of field samples for mechanical tests: (a) cored sample from in-service pavement (b) cutting layers of hockey pucks, (c) side coring and cutting for mechanical tests, and (d) dimensions of test samples.

3.1.4 Determination of Mix Design Parameters

Air void content

The air void contents of the hockey pucks can be measured by either the saturated surface dry (SSD) method or the Corelok vacuum sealing method. For consistency, the air void contents of the prepared hockey pucks were measured by the Corelok method, because the SSD method is limited in measuring the air void content of mixtures that have interconnecting voids, such as open-graded mixtures. Also, the Corelok method does not require an additional sample drying procedure for the next step, which is aggregate separation. Before measuring the air void contents, the hockey pucks were dried by an automatic rapid-drying laboratory apparatus using vacuum technology, CoreDry. The detailed test procedures for measuring air void content are presented in standard specifications, ASTM D2726, ASTM D6752, ASTM D7227, for the SSD, Corelok, and CoreDry methods, respectively. Figure 3.3 shows the experimental equipment used for measuring air void content. (Note: Figure 3.3 (a) and (b) were taken from the InstroTek website.) The values measured for each mixture were recorded in the master database to help identify causes of systematic mix design flaws.

Figure 3.3 (a): CoreDry, (b), Corelock, and (c) Gilson water tank.

Theoretical Maximum Specific Gravity

The theoretical maximum specific gravity (G_{mm}) value is used with bulk-specific gravity values measured from field cores to calculate the air void content in a mixture. The maximum specific gravity is determined using samples in a so-called loose-mixture condition. Therefore, for this research, the hockey pucks used for air void measurements were used to create the measurable loose-mixture condition for the samples. In order to change the condition of the field cores to a loose-mix condition, the hockey pucks were placed in an oven at 110 ± 5°C for 15 minutes. Once the mixture was soft enough to be able to separate the cut aggregate from the aggregate that was fully covered with binder, all of the cut aggregate samples were removed by hand. Then, the particles of fine aggregate were gently separated in order to retain particles no larger than a nominal maximum size of aggregate (NMSA) of 6 mm. The minimum required sample sizes (by weight) are presented in Table 2.1. The detailed test procedure for the maximum specific gravity measurements is presented in standard specifications, ASTM D2041 or AASHTO T209. Figure 3.4 shows a test-ready sample in the loose-mixture condition and the vacuum assembly used for research at NCSU.

Table 3.1 Mass requirement for the theoretical maximum specific gravity measurement

Nominal Maximum Size of Aggregates	Minimum Sample Size
37.5 mm or greater	5,000 g
19 mm to 25 mm	2,500 g
12.5 mm or smaller	1,500 g

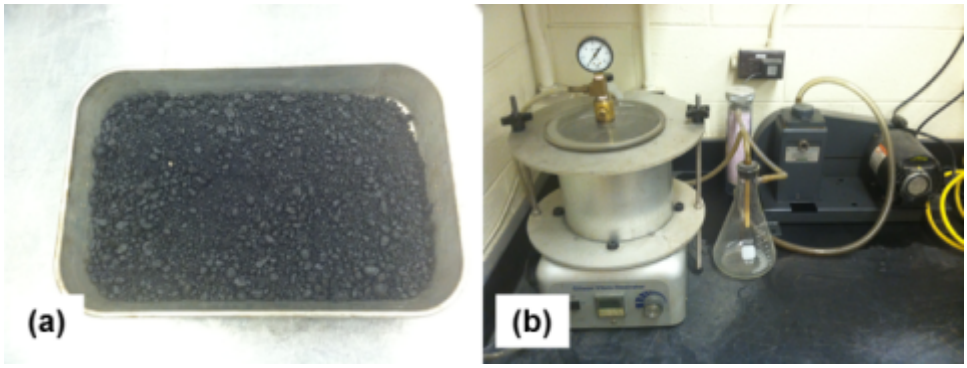

Figure 3.4 (a) Test-ready separated sample and (b) vacuum assembly with metal bowl.

Asphalt Binder Content

The asphalt binder content is measured as the difference between the initial mass of the material and the mass of the binder removed in an ignition chamber. The materials used for measuring the theoretical maximum specific gravity were used to obtain the asphalt content in the mixture. The water that remained in the material that was used for the maximum specific gravity measurements was carefully removed and dried at room temperature in a pan. Once no moisture was observed (visually) in the material, it was oven-dried again to a constant weight at a temperature of 110 ± 5°C. The required minimum amount of sample for this test is presented in Table 2.1. The detailed test procedure for determining asphalt binder content is presented in the standard specification, AASHTO T308-08. Figure 3.5 (a) and (b) show the materials contained in the ignition basket before and after ignition, and the Troxler NTO ignition chamber used for the research, respectively. The values measured for each mixture were recorded in the master database to help identify causes of systematic mix design flaws.

Table 3.2 Mass requirement for determining the asphalt content by the ignition method

Nominal Maximum Size of Aggregates	Minimum Sample Size (g)
4.75 mm	1,200
9.5 mm	1,200
12.5 mm	1,500
19.0 mm	2,000
25.0 mm	3,000
37.5 mm	4,000

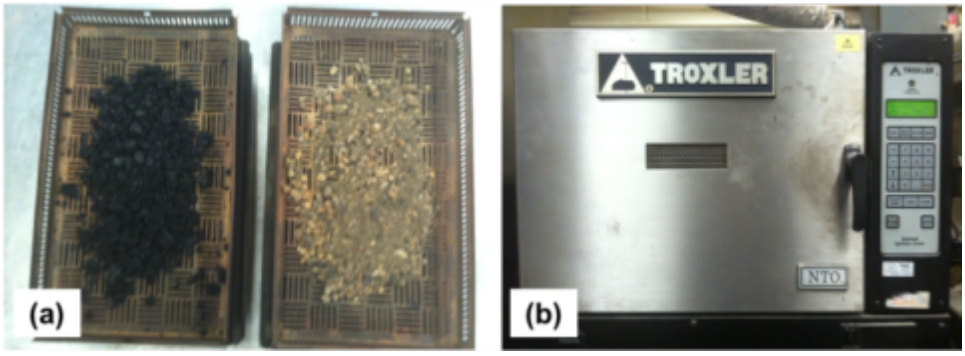

Figure 3.5 (a) Material before ignition and after ignition, and (b) Troxler NTO ignition chamber.

3.2 Mechanical Experiment

3.2.1 Test Setup

A closed-loop servo-hydraulic testing machine manufactured by MTS was used for the mechanical experiments for this research. The test machine is a MTS 810 loading frame equipped with either a 25 kN or 8.9kN load cell, depending on the nature of the test. It is capable of applying loads up to 20 kips, from 0.01 Hz to 25 Hz. Vertical deformations were measured using linear variable differential transformers (LVDTs). In order to mount the LVDTs on the test specimens, round targets were glued to the specimens beforehand. Loose-core LVDTs were used for taking the measurements and were located 90° apart from each other. The gauge length of 50 mm was adopted for measuring the deformations of specimens with small geometries. For accurate and consistent measurements, a target gluing jig was developed for these smaller geometries. A temperature control chamber was used to measure material performance at different temperatures with consistency. This chamber is capable of maintaining temperatures ranging from -15°C to 100°C.

The data acquisition system used in this research is a fully computer-controlled system based on LabView software. The LabView program is capable of measuring and recording real-time information from up to 16 channels simultaneously. Six channels were used for the mechanical tests: four for the vertical LVDTs, one for the load cell, and one for the actuator.

3.2.2 Theoretical Background

Viscoelastic materials such as asphalt mixtures exhibit time- and temperature-dependent characteristics, which means that the response of the asphalt material is not only a function of the current input but also the past input history, unlike the responses of pure elastic materials that reflect only the behavior that is dependent on the current input.

For linear viscoelastic materials, the input and response relationship can be expressed by the hereditary integral function (Equation (3)). The response to past and current inputs can be obtained by a known unit response function.

$$R = \int_{-\infty}^{t} R_H(t,\tau)\frac{dI}{d\tau}d\tau \tag{3}$$

where

R = response,

R_H = unit response function,

t = time of interest,

τ = integration variable, and

I = input.

For uniaxial loading, the linear viscoelastic stress and strain relationship is expressed in the convolution integral function, as shown in Equations (4) and(5).

$$\sigma = \int_{0}^{t} E(t-\tau)\frac{d\varepsilon}{d\tau}d\tau \tag{4}$$

$$\varepsilon = \int_{0}^{t} D(t-\tau)\frac{d\sigma}{d\tau}d\tau \tag{5}$$

where

σ = stress,

ε = strain,

$E(t)$ = relaxation modulus, and

$D(t)$ = creep compliance.

Both the relaxation modulus and creep compliance are referred to as unit response functions, because these properties are the responses for respective unit inputs. Therefore, in linear viscoelastic theory, these two properties and the complex modulus are important material properties. These unit response properties (functions) can be obtained by mechanical experiments in the linear viscoelastic state.

Schapery (1984) suggests that the elastic-viscoelastic correspondence principle is applicable to both linear and nonlinear viscoelastic material behavior. In short, the stress and strain in a viscoelastic body can be handled with an elastic solution once the physical quantities are replaced by pseudo variables in a convolution integral form. According to Schapery, the uniaxial pseudo strain, ε^R, is defined as in Equation (6).

$$\varepsilon^R = \frac{1}{E_R}\int_o^t E(t-\tau)\frac{d\varepsilon}{d\tau}d\tau \tag{6}$$

where

$E_R = reference\ modulus\ set\ as\ an\ arbitrary\ constant,$
$E(t) = uniaxial\ relaxation\ modulus,$
$t = time\ of\ interest,\ and$
$\tau = integration\ constant.$

Using the pseudo strain in Equation (6), Equation (4) can be rewritten as

$$\sigma = E_R\varepsilon^R \tag{7}$$

This Equation (7) corresponds to Hooke's Law, which describes the linear elastic stress-strain relationship. The use of pseudo strain simplifies modeling by separating viscoelastic behavior from accumulated damage. The basic concept of continuum damage theory is that the reduction in stiffness is related to damage in a body. For the viscoelastic material case, a reduction in the secant modulus is related to time effects. Note that the instantaneous secant modulus is used to assess the effective modulus in macro scale. Thus, the removal of the time effect in stress-pseudo strain space enables the direct coupling of the reduction of the pseudo secant modulus and damage.

3.2.3 Dynamic Modulus Testing

It is well known that asphalt concrete mixtures are thermorheologically simple (TRS) materials in the linear viscoelastic state. Therefore, the time-temperature superposition (t-TS) concept can be applied to the material when it is in an undamaged state. Thus, the effect of loading time (or frequency) and temperature can be combined into a single parameter, which is referred to as *reduced frequency*, to yield a single continuous mastercurve that describes the dynamic modulus of the material. The mastercurve is represented by a sigmoidal functional form given in Equation (8).

$$\log|E^*| = a + \frac{b}{1 + \frac{1}{e^{d+g*\log(f_R)}}} \tag{8}$$

$$f_R = a_T f \tag{9}$$

where

$a, b, d, \text{ and } g = \text{regression constants},$

$f_R = \text{reduced frequency},$

$f = \text{loading frequency}, \text{ and}$

$a_T = \text{time} - \text{temperature shift factor}.$

The t-TS principle states that unit response functions can be shifted along the abscissa (frequency domain) to produce a mastercurve in the TRS material state. The relationship between the shift factor and temperature can be fitted to a second-order polynomial function.

$$\log(a_T) = \alpha_1 T^2 + \alpha_2 T + \alpha_3 \tag{10}$$

where

$a_1, a_2, \text{ and } a_3 = \text{constants}.$

In this research, dynamic modulus testing was conducted at 5°C, 20°C, and 40°C and at 25, 10, 5, 1, 0.5, 0.1, 0.05, and 0.01 Hz. The detailed procedure is presented in the standard specification, AASHTO T 342. For quality testing, the target resultant strain amplitude was set from 50 to 75 micro strains, and the corresponding load level was determined by trial and error using the same material throughout the procedure.

3.2.4 Controlled Crosshead Cyclic Tension Testing with S-VECD Program

The simplified viscoelastic continuum damage (S-VECD) program is, as the name suggests, a simplified modeling approach for the viscoelastic continuum damage (VECD) model. The universally accepted VECD model has disadvantages with regard to its lengthy computing time and its inability to simulate actual in-service pavement loading conditions. The S-VECD model was developed to resolve these shortcomings by employing a piecewise approach. The S-VECD model separates the analysis of the first loading cycle from the analysis of the entire loading history, because 15%~25% reduction in pseudo stiffness occurs during the first loading cycle. After a full analysis of the data points obtained from the first loading cycle, the successive peak data points from the subsequent load cycles are used to calculate the pseudo stiffness and damage using the load shape function obtained from the first load cycle analysis. Detailed information about the S-VECD model is available from Underwood et al. (2010).

$$C = e^{aS^b}, \tag{11}$$

where

$C = the\ loss\ in\ pseudo\ stiffness\ (or\ material\ intigrity)$;

$S = damage\ parameter,\ and$

$a, b = fiitting\ coefficients.$

Material damage characteristics were determined by conducting controlled cross-head (CX) cyclic tension tests at 19°C and 10 Hz. In order to verify sample-to-sample variability, the fingerprint dynamic modulus test was conducted at 19°C and 10 Hz prior to CX cyclic tension testing.

3.3 Small Geometry Specimens

3.3.1 Introduction

Performing laboratory fatigue tests on field cores presents a unique set of difficulties. The typical test methods that use cylinders require specimens that are 75 mm to 100 mm (3-4 in.) in diameter and 150 mm (6 in.) in height. In-service pavement layers are typically only 50 mm to 100 mm (2-4 in.) thick. To extract standard geometry test specimens from in-service pavements,

the research team must find pavements with layers that are at least 75 mm thick and then must either cut a pavement trench and core horizontally, or extract a 20 mm (8 in.) core from the pavement and core horizontally through the core. Of course, other geometries also can be used, such as those for indirect tension testing that require specimens 150 mm in diameter by approximately 38 mm (1.5 in.), or beam specimens that are 380 mm long, 63 mm wide, and 50 mm thick (15 in. x 2.5 in. x 2 in.). However, uniaxial direct tension testing of cylindrical specimens has a key advantage over these other test geometries in that the state of stress is much simpler, and thus, the material responses measured during testing can be related more easily to the fundamental material properties.

3.3.2 38 mm Diameter Cylindrical Specimens

To resolve the difficulty in performing laboratory tests on field-extracted materials, the researchers at the Turner-Fairbank Highway Research Facility (TFHRC) have devised a method to use small cylindrical test specimens (Kutay et al. 2009) that are 38 mm (1.5 in.) in diameter and 100 mm in height. The importance of this geometry (hereinafter called the 38 mm geometry) is that specimens can be obtained from pavement layers as thin as 44.5 mm (1.75 in.) and also from 150 mm field-extracted cores. Using this geometry, Kutay et al. (2009) were able to show that the fundamental fatigue behavior of asphalt concrete could be determined reliably. Based on the findings from the Kutay et al. work, the 38 mm by 100 mm test geometry was selected for this research to perform the forensic study of in-service asphalt concrete pavements.

3.3.3 Prismatic Specimens

To fabricate 38 mm diameter by 100 mm tall cylindrical specimens, the minimum asphalt concrete layer thickness must be 44 mm (1.7 in.) due to the edge thickness of the core drill bit. The research team performed a limited study to identify a potential experimental method for such situations. This limited study was initiated before finalization of the candidate test sections, and at the time it was not clear that all test sections would have layers thicker than 44 mm. Even though it was realized that 44-mm thick layers were available in all sections, this small study was completed because as-constructed and as-designed thicknesses sometimes vary. In addition, in the case of pavement rehabilitation, milling the damaged pavement surface usually takes

precedence over other rehabilitation techniques. Therefore, it is likely that the actual thickness of a pavement from the field is less than 38 mm, and this hypothesis was verified from field-extracted cores. The area of a cylindrical specimen is similar to that of a prismatic specimen, but a thinner pavement can be used for the prismatic specimen geometry. Therefore, the prismatic specimen geometry of 25 mm thick, 50 mm wide, and 100 mm long was adopted for this study.

3.3.4 Ancillary Devices for Small Geometries

Ancillary devices were necessary in order to perform tests on small samples reliably. These devices include: 1) a jig to hold the pavement cores so that the test cores can be extracted, 2) end plates for gripping the test specimen and applying tensile force, 3) a jig to glue the end plates to the sample, and 4) a fixture to mount measuring devices such as LVDTs to the specimen in a reliable manner. Accordingly, a new set of end platens and a new end platen alignment gluing jig for both the prismatic and small geometries were developed for this study. The photographs in Figure 3.6 show a newly designed core-holding vise for the horizontal coring of field and laboratory-fabricated specimens. Figure 3.6 (a) shows the initial design for one coring for each layer, and Figure 3.6 (b) shows the developed core-holding vise for two corings of each layer to maximize the use of the field material. The photographs in Figure 3.7 show the newly developed end platen gluing jig with alignment adjusting system for a 38 mm specimen and a prismatic specimen. The photographs in Figure 3.8 show the newly designed target gluing jig for both a 38 mm specimen and a prismatic specimen. The photographs in Figure 3.9 show the newly designed LVDT bracket attached to test-ready samples and end platens for both prismatic and 38 mm specimens. These pieces of equipment were fabricated at the precision machine shop at NCSU.

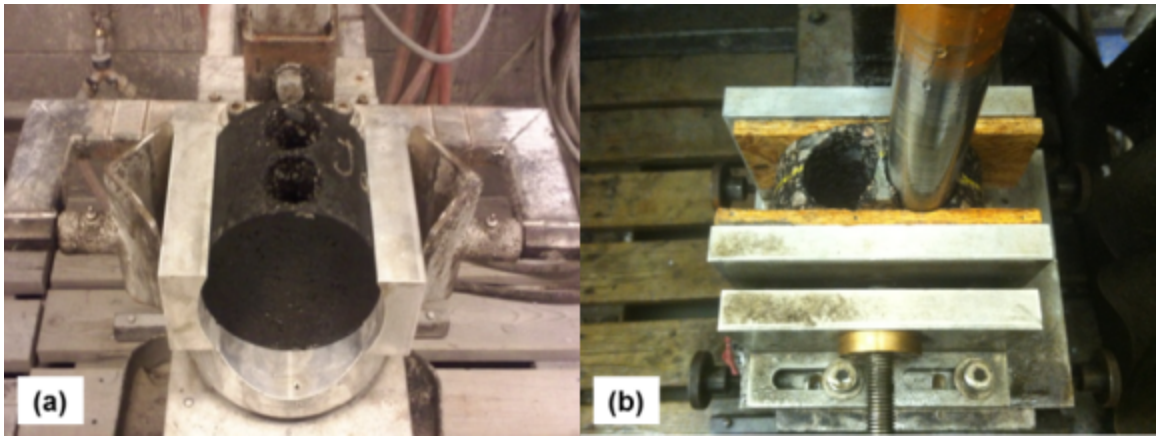

Figure 3.6 Core-holding vise for horizontal coring: (a) initial design for one coring per layer and (b) developed vise for 2 corings per layer.

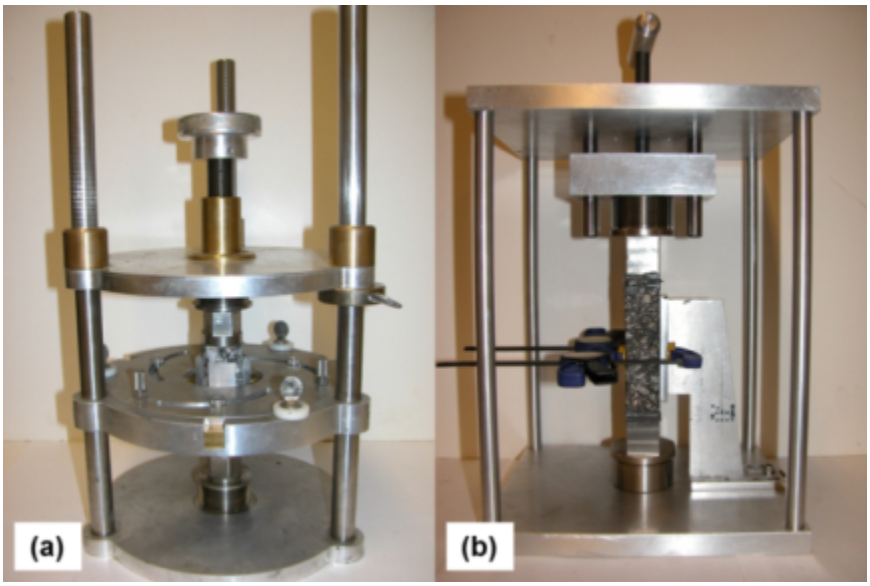

Figure 3.7 End platens gluing jig with alignment adjuster: (a) 38 mm diameter cylindrical specimen and (b) prismatic specimen.

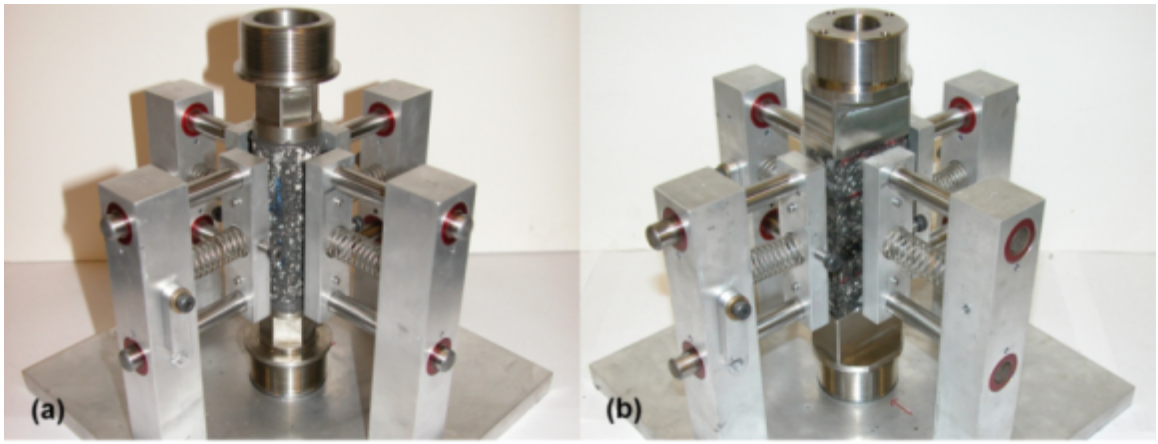

Figure 3.8 Multi-use target gluing jig: (a) 38 mm diameter cylindrical specimen and (b) prismatic specimen.

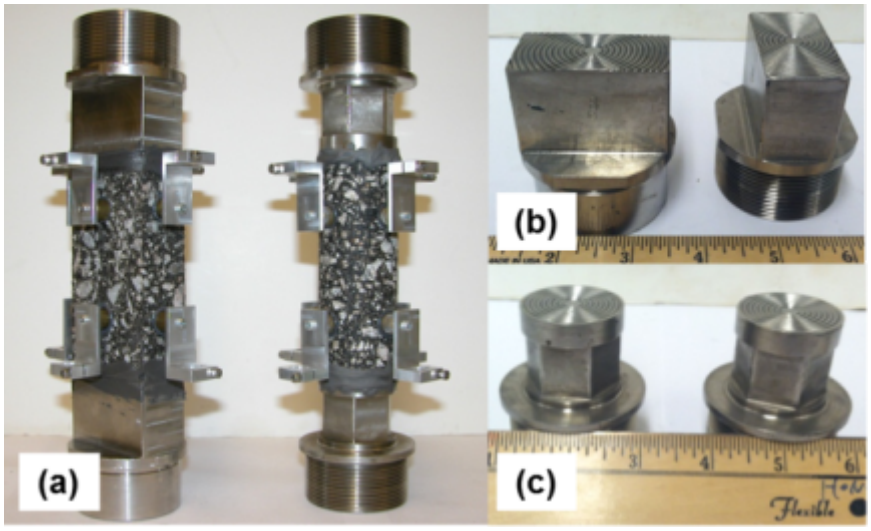

Figure 3.9 Mechanical test-ready samples and new design of end platens for prismatic and small geometric specimens: (a) new LVDT bracket attached to test-ready samples, (b) end platens for prismatic geometry specimens, and (c) end platens for small geometry samples.

3.3.5 Verification of Small Geometry Specimens

3.3.5.1 Specimen Fabrication

Gyratory specimens were fabricated in order to verify the uniformity of the mechanical responses from the different geometries but with the same material. For this purpose, all of the specimens were compacted using a Servopac gyratory compactor by IPC Global. For standard-sized cylindrical specimens, the specimens were compacted to 178 mm in height and 150 mm in

diameter. For small geometries, the height was reduced to 150 mm because the required height for the small geometry is 100 mm. In order to maintain consistent air void distribution in the small geometry specimens, all three 38 mm diameter and prismatic specimens were extracted in the range of 100 mm diameter for the gyratory specimens. In order to accomplish this size, as shown in Figure 3.10, a 100 mm diameter circle was drawn on top of the gyratory specimens, and then small geometry specimens were obtained by cutting and coring the prismatic specimens and 38 mm diameter cylindrical specimens within the 100 mm diameter circle. After vertical cutting and coring, the top 25 mm and bottom 25 mm were removed to achieve air void content consistency. A study of air void distribution in Superpave gyratory specimens can be found elsewhere (Chehab 2002).

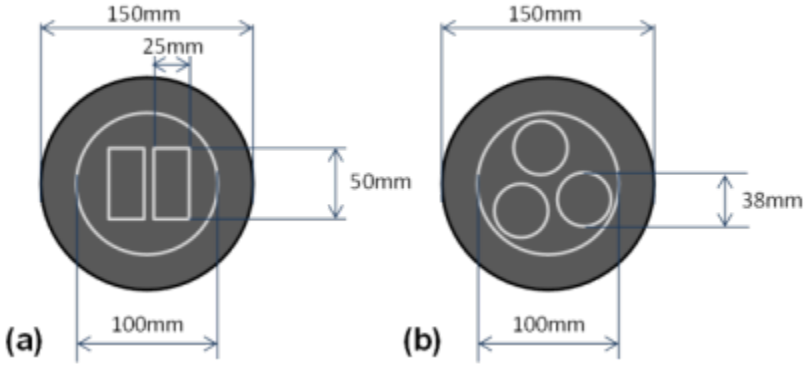

Figure 3.10 Top view of gyratory specimen for cutting and coring small geometries.

In order to verify the test design, aggregate obtained from the Martin-Marietta quarry in Garner, North Carolina was used. The NMSA of the mixture was 9.5 mm, and the mixture was comprised of 36% 78M stone, 25% dry screenings, 38% washed screening, 1%, baghouse fines, and PG 70-22 SBS-modified binder from Kumho Petrochemical Co. The blended gradation is presented in Figure 3.11.

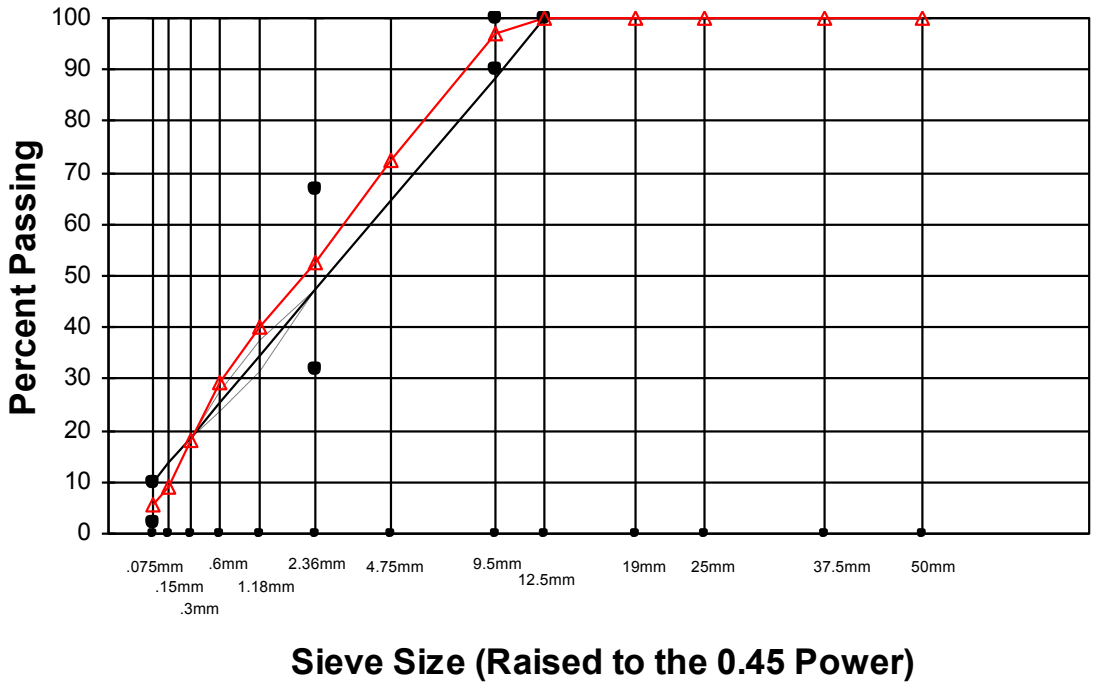

Figure 3.11 Mixture gradation chart.

3.3.5.2 Mechanical Experimental Results from Different Geometries

Dynamic modulus and S-VECD tests were performed for the prismatic geometry, the 38 mm geometry, and the standard (75 mm diameter) cylindrical geometry; the results are summarized in Figure 3.12 (a) to (d). The data presented in Figure 3.12 (a) to (c) provide the dynamic modulus values measured at -10°C to 40°C and at frequencies from 25 to 0.1 Hz for the three geometries. Note that, in Figure 3.12, the 38-1 and 38-2 data series are obtained from measurements taken for the 38 mm geometry, the P-1 and P-2 data series are from measurements taken for the prismatic geometry, and the 75-1 and 75-2 data series are obtained from measurements taken for the standard geometry. It is noted that the 75 mm diameter sample typically is used in lieu of the AASHTO T-342-11 standard 100 mm diameter geometry when measuring the dynamic modulus using the tension-compression protocol. Data for 54°C are not presented due to experimental difficulties with the small geometry at this elevated temperature. Since fatigue cracking is active primarily at cooler temperature, it is believed that this issue does not affect the work in this study.

A comparison of the dynamic modulus values presented in Figure 3.12 (a) to (c) shows that the three geometries are very close in terms of dynamic modulus value. The prismatic

specimens are slightly stiffer than the 38 mm geometry specimens; however, the difference between the prisms and the 38 mm cylinders is well within the sample-to-sample variability observed in the standard geometry. For each of the three geometries, S-VECD characterization (via the cyclic direct tension test) was performed. Although the damage characteristic curves for the 75 mm geometry are located slightly below those for the 38 mm and prism geometries, as shown in Figure 3.12 (d), the same conclusions can be drawn as for the dynamic moduli comparison with respect to the damage characteristic curves based on sample-to-sample variability. The standard-sized specimens were extracted from specimens 150 mm in diameter and 178 mm in height. The prismatic and small geometries were extracted from laboratory-fabricated specimens 150 mm in diameter and 150 mm in height. Therefore, the air void distribution may affect the variability in the damage characteristic curves for the different geometries. Also, the benefits of being able to test thin field cores for the S-VECD characterization outweigh the possibility of errors that might be caused by the small differences in the damage characteristic curves, if indeed such errors even exist.

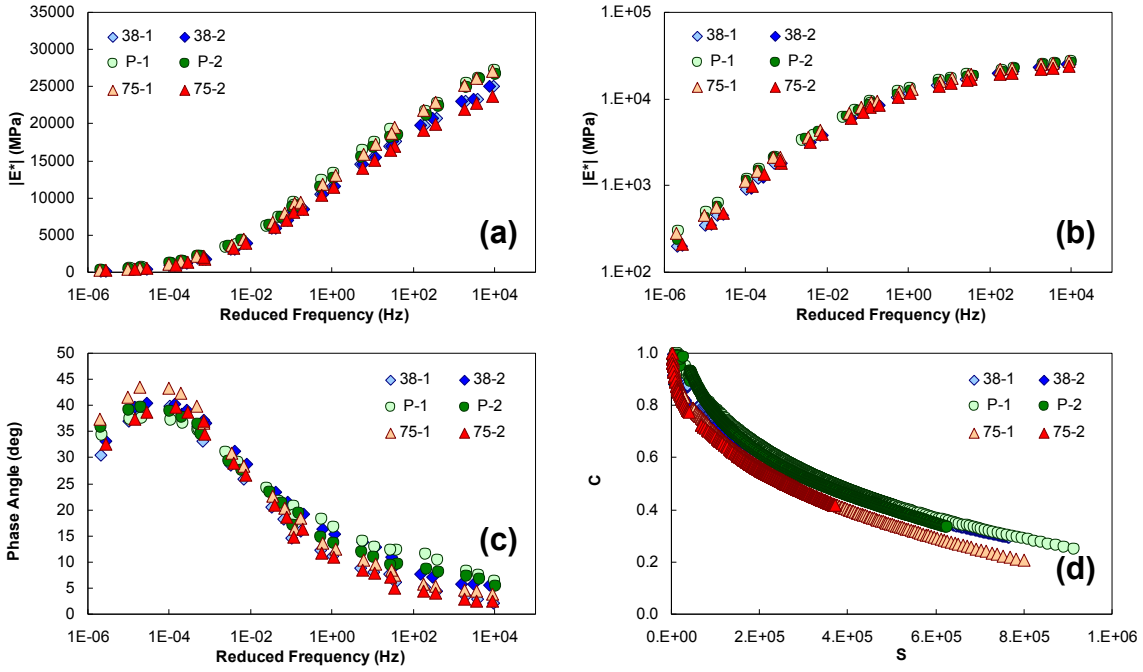

Figure 3.12 Comparison of material properties measured from standard, 38 mm, and prismatic geometry specimens: (a) dynamic modulus in semi-log space, (b) dynamic modulus in log-log space, (c) phase angle, and (d) damage characteristic curve.

3.3.5.3 Verification of Anisotropic Aggregate Orientation Effect in Small Geometries

In the previous subsections 3.3.5.1 and 3.3.5.2, the material responses from different geometries were compared using the specimens obtained by vertical coring and cutting, as shown in Figure 3.10. However, in the case of field-extracted materials the cutting and coring direction would be perpendicular to the compaction direction. Therefore, the effect of anisotropic aggregate orientation needs to be verified for the small geometry specimens. Underwood et al. (2005) presented experimental study results of the effect of anisotropy of aggregate orientation on the mechanical responses of asphalt concrete mixtures. These researchers concluded that the inherent anisotropy does not affect dynamic modulus results and the mechanical responses of asphalt concrete in tensile mode. Despite this detailed research into the effects of aggregate orientation, another verification process was conducted for this research because the specimen geometry used in the Underwood study was 75 mm in diameter and 90 mm in height, whereas the small specimen geometries used in this study are much smaller. Therefore, gyratory specimens were cored in both the vertical (Figure 3.13) and horizontal (Figure 3.6 (a)) directions and the mechanical responses were compared. This same directional approach was applied to the prismatic specimens. The test-ready specimens produced by vertical and horizontal cutting are presented in Figure 3.14. Clear aggregate orientations that are perpendicular to compaction direction are presented in Figure 3.15. Vertical coring means compaction direction and coring and cutting direction is parallel, and horizontal coring means compaction direction and coring and cutting direction is perpendicular.

Figure 3.13 Photograph of vertical coring for 38 mm specimen.

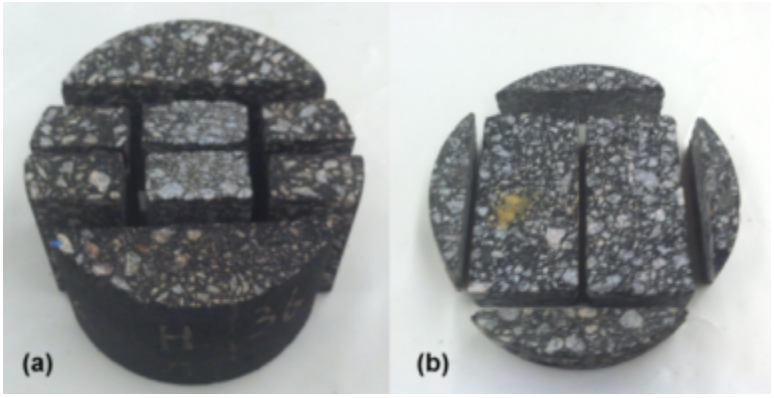

Figure 3.14 Photographs of test-ready prismatic specimens: (a) from vertical direction and (b) horizontal direction.

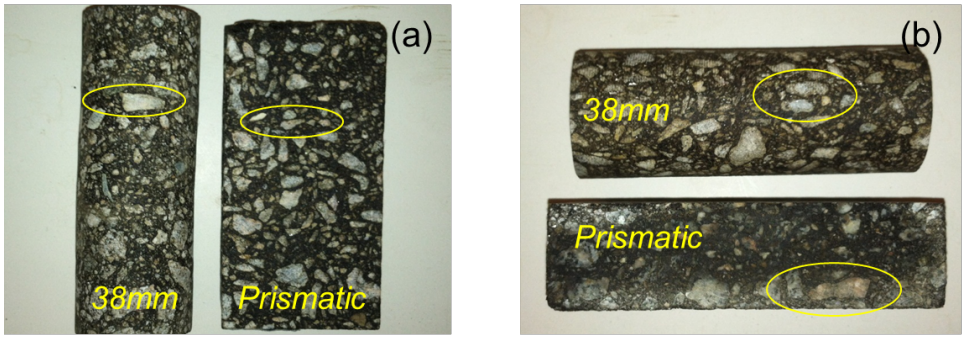

Figure 3.15 Photpgraphs of aggregate orientation perpendicular to compaction direction: (a) from vertical direction and (b) horizontal direction

The same test protocol that was described in the previous subsection 3.4.5.2 was used also for this verification of the anisotropic aggregate orientation effect. Note that the mixture used for this verification is not the same as that described in the previous subsection 3.4.5.2. Figure 3.16 (a) to (c) show that, except for the results for the prismatic specimens that were cut from the side (perpendicular to the compaction direction), all of the dynamic modulus test results obtained from the different geometries and coring directions fall within reasonable sample-to-sample variation. For the case of the side coring of the prismatic specimens, it is believed that the sample came from the center of the specimen where the air void distribution is low. Figure 3.16 (d) shows the damage characteristic curves obtained from the different coring directions and geometries. Although the curves for the vertical cutting of the prismatic specimens are located slightly lower than those for the other conditions, all the test results show similar trends.

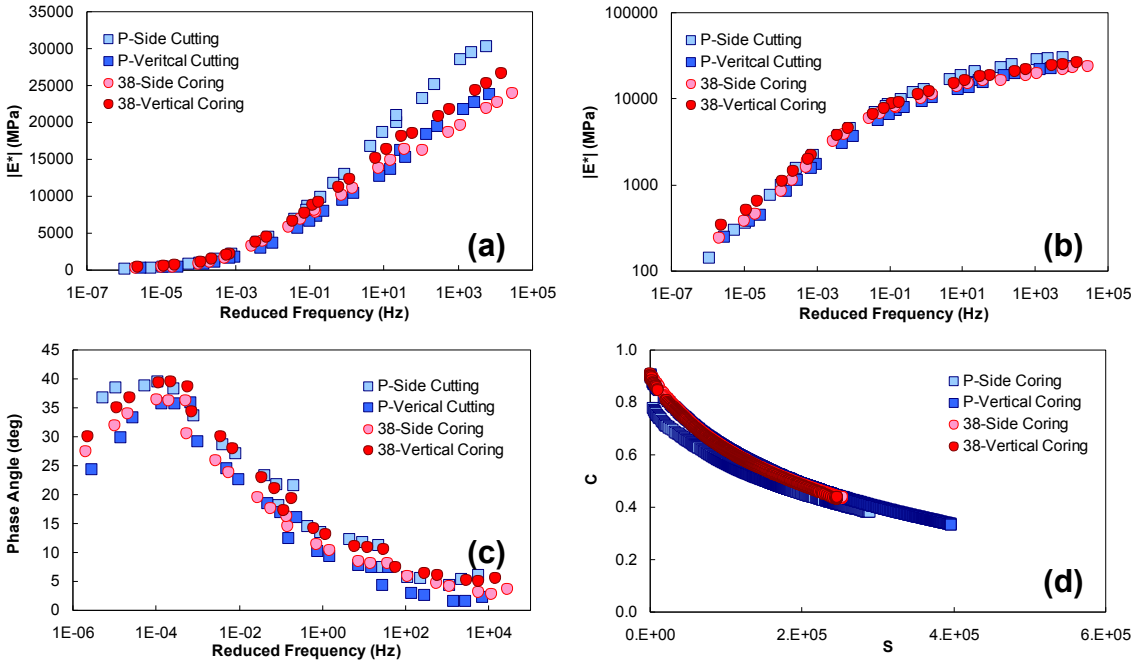

Figure 3.16 Comparison of material properties measured from vertical and side coring of 38 mm and prismatic geometry specimens: (a) dynamic modulus in semi-log space, (b) dynamic modulus in log-log space, (c) phase angle, and (d) damage characteristic curve.

3.4 Rheological Properties of Asphalt Binder

3.4.1 Introduction

The Superpave performance grading (PG) system was developed as part of the SHRP. This system led to the transition from asphalt binder specifications based on index properties to those based on mechanical properties. The PG specification for binder fatigue is based on minimizing the dissipated energy per cycle, which implies that a low dynamic shear modulus (|G*|) value and phase angle ($\sin\delta$), as measured by the dynamic shear rheometer (DSR), leads to a more fatigue-resistant material. However, weak correlations between the mixture fatigue damage properties and the $|G^*|\sin\delta$ were identified in subsequent research efforts (Bahia et al. 2001, Bahia et al. 2002, and Tsai et al. 2005). This finding is not entirely surprising as the PG specification is based on linear viscoelastic properties that do not consider actual damage resistance. Accordingly, in order to improve this limitation of the current specifications, the time-sweep (TS) test method was introduced as a result of the NCHRP 9-10 project. The TS test method applies repeated sinusoidal cyclic loading at a fixed amplitude to asphalt binder specimens using 8 mm diameter parallel plates and DSR geometry. However, this TS method also has practical shortcomings for specification purposes because it requires an extended testing time and has associated equipment limitations that correspond to the lengthy test time (Johnson and Bahia 2010). Among alternatives to the TS test, the linear amplitude sweep (LAS) test was adopted for this research. The LAS test is similar to the TS test in that it consists of applying cyclic loading in the DSR using 8 mm diameter parallel plate geometry; however, in the LAS test the load amplitude is increased gradually to accelerate damage in the specimen. A VECD-based analysis framework can be applied to the LAS test results to estimate the fatigue life of specimens at any strain amplitude (Hintz and Bahia 2013).

3.4.2 Sample Extraction and Recovery

In order to test the performance of the asphalt binder in field-extracted materials, asphalt binder was extracted from each layer in two different condition regions from Level 1 sites. Field-extracted cores were cut for this purpose, and the materials were placed in flat pans and warmed to 110 ± 5°C for about 10 minutes and then separated. The required asphalt mixture sample size for extraction and recovery was determined based on the NMSA of the field materials, as

specified in Table 3.3. Prepared samples in the loose-mixture condition were disintegrated using a chemical solvent (trichloethylene, propyl bromide, or methylene chloride), and the asphalt binder was extracted from the aggregate by the turning force in a centrifuge (extraction unit bowl) according to ASTM D2172. Figure 3.17 (a) shows the extraction unit bowl. The extracted soluble binder was recovered using a rotary evaporator and recovery system (Figure 3.17 (b)) according to ASTM D5404. The extraction and recovery process of the binder from the field cores was performed by Trimat.

Table 3.3 Required minimum mass of sample for extraction

Norminal Maximum Size of Aggregate (mm)	Minimum Mass of Sample (g)
4.75	500
9.5	1,000
12.5	1,500
19	2,000
25	3,000
37.5	4,000

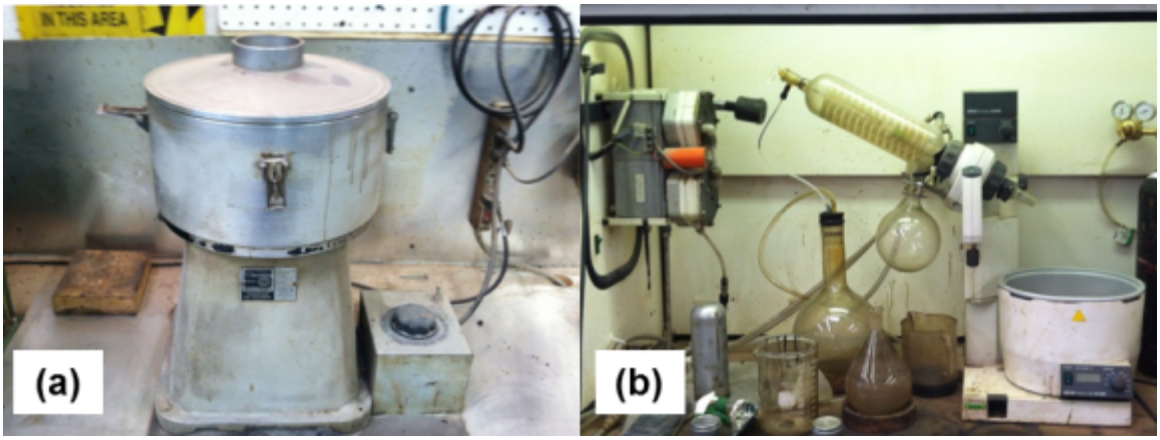

Figure 3.17 (a) Extraction unit bowl and (b) rotary evaporator and recovery system.

3.4.3 Specimen Preparation

An AR-G2 DSR manufactured by TA Instruments was used for all binder testing in this research. In order to make specimens for DSR testing, the field-extracted asphalt binder was heated gradually in the oven. This gradual increase of temperature started at 100ºC and rose to higher temperatures where the binder could become fluid enough to pour. When the binder became fluid, it was poured into a 8 mm silicon mold. This 8 mm parallel plate geometry was used also for both the frequency sweep test over a range of temperatures to generate the linear viscoelastic mastercurves and for the LAS test to measure fatigue resistance.

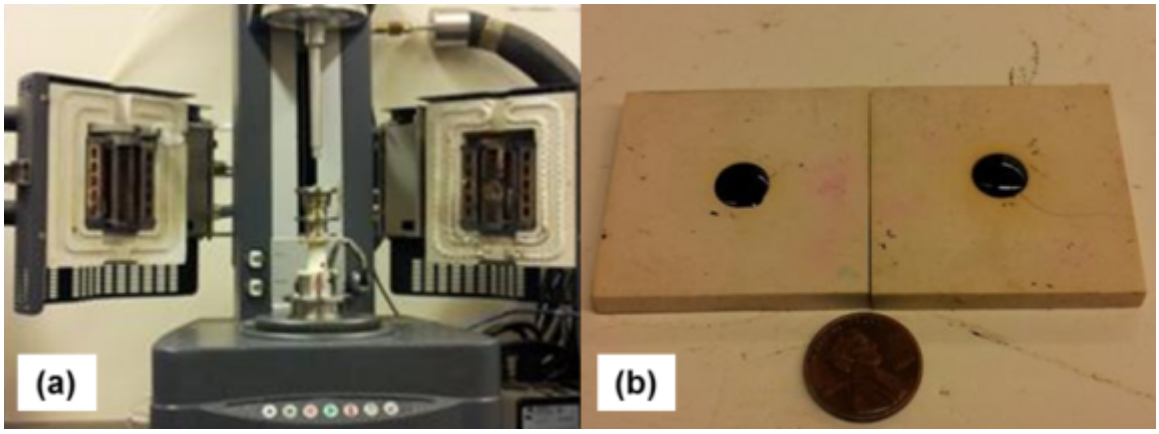

Figure 3.18 (a) AR-G2 rheometer and (b) 8 mm silicon mold with asphalt binder.

3.4.4 Frequency Sweep Test

In order to obtain the mechanical responses of the asphalt binder in the linear viscoelastic range, the temperature range was selected as 30ºC to 5ºC in 5ºC increments at frequencies ranging from 0 to 150 rad/sec. Before starting oscillation at each temperature, each specimen was conditioned for 10 minutes to stabilize at the specific temperature. After the test, the t-TS principle was employed to form the mastercurve.

3.4.5 Linear Amplitude Sweep (LAS) Test

As stated in the previous subsection 3.4.1, the LAS test is an accelerated cyclic fatigue test and is conducted in two steps. The first step is the frequency sweep test to obtain a fingerprint of the undamaged material properties, and the second step is the amplitude sweep test. In the frequency sweep step, the frequency is increased from 1 to 150 rad/sec with constant strain amplitude of 1 percent. In the amplitude sweep test, the amplitude is increased from 1% to 30% strain over 300 seconds with a frequency 10 Hz. Then, the VECD model approach is used to predict the fatigue life of the binder. The test temperature is selected as the intermediate PG temperature.

Chapter 4 Causes of Cracking

4.1 Introduction

The common understanding of the fatigue cracking phenomenon suggests that repeated applications of load cycles create areas of tensile strain at the bottom of the pavement layer, which in turn lead to the initiation of microcracks. Under repeated loadings these microcracks densify, coalesce, propagate and eventually develop into visible macrocracks on the pavement surface. The new NCHRP 1-37A MEPDG provides a mechanistic means of exploring this traditional fatigue damage process. The MEPDG computes stress and strain levels at critical locations within the pavement structure to predict the performance of the asphalt pavement. The critical strain is the tensile strain, and the location of bottom-up fatigue is at the bottom of the asphalt layer. The MEPDG adopts the following phenomenological relationship between the fatigue life and the tensile strain at the bottom of the asphalt layer (NCHRP 2004a).

$$N_f = K_1 \left(\frac{1}{\varepsilon_t} \right)^{K_2} \left| E^* \right|^{K_3}, \tag{12}$$

where

N_f = *number of cycles to failure, i.e., fatigue life*;
ε_t = *tensile strain at the bottom of asphalt layer*;
$\left|E^*\right|$ = *dynamic modulus of asphalt mixture; and*
K_1, K_2, K_3 = *material constants*.

Equation (12) indicates that bottom-up fatigue is both material-dependent (expressed through coefficients K_1, K_2, K_3, and the material property $|E^*|$) and structure-dependent (ε_t, tensile strain at the bottom of the asphalt layer).

The aforementioned common understanding of fatigue failure has been challenged in recent years as more and more agencies have begun to report on another form of failure, top-down fatigue (Myers et al. 1998, Pellinen 2002, Myers and Roque 2001, Uhlmeyer 2000). At the outset of this research into top-down fatigue cracking universal agreement had not yet been

reached as to the exact causes of this type of distress (Myers et al. 1998, Al-Qadi and Yoo 2007). Nevertheless, it could still be stated with certainty that the overall driving conditions appeared to differ from those that cause the more traditional bottom-up fatigue cracking. Thus, the material characteristics most closely tied to performance in bottom-up and top-down fatigue cracking also may differ. For example, pavements constructed with materials that exhibit a strong propensity to age may be significantly more sensitive to the top-down cracking phenomenon than pavements constructed with materials that have a relatively weak propensity to age. However, because aging is a top-down process, the bottom-up cracking phenomenon may be affected only slightly.

The differentiation between bottom-up and top-down fatigue cracking has important implications in pavement management because the type of cracking will affect decisions as to the most structurally-effective and cost-effective rehabilitation strategies to take for design and construction. Bottom-up and top-down fatigue cracks look identical on the pavement surface, and as a result, most studies that delve into differentiating between them involve coring or trenching the pavement (Myers et al. 1998). Some promising results using nondestructive techniques have been produced, but these have been limited to laboratory studies only (Underwood and Kim 2003).

Research has shown that numerous mixture factors affect the fatigue response of asphalt concrete mixtures. The most important factors include asphalt type, filler content, percentage of air voids, and asphalt content. Secondary factors that also have been shown to contribute to the fatigue performance of certain mixtures include aggregate gradation, angularity, source and construction temperature (Epps and Monismith 1969, Pell and Taylor 1969, Maupin 1970, Epps and Monismith 1972, Malan et al. 1989, Tayebali and Huang 2004). It has also been found that certain materials and certain combinations of materials promote aging, which ultimately would make these materials more prone to fatigue cracking (Glover et al. 2009, Freeman et al. 2009). A similar phenomenon exists with regard to resistance to moisture damage. It has been found that the fatigue resistance of asphalt concrete decreases when moisture damage is present in the system (Sebaaly et al. 2001). Studies of the physico-chemical behavior of aggregate and asphalt surfaces have shown that certain materials may promote or mitigate these behaviors (Hefer et al. 2005). Many of these same factors may also have a significant effect on the rutting performance of asphalt concrete mixes (Ahlrich 1996, Kandhall 2002, Epps et al. 2002). Christensen and

Bonaquist have classified the factors that contribute to top-down cracking (NCHRP 2004b); a summary of these researchers' findings is shown in Table 1. Many of these same factors may also have a significant effect on the permanent deformation performance of asphalt concrete mixes (Ahlrich 1996, Kandhall 2002, Epps et al. 2002).

These observations, coupled with reported observations by the NCDOT that North Carolina pavements exhibit a disproportional amount of fatigue cracking, have led to the belief that mixtures used in North Carolina are systematically biased towards conditions (i.e., design and procedures) that promote fatigue cracking. Specifically, among the aforementioned mixture factors, the asphalt contents are believed to be too low; i.e., North Carolina mixtures are dry. This belief may be true because, in general, asphalt contents have been decreasing for the past twenty to thirty years as agencies have developed procedures and specifications aimed at reducing permanent deformation-related distresses in their pavements (Valkering and Van Gooswilligen 1989). However, as the cited literature indicates, other mixture factors may affect fatigue performance as significantly as or more than the asphalt content.

Additional changes brought about by Superpave, such as the increased use of coarse-graded mixtures and a purported systematic reduction in asphalt content, have further complicated this problem of fatigue cracking (Epps and Hand 2001, Christensen and Bonaquist 2006). Coarse Superpave mixtures also have been noted to exhibit substantially more permeability than their fine counterparts (Choubane et al. 1998, Khosla and Sadasivam 2004). Such permeability is known to reduce the fatigue life of asphalt concrete mixtures in the laboratory, but it also has a substantial effect under real-world conditions because it allows water to enter the pavement system more easily than when fine-graded mixtures are used.

No simple fix is readily available for correcting the trend toward reduced asphalt contents because all the factors in a volumetric mix design are interrelated. Additionally, most factors that are beneficial for preventing permanent deformation have the opposite effect on fatigue. As a consequence, many researchers have recognized the need to balance the effects of both fatigue and permanent deformation in mix design (Lee 2007, Zhou et al. 2007). Further, the effect of transferring a laboratory-based mix design to the field may introduce a host of other considerations specifically related to quality control/quality assurance (QC/QA) practices at both the mixing and construction stages (Christensen and Bonaquist 2006). These QC/QA issues can be magnified by the chosen mix design. Epps and Hand (2001) report that coarse Superpave

mixtures exhibit significantly higher sensitivity to variations in asphalt content and air void content than similar fine-graded mixtures.

Although not a comprehensive fix, relatively simple modifications to their mix design processes have been reported by some agencies in an attempt to obtain more effective asphalt concrete mixtures for their specific circumstances. The three most commonly reported modifications include: 1) using design air void contents of 3% to 5% instead of a constant 4%, 2) establishing a maximum *voids in the mineral aggregate* (VMA) requirement that is 1.5% to 2% above the minimum value, and 3) slightly increasing the minimum VMA requirement by about 0.5% (Christensen and Bonaquist 2006).

In addition to these material-level factors, structural and environmental conditions must also be considered, which may invalidate implied assumptions regarding the mixture design process (Deacon et al. 1995). For example, when designing an asphalt concrete mixture, it is assumed that: 1) the temperature will never exceed some historical magnitude adjusted for reliability; 2) the total pavement thickness will be thick enough that the load on the subgrade surface does not exceed a critical threshold; 3) the thickness is substantial enough that the strain at the bottom of the asphalt concrete layer is not so large as to promote quick cracking; and 4) the traffic (load magnitude and load repetitions) is below some given threshold. If the third or fourth assumption is violated, then it should be expected that the resulting pavement would fail by fatigue regardless of the mix design.

Table 4.1 Summary of research into top-down cracking (NCHRP 2004c)

Authors	Year / Location	Identified Contributing Factors					Proposed Models	Primary Causes	Suggested Remedial Measures
		Mix Properties	Load-Related	Environ-mental	Structural	Construction-Related			
Harmelink and Aschenbner	2003/ Colorado					Segregation		Segregation	Increase asphalt content, modify desing of paver
Holewinski et al.			Contact stress				Contact mechanics, finite element analysis		
Hugo and Kennedy	1985/ South Africa	Gap-grading, high stiffness at low temp.		Age hardening, thermal stress	Deflection/ curvature, plasticity profile		Layered elastic elasto-plastic analysis	Gap-graded mixes in severe climate	Avoid gap-graded mixtures in severe climates; use lowest possible viscosity in surface course
Mahoney	2001/ Wash. State			Binder age hardening	Surface tensile stress			Age hardening	
Masuno and Nishzawa	1992/ Japan		High traffic levels	High surface temp. (thermal gradients)			Finite element analysis	High pavement surface temp.	
Merrill	2000/ Wales, UK		Contact stress	Thermal stress, thermal gradient	Pavement thickness	Surface flaws during compaction	Finite element analysis	Thermal stress and tire contact stress	Improve pavement design methods
Myers	2001-2002/ Florida	Inadequate fracture resistance	Contact stress	Thermal stress	Stiffness gradient		Finite element analysis, fracture mechanics	Contact stress and thermal stress	Improve mixture fracture resistance, high performance overlay
Myers and Roque	2001/ Florida				Stiffness gradient, load-position spectra		Finite element and fracture mechanics	Tensile stress at surface	
Myers et al.	1998/ Florida				Stiffness gradient, load		Layered elastic with contact stress, thermal stress analysis	Tire contact stress	Use fracture-resistant mixtures
Minnesota DOT (MnRoad)	2002/ Minnesota	High mix stiffness	Traffic loading	Pavement age					
Mun	2003/ North Carolina		Contact stress		Pavement thickness, base course stiffness		Finite element and continuum damage	Contact stress and shear	
Roque	2002/ Florida	Inadequate fracture resistance, low temp. properties	Contact stress, load-position spectra	Thermal stress	Stiffness gradient		Finite element and fracture mechanics		Use fracture-resistant mixtures, and specialized thin wearing courses
Schorsch and Baladi	2004/ Michigan	Poor moisture resistance				Segregation	Empirical model for predicting loss of pavement service life	Segregation and moisture damage	Improve construction and maintenance practices
Soon et al.	2003/ Minnesota		Contact stress				Contact mechanics, finite element analysis		
Svasdisant et al.	2002/ Michigan	Excessive mineral filler		Age hardening and loss of strength	Stiffness gradients from temp. difference, age hardening and difference in lifts	Poor compaction from screed	Layered elastic analysis, finite element analysis	Traffic-induced tensile radial stress	
Ulmeyer et al.	2000/ Wash. State	Poor moisture resistance	Traffic-induced stress	Moisture damage	Thick pavement	Streaking from screed			Use overlay, mill and inlay or overlay
Wamburga et al.	1999/ Kenya			Age hardening thermal stress	Extreme stiffness gradients due to age hardening traffic-induced stress			Extreme stiffness gradients due to age hardening along with heavy traffic loads	
Wang et al.	2003/ N/A	Weak mastic		High temp.			Micro-mechanics	Tensile and shear stress induced by traffic loading at or near surface	
Washington State DOT	2003/ Wash. State		Contact stress	Age hardening thermal stress	Stiffness gradients from temp. difference, age hardening and difference in lifts			High tire contact stress, age hardening and thermal stress	
Worel	2003/ Minnesota	High binder grade/ mixture stiffness	Traffic loading	Age hardening, pre-existing transverse cracks					

4.2 Master Database

Although the absence of both job mix formulae (JMFs) for the mixtures and a detailed construction database is somewhat understandable, this lack of information was challenging to this research. Because the objectives of this research are to find the primary causes of fatigue cracking in North Carolina pavements, the use of field-extracted materials and associated data is indispensable. Accordingly, as much historical information as possible has been obtained about field materials and supplementary construction and environmental records, such as locational natural disasters that may have caused accelerated damage to both a pavement and its substructure, the latest traffic distribution, the latest temperature records, and so on. All possible data from both the field and laboratory were recorded, and a master database was built for effective and comprehensive analysis. This developed master database contains section identifications and locations, pavement condition ratings, pavement structural information, pavement layer properties, aggregate gradations and asphalt content, air void content, recovered binder properties, etc. It is used in this research to identify the causes of systematic mix design flaws. The master database is presented in Appendix 1.

4.3 Pavement Condition Index

As the first step in the comprehensive analysis of the tested and observed data, a practical condition index needed to be devised to fit the purposes of the research. For pavement management purposes, the NCDOT, along with most state agencies, uses a pavement condition rating (PCR) index for both asphalt and concrete pavements. This PCR index was used initially to find the optimal field sites for this project. However, the length of the field site that was selected according to the PCR index in the NCDOT database is longer than most of the lengths of the actual sites selected for this research. This difference in length between the PCR-selected site and the condition regions at the test sites is due to issues related to traffic consistency and safety matters. In order to evaluate the mix design and structural design factors without complications from traffic patterns and volumes, the field sites were selected to avoid major intersections, which resulted in the lengths of most of the selected field sites being shorter than the length of the site reported in the PCR index of the NCDOT database. Specifically, the test

sites are located between intersections in order to keep the traffic volume the same at each selected site; this criterion necessitated relatively short test sections. Also, on the day of the field testing, in order to secure the safety of the field workers on the roads during a partial lane closure, a straight section of the site was selected for field testing and material extraction. Furthermore, because the pavement within a single site is divided into different condition regions (i.e., relatively *good* condition regions and *poor* condition regions), detailed PCR indices were needed for each condition region because the PCR is a function of the amount of distress and the length of the site.

In order to determine the severity of the surface distresses for the asphalt pavements in this research, the research team adopted the Long-Term Pavement Performance (LTPP) program's condition rating method. In the LTPP data analysis support report, the deduction values for alligator cracking are obtained by combining all three severity levels of alligator cracking. Table 4.2 presents the deduction values for the three severity levels that reflect the total (summed) value for each distress. The deduct value obtained for each of the three severity levels for each distress is computed using Equations (13) to (16), as presented in the LTPP data analysis support report (Jackson and Puccinelli 2006).

$$D_L = 3.4082 \times P_L^{0.514} \tag{13}$$

$$D_M = 4.4575 \times P_M^{0.6107} \tag{14}$$

$$D_L = 5.2064 \times P_H^{0.6956} \tag{15}$$

$$D_T = D_L + D_M + D_H \tag{16}$$

where

$D_L = low\ severity\ deduct\ value$,
$D_M = moderate\ severity\ deduct\ value$,
$D_H = high\ severity\ deduct\ value$,
$D_T = total\ deduct\ value$,
$P_L = recorded\ percentage\ of\ low\ severity\ distress$,
$P_M = recorded\ percentage\ of\ moderate\ severity\ distress$, *and*
$P_H = recorded\ percentage\ of\ high\ severity\ distress$.

The recorded amounts of alligator cracking and longitudinal cracking on the wheel path (LWP), as obtained from field surveys, were converted into percentages based on the total area of the site. In order to obtain the LWP value, the length of the LWP is converted to a unit of area by applying a standard width of the wheel path (0.3 m or 1 ft.) to the length of the LWP, as suggested by Jackson and Puccinelli (2006). The severity of the LWP is considered to be *low* for calculating the deduct value of the combined indices (Jackson and Puccinelli 2006). Accordingly, the alligator cracking and LWP data are combined together and corresponding deduct values are subtracted from 100 to determine the so-called *alligator cracking index* (ACI).

Jackson et al. (1996) developed an index for transverse cracking (TC) for the enhanced South Dakota DOT pavement management system. The severity of TC is developed on the basis of the distance between transverse cracks instead of the width of the TC, which is adopted by many agencies. The Jackson et al. approach is adopted for this research due to the lack of TC width information from the field. Jackson et al. categorized TC into three severity levels with the following category limits: greater than 15.2 m spacing, 15.2 m to 7.6 m spacing, and less than 7.6 m spacing for high, medium, and low severity TC, respectively. Based on this concept of 7.6 m intervals between severity levels, the research team developed a revised *transverse cracking index* (TCI) by giving 15 points of deduct value for each level of three TC severities. In other words, a deduct value of zero spacing indicates 45 points of deduction, and a deduction point of 22.8 m (3 times 7.6 m) indicates zero point deduction. Then, the averaged value of the TC space for a given condition region is used to calculate the deduction points via interpolation. Then, the percentage of the area that shows the amount of TC out of an entire condition region is multiplied to obtain the final TCI value. Table 4.2 shows the numerical values of the ACI and TCI of the field sites. Higher ACI and TCI values indicate a better condition than lower ACI and TCI values suggest.

Table 4.2 Alligator cracking index and transverse cracking index with numerical values of distress obtained from condition survey data

	Site	Condition Region	Length (ft.)	Lane Width (ft.)	Transvers Cracking (ft.)					Longitudinal Cracking (ft.)	Alligator Cracking Area(ft.^{2})			ACI	TCI
					Summed Length	Occurence (Partial)	Occurence (full)	Occurrence Distance	Average Space	Length	Light	Moderate	Severe		
Test Level 1	I-540	B1	100	12	53	2	3	110	22	19	288	224	0	55.33	98.61
		A1	94	12	24	0	2	33	33	0	68	0	0	91.42	-
		B2	196	12	24	0	2	56	56	0	502	276	304	32.63	-
		A2	100	12	0	0	0	0	0	0	6	0	0	97.61	-
	NC-24	B1	400	12	21	1	1	39	39	32	364	118	316	62.88	-
		A1	124	12	34	6	0	40	8	7	30	52	58	71.57	90.58
		B2	82	12	7	1	0	0	0	10	13.5	54	0	82.06	-
	US 70	B1	100	12	0	0	0	0	0	50	0	0	0	92.90	-
		B2	100	12	0	0	0	0	0	55	26	0	0	90.91	-
		A1	100	12	0	0	0	0	0	11	0	0	0	96.74	-
		A2	100	12	0	0	0	0	0	0	0	0	0	100.00	-
	US-17	B1	98	12	21	1	1	73	73	49	16	0	0	91.79	-
		B2	70	12	4	1	0	0	0	30	18	0	0	91.65	-
		A1	70	12	0	0	0	0	0	44	0	0	0	92.02	-
		A2	66	12	0	0	0	0	0	58	0	0	0	90.52	-
	US-601	A1	148	11.5	104.5	1	9	97	10.78	13	90	0	0	91.40	84.45
		B1	198	11.5	193.5	13	9	168	8.84	42	411.5	0	0	84.14	76.62
		B2	286	11.5	48.5	2	3	20	5	147	542	0	0	83.72	97.54
	NC-87	A1	122	12	0	0	0	0	0	17	0	0	0	96.32	96.04
		B1	118	12	96	2	7	106	13.25	39	110	0	0	88.57	-
		A2	114	12	36	0	3	50	25	24	0	0	0	95.45	-
		B2	240	12	106	6	5	202	20.2	127	212	0	0	87.90	83.07
	US-76	B1	150	13	60	2	3	16	4	110	398	0	24	75.78	-
		A1	196	13	18	2	0	70	70	24	0	0	0	96.70	95.68
	US-74	B1	290	12	48	10	0	150	16.67	162	112	48	176	68.65	93.74
		A1	266	12	101	7	5	210	19.1	237	66	0	60	81.09	94.23
	NC-209	A1	106	10	0	0	0	0	0	0	0	0	0	100.00	-
		B1	148	10	0	0	0	0	0	21	0	0	0	95.92	-
		A2	116	10	0	0	0	0	0	0	0	0	0	100.00	-
Test Level 2	US-13	A1	70	12	12	0	1	0	0	19	45	8	0	85.99	-
		B1	134	12	0	0	0	0	0	40	166	78	84	59.22	-
		B2	66	12	0	0	0	0	0	36	92	28	8	70.87	-
		A2	134	12	0	0	0	0	0	58	44	47	10	78.87	-
	NC-177	B1	284	11	64	8	1	280	40	194	115	118	0	78.90	-
		A1	180	11	64	10	1	168	16.8	58	106	0	0	89.90	88.95
		A2	288	11	144	18	1	259	14.39	38	52	0	0	94.17	85.07
		B2	280	11	37	7	0	194	32.33	26	142	172	280	54.93	-
	SR-1530	B1	60	11	4	1	0	0	0	68	4	0	0	88.36	-
		B2	50	11	0	0	0	0	0	40	28	14	0	79.70	-
		A1	48	11	0	0	0	0	0	54	0	0	0	88.74	-
	US-220	B1	252	9	77	4	5	200	25	167	0	0	0	90.49	-
		A1	368	9	174	10	11	346	34.6	148	0	0	0	92.64	-
	NC-47	B1	164	10	0	0	0	0	0	11	373	0	100	64.45	-
		A1	100	10	0	0	0	0	0	24	56	0	0	90.08	-
		B2	246	10	12.5	2	0	1	1	27	172	0	168	70.21	99.83
	NC-82	B1	328	10.5	402.5	27	27	318	6	554	0	0	0	85.79	67.85
		A1	200	10.5	153	5	12	184	11.5	81	0	0	0	93.18	79.48
	US-401	A1	320	10	139	17	2	272	15.11	48	355.5	0	0	87.46	87.10
		B1	394	10	57	7	1	202	28.86	68	180	188	0	79.65	-
	NC-55	A1	126	11	14	3	0	90	45	19	74	0	0	90.93	-
		B1	242	11	120	9	5	236	18.15	40	326	0	0	86.89	91.05
	NC-194	B1	182	9	52.5	4	3	140	23.33	16	212	0	0	86.81	-
		A1	168	9	92	18	1	140	9.33	16	128	0	0	89.14	77.85
		A2	124	9	67	9	2	79	8.78	21	34	28	0	84.45	82.37
		B2	244	9	69	12	1	173	17.3	81	135	257.5	0	68.92	92.30
	NC-179	A1	174	11	56	11	1	160	14.55	148	44	40	0	81.86	85.03
		B1	100	11	5	1	0	0	0	24	0	0	0	94.91	-

4.4 Mix Deign

4.4.1 Introduction

As noted early in this chapter, the absence of historical data about mixtures used for in-service pavements has limited the possible approaches for this research. In spite of the time and effort spent to find mixture- and construction-related records, no valid information about the mixtures used in this research was available. Therefore, in order to identify systematic mix design flaws, the research team focused on finding general trends of mix design constitutive factors that are related to pavement's cracking conditions.

It is well known that TC is associated with the shrinkage of pavement during winter; this phenomenon is called *thermal cracking*. Rapid temperature changes in winter produce thermal stress in asphalt pavement. When the pavement temperature drops in winter the asphalt binder is contracting more than aggregates in mixture, which eventually makes the *asphalt film thickness* (AFT) thinner around the aggregate particles (Boutin and Claude 2000). This process makes mixtures brittle and triggers TC. Therefore, the film thickness of each layer was calculated by the values obtained from fundamental experiments. Campen et al. (1959) recognized that thin asphalt film tends to produce brittle mixtures that have a short service life, but thick asphalt film tends to produce durable mixtures (Campen et al. 1959).

4.4.2 Analysis Results

The 19 sites selected for this research contain 56 different condition regions. Among the 56 condition regions, 25 regions have top-down cracking (TDC) or bi-directional cracking (BDC) propensity; 16 regions have only TDC propensity; 12 regions have bottom-up cracking (BUC) or BDC; and 4 regions have BUC only. Figure 4.1 presents comparisons between ACI values for both air void content and asphalt content. It is well known that a pavement with low asphalt content is more likely to exhibit fatigue cracking than a pavement with high asphalt content and that a pavement with higher than optimal air void content is more likely to exhibit fatigue cracking than a pavement with low air void content. These facts indicate that it is hard to find a relationship between pavement conditions (i.e., ACI values) and air void content and asphalt content simultaneously from the field-extracted materials. In order to simplify the cause and effect of the air void content and asphalt content with regard to pavement condition and cracking

direction, the intermediate layers again are excluded for this analysis. As indicated by the TDC or BDC observed in the top layers, the condition regions with high asphalt contents tend to have high ACI values, as presented in Figure 4.1 (b) and (d). Although these trends are not clear due to the canceling-out effect of the air void content and asphalt content in the mixtures, somewhat reasonable relationships are found in regions where TDC or BDC are observed. Another noteworthy finding is that higher air void contents tend to have lower ACI values, as indicated from the bottom layers of BUC or BDC pavements, as presented in Figure 4.1 (e) and (g).

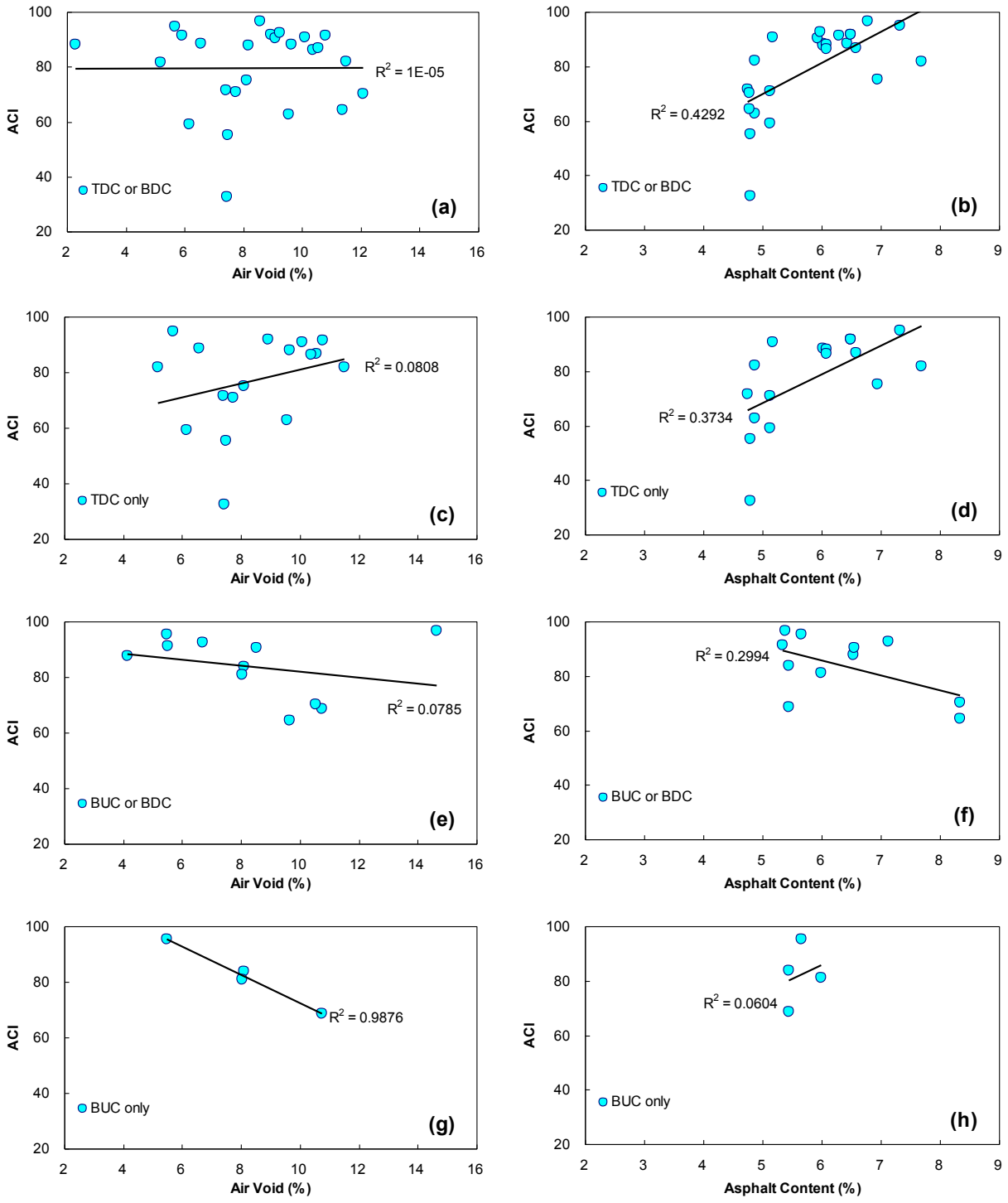

Figure 4.1 Comparison of alligator cracking index to air void and asphalt content: (a) and (b) from TDC or BDC observed condition regions, (c) and (d) TDC observed condition regions, (e) and (f) BUC or BDC observed condition regions, and (g) and (h) BUC observed condition regions.

For quality analysis, the data presented in Figure 4.1 (a) and (b) are divided into different nominal maximum size of aggregate (NMSA) values and aggregate gradation categories, i.e., coarse, fine and penetrating aggregate gradations. Figure 4.2 (a) and (c) and Figure 4.2 (b) and (d) include the data presented in Figure 4.1 (a) and (b), respectively. The data are derived from top layer with the TDC or BDC. Two different NMSAs (9.5 mm and 12.5 mm) can be seen in Figure 4.2 (a) and (b). In Figure 4.2 (a), no correlation is found in the comparison between the ACI values and air void contents. However, in Figure 4.2 (b), a reasonable and strong correlation is observed from the comparison between the ACI values and asphalt contents for the 12.5 mm NMSA mixture. Although the coefficient of determination for the 9.5 mm NMSA is less than that for the 12.5 mm NMSA, a proportional trend also is observed. Figure 4.2 (c) and (d) include the data presented in Figure 4.1 (a) and (b) where the data are divided into different aggregate gradation types. In Figure 4.2 (c), no reasonable correlation is observed from the comparison between the ACI values and the air void contents under data partitioning. However, in Figure 4.2 (d), proportional correlations are observed from the comparison between the ACI values and asphalt contents, regardless of aggregate gradation category.

Figure 4.2 (e) and (g) and Figure 4.2 (f) and (h) include the data presented in Figure 4.1 (c) and (d), respectively. The data are derived from the top layer with TDC only and are divided into the different categories described above (i.e., the different NMSAs and aggregate gradation types). Two different NMSAs (9.5 mm and 12.5 mm) are seen in Figure 4.2 (e) and (f). In Figure 4.2 (e), no correlation is observed in the comparison between the ACI values and air void contents. However, in Figure 4.2 (f), a strong correlation is seen in the comparison of the ACI values and asphalt contents for the 12.5 mm NMSA mixture. Although the coefficient of determination for the 9.5 mm NMSA is less than that for the 12.5 mm NMSA, a proportional trend also is observed, which is a reasonable relationship between the ACI values and the asphalt contents. In Figure 4.2 (g), no reasonable correlation is observed in the comparison between the ACI values and air void contents under data partitioning. However, in Figure 4.2 (h), proportional correlations are seen from the comparison between the ACI values and asphalt contents for the *fine* and *penetrating aggregate gradation* categories. Because only two data points could be derived from the coarse aggregate gradation shown in Figure 4.2 (g) and (h), those data points are not described.

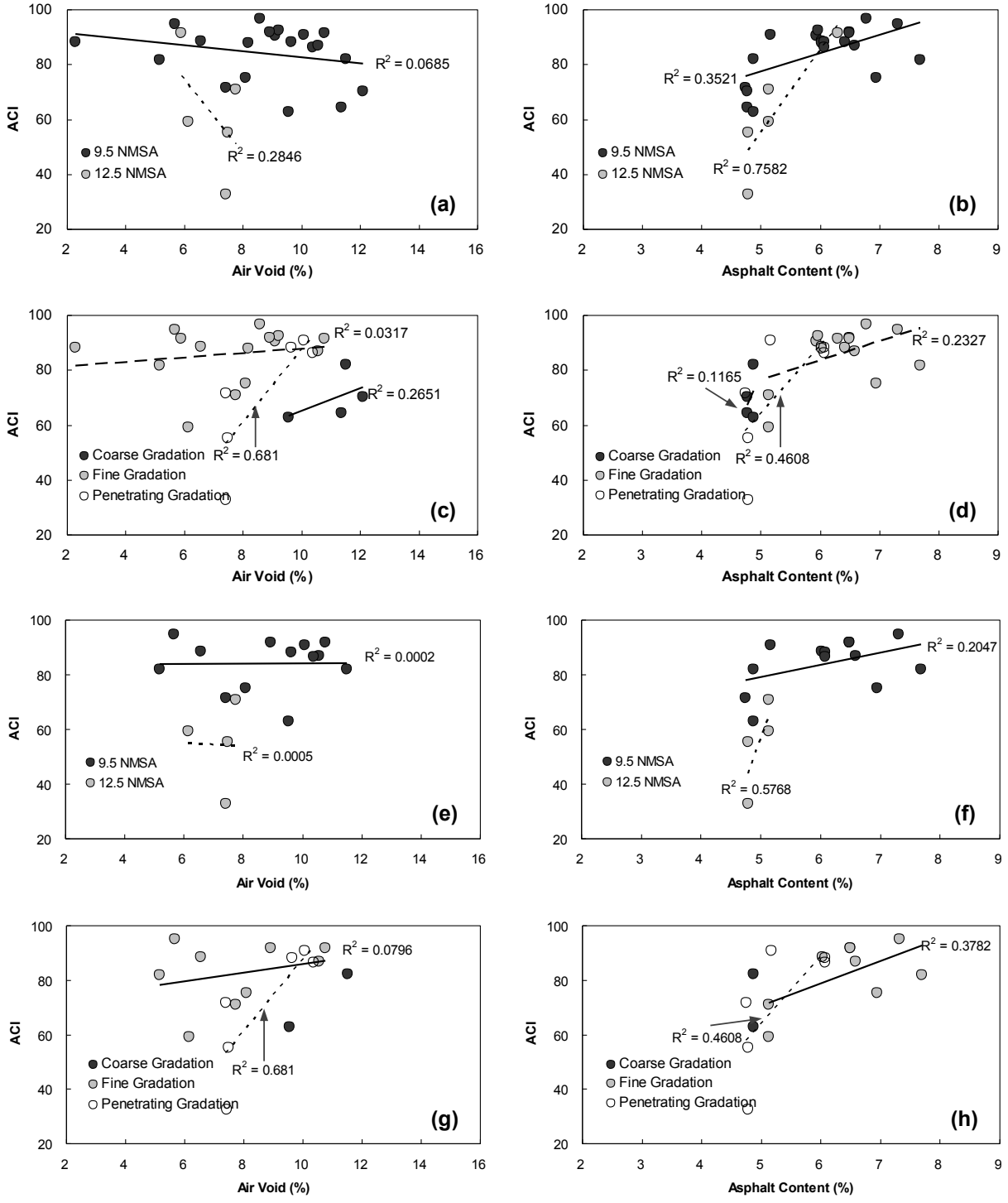

Figure 4.2 Comparison of alligator cracking index to air void content and asphalt content: (a) and (b) divided NMSAs for TDC or BDC observed condition regions, (c) and (d) divided aggregate gradations for TDC or BDC observed condition regions, (e) and (f) divided NMSAs for TDC only observed condition regions, and (g) and (h) divided aggregate gradations for TDC only observed condition regions.

Figure 4.3 (a) and (c) and Figure 4.3 (b) and (d) include the data presented in Figure 4.1 (a) and (b), respectively. The data are derived from the bottom layer with BUC or BDC and are divided into different categories. Two different NMSAs (9.5 mm and 19.0 mm) are observed in Figure 4.3 (a) and (b). In Figure 4.3 (a), a reasonable and strong correlation can be seen in the comparison of the ACI values and air void contents for the 9.5 mm NMSA, but no clear correlation is seen for the 19.0 mm NMSA. Figure 4.3 (b) shows an inverse correlation in the comparison between the ACI values and asphalt contents for the 9.5 mm NMSA, but this result is not a reasonable correlation. The comparison between the ACI values and asphalt contents for the 19.0 mm NMSA is not clear. Figure 4.3 (c) shows a reasonable and strong correlation in the comparison between the ACI values and air void contents for the penetrating aggregate gradation, but no clear correlation for the fine aggregate gradation. Figure 4.3 (f) shows that, although an inverse relationship is evident in the comparison of the ACI values and asphalt contents for the penetrating aggregate gradation, it is not a reasonable relationship. A somewhat reasonable correlation is observed in the comparison between the ACI values and asphalt contents for the fine aggregate gradation, but the correlation is insignificant in terms of the coefficient of determination value.

Figure 4.3 (e) and (f) include the data presented in Figure 4.1 (a) and (b), respectively. The data are derived from the bottom layer with BUC only, and only the 19.0 mm NMSA and two different aggregate gradation categories (fine and penetrating gradation) are observed in those figures. Figure 4.3 (e) shows a reasonable and strong correlation in the comparison between the ACI values and air void contents for the fine aggregate gradation. Figure 4.3 (f) shows a correlation between the ACI values and asphalt contents for the fine aggregate gradation, but the correlation is insignificant in terms of the coefficient of determination value. In summary, the asphalt content seems to have a more pronounced effect on the cracking performance than the air void content seems to have. Also, this effect is more evident in the pavements that exhibit top-down cracking than the ones with bottom-up cracking.

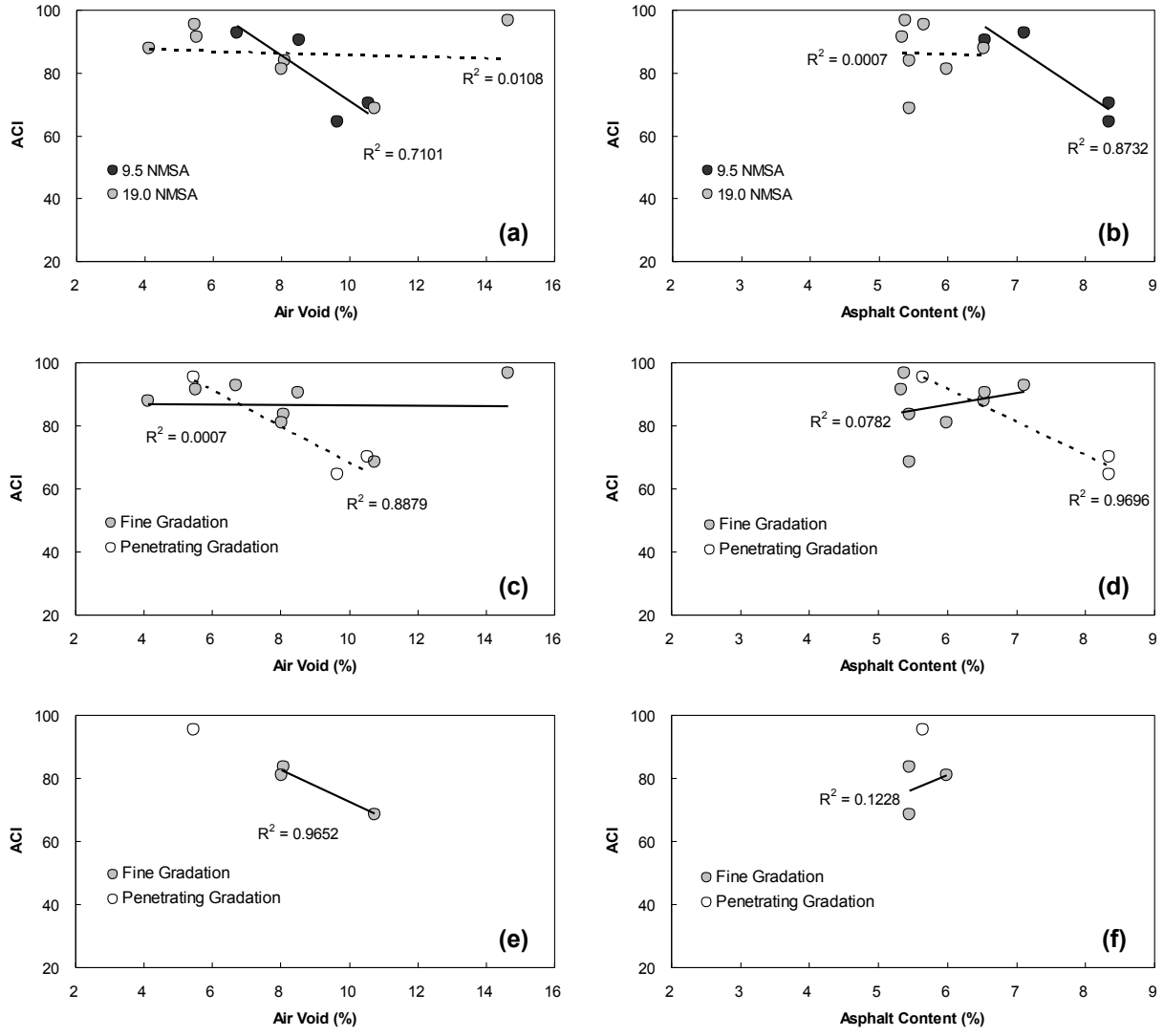

Figure 4.3 Comparison of alligator cracking index to air void content and asphalt content for the BUC or BDC observed condition regions: (a) and (b) divided NMSA for BUC or BDC observed condition regions, (c) and (d) divided aggregate gradation for BUC or BDC observed condition regions, and (e) and (f) divided aggregate gradation for BUC only observed condition regions.

In aggregate gradation, nominal maximum size of aggregates means one sieve size larger than the first sieve to retain more than 10% of total aggregate, and maximum aggregate size means one sieve size larger than the NMSA. An example of aggregate gradation chart of 9.5mm NMSA used in NCODT is presented in Figure 4.4. The function of control points is limiting the master range that given NMSA gradation must pass. The maximum density line represents a gradation line that meets aggregate proportion in densest arrangement. According to the

Superpave procedure, the restricted zone forms a band where given NMSA gradation should not pass. Although it was known that aggregate gradation that pass through restricted zone practically result in tender mixture performance due to excessive contain of fine sand in relation to total sand, Cooley et al. (2002) claimed that no relationship exist between Superpave restricted zone and permanent deformation or fatigue performance of hot mix asphalt pavement.

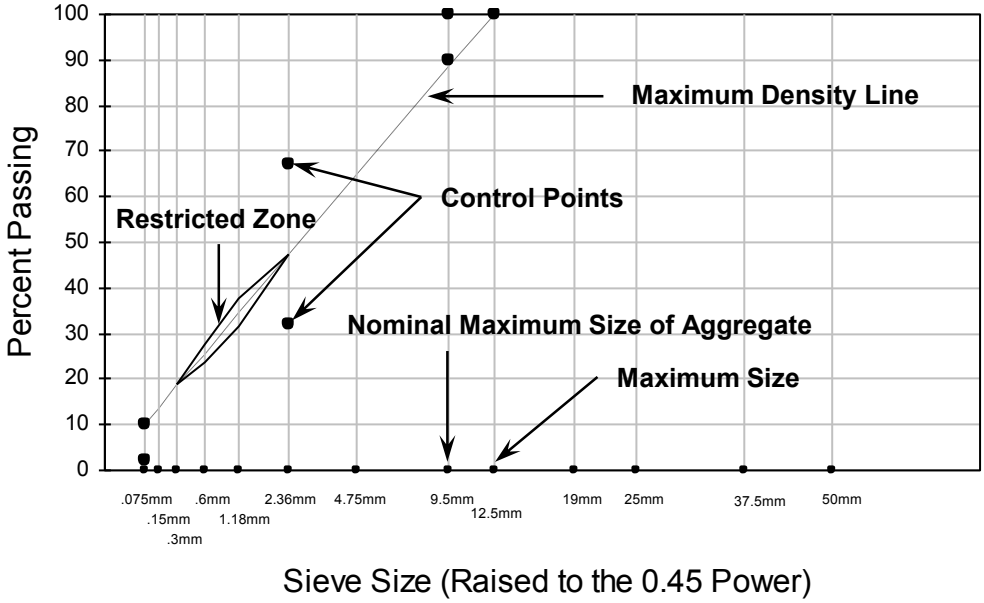

Figure 4.4 Example of 0.45 power aggregate gradation chart used NCDOT

Aggregate gradation that passes above restricted zone is fine aggregate gradation, and aggregate gradation that passes below restricted zone is coarse aggregate gradation. In order to compare the effect of gradation types on the cracking resistance of pavement, aggregate gradation types were divided into three different gradation type: coarse, fine, and penetrating gradation that pass through restricted zone. Penetrating gradation has often been called as a humped gradation. In Figure 4.5, ACI values of the three different gradation types from top layer are presented. From the Figure 4.5, higher average ACI value was observed from fine gradation comparing to other gradation types regardless of cracking direction.

In order to compare the effect of gradation type on the performance of pavements selected for this research, the aggregate gradation types are divided into coarse, fine, and penetrating aggregate gradations, and their ACI values are compared to each other. Also, in order

to simplify the cause and effect of aggregate gradation type in terms of pavement condition, the intermediate layers are excluded in this analysis.

Figure 4.5 and Figure 4.6 present the ACI values of the three different gradation types for the top layer and bottom layer. The data presented in Figure 4.5 (a) and (b) and Figure 4.6 (a) and (b) are taken respectively from the top layers and bottom layers of the condition regions. The averaged ACI values from each aggregate gradation type are presented next to the bar chart in each subfigure. Figure 4.5 and Figure 4.6 show higher average ACI values for the fine gradation than for the other gradation types, regardless of cracking direction and layer location. A similar conclusion was reported by Sausa et al. (*16*). They investigated the effect of aggregate gradation on the fatigue performance of asphalt mixtures using the bending beam fatigue test and concluded that mixtures with fine aggregate exhibit better fatigue resistance than those with other gradation types (*16*).

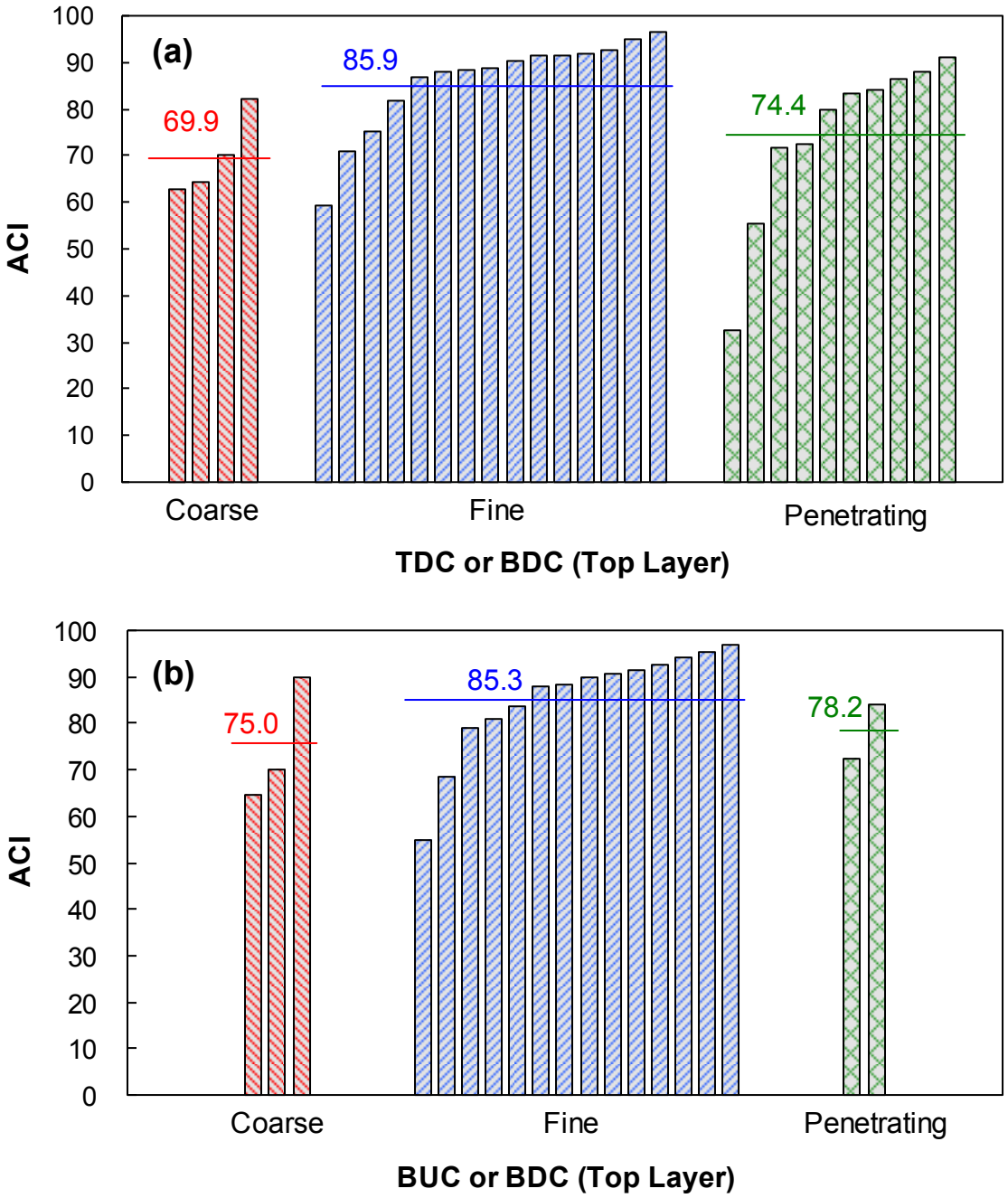

Figure 4.5 Comparison of alligator cracking index to aggregate gradation from top layer: (a) data with TDC only or BDC (b) data with BUC only or BDC.

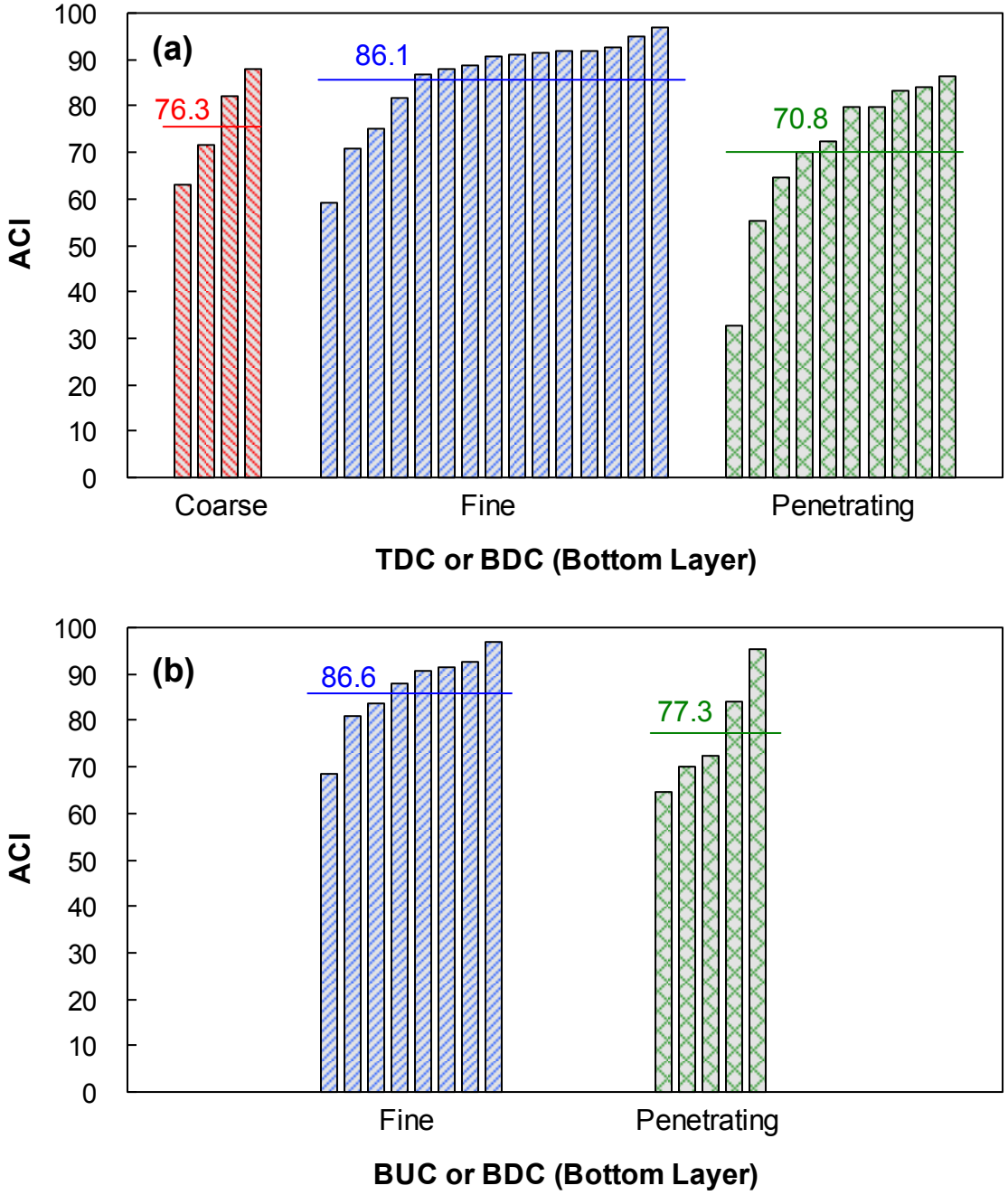

Figure 4.6 Comparison of alligator cracking index to aggregate gradation from bottom layer: (a) data with TDC only or BDC (b) data with BUC only or BDC.

AFTs were calculated following the specifications of the Minnesota Department of Transportation (MnDOT). The detailed process is presented in Lab Manual 1854.0 of the MnDOT that includes the surface area adjustment procedure adopted for this research. In the Lab Manual, the AFT is a function of the effective binder content (P_{be}), the percentage of aggregate in the mixture (P_s) and the percentage of the total asphalt binder in the mixture (P_b). However, the effective binder contents used for this analysis are not derived from the measured values. The effective binder contents were calculated using the averaged values of the effective specific gravity of aggregate commonly used in North Carolina; the averaged values for each different NMSA are found in the mix design database of the NCDOT Materials and Test Unit (MTU).

Among the 56 condition regions described earlier in this section, TC was observed in 32 condition regions. A comparison between the ACI values and AFTs from the TC-observed top layers is presented in Figure 4.7; no noticeable correlation was observed in Figure 4.7 (a). It is not surprising that there is no correlation between those values because of the different aging levels of each condition region, other volumetric design factors, and the assumed value of the effective specific gravity of the aggregate. Data presented in Figure 4.7 (a) contains film thickness data from 9.5mm NMSA and 12.5mm NMSA with air void content range from 2.3%to 12.1% and 5.9% to 7.5%, respectively. For quality analysis, the air void content range was reduced to 4~10%. Figure 4.7 (b) includes the data presented in Figure 4.7 (a) and is divided into different NMSA values. Figure 4.7 (b) shows that 12.5 mm NMSA show slightly proportional trends in the comparison between the ACI and AFT. However, 9.5mm NMSA still do not show any correlation between ACI and AFT.

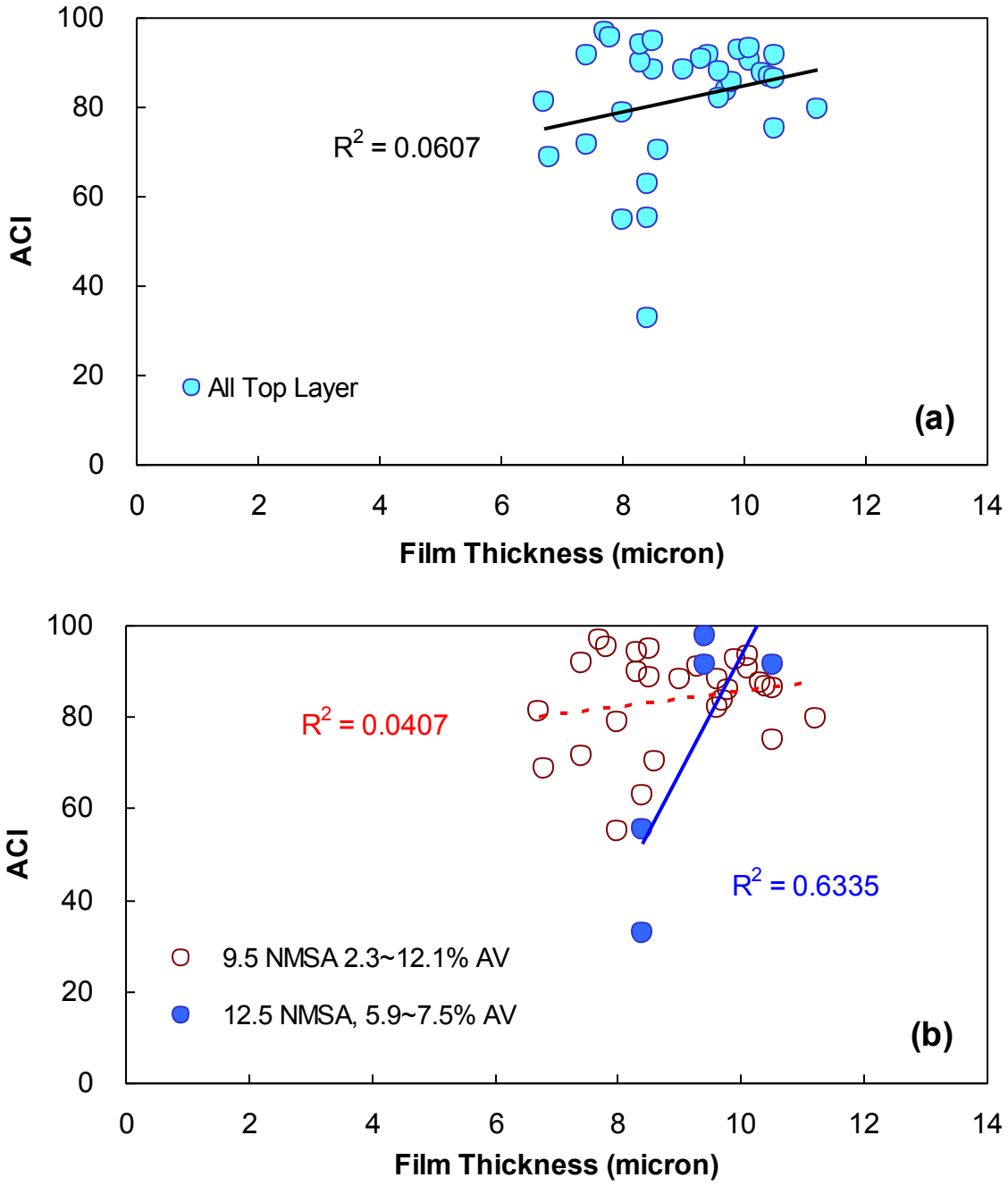

Figure 4.7 Comparison of alligator cracking index to asphalt film thickness of top layer: (a) data from all top layers with TC and (b) data from different NMSA values.

4.4.3 Summary

The asphalt contents of the top layers that exhibit TDC or BDC show a proportional relationship to the ACI values. The air void contents of the bottom layers that exhibit BUC or BDC show an inverse proportional relationship to the ACI values. These observations reflect quite reasonable results. For quality analysis, the given data were partitioned into different categories: different NMSAs and aggregate gradation types. In case of top layer exhibiting TDC or BDC, same conclusions can be drawn in comparison of ACI values and asphalt content regardless of sizes of NMSA and aggregate gradation types. However, for the case of bottom layer exhibiting BUC or BDC, reasonable correlations were observed in specific categories: 9.5mm NMSA and penetrating aggregate gradation for BUC or BDC and fine aggregate gradation for only BUC exhibit bottom layer. If mix design information of each condition region was available for this research, quality analysis could be conducted to find out why poor relationships were observed in the comparison of ACI values and air void and asphalt contents showing undesirable relationship. For the analysis of aggregate gradation types against ACI values, it was observed that fine aggregate gradation showed higher average ACI values than other aggregate gradation types regardless layer location and cracking direction. For the analysis of AFTs against ACI values, no noteworthy findings were found in the comparison between the ACI values and AFTs, but a somewhat reasonable result was found once the range of comparison was narrowed down to 12.5mm NMSA. In short, thick asphalt films indicate high ACI values.

Because lack of mix design and material information, it would be controversial statement if the research team comment all findings from the aforementioned analyses are directly describe the fatigue cracking performance of given pavements. Analysis approaches hereinbefore conducted from the mix design aspects are possible analyses under given situation that need to rely on field extracted material and pavement condition survey. Therefore, the lack of mix design and material information left much to be desired.

4.5 Structural Uniformity

4.5.1 Pavement Substructure Analysis

The DCP is used to assess the pavement substructure (i.e., thickness of the base layer, base layer modulus and subgrade modulus) in field sites. It is used to determine the California

bearing ratio (CBR); then, the measured CBR can be used to determine the elastic modulus value of the soil. For this research, DCP test results were used to determine the modulus values of the base layer and subgrade layers, verify the consistency of the pavement substructure by showing the different levels of deterioration on the pavement surface, and determine the thickness of the base layer that could not be found in the NCDOT pavement profile database.

A DCP was developed originally by Scala (1959), and then various researchers further developed the test device and procedure. The cone at the tip of the drive rod has a 60° angle with a base diameter of 20 mm (0.79 in.). A DCP test is performed by dropping an 8 kg (17.6 lb) weight through a 575 mm (22.6 in.) slide rod and then measuring the penetration depth of the cone per blow or by measuring the number of blows it takes to achieve 150 mm of penetration. Figure 4.8 presents a schematic of a DCP.

The total number of blows and the depth of the penetration are recorded for each test. Then, the *penetration ratio* (PR) is calculated as the penetration depth (mm) over the number of blows. This PR, presented in Equation (17), is then used to calculate the *in situ* CBR values. Various researchers recommend different correlations between the DCP measurements and CBR values, but Equation (18), which is recommend by the US Army Corps of Engineers (Webster et al. 1992), is adopted for this research to obtain the CBR values for the base and subgrade layers. Equation (19) is used to calculate the modulus values of the base and subgrade layers. (Note: Equations (18) and (19) are presented in NCHRP 1-37A Project, Part 2 (NCHRP 2004b)).

$$PR = \frac{Penetration\ Depth\ (mm)}{Number\ of\ Blows} \tag{17}$$

$$CBR = \frac{292}{PR^{1.12}} \tag{18}$$

$$E_{base} = 2555 \times CBR^{0.64} \tag{19}$$

where

$PR = penetration\ rate\ (mm/blow)$,
$CBR = California\ bearing\ ratio, and$
$E_{Base} = Modulus\ of\ aggregate\ base\ (psi)$.

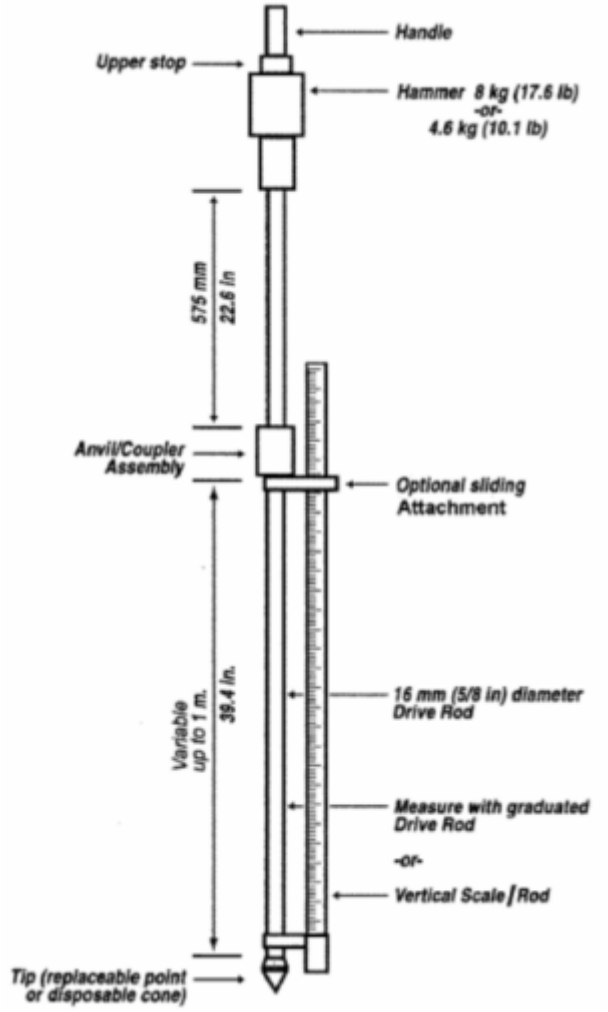

Figure 4.8 Schematic of DCP device (ASTM D6951/D6951M).

The stiffness of the substructure is defined by the PR. A high PR value indicates soft soil, and a low PR value indicates hard soil. However, as shown in Figure 4.9, the first few DCP blows show different PR values at the beginning of the DCP testing up to a certain depth. These different PR values are due to the presence of water that has penetrated through the pavement during the coring procedure and/or cone stabilization progress. Accordingly, these first few blows are discounted in calculating the elastic modulus value of the base layer. The depth measurements that are affected by water and cone stabilization can be defined by the visual observation of the PR vs. depth plots. For example, Figure 4.9 shows that the first few PR values are higher than the next PR values. Thus, those data points for the high PR values are removed for calculating the elastic modulus of the base layer.

After removing the unusable data points, the penetration depths for the *in situ* DCP data are plotted against the number of blows. As presented in Figure 4.10 (a), the plotted data show two dramatically changing PR slopes for one DCP test location. The change in the penetration depth vs. number of blows slope indicates the existence of new material under the point of the change in slope. This change in slope reflects the depth of the base layer for each DCP-tested location. After this depth (i.e., at the base layer), the new layer is considered to be the subgrade layer. In the case of an unclear slope change at the bottom of the base layer, linear regression analysis is performed on data points that constitute two distinctively different slopes, and the intersection of the two lines is used to define the depth of the base layer. Figure 4.11 shows the DCP data and the regression equations that were used to determine both the base and subgrade layers for the four different condition regions of the US-601 pavement.

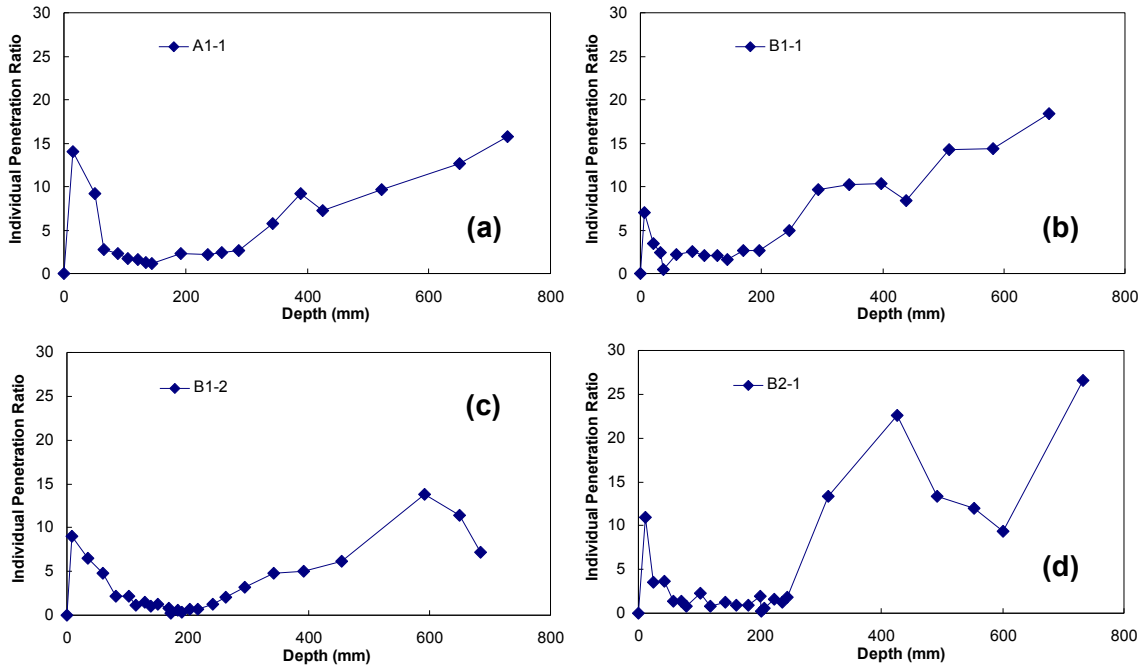

Figure 4.9 Penetration ratio vs. penetration depth for four US 601 pavement regions: (a) DCP data from A1 condition region, (b) 1st DCP data from B1 condition region, (c) 2nd DCP data from B1 condition region, and (d) DCP data from B2 condition region.

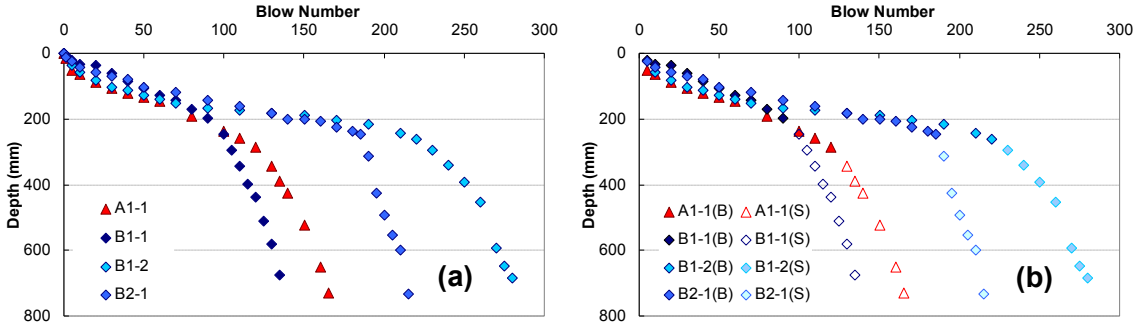

Figure 4.10 Plots of penetration depth vs. number of blows for four US 601 pavement regions: (a) raw data and (b) modified data for base and subgrade layers.

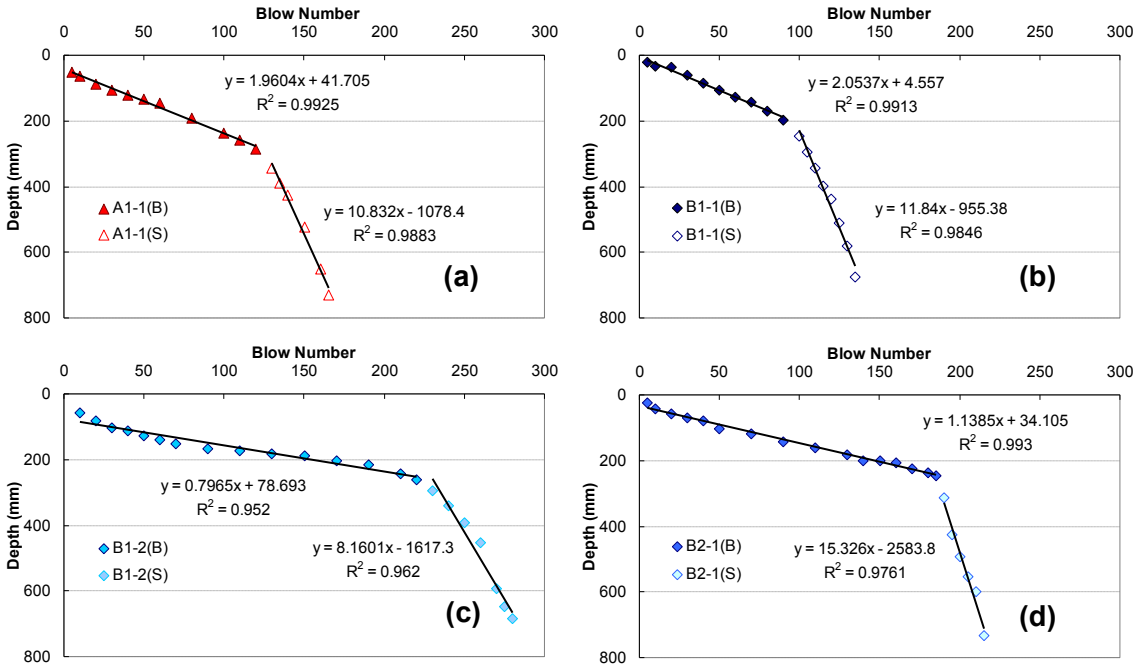

Figure 4.11 Modified DCP data for base and subgrade layers showing PR values and coefficients of determination for four US 601 pavement regions: (a) DCP data from A1 condition region, (b) 1st DCP data from B1 condition region, (c) 2nd DCP data from B1 condition region, and (d) DCP data from B2 condition region.

Table 4.3 provides a summary of the pavement substructure properties of all the field sites. DCP analysis for each field site was performed according to the method described above for the three different pavement condition regions at the US 601 site.

Table 4.3 Substructure properties of selected field sites from *in situ* DCP test results

	Site	Condition Region	Modulus (ksi)		Base Depth (mm)	Note
			Base Layer	Subgrade layer		
Test Level 1	I-540	B1	1,500,000	11,835	200	Thickness of base layer came from NCDOT database, Base layer is Cement Treated Aggregate Base Course
		A1	1,500,000	14,259	200	
		B2	1,500,000	15,649	200	
		A2	1,500,000	19,268	200	
	NC-24	B1	54,635	16,242	230	-
		A1	58,884	12,851	380	
		B2	31,559	17,164	180	
	US 70	B1	119,925	43,486	230	-
		B2	54,294	21,834	240	
		A1	60,092	15,215	240	
		A2	74,186	26,792	240	
	US-17	B1	25,971	26,259	200	Thickness of base layer came from NCDOT database
		B2	23,851	22,916	200	
		A1	17,171	21,861	200	
		A2	12,868	26,114	200	
	US-601	A1	59,660	17,521	289	-
		B1	85,741	18,951	234	
		B2	88,074	13,662	244	
	NC-87	A1	27,354	29,685	350	-
		B1	25,849	6,254	230	
		A2	29,786	17,359	290	
		B2	31,895	14,060	380	
	US-76	B1	73,730	28,668	240	-
		A1	32,897	28,370	290	
	US-74	B1	88,331	20,638	260	-
		A1	89,583	25,258	300	
	NC-209	A1	63,476	19,022	330	-
		B1	50,199	16,256	280	
		A2	41,926	20,980	180	
Test Level 2	US-13	A1	62,619	27,759	260	-
		B1	84,411	28,162	230	
		B2	57,986	38,928	380	
		A2	30,603	19,174	260	
	NC-177	B1	14,507	9,507	360	-
		A1	21,804	13,332	300	
		A2	31,259	18,908	230	
		B2	12,317	6,769	330	
	SR-1530	B1	30,735	10,327	160	-
		B2	40,946	10,041	200	
		A1	8,944	7,999	60	
	US-220	A1	-	5,219	-	Concrete pavement under asphalt pavement
	NC-47	B1	26,524	11,174	270	-
		A1	30,683	9,872	210	
		B2	30,308	8,943	190	
	NC-82	B1	33,775	6,393	310	-
		A1	18,284	4,964	340	
	US-401	A1	36,800	21,896	310	-
		B1	23,207	12,869	310	
	NC-55	A1	28,597	12,170	260	-
		B1	25,196	9,056	270	
	NC-194	B1	20,106	5,785	100	-
		A1	35,564	22,583	100	
		B2	34,559	20,817	440	
	NC-179	A1	59,651	22,997	310	-
		B1	45,674	13,876	320	

4.5.2 Roadway Widening

Fatigue cracking can be defined by the longitudinal direction of clusters of interconnected cracks that are caused by the fatigue failure of hot mix asphalt (HMA) pavement. Longitudinal cracking is the early phase of fatigue cracking, i.e., before the cracks become interconnected. Potentially, longitudinal cracks under the wheel path can develop into fatigue cracking. Given this situation, it is also cost-effective to rehabilitate a pavement before it requires full reconstruction. In particular, the maintenance threshold for the primary roads selected for this research, as described in Section 1.2, is higher than that of secondary roads. Therefore, most of the pavement sites selected for this research are in the early phase of fatigue cracking, which is longitudinal cracking with localized interconnected cracks.

In order to verify the condition survey results using database analysis, the research team visited candidate sites in the *young age and poor performance* category. The most of the pavement sites selected for this research are in the early phase of fatigue cracking, which is longitudinal cracking with localized interconnected cracks. The most significant outcome from the field visits and field testing stems from the lack of construction history records, because several sites tested (5 out of 19) show evidence of road widening that had not been recorded in the NCDOT database. Out of those five sites with evidence of road widening, three sites show road widening throughout the entire length of the section. Those sites are US 220, NC 47 and NC 194, which were initially constructed in 1926, 1946, and 1931, respectively. It is suspected that these three primary roads were designed initially to accommodate smaller vehicles than those currently on the roads. Therefore, the decision to widen these roadways may have been necessitated by safety concerns.

Evidence of road widening includes pavement marking/paint lines in the cores taken from the outer wheel path as well as characteristics of the actual structure of a pavement that clearly indicate that the road has been widened beyond the original substructure. Figure 4.12 (a), (b) and (c) show the pavement substructure as evidence of road widening. Figure 4.12 (a) shows the cracking pattern at the site (US 220). Figure 4.12 (b) and (c) clearly show evidence of road widening that extends beyond the original pavement structure. Figure 4.13 is a schematic illustration based on the findings for the pavement structure shown in Figure 4.12 (a), (b) and (c). In Figure 4.14 (a) to (c), the ovals show traces of marking paint on the delaminated surface and in the middle of cores extracted from the outer wheel path; these paint lines indicate road

widening. Even clearer evidence of road widening from marking paint lines is presented in Figure 4.15 (a) to (e). Figure 4.15 (a) shows the condition survey from the NC 87 pavement site and also shows the coring locations and pavement conditions presented in the condition survey map. As indicated in Figure 4.15 (a), the cores shown in Figure 4.15 (b) and (e) were extracted from slightly outside the outer wheel path area, and the cores shown in Figure 4.15 (c) and (d) were extracted from inside the outer wheel path area. The cores taken from outside the outer wheel path area exhibit a different pavement structure than those extracted from the inside of the wheel path, and the core shown in Figure 4.15 (c) has a paint line on the core. These observations clearly indicate that pavement marking was on top of the core in Figure 4.15 (c) and the road was widened at least the distance between the core location and the current pavement marking location that is presented in Figure 4.15 (a).

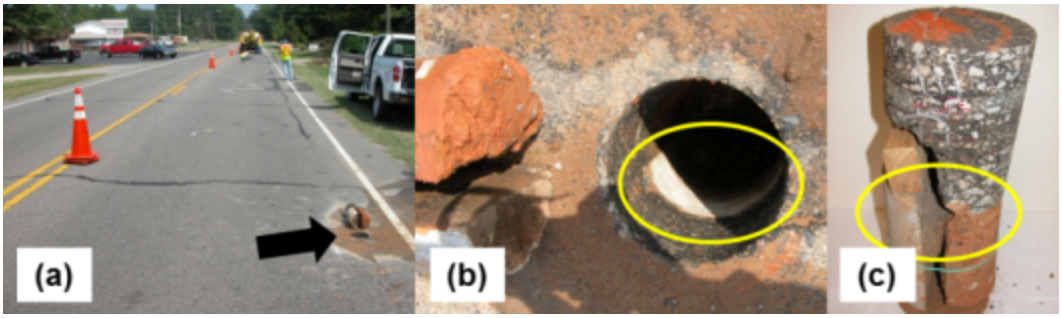

Figure 4.12 Field core with pavement substructure as evidence of road widening.

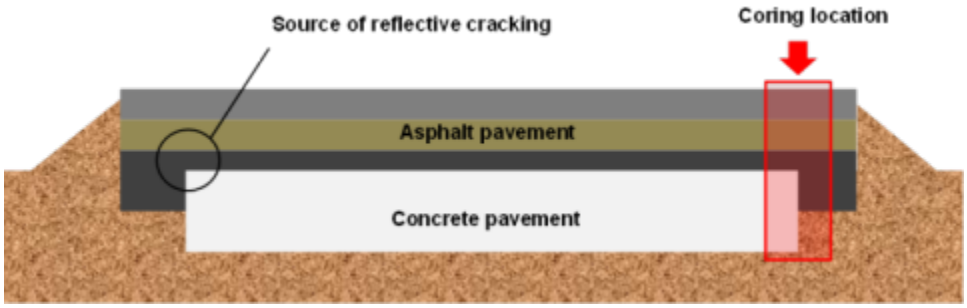

Figure 4.13 Illustration of pavement structure shown in Figure 4.12 (US 220, Montgomery County).

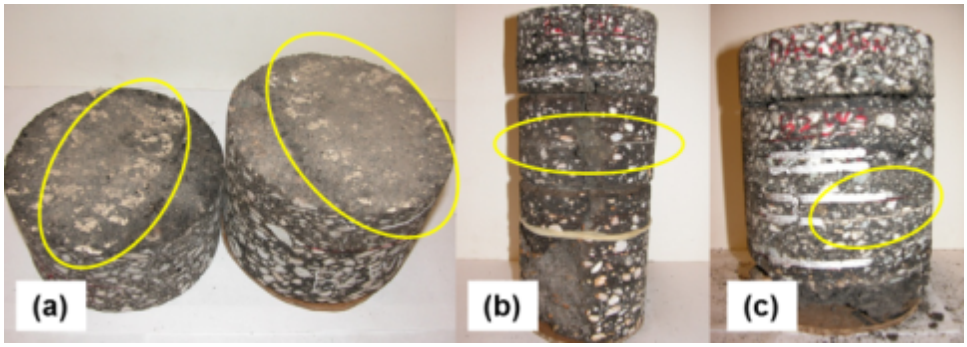

Figure 4.14 Field cores with marking paint as evidence of road widening.

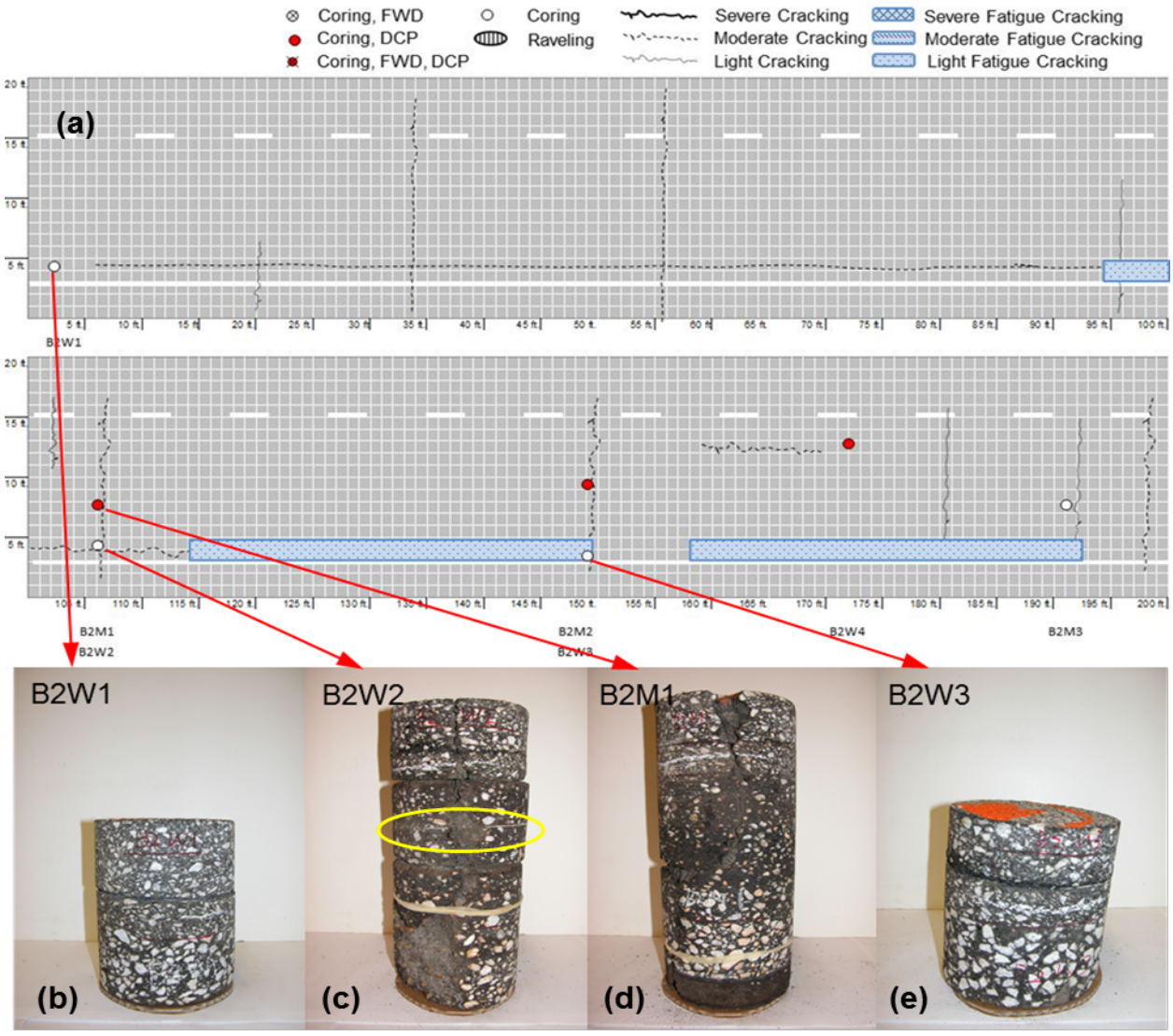

Figure 4.15 Pavement condition survey from NC87 and field cores: (a) condition survey and (b) to (e) cores presented in the condition survey map

4.6 Layer Interface Separation

4.6.1 Introduction

Layer interface separation (debonding) is caused by the lack of sufficient bonding between two different pavement layers. This insufficient bonding leads to non-uniform structural movement, which eventually shortens the pavement life cycle because of slippage and corrugation on the surface and cracking from the bottom of the upper separated asphalt layer. Accordingly, several researchers stress the important role that bonding plays in the pavement life cycle (Walubita and Scullion 2007, Metcalf et al. 1999, Hu and Walubita 2011). It is well known that high temperatures and high traffic loads (especially horizontal loads) or a combination of these two factors with poor bonding can lead to interface separation in asphalt layers. Also, water that has penetrated into the partially separated layer propagates debonding in the entire layer. Walubita and Scullion (2007) point out that poor construction practices and poor quality or insufficient bonding material are major causes of debonding. Because finding the mechanisms of debonding is outside the scope of this research, debonding is discussed from the QC/QA perspective. Based on the research findings from three-dimensional finite element methods, Hu and Walubita (2011) conclude that tensile stress-induced fatigue cracking failure occurs in both traffic directions and perpendicular to the traffic direction and, inevitably, leads to premature alligator cracking under the debonding condition.

4.6.2 Field Observations of Debonding

As noted earlier, the 19 sites selected for this research contain 56 different condition regions. Debonding was observed in 29 different condition regions; 23 out of these 29 condition regions showed a history of overlay and 6 regions had single-construction histories. Table 4.4 and Figure 4.16 present details regarding the debonding occurrence in terms of frequency and frequency percentages. Debonding was observed in cores extracted from both cracked areas and areas with no cracking. Because the size of the drill bit used for the research is 6 inches for its inner diameter, high torsional shear force during coring may have caused or accelerated debonding in the cores. Sometimes the layer interface separation can be clearly observed in a cored hole (e.g., as seen in the photograph in Figure 4.17), but not all cases of debonding are so obvious. The photograph in Figure 4.17 was taken immediately after the core was extracted and

shows the water used for coring coming out of the separated layer interface. Therefore, it is noted that all observations and records are based on the visual observation of both cores and core-extracted holes.

One major cause of debonding that can be discussed with confidence is the quality of the bonding material (tack coat) or poor construction practices for applying tack coats. Many cores that show debonding have a very smooth surface where the debonding occurred. If a quality tack coat was used at a certain site, and debonding was caused only by the penetration of water, at least one of the cores should have partial debonding with a non-smooth surface. However, most of the field sites with cores with smooth debonding surfaces do not have cores with partial debonding. Figure 4.18 (a) and (b) show a smooth debonding surface for cores extracted from US-70 and NC-24, respectively.

Table 4.4 Frequency of debonding and no debonding under different construction scenarios

	Overlay	One-construction
Debonding	23	6
No Debonding	21	6

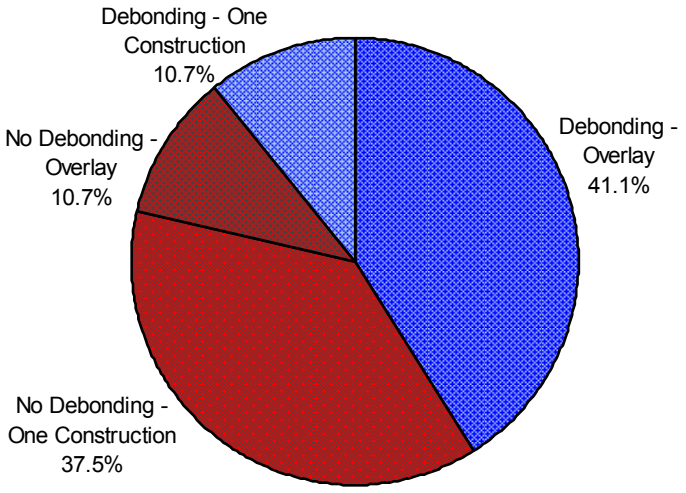

Figure 4.16 Percentage of debonding frequency for different construction histories of all condition regions.

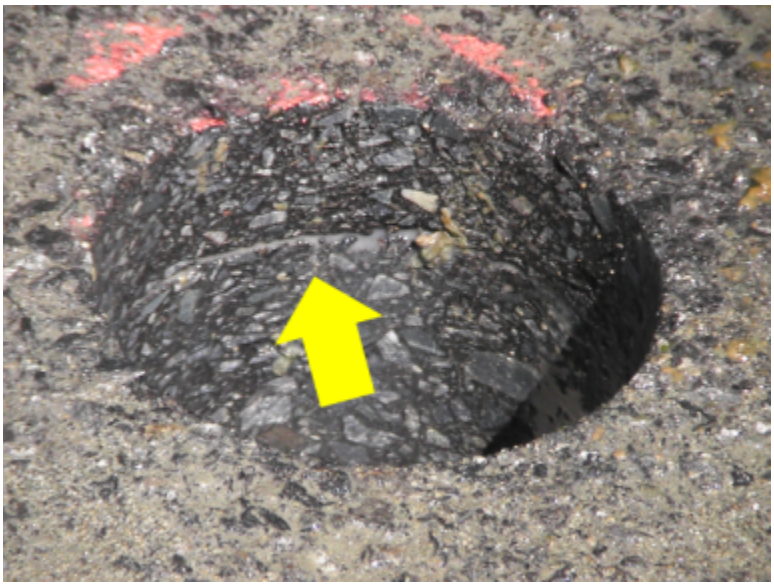

Figure 4.17 Debonding (layer interface separation) in core-extracted hole (NC-24).

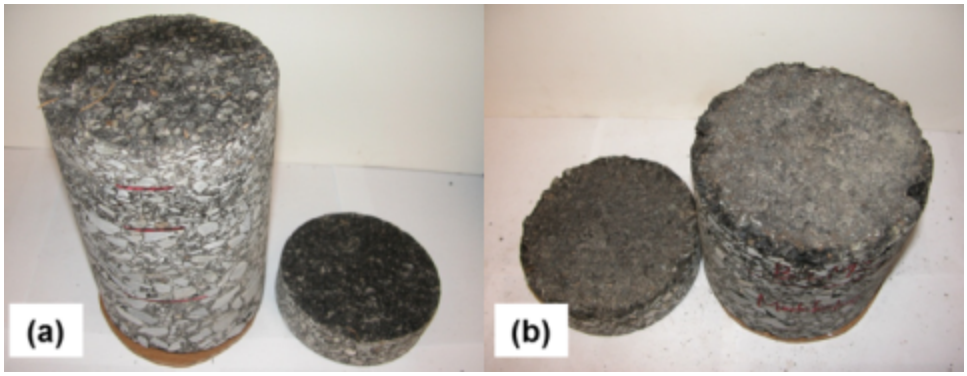

Figure 4.18 Photographs of smooth debonding (layer interface separation) surfaces in field cores.

4.6.3 Summary

The master database indicates that condition regions without debonding have relatively higher ACI values than those from condition regions with debonding, as shown in Figure 4.19. That is, regions with observed debonding exhibit poorer pavement conditions than regions without records of debonding. Figure 4.20 to Figure 4.22 support this conclusion by comparing cracked areas of regions where debonding was observed with those of regions where debonding was not observed in terms of severity level.

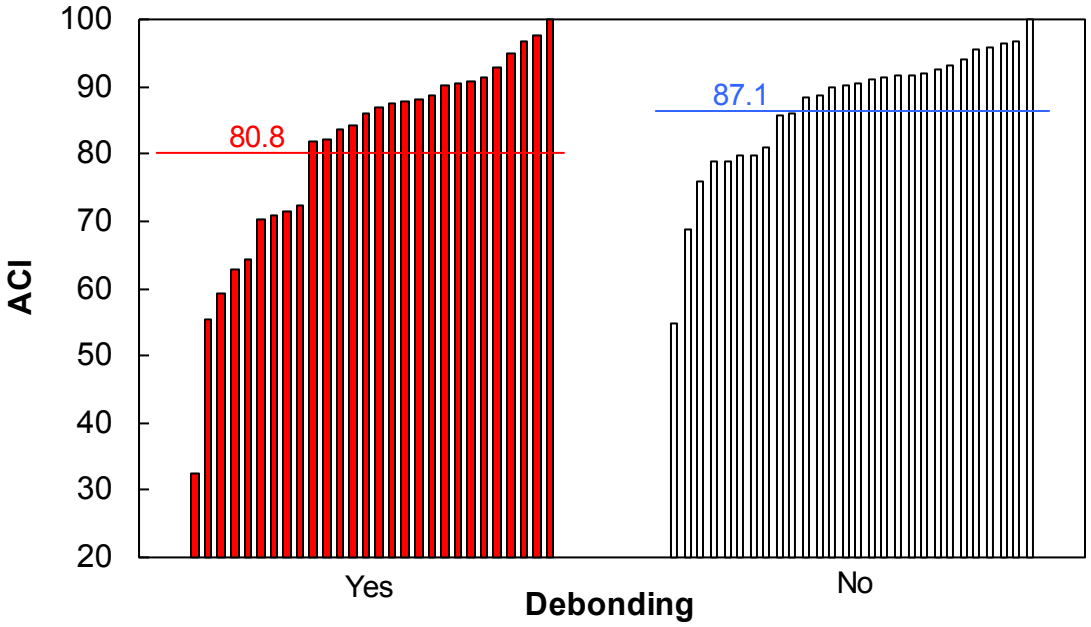

Figure 4.19 Alligator cracking index values from the condition regions with or without debonding.

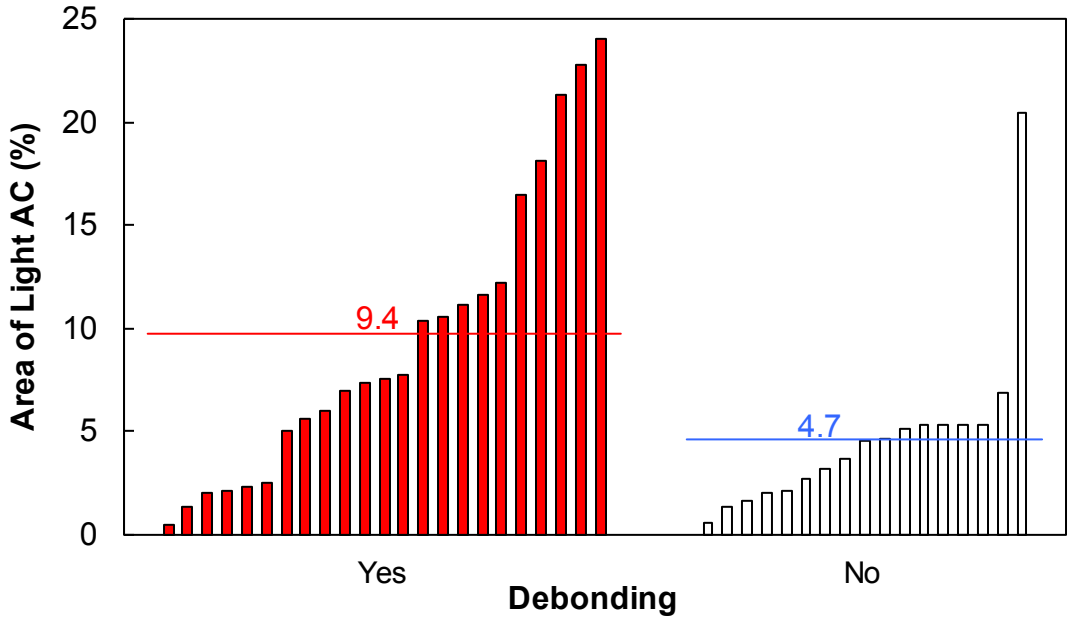

Figure 4.20 Percentage of area with light alligator cracking in condition regions with or without debonding.

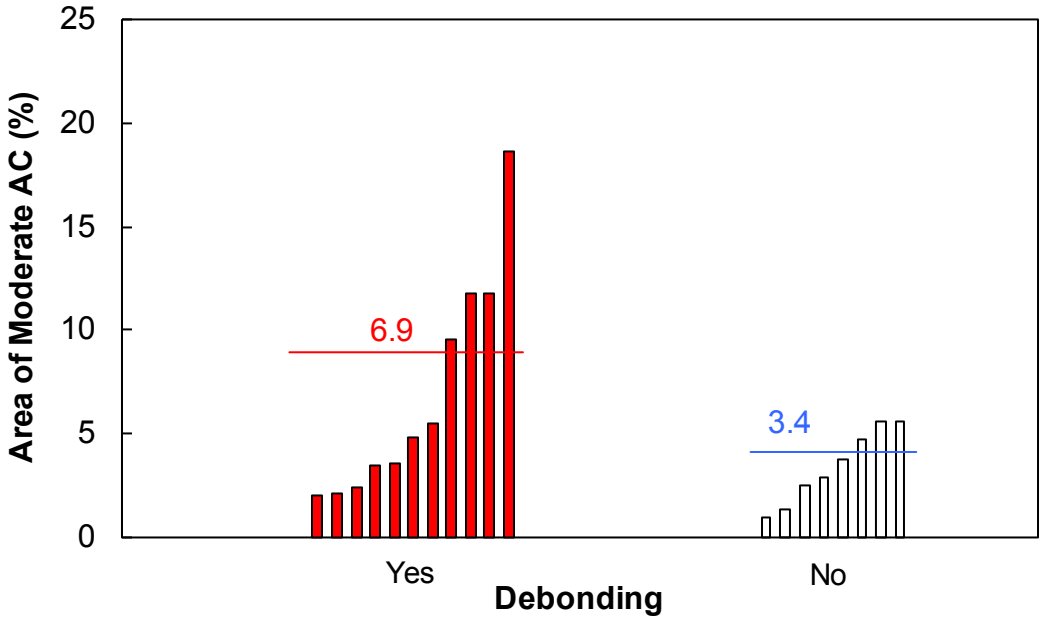

Figure 4.21 Percentage of area with moderate alligator cracking in condition regions with or without debonding.

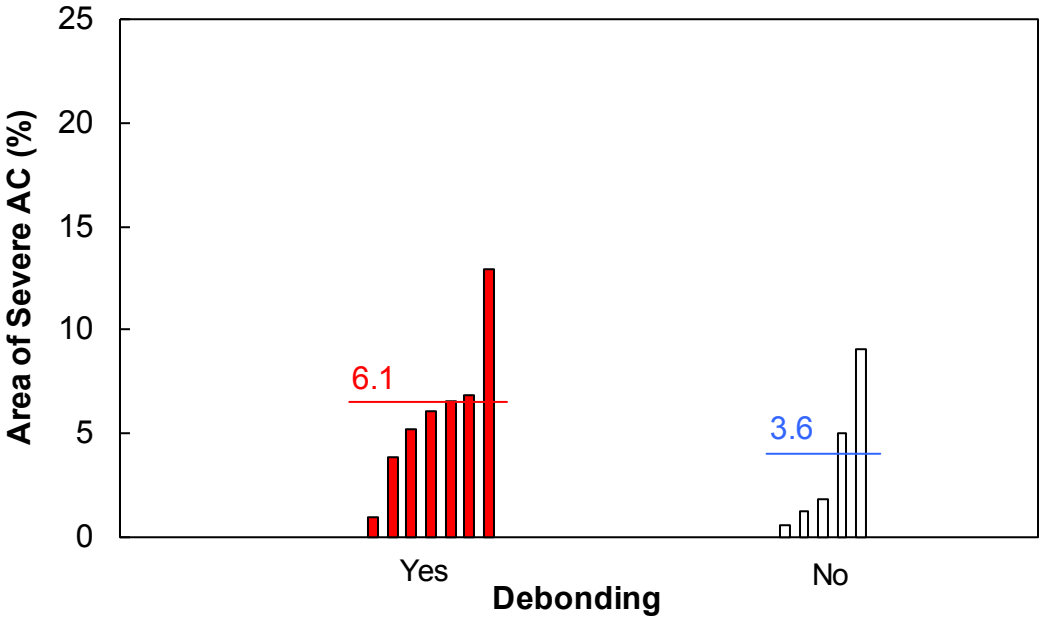

Figure 4.22 Percentage of area with severe alligator cracking in condition regions with or without debonding.

4.7 Top-Down Cracking Identification

It is now well accepted that load-related top-down fatigue cracking (i.e., cracking that initiates at the surface of the pavement and propagates downward) commonly occurs in HMA pavements. This phenomenon has been reported to occur in many parts of the United States as well as in Europe, Japan, and other countries (Myers et al. 1998, Jacobs 1995, Matsuno and Nishizawa 1992, Pellinen 2002, Myers and Roque 2001, Uhlmeyer et al. 2000). Top-down cracking cannot be explained by the traditional fatigue mechanisms that are used to explain load-associated fatigue cracking that initiates at the bottom of the pavement layers. Furthermore, conventional pavement analysis models that consider bending stress in a layered pavement system are incapable of predicting pavement responses that could result in stress-strain conditions that would explain the initiation and propagation of top-down longitudinal cracks.

Top-down cracks and full-depth cracks caused by bottom-up cracking look identical on the pavement surface, and as a result, most studies that attempt to differentiate between them involve coring or trenching the pavement (Myers et al. 1998). The differentiation between top-down and full-depth cracking caused by bottom-up cracking has important implications in pavement management because the type of cracking will affect the determination of the most structurally-effective and cost-effective rehabilitation strategies. In other words, if top-down cracking is identified in an asphalt concrete pavement, replacing the top layer after milling off the distressed layer will restore the asphalt pavement to the condition of a new pavement. (This concept is the basis for perpetual pavements.) Therefore, identifying the cracking pattern from surface cracks is crucial for project-level pavement management systems.

4.7.1 *AREA* Parameter Method

Uhlmeyer et al. (2000) conclude from their field study that top-down cracking occurs in pavement layers that typically are more than 160 mm (6.3 in.) thick. In addition, in sections that exhibit top-down cracking, FWD data do not show as much reduction in structural stiffness as sections that exhibit full-depth cracking.

The findings from the Uhlmeyer et al. study were applied to the FWD deflections and thickness information obtained from each of the sites listed in Table 4.5. As shown in Figure 4.23, the so-called *AREA* values, Equation(20), were computed from deflections measured from

the top-down cracking and bottom-up cracking sections. Note that the deflections have been corrected for temperature effects and normalized to a load level of 40 kN (9,000 lbs) according to the method given elsewhere (Pierce and Sivaneswaran 1999).

$$AREA = \frac{6\left(D_0 + 2D_1 + 2D_2 + D_3\right)}{D_0} \tag{20}$$

where D_0 is the surface deflection at the test load center, and $D_{1\text{-}3}$ are the measured surface deflections at 30.48 cm (12 in.), 60.96 cm (24 in.), and 91.44 cm (36 in.) from the load center.

Table 4.5 Summary of pavement information for the selected sites

Crack Type	Site	Pvmt Layer	Material Type	Material Sub-Type	Thickness, cm (in.)	Modulus, MPa (ksi)
TDC	I 540	1	Asphalt Concrete	12.5 mm NMSA	3.75 (1.5)	Presented in Appendix
		2		12.5 mm NMSA	5.46 (2.1)	
		3		19.0 mm NMSA	8.62 (3.4)	
		4		25.0 mm NMSA	12.21 (4.8)	
		5	Base	Cement Treated ABC	20.28 (8)	10342 (1500)
		6	Subgrade	A-4 (top 11 in.)	Semi-infinite	83(12)
	NC24	1	Asphalt Concrete	9.5 mm NMSA	4.1 (1.6)	Presented in Appendix
		2		9.5 mm NMSA	3.49 (1.4)	
		3		19.0 mm NMSA	9.7 (3.8)	
		4	Base	Stabilized ABC	29.5 (11.6)	352 (51)
		5	Subgrade	A-4 (top 6 in.)	Semi-infinite	83 (12)
	US 17	1	Asphalt	HMA (4 layers)	20.45 (9.47)	n/a
		2	Base	Aggregate Base Course	20.32 (8)	n/a
		3	Subgrade	A-2 (top 21 in)	Semi-infinite	116 (16.8)
	US 70	1	Asphalt	HMA (5 layers)	27.67 (10.89)	n/a
		2	Base	Aggregate Base Course	20.32 (8)	n/a
		3	Subgrade	A-2-4 (top 14 in)	Semi-infinite	116 (16.8)
BUC	US 74	1	Asphalt	HMA (3 layers)	16.66 (6.56)	n/a
		2	Base	Coarse Aggregate Base Course	33.02 (13)	n/a
		3	Subgrade	A-5 (top 11 in)	Semi-infinite	133 (19.3)
	NC 87	1	Asphalt	HMA (6 layers)	29.22 (11.50)	n/a
		2	Subgrade	A-4 (top 7 in)	Semi-infinite	90 (13.1)

The *AREA* index was identified by Uhlmeyer et al. (2000) as an important index to identify top-down cracking when surface cracks are present. The *AREA* value is affected by both

the thickness of the pavement and also the condition of the pavement, i.e., the structural stiffness of the site, and can be used as a method for selecting the proper pavement rehabilitation strategy. Figure 4.23 presents the *AREA* values determined in this research along with the respective pavement thickness values. It is noted that the deflection data used to generate Figure 4.23 were obtained from FWD tests on surface cracks and the areas immediately next to those surface cracks. A clear differentiation is observed between the top-down cracking and full-depth cracking areas. Specifically, the *AREA* values are much smaller, given the pavement thicknesses, in the full-depth cracking sections, which suggests that the structural damage in these sections is more severe than in the top-down cracking sections. This observation is confirmed from the cores taken at each test site. Also, this observation is similar to that of Uhlmeyer et al. and verifies that FWD measurements used in conjunction with the known pavement structure may yield important information for identifying pavements with top-down cracking when surface cracks are present.

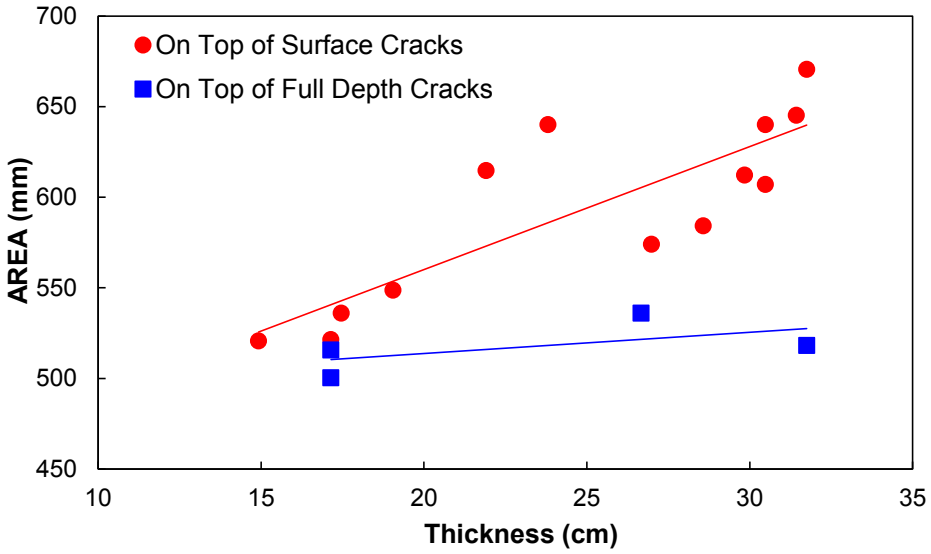

Figure 4.23 Comparison of *AREA* values for TDC and BUC sections.

4.8 Bottom-Up Cracking Identification

Because bottom-up cracking is caused by the bending moment in the bottom layer, the actual tensile strain response at the bottom of the asphalt layer needs to be investigated. Therefore, simulations were conducted using the LVECD program for pavement sites that

clearly showed bottom-up crack propensity and top-down crack propensity from field-extracted cores. The list of these sites and associated pavement structural information are presented in Table 4.6. Because these tensile strain responses were obtained as part of a long-term performance simulation process, the actual in-service pavement conditions, i.e., temperature gradient, traffic speed and loading, substructure strength, etc., were considered for these simulations. Accordingly, the simulation results show the movement of the pavement structure under in-service pavement conditions.

BUC is caused by the bending moment at the bottom of the asphalt layer. Accordingly, the actual tensile strain response at the bottom of the asphalt layer needs to be investigated to verify the cause(s) of BUC. Therefore, in order to compare the tensile strain at the bottom of the asphalt layer for TDC and BUC pavements, simulations were conducted using the layered viscoelastic analysis (LVEA) program for pavement sites that clearly show BUC propensity and TDC propensity from field-extracted cores. The LVEA program performs three-dimensional analysis to calculate pavement responses under moving traffic loads (Eslaminia et al. 2012).

The list of the sites and associated pavement structural information used in the LVEA simulations are presented in Table 4.6. For these simulations, the actual in-service pavement conditions are used as inputs, i.e., the loading speed derived from the speed limit, the temperature profile in asphalt layers at 2 pm on March 1 averaged from the most recent three years in the EICM database, the substructure layer modulus and thickness values obtained from the dynamic cone penetrometer (DCP), the asphalt layer thickness obtained from the field cores, and the asphalt layer modulus values obtained from the dynamic modulus tests. It is noted that the temperature at the bottom of asphalt layer varies between 12.2°C and 16.5°C among all the simulated sections. The 18-kip single axle load was used in all the simulations. A flow chart describing this simulation process is given in Figure 4.24.

The conversion of the DCP values to the modulus values of the unbound layers is performed using the following equation, which is derived from the equations given in the NCHRP 1-37A report, Part 2 (NCHRP 2004b):

$$E_{base} = 666.4 \times \left(\frac{number\ of\ blows}{penetration\ depth} \right)^{0.7168} \tag{21}$$

where E_{base} is the modulus of the aggregate base in MPa, and *penetration depth* is in mm.

The dynamic modulus values of the asphalt layers were measured either from the 38 mm diameter, 100 mm tall side cores obtained from 150 mm diameter field cores when the layer thickness is greater than 44 mm, or from 25 mm thick, 50 mm wide, 100 mm long prismatic specimens when the layer thickness is less than 44 mm. Details regarding the testing of these small specimens are described in (Kutay et al. 2009).

Figure 4.25 (a) and (b) present the tensile strain kernels and maximum tensile strains calculated from the LVEA program for the pavements with three different cracking types. Overall, the BUC sites exhibit higher tensile strain at the bottom of the asphalt layer than the TDC sites, indicating the possibility of structural deficiency in the BUC sites.

Table 4.6 List of regions selected for simulation

Condition group	Region		ACI	AC layer thick. (mm)	Base type	Base thick. (mm)	E_{base} (psi)	$E_{subgrade}$ (psi)	Tensile strain (μs)	Crack type
Y & P	NC24	B1	62.88	175.3	SABC	230	54,635	16,242	104.5	TDC
Y & P	NC24	A1	71.57	188.0	SABC	380	58,884	12,851	90	TDC
O & G	US-70	B2	90.91	271.8	ABC	238	54,294	21,834	53.6	TDC
O & G	US17	B2	91.65	233.7	ABC	203	23,851	22,916	58.8	TDC
Y & P	US601	A1	91.40	175.3	ABC	289	59,660	17,521	79	BUC
Y & P	US601	B1	84.14	160.0	ABC	234	85,741	18,951	80.6	Both (BDC)
Y & P	US601	B2	83.72	167.6	ABC	244	88,074	13,662	76.4	Both (BDC)
Y & P	**US76**	**B1**	**75.16**	**114.3**	**ABC**	**240**	**73,730**	**28,668**	**173.2**	BUC
Y & P	**US76**	**A1**	**96.70**	**215.9**	**ABC**	**290**	**32,897**	**28,370**	**91**	TDC
Y & P	NC87	A1	96.32	292.1	Soil	349	27,354	29,685	36.2	BUC
Y & P	NC87	B1	88.57	322.6	Soil	228	25,849	6,254	60.3	TDC
Y & P	US74	B1	68.65	172.7	C ABC	260	88,331	20,638	137	BUC
Y & P	US74	A1	81.09	180.3	C ABC	300	89,583	25,258	94	BUC

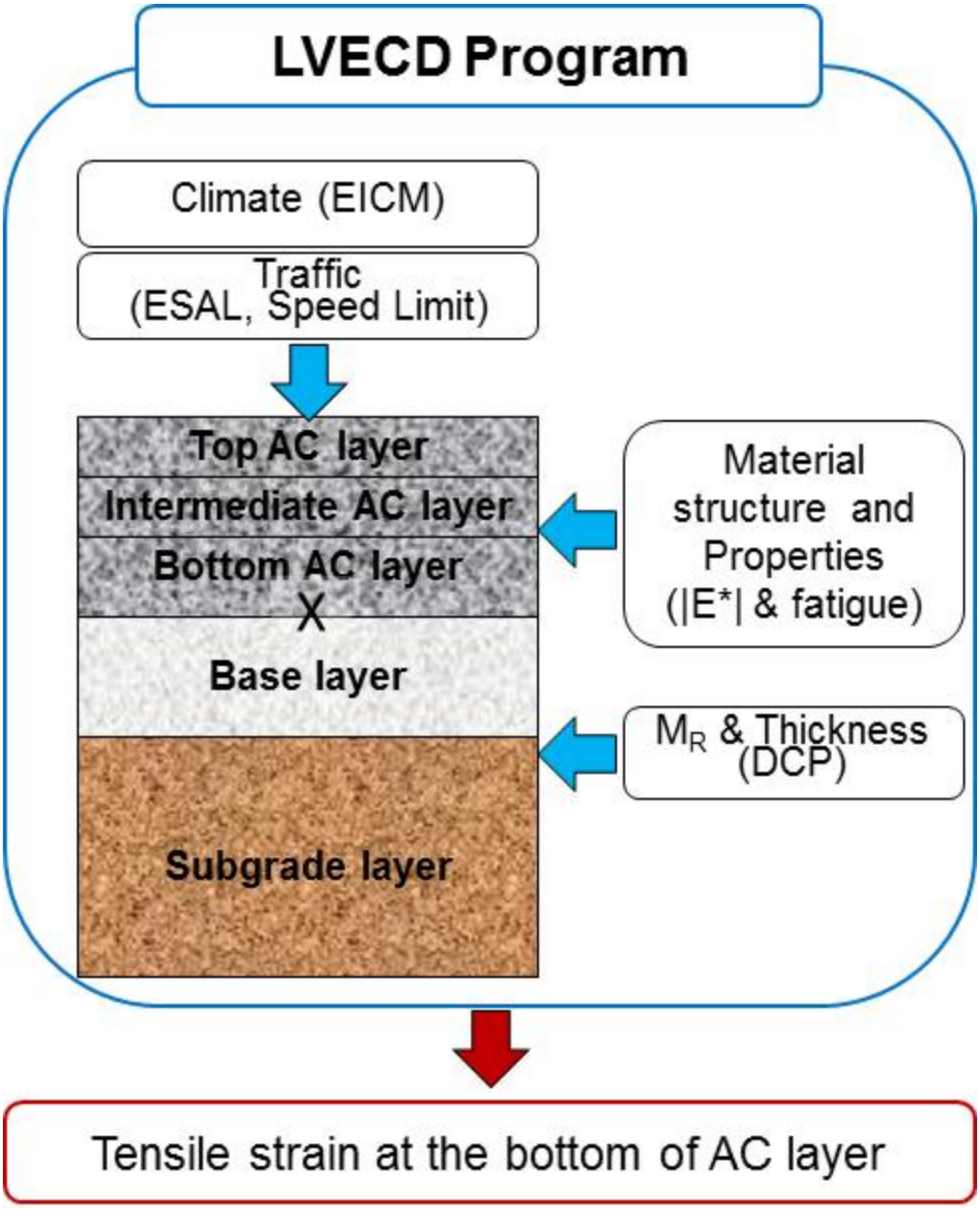

Figure 4.24 Simulation flow chart

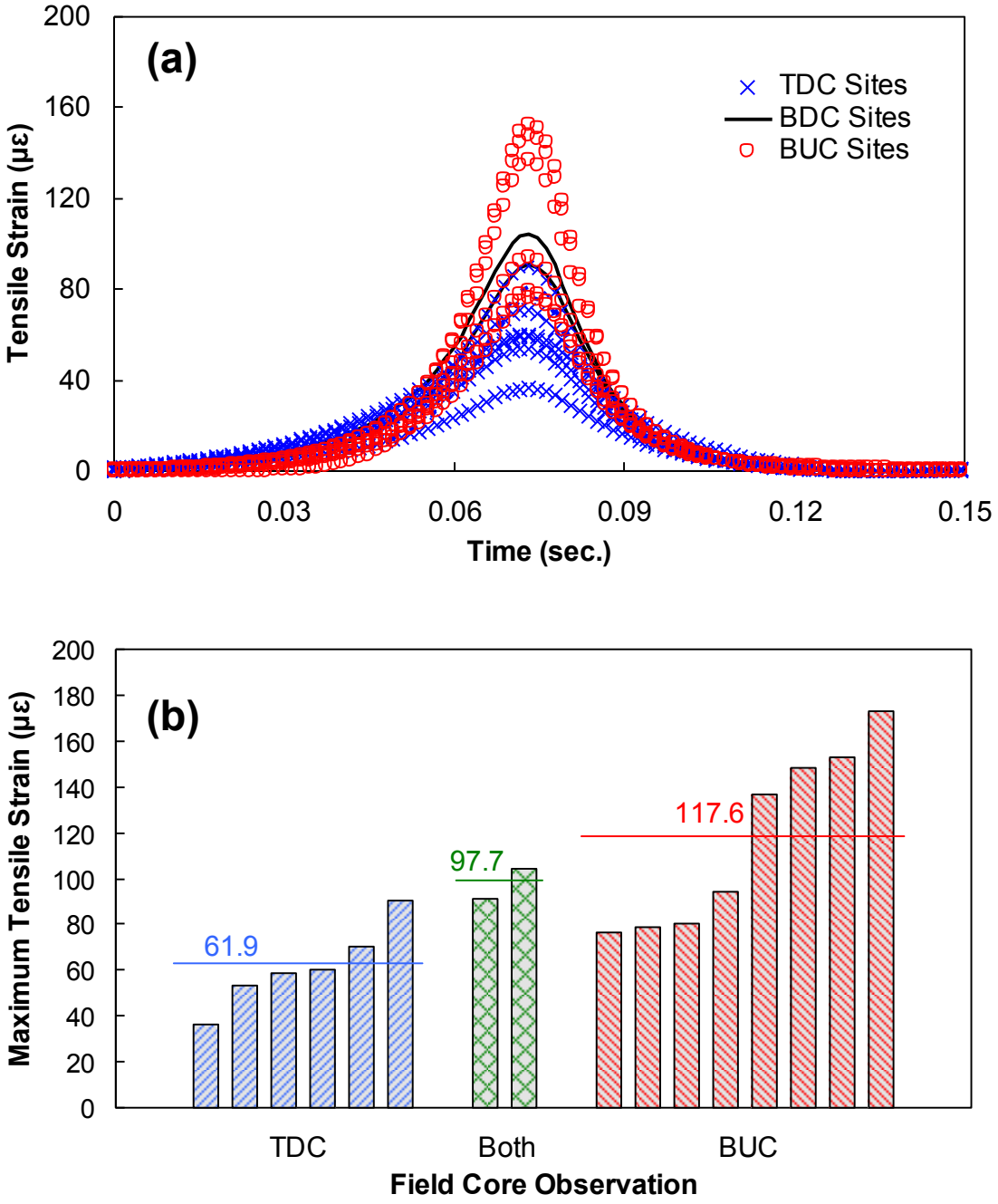

Figure 4.25 Tensile strain result for the investigation of bottom-up cracking: (a) tensile strain kernel at the bottom of asphalt layer and (b) maximum tensile strain at the bottom of asphalt layer.

4.9 Rheological Properties

4.9.1 Analysis Results

As stated in Acknowledgement, all extracted binder experiments were conducted by Mohammad Ilias and Farinaz Safaei.

According to Kose et al.'s research, binder has a strain value that is approximately 50 times of mixture strain value (Kose et al. 2000). Therefore, number of cycles to failure (N_f, which represents the fatigue life) of mixtures and binder extracted from the mixture was compared at same strain level and the result presented in Figure 4.26. Since no noteworthy finding observed from Figure 4.26, the research team divided the data presented in Figure 4.26 into different categories as *old and good* condition sites and *young and poor* condition sites. In spite of data partitioning, no clear correlation in the comparison of mixture and binder observed.

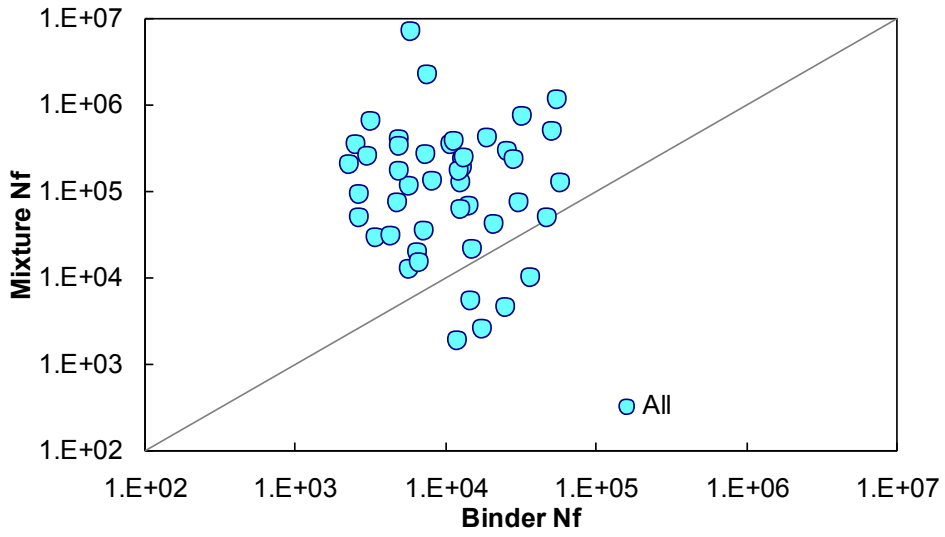

Figure 4.26 Comparison of number of cycles to failure of asphalt binder and mixture.

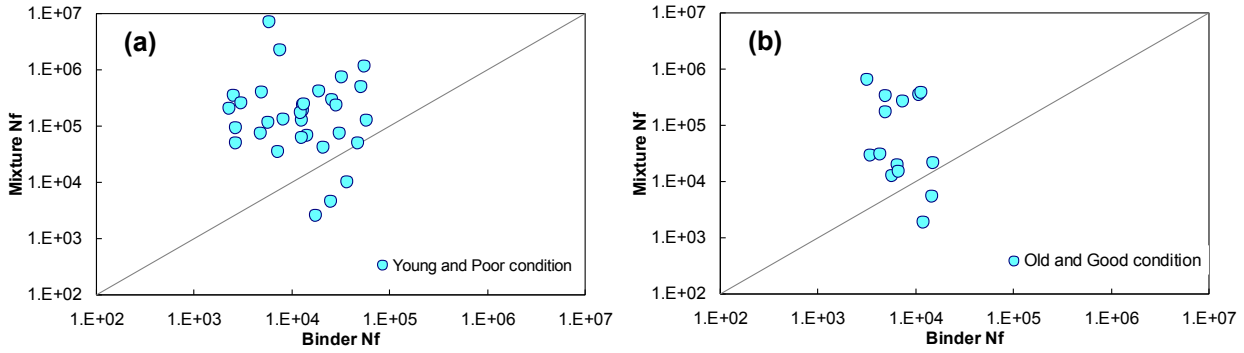

Figure 4.27 Comparison of number of cycles to failure of asphalt binder and mixtures from different information categories: (a) young and poor condition regions and (b) old and good condition regions.

A comparison of the LAS test results for a relatively *good* condition region and *bad* condition region within one site indicates that the number of cycles to failure for the asphalt binder in different condition regions correlates in log-log space, as presented in Figure 4.28. Note that all the presented values of the number of cycles to failure of asphalt binder in different condition regions were calculated at 2% strain amplitude. The linear correlation of the number of cycles to failure obtained from different condition regions indicates that the pavement performance condition at the material level is not directly related to the asphalt binder. This phenomenon can be seen more clearly by comparing the figures in Figure 4.29. The numbers of cycles to failure from the A condition region (relatively *good* condition region) are higher than those from the B condition region, and there is no linear relationship found between the values from the different condition regions shown in Figure 4.29 (b).

Asphalt binder testing was conducted to determine if asphalt binder plays a significant role in the relative performance of condition A regions (relatively *good* condition) and condition B regions (relatively *poor* condition) for given test sites. A comparison between the LAS test predicted fatigue life (N_f) of the binders at 2% strain from the corresponding A and B regions for each site considered is presented in Figure 4.28. It is seen that all the data points fall close to the LOE, indicating little difference between the binder properties of the corresponding A and B regions for each site evaluated. These results suggest that the binder properties of the *good* and *poor* regions of a given site are not dependent on the change in the binder properties. This finding is not entirely surprising as a given site presumably has one consistent binder and, thus, the only source of difference is the extent of oxidation for the different locations as a result of

differing mixture volumetric properties. This observation is reflected more clearly by comparing the relative fatigue life data of asphalt mixtures from the corresponding condition A and B regions, as presented in Figure 4.29. From the asphalt mixture results, it is seen that the numbers of cycles to failure from the A condition region are consistently higher than those from the B condition region, as expected. Thus, the results suggest that mixture variables, other than the constituent asphalt binder, can lead to differences in the performance of the condition A and B regions (in terms of air void content, asphalt content, etc.).

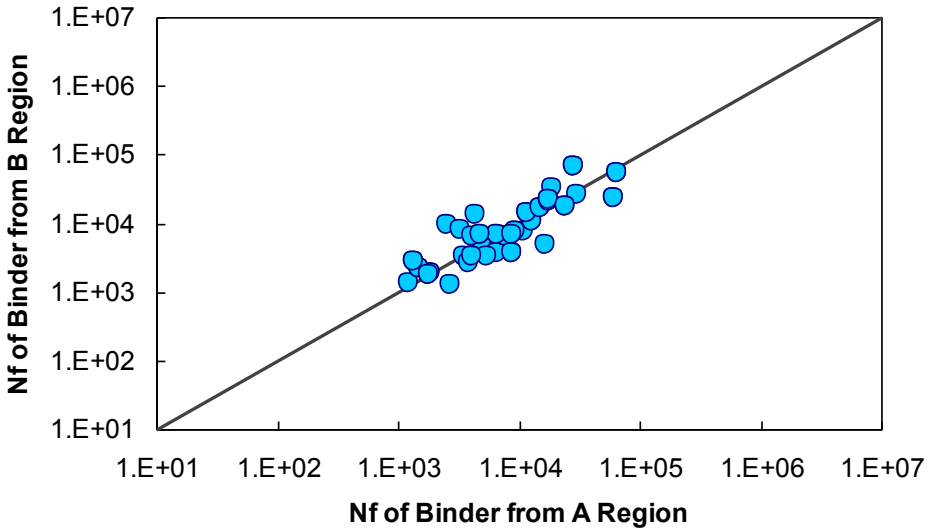

Figure 4.28 Comparison of number of cycles to failure of asphalt binder from different condition regions.

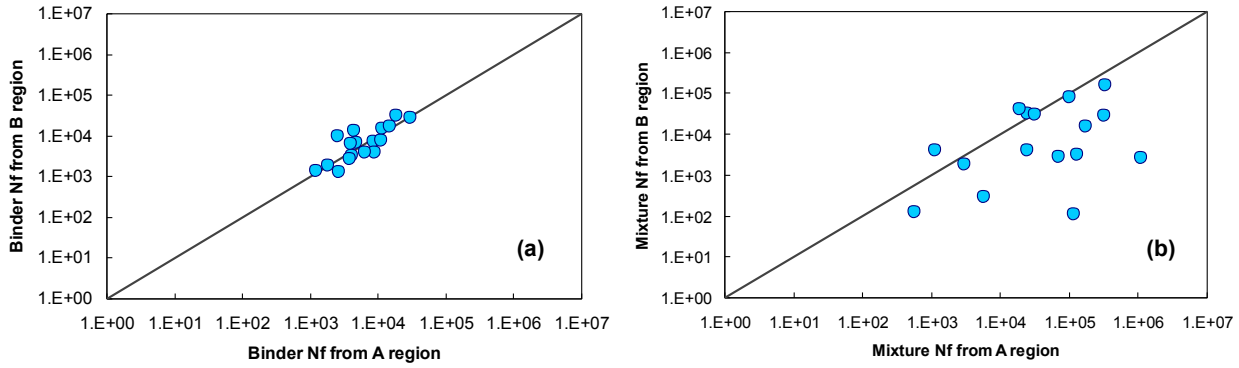

Figure 4.29 Comparison of number of cycles to failure of (a) asphalt binder and (b) mixtures from different condition regions.

In Figure 4.30, all the data points are the same as those in Figure 4.28, but the research team divided those data into different categories as *old and good* condition sites and *young and poor* condition sites. It is observed that more data points from the *old and good* condition sites converge on the line of equality (LOE) than the data points from the *young and poor* condition sites. This finding may indicate that the less variable the material property, the better the pavement condition.

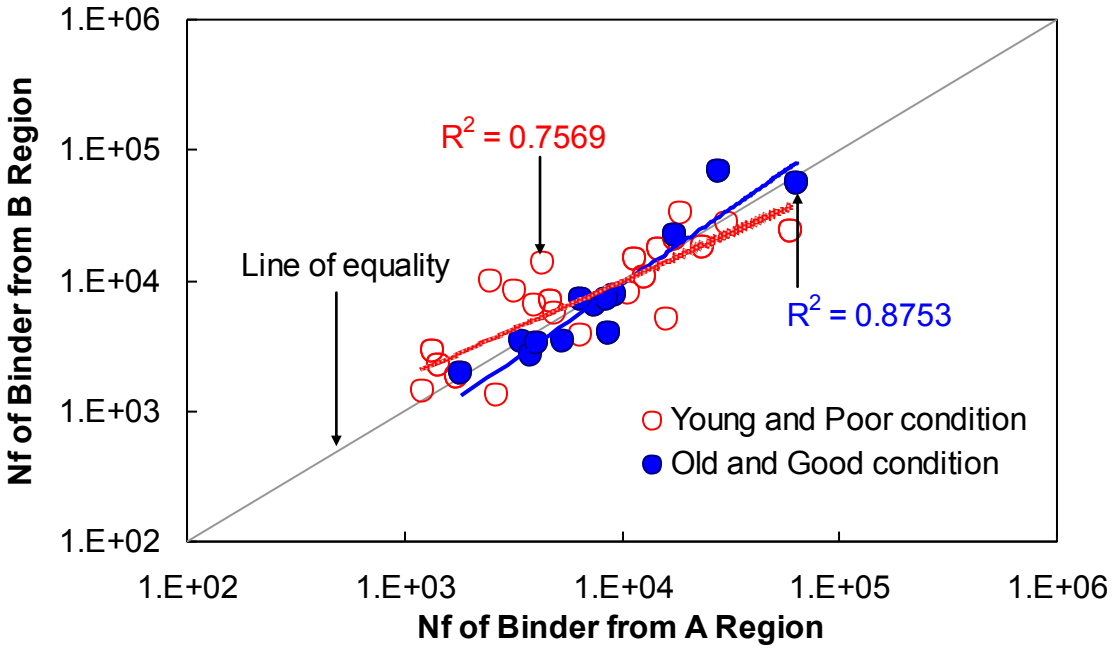

Figure 4.30 Comparison of number of cycles to failure of asphalt binder from different condition regions in different categories.

4.9.2 Summary

At the network level, there is little difference between the fatigue resistance of *good* and *bad* condition regions within the same site. However, the laboratory mixture fatigue test results indicate that mixtures from *poor* condition regions have less fatigue resistance than those from *good* condition regions within the same site. The binder fatigue test results indicate that the cracking performance difference between *good* and *poor* regions in a given site is not dependent on the change in binder properties. Hence, other mixture design factors must be at work in controlling the variability in fatigue resistance at the different sites.

Chapter 5 Long-Term Performance Simulations

5.1 Introduction

Asphalt pavement is composed of layers of asphalt mixture and substructure, i.e. the base layer and subgrade layer. Material-level analysis, based on stiffness (dynamic modulus) and fatigue resistance (S-VECD) test results, is focused on characterizing the material itself. However, actual pavements have internal structural factors, such as the thickness of the layers and structural support underneath the layers, which need to be considered as part of long-term performance simulations.

5.2 Layered Viscoelastic Continuum Damage Program

In order to predict long-term pavement performance under moving traffic loads, a layered viscoelastic structural model and fast-Fourier transform-based finite element analysis program were used in this research. The resultant simulation program, called the LVECD program, was developed by Eslamania et al. (2012) at NCSU. It can perform three-dimensional analysis of pavements under moving loads in a computationally efficient manner and can capture the effects of the viscoelasticity of asphalt concrete, thermal stress and viscoelastic property changes caused by temperature and traffic loading conditions. The framework of the LVECD program was developed based on a combination of the following ideas (Eslaminia et al. 2012):

- Utilizing the vast difference in time scales associated with temperature and traffic load variations reduces the number of stress analysis runs from several million to a few dozen.
- Using Fourier transform-based analysis reduces the number of stress analysis runs from several million to fewer than a hundred.

5.2.1 LVECD Inputs

As described previously, all the cores taken for material characterization were extracted from the center of the lane and from areas with no visible cracking (i.e., invisible by visual inspection) in order to avoid the effects of traffic-induced damage and existing damage. The

material properties obtained from the cores for Test Level 1 were used as inputs for the pavement simulations. The simulations were performed for the equivalent single axle loads (ESALs) of actual field traffic as obtained from the NCDOT Traffic Survey Unit. The design load was based on actual field conditions as follows: rectangular with a width of 17.78 cm (7 in.), length of 27.94 cm (11 in.), load of 40 kN (9,000 lb), constant contact pressure of 805.9 kPa (116.9 psi), and constant velocity based on the speed limit at each site. All of the simulations were conducted with temperature variables obtained from the Enhanced Integrated Climate Model (EICM). Other inputs for the simulations were taken from the master database (Appendix A) and forensic study (Appendix C). The base layer modulus values, thicknesses, and subgrade modulus values were taken from the DCP test results, as provided in Table 4.3.

5.2.2 LVECD Simulation Results

The damage contours presented in Figure 5.1 to Figure 5.20 are the contours of normalized pseudo stiffness, which starts from 1.0 in an intact condition and decreases as the level of damage increases. The same grayscale (i.e., between 0.25 and 0.8) is used in presenting all the damage contours shown in those figures. A small value of normalized stiffness, which is represented by the white color in the sub-figures in Figure 5.1 to Figure 5.20, corresponds to areas with high levels of damage and, consequently, areas where cracking is more likely to occur. The crack propagation propensity of each region selected for LVECD simulation and corresponding ACI values are presented in Table 5.1. In Table 5.1, italic-bold font indicates that the simulation results do not match the field core and field condition observations. Because a damage contour is not a numerical value, the rank of the level of damage predicted from the damage contours is used for comparison with the ACI ranking for the same site. That is, the ranking of the ACI values from different condition regions in a single site is compared to that for the area or severity of normalized stiffness, which is represented by the white color in the damage contour plots, as described earlier, in order to verify the sensitivity of the LVECD program under the same environmental and traffic conditions.

Several important observations can be made from the damage contours presented in Figure 5.1 to Figure 5.20 and the cracking conditions summarized in Table 5.1, as follows.

- In general, the predicted simulation results presented in Figure 5.1 to Figure 5.20 indicate better conditions in the A condition regions than in the B condition regions.

- The *old* and *good* pavements, i.e., US 17 and NC 209, show relatively minor damage from the 20-year pavement simulations.
- The predicted simulation results presented in Figure 5.3 and Figure 5.5 and Figure 5.13 to Figure 5.14 indicate that the TDC simulation results for US-70 and I-540 are in agreement with the field core observations.
- A noteworthy finding from NC-24 and US-74 is presented in Figure 5.1 to Figure 5.2 and Figure 5.15 to Figure 5.16. The thicknesses of the asphalt layers in these two sections are similar (about 7 in.), and higher base and subgrade modulus values were measured from US-74 than from NC-24. If the asphalt layer properties were the same, these conditions would give the NC-24 section a greater potential for BUC. However, TDC was observed from NC-24 and BUC was observed from US-74 due to the different asphalt mixtures used in these two sections. The predicted simulation results shown in Figure 5.1 to Figure 5.2 and Figure 5.15 to Figure 5.16 match these field core observations.
- The predicted results from the A condition region of US-76 presented in Figure 5.18 match the field core observations, but none of the field core observations are captured by the simulations of the B condition region. According to the 2010 NCDOT condition survey, as denoted by the highlighted areas of Table 5.1, this site contains oxidized pavement. Accordingly, it appears that the TDC observed from the field cores is caused by excessive oxidization. This oxidization is not captured by the LVECD program because an aging model has not been implemented in the LVECD model yet.
- The A condition region of NC 87 has a thicker base layer and stiffer substructure than the B condition region. However, BUC is observed from the A condition region, whereas TDC is observed from the B condition region. These field observations indicate that the BUC and TDC propensity is governed not only by the pavement structure, but also by the material properties, which are shown to affect such propensity significantly. The predicted simulation results match the field core observations.
- The TDC that is observed in the field cores from the A condition region of US-601 is not observed in the predicted simulations presented in Figure 5.6 to Figure 5.8.

- Overall, the expected crack directions of 26 out of 36 (72%) condition regions match the field core observations. This agreement rate increases to 78% once the severity rankings of the different condition regions in a single site are included.

Table 5.1 Cracking Severity and Propagation Direction Observed from Field Cores and Their Agreement with LVECD Prediction Results

Route	Field Observation				
	Condition Region	Field Cores		Condition Survey	NCDOT Database
		TDC?	BUC?	Local ACI	No
NC-24	B1	Yes	***No***	***62.88***	No
NC-24	A1	Yes	***No***	***71.57***	No
I-540	A1	No	No	91.42	No
I-540	B2	Yes	No	32.63	No
I-540	A2	No	No	97.61	No
US-601	A1	***Yes***	Yes	91.40	No
US-601	B1	***Yes***	Yes	84.14	No
US-601	B2	No	Yes	83.72	No
US-17	B2	Yes	No	***91.65***	***Yes***
US-17	A2	No	No	***90.52***	***Yes***
NC-209	A1	No	***No***	100.00	No
NC-209	B1	No	***No***	95.92	No
US-70	B2	Yes	No	90.91	No
US-70	A2	No	No	100.00	No
US-74	B1	No	Yes	68.65	No
US-74	A1	No	Yes	81.09	No
US-76	B1	***Yes***	***No***	75.16	***Yes***
US-76	A1	Yes	Yes	96.70	***Yes***
NC-87	A1	No	***No***	96.32	No
NC-87	B1	Yes	No	88.57	No

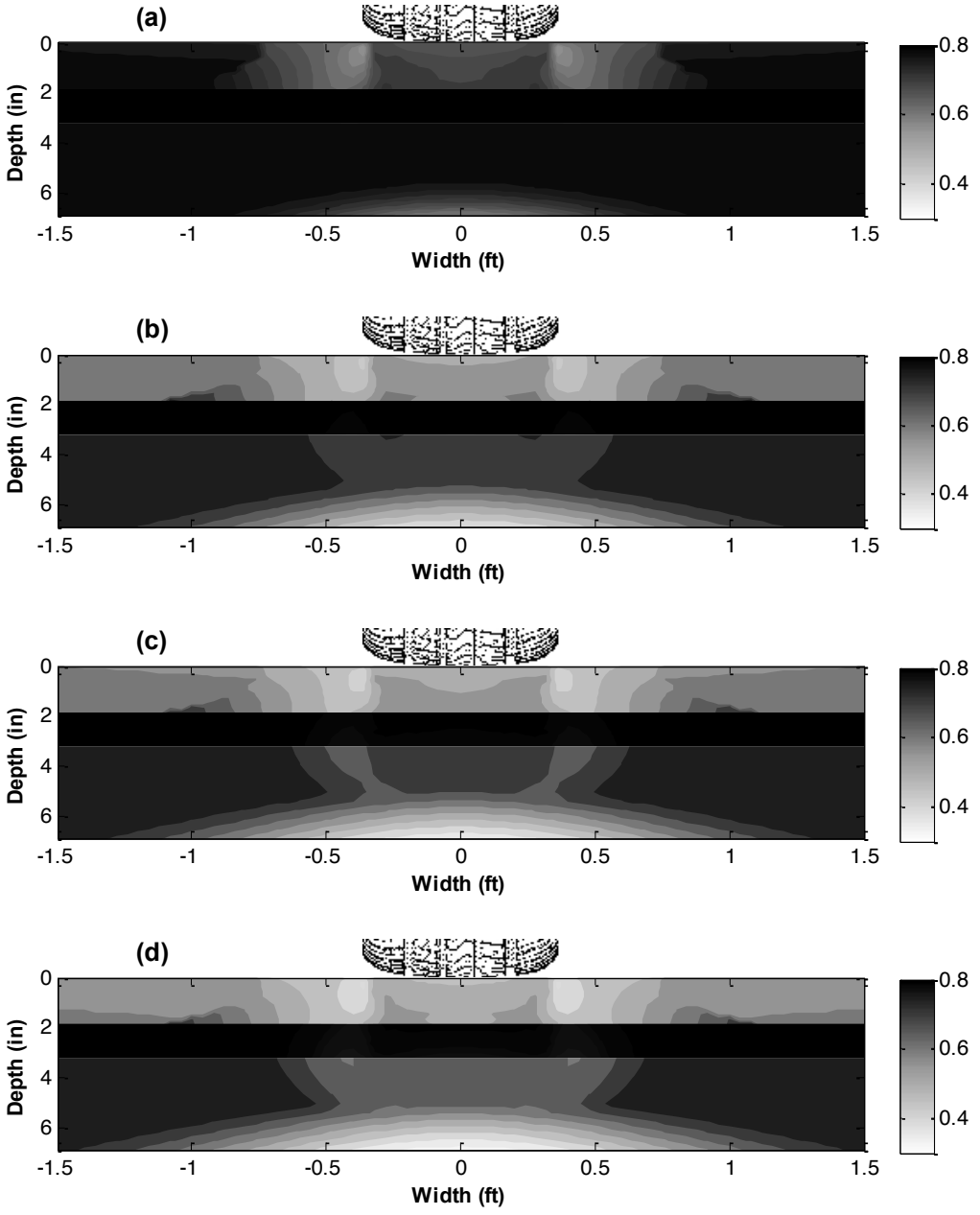

Figure 5.1 Damage contours for the B1 region in NC 24 pavement: (a) 1 year, (b) 5 years, (c) 10 years, and (d) 20 years.

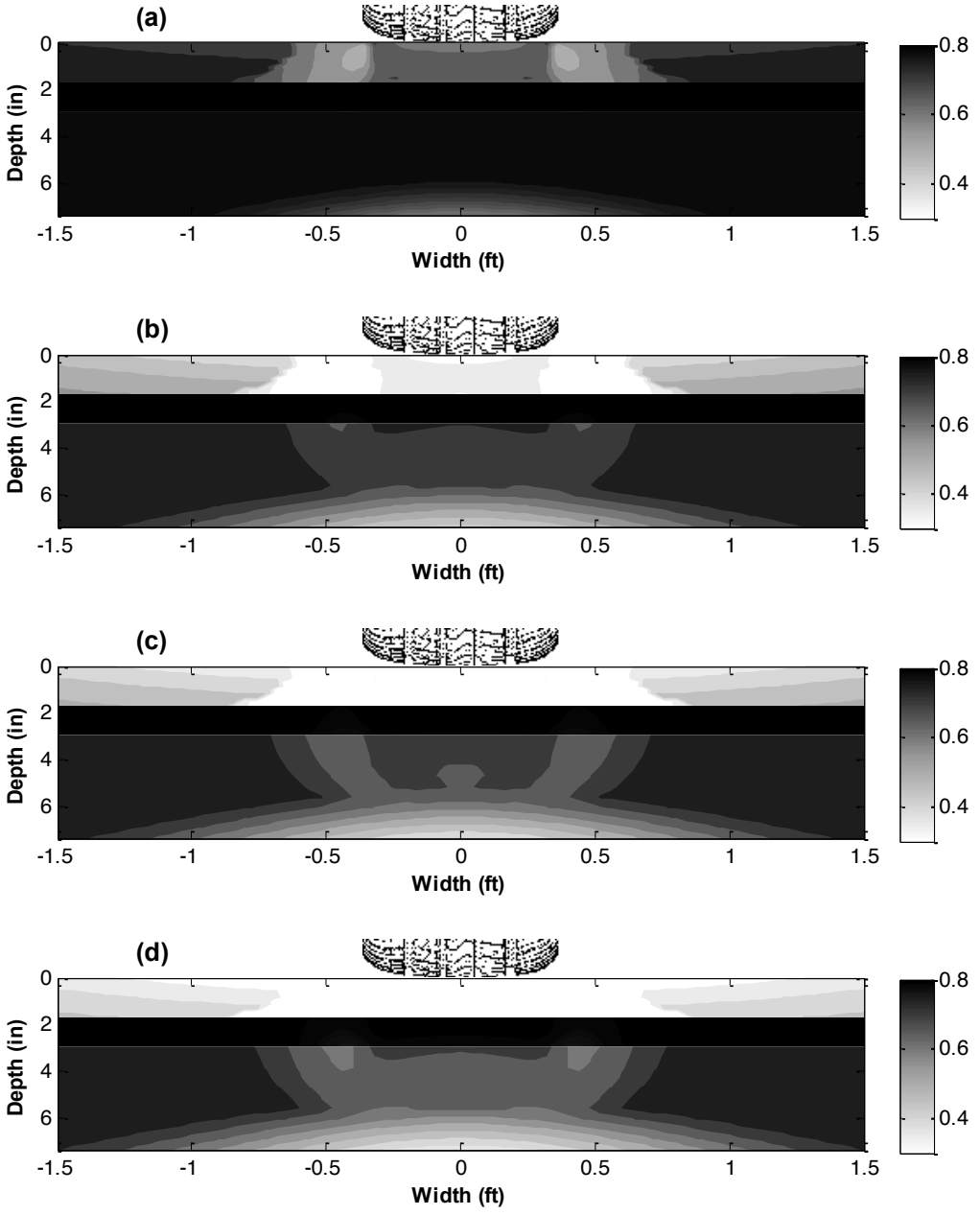

Figure 5.2 Damage contours for the A1 region in NC 24 pavement: (a) 1 year, (b) 5 years, (c) 10 years, and (d) 20 years.

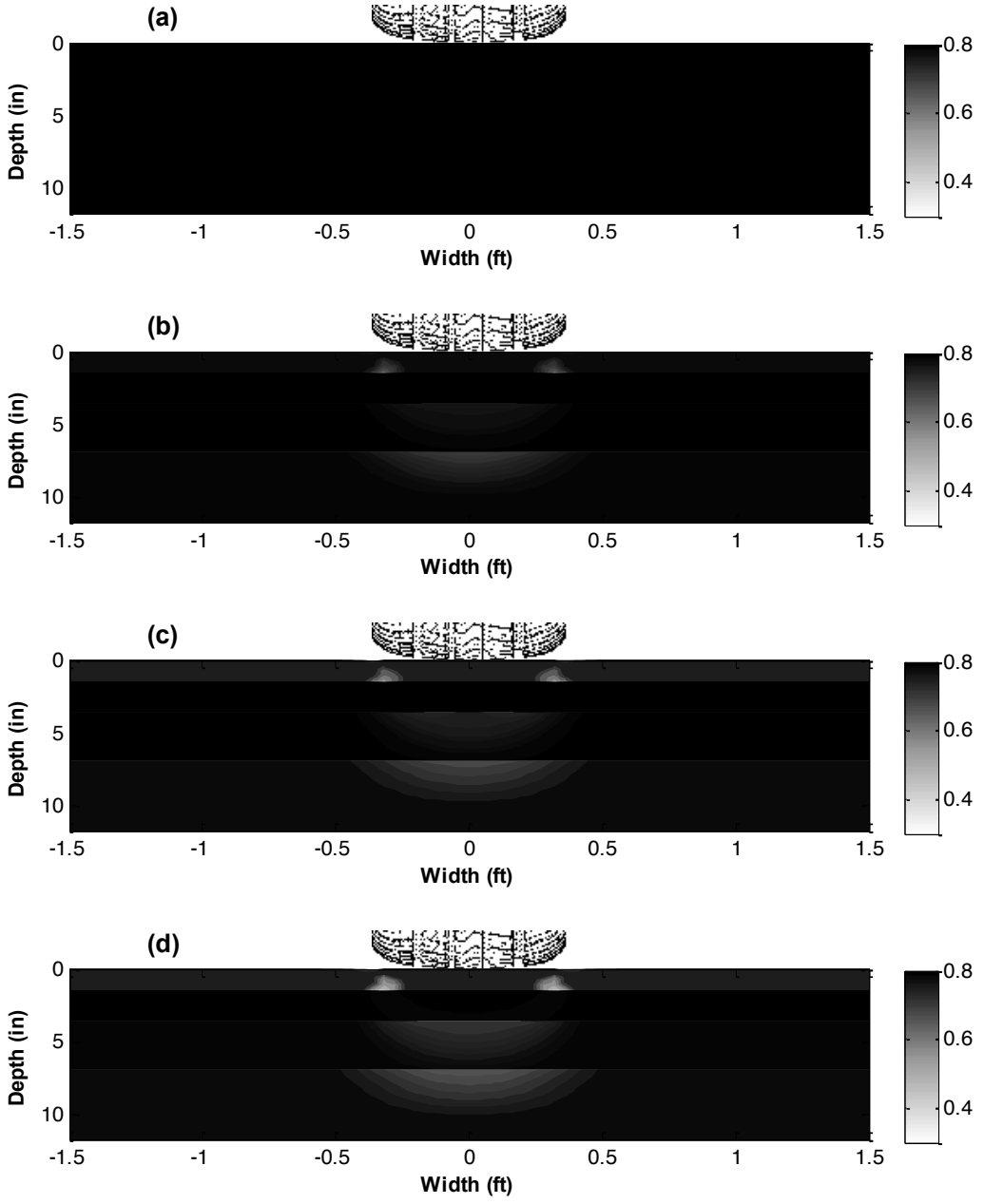

Figure 5.3 Damage contours for the B2 region in I 540 pavement: (a) 1 year, (b) 5 years, (c) 10 years, and (d) 20 years.

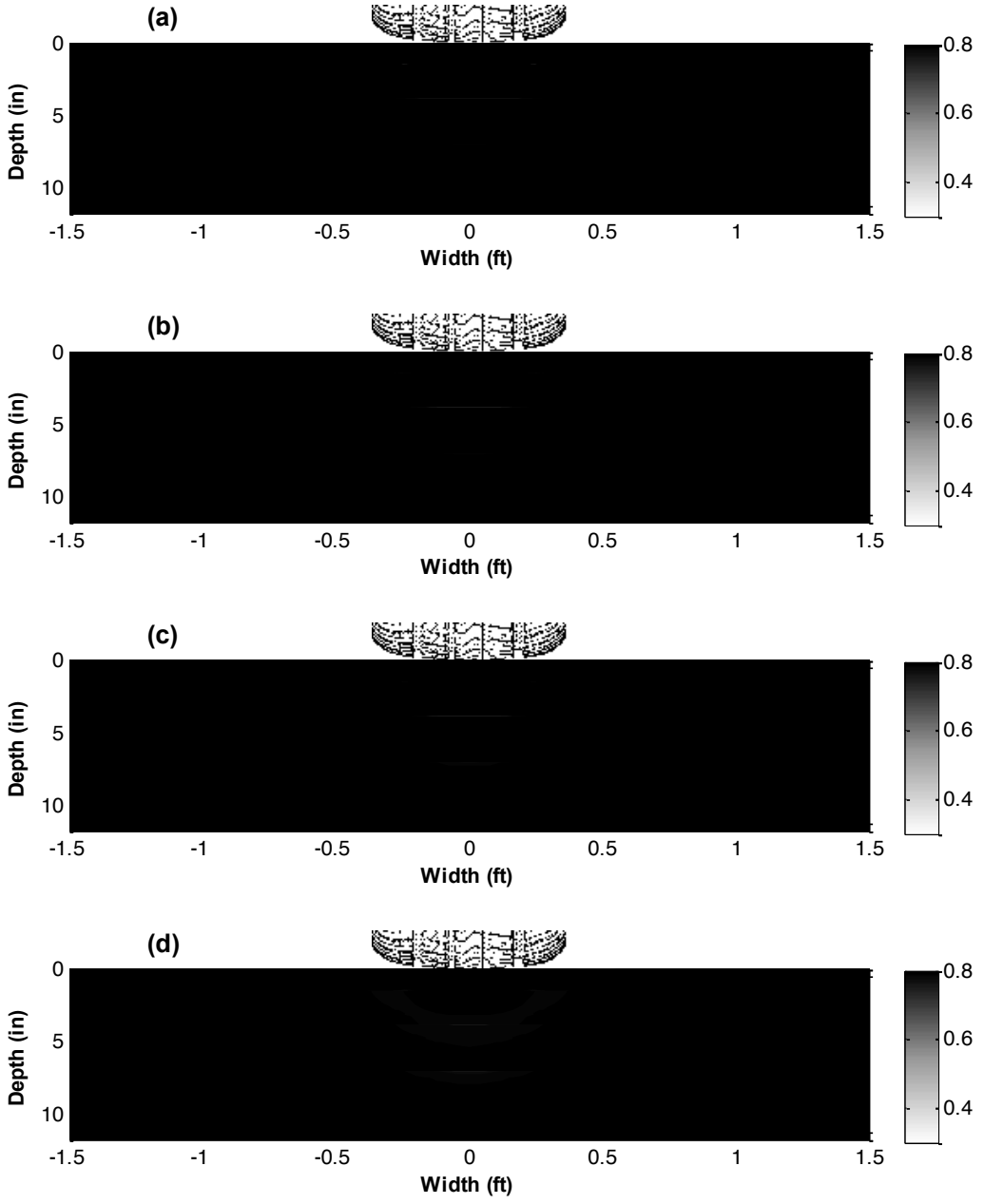

Figure 5.4 Damage contours for the A1 region in I 540 pavement: (a) 1 year, (b) 5 years, (c) 10 years, and (d) 20 years.

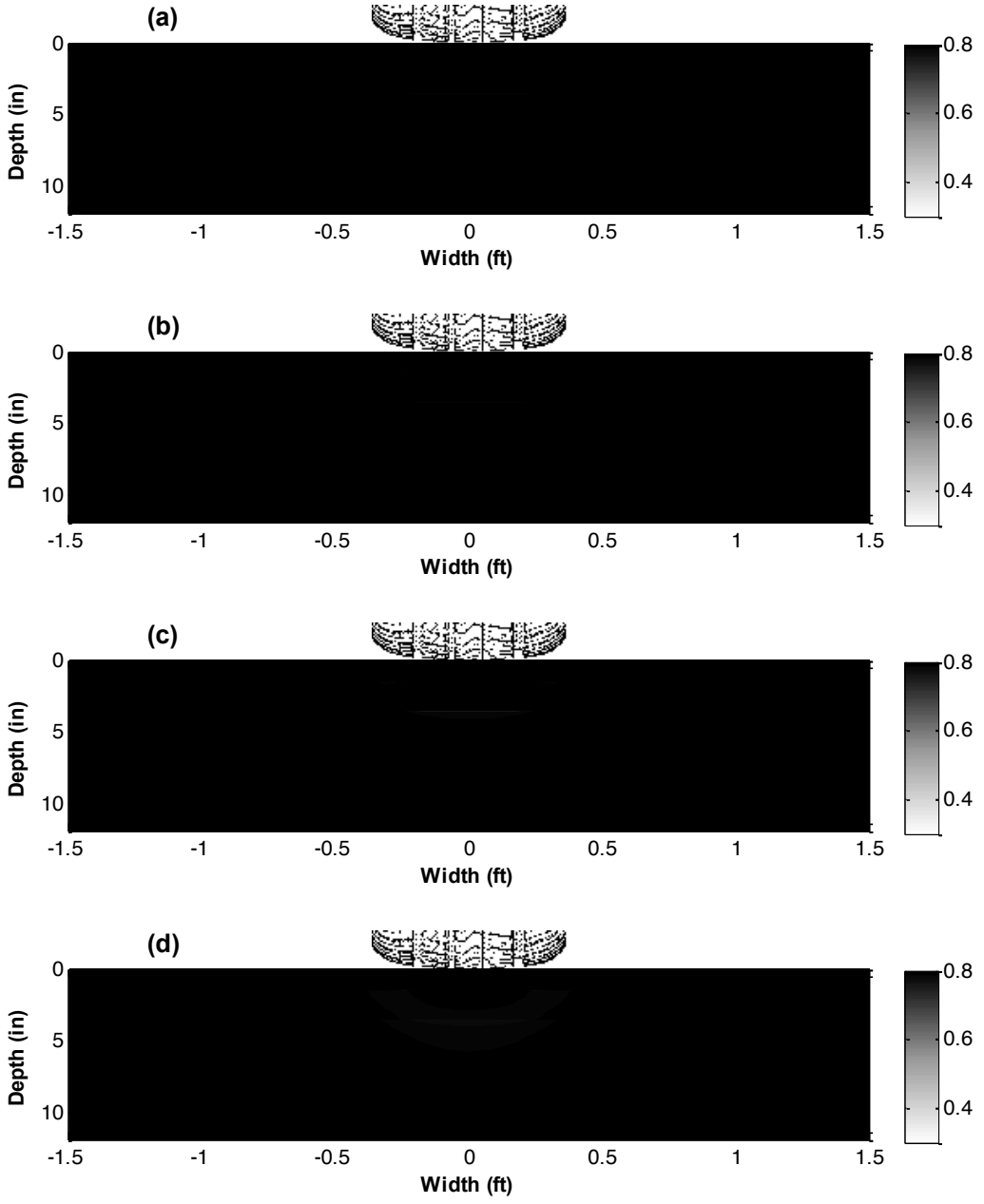

Figure 5.5 Damage contours for the A2 region in I 540 pavement: (a) 1 year, (b) 5 years, (c) 10 years, and (d) 20 years.

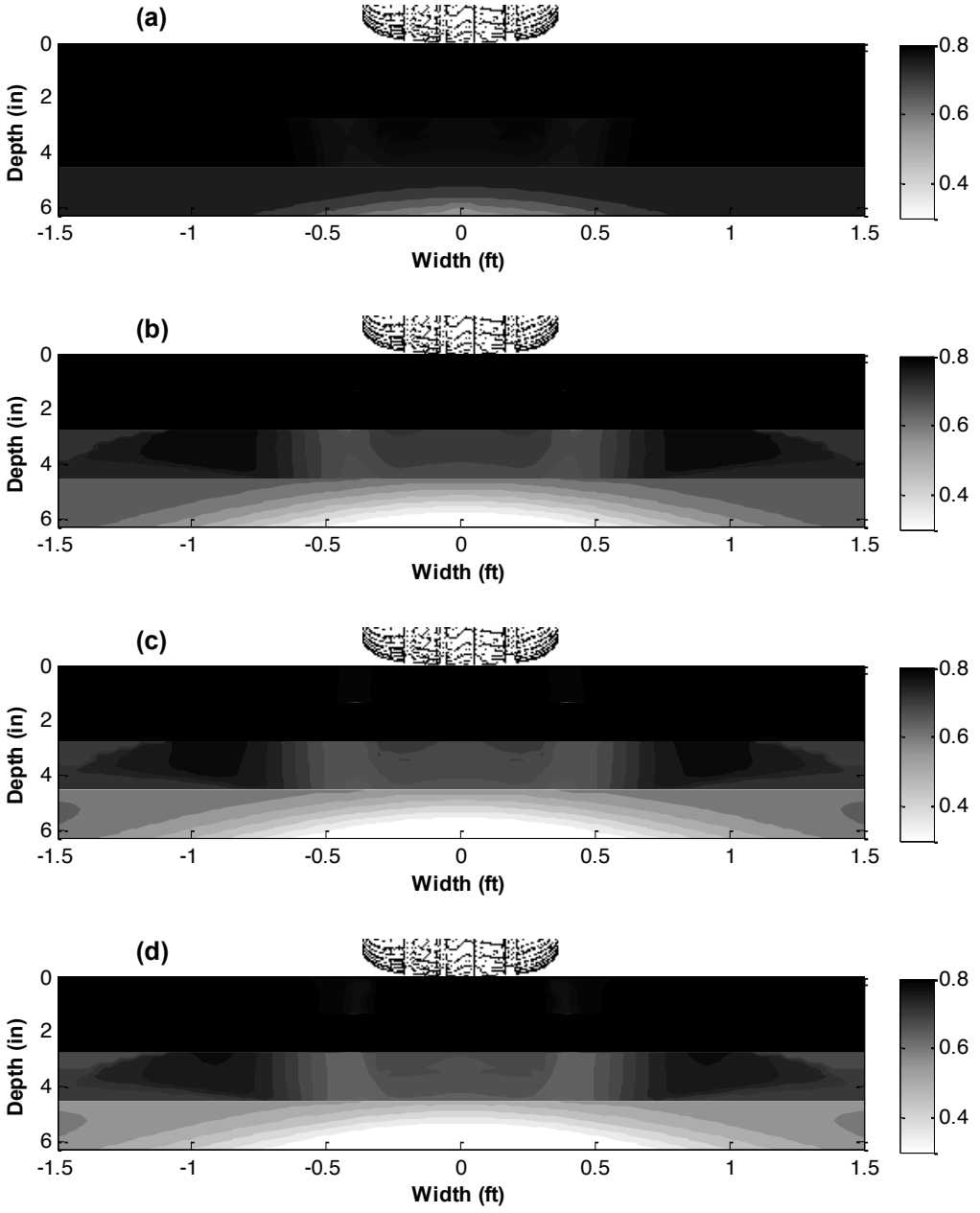

Figure 5.6 Damage contours for the B1 region in US 601 pavement: (a) 1 year, (b) 5 years, (c) 10 years, and (d) 20 years.

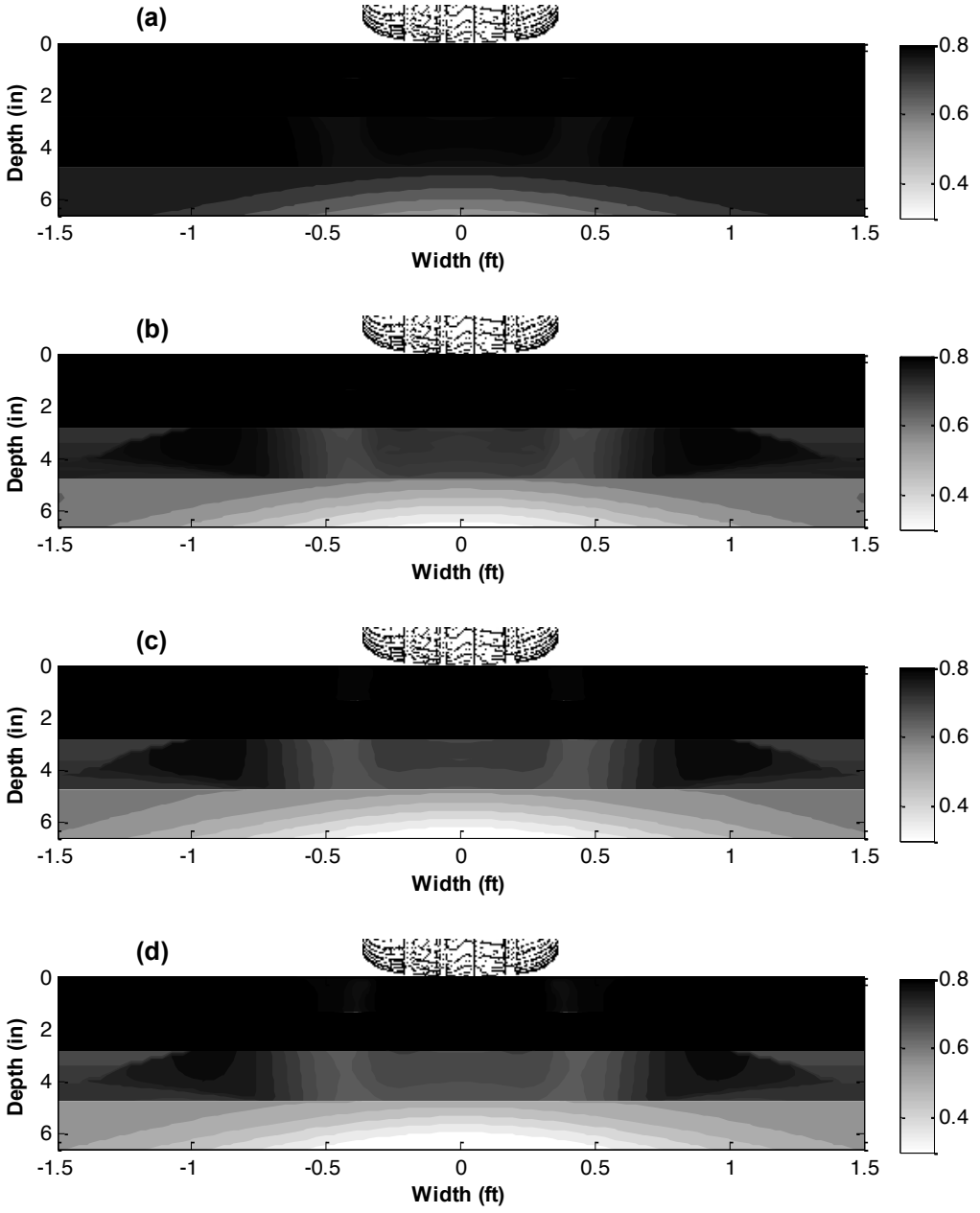

Figure 5.7 Damage contours for the B2 region in US 601 pavement: (a) 1 year, (b) 5 years, (c) 10 years, and (d) 20 years.

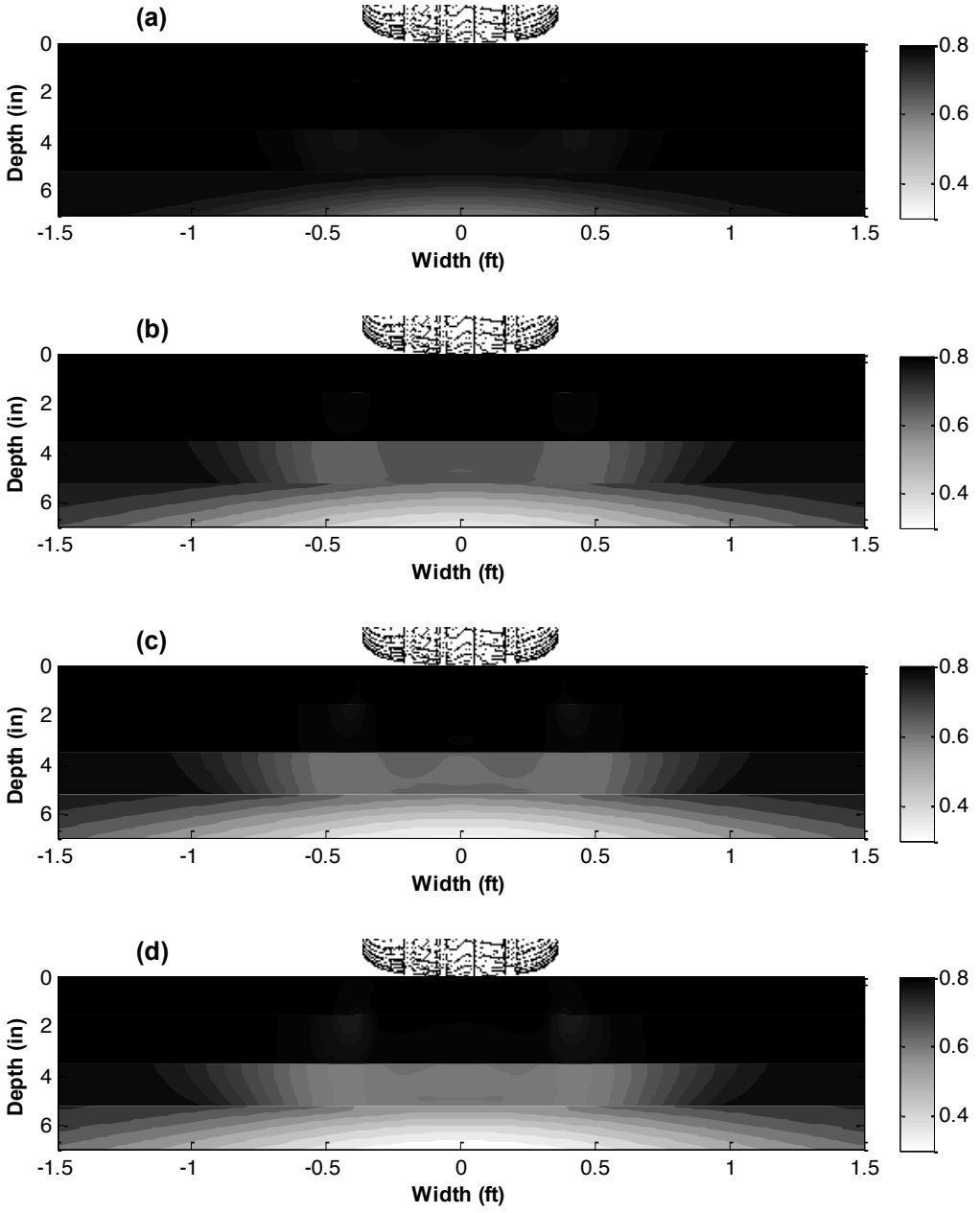

Figure 5.8 Damage contours for the A1 region in US 601 pavement: (a) 1 year, (b) 5 years, (c) 10 years, and (d) 20 years.

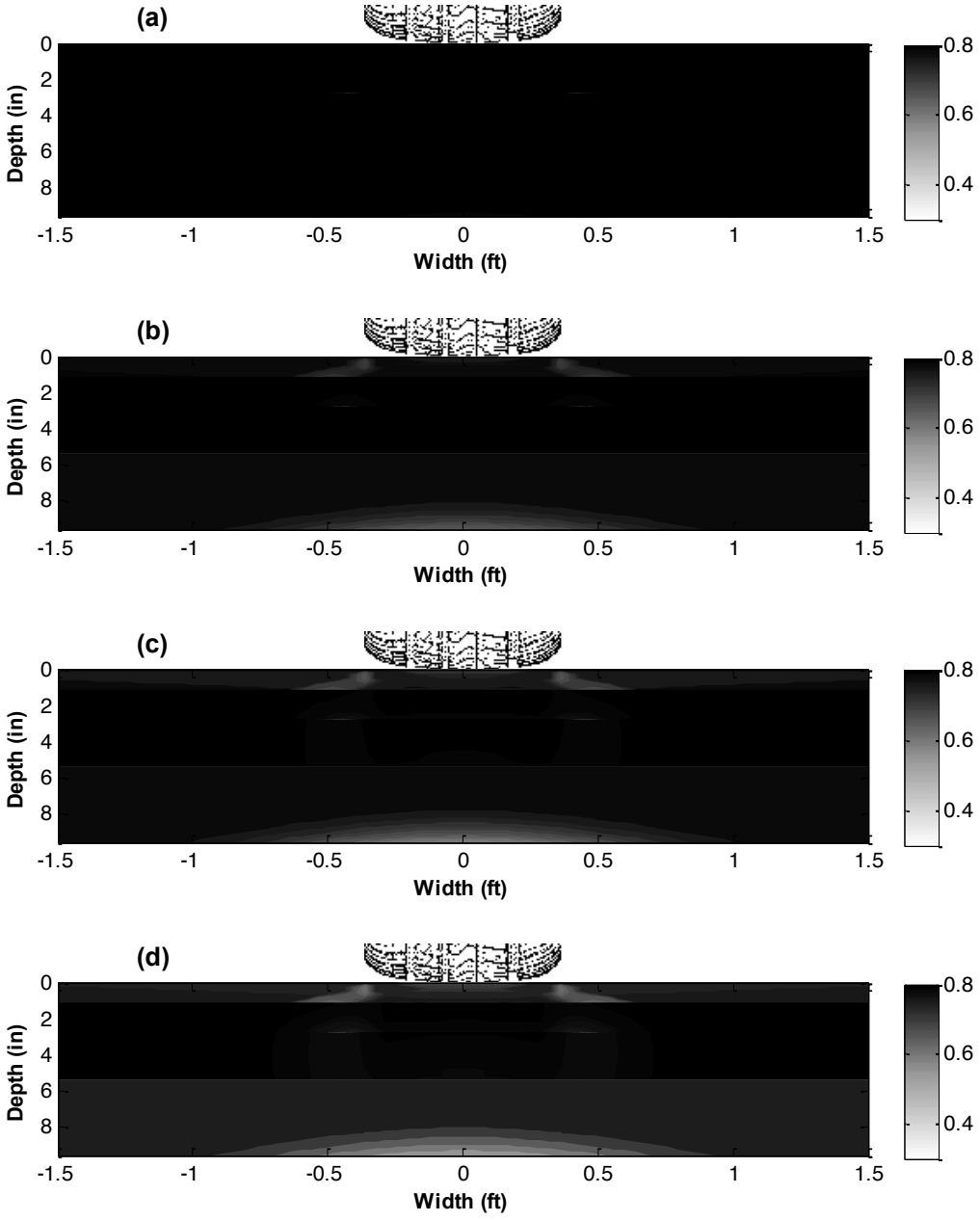

Figure 5.9 Damage contours for the B2 region in NC 17 pavement: (a) 1 year, (b) 5 years, (c) 10 years, and (d) 20 years.

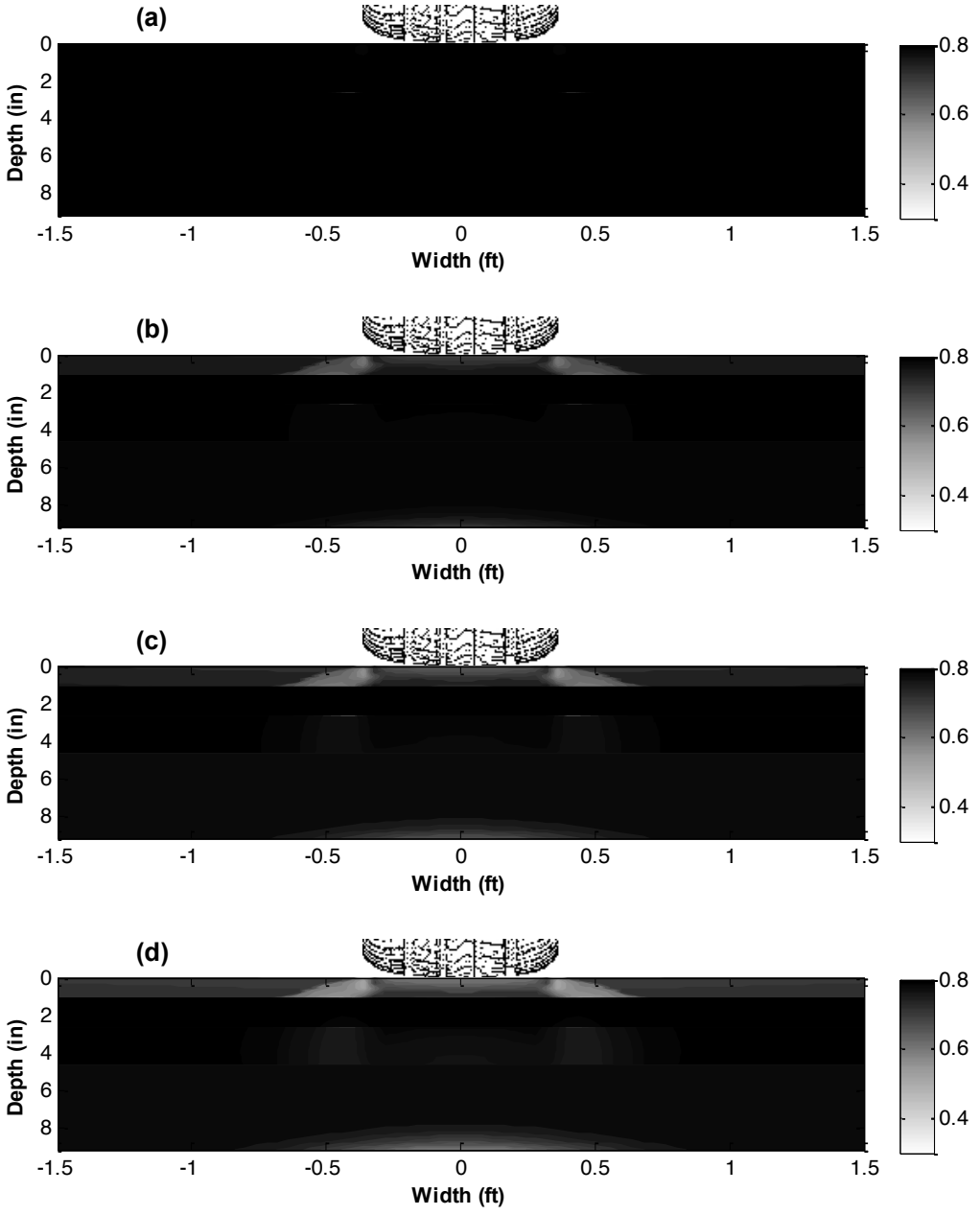

Figure 5.10 Damage contours for the A2 region in NC 17 pavement: (a) 1 year, (b) 5 years, (c) 10 years, and (d) 20 years.

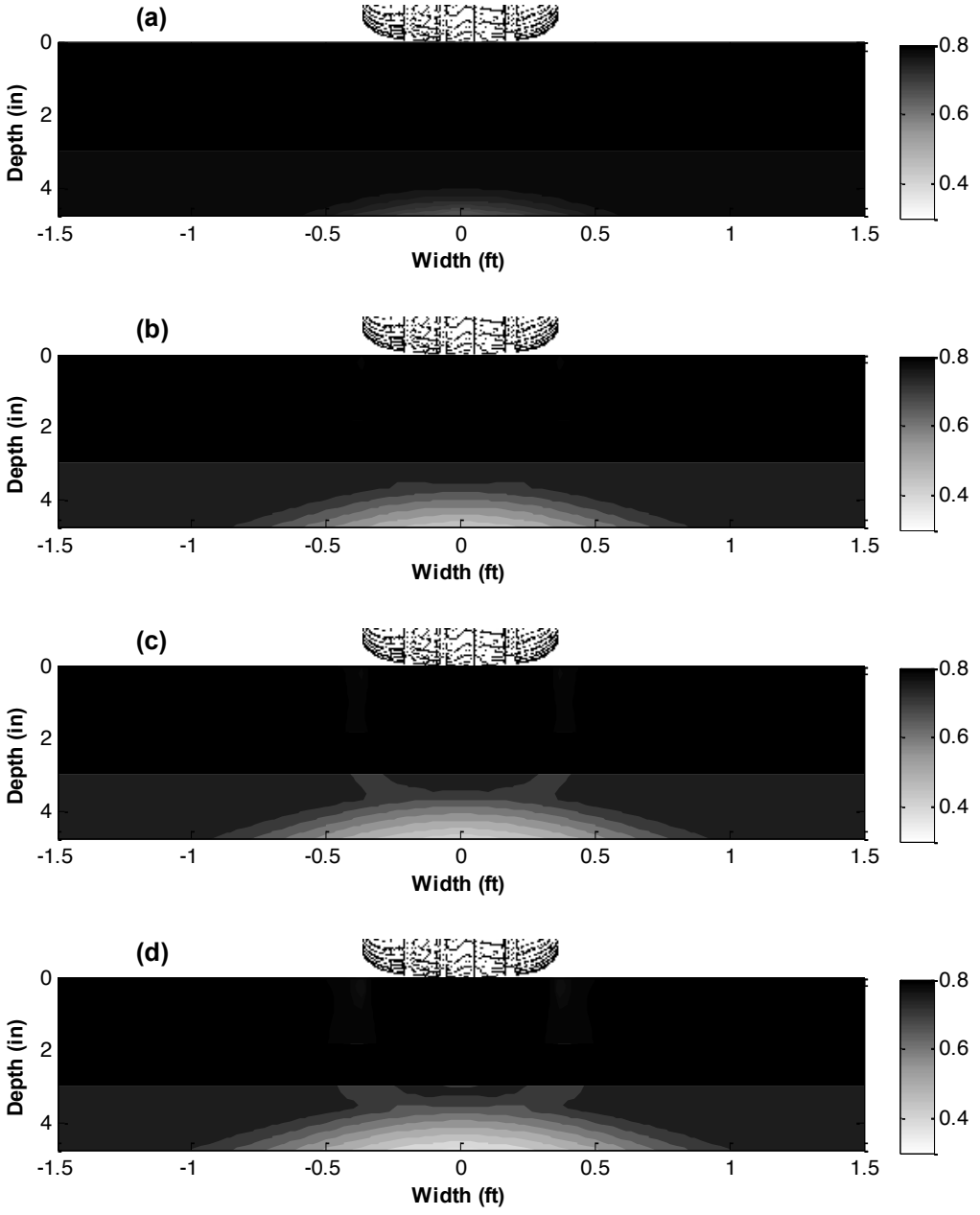

Figure 5.11 Damage contours for the B1 region in NC 209 pavement: (a) 1 year, (b) 5 years, (c) 10 years, and (d) 20 years.

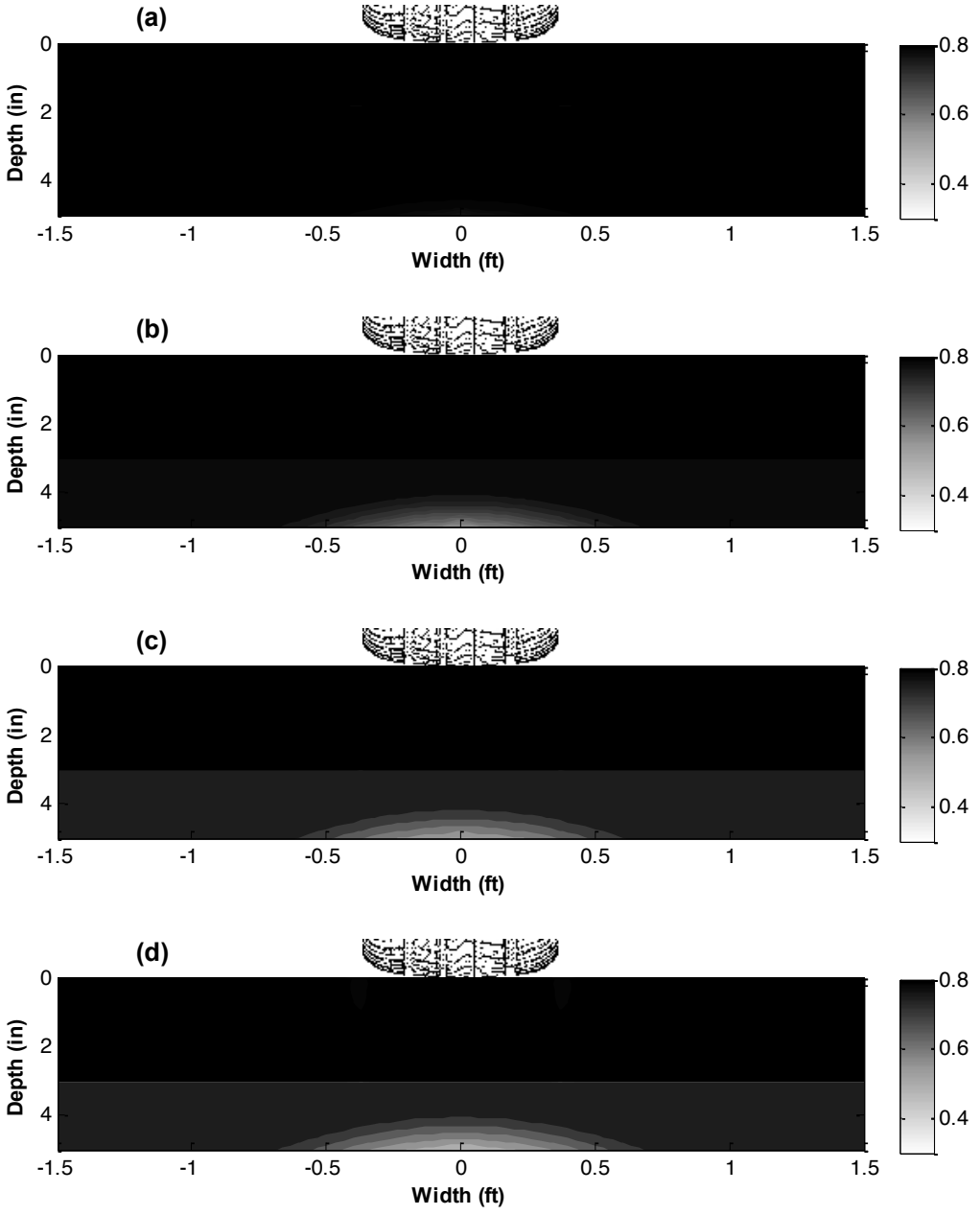

Figure 5.12 Damage contours for the A1 region in NC 209 pavement: (a) 1 year, (b) 5 years, (c) 10 years, and (d) 20 years.

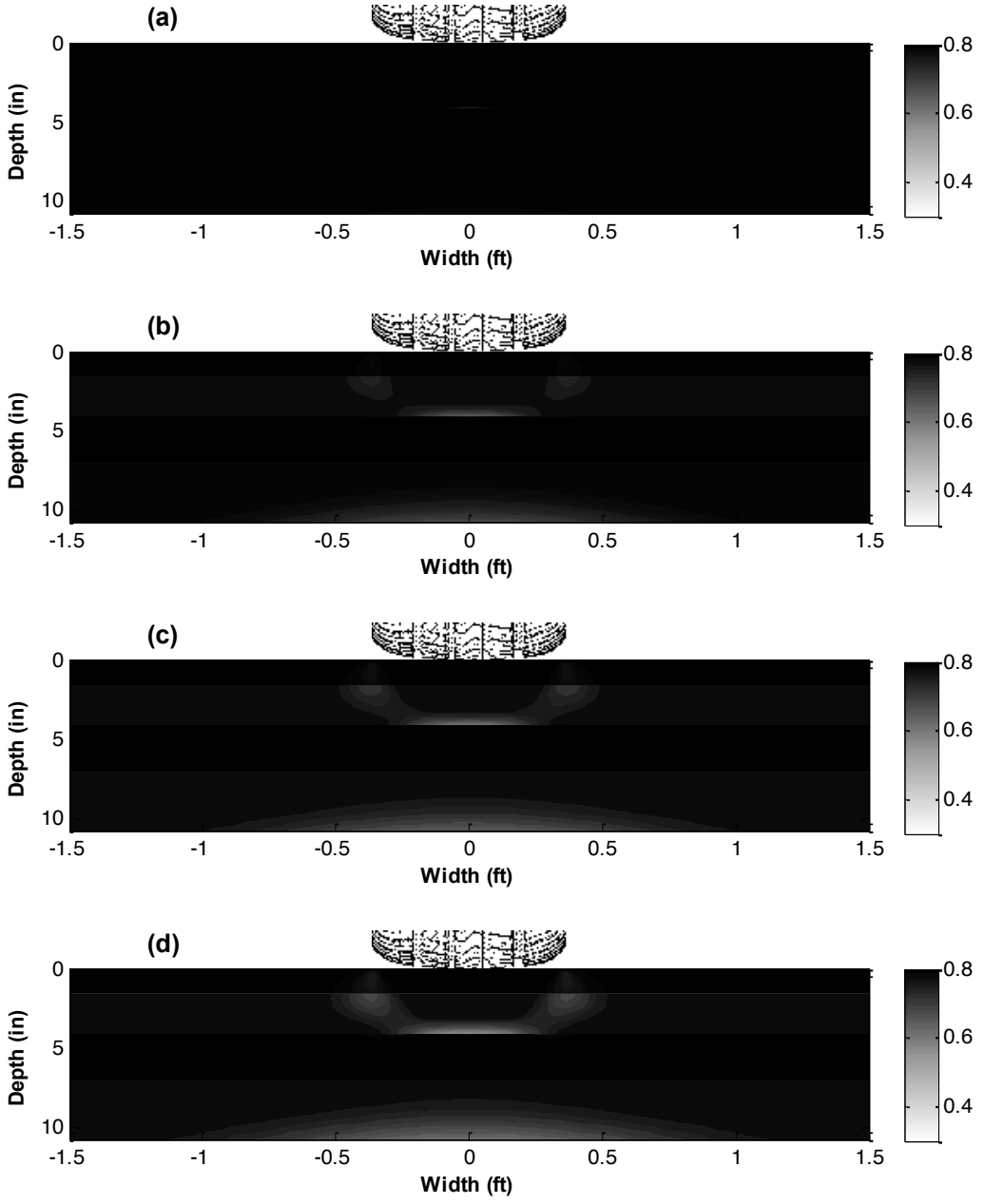

Figure 5.13 Damage contours for the B2 region in US 70 pavement: (a) 1 year, (b) 5 years, (c) 10 years, and (d) 20 years.

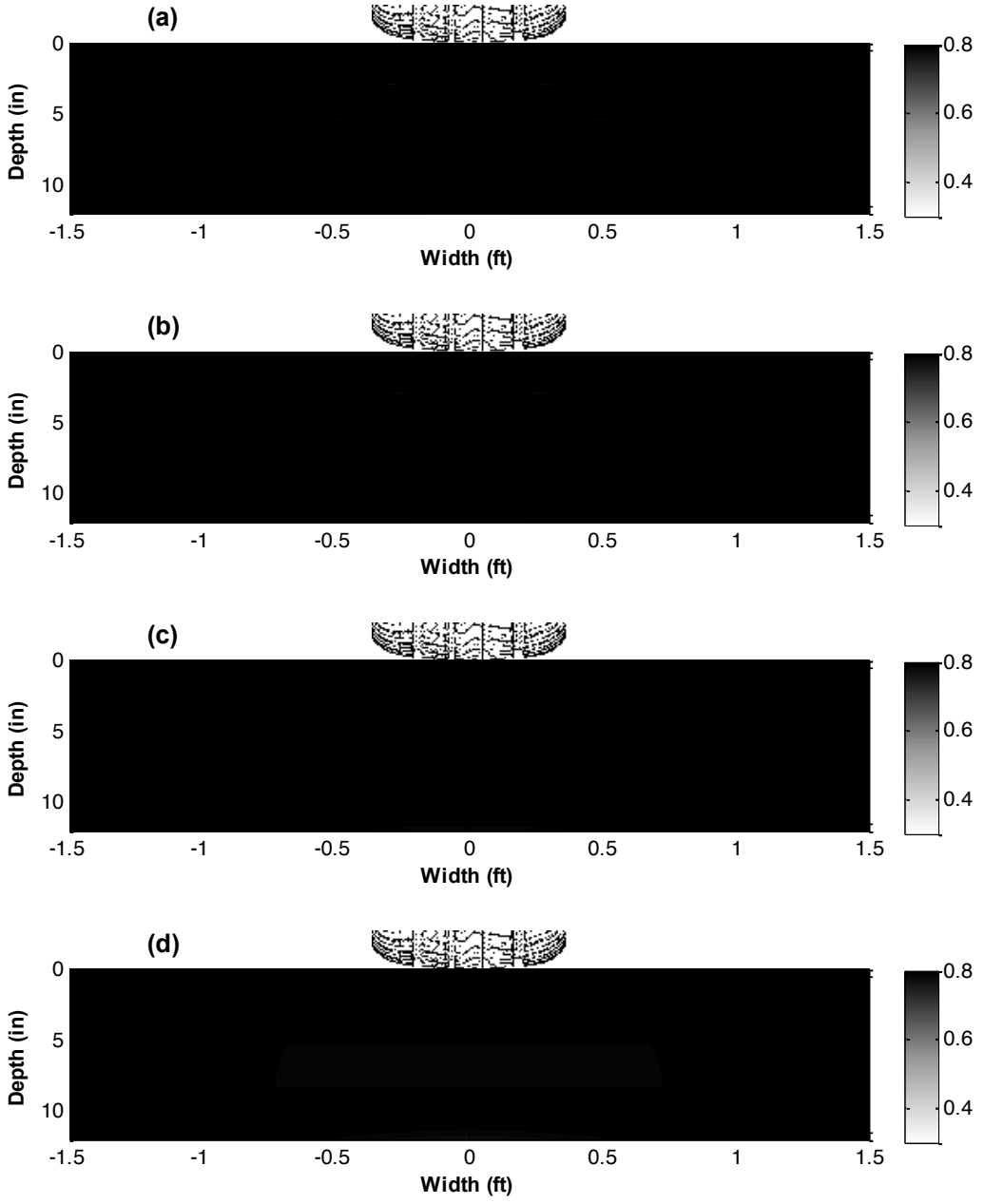

Figure 5.14 Damage contours for the A2 region in US 70 pavement: (a) 1 year, (b) 5 years, (c) 10 years, and (d) 20 years.

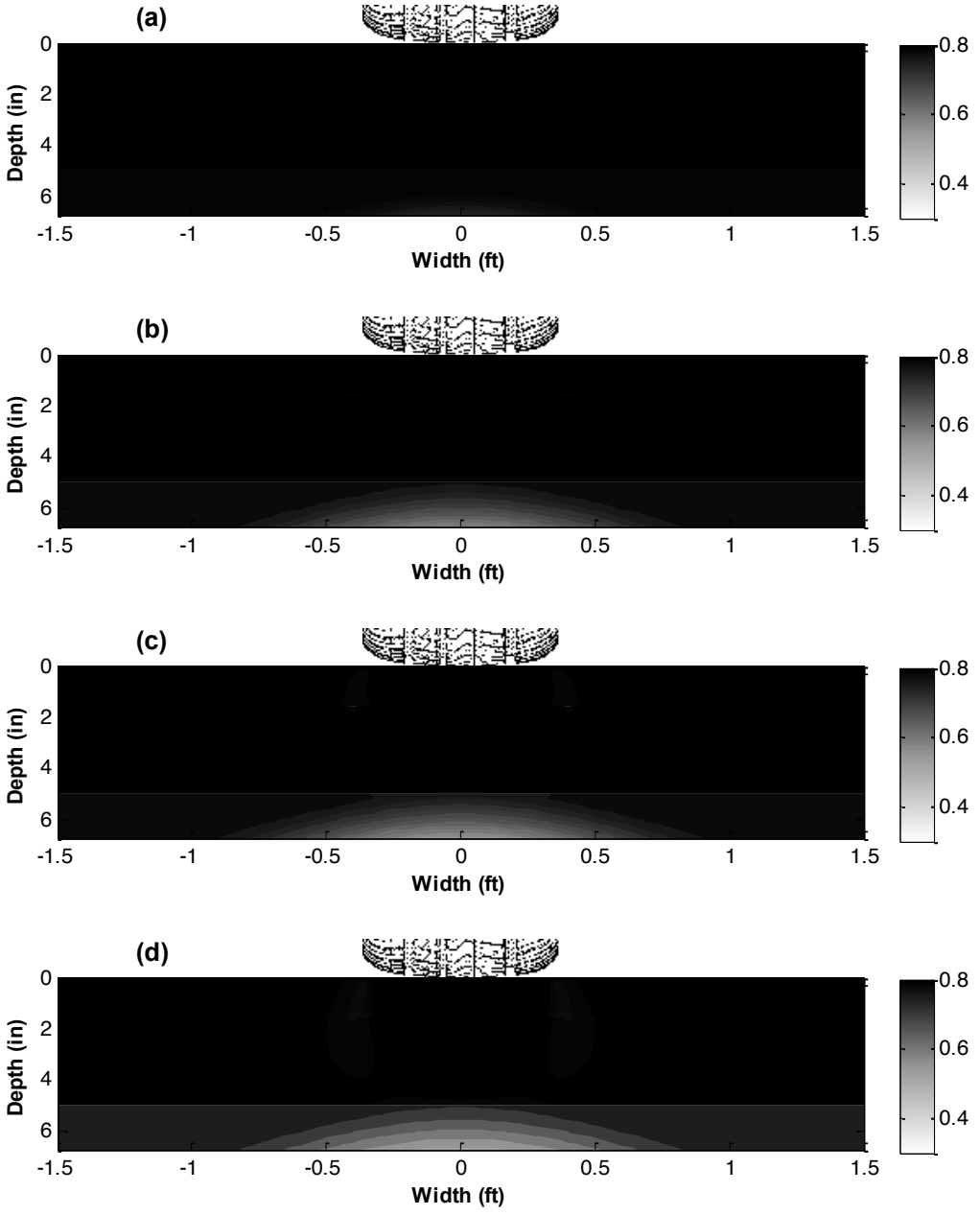

Figure 5.15 Damage contours for the B1 region in US 74 pavement: (a) 1 year, (b) 5 years, (c) 10 years, and (d) 20 years.

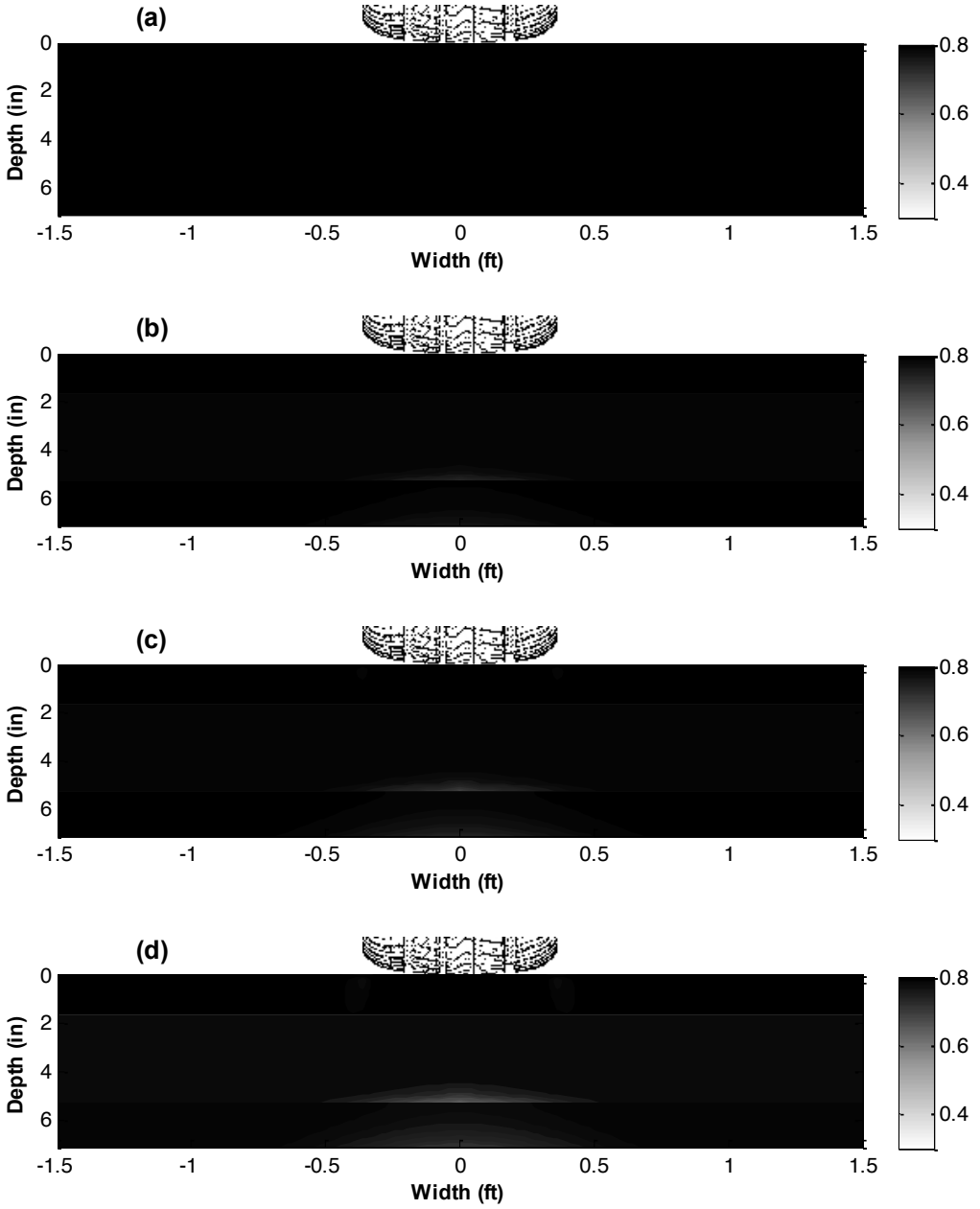

Figure 5.16 Damage contours for the A1 region in US 74 pavement: (a) 1 year, (b) 5 years, (c) 10 years, and (d) 20 years.

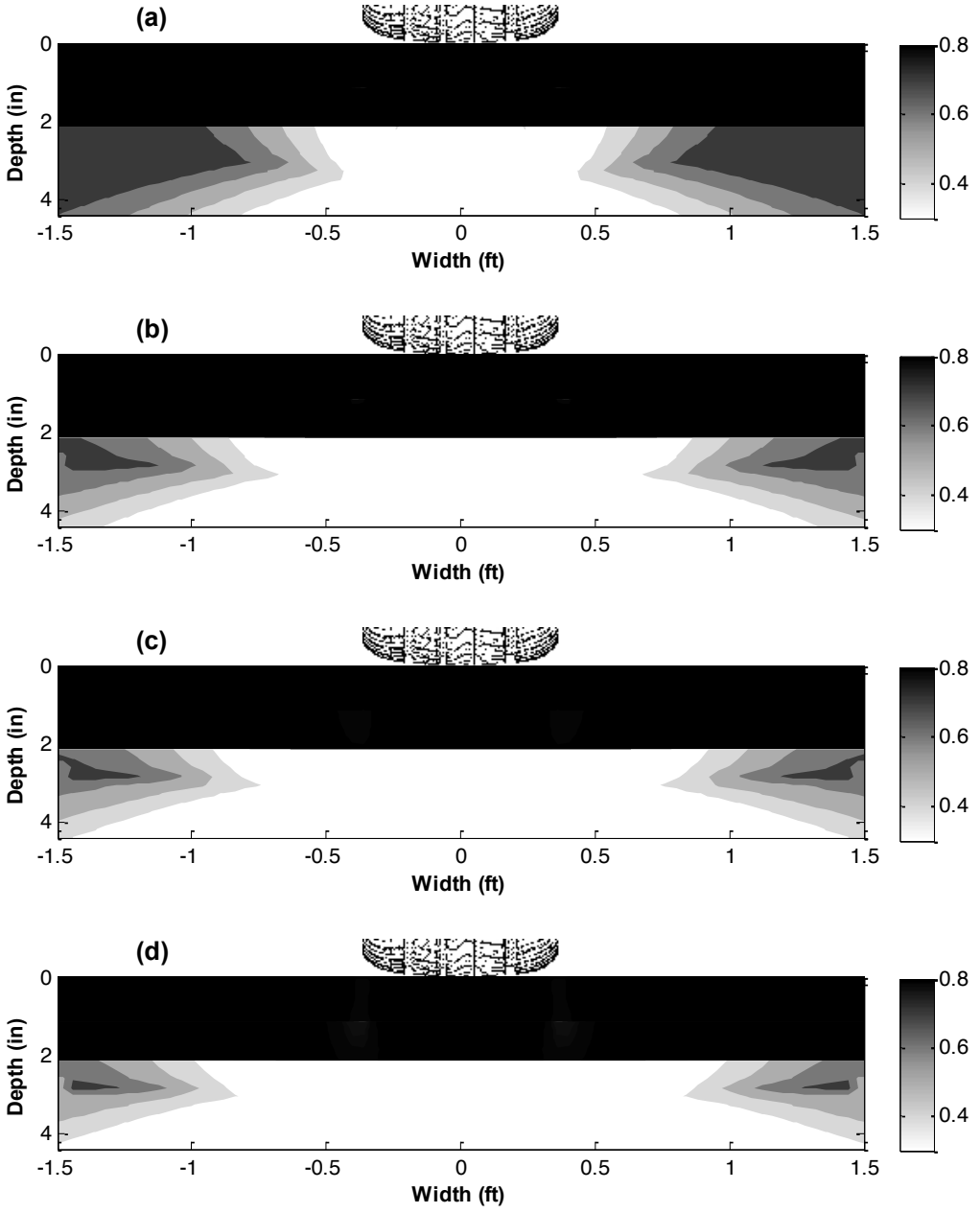

Figure 5.17 Damage contours for the B1 region in US 76 pavement: (a) 1 year, (b) 5 years, (c) 10 years, and (d) 20 years.

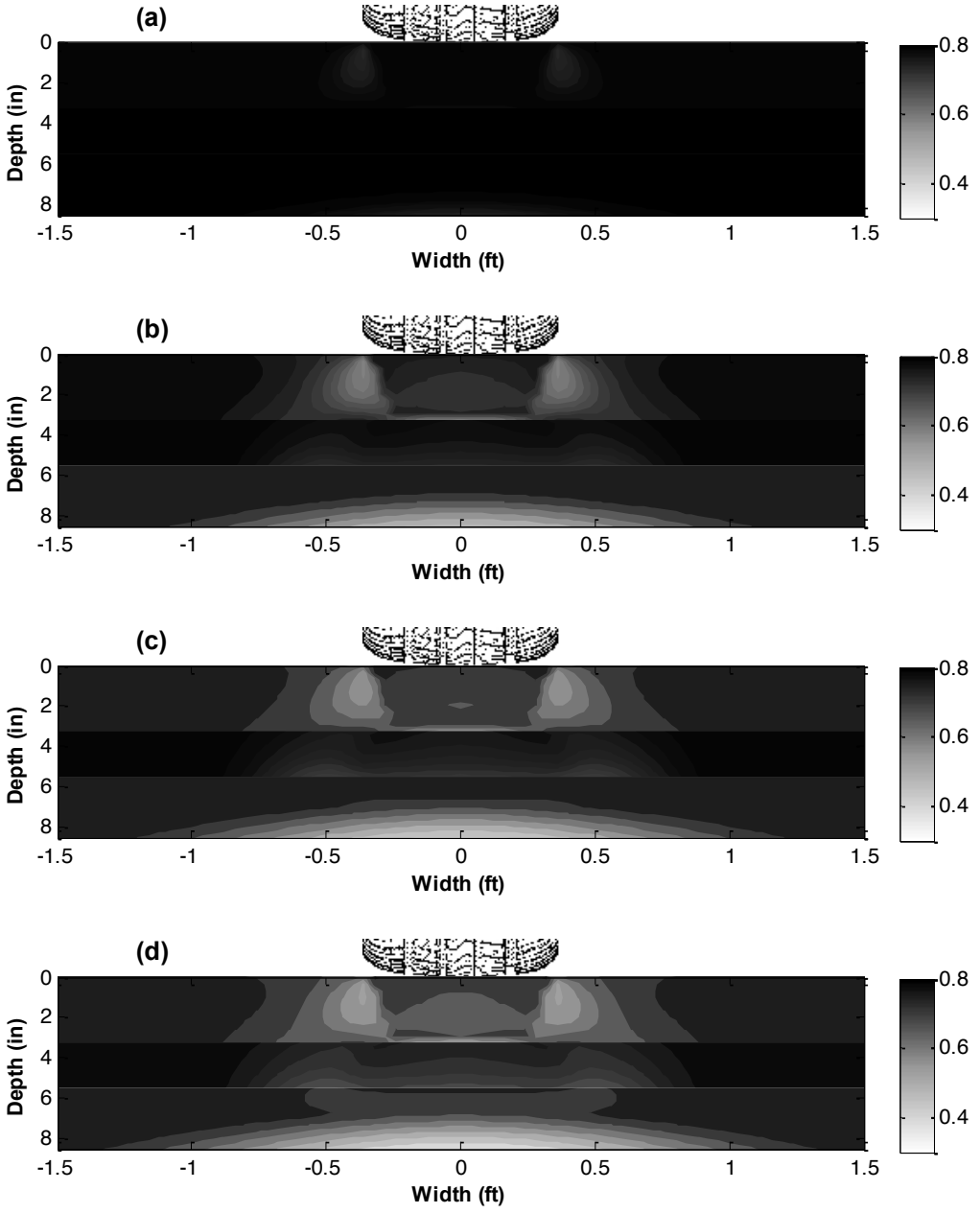

Figure 5.18 Damage contours for the A1 region in US 76 pavement: (a) 1 year, (b) 5 years, (c) 10 years, and (d) 20 years.

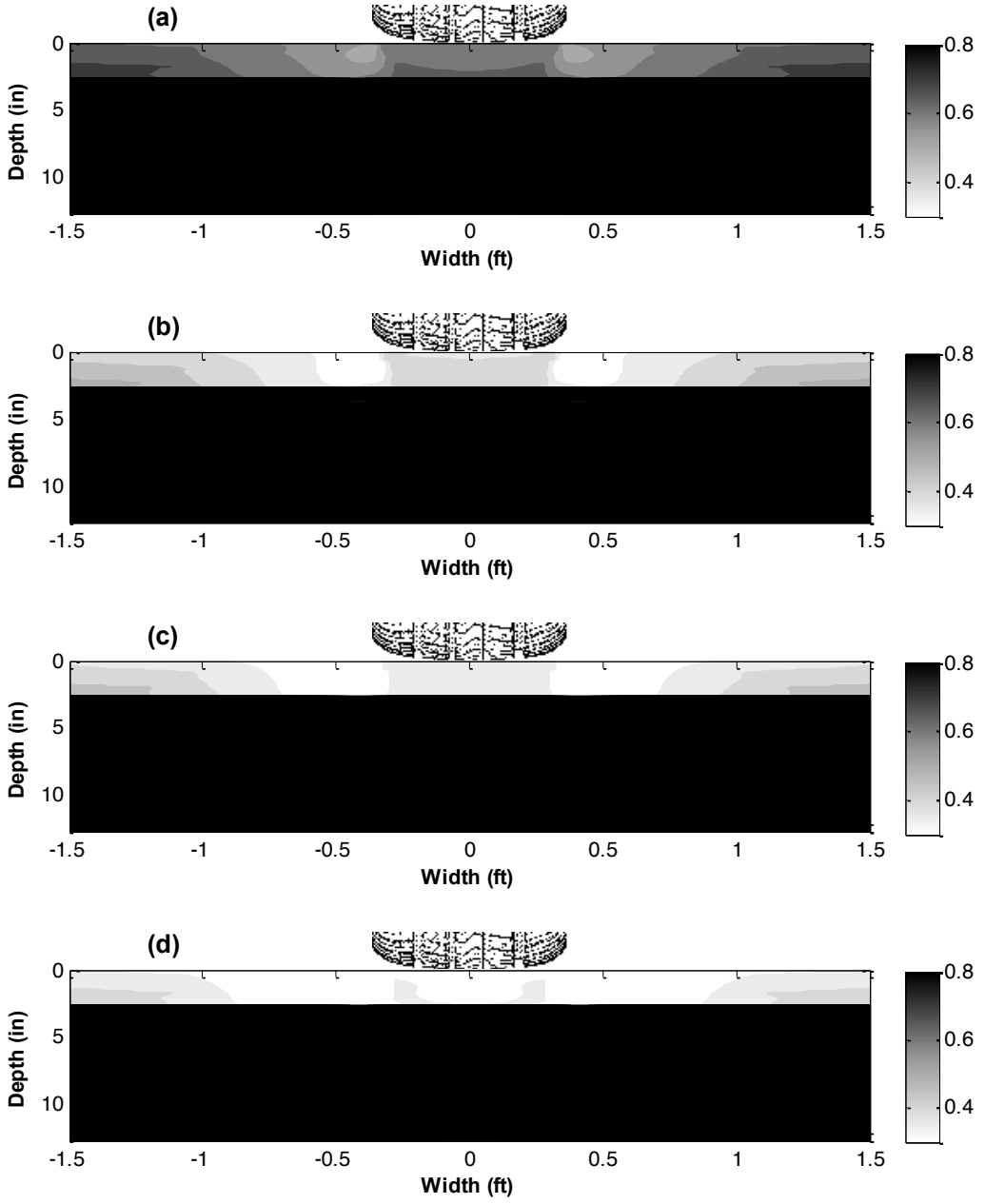

Figure 5.19 Damage contours for the B1 region in US 87 pavement: (a) 1 year, (b) 5 years, (c) 10 years, and (d) 20 years.

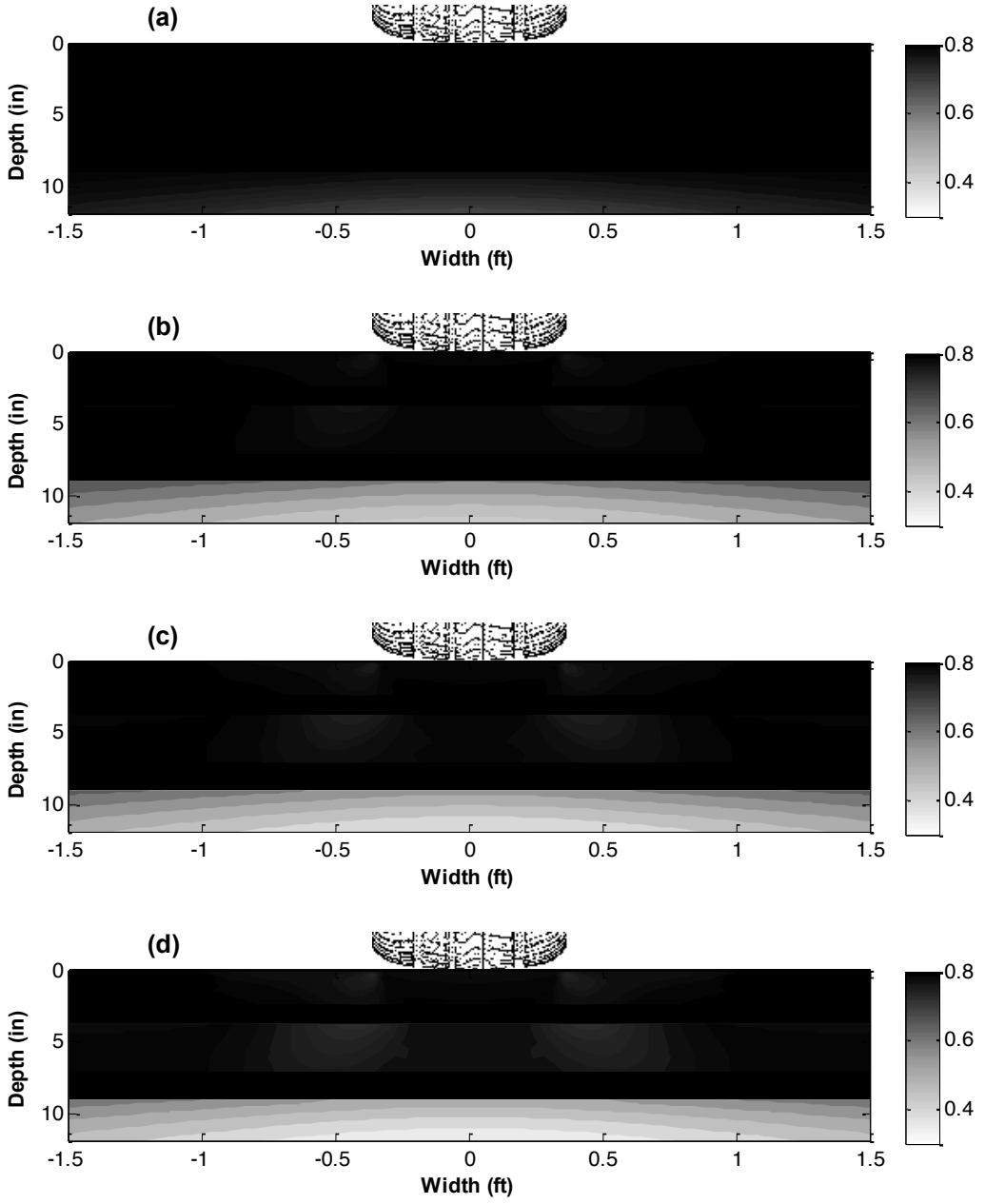

Figure 5.20 Damage contours for the A1 region in US 87 pavement: (a) 1 year, (b) 5 years, (c) 10 years, and (d) 20 years.

5.3 DARWin-ME Pavement ME Design

DARWin-ME is a software package that is based on the MEPDG. DARWin-ME makes it possible to design and analyze both HMA and Portland cement concrete (PCC) pavement structures. DARWin-ME also can evaluate long-term pavement performance under design traffic loading and climate conditions. Therefore, in this research, the long-term pavement conditions of all the tested sites were evaluated using this software. All required inputs were obtained through laboratory tests using field-extracted materials. Detailed information about DARWin-ME is available in the MEPDG, Interim Edition: Manual of Practice.

DARWin-ME is pavement design software that supports pavement design and analysis based on mechanistic and empirical analysis. This software considers traffic, climate, subgrade and pavement materials. The trial design that uses this software is evaluated based on the prediction of distresses. DARWin-ME considers asphalt concrete surfaced pavements as flexible pavements. In this project, the analysis was performed for conventional flexible pavements that include relatively thin asphalt concrete surfaces, aggregate base layers (crushed stone or gravel) and subgrade (foundation soil).

The goal of these long-term simulations is to verify current crack propagation using current material response inputs. If the long-term simulation results show a similar trend for cracking that is observed for certain crack propagation trends, then this simulation tool can be used effectively by state agencies for building cost-effective roadways.

5.3.1 Required Inputs

For performing conventional flexible pavement analysis, the required inputs can be divided into four main categories: traffic, climate, material properties, and layer thickness.

Traffic:

One of the major inputs required for the structural design/analysis of pavement structures is traffic data. Traffic data are required to estimate the load that is applied to the pavement for the design life. They also are required to calculate the frequency with which those given loads are applied throughout the pavement's design life. Different types of load-associated distress usually occur because of repeated traffic loading. For these reasons, traffic data are very important for

pavement design and analysis. Table 5.2 provides a comprehensive list of the input traffic parameters required by DARWin-ME.

For this project, some data were collected from the NCDOT Traffic Survey Unit; these data include average annual daily truck traffic (AADTT) and vehicle class distribution (VCD). The DARWin-ME software has the option to include built-in national average default values for many of the traffic parameters listed in Table 5.2. These values, such as those for tire pressure and axle spacing, can be used by almost all state highway agencies because they are generally not dependent on location or traffic stream characteristics. Other factors, however, can be dependent on local traffic characteristics, so statewide averages are used as much as possible.

Table 5.2 Required traffic inputs

Item		Source
AADTT	Initial two-way average annual daily truck traffic (AADTT)	NCDOT
	Number of lanes in design direction	Field data
	Percentage of trucks in design direction	Default
	Percentage of trucks in design lane	Default
	Operational speed	Default
Traffic Capacity		NA
Axle Configuration	Average axle width	Default
	Dual tire spacing	Default
	Tire pressure	Default
	Tandem axle spacing	Statewide Average
	Tridem axle spacing	Statewide Average
	Quad axle spacing	Statewide Average
Lateral Wander	Mean wheel location	Default
	Traffic wander standard deviation	Default
	Design lane width	Field data
Wheelbase	Average spacing of short axles	Default
	Average spacing of medium axles	Default
	Average spacing of long axles	Default
	Percentage of trucks with short axles	Default
	Percentage of trucks with medium axles	Default
	Percentage of trucks with long axles	Default
Monthly adjustment factors (MAF)		Statewide Average
Vehicle class distribution (VCD)		NCDOT
Hourly distribution factors (HDF)		Default
Traffic growth		Default
Number of different axle types per truck class (APT)		Statewide Average
Axle load distribution factor		Default

Climate:

The performance of flexible pavements is directly affected by environmental conditions. Factors such as precipitation, temperature, freeze-thaw cycles, and depth to water table affect the temperature and moisture content of unbound materials, which, in turn, directly affect the load-

carrying capacity of the pavement. The DARWin-ME software considers the effects of these environmental factors. The ground water table depth, precipitation/infiltration, freeze-thaw cycles, and other external factors also are considered as required inputs for pavement design. The DARWin-ME database includes EICM data for throughout the United States. Users can select a single weather station or group of weather stations from which to gather information such as air temperature, relative humidity (RH), precipitation, wind speed, sunshine percentage, and rainfall. This information and depth of water table information are both utilized by the EICM to account for the effects of changing temperature and moisture profiles on the performance of unbound and bound materials. The climatic data used for this project are presented in Table 5.3.

Table 5.3 Required climatic inputs

Item	Source
Latitude	Field Data
Longitude	Field Data
Elevation	Field Data
Depth of Water table	N/A

Material properties:

(1) Asphalt concrete layers:

The key material inputs required for asphalt concrete layers include:

- Dynamic modulus values of the asphalt mixtures
- Rheological properties (i.e., viscosity, penetration, complex modulus values and phase angle) of the asphalt binder
- Creep compliance and indirect tensile strength values
- Mix-related and other properties (e.g., effective binder content, air void content, heat capacity, and thermal conductivity)

These inputs are required for predicting pavement responses, climatic conditions, asphalt aging as well as pavement performance.

(2) Base layers:

The required inputs for base layers are presented in Table 5.4. Some of these required inputs were used as default values in this research.

Table 5.4 Required base layer inputs

Item	Source
Material	Field Data
Thickness	Field Data
Poisson's ratio	Default
Coefficient of lateral earth pressure	Default
Resilient modulus (psi)	Field Data
Gradation & other engineering properties	Default

(3) Subgrade:

The subgrade materials include soil classes A-1 through A-7-6, as defined in accordance with the AASHTO soil classification system. The inputs required for the subgrade materials are the same as those for non-stabilized materials and include physical and engineering properties such as dry density, moisture content, hydraulic conductivity, specific gravity, soil-water characteristic curve (SWCC) parameters, classification properties, and resilient modulus values. The NCHRP 9-23A project produced a comprehensive nationwide soils database that includes SWCC parameters and other soil properties that are required by the EICM. This database can account for changes in the modulus values of bound and unbound materials due to changes in temperature and moisture profiles within a pavement structure. The SWCC parameter represents a measure of the water-holding capacity of a given soil, which is very important in predicting permeability, volume change, deformability and the shear strength of unsaturated soils. The NCHRP 9-23A (2010) project products include Geographic Information System (GIS) -based soil maps for all states. These maps were transformed into image files and stored as PDF documents. These files can be used to superimpose any road sites onto a soil map and, consequently, to select the most accurate soil type for that road section for a given project. The required inputs for the subgrade are presented in Table 5.5.

Table 5.5 Required subgrade inputs

Item	Source
Material	NCHRP 9-23A
Resilient modulus (psi)	Field Investigation (DCP)
Gradation & other engineering properties	NCHRP 9-23A

Evaluation of project data:

The extraction of structural materials and collection of traffic data is a vital step for the successful analysis of pavement performance. After gathering all the data, analysis was performed for the 19 sites for each region using as much data as possible. Design analysis was performed for 20 years for all sites, which means 20 years from the completion of construction at which time the pavement is expected to perform adequately without significant loss of function or structural integrity. Pavement performance was predicted over the design life beginning from the month the pavement was opened to traffic.

The design procedure is based on pavement performance, and therefore, the critical levels of pavement distress at the selected level of reliability are specified at the outset of the analysis. The distress types considered in this analysis procedure are:

- Terminal International Roughness Index (IRI) value (in./mile)
- Permanent deformation of total pavement (in.)
- Asphalt concrete bottom-up fatigue cracking (%)
- Asphalt concrete thermal cracking (ft/mile)
- Asphalt concrete top-down fatigue cracking (ft/mile)
- Permanent deformation of asphalt concrete only (in.)

5.3.2 DARWin-ME Analysis Results

As stated in Acknowledgement, all DARWin-ME simulations were conducted by Nasrin Sumee.

The DARWin-ME simulations can be used with different levels of input data. Because the dynamic modulus values were measured from test level 1 sites, Level 1 DARWin-ME simulations were performed for the test level 1 sites. For the remaining sites, Level 3 DARWin-ME simulations were performed. Table 5.6 shows the 20-year simulation results obtained from

the both Level 1 and Level 3 input along with the field observations. In order to compare field observed cracking direction to DARWin-ME simulation result, pass or fail results of TDC and BUC were used for this comparison. In Table 5.6, values in italic-bold font indicate that the core and field condition observations do not match the simulation results in terms of cracking direction. Pass or fail for TDC or BUC were decided by certain distress values at 90% reliability of 20 years simulation result. Several important observation can be made from DARWin-Me simulation are presented as following.

- All of BUC observed condition regions were not captured by Level 1 simulation.
- 8 out of 13 TDC observed condition regions were captured by Level 1simulation, but significantly higher distress observed from I-540 A1 region in which no TDC observed.
- TDC capturing rate (34%) of Level 3 DARWin-ME simulation was significantly lower than high-level simulation.
- About 70% of cracking directions were match with field core observation from higher-level simulation, and about 60% of cracking directions were match with lower-level simulation result.

DARWin-ME tends to capture more crack propensity trends in the bottom-up cracking (BUC) sites than in the top-down cracking (TDC) sites. Because DARWin-ME uses static loads, unlike the LVECD program that uses moving loads, for simulations, it is not surprising to observe weakness in the DARWin-ME simulations for the TDC-observed sites.

Table 5.6 Crack Propagation Propensity Observed from Field Cores and 20-year Simulation Results of DARWin-ME for Input Levels 1 and 3

Input Level	Condition region ID		DARWin-ME 20-year Simulation Results										Field Observation	
			TDC Target		Expected TDC			BUC Target		Expected BUC				
			Distress @ Specified Reliability	Reliability (%)	Distress @ Specified Reliability Predicted	Reliability (%) Achieved	Criterion Satisfied?	Distress @ Specified Reliability	Reliability (%)	Distress @ Specified Reliability Predicted	Reliability (%) Achieved	Criterion Satisfied?	TDC?	BUC?
Input Level	I-540	A1	2000	90	10894.64	1.0	Fail	25	90	1.45	100.0	Pass	***No***	No
	I-540	B2	2000	90	2960.01	78.8	Fail	25	90	1.45	100.0	Pass	Yes	No
	NC24	B1	2000	90	4212.15	61.6	Fail	25	90	2.05	100.0	Pass	Yes	No
	NC24	A1	2000	90	2506.41	84.1	Fail	25	90	2.18	100.0	Pass	Yes	No
	US-70	B2	2000	90	2382.12	85.6	Fail	25	90	1.49	100.0	Pass	Yes	No
	US-70	A2	2000	90	1205.47	98.4	Pass	25	90	1.46	100.0	Pass	No	No
	US17	B2	2000	90	2851.48	80.1	Fail	25	90	1.61	100.0	Pass	Yes	No
	US17	A1	2000	90	1120.63	98.9	Pass	25	90	1.53	100.0	Pass	No	No
	US601	A1	2000	90	1300.36	97.6	Pass	25	90	1.69	100.0	Pass	***Yes***	***Yes***
	US601	B2	2000	90	620.29	100.0	Pass	25	90	1.73	100.0	Pass	No	***Yes***
	US76	B1	2000	90	1371.75	97.0	Pass	25	90	14.13	99.2	Pass	***Yes***	No
	US76	A1	2000	90	1503.99	95.7	Pass	25	90	1.98	100.0	Pass	***Yes***	***Yes***
	NC87	B1	2000	90	260.49	100.0	Pass	25	90	1.47	100.0	Pass	***Yes***	No
	NC87	A2	2000	90	307.70	100.0	Pass	25	90	1.46	100.0	Pass	No	***Yes***
	US74	B1	2000	90	411.45	100.0	Pass	25	90	1.85	100.0	Pass	No	***Yes***
	US74	A1	2000	90	349.43	100.0	Pass	25	90	1.55	100.0	Pass	No	***Yes***
	NC209	A1	2000	90	569.04	100.0	Pass	25	90	1.61	100.0	Pass	No	No
	NC209	B1	2000	90	392.00	100.0	Pass	25	90	1.52	100.0	Pass	No	No
Level 3	I 540	A1	2000	90	3868.00	66.7	Fail	25	90	1.45	100.0	Pass	***No***	No
	I 540	B2	2000	90	2996.48	78.4	Fail	25	90	1.45	100.0	Pass	Yes	No
	NC 24	B1	2000	90	419.10	100.0	Pass	25	90	2.29	100.0	Pass	***Yes***	No
	NC 24	A1	2000	90	5252.03	45.2	Fail	25	90	17.46	97.4	Pass	Yes	No
	US 70	B2	2000	90	1556.18	95.1	Pass	25	90	1.47	100.0	Pass	***Yes***	No
	US 70	A2	2000	90	4048.90	64.1	Fail	25	90	1.48	100.0	Pass	***No***	No
	US 17	B2	2000	90	2031.38	89.6	Fail	25	90	1.59	100.0	Pass	Yes	No
	US 17	A1	2000	90	2735.19	81.5	Fail	25	90	1.66	100.0	Pass	***No***	No
	US 601	A1	2000	90	710.26	100.0	Pass	25	90	2.00	100.0	Pass	***Yes***	***Yes***
	US 601	B2	2000	90	457.40	100.0	Pass	25	90	2.11	100.0	Pass	No	***Yes***
	US 76	B1	2000	90	1669.29	93.9	Pass	25	90	1.93	100.0	Pass	***Yes***	No
	US 76	A1	2000	90	1533.73	95.4	Pass	25	90	15.06	98.8	Pass	***Yes***	***Yes***
	NC 87	B1	2000	90	578.84	100.0	Pass	25	90	1.47	100.0	Pass	***Yes***	No
	NC 87	A2	2000	90	459.23	100.0	Pass	25	90	1.46	100.0	Pass	No	***Yes***
	US 74	B1	2000	90	331.89	100.0	Pass	25	90	1.55	100.0	Pass	No	***Yes***
	US 74	A1	2000	90	347.56	100.0	Pass	25	90	1.88	100.0	Pass	No	***Yes***
	NC 209	A1	2000	90	542.46	100.0	Pass	25	90	1.66	100.0	Pass	No	No
	NC 209	B1	2000	90	345.99	100.0	Pass	25	90	1.55	100.0	Pass	No	No
	US 13	A	2000	90	3045.30	77.8	Fail	25	90	22.14	93.1	Pass	***No***	No
	US 13	B	2000	90	2724.06	81.6	Fail	25	90	7.94	100.0	Pass	Yes	No
	NC 177	A	2000	90	5316.18	44.2	Fail	25	90	19.90	95.0	Pass	***No***	***Yes***
	NC 177	B	2000	90	10070.28	2.2	Fail	25	90	31.81	78.8	Fail	***No***	Yes
	NC 47	A	2000	90	5667.79	38.7	Fail	25	90	35.91	69.5	Fail	***No***	Yes
	NC 47	B	2000	90	7212.85	18.4	Fail	25	90	23.79	91.4	Pass	Yes	***Yes***
	US 401	A	2000	90	2344.83	86.0	Fail	25	90	2.12	100.0	Pass	***No***	No
	US 401	B	2000	90	5047.01	48.4	Fail	25	90	2.69	100.0	Pass	***No***	No
	NC 55	A	2000	90	1590.27	94.7	Pass	25	90	1.48	100.0	Pass	No	No
	NC 55	B	2000	90	1912.25	91.0	Pass	25	90	1.48	100.0	Pass	***Yes***	No
	NC 179	A	2000	90	406.62	100.0	Pass	25	90	1.69	100.0	Pass	***Yes***	No
	NC 179	B	2000	90	406.62	100.0	Pass	25	90	1.74	100.0	Pass	***Yes***	No
	NC 194	A	2000	90	1044.44	99.3	Pass	25	90	1.45	100.0	Pass	***Yes***	No
	NC 194	B	2000	90	1731.58	93.1	Pass	25	90	1.70	100.0	Pass	***Yes***	No

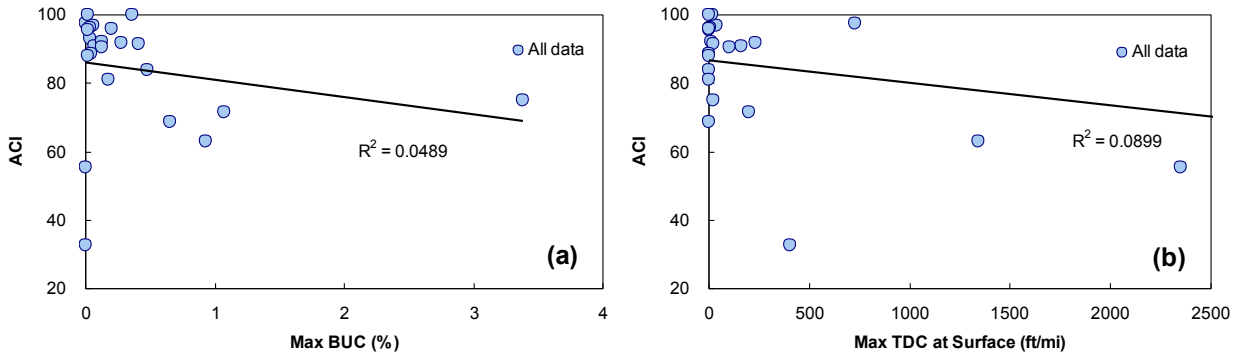

Figure 5.21 Comparison between ACI values and 20-year simulation results from DARWin-ME with Level 1 input: (a) maximum BUC% and (b) length of maximum TDC at surface.

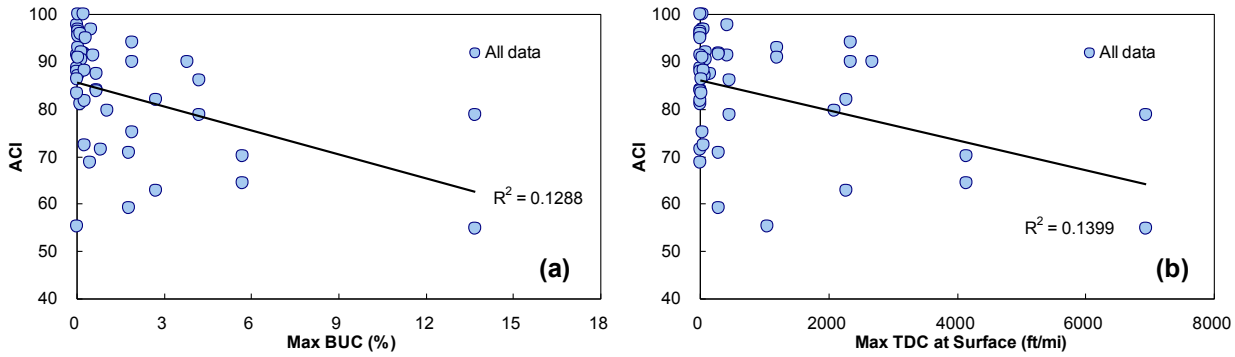

Figure 5.22 Comparison between ACI values and 20-year simulation results from DARWin-ME with Level 3 input: (a) maximum BUC% and (b) length of maximum TDC at surface.

Among the key distress types that were generated by the DARWin-ME simulations (i.e., the terminal international roughness index (IRI), permanent deformation of the total pavement, bottom-up fatigue cracking, thermal cracking on the surface, and top-down cracking on the surface), the *asphalt concrete BUC (%)* and *asphalt concrete TDC (ft/mile)* were considered for comparison with the ACI values described in Section 4.3. Note that *BUC (%)* indicates the possibility of BUC at a certain percentage after 20 years of service, and *asphalt concrete TDC (ft/mile)* indicates that a certain amount of TDC will appear on the surface after 20 years of service. A summary of the comparison results is presented in Figure 5.21 and Figure 5.23 for Level 1 input and in Figure 5.22 and Figure 5.24 for Level 3 input. The data presented in subfigures (a) and (b) in Figure 5.21 and Figure 5.22 present all of the data points, which are divided into different cracking direction groups in the subsequent subfigures in Figure 5.23 and Figure 5.24. These comparative results show a very weak correlation between the ACI values

and simulation results, although the overall trend is reasonable. Among those subfigures presented in Figure 5.23, Figure 5.23 (b), (d), (e), and (g) show better correlations than the other subfigures. This observation is quite reasonable because the value of the length of the TDC at the surface needs to correlate with the ACI values from the TDC-observed condition regions. Likewise, a maximum BUC percentage needs to correlate with the ACI values from the BUC-observed sites. It is noteworthy that strong correlations are observed from the comparison between the maximum BUC percentage and the ACI values from the BUC-observed sites, although the pass and fail comparisons with the field core observations do not capture the BUC propensity. Among those subfigures presented in Figure 5.24, Figure 5.24 (a), (c), (f), and (h) show slightly better correlations than the other subfigures. For these subfigures of Figure 5.24, the same conclusions can be drawn as described for Figure 5.23, which is the Level 1 input simulation case; however, the correlations are significantly lower in Figure 5.24 than in Figure 5.23.

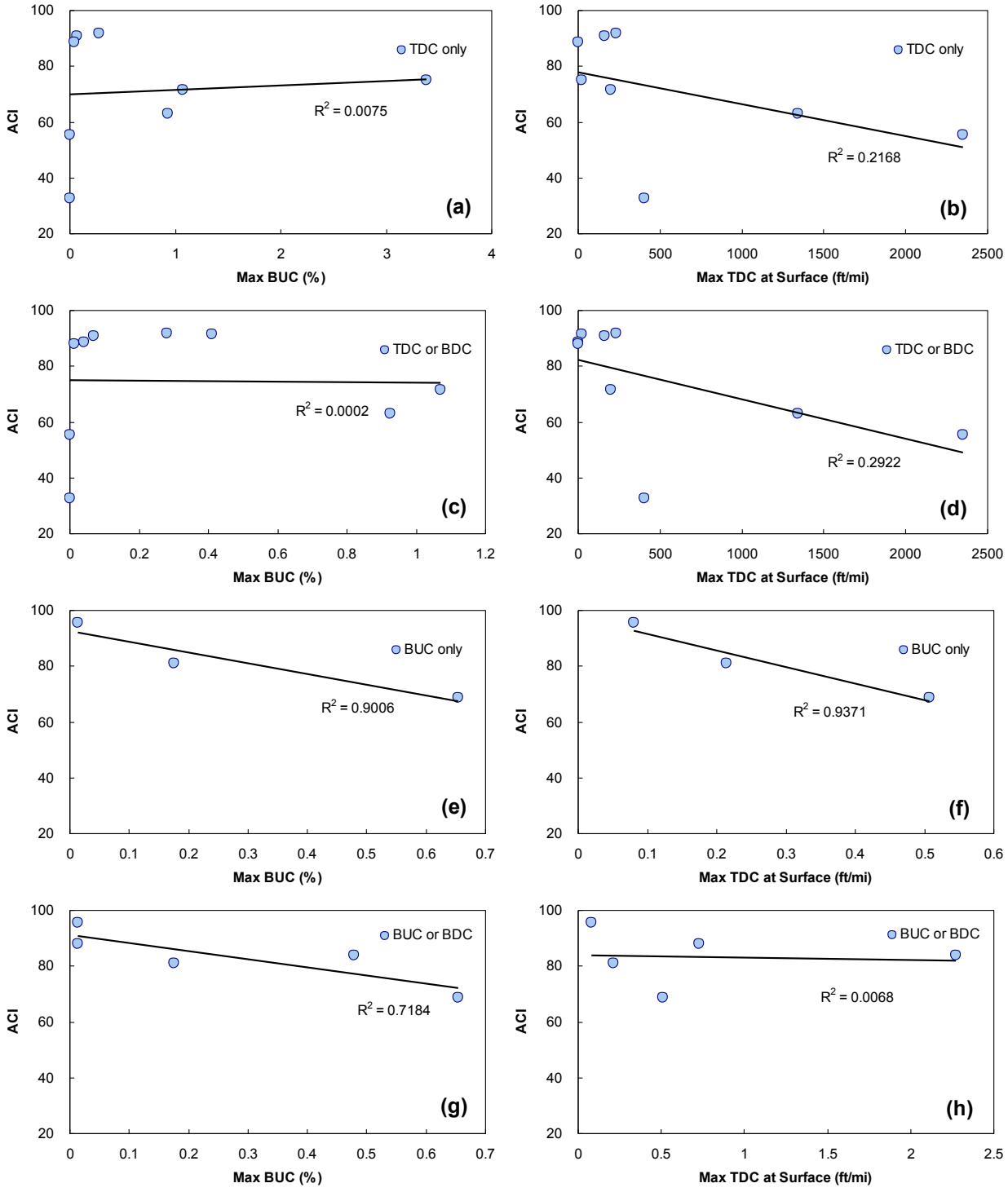

Figure 5.23 Comparison between ACI values and 20-year simulation results of maximum BUC% and maximum length of TDC at surface from DARWin-ME with higher-level inputs: (a) and (b) from TDC observed sites, (c) and (d) from TDC or BDC observed sites, (e) and (f) BUC observed sites, (g) and (h) from TDC or BDC observed sites.

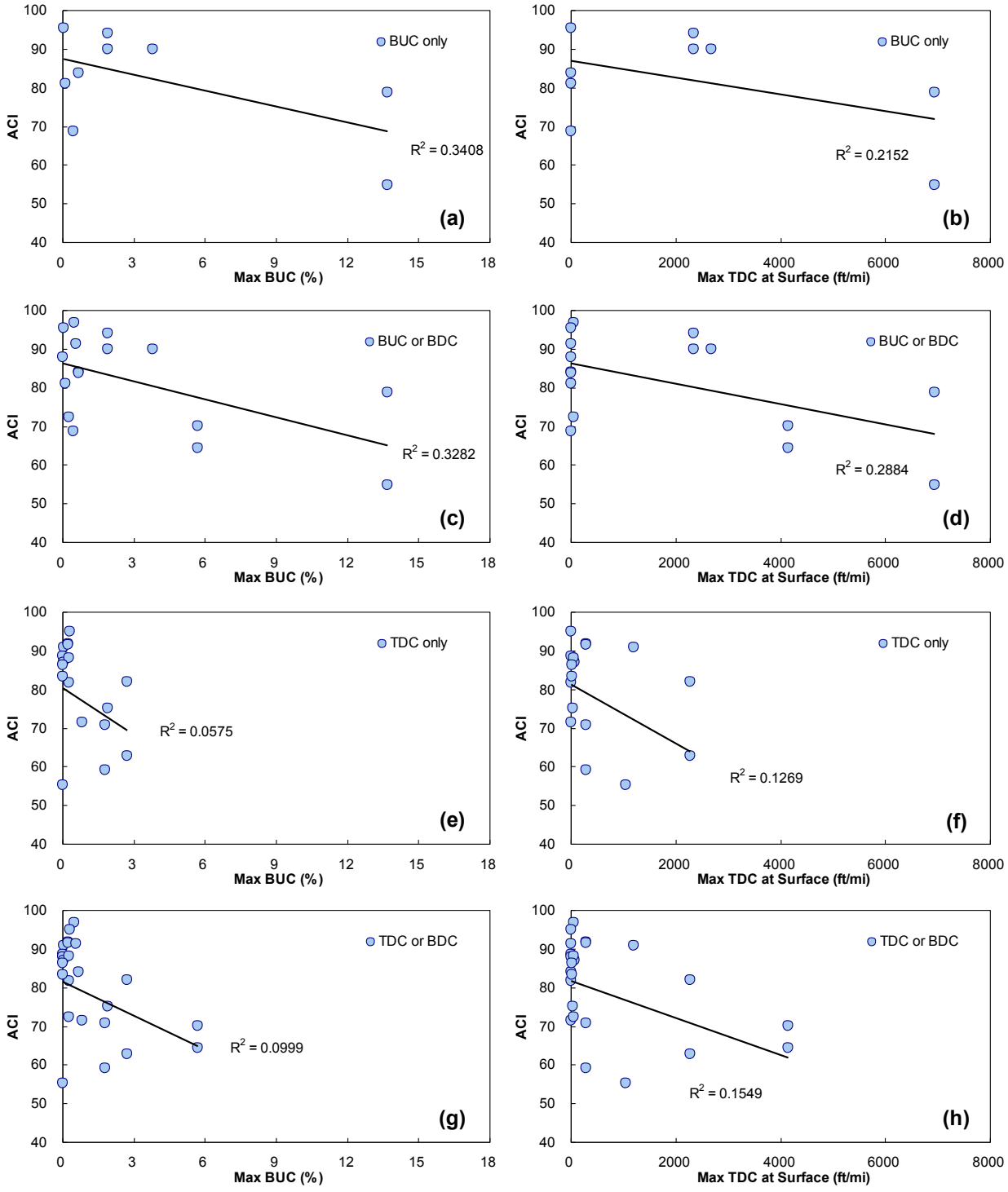

Figure 5.24 Comparison between ACI values and 20-year simulation results of maximum BUC% and maximum length of TDC at surface from DARWin-ME with lower-level inputs: (a) and (b) from BUC observed sites, (c) and (d) from BUC or BDC observed sites, (e) and (f) TDC observed sites, (g) and (h) from TDC or BDC observed sites.

5.4 Summary

Cost-effective and structurally-effective pavement maintenance strategies begin from the identification of the different causes of cracking. Accordingly, maintenance engineers should design different rehabilitation plans according to the crack initiation locations and the cracking propensity of the asphalt pavements. Replacing the surface after milling and placing a new pavement layer, which is an appropriate approach for TDC pavements, will never remedy BUC that is caused by structural deficiencies of the pavement. This study verifies the capability of the LVECD model and DARWin-ME simulation program to capture crack initiation locations and propagation propensity compared to the observations of field cores and the field condition survey of in-service pavements in North Carolina. Overall, the agreement rate between the field core observations and field condition survey and the predicted LVECD simulation results is about 78% in terms of crack propensity and damage severity as ranked from two different condition regions in a single site. The agreement rate between the field core observations and the predicted DARWin-ME simulation results using Level 1 inputs is about 69% in terms of crack propensity. This ability of the DARWin-ME simulations to capture crack propensity drops to 58% for Level 3 inputs. Considering the fact that the simulation binder parameters are not the same as the extracted binder of the field material, this agreement rate is fairly reasonable; however, it is noteworthy that none of the existing BUC was captured by the DARWin-ME simulations with Level 1 input. This finding may indicate that pass and fail simulations of the DARWin-ME program cannot effectively capture the crack propagation observed from the field cores, even though strong correlations were observed from the comparison between the maximum BUC percentage and the ACI values for the BUC-observed sites. Based on this finding, it is expected that the reliability threshold for the pass or fail guidelines needs to be modified for better accuracy. A direct comparison of the capability of DARWin-ME and the LVECD program is difficult, but it appears that the LVECD program tends to capture cracking propensity better than DARWin-ME, based on field observations. Accordingly, the LVECD-based mechanistic approach can be used as a performance prediction model for pavement design and maintenance and can help maintenance engineers to create cost-effective rehabilitation strategies for project-level pavement management systems.

Chapter 6 Conclusions and Recommendations

6.1 Conclusions

Specific conclusions drawn from this research into the primary causes of cracking are summarized below.

- The asphalt content in the top layer that exhibits top-down cracking or bi-directional cracking has a proportional relationship to ACI values. The air void content in a bottom layer that exhibits bottom-up racking or bi-directional cracking shows an inverse proportional relationship to ACI values. For quality analysis, the given data were partitioned into different categories: different NMSAs and aggregate gradation types. In case of top layer exhibiting top-down cracking or bi-directional cracking, same conclusions can be drawn in comparison of ACI values and asphalt content regardless of sizes of NMSA and aggregate gradation types. However, for the case of bottom layer exhibiting bottom-up racking or bi-directional cracking, reasonable correlations were observed in specific categories: 9.5 mm NMSA and penetrating aggregate gradation for bottom-up racking or bi-directional cracking and fine aggregate gradation for only BUC exhibit bottom layer. If mix design information of each condition region was available for this research, quality analysis could be conducted to find out why poor relationships were observed in the comparison of ACI values and air void and asphalt contents showing undesirable relationship.
- A comparison between ACI and AFT values does not produce noteworthy findings, but somewhat reasonable results are evident once the range of comparison is narrowed down. Thicker film thicknesses show higher ACI values.
- From field core visual observations, road widening is identified as a major cause of longitudinal cracking.
- Regions with observed layer interface separation (debonding) tend to have low ACI values.

- Layer interface separation was observed from 29 out of 56 condition regions, which is more than 51%. This indicates that layer interface separation is one of major cause of cracking but can be relatively easily resolved by QC and QA.
- Overall, it is observed that sites with observed bottom-up cracking have higher tensile strain levels at the bottom of the asphalt layer than sites with observed top-down cracking.
- The *AREA* parameter versus pavement thickness relationship differentiates the top-down cracking sections from pavements with full-depth cracking that is caused by the bottom-up cracking mechanism. Therefore, the FWD-based *in situ* method will allow pavement engineers to identify the existence and likelihood of top-down cracking. This simplified method will not only reduce the time and cost involved for the engineer to verify the structural soundness of the pavement, but will also lead to selecting the optimal maintenance treatment and rehabilitation designs.
- Binder fatigue test results indicate that binder properties between *good* and *poor* sections of a given site are not the result of differences in the binder properties. Hence, other mixture design factors are at work in controlling the site variability in terms of fatigue resistance.
- The fact that the predicted cracking propensity and locations obtained from the LVECD simulations are in good agreement with the condition survey results and with the visual observations from the cores suggests that the LVECD program analysis can be an effective tool in determining the top-down cracking propensity of asphalt pavements, if the mechanical properties of the individual layers are available. When an accurate aging model and healing model become available and are implemented into the LVED program, the prediction results can be calibrated against the field performance data to develop a powerful and accurate pavement cracking performance prediction program that allows cracks to initiate at any location and propagate in whatever direction within the pavement structure based on the law of physics.
- The ability to identify top-down cracking and bottom-up cracking based on surface cracks is one of the most important starting points for creating cost-effective rehabilitation strategies for project-level pavement management systems. Therefore, the

LVECD program and the *AREA* parameter method can be effective tools for building a cost-effective pavement management system.

- DARWin-ME cannot effectively capture the direction of cracking using lower level simulation inputs.
- A direct comparison of the capability of DARWin-ME and the LVECD program is difficult, but it appears that the LVECD program tends to capture cracking propensity better than DARWin-ME, based on field observations. Accordingly, the LVECD-based mechanistic approach also can be used as a performance prediction model for pavement design.

6.2 Recommendations for Future Research

Recommendations for future research regarding field-extracted materials are summarized as follows.

- Integrated materials and pavement condition database development. A significant challenge for this project was the lack of JMF and material data, which made it difficult to find systematic flaws in the mix design. If the JMF of each material had been available to the research team, an enormous amount of information, such as construction quality, material quality, aggregate blending, density records during onsite compaction, etc., could have been obtained for the field-extracted materials. Also, if local or Division engineers had accurate records of the need for past rehabilitation efforts, a more effective analysis approach could have been taken for this research. Also, the process of finding valid field sites was lengthy for this research project. The depth of this research could have been more extensive if the NCDOT had test tracks or test roads and a full construction and materials database. Therefore, future research is needed into the development of an integrated materials and pavement condition database.
- Road widening. A sand mix layer was observed in many of the road-widening locations. According to a Division engineer, sand mixes typically are used for elevation purposes. A higher quality mix needs to be developed for these purposes, and the effect of poor quality patching mix on pavement service life needs to be evaluated.

- AREA parameter. In order to predict the top-down cracking potential and to determine the direction of cracking of new pavement, applicability of AREA nomography needs to be studied.
- DARWin-ME. The simulation results obtained from Level 3 inputs could not capture field-observed deterioration in terms of crack location. The usefulness of low-level inputs for simulations needs to be investigated, and an approach to mediate this problem needs to be studied.
- DAWRin-ME. Pass and fail result of long-term simulation could not effectively capture crack propagation observed from field cores, even though strong correlation observed from the comparison between maximum BUC % and ACI values from BUC observed sites. This problem need to be studied to build effective design and evaluation tool.
- Implementation and calibration of the LVECD program and associated material test methods. The LVECD program and associated material testing have shown potential to be used as a reliable performance prediction approach for the State of North Carolina. This approach serves as the basis for the FHWA's newly developed Performance-Related Specifications for asphalt concrete and is now being verified using field performance results obtained for various pavements in the U.S. and other countries. Specifications for these test methods are currently being evaluated by the AASHTO Subcommittee of Materials for acceptance as provisional standards. The LVECD program will be released to the FHWA during the month of July 2013 and eventually to the public for routine use for pavement design and analysis.

REFERENCES

1. Ahlrich, R. C. (1996). "Influence of Aggregate Gradation and Particle Shape/Texture on Permanent Deformation of Hot Mix Asphalt Pavements," Final Report. DTFA01-90-Z-02069. Army Engineering Waterways Station, Vicksburg, MS.

2. Al-Qadi, I. and P. J. Yoo (2007). "Surface Tangential Contact Stresses Effect on Flexible Pavement Response," *Journal of Association of Asphalt Paving Technologists*, Vol. 76, pp. 663-692.

3. American Association of State Highway Transportation Officials (AASHTO) (2011). "AASHTO T209-11: Theoretical Maximum Specific Gravity and Density of Hot-Mix Asphalt Paving Mixtures," *AASHTO*, Washington, D.C.

4. American Association of State Highway Transportation Officials (AASHTO) (2008). "AASHTO T308-08: Determining the Asphalt binder content of HMA by the ignition method, *AASHTO*, Washington, D.C.

5. American Association of State Highway Transportation Officials (AASHTO) (2011). "AASHTO T341-11: Standard Method of Test for Determining Dynamic Modulus of Hot-Mix Asphalt Concrete Mixtures," *AASHTO*, Washington, D.C.

6. American Society for Testing and Materials (ASTM) (2011). "ASTM D2726-11: Standard Test Method for Bulk Specific Gravity and Density of Non-Absorptive Compacted Bituminous Mixtures," *ASTM International*, West Conshohocken, PA.

7. American Society for Testing and Materials (ASTM) (2011). "ASTM D2172/D2172M-11: Standard Test Methods for Quantitative Extraction of Bitumen From Bituminous Paving Mixtures," *ASTM International*, West Conshohocken, PA.

8. American Society for Testing and Materials (ASTM) (2012). "ASTM D5404-12: Standard Practice for Recovery of Asphalt from Solution Using the Rotary Evaporator," *ASTM International*, West Conshohocken, PA.

9. American Society for Testing and Materials (ASTM) (2009). "ASTM D6951/D6951M-09 Standard Test Method for Use of the Dynamic Cone Penetrometer in Shallow Pavement Applications," *ASTM International*, West Conshohocken, PA.

10. American Society for Testing and Materials (ASTM) (2011). " ASTM D6752-11: Standard Test Method for Bulk Specific Gravity and Density of Compacted Bituminous Mixtures Using Automatic Vacuum Sealing Method," *ASTM International*, West Conshohocken, PA.

11. American Society for Testing and Materials (ASTM) (2011). "ASTM D7227: Standard Practice for Rapid Drying of Compacted Asphalt Specimens Using Vacuum Drying Apparatus," *ASTM International*, West Conshohocken, PA.

12. American Society for Testing and Materials (ASTM) (2011). "ASTM D2041: Standard Test Method for Theoretical Maximum Specific Gravity and Density of Bituminous Paving Mixtures," *ASTM International*, West Conshohocken, PA.

13. Anderson, D., R. Dongre, D. W. Christensen and L. Dukatz (1992). "Effects of Minus 200 Sized Aggregate on Fracture Behavior of Dense Graded Hot Mix Asphalt," In Effects of Aggregate and Mineral Fillers on Asphalt Mix Performance: ASTM STP 1147, Richard C. Meininger (ed.) ASTM. Philadelphia.

14. Bahia, H. U., Hanson, D. I., Zeng, M., Zhai, H., Khatri, M. A., and Anderson, R. M. (2001). "*Characterization of Modified Asphalt Binders in Superpave Mix Design*," NCHRP Report 459, National Academy Press.

15. Bahia, H. U., H. Zhai, M. Zeng, Y. Hu, and P. Turner (2002). "Development of binder specification parameters based on characterization of damage behavior," *J. Assn. Asphalt Paving Technologists,* Vol. 70, pp. 442-470.

16. Boutin, G. and L. Claude (2000). "Thermal Cracking of Asphalt Pavement," 2nd Euroasphalt & Eurobitumen Congress Barcelona. 0267. UK.

17. Campen, W.H., J.R. Smith, L.G. Erickson, and L.R. Mertz (1959). "The Relationships Between Voids, Surface Area, Film Thickness and Stability in Bituminous Paving Mixtures," Proceedings of the AAPT, 28, pp. 149–178.

18. Christensen, D. W. and R. F. Bonaquist (2006). "Volumetric Requirements for Superpave Mix Design," NCHRP Report 567. National Cooperative Highway Research Program. Transportation Research Board. National Research Council, Washington, D.C.

19. Chehab, G. R. (2002). Characterization of Asphalt Concrete in Tension Using a ViscoElastoPlastic model, Ph.D. Dissertation, North Carolina State University, Raleigh, NC.

20. Choubane, B., G. Page, and J. Musselman (1998). "Investigation of Water Permeability of Coarse-Graded Superpave Pavements," *Journal of Association of Asphalt Paving Technologists*, Vol. 67, pp. 254-276.

21. Cooley, L. A., J. Zhang, P. S. Kandhal, A. J. Hand, and A. E, Martin (2002). "Significance of Restricted Zone in Superpave Aggregare Gradation Specification," *Transportation Research Circular*, Transportation Research Board, National Research Council, Washington, D.C. E-C043.

22. Corley-Lay, J., F. M. Jadoun, J. N. Mastin, and Y. R. Kim (2010). "Comparison of NCDOT and LTPP Monitored Flexible Pavement Distresses," *Transportation Research Record: Journal of the Transportation Research Board,* Transportation Research Board, National Research Council, Washington, D.C.

23. Deacon, J. A., A. A. Tayebali, G. M. Rowe and C. L. Monismith (1995). "Validation of SHRP A-003A Flexural Beam Fatigue Test. In Engineering Properties of Asphalt Mixtures and the Relationship to Their Performance," ASTM STP 1265, pp. 21-36.

24. Epps, A. L. and A. J. Hand (2001). "A Comparison of HMA Field Performance and Laboratory Volumetric Sensitivies," *Journal of Association of Asphalt Paving Technologists*, Vol. 70, pp. 671-711.

25. Epps, J. A. and C. L. Monismith (1969). "Influence of Mixture Variables on the Flexural Fatigue Properties of Asphalt Concrete," *Journal of Association of Asphalt Paving Technologists*, Vol. 38, pp. 423-464.

26. Epps, J. A. and C. L. Monismith (1972) "Fatigue of Asphalt Concrete Mixtures Summary of Existing Information," In Fatigue of Compacted Bituminous Aggregate Mixtures, ASTM STP 508, ASTM, pp. 59-45.

27. Epps, J. A, A. Hand, S. Seeds, T. Schulz, S. Alavi, C. Ashmore, C. L. Monismith, J. A. Deacon, J. T. Harvey and R. Leahy (2002). "Recommended Performance Related Specification for Hot-Mix Asphalt Construction: Results of the Westrack Project," NCHRP Report 455. National Cooperative Highway Research Program. Transportation Research Board. National Research Council, Washington, D.C.

28. Eslaminia, M., S. Thirunavukkarasu, M. N. Guddati, and Y. R. Kim (2012). "Accelerated Pavement Performance Modeling Using Layered Viscoelastic Analysis," *7th International RILEM Conference on Cracking in Pavements*, Delft, The Netherlands, pp. 20-22.

29. Freeman, R. B., H. Bell, R. Brown, and M. Mariely (2009). "Fatigue Evaluation Criteria for Aged Asphalt Concrete Surfaces," 88th Annual Meeting of the Transportation Research Board. National Research Council, Washington, D.C. DVD-ROM.

30. Ghuzlan, K. A. and S. H. Carpenter (2002). "Traditional Fatigue Analysis of Asphalt Concrete Mixtures," Transportation Research Record, Annual Meeting CD-ROM.

31. Glover, C. J., A.E. Martin, A. Chowdhury, R. Han, N. Paraitrakul, X. Jin, and J. Lawrence (2009), "Evaluation of Binder Aging and Its Influence on Hot Mix Asphalt Concrete: Literature Review and Experimental Design," Texas Transportation Institute, Texas Department of Transportation, Federal Highway Administration.

32. Harmelink, D. and T. Aschenbrener (2003). Extent of Top-Down Cracking in Colorado, Report No. CDOT-DTD-R-2003-7, Denver, CO: Colorado Department of Transportation, 53 pp.

33. Hefer, A. W., D. N. Little, and R. L. Lytton (2005). "A Synthesis of Theories and Mechanisms of Bitumen-Aggregate Adhesion Including Recent Advances in Quantifying the Effects of Water," *Journal of the Association of Asphalt Paving Technologists* 74: pp. 139-196.

34. Hintz, C and H. U. Bahia (2013). "Simplification of the Linear Amplitude Sweep Test and Specification Parameter," *Transportation Research Record: Journal of the transportation Research Board,* Transportation Research Board, National Research Council, Washington, D.C.

35. Holewinski, J. M., S. Soon, A. Drescher and H. Stolarski (2003). Investigation of Factors Related to Surface-Initiated Cracks in Flexible Pavements, Final Report to the Minnesota Department of Transportation, Report No. MN/RC-2003-07, Springfield, VA: National Technical Information Services, 191 pp.

36. Hu, X. and L. F. Walubita (2011). "Effects of layer Interfacial Bonding Conditions on the Mechanistic Responses in Asphalt Pavements," ASCE *Journal of Transportation Engineering.*

37. Hugo, F. and T. W. Kennedy (1985). "Surface Cracking of Asphalt Mixtures in Southern Africa," Proceedings of the Association of Asphalt Paving Technologists, Vol. 54, pp. 454-496.

38. Jackson, N. C., R. Deighton and D. L. Huft (1996). "Development of Pavement Performance Curves for Individual Distress Indexes in South Dakota Based on Expert Opinion," *Transportation Research Record*: *Journal of the Transportation Research Board,* No. 1524, National Research Council, Washington, D.C. pp. 130-136.

39. Jackson, N. and J. Puccinelli (2006). "*Long-Term Pavement Performance (LTPP) Data Analysis Support: National Pooled Fund Study TPF-5(013)-Effect of Multiple Freeze Cycles and Deep Frost Penetration on Pavement performance and Cost,"* Publication FHWA-HRT-06-121. FHWA, U.S. Department of Transportation.

40. Jacobs, M. J. (1995). Crack Growth in Asphaltic Mixes. Ph.D. Dissertation, Delft Technical University, Delft, Netherlands.

41. Johnson, C.M. and H.U. Bahia (2010). "Evaluation of an Accelerated Procedure for Fatigue Characterization of Asphalt Binders," Submitted for publication in *Road Materials and Pavement Design*, 2010.

42. Kandhall, P. S. and L. A. Cooley (2002). "Coarse- Versus Fine-Graded Superpave Mixtures: Comparative Evaluation of Resistance to Rutting," Transportation Research

Record. No. 1789, *Transportation Research Board*, National Research Council, Washington, D.C., pp. 216-224.

43. Khosla, N. P. and S. Sadasivam (2004). "Determinaton of Optimum Gradation for Resistance to Permeability, Rutting and Fatigue Cracking," Final Report. Report No. FHWA/NC/2004-012.

44. Kim, Y. R., J. S. Daniel, and H. Wen (2002). "Fatigue Performance Evaluation of WesTrack Asphalt Mixtures using Viscoelastic Continuum Damage Approach," Final Report. Report No. FHWA/NC/2002-004.

45. Kim, Y. R., M. Momen, M. King (2005). "Typical Dynamic Moduli for North Carolina Asphalt Concrete Mixtures," Final Report. Report No. FHWA/NC/2005-03.

46. Kose, S., M. Guler, H. U. Bahia, and E Masad (2000). "Distribution of Strains Within Hot-Mix Asphalt Binders," *Transportation Research Record*: *Journal of the Transportation Research Board,* No. 1728, National Research Council, Washington, D.C., pp. 21-27.

47. Kutay, M. E., N. H. Gibson, J. Youtcheff, and R. Dongre (2009). "Use of Small Samples to Predict Fatigue Lives of Field Cores: Newly Developed Formulation Based on Viscoelastic Continuum Damage Theory," *Transportation Research Record*: *Journal of the Transportation Research Board,* No. 2127, National Research Council, Washington, D.C., pp. 90-97.

48. Lee, S. (2007). Investigation of the Effects of Lime on the Performance of HMA using Advanced Testing and Modeling Techniques. Ph.D. Dissertation. North Carolina State University, Raleigh, NC.

49. Mahoney, J. P. (2001). "Study of Long-Lasting Pavements in Washington State," Perpetual Bituminous Pavements, Transportation Research Circular No. 503, Washington, D.C.: Transportation Research Board, pp. 88-95.

50. Malan, G. W., P. J. Straus, and F. Hugo (1989). "A Field Study of Premature Surface Cracking in Asphalt," *Journal of Association of Asphalt Paving Technologists*, Vol. 58, pp. 142-162.

51. Matsuno, S. and T. Nishizawa (1992). "Mechanism of Longitudinal Surface Cracking in Asphalt Pavements," Proceedings of the Seventh International Conference on Asphalt Pavements, Vol. 2, Nottingham, U.K., pp. 277-291.

52. Maupin, G. W. (1970). "Effect of Particle Shape and Surface Texture on the Fatigue Behavior of Asphaltic Concrete," Highway Research Record No. 313. Highway Research Board, pp. 55-62.

53. Merrill, D. (2000). Investigating the Causes of Surface Cracking in Flexible Pavements Using Improved Mathematical Models, Ph.D. Dissertation, Swansea, Wales, U.K.: University of Wales.

54. Metcalf, J. B., Li, Y., S. A. Romanoschi, and M. Rasoulian (1999). "Comparison of Louisiana's conventional and alternative base courses under accelerated loading: Final report," Rep. No. 93-2ALF, Louisiana Transportation Research Center, Baton Rouge, LA.

55. Minnesota Department of Transportation (2002). "MnRoad Mainline Test Road Top-Down Cracking," Distributed at the FHWA Mixture Expert Task Group Meeting, August 2002, Minneapolis, MN.

56. Mun, S. (2003). Nonlinear Finite Element Analysis of Pavements and Its Application to Performance Evaluation, Ph.D. Dissertation, Department of Civil Engineering, North Carolina State University, 106 pp.

57. Myers, L. A., R. Roque and B. E. Ruth (1998). "Mechanisms of Surface-Initiated Longitudinal Wheel Path Cracks in High Type Bituminous Pavements," *Journal of Association of Asphalt Paving Technologists*, Vol. 65, pp. 401-432.

58. Myers, L. (2000). Development and Propagation of Surface-Initiated Longitudinal Wheel Path Cracks in Flexible Highway Pavements, Ph.D. Disseration, Gainesville, FA: University of Florida.

59. Myers, L. A. and R. Roque (2001). "Evaluation of Top-Down Cracking in Thick Asphalt Pavements and the Implications for Pavement Design," Transportation Research Circular: Perpetual Bituminous Materials. Washington, D.C.

60. NCHRP (2004a). "2002 Design Guide: Design of New and Rehabilitated Pavement Structures," NCHRP 1-37A Project, National Cooperative Highway Research Program. National Research Council, Washington, D.C.

61. NCHRP (2004 b). "*Guide for Mechanistic-Empirical Design of New and Rehabilitated Pavement Structures*," NCHRP 1-37A Project, Part 2 *National Cooperative Highway Research Program.* National Research Council, Washington, D.C.

62. NCHRP (2004c). "Top-Down Fatigue Cracking of Hot-Mix Asphalt Layers," NCHRP 1-42 Project, National Research Council, Washington, D.C.

63. Rao Tangella, S. C., J. Craus, J. A. Deacon and C. L. Monismith (1990). "Summary Report on Fatigue Response of Asphalt Mixtures," Report TM-UCB-A-003A-89-3. Strategic Highway Research Program. National Research Council, Washington, D.C.

64. Pell, P. S. and I. F. Taylor (1969). "Asphaltic Road Mixtures in Fatigue," *Journal of Association of Asphalt Paving Technologists*, Vol. 38, pp. 371-422.

65. Pellinen, T. (2002). "Evaluation of Surface (top-down) Longitudinal Wheel Path Cracking in Indiana," Joint Transportation Research Program. Purdue University, West Lafayette, IN.

66. Pierce, L. and N. Sivaneswara (1999). FWD AREA Program. WSDOT web document.

67. Roque, R. (2002). "Top-Down Cracking: Causes and Potential Solutions," Presented at the Southeast Asphalt User/Producer Group Meeting.

68. Scala, A. J. (1959), "Simple Method of Flexible Pavement Design Using Cone Penetrometers," *Proceedings of 2nd Australian – New Zealand Conference on Soil Mechanics and Foundation Engineering,* New Zealand.

69. Schapery, R.A. (1984). "Correspondence principles and a generalized J-integral for large deformation and fracture analysis of viscoelastic media," *Int. J. Fract.*, Vol. 25, pp.195-223.

70. Schorsch, M. and G. Y. Baladi (2004). "Effects of Moisture Damage and Segregation on TopDown Cracking in Flexible Pavements," Submitted to the Transportation Research Board 83d Annual Meeting, Washington, D.C.

71. Sebaaly, P. E., Z. Eid, and J. A. Epps (2001). "Evaluation of Moisture Sensitivity Properties of ADOT Mixtures on US93," Volume I: Final Report. Report No. FHWA-AZ98-402-01. Arizona Department of Transportation.

72. Soon, S., A. Drescher, H. K. Stolarski (2003). "Tire-Induced Surface Stresses in Flexible Pavements," Submitted to the Transportation Research Board 82nd Annual Meeting, Washington, D.C.

73. Svasdisant, T., M. Schorsch, G. Y. Baladi and S. Pinyosunun (2002). "Mechanistic Analysis of Top-Down Cracks in Asphalt Pavements," Submitted to the Transportation Research Board 81st Annual Meeting, Washington, D.C.

74. Tayebali, A. A. and Y. Huang (2004). "Material Characterization and Performance Properties of Superpave Mixtures," Final Report. Report No. FHWA/NC/2004-011.

75. Tsai, B.W., C. L. Monismith, M. Dunning, N. Gibson, J. D'Angelo, R. Leahy, G. King, D. Christensen, D. Anderson, R. Davis, and D. Jones (2005). "Influence of asphalt binder properties on the fatigue performance of asphalt concrete pavements," *J. Assn. Asphalt Paving Technologists,* Vol. 74, pp. 733-789.

76. Uhlmeyer, J. S., K. Willoughby, L. M. Pierce and J. P. Mahoney (2000). "Top-Down Cracking in Washington State Asphalt Concrete Wearing Courses," *Transportation Research Record*. No. 1730, Transportation Research Board, National Research Council, Washington, D.C., pp. 110-116.

77. Underwood, S., A.H. Heidari, M. Guddati, and Y.R. Kim (2005). "Experimental Investigation of Anisotropy in Asphalt Concrete," *Transportation Research Record*, 1929, National Research Council, Washington, D.C., pp. 238-247.

78. Underwood, B. S. and Y. R. Kim (2003). "Determination of Depth of Surface Cracks in Asphalt Pavements," *Transportation Research Record*. No. 1853, Transportation Research Board, National Research Council, Washington, D.C., pp. 143-149.

79. Underwood, B.S., Y.R. Kim, and M.N. Guddati (2010). "Improved Calculation Method of Damage Parameter in Viscoelastic Continuum Damage Model," *International Journal of Pavement Engineering.*

80. Valkering, C. P. and G. VanGooswilligen (1989). "The Role of the Binder Content in The Performance of Asphaltic Mixes for Surface Layers." *Journal of Association of Asphalt Paving Technologists*, Vol. 58, pp. 238-255.

81. Walubita, L. F., and S. Scullion (2007). "Perpetual pavements in Texas: The fort worth SH 114 perpetual pavement in Wise County," Technical Rep. No. FHWA/TX-05/0-4822-2, TTI, College Station, TX.

82. Wamburga, J. H. G., J. N. Maina and H. R. Smith (1999). "Kenya Asphaltic Materials Study," submitted to the Transportation Research Board 78th Annual Meeting, Washington, D.C.

83. Wang, L. B., L. A. Myers, L. N. Mohammad, and Y. R. Fu (2003). "A Micromechanics Study on Top-Down Cracking," Submitted to the Transportation Research Board 82nd Annual Meeting, Washington, D.C.

84. Worel, B. (2003). "MnRoad HMA Performance," Presented at the MnRoad Workshop, Mn/Road Office of Materials, http://mnroad.dot.state.mn.us, Maplewood, MN.

85. Washington State Department of Transportation, "Top-Down Cracking: Pavement Evaluation Module 9," at http://hotmix.ce.washington.edu/wsdot_web/Modules/09_pavement_evaluation/top_down.

86. Webster, S. L., R. H. Grau and T. P. Williams (1992). "*Description and Application of Dual Mass Dynamic Cone Penetrometer*," Report GL-92-3, Department of the Army, Washington, DC.

87. Zhou, F., H. Sheng, T. Scullion, M. Mikhail and L. Walubita (2007). "A Balanced HMA Mix Design Procedure for Overlays," Journal of Association of Asphalt Paving Technologists, Vol. 76, pp. 823-850.

APPENDICES

Appendix A: Master Database for the Research

Master Database for the Research

Table A.1 Master Database part 1 of test level 1

	from NCDOT Database				Field Observation															Longitudinal Cracking (ft.)
Test Level	Cond group (2010)	County	Route	age (2010)	Loc ID	Lane Width	Number of Lanes	Shldr Type	Shldr Width (ft.)	TDC?	BUC?	Widening?	Debonding?	Patching?	T Cracking?	Oxidization	Condition region lane length	Transvers Cracking (ft.) Total Crack Length	Occurence (Partial)	Occurence (full)	Occurrence Length	Average Space	Length
1	Y & P	Wake	I-540	9	B1	12	3	Paved	5	Yes	No	No	Yes	No	Yes	No	100	53	2	3	88	22	19
1	Y & P	Wake	I-540	9	B1	12	3	Paved	5	Yes	No	No	Yes	No	Yes	No	100	53	2	3	88	22	19
1	Y & P	Wake	I-540	9	B1	12	3	Paved	5	Yes	No	No	Yes	No	Yes	No	100	53	2	3	88	22	19
1	Y & P	Wake	I-540	9	B1	12	3	Paved	5	Yes	No	No	Yes	No	Yes	No	100	53	2	3	88	22	19
1	Y & P	Wake	I-540	9	A1	12	3	Paved	5	No	No	No	Yes	No	Yes	No	94	24	0	2	33	33	0
1	Y & P	Wake	I-540	9	A1	12	3	Paved	5	No	No	No	Yes	No	Yes	No	94	24	0	2	33	33	0
1	Y & P	Wake	I-540	9	A1	12	3	Paved	5	No	No	No	Yes	No	Yes	No	94	24	0	2	33	33	0
1	Y & P	Wake	I-540	9	A1	12	3	Paved	5	No	No	No	Yes	No	Yes	No	94	24	0	2	33	33	0
1	Y & P	Wake	I-540	9	B2	12	3	Paved	5	Yes	No	No	Yes	No	Yes	No	196	24	0	2	56	56	0
1	Y & P	Wake	I-540	9	B2	12	3	Paved	5	Yes	No	No	Yes	No	Yes	No	196	24	0	2	56	56	0
1	Y & P	Wake	I-540	9	B2	12	3	Paved	5	Yes	No	No	Yes	No	Yes	No	196	24	0	2	56	56	0
1	Y & P	Wake	I-540	9	B2	12	3	Paved	5	Yes	No	No	Yes	No	Yes	No	196	24	0	2	56	56	0
1	Y & P	Wake	I-540	9	A2	12	3	Paved	5	No	No	No	Yes	No	No	No	100	0	0	0	0	0	0
1	Y & P	Wake	I-540	9	A2	12	3	Paved	5	No	No	No	Yes	No	No	No	100	0	0	0	0	0	0
1	Y & P	Wake	I-540	9	A2	12	3	Paved	5	No	No	No	Yes	No	No	No	100	0	0	0	0	0	0
1	Y & P	Wake	I-540	9	A2	12	3	Paved	5	No	No	No	Yes	No	No	No	100	0	0	0	0	0	0
1	Y & P	Mecklenburg	NC24	6	B1	12	2	no/ curb	0	Yes	No	No	Yes	No	Yes	No	400	21	1	1	39	39	32
1	Y & P	Mecklenburg	NC24	6	B1	12	2	no/ curb	0	Yes	No	No	Yes	No	Yes	No	400	21	1	1	39	39	32
1	Y & P	Mecklenburg	NC24	6	B1	12	2	no/ curb	0	Yes	No	No	Yes	No	Yes	No	400	21	1	1	39	39	32
1	Y & P	Mecklenburg	NC24	6	A1	12	2	no/ curb	0	Yes	No	No	Yes	No	Yes	No	124	34	6	0	40	8	7
1	Y & P	Mecklenburg	NC24	6	A1	12	2	no/ curb	0	Yes	No	No	Yes	No	Yes	No	124	34	6	0	40	8	7
1	Y & P	Mecklenburg	NC24	6	A1	12	2	no/ curb	0	Yes	No	No	Yes	No	Yes	No	124	34	6	0	40	8	7
1	Y & P	Mecklenburg	NC24	6	B2	12	2	no/ curb	0	Yes	No	No	Yes	No	No	No	82	7	1	0	0	0	10
1	Y & P	Mecklenburg	NC24	6	B2	12	2	no/ curb	0	Yes	No	No	Yes	No	No	No	82	7	1	0	0	0	10
1	Y & P	Mecklenburg	NC24	6	B2	12	2	no/ curb	0	Yes	No	No	Yes	No	No	No	82	7	1	0	0	0	10
1	O & G	Johnston	US-70	3	B1	12	2	No	0	No	No	No	Yes	No	No	No	100	0	0	0	0	0	50
1	O & G	Johnston	US-70	3	B1	12	2	No	0	No	No	No	Yes	No	No	No	100	0	0	0	0	0	50
1	O & G	Johnston	US-70	3	B1	12	2	No	0	No	No	No	Yes	No	No	No	100	0	0	0	0	0	50
1	O & G	Johnston	US-70	3	B1	12	2	No	0	No	No	No	Yes	No	No	No	100	0	0	0	0	0	50
1	O & G	Johnston	US-70	3	B2	12	2	No	0	Yes	No	No	Yes	No	No	No	100	0	0	0	0	0	55
1	O & G	Johnston	US-70	3	B2	12	2	No	0	Yes	No	No	Yes	No	No	No	100	0	0	0	0	0	55
1	O & G	Johnston	US-70	3	B2	12	2	No	0	Yes	No	No	Yes	No	No	No	100	0	0	0	0	0	55
1	O & G	Johnston	US-70	3	B2	12	2	No	0	Yes	No	No	Yes	No	No	No	100	0	0	0	0	0	55
1	O & G	Johnston	US-70	3	A1	12	2	No	0	No	No	No	Yes	No	No	No	100	0	0	0	0	0	11
1	O & G	Johnston	US-70	3	A1	12	2	No	0	No	No	No	Yes	No	No	No	100	0	0	0	0	0	11
1	O & G	Johnston	US-70	3	A1	12	2	No	0	No	No	No	Yes	No	No	No	100	0	0	0	0	0	11
1	O & G	Johnston	US-70	3	A1	12	2	No	0	No	No	No	Yes	No	No	No	100	0	0	0	0	0	11
1	O & G	Johnston	US-70	3	A2	12	2	No	0	No	No	No	Yes	No	No	No	100	0	0	0	0	0	0
1	O & G	Johnston	US-70	3	A2	12	2	No	0	No	No	No	Yes	No	No	No	100	0	0	0	0	0	0
1	O & G	Johnston	US-70	3	A2	12	2	No	0	No	No	No	Yes	No	No	No	100	0	0	0	0	0	0
1	O & G	Johnston	US-70	3	A2	12	2	No	0	No	No	No	Yes	No	No	No	100	0	0	0	0	0	0
1	O & G	Brunswick	US17	20	B1	12	2	Paved	5	Yes	No	No	No	No	Yes	Yes	98	21	1	1	73	73	49
1	O & G	Brunswick	US17	20	B1	12	2	Paved	5	Yes	No	No	No	No	Yes	Yes	98	21	1	1	73	73	49
1	O & G	Brunswick	US17	20	B1	12	2	Paved	5	Yes	No	No	No	No	Yes	Yes	98	21	1	1	73	73	49
1	O & G	Brunswick	US17	20	B1	12	2	Paved	5	Yes	No	No	No	No	Yes	Yes	98	21	1	1	73	73	49
1	O & G	Brunswick	US17	20	B2	12	2	Paved	5	Yes	No	No	No	No	No	Yes	70	4	1	0	0	0	30
1	O & G	Brunswick	US17	20	B2	12	2	Paved	5	Yes	No	No	No	No	No	Yes	70	4	1	0	0	0	30
1	O & G	Brunswick	US17	20	B2	12	2	Paved	5	Yes	No	No	No	No	No	Yes	70	4	1	0	0	0	30
1	O & G	Brunswick	US17	20	B2	12	2	Paved	5	Yes	No	No	No	No	No	Yes	70	4	1	0	0	0	30
1	O & G	Brunswick	US17	20	A1	12	2	Paved	5	No	No	No	No	No	No	Yes	70	0	0	0	0	0	44
1	O & G	Brunswick	US17	20	A1	12	2	Paved	5	No	No	No	No	No	No	Yes	70	0	0	0	0	0	44
1	O & G	Brunswick	US17	20	A1	12	2	Paved	5	No	No	No	No	No	No	Yes	70	0	0	0	0	0	44
1	O & G	Brunswick	US17	20	A1	12	2	Paved	5	No	No	No	No	No	No	Yes	70	0	0	0	0	0	44
1	O & G	Brunswick	US17	20	A2	12	2	Paved	5	No	No	No	No	No	No	Yes	66	0	0	0	0	0	58
1	O & G	Brunswick	US17	20	A2	12	2	Paved	5	No	No	No	No	No	No	Yes	66	0	0	0	0	0	58
1	O & G	Brunswick	US17	20	A2	12	2	Paved	5	No	No	No	No	No	No	Yes	66	0	0	0	0	0	58
1	O & G	Brunswick	US17	20	A2	12	2	Paved	5	No	No	No	No	No	No	Yes	66	0	0	0	0	0	58
1	Y & P	Union	US601	10	A1	11.5	2	Paved	4	Yes	Yes	No	No	No	Yes	No	148	104.5	1	9	97	10.78	13
1	Y & P	Union	US601	10	A1	11.5	2	Paved	4	Yes	Yes	No	No	No	Yes	No	148	104.5	1	9	97	10.78	13
1	Y & P	Union	US601	10	A1	11.5	2	Paved	4	Yes	Yes	No	No	No	Yes	No	148	104.5	1	9	97	10.78	13
1	Y & P	Union	US601	10	A1	11.5	2	Paved	4	Yes	Yes	No	No	No	Yes	No	148	104.5	1	9	97	10.78	13
1	Y & P	Union	US601	10	B1	11.5	2	Paved	4	Yes	Yes	No	Yes	No	Yes	No	198	193.5	13	9	168	8.84	42
1	Y & P	Union	US601	10	B1	11.5	2	Paved	4	Yes	Yes	No	Yes	No	Yes	No	198	193.5	13	9	168	8.84	42
1	Y & P	Union	US601	10	B1	11.5	2	Paved	4	Yes	Yes	No	Yes	No	Yes	No	198	193.5	13	9	168	8.84	42
1	Y & P	Union	US601	10	B1	11.5	2	Paved	4	Yes	Yes	No	Yes	No	Yes	No	198	193.5	13	9	168	8.84	42
1	Y & P	Union	US601	10	B2	11.5	2	Paved	4	No	Yes	No	Yes	No	Yes	No	286	48.5	2	3	20	5	147
1	Y & P	Union	US601	10	B2	11.5	2	Paved	4	No	Yes	No	Yes	No	Yes	No	286	48.5	2	3	20	5	147
1	Y & P	Union	US601	10	B2	11.5	2	Paved	4	No	Yes	No	Yes	No	Yes	No	286	48.5	2	3	20	5	147
1	Y & P	Union	US601	10	B2	11.5	2	Paved	4	No	Yes	No	Yes	No	Yes	No	286	48.5	2	3	20	5	147
1	Y & P	New Hanover	US76	11	B1	13	2	no/ curb	0	Yes	No	No	No	No	Yes	Yes	150	60	2	3	16	4	110
1	Y & P	New Hanover	US76	11	B1	13	2	no/ curb	0	Yes	No	No	No	No	Yes	Yes	150	60	2	3	16	4	110
1	Y & P	New Hanover	US76	11	B1	13	2	no/ curb	0	Yes	No	No	No	No	Yes	Yes	150	60	2	3	16	4	110
1	Y & P	New Hanover	US76	11	A1	13	2	no/ curb	0	Yes	Yes	No	No	No	Yes	Yes	196	18	2	0	70	70	24
1	Y & P	New Hanover	US76	11	A1	13	2	no/ curb	0	Yes	Yes	No	No	No	Yes	Yes	196	18	2	0	70	70	24
1	Y & P	New Hanover	US76	11	A1	13	2	no/ curb	0	Yes	Yes	No	No	No	Yes	Yes	196	18	2	0	70	70	24
1	Y & P	Cumberland	NC87	8	A1	12	2	Paved	3	No	No	No	No	No	No	No	122	0	0	0	0	0	17
1	Y & P	Cumberland	NC87	8	A1	12	2	Paved	3	No	No	No	No	No	No	No	122	0	0	0	0	0	17
1	Y & P	Cumberland	NC87	8	A1	12	2	Paved	3	No	No	No	No	No	No	No	122	0	0	0	0	0	17
1	Y & P	Cumberland	NC87	8	A1	12	2	Paved	3	No	No	No	No	No	No	No	122	0	0	0	0	0	17
1	Y & P	Cumberland	NC87	8	A1	12	2	Paved	3	No	No	No	No	No	No	No	122	0	0	0	0	0	17
1	Y & P	Cumberland	NC87	8	B1	12	2	Paved	3	Yes	No	No	Yes	No	Yes	No	118	96	2	7	106	13.25	39
1	Y & P	Cumberland	NC87	8	B1	12	2	Paved	3	Yes	No	No	Yes	No	Yes	No	118	96	2	7	106	13.25	39
1	Y & P	Cumberland	NC87	8	B1	12	2	Paved	3	Yes	No	No	Yes	No	Yes	No	118	96	2	7	106	13.25	39
1	Y & P	Cumberland	NC87	8	B1	12	2	Paved	3	Yes	No	No	Yes	No	Yes	No	118	96	2	7	106	13.25	39
1	Y & P	Cumberland	NC87	8	B1	12	2	Paved	3	Yes	No	No	Yes	No	Yes	No	118	96	2	7	106	13.25	39
1	Y & P	Cumberland	NC87	8	A2	12	2	Paved	3	No	Yes	No	No	No	Yes	No	114	36	0	3	50	25	24
1	Y & P	Cumberland	NC87	8	A2	12	2	Paved	3	No	Yes	No	No	No	Yes	No	114	36	0	3	50	25	24
1	Y & P	Cumberland	NC87	8	A2	12	2	Paved	3	No	Yes	No	No	No	Yes	No	114	36	0	3	50	25	24
1	Y & P	Cumberland	NC87	8	A2	12	2	Paved	3	No	Yes	No	No	No	Yes	No	114	36	0	3	50	25	24
1	Y & P	Cumberland	NC87	8	A2	12	2	Paved	3	No	Yes	No	No	No	Yes	No	114	36	0	3	50	25	24
1	Y & P	Cumberland	NC87	8	B2	12	2	Paved	3	Yes	Yes	Yes	Yes	No	Yes	No	240	106	6	5	202	20.2	127
1	Y & P	Cumberland	NC87	8	B2	12	2	Paved	3	Yes	Yes	Yes	Yes	No	Yes	No	240	106	6	5	202	20.2	127
1	Y & P	Cumberland	NC87	8	B2	12	2	Paved	3	Yes	Yes	Yes	Yes	No	Yes	No	240	106	6	5	202	20.2	127
1	Y & P	Cumberland	NC87	8	B2	12	2	Paved	3	Yes	Yes	Yes	Yes	No	Yes	No	240	106	6	5	202	20.2	127
1	Y & P	Cumberland	NC87	8	B2	12	2	Paved	3	Yes	Yes	Yes	Yes	No	Yes	No	240	106	6	5	202	20.2	127
1	Y & P	Swain	US74	9	B1	12	2	Paved	8	No	Yes	No	No	No	Yes	No	290	48	10	0	150	16.67	162
1	Y & P	Swain	US74	9	B1	12	2	Paved	8	No	Yes	No	No	No	Yes	No	290	48	10	0	150	16.67	162
1	Y & P	Swain	US74	9	B1	12	2	Paved	8	No	Yes	No	No	No	Yes	No	290	48	10	0	150	16.67	162
1	Y & P	Swain	US74	9	A1	12	2	Paved	8	No	Yes	No	No	No	Yes	No	266	101	7	5	210	19.1	237
1	Y & P	Swain	US74	9	A1	12	2	Paved	8	No	Yes	No	No	No	Yes	No	266	101	7	5	210	19.1	237
1	Y & P	Swain	US74	9	A1	12	2	Paved	8	No	Yes	No	No	No	Yes	No	266	101	7	5	210	19.1	237
1	O & G	Haywood	NC209	17	A1	10	1	Paved	1	No	No	No	No	No	No	No	106	0	0	0	0	0	0
1	O & G	Haywood	NC209	17	A1	10	1	Paved	1	No	No	No	No	No	No	No	106	0	0	0	0	0	0
1	O & G	Haywood	NC209	17	A1	10	1	Paved	1	No	No	No	No	No	No	No	106	0	0	0	0	0	0
1	O & G	Haywood	NC209	17	B1	10	1	Paved	1	No	No	No	No	Yes	No	No	148	0	0	0	0	0	21
1	O & G	Haywood	NC209	17	B1	10	1	Paved	1	No	No	No	No	Yes	No	No	148	0	0	0	0	0	21
1	O & G	Haywood	NC209	17	B1	10	1	Paved	1	No	No	No	No	Yes	No		148	0	0	0	0	0	21

Table A.2 Master Database part 1 of test level 2

	from NCDOT Database				Field Observation													Transvers Cracking (ft.)					
Test Level	Cond group (2010)	County	Route	age (2010)	Loc ID	Lane Width	Number of Lanes	Shldr Type	Shldr Width (ft.)	TDC?	BUC?	Widening?	Debonding?	Patching?	T Cracking?	Oxidization	Condition region lane length	Total Crack	Occurence	Occurence	Occurrence	Average	Longitudinal Length
2	O & G	Martin	US13	7	A1	12	2	Paved	2	No	No	No	No	No	No	No	70	12	0	1	0	0	19
2	O & G	Martin	US13	7	A1	12	2	Paved	2	No	No	No	No	No	No	No	70	12	0	1	0	0	19
2	O & G	Martin	US13	7	A1	12	2	Paved	2	No	No	No	No	No	No	No	70	12	0	1	0	0	19
2	O & G	Martin	US13	7	B1	12	2	Paved	2	Yes	No	No	Yes	No	No	No	134	0	0	0	0	0	40
2	O & G	Martin	US13	7	B1	12	2	Paved	2	Yes	No	No	Yes	No	No	No	134	0	0	0	0	0	40
2	O & G	Martin	US13	7	B1	12	2	Paved	2	Yes	No	No	Yes	No	No	No	134	0	0	0	0	0	40
2	O & G	Martin	US13	7	B2	12	2	Paved	2	Yes	No	No	Yes	No	No	No	66	0	0	0	0	0	36
2	O & G	Martin	US13	7	B2	12	2	Paved	2	Yes	No	No	Yes	No	No	No	66	0	0	0	0	0	36
2	O & G	Martin	US13	7	B2	12	2	Paved	2	Yes	No	No	Yes	No	No	No	66	0	0	0	0	0	36
2	O & G	Martin	US13	7	A2	12	2	Paved	2	No	No	No	No	No	No	No	134	0	0	0	0	0	58
2	O & G	Martin	US13	7	A2	12	2	Paved	2	No	No	No	No	No	No	No	134	0	0	0	0	0	58
2	O & G	Martin	US13	7	A2	12	2	Paved	2	No	No	No	No	No	No	No	134	0	0	0	0	0	58
2	Y & P	Richmond	NC177	7	B1	11	1	Paved	1	No	Yes	No	No	No	Yes	No & Yes	284	64	8	1	280	40	194
2	Y & P	Richmond	NC177	7	B1	11	1	Paved	1	No	Yes	No	No	No	Yes	No & Yes	284	64	8	1	280	40	194
2	Y & P	Richmond	NC177	7	A1	11	1	Paved	1	No	Yes	No	No	No	Yes	No & Yes	180	64	10	1	168	16.8	58
2	Y & P	Richmond	NC177	7	A1	11	1	Paved	1	No	Yes	No	No	No	Yes	No & Yes	180	64	10	1	168	16.8	58
2	Y & P	Richmond	NC177	7	A2	11	1	Paved	1	No	Yes	No	No	No	Yes	No & Yes	288	144	18	1	259	14.39	38
2	Y & P	Richmond	NC177	7	A2	11	1	Paved	1	No	Yes	No	No	No	Yes	No & Yes	288	144	18	1	259	14.39	38
2	Y & P	Richmond	NC177	7	B2	11	1	Paved	1	No	Yes	No	No	No	Yes	No & Yes	280	37	7	0	194	32.33	26
2	Y & P	Richmond	NC177	7	B2	11	1	Paved	1	No	Yes	No	No	No	Yes	No & Yes	280	37	7	0	194	32.33	26
2	Y & P	Montgomery	US220	7	B1	9	1	Paved	3	Yes	Yes	Yes	Yes	No	Yes	No	252	77	4	5	200	25	167
2	Y & P	Montgomery	US220	7	B1	9	1	Paved	3	Yes	Yes	Yes	Yes	No	Yes	No	252	77	4	5	200	25	167
2	Y & P	Montgomery	US220	7	B1	9	1	Paved	3	Yes	Yes	Yes	Yes	No	Yes	No	252	77	4	5	200	25	167
2	Y & P	Montgomery	US220	7	A1	9	1	Paved	3	Yes	Yes	Yes	No	No	Yes	No	368	174	10	11	346	34.6	148
2	Y & P	Montgomery	US220	7	A1	9	1	Paved	3	Yes	Yes	Yes	No	No	Yes	No	368	174	10	11	346	34.6	148
2	Y & P	Montgomery	US220	7	A1	9	1	Paved	3	Yes	Yes	Yes	No	No	Yes	No	368	174	10	11	346	34.6	148
2	Y & P	Davidson	NC47	9	B1	10	1	No	0	Yes	Yes	Yes	Yes	No	No	No	164	0	0	0	0	0	11
2	Y & P	Davidson	NC47	9	B1	10	1	No	0	Yes	Yes	Yes	Yes	No	No	No	164	0	0	0	0	0	11
2	Y & P	Davidson	NC47	9	B1	10	1	No	0	Yes	Yes	Yes	Yes	No	No	No	164	0	0	0	0	0	11
2	Y & P	Davidson	NC47	9	A1	10	1	No	0	No	Yes	Yes	Yes	No	No	No	100	0	0	0	0	0	24
2	Y & P	Davidson	NC47	9	A1	10	1	No	0	No	Yes	Yes	Yes	No	No	No	100	0	0	0	0	0	24
2	Y & P	Davidson	NC47	9	B2	10	1	No	0	Yes	Yes	Yes	Yes	No	Yes	No	246	12.5	2	0	1	1	27
2	Y & P	Davidson	NC47	9	B2	10	1	No	0	Yes	Yes	Yes	Yes	No	Yes	No	246	12.5	2	0	1	1	27
2	Y & P	Davidson	NC47	9	B2	10	1	No	0	Yes	Yes	Yes	Yes	No	Yes	No	246	12.5	2	0	1	1	27
2	Y & P	Cumberland	NC82	6	B1	10.5	1	No	0	No	No	No	No	No	Yes	No	328	402.5	27	27	318	6	554
2	Y & P	Cumberland	NC82	6	B1	10.5	1	No	0	No	No	No	No	No	Yes	No	328	402.5	27	27	318	6	554
2	Y & P	Cumberland	NC82	6	B1	10.5	1	No	0	No	No	No	No	No	Yes	No	328	402.5	27	27	318	6	554
2	Y & P	Cumberland	NC82	6	A1	10.5	1	No	0	No	No	No	No	No	Yes	No	200	153	5	12	184	11.5	81
2	Y & P	Cumberland	NC82	6	A1	10.5	1	No	0	No	No	No	Yes	No	Yes	No	200	153	5	12	184	11.5	81
2	Y & P	Cumberland	NC82	6	A1	10.5	1	No	0	No	No	No	Yes	No	Yes	No	200	153	5	12	184	11.5	81
2	Y & P	Cumberland	NC82	6	A1	10.5	1	No	0	No	No	No	Yes	No	Yes	No	200	153	5	12	184	11.5	81
2	Y & P	Cumberland	US401	10	A1	10	1	Paved	3	No	No	No	Yes	No	Yes	No	320	139	17	2	272	15.11	48
2	Y & P	Cumberland	US401	10	A1	10	1	Paved	3	No	No	No	Yes	No	Yes	No	320	139	17	2	272	15.11	48
2	Y & P	Cumberland	US401	10	A1	10	1	Paved	3	No	No	No	Yes	No	Yes	No	320	139	17	2	272	15.11	48
2	Y & P	Cumberland	US401	10	A1	10	1	Paved	3	No	No	No	Yes	No	Yes	No	320	139	17	2	272	15.11	48
2	Y & P	Cumberland	US401	10	A1	10	1	Paved	3	No	No	No	Yes	No	Yes	No	320	139	17	2	272	15.11	48
2	Y & P	Cumberland	US401	10	B1	10	1	Paved	3	No	No	No	No	No	Yes	No	394	57	7	1	202	28.86	68
2	Y & P	Cumberland	US401	10	B1	10	1	Paved	3	No	No	No	No	No	Yes	No	394	57	7	1	202	28.86	68
2	Y & P	Cumberland	US401	10	B1	10	1	Paved	3	No	No	No	No	No	Yes	No	394	57	7	1	202	28.86	68
2	Y & P	Cumberland	US401	10	B1	10	1	Paved	3	No	No	No	No	No	Yes	No	394	57	7	1	202	28.86	68
2	Y & P	Cumberland	US401	10	B1	10	1	Paved	3	No	No	No	No	No	Yes	No	394	57	7	1	202	28.86	68
2	Y & P	Harnett	NC55	11	A1	11	1	Paved	2	No	No	No	No	No	Yes	No	126	14	3	0	90	45	19
2	Y & P	Harnett	NC55	11	A1	11	1	Paved	2	No	No	No	No	No	Yes	No	126	14	3	0	90	45	19
2	Y & P	Harnett	NC55	11	A1	11	1	Paved	2	No	No	No	No	No	Yes	No	126	14	3	0	90	45	19
2	Y & P	Harnett	NC55	11	A1	11	1	Paved	2	No	No	No	No	No	Yes	No	126	14	3	0	90	45	19
2	Y & P	Harnett	NC55	11	B1	11	1	Paved	2	Yes	No	No	Yes	No	Yes	No	242	120	9	5	236	18.15	40
2	Y & P	Harnett	NC55	11	B1	11	1	Paved	2	Yes	No	No	Yes	No	Yes	No	242	120	9	5	236	18.15	40
2	Y & P	Harnett	NC55	11	B1	11	1	Paved	2	Yes	No	No	Yes	No	Yes	No	242	120	9	5	236	18.15	40
2	Y & P	Harnett	NC55	11	B1	11	1	Paved	2	Yes	No	No	Yes	No	Yes	No	242	120	9	5	236	18.15	40
2	Y & P	Brunswick	NC179	3	A1	11	1	Paved	2	Yes	No	No	Yes	No	Yes	Yes	174	56	11	1	160	14.55	148
2	Y & P	Brunswick	NC179	3	A1	11	1	Paved	2	Yes	No	No	Yes	No	Yes	Yes	174	56	11	1	160	14.55	148
2	Y & P	Brunswick	NC179	3	A1	11	1	Paved	2	Yes	No	No	Yes	No	Yes	Yes	174	56	11	1	160	14.55	148
2	Y & P	Brunswick	NC179	3	B1	11	1	Paved	2	Yes	No	No	Yes	No	Yes	Yes	100	5	1	0	0	0	24
2	Y & P	Brunswick	NC179	3	B1	11	1	Paved	2	Yes	No	No	Yes	No	Yes	Yes	100	5	1	0	0	0	24
2	Y & P	Brunswick	NC179	3	B1	11	1	Paved	2	Yes	No	No	Yes	No	Yes	Yes	100	5	1	0	0	0	24
2	Y & P	Avery	NC194	10	B1	11	1	Paved	1	Yes	No	Yes	Yes	No	Yes	No	182	52.5	4	3	140	23.33	16
2	Y & P	Avery	NC194	10	B1	11	1	Paved	1	Yes	No	Yes	Yes	No	Yes	No	182	52.5	4	3	140	23.33	16
2	Y & P	Avery	NC194	10	B1	11	1	Paved	1	Yes	No	Yes	Yes	No	Yes	No	182	52.5	4	3	140	23.33	16
2	Y & P	Avery	NC194	10	B1	11	1	Paved	1	Yes	No	Yes	Yes	No	Yes	No	182	52.5	4	3	140	23.33	16
2	Y & P	Avery	NC194	10	A1	11	1	Paved	1	Yes	No	Yes	No	No	Yes	No	168	92	18	1	140	9.33	16
2	Y & P	Avery	NC194	10	A1	11	1	Paved	1	Yes	No	Yes	No	No	Yes	No	168	92	18	1	140	9.33	16
2	Y & P	Avery	NC194	10	A1	11	1	Paved	1	Yes	No	Yes	No	No	Yes	No	168	92	18	1	140	9.33	16
2	Y & P	Avery	NC194	10	A1	11	1	Paved	1	Yes	No	Yes	No	No	Yes	No	168	92	18	1	140	9.33	16
2	Y & P	Avery	NC194	10	A1	11	1	Paved	1	Yes	No	Yes	No	No	Yes	No	168	92	18	1	140	9.33	16
2	Y & P	Avery	NC194	10	A2	11	1	Paved	1	Yes	No	Yes	Yes	No	Yes	No	124	67	9	2	79	8.78	71
2	Y & P	Avery	NC194	10	A2	11	1	Paved	1	Yes	No	Yes	Yes	No	Yes	No	124	67	9	2	79	8.78	71
2	Y & P	Avery	NC194	10	A2	11	1	Paved	1	Yes	No	Yes	Yes	No	Yes	No	124	67	9	2	79	8.78	71
2	Y & P	Avery	NC194	10	A2	11	1	Paved	1	Yes	No	Yes	Yes	No	Yes	No	124	67	9	2	79	8.78	71
2	Y & P	Avery	NC194	10	A2	11	1	Paved	1	Yes	No	Yes	Yes	No	Yes	No	124	67	9	2	79	8.78	71
2	Y & P	Avery	NC194	10	B2	11	1	Paved	1	Yes	Yes	Yes	Yes	Yes	Yes	No	244	69	12	1	173	17.3	81
2	Y & P	Avery	NC194	10	B2	11	1	Paved	1	Yes	Yes	Yes	Yes	Yes	Yes	No	244	69	12	1	173	17.3	81
2	Y & P	Avery	NC194	10	B2	11	1	Paved	1	Yes	Yes	Yes	Yes	Yes	Yes	No	244	69	12	1	173	17.3	81
2	Y & P	Avery	NC194	10	B2	11	1	Paved	1	Yes	Yes	Yes	Yes	Yes	Yes	No	244	69	12	1	173	17.3	81
2	Y & P	Alamance	SR1530	7	B1	11	1	No	0	Yes	Yes	Yes	No	No	Yes	No	60	4	1	0	0	0	68
2	Y & P	Alamance	SR1530	7	B1	11	1	No	0	Yes	Yes	Yes	No	No	Yes	No	60	4	1	0	0	0	68
2	Y & P	Alamance	SR1530	7	B1	11	1	No	1	Yes	Yes	Yes	No	No	Yes	No	60	4	1	0	0	0	68
2	Y & P	Alamance	SR1530	7	B1	11	1	No	2	Yes	Yes	Yes	No	No	Yes	No	60	4	1	0	0	0	68
2	Y & P	Alamance	SR1530	7	B2	11	1	No	2	Yes	No	No	No	No	No	No	50	0	0	0	0	0	40
2	Y & P	Alamance	SR1530	7	B2	11	1	No	2	Yes	No	No	No	No	No	No	50	0	0	0	0	0	40
2	Y & P	Alamance	SR1530	7	B2	11	1	No	2	Yes	No	No	No	No	No	No	50	0	0	0	0	0	40
2	Y & P	Alamance	SR1530	7	B2	11	1	No	2	Yes	No	No	No	No	No	No	50	0	0	0	0	0	40
2	Y & P	Alamance	SR1530	7	G1	11	1	No	2	No	No	No	No	No	No	No	48	0	0	0	0	0	54
2	Y & P	Alamance	SR1530	7	G1	11	1	No	2	No	No	No	No	No	No	No	48	0	0	0	0	0	54
2	Y & P	Alamance	SR1530	7	G1	11	1	No	2	No	No	No	No	No	No	No	48	0	0	0	0	0	54
2	Y & P	Alamance	SR1530	7	G1	11	1	No	2	No	No	No	No	No	No	No	48	0	0	0	0	0	54
2	Y & P	Alamance	SR1530	7	G1	11	1	No	2	No	No	No	No	No	No	No	48	0	0	0	0	0	54

Table A.3 Master Database part 2 of test level 1

		Field Observation					Step Calculation											local condition idx						
County	Route	Loc ID	Alligator Cracking Area(ft.^{2})			Longitudin	Alligator Cracking											Local ACI	Local TCI	AC thickness (inch)	Layer	Thickness (inch)	Layer	Overlay?
			Light	Moderate	Severe	PL	PL	PM	PH	DL	DM	DH	ACI				TCI							
Wake	I-540	B1	288	224	0	1.583	24.000	18.667	0.000	18.039	26.628	0.000	55.333	22	1.578947	0.88	98.61053	55.33	98.61	11.97	1	1.45	T	No
Wake	I-540	B1	288	224	0	1.583	24.000	18.667	0.000	18.039	26.628	0.000	55.333	22	1.578947	0.88	98.61053	55.33	98.61	11.97	2	2.16	I	No
Wake	I-540	B1	288	224	0	1.583	24.000	18.667	0.000	18.039	26.628	0.000	55.333	22	1.578947	0.88	98.61053	55.33	98.61	11.97	3	3.53	I	No
Wake	I-540	B1	288	224	0	1.583	24.000	18.667	0.000	18.039	26.628	0.000	55.333	22	1.578947	0.88	98.61053	55.33	98.61	11.97	4	4.83	B	No
Wake	I-540	A1	68	0	0	0.000	6.028	0.000	0.000	8.581	0.000	0.000	91.419	0	0	0.351064	100	91.42	100.00	11.75	1	1.45	T	No
Wake	I-540	A1	68	0	0	0.000	6.028	0.000	0.000	8.581	0.000	0.000	91.419	0	0	0.351064	100	91.42	100.00	11.75	2	2.33	I	No
Wake	I-540	A1	68	0	0	0.000	6.028	0.000	0.000	8.581	0.000	0.000	91.419	0	0	0.351064	100	91.42	100.00	11.75	3	3.28	I	No
Wake	I-540	A1	68	0	0	0.000	6.028	0.000	0.000	8.581	0.000	0.000	91.419	0	0	0.351064	100	91.42	100.00	11.75	4	4.70	B	No
Wake	I-540	B2	502	276	304	0.000	21.344	11.735	12.925	16.435	20.055	30.878	32.632	0	0	0.285714	100	32.63	100.00	11.72	1	1.51	T	No
Wake	I-540	B2	502	276	304	0.000	21.344	11.735	12.925	16.435	20.055	30.878	32.632	0	0	0.285714	100	32.63	100.00	11.72	2	2.10	I	No
Wake	I-540	B2	502	276	304	0.000	21.344	11.735	12.925	16.435	20.055	30.878	32.632	0	0	0.285714	100	32.63	100.00	11.72	3	3.24	I	No
Wake	I-540	B2	502	276	304	0.000	21.344	11.735	12.925	16.435	20.055	30.878	32.632	0	0	0.285714	100	32.63	100.00	11.72	4	4.86	B	No
Wake	I-540	A2	6	0	0	0.000	0.500	0.000	0.000	2.387	0.000	0.000	97.613	0	45	0	100	97.61	100.00	11.88	1	1.47	T	No
Wake	I-540	A2	6	0	0	0.000	0.500	0.000	0.000	2.387	0.000	0.000	97.613	0	45	0	100	97.61	100.00	11.88	2	2.03	I	No
Wake	I-540	A2	6	0	0	0.000	0.500	0.000	0.000	2.387	0.000	0.000	97.613	0	45	0	100	97.61	100.00	11.88	3	3.59	I	No
Wake	I-540	A2	6	0	0	0.000	0.500	0.000	0.000	2.387	0.000	0.000	97.613	0	45	0	100	97.61	100.00	11.88	4	4.78	B	No
Mecklenburg	NC24	B1	364	118	316	0.667	7.583	2.458	6.583	10.083	7.721	19.313	62.884	0	0	0.0975	100	62.88	100.00	6.90	1	1.83	T	Yes
Mecklenburg	NC24	B1	364	118	316	0.667	7.583	2.458	6.583	10.083	7.721	19.313	62.884	0	0	0.0975	100	62.88	100.00	6.90	2	1.38	I	Yes
Mecklenburg	NC24	B1	364	118	316	0.667	7.583	2.458	6.583	10.083	7.721	19.313	62.884	0	0	0.0975	100	62.88	100.00	6.90	3	3.69	B	Yes
Mecklenburg	NC24	A1	30	52	58	0.470	2.016	3.495	3.898	5.443	9.571	13.413	71.573	8	29.21053	0.322581	90.57725	71.57	90.58	7.35	1	1.67	T	Yes
Mecklenburg	NC24	A1	30	52	58	0.470	2.016	3.495	3.898	5.443	9.571	13.413	71.573	8	29.21053	0.322581	90.57725	71.57	90.58	7.35	2	1.27	I	Yes
Mecklenburg	NC24	A1	30	52	58	0.470	2.016	3.495	3.898	5.443	9.571	13.413	71.573	8	29.21053	0.322581	90.57725	71.57	90.58	7.35	3	4.42	B	Yes
Mecklenburg	NC24	B2	13.5	54	0	1.016	1.372	5.488	0.000	5.332	12.608	0.000	82.061	0	45	0	100	82.06	100.00	6.77	1	1.46	T	Yes
Mecklenburg	NC24	B2	13.5	54	0	1.016	1.372	5.488	0.000	5.332	12.608	0.000	82.061	0	45	0	100	82.06	100.00	6.77	2	1.42	I	Yes
Mecklenburg	NC24	B2	13.5	54	0	1.016	1.372	5.488	0.000	5.332	12.608	0.000	82.061	0	45	0	100	82.06	100.00	6.77	3	3.90	B	Yes
Johnston	US-70	B1	0	0	0	4.167	0.000	0.000	0.000	7.097	0.000	0.000	92.903	0	45	0	100	92.90	100.00	10.38	1	1.66	T	Yes
Johnston	US-70	B1	0	0	0	4.167	0.000	0.000	0.000	7.097	0.000	0.000	92.903	0	45	0	100	92.90	100.00	10.38	2	2.59	I	Yes
Johnston	US-70	B1	0	0	0	4.167	0.000	0.000	0.000	7.097	0.000	0.000	92.903	0	45	0	100	92.90	100.00	10.38	3	3.06	I	Yes
Johnston	US-70	B1	0	0	0	4.167	0.000	0.000	0.000	7.097	0.000	0.000	92.903	0	45	0	100	92.90	100.00	10.38	4	3.06	B	Yes
Johnston	US-70	B2	26	0	0	4.583	2.167	0.000	0.000	9.095	0.000	0.000	90.905	0	45	0	100	90.91	100.00	10.73	1	1.58	T	Yes
Johnston	US-70	B2	26	0	0	4.583	2.167	0.000	0.000	9.095	0.000	0.000	90.905	0	45	0	100	90.91	100.00	10.73	2	2.50	I	Yes
Johnston	US-70	B2	26	0	0	4.583	2.167	0.000	0.000	9.095	0.000	0.000	90.905	0	45	0	100	90.91	100.00	10.73	3	3.00	I	Yes
Johnston	US-70	B2	26	0	0	4.583	2.167	0.000	0.000	9.095	0.000	0.000	90.905	0	45	0	100	90.91	100.00	10.70	4	3.65	B	Yes
Johnston	US-70	A1	0	0	0	0.917	0.000	0.000	0.000	3.259	0.000	0.000	96.741	0	45	0	100	96.74	100.00	10.50	1	1.91	T	Yes
Johnston	US-70	A1	0	0	0	0.917	0.000	0.000	0.000	3.259	0.000	0.000	96.741	0	45	0	100	96.74	100.00	10.50	2	2.56	I	Yes
Johnston	US-70	A1	0	0	0	0.917	0.000	0.000	0.000	3.259	0.000	0.000	96.741	0	45	0	100	96.74	100.00	10.50	3	3.03	I	Yes
Johnston	US-70	A1	0	0	0	0.917	0.000	0.000	0.000	3.259	0.000	0.000	96.741	0	45	0	100	96.74	100.00	10.50	4	3.00	B	Yes
Johnston	US-70	A2	0	0	0	0.000	0.000	0.000	0.000	0.000	0.000	0.000	100.000	0	45	0	100	100.00	100.00	11.93	1	2.92	T	Yes
Johnston	US-70	A2	0	0	0	0.000	0.000	0.000	0.000	0.000	0.000	0.000	100.000	0	45	0	100	100.00	100.00	11.93	2	2.41	I	Yes
Johnston	US-70	A2	0	0	0	0.000	0.000	0.000	0.000	0.000	0.000	0.000	100.000	0	45	0	100	100.00	100.00	11.93	3	2.91	I	Yes
Johnston	US-70	A2	0	0	0	0.000	0.000	0.000	0.000	0.000	0.000	0.000	100.000	0	45	0	100	100.00	100.00	11.93	4	3.69	B	Yes
Brunswick	US17	B1	16	0	0	4.167	1.361	0.000	0.000	8.207	0.000	0.000	91.793	0	0	0.744898	100	91.79	100.00	9.06	1	1.21	T	No
Brunswick	US17	B1	16	0	0	4.167	1.361	0.000	0.000	8.207	0.000	0.000	91.793	0	0	0.744898	100	91.79	100.00	9.06	2	1.46	I	No
Brunswick	US17	B1	16	0	0	4.167	1.361	0.000	0.000	8.207	0.000	0.000	91.793	0	0	0.744898	100	91.79	100.00	9.06	3	2.33	I	No
Brunswick	US17	B1	16	0	0	4.167	1.361	0.000	0.000	8.207	0.000	0.000	91.793	0	0	0.744898	100	91.79	100.00	9.06	4	4.06	B	No
Brunswick	US17	B2	18	0	0	3.571	2.143	0.000	0.000	8.348	0.000	0.000	91.652	0	45	0	100	91.65	100.00	9.19	1	1.10	T	No
Brunswick	US17	B2	18	0	0	3.571	2.143	0.000	0.000	8.348	0.000	0.000	91.652	0	45	0	100	91.65	100.00	9.19	2	1.52	I	No
Brunswick	US17	B2	18	0	0	3.571	2.143	0.000	0.000	8.348	0.000	0.000	91.652	0	45	0	100	91.65	100.00	9.19	3	2.02	I	No
Brunswick	US17	B2	18	0	0	3.571	2.143	0.000	0.000	8.348	0.000	0.000	91.652	0	45	0	100	91.65	100.00	9.19	4	4.54	B	No
Brunswick	US17	A1	0	0	0	5.238	0.000	0.000	0.000	7.983	0.000	0.000	92.017	0	45	0	100	92.02	100.00	9.58	1	1.15	T	No
Brunswick	US17	A1	0	0	0	5.238	0.000	0.000	0.000	7.983	0.000	0.000	92.017	0	45	0	100	92.02	100.00	9.58	2	1.60	I	No
Brunswick	US17	A1	0	0	0	5.238	0.000	0.000	0.000	7.983	0.000	0.000	92.017	0	45	0	100	92.02	100.00	9.58	3	2.63	I	No
Brunswick	US17	A1	0	0	0	5.238	0.000	0.000	0.000	7.983	0.000	0.000	92.017	0	45	0	100	92.02	100.00	9.58	4	4.21	B	No
Brunswick	US17	A2	0	0	0	7.323	0.000	0.000	0.000	9.484	0.000	0.000	90.516	0	45	0	100	90.52	100.00	10.10	1	1.54	T	No
Brunswick	US17	A2	0	0	0	7.323	0.000	0.000	0.000	9.484	0.000	0.000	90.516	0	45	0	100	90.52	100.00	10.10	2	1.60	I	No
Brunswick	US17	A2	0	0	0	7.323	0.000	0.000	0.000	9.484	0.000	0.000	90.516	0	45	0	100	90.52	100.00	10.10	3	2.56	I	No
Brunswick	US17	A2	0	0	0	7.323	0.000	0.000	0.000	9.484	0.000	0.000	90.516	0	45	0	100	90.52	100.00	10.10	4	4.40	B	No
Union	US601	A1	90	0	0	0.764	5.288	0.000	0.000	8.598	0.000	0.000	91.402	10.78	23.72368	0.655405	84.45137	91.40	84.45	6.92	1	1.55	T	Yes
Union	US601	A1	90	0	0	0.764	5.288	0.000	0.000	8.598	0.000	0.000	91.402	10.78	23.72368	0.655405	84.45137	91.40	84.45	6.92	2	1.94	I	Yes
Union	US601	A1	90	0	0	0.764	5.288	0.000	0.000	8.598	0.000	0.000	91.402	10.78	23.72368	0.655405	84.45137	91.40	84.45	6.92	3	1.73	I	Yes
Union	US601	A1	90	0	0	0.764	5.288	0.000	0.000	8.598	0.000	0.000	91.402	10.78	23.72368	0.655405	84.45137	91.40	84.45	6.92	4	1.70	B	Yes
Union	US601	B1	411.5	0	0	1.845	18.072	0.000	0.000	15.861	0.000	0.000	84.139	8.84	27.55263	0.848485	76.62201	84.14	76.62	6.27	1	1.35	T	Yes
Union	US601	B1	411.5	0	0	1.845	18.072	0.000	0.000	15.861	0.000	0.000	84.139	8.84	27.55263	0.848485	76.62201	84.14	76.62	6.27	2	1.38	I	Yes
Union	US601	B1	411.5	0	0	1.845	18.072	0.000	0.000	15.861	0.000	0.000	84.139	8.84	27.55263	0.848485	76.62201	84.14	76.62	6.27	3	1.79	I	Yes
Union	US601	B1	411.5	0	0	1.845	18.072	0.000	0.000	15.861	0.000	0.000	84.139	8.84	27.55263	0.848485	76.62201	84.14	76.62	6.27	4	1.75	B	Yes
Union	US601	B2	542	0	0	4.469	16.479	0.000	0.000	16.278	0.000	0.000	83.722	5	35.13158	0.06993	97.54325	83.72	97.54	6.58	1	1.35	T	Yes
Union	US601	B2	542	0	0	4.469	16.479	0.000	0.000	16.278	0.000	0.000	83.722	5	35.13158	0.06993	97.54325	83.72	97.54	6.58	2	1.45	I	Yes
Union	US601	B2	542	0	0	4.469	16.479	0.000	0.000	16.278	0.000	0.000	83.722	5	35.13158	0.06993	97.54325	83.72	97.54	6.58	3	1.95	I	Yes
Union	US601	B2	542	0	0	4.469	16.479	0.000	0.000	16.278	0.000	0.000	83.722	5	35.13158	0.06993	97.54325	83.72	97.54	6.58	4	1.83	B	Yes
New Hanover	US76	B1	432	0	24	5.641	22.154	0.000	1.231	18.824	0.000	6.015	75.160	4	37.10526	0.106667	96.04211	75.16	96.04	4.51	1	1.16	T	Yes
New Hanover	US76	B1	432	0	24	5.641	22.154	0.000	1.231	18.824	0.000	6.015	75.160	4	37.10526	0.106667	96.04211	75.16	96.04	4.51	2	1.00	I	Yes
New Hanover	US76	B1	432	0	24	5.641	22.154	0.000	1.231	18.824	0.000	6.015	75.160	4	37.10526	0.106667	96.04211	75.16	96.04	4.51	3	2.35	B	Yes
New Hanover	US76	A1	0	0	0	0.942	0.000	0.000	0.000	3.305	0.000	0.000	96.695	0	0	0.357143	100	96.70	100.00	8.50	1	3.21	T	Yes
New Hanover	US76	A1	0	0	0	0.942	0.000	0.000	0.000	3.305	0.000	0.000	96.695	0	0	0.357143	100	96.70	100.00	8.50	2	2.29	I	Yes
New Hanover	US76	A1	0	0	0	0.942	0.000	0.000	0.000	3.305	0.000	0.000	96.695	0	0	0.357143	100	96.70	100.00	8.50	3	3.00	B	Yes
Cumberland	NC87	A1	0	0	0	1.161	0.000	0.000	0.000	3.680	0.000	0.000	96.320	0	45	0	100	96.32	100.00	11.48	1	1.40	T	Yes
Cumberland	NC87	A1	0	0	0	1.161	0.000	0.000	0.000	3.680	0.000	0.000	96.320	0	45	0	100	96.32	100.00	11.48	2	1.28	I	Yes
Cumberland	NC87	A1	0	0	0	1.161	0.000	0.000	0.000	3.680	0.000	0.000	96.320	0	45	0	100	96.32	100.00	11.48	3	2.03	I	Yes
Cumberland	NC87	A1	0	0	0	1.161	0.000	0.000	0.000	3.680	0.000	0.000	96.320	0	45	0	100	96.32	100.00	11.48	4	1.93	I	Yes
Cumberland	NC87	A1	0	0	0	1.161	0.000	0.000	0.000	3.680	0.000	0.000	96.320	0	45	0	100	96.32	100.00	11.48	5	4.85	B	Yes
Cumberland	NC87	B1	110	0	0	2.754	7.768	0.000	0.000	11.426	0.000	0.000	88.574	13.25	18.84868	0.898305	83.06813	88.57	83.07	12.69	1	2.56	T	Yes
Cumberland	NC87	B1	110	0	0	2.754	7.768	0.000	0.000	11.426	0.000	0.000	88.574	13.25	18.84868	0.898305	83.06813	88.57	83.07	12.69	2	1.09	I	Yes
Cumberland	NC87	B1	110	0	0	2.754	7.768	0.000	0.000	11.426	0.000	0.000	88.574	13.25	18.84868	0.898305	83.06813	88.57	83.07	12.69	3	3.56	I	Yes
Cumberland	NC87	B1	110	0	0	2.754	7.768	0.000	0.000	11.426	0.000	0.000	88.574	13.25	18.84868	0.898305	83.06813	88.57	83.07	12.69	4	1.50	I	Yes
Cumberland	NC87	B1	110	0	0	2.754	7.768	0.000	0.000	11.426	0.000	0.000	88.574	13.25	18.84868	0.898305	83.06813	88.57	83.07	12.69	5	3.97	B	Yes
Cumberland	NC87	A2	0	0	0	1.754	0.000	0.000	0.000	4.550	0.000	0.000	95.450	0	0	0.438596	100	95.45	100.00	11.87	1	2.38	T	Yes
Cumberland	NC87	A2	0	0	0	1.754	0.000	0.000	0.000	4.550	0.000	0.000	95.450	0	0	0.438596	100	95.45	100.00	11.87	2	1.39	I	Yes
Cumberland	NC87	A2	0	0	0	1.754	0.000	0.000	0.000	4.550	0.000	0.000	95.450	0	0	0.438596	100	95.45	100.00	11.87	3	3.30	I	Yes
Cumberland	NC87	A2	0	0	0	1.754	0.000	0.000	0.000	4.550	0.000	0.000	95.450	0	0	0.438596	100	95.45	100.00	11.87	4	1.93	I	Yes
Cumberland	NC87	A2	0	0	0	1.754	0.000	0.000	0.000	4.550	0.000	0.000	95.450	0	0	0.438596	100	95.45	100.00	11.87	5	2.88	B	Yes
Cumberland	NC87	B2	212	0	0	4.410	7.361	0.000	0.000	12.104	0.000	0.000	87.896	20.2	5.131579	0.841667	95.68092	87.90	95.68	11.95	1	2.29	T	Yes
Cumberland	NC87	B2	212	0	0	4.410	7.361	0.000	0.000	12.104	0.000	0.000	87.896	20.2	5.131579	0.841667	95.68092	87.90	95.68	11.95	2	1.17	I	Yes
Cumberland	NC87	B2	212	0	0	4.410	7.361	0.000	0.000	12.104	0.000	0.000	87.896	20.2	5.131579	0.841667	95.68092	87.90	95.68	11.95	3	3.75	I	Yes
Cumberland	NC87	B2	212	0	0	4.410	7.361	0.000	0.000	12.104	0.000	0.000	87.896	20.2	5.131579	0.841667	95.68092	87.90	95.68	11.95	4	1.75	I	Yes
Cumberland	NC87	B2	212	0	0	4.410	7.361	0.000	0.000	12.104	0.000	0.000	87.896	20.2	5.131579	0.841667	95.68092	87.90	95.68	11.95	5	3.00	B	Yes
Swain	US74	B1	112	48	176	4.655	3.218	1.379	5.057	9.844	5.425	16.077	68.655	16.67	12.09868	0.517241	93.74206	68.65	93.74	6.77	1	1.56	T	Yes
Swain	US74	B1	112	48	176	4.655	3.218	1.379	5.057	9.844	5.425	16.077	68.655	16.67	12.09868	0.517241	93.74206	68.65	93.74	6.77	2	3.47	I	Yes
Swain	US74	B1	112	48	176	4.655	3.218	1.379	5.057	9.844	5.425	16.077	68.655	16.67	12.09868	0.517241	93.74206	68.65	93.74	6.77	3	1.73	B	Yes
Swain	US74	A1	66	0	60	7.425	2.068	0.000	1.880	10.837	0.000	8.076	81.087	19.1	7.302632	0.789474	94.23476	81.09	94.23	7.10	1	1.61	T	Yes
Swain	US74	A1	66	0	60	7.425	2.068	0.000	1.880	10.837	0.000	8.076	81.087	19.1	7.302632	0.789474	94.23476	81.09	94.23	7.10	2	3.67	I	Yes
Swain	US74	A1	66	0	60	7.425	2.068	0.000	1.880	10.837	0.000	8.076	81.087	19.1	7.302632	0.789474	94.23476	81.09	94.23	7.10	3	1.82	B	Yes
Haywood	NC209	A1	0	0	0	0.000	0.000	0.000	0.000	0.000	0.000	0.000	100.000	0	45	0	100	100.00	100.00	3.03	1	1.81	T	No
Haywood	NC209	A1	0	0	0	0.000	0.000	0.000	0.000	0.000	0.000	0.000	100.000	0	45	0	100	100.00	100.00	3.03	2	1.22	I	No
Haywood	NC209	A1	0	0	0	0.000	0.000	0.000	0.000	0.000	0.000	0.000	100.000	0	45	0	100	100.00	100.00	3.03	3	1.96	B	No
Haywood	NC209	B1	0	0	0	1.419	0.000	0.000	0.000	4.080	0.000	0.000	95.920	0	45	0	100	95.92	100.00	3.14	1	1.82	T	No
Haywood	NC209	B1	0	0	0	1.419	0.000	0.000	0.000	4.080	0.000	0.000	95.920	0	45	0	100	95.92	100.00	3.14	2	1.15	I	No
Haywood	NC209	B1	0	0	0	1.419	0.000	0.000	0.000	4.080	0.000	0.000	95.920	0	45	0	100	95.92	100.00	3.15	3	1.79	B	No

Table A.4 Master Database part 2 of test level 2

		Field Observation	Step Calculation															local condition idx						
County	Route	Loc ID	Alligator Cracking Area(ft.^{2})			Longitudin	Alligator Cracking											Local ACI	Local TCI	AC thickness (inch)	Layer	Thickness (inch)	Layer	Overlay?
			Light	Moderate	Severe	PL	PL	PM	PH	DL	DM	DH	ACI				TCI							
Martin	US13	A1	45	8	0	2.262	5.357	0.952	0.000	9.679	4.327	0.000	85.995	0	45	0	100	85.99	100.00	6.00	1	1.00	T	Yes
Martin	US13	A1	45	8	0	2.262	5.357	0.952	0.000	9.679	4.327	0.000	85.995	0	45	0	100	85.99	100.00	6.00	2	2.50	I	Yes
Martin	US13	A1	45	8	0	2.262	5.357	0.952	0.000	9.679	4.327	0.000	85.995	0	45	0	100	85.99	100.00	6.00	3	2.50	B	Yes
Martin	US13	B1	166	78	84	2.488	10.323	4.851	5.224	12.642	11.693	16.443	59.222	0	45	0	100	59.22	100.00	6.23	1	1.42	T	Yes
Martin	US13	B1	166	78	84	2.488	10.323	4.851	5.224	12.642	11.693	16.443	59.222	0	45	0	100	59.22	100.00	6.23	2	2.25	I	Yes
Martin	US13	B1	166	78	84	2.488	10.323	4.851	5.224	12.642	11.693	16.443	59.222	0	45	0	100	59.22	100.00	6.23	3	2.56	B	Yes
Martin	US13	B2	92	28	8	4.545	11.616	3.535	1.010	14.246	9.639	5.243	70.873	0	45	0	100	70.87	100.00	6.19	1	1.59	T	Yes
Martin	US13	B2	92	28	8	4.545	11.616	3.535	1.010	14.246	9.639	5.243	70.873	0	45	0	100	70.87	100.00	6.19	2	1.72	I	Yes
Martin	US13	B2	92	28	8	4.545	11.616	3.535	1.010	14.246	9.639	5.243	70.873	0	45	0	100	70.87	100.00	6.19	3	2.88	B	Yes
Martin	US13	A2	44	47	10	3.607	2.736	2.923	0.622	8.809	8.581	3.741	78.868	0	45	0	100	78.87	100.00	6.01	1	1.58	T	Yes
Martin	US13	A2	44	47	10	3.607	2.736	2.923	0.622	8.809	8.581	3.741	78.868	0	45	0	100	78.87	100.00	6.01	2	1.81	I	Yes
Martin	US13	A2	44	47	10	3.607	2.736	2.923	0.622	8.809	8.581	3.741	78.868	0	45	0	100	78.87	100.00	6.01	3	2.63	B	Yes
Richmond	NC177	B1	115	118	0	6.210	3.681	3.777	0.000	11.068	10.036	0.000	78.895	0	0	0.985915	100	78.90	100.00	4.84	1	1.65	T	Yes
Richmond	NC177	B1	115	118	0	6.210	3.681	3.777	0.000	11.068	10.036	0.000	78.895	0	0	0.985915	100	78.90	100.00	4.84	2	0.78	B(not really)	Yes
Richmond	NC177	A1	106	0	0	2.929	5.354	0.000	0.000	10.103	0.000	0.000	89.897	16.8	11.84211	0.933333	88.94737	89.90	88.95	4.88	1	1.77	T	Yes
Richmond	NC177	A1	106	0	0	2.929	5.354	0.000	0.000	10.103	0.000	0.000	89.897	16.8	11.84211	0.933333	88.94737	89.90	88.95	4.88	2	0.77	B(not really)	Yes
Richmond	NC177	A2	52	0	0	1.199	1.641	0.000	0.000	5.829	0.000	0.000	94.171	14.39	16.59868	0.899306	85.07271	94.17	85.07	4.88	1	1.80	T	Yes
Richmond	NC177	A2	52	0	0	1.199	1.641	0.000	0.000	5.829	0.000	0.000	94.171	14.39	16.59868	0.899306	85.07271	94.17	85.07	4.88	2	0.95	B(not really)	Yes
Richmond	NC177	B2	142	172	280	0.844	4.610	5.584	9.091	8.151	12.743	24.174	54.932	0	0	0.692857	100	54.93	100.00	4.84	1	1.38	T	Yes
Richmond	NC177	B2	142	172	280	0.844	4.610	5.584	9.091	8.151	12.743	24.174	54.932	0	0	0.692857	100	54.93	100.00	4.84	2	0.88	B(not really)	Yes
Montgomery	US220	B1	0	0	0	7.363	0.000	0.000	0.000	9.510	0.000	0.000	90.490	0	0	0.793651	100	90.49	100.00	4.28	1	1.81	T	Yes
Montgomery	US220	B1	0	0	0	7.363	0.000	0.000	0.000	9.510	0.000	0.000	90.490	0	0	0.793651	100	90.49	100.00	4.28	2	0.94	I	Yes
Montgomery	US220	B1	0	0	0	7.363	0.000	0.000	0.000	9.510	0.000	0.000	90.490	0	0	0.793651	100	90.49	100.00	4.28	3	1.53	B	Yes
Montgomery	US220	A1	0	0	0	4.469	0.000	0.000	0.000	7.357	0.000	0.000	92.643	0	0	0.940217	100	92.64	100.00	4.68	1	1.74	T	Yes
Montgomery	US220	A1	0	0	0	4.469	0.000	0.000	0.000	7.357	0.000	0.000	92.643	0	0	0.940217	100	92.64	100.00	4.68	2	0.84	I	Yes
Montgomery	US220	A1	0	0	0	4.469	0.000	0.000	0.000	7.357	0.000	0.000	92.643	0	0	0.940217	100	92.64	100.00	4.68	3	2.09	B	Yes
Davidson	NC47	B1	373	0	100	0.671	22.744	0.000	6.098	17.236	0.000	18.310	64.454	0	45	0	100	64.45	100.00	4.11	1	1.85	T	Yes
Davidson	NC47	B1	373	0	100	0.671	22.744	0.000	6.098	17.236	0.000	18.310	64.454	0	45	0	100	64.45	100.00	4.11	2	1.30	I	Yes
Davidson	NC47	B1	373	0	100	0.671	22.744	0.000	6.098	17.236	0.000	18.310	64.454	0	45	0	100	64.45	100.00	4.11	3	0.96	B	Yes
Davidson	NC47	A1	56	0	0	2.400	5.600	0.000	0.000	9.925	0.000	0.000	90.075	0	45	0	100	90.08	100.00	4.31	1	2.02	T	Yes
Davidson	NC47	A1	56	0	0	2.400	5.600	0.000	0.000	9.925	0.000	0.000	90.075	0	45	0	100	90.08	100.00	4.31	2	1.42	I	Yes
Davidson	NC47	B2	172	0	168	1.098	6.992	0.000	6.829	9.981	0.000	19.812	70.207	1	43.02632	0.004065	99.8251	70.21	99.83	5.01	1	1.78	T	Yes
Davidson	NC47	B2	172	0	168	1.098	6.992	0.000	6.829	9.981	0.000	19.812	70.207	1	43.02632	0.004065	99.8251	70.21	99.83	5.01	2	1.80	I	Yes
Davidson	NC47	B2	172	0	168	1.098	6.992	0.000	6.829	9.981	0.000	19.812	70.207	1	43.02632	0.004065	99.8251	70.21	99.83	5.01	3	1.44	B	Yes
Cumberland	NC82	B1	0	0	0	16.086	0.000	0.000	0.000	14.211	0.000	0.000	85.789	6	33.15789	0.969512	67.85302	85.79	67.85	4.89	1	2.00	T	Yes
Cumberland	NC82	B1	0	0	0	16.086	0.000	0.000	0.000	14.211	0.000	0.000	85.789	6	33.15789	0.969512	67.85302	85.79	67.85	4.89	2	2.37	I	Yes
Cumberland	NC82	B1	0	0	0	16.086	0.000	0.000	0.000	14.211	0.000	0.000	85.789	6	33.15789	0.969512	67.85302	85.79	67.85	4.89	3	0.52	B	Yes
Cumberland	NC82	A1	0	0	0	3.857	0.000	0.000	0.000	6.821	0.000	0.000	93.179	11.5	22.30263	0.92	79.48158	93.18	79.48	6.55	1	2.02	T	Yes
Cumberland	NC82	A1	0	0	0	3.857	0.000	0.000	0.000	6.821	0.000	0.000	93.179	11.5	22.30263	0.92	79.48158	93.18	79.48	6.55	2	1.03	I	Yes
Cumberland	NC82	A1	0	0	0	3.857	0.000	0.000	0.000	6.821	0.000	0.000	93.179	11.5	22.30263	0.92	79.48158	93.18	79.48	6.55	3	1.41	I	Yes
Cumberland	NC82	A1	0	0	0	3.857	0.000	0.000	0.000	6.821	0.000	0.000	93.179	11.5	22.30263	0.92	79.48158	93.18	79.48	6.55	4	2.09	B	Yes
Cumberland	US401	A1	355.5	0	0	1.500	11.109	0.000	0.000	12.540	0.000	0.000	87.460	15.11	15.17763	0.85	87.09901	87.46	87.10	6.98	1	1.19	T	Yes
Cumberland	US401	A1	355.5	0	0	1.500	11.109	0.000	0.000	12.540	0.000	0.000	87.460	15.11	15.17763	0.85	87.09901	87.46	87.10	6.98	2	1.89	I	Yes
Cumberland	US401	A1	355.5	0	0	1.500	11.109	0.000	0.000	12.540	0.000	0.000	87.460	15.11	15.17763	0.85	87.09901	87.46	87.10	6.98	3	1.94	I	Yes
Cumberland	US401	A1	355.5	0	0	1.500	11.109	0.000	0.000	12.540	0.000	0.000	87.460	15.11	15.17763	0.85	87.09901	87.46	87.10	6.98	4	0.83	I	Yes
Cumberland	US401	A1	355.5	0	0	1.500	11.109	0.000	0.000	12.540	0.000	0.000	87.460	15.11	15.17763	0.85	87.09901	87.46	87.10	6.98	5	1.13	B	Yes
Cumberland	US401	B1	180	188	0	1.726	4.569	4.772	0.000	8.774	11.576	0.000	79.650	0	0	0.51269	100	79.65	100.00	6.65	1	1.35	T	Yes
Cumberland	US401	B1	180	188	0	1.726	4.569	4.772	0.000	8.774	11.576	0.000	79.650	0	0	0.51269	100	79.65	100.00	6.65	2	1.63	I	Yes
Cumberland	US401	B1	180	188	0	1.726	4.569	4.772	0.000	8.774	11.576	0.000	79.650	0	0	0.51269	100	79.65	100.00	6.65	3	2.03	I	Yes
Cumberland	US401	B1	180	188	0	1.726	4.569	4.772	0.000	8.774	11.576	0.000	79.650	0	0	0.51269	100	79.65	100.00	6.65	4	0.64	I	Yes
Cumberland	US401	B1	180	188	0	1.726	4.569	4.772	0.000	8.774	11.576	0.000	79.650	0	0	0.51269	100	79.65	100.00	6.65	5	1.00	B	Yes
Harnett	NC55	A1	74	0	0	1.371	5.339	0.000	0.000	9.067	0.000	0.000	90.933	0	0	0.714286	100	90.93	100.00	6.48	1	1.41	T	Yes
Harnett	NC55	A1	74	0	0	1.371	5.339	0.000	0.000	9.067	0.000	0.000	90.933	0	0	0.714286	100	90.93	100.00	6.48	2	2.23	I	Yes
Harnett	NC55	A1	74	0	0	1.371	5.339	0.000	0.000	9.067	0.000	0.000	90.933	0	0	0.714286	100	90.93	100.00	6.48	3	1.14	I	Yes
Harnett	NC55	A1	74	0	0	1.371	5.339	0.000	0.000	9.067	0.000	0.000	90.933	0	0	0.714286	100	90.93	100.00	6.48	4	1.69	B	Yes
Harnett	NC55	B1	326	0	0	1.503	12.246	0.000	0.000	13.110	0.000	0.000	86.890	18.15	9.177632	0.975207	91.04991	86.89	91.05	7.15	1	1.15	T	Yes
Harnett	NC55	B1	326	0	0	1.503	12.246	0.000	0.000	13.110	0.000	0.000	86.890	18.15	9.177632	0.975207	91.04991	86.89	91.05	7.15	2	1.52	I	Yes
Harnett	NC55	B1	326	0	0	1.503	12.246	0.000	0.000	13.110	0.000	0.000	86.890	18.15	9.177632	0.975207	91.04991	86.89	91.05	7.15	3	1.47	I	Yes
Harnett	NC55	B1	326	0	0	1.503	12.246	0.000	0.000	13.110	0.000	0.000	86.890	18.15	9.177632	0.975207	91.04991	86.89	91.05	7.15	4	3.01	B	Yes
Brunswick	NC179	A1	44	40	0	7.732	2.299	2.090	0.000	11.149	6.992	0.000	81.860	14.55	16.28289	0.91954	85.02722	81.86	85.03	4.25	1	1.15	T	No
Brunswick	NC179	A1	44	40	0	7.732	2.299	2.090	0.000	11.149	6.992	0.000	81.860	14.55	16.28289	0.91954	85.02722	81.86	85.03	4.25	2	1.43	I	No
Brunswick	NC179	A1	44	40	0	7.732	2.299	2.090	0.000	11.149	6.992	0.000	81.860	14.55	16.28289	0.91954	85.02722	81.86	85.03	4.25	3	1.66	B	No
Brunswick	NC179	B1	0	0	0	2.182	0.000	0.000	0.000	5.090	0.000	0.000	94.910	0	45	0	100	94.91	100.00	4.92	1	1.47	T	No
Brunswick	NC179	B1	0	0	0	2.182	0.000	0.000	0.000	5.090	0.000	0.000	94.910	0	45	0	100	94.91	100.00	4.92	2	1.19	I	No
Brunswick	NC179	B1	0	0	0	2.182	0.000	0.000	0.000	5.090	0.000	0.000	94.910	0	45	0	100	94.91	100.00	4.92	3	2.26	B	No
Avery	NC194	B1	212	0	0	0.799	10.589	0.000	0.000	11.900	0.000	0.000	88.100	0	0	0.769231	100	88.10	100.00	8.40	1	1.28	T	Yes
Avery	NC194	B1	212	0	0	0.799	10.589	0.000	0.000	11.900	0.000	0.000	88.100	0	0	0.769231	100	88.10	100.00	8.40	2	1.75	I	Yes
Avery	NC194	B1	212	0	0	0.799	10.589	0.000	0.000	11.900	0.000	0.000	88.100	0	0	0.769231	100	88.10	100.00	8.40	3	2.13	I	Yes
Avery	NC194	B1	212	0	0	0.799	10.589	0.000	0.000	11.900	0.000	0.000	88.100	0	0	0.769231	100	88.10	100.00	8.40	4	3.25	B	Yes
Avery	NC194	A1	44	42	0	0.866	2.381	2.273	0.000	6.243	7.359	0.000	86.397	9.33	26.58553	0.833333	77.84539	86.40	77.85	6.58	1	1.47	T	Yes
Avery	NC194	A1	44	42	0	0.866	2.381	2.273	0.000	6.243	7.359	0.000	86.397	9.33	26.58553	0.833333	77.84539	86.40	77.85	6.58	2	1.53	I	Yes
Avery	NC194	A1	44	42	0	0.866	2.381	2.273	0.000	6.243	7.359	0.000	86.397	9.33	26.58553	0.833333	77.84539	86.40	77.85	6.58	3	1.17	I	Yes
Avery	NC194	A1	44	42	0	0.866	2.381	2.273	0.000	6.243	7.359	0.000	86.397	9.33	26.58553	0.833333	77.84539	86.40	77.85	6.58	4	0.96	I	Yes
Avery	NC194	A1	44	42	0	0.866	2.381	2.273	0.000	6.243	7.359	0.000	86.397	9.33	26.58553	0.833333	77.84539	86.40	77.85	6.58	5	1.46	B	Yes
Avery	NC194	A2	34	28	0	5.205	2.493	2.053	0.000	9.730	6.916	0.000	83.354	8.78	27.67105	0.637097	82.37086	83.35	82.37	6.90	1	1.16	T	Yes
Avery	NC194	A2	34	28	0	5.205	2.493	2.053	0.000	9.730	6.916	0.000	83.354	8.78	27.67105	0.637097	82.37086	83.35	82.37	6.90	2	1.78	I	Yes
Avery	NC194	A2	34	28	0	5.205	2.493	2.053	0.000	9.730	6.916	0.000	83.354	8.78	27.67105	0.637097	82.37086	83.35	82.37	6.90	3	1.00	I	Yes
Avery	NC194	A2	34	28	0	5.205	2.493	2.053	0.000	9.730	6.916	0.000	83.354	8.78	27.67105	0.637097	82.37086	83.35	82.37	6.90	4	1.42	I	Yes
Avery	NC194	A2	34	28	0	5.205	2.493	2.053	0.000	9.730	6.916	0.000	83.354	8.78	27.67105	0.637097	82.37086	83.35	82.37	6.90	5	1.54	B	Yes
Avery	NC194	B2	135	257.5	0	3.018	5.030	9.594	0.000	9.955	17.734	0.000	72.311	17.3	10.85526	0.709016	92.30344	72.31	92.30	5.20	1	1.38	T	Yes
Avery	NC194	B2	135	257.5	0	3.018	5.030	9.594	0.000	9.955	17.734	0.000	72.311	17.3	10.85526	0.709016	92.30344	72.31	92.30	5.20	2	1.45	I	Yes
Avery	NC194	B2	135	257.5	0	3.018	5.030	9.594	0.000	9.955	17.734	0.000	72.311	17.3	10.85526	0.709016	92.30344	72.31	92.30	5.20	3	1.25	I	Yes
Avery	NC194	B2	135	257.5	0	3.018	5.030	9.594	0.000	9.955	17.734	0.000	72.311	17.3	10.85526	0.709016	92.30344	72.31	92.30	5.20	4	1.13	B	Yes
Alamance	SR1530	B1	4	0	0	10.303	0.606	0.000	0.000	11.640	0.000	0.000	88.360	0	45	0	100	88.36	100.00		1		T	Yes
Alamance	SR1530	B1	4	0	0	10.303	0.606	0.000	0.000	11.640	0.000	0.000	88.360	0	45	0	100	88.36	100.00		2		I	Yes
Alamance	SR1530	B1	4	0	0	10.303	0.606	0.000	0.000	11.640	0.000	0.000	88.360	0	45	0	100	88.36	100.00		3		I	Yes
Alamance	SR1530	B1	4	0	0	10.303	0.606	0.000	0.000	11.640	0.000	0.000	88.360	0	45	0	100	88.36	100.00		4		I	Yes
Alamance	SR1530	B2	28	14	0	7.273	5.091	2.545	0.000	12.413	7.887	0.000	79.700	0	45	0	100	79.70	100.00		1		B	Yes
Alamance	SR1530	B2	28	14	0	7.273	5.091	2.545	0.000	12.413	7.887	0.000	79.700	0	45	0	100	79.70	100.00		2		T	Yes
Alamance	SR1530	B2	28	14	0	7.273	5.091	2.545	0.000	12.413	7.887	0.000	79.700	0	45	0	100	79.70	100.00		3		I	Yes
Alamance	SR1530	B2	28	14	0	7.273	5.091	2.545	0.000	12.413	7.887	0.000	79.700	0	45	0	100	79.70	100.00		4		B	Yes
Alamance	SR1530	G1	0	0	0	10.227	0.000	0.000	0.000	11.260	0.000	0.000	88.740	0	45	0	100	88.74	100.00		1		T	Yes
Alamance	SR1530	G1	0	0	0	10.227	0.000	0.000	0.000	11.260	0.000	0.000	88.740	0	45	0	100	88.74	100.00		2		I	Yes
Alamance	SR1530	G1	0	0	0	10.227	0.000	0.000	0.000	11.260	0.000	0.000	88.740	0	45	0	100	88.74	100.00		3		I	Yes
Alamance	SR1530	G1	0	0	0	10.227	0.000	0.000	0.000	11.260	0.000	0.000	88.740	0	45	0	100	88.74	100.00		4		I	Yes
Alamance	SR1530	G1	0	0	0	10.227	0.000	0.000	0.000	11.260	0.000	0.000	88.740	0	45	0	100	88.74	100.00		5		B	Yes

Table A.5 Master Database part 3 of test level 1

			Dynamic Modulus				Fatigue							Extracted Binder				
County	Route	Loc ID	shift factor							Exp. Coefficient		Power. Coefficient		DSR			LAS	
			Geometry	a1	a2	a3	Geometry	Cf	alpha	a	b	Y	Z	G*	phase angle	G* sine delta	a	b
Wake	I-540	B1												6614531.8	46.704	48142.2	5.672	-1.927
Wake	I-540	B1												1267051.2	53.257	10153.2	9.723	-1.871
Wake	I-540	B1												1134533.4	56.098	9416.6	13.296	-1.829
Wake	I-540	B1												3024164.3	53.013	24156.1	9.643	-1.964
Wake	I-540	A1	P	6.32E-04	-1.62E-01	2.99E+00	P	0.25	3.82	-7.40109E-05	0.8180258	0.00057718	0.60397294	4749832.2	48.895	35790.4	4.985	-2.008
Wake	I-540	A1	P	9.04E-04	-1.68E-01	2.99E+00	P	0.37	3.61	-0.000170055	0.78187958	0.00064485	0.62666892	19806398.1	43.220	135634.5	3.698	-2.056
Wake	I-540	A1	38	6.17E-04	-1.50E-01	2.76E+00	38	0.21	3.18	-0.000351673	0.71408807	0.00441927	0.4439635	6543165.6	50.674	50614.6	5.834	-2.002
Wake	I-540	A1	38	6.06E-04	-1.47E-01	2.69E+00	38	0.25	3.01	-0.001071909	0.6425839	0.00763991	0.4139297	2084964.1	54.893	17056.6	8.859	-1.940
Wake	I-540	B2	P	7.85E-04	-1.58E-01	2.84E+00	P	0.25	4.80	-5.8408E-06	1.16379515	0.00017782	0.78839432	6614531.8	46.704	48142.2	5.672	-1.927
Wake	I-540	B2	P	9.94E-04	-1.76E-01	3.11E+00	P	0.37	3.46	-0.002243526	0.52469741	0.0051108	0.41912382	1267051.2	53.257	10153.2	9.723	-1.871
Wake	I-540	B2	38	5.03E-04	-1.44E-01	2.69E+00	38	0.21	3.21	-0.00255847	0.5623861	0.0175247	0.33637331	1134533.4	56.098	9416.6	13.296	-1.829
Wake	I-540	B2	38	6.44E-04	-1.47E-01	2.69E+00	38	0.25	2.95	-0.017152203	0.38856872	0.02786169	0.2995021	3024164.3	53.013	24156.1	9.643	-1.964
Wake	I-540	A2					P	0.25	3.82	-0.000496695	0.63159931	2.5317E-05	0.86258225	4749832.2	48.895	35790.4	4.985	-2.008
Wake	I-540	A2					P	0.25	3.61	-4.56347E-06	1.16963767	8.3462E-05	0.84906044	19806398.1	43.220	135634.5	3.698	-2.056
Wake	I-540	A2					38	0.25	3.18	-0.000608896	0.66284184	0.00513786	0.42983579	6543165.6	50.674	50614.6	5.834	-2.002
Wake	I-540	A2					38	0.24	3.01	-0.000171687	0.80876454	0.00225107	0.5245226	2084964.1	54.893	17056.6	8.859	-1.940
Mecklenburg	NC24	B1	P	0.001536216	-0.222363717	3.83278789	P	0.25	4.23	-0.013769057	0.41733063	0.02361108	0.32373298	19194421.1	38.942	120642.1	1.939	-2.034
Mecklenburg	NC24	B1	P	0.000711105	-0.159115818	2.89787431	P	0.17	3.56	-0.00035433	0.67894059	0.00645234	0.38986278	7817502.8	47.762	57877.4	5.224	-2.188
Mecklenburg	NC24	B1	38	0.000766423	-0.159017685	2.87378443	38	0.27	3.44	-0.001124041	0.60227355	0.0038881	0.45258294	2220326.3	55.306	18255.5	9.658	-2.075
Mecklenburg	NC24	A1	38	0.001811321	-0.269783453	4.67114067	38	0.25	2.14	-0.005296594	0.56123749	0.01221266	0.42357695	24782775.4	39.277	156891.6	2.057	-1.990
Mecklenburg	NC24	A1	P	0.000971615	-0.172105077	3.05345537	P	0.26	4.13	-0.000671318	0.64545073	0.00529862	0.42166249	4518133.3	51.760	35486.6	7.277	-2.131
Mecklenburg	NC24	A1	38	0.000572546	-0.147741046	2.72580241	38	0.19	3.34	-0.003270391	0.51358596	0.02444145	0.2906194	1178916.7	55.176	9677.9	9.636	-1.935
Mecklenburg	NC24	B2												19194421.1	38.942	120642.1	1.939	-2.034
Mecklenburg	NC24	B2												7817502.8	47.762	57877.4	5.224	-2.188
Mecklenburg	NC24	B2												2220326.3	55.306	18255.5	9.658	-2.075
Johnston	US-70	B1												66985642.9	35.060	384785.3	0.294	-2.383
Johnston	US-70	B1												79349607.5	29.350	388925.7	0.700	-2.022
Johnston	US-70	B1												11828270.3	45.221	83960.6	3.323	-1.937
Johnston	US-70	B1												14667491.1	43.591	101132.6	3.862	-1.938
Johnston	US-70	B2	38	0.000758689	-0.170639759	3.10931971	38	0.42	3.2	-0.000477222	0.62363035	0.00202681	0.47153119	66985642.9	35.060	384785.3	0.294	-2.383
Johnston	US-70	B2	38	0.000590826	-0.164457049	3.05281064	38	0.27	3.8	-0.000524329	0.67563119	0.00415494	0.44885985	79349607.5	29.350	388925.7	0.700	-2.022
Johnston	US-70	B2	38	0.000802469	-0.165554504	2.99010234	38	0.16	3.87	-0.001901715	0.55092844	0.00519386	0.42459493	11828270.3	45.221	83960.6	3.323	-1.937
Johnston	US-70	B2	38	0.000809811	-0.1587663	2.85140149	38	0.25	3.26	-0.002295336	0.53168475	0.00500932	0.42824959	14667491.1	43.591	101132.6	3.862	-1.938
Johnston	US-70	A1												36051200.5	38.592	224874.4	1.039	-2.113
Johnston	US-70	A1												44794112.2	33.662	248291.1	0.994	-1.922
Johnston	US-70	A1												11211175.2	46.449	81254.3	4.728	-1.884
Johnston	US-70	A1												9331368.6	43.954	64767.2	5.489	-1.902
Johnston	US-70	A2	38	0.000651267	-0.16358458	3.01118486	38	0.26	3.57	-0.000496695	0.63159931	0.004432	0.41106662	36051200.5	38.592	224874.4	1.039	-2.113
Johnston	US-70	A2	38	0.000792597	-0.16165734	2.91610814	38	0.19	4.39	-0.001254439	0.59865918	0.01268769	0.34861185	44794112.2	33.662	248291.1	0.994	-1.922
Johnston	US-70	A2	38	0.000556866	-0.140496929	2.58719227	38	0.25	3.21	-0.003039371	0.52189799	0.00831636	0.3916696	11211175.2	46.449	81254.3	4.728	-1.884
Johnston	US-70	A2	38	0.000624347	-0.151681334	2.78388793	38	0.25	3.46	-2.25627E-05	0.93239564	0.0001562	0.7274177	9331368.6	43.954	64767.2	5.489	-1.902
Brunswick	US17	B1																
Brunswick	US17	B1												8951412.1	47.959	66479.5	6.918	-1.771
Brunswick	US17	B1												10251335.8	51.249	79947.6	5.014	-1.855
Brunswick	US17	B1												8707378.0	53.302	69815.1	2.034	-1.930
Brunswick	US17	B2	P	0.00046634	-0.170054955	3.21456309	P	0.25	2.69	-0.00061124	0.60442687	0.00231678	0.45998439					
Brunswick	US17	B2	P	0.000764413	-0.161920772	2.93265019	P	0.39	3.36	-0.000785261	0.60975298	0.00188057	0.50295351	8951412.1	47.959	66479.5	6.918	-1.771
Brunswick	US17	B2	P	0.000541871	-0.140893631	2.60112441	P	0.44	3.16	-0.002013266	0.54588984	0.00394876	0.45345161	10251335.8	51.249	79947.6	5.014	-1.855
Brunswick	US17	B2	P	0.000489073	-0.142813323	2.66063737	P	0.37	3.28	-2.54841E-05	0.89270616	0.00016051	0.70264282	8707378.0	53.302	69815.1	2.034	-1.930
Brunswick	US17	A1	P	0.000754211	-0.189377197	3.48585969	P	0.26	3.16	-0.00253178	0.48991862	0.00627594	0.37948376					
Brunswick	US17	A1	P	0.000720423	-0.14523604	2.61655165	P	0.16	3.42	-0.002267702	0.52523259	0.00678726	0.3916139	9787200.5	44.691	68831.9	5.732	-1.796
Brunswick	US17	A1	P	0.000520703	-0.139617256	2.58406409	P	0.5	3.03	-0.002069506	0.53044421	0.00379445	0.44803567	9789270.7	50.759	75817.3	5.362	-1.886
Brunswick	US17	A1	P	0.001051837	-0.176995328	3.11917187	P	0.32	3.23	-0.000398577	0.68108564	0.00133931	0.53991966	11020954.7	49.231	83467.5	6.372	-1.848
Brunswick	US17	A2																
Brunswick	US17	A2												9787200.5	44.691	68831.9	5.732	-1.796
Brunswick	US17	A2												9789270.7	50.759	75817.3	5.362	-1.886
Brunswick	US17	A2												11020954.7	49.231	83467.5	6.372	-1.848
Union	US601	A1	P	0.00039991	-0.150055618	2.84114826	P	0.22	3.1	-0.000492309	0.64871159	0.00558699	0.40134948	5231702.1	48.946	39451.5	4.655	-1.982
Union	US601	A1	P	0.000569364	-0.171056952	3.19339355	P	0.36	2.57	-0.000141242	0.72486154	0.00096518	0.53211481					
Union	US601	A1	P	0.000536093	-0.174968667	3.28493596	P	0.29	2.98	-0.013725892	0.37585459	0.0440908	0.23286165	19093165.9	33.884	106448.3	0.056	-2.550
Union	US601	A1	P	0.001180079	-0.205606516	3.6400989	P	0.21	2.53	-0.00527168	0.46426536	0.02598768	0.28151775	18713392.5	36.607	111591.4	0.711	-2.102
Union	US601	B1	P	0.000635584	-0.155483008	2.85542667	P	0.25	3.04	-0.0006266	0.6170156	0.00481195	0.40762336	10506093.3	43.520	72345.8	2.485	-2.060
Union	US601	B1	P	0.000778892	-0.170229253	3.09302835	P	0.18	3.05	-6.02668E-05	0.80004485	0.00062706	0.56807868	17043764.5	42.192	114469.6	1.366	-2.180
Union	US601	B1	P	0.000387772	-0.16174187	3.07972863	P	0.5	4.27	-0.013725892	0.37585459	0.02450319	0.2897398	36649187.2	28.173	173033.7	0.187	-2.282
Union	US601	B1	P	0.000723303	-0.192981659	3.57031199	P	0.1	2.59	-0.000849678	0.65141217	0.01989252	0.31746737	22561047.1	34.357	127322.1	0.084	-2.468
Union	US601	B2	P	0.000635584	-0.155483008	2.85542667	P	0.42	3.04	-0.001396004	0.54235166	0.00474287	0.40672092	10506093.3	43.520	72345.8	2.485	-2.060
Union	US601	B2	P	0.000778892	-0.170229253	3.09302835	P	0.29	3.05	-0.000162811	0.70767591	0.0015661	0.48687983	17043764.5	42.192	114469.6	1.366	-2.180
Union	US601	B2	P	0.000387772	-0.16174187	3.07972863	P	0.5	4.27	-0.013725892	0.37585459	0.02450319	0.2897398	36649187.2	28.173	173033.7	0.187	-2.282
Union	US601	B2	P	0.000723303	-0.192981659	3.57031199	P	0.15	2.59	-0.005315202	0.4821318	0.04259332	0.2475449	22561047.1	34.357	127322.1	0.084	-2.468
New Hanover	US76	B1	P	0.000567504	-0.160229338	2.97758507	P	0.57	3.85	-0.001414768	0.51650835	0.00215155	0.46049036	48252508.3	36.560	287425.5	0.583	-2.246
New Hanover	US76	B1	P	0.000624889	-0.162647505	3.00299438	P	0.63	3.95	-0.000119012	0.7468649	0.00049854	0.59634052	16804891.0	45.785	120446.4	2.770	-2.086
New Hanover	US76	B1	38	0.001306773	-0.193513846	3.34756787	38	0.25	2.18	-0.011404605	0.52433756	0.0212581	0.40133445	69120982.3	26.913	312870.0	7.704	-1.299
New Hanover	US76	A1	38	0.000749246	-0.163800304	2.97630779	38	0.15	3.63	-0.006653757	0.47347164	0.01952323	0.32564388	59536967.1	34.252	335097.2	0.717	-2.327
New Hanover	US76	A1	38	0.000721984	-0.156281975	2.83684599	38	0.32	3.61	-0.003750529	0.51690563	0.02408291	0.30100794	59536967.1	34.252	335097.2	0.279	-2.329
New Hanover	US76	A1	38	0.000356444	-0.163059625	3.11861508	38	0.32	2.65	-0.001369306	0.57656842	0.00375729	0.45212417	##########	32.174	555463.0	0.000	-9.280
Cumberland	NC87	A1												25362402.0	39.705	162023.5	1.848	-1.983
Cumberland	NC87	A1												19113189.4	36.366	113329.7	3.293	-1.860
Cumberland	NC87	A1												15855831.5	35.616	92335.6	2.789	-1.599
Cumberland	NC87	A1												26608015.7	31.091	137405.0	0.812	-1.964
Cumberland	NC87	A1												57804925.9	28.079	272080.3	8.987	-1.281
Cumberland	NC87	B1	38	0.001407613	-0.214894387	3.73484251	38	0.22	1.94	-0.019718066	0.40002054	0.05524362	0.24764557	##########	32.180	791460.1	0.013	-3.539
Cumberland	NC87	B1	P	0.000997896	-0.179825667	3.19735493	P	0.31	3.95	-0.001132726	0.56033239	0.00642409	0.37921291	22722525.0	37.282	137637.9	2.976	-1.982
Cumberland	NC87	B1	38	0.000566535	-0.164190406	3.05719405	38	0.25	4.39	-0.001602804	0.53880934	0.01109556	0.33752195	12980573.2	38.758	81262.4	3.400	-1.657
Cumberland	NC87	B1	P	0.000488428	-0.166609906	3.13682701	P	0.26	4.21	-0.000167831	0.71768678	0.00197103	0.47574284	35782809.9	28.859	172708.6	1.414	-1.828
Cumberland	NC87	P	0.001032224	-0.181242753	3.21196536	P	0.17	5.19	-0.000541023	0.67198809	0.00811878	0.38710627	68045105.1	25.538	293350.9	0.165	-2.494
Cumberland	NC87	A2	38	0.000364247	-0.143261034	2.71952169	38	0.28	3.69	-0.021575471	0.29705454	0.06301425	0.17813544	25362402.0	39.705	162023.5	1.848	-1.983
Cumberland	NC87	A2	P	0.000547057	-0.164786198	3.07690098	P	0.3	3.34	-0.000499401	0.63253769	0.0035878	0.43034123	19113189.4	36.366	113329.7	3.293	-1.860
Cumberland	NC87	A2	38	0.001308433	-0.209737951	3.67138592	38	0.2	2.95	-0.003269072	0.51377233	0.02312944	0.29564933	15855831.5	35.616	92335.6	2.789	-1.599
Cumberland	NC87	A2	P	0.001270221	-0.233575974	4.20743123	P	0.25	3.95	-0.00427876	0.4687314	0.02217407	0.28703943	26608015.7	31.091	137405.0	0.812	-1.964
Cumberland	NC87	A2	38	0.000567375	-0.188635922	3.54576845	38	0.25	1.62	-0.015669155	0.37707683	0.05364439	0.22303307	57804925.9	28.079	272080.3	8.987	-1.281
Cumberland	NC87	B2												##########	32.180	791460.1	0.013	-3.539
Cumberland	NC87	B2												22722525.0	37.282	137637.9	2.976	-1.982
Cumberland	NC87	B2												12980573.2	38.758	81262.4	3.400	-1.657
Cumberland	NC87	B2												35782809.9	28.859	172708.6	1.414	-1.828
Cumberland	NC87	B2												68045105.1	25.538	293350.9	0.165	-2.494
Swain	US74	B1	P	8.04E-04	-1.65E-01	2.98E+00	P	0.25	3.09	-1.27E-03	5.55E-01	2.90E-03	4.55E-01	26713435.6	36.379	158444.7	40.892	-1.233
Swain	US74	B1	P	4.58E-04	-1.45E-01	2.73E+00	P	0.27	3.51	-5.49E-04	6.30E-01	2.27E-03	4.76E-01	18399134.8	40.083	118472.1	22.929	-1.506
Swain	US74	B1	P	6.83E-04	-1.69E-01	3.11E+00	P	0.15	4.23	-1.75E-03	5.67E-01	9.31E-03	3.76E-01	38993725.3	25.648	168782.5	0.266	-2.579
Swain	US74	A1	P	4.92E-04	-1.54E-01	2.88E+00	P	0.36	3.84	-5.35E-04	6.28E-01	2.73E-03	4.56E-01	53854952.5	24.014	219164.4	0.007	-3.735
Swain	US74	A1	P	2.62E-04	-1.38E-01	2.65E+00	P	0.25	3.44	-7.29E-05	8.02E-01	6.62E-04	5.79E-01	32407531.9	35.499	188188.6	19.330	-1.308
Swain	US74	A1	P	7.72E-04	-1.70E-01	3.10E+00	P	0.251	3.85	-5.90E-04	6.41E-01	3.77E-03	4.42E-01	26293085.8	37.826	161246.4	31.782	-1.236
Haywood	NC209	A1	38	0.000354284	-0.148223216	2.82275058	38	0.25	3.62	-0.000535449	0.62753536	0.00273234	0.45531253	2108860.1	47.964	15663.0	10.936	-1.585
Haywood	NC209	A1	38	0.000716491	-0.15658144	2.84503229	38	0.25	3.71	-7.28699E-05	0.80247825	0.00067651	0.57729732	9514743.3	42.308	64045.2	4.202	-1.716
Haywood	NC209	A1	38	0.00032844	-0.153360904	2.93584209	38	0.49	3.62	-0.000589931	0.64146134	0.00374045	0.44288666	5315662.4	44.659	37362.9	15.948	-1.402
Haywood	NC209	B1	38	0.000458674	-0.157828873	2.97310768	38	0.24	3.58	-0.001270696	0.55504966	0.00290748	0.4545294	4646123.1	46.422	33658.4	18.871	-1.328
Haywood	NC209	B1	38	0.000506276	-0.156865648	2.93480254	38	0.251	3.66	-0.000549488	0.63022424	0.00223012	0.47748533	1324347.5	50.606	10234.5	22.750	-1.282
Haywood	NC209	B1	38	0.000698034	-0.166407899	3.04894435	38	0.29	3.53	-0.00174695	0.56696962	0.00925635	0.37690182	17926542.9	37.805	109885.8	4.181	-1.653

Table A.6 Master Database part 4 of test level 1

		Field Observed	Mixture info.																
						Gradation (% Passing)													
County	Route	Loc ID	Gmm	%AV	%AC	NMSA	1.50" (37.5mm)	1" (25mm)	3/4" (19mm)	1/2" (12.5mm)	3/8" (9.5mm)	#4 (4.75mm)	#8 (2.36mm)	#16 (1.18mm)	#30 (0.6mm)	#50 (0.3mm)	#100 (0.15mm)	#200 (0.075mm)	
Wake	I-540	B1	2.45	7.47	4.78	12.5	100.00	100.00	98.52	93.77	85.46	55.11	37.13	28.17	21.38	15.18	8.97	4.50	P
Wake	I-540	B1	2.44	8.58	5.17	9.5	100.00	100.00	100.00	97.89	91.47	61.88	39.81	27.81	18.83	11.52	5.31	2.23	C
Wake	I-540	B1	2.46	11.96	4.76	19	100.00	100.00	97.41	82.56	70.30	48.35	35.37	26.04	18.52	12.00	6.18	2.88	P
Wake	I-540	B1	2.46	5.56	4.84	25	100.00	98.21	89.74	77.33	68.33	40.94	25.55	18.50	13.42	9.18	5.26	2.59	P
Wake	I-540	A1	2.45	7.52	5.19	12.5	100.00	100.00	98.52	93.77	85.46	55.11	37.13	28.17	21.38	15.18	8.97	4.50	P
Wake	I-540	A1	2.45	6.30	5.09	12.5	100.00	100.00	98.70	94.64	87.51	55.69	33.35	23.71	16.54	10.58	5.28	2.27	C
Wake	I-540	A1	2.47	12.37	4.60	19	100.00	100.00	99.27	86.40	72.40	45.98	31.71	23.17	16.65	10.94	5.71	2.72	P
Wake	I-540	A1	2.45	5.21	4.84	25	100.00	97.27	88.92	74.48	59.41	38.58	28.50	21.78	16.28	11.49	6.90	3.71	P
Wake	I-540	B2	2.45	7.42	4.78	12.5	100.00	100.00	98.52	93.77	85.46	55.11	37.13	28.17	21.38	15.18	8.97	4.50	P
Wake	I-540	B2	2.44	7.56	5.17	9.5	100.00	100.00	100.00	97.89	91.47	61.88	39.81	27.81	18.83	11.52	5.31	2.23	C
Wake	I-540	B2	2.46	11.30	4.76	19	100.00	100.00	97.41	82.56	70.30	48.35	35.37	26.04	18.52	12.00	6.18	2.88	P
Wake	I-540	B2	2.46	5.49	4.84	25	100.00	98.21	89.74	77.33	68.33	40.94	25.55	18.50	13.42	9.18	5.26	2.59	P
Wake	I-540	A2	2.45	6.20	5.19	12.5	100.00	100.00	98.52	93.77	85.46	55.11	37.13	28.17	21.38	15.18	8.97	4.50	P
Wake	I-540	A2	2.45	9.99	5.09	12.5	100.00	100.00	98.70	94.64	87.51	55.69	33.35	23.71	16.54	10.58	5.28	2.27	C
Wake	I-540	A2	2.47	4.77	4.60	19	100.00	100.00	99.27	86.40	72.40	45.98	31.71	23.17	16.65	10.94	5.71	2.72	P
Wake	I-540	A2	2.45	3.43	4.84	25	100.00	97.27	88.92	74.48	59.41	38.58	28.50	21.78	16.28	11.49	6.90	3.71	P
Mecklenburg	NC24	B1	2.58	9.54	4.87	9.5	100.00	100.00	100.00	99.60	95.32	64.96	41.57	29.95	21.52	13.70	8.14	4.98	C
Mecklenburg	NC24	B1	2.55	7.49	5.40	9.5	100.00	100.00	99.28	98.09	91.82	60.76	40.77	29.95	21.06	12.84	7.49	4.57	C
Mecklenburg	NC24	B1	2.58	6.31	4.98	19	100.00	100.00	96.87	78.56	65.87	38.89	25.90	19.76	14.37	8.93	5.23	3.37	C
Mecklenburg	NC24	A1	2.58	7.40	4.74	9.5	100.00	100.00	100.00	98.41	93.72	63.44	42.68	32.31	24.02	16.51	8.68	5.23	P
Mecklenburg	NC24	A1	2.56	6.39	5.47	9.5	100.00	100.00	98.89	97.49	91.18	62.77	43.18	32.64	23.35	14.32	6.29	3.58	P
Mecklenburg	NC24	A1	2.60	7.50	4.96	19	100.00	100.00	93.54	78.06	68.71	42.42	26.80	19.26	14.16	9.70	5.60	3.91	C
Mecklenburg	NC24	B2	2.58	11.50	4.87	9.5	100.00	100.00	100.00	99.60	95.32	64.96	41.57	29.95	21.52	13.70	8.14	4.98	C
Mecklenburg	NC24	B2	2.55	7.40	5.40	9.5	100.00	100.00	99.28	98.09	91.82	60.76	40.77	29.95	21.06	12.84	7.49	4.57	C
Mecklenburg	NC24	B2	2.58	7.55	4.98	19	100.00	100.00	96.87	78.56	65.87	38.89	25.90	19.76	14.37	8.93	5.23	3.37	C
Johnston	US-70	B1	2.50		5.17	9.5	100.00	100.00	100.00	99.08	93.65	68.33	50.65	37.10	24.44	13.50	7.68	5.26	P
Johnston	US-70	B1	2.50		5.01	9.5	100.00	100.00	100.00	99.57	96.67	66.84	45.01	31.51	21.07	10.85	7.09	5.19	C
Johnston	US-70	B1	2.48		5.66	9.5	100.00	100.00	100.00	100.00	96.62	66.28	45.39	32.49	22.38	11.41	7.67	5.77	P
Johnston	US-70	B1	2.50		4.39	25	100.00	98.47	84.61	70.75	60.32	45.57	35.90	28.62	21.05	10.39	6.65	4.75	F
Johnston	US-70	B2	2.50	10.07	5.17	9.5	100.00	100.00	100.00	99.08	93.65	68.33	50.65	37.10	24.44	13.50	7.68	5.26	P
Johnston	US-70	B2	2.50	12.06	5.01	9.5	100.00	100.00	100.00	99.57	96.67	66.84	45.01	31.51	21.07	10.85	7.09	5.19	C
Johnston	US-70	B2	2.48	7.58	5.66	9.5	100.00	100.00	100.00	100.00	96.62	66.28	45.39	32.49	22.38	11.41	7.67	5.77	P
Johnston	US-70	B2	2.50	4.53	4.39	25	100.00	98.47	84.61	70.75	60.32	45.57	35.90	28.62	21.05	10.39	6.65	4.75	F
Johnston	US-70	A1	2.50	8.57	5.28	9.5	100.00	100.00	100.00	99.13	94.62	70.95	51.95	37.68	24.65	13.51	7.71	5.31	P
Johnston	US-70	A1	2.49	11.43	5.09	9.5	100.00	100.00	100.00	100.00	97.05	70.51	51.42	37.09	24.97	13.81	8.46	6.05	P
Johnston	US-70	A1	2.47	3.83	5.77	9.5	100.00	100.00	100.00	99.44	95.09	63.05	44.21	32.24	22.32	11.36	7.69	5.73	P
Johnston	US-70	A1	2.50	5.42	4.33	25	100.00	96.36	80.55	65.99	58.37	46.74	37.80	29.18	20.94	11.23	8.03	6.47	F
Johnston	US-70	A2	2.50	10.34	5.28	9.5	100.00	100.00	100.00	99.13	94.62	70.95	51.95	37.68	24.65	13.51	7.71	5.31	P
Johnston	US-70	A2	2.49	9.11	5.09	9.5	100.00	100.00	100.00	100.00	97.05	70.51	51.42	37.09	24.97	13.81	8.46	6.05	P
Johnston	US-70	A2	2.47	3.53	5.77	9.5	100.00	100.00	100.00	99.44	95.09	63.05	44.21	32.24	22.32	11.36	7.69	5.73	P
Johnston	US-70	A2	2.50	6.57	4.33	25	100.00	96.36	80.55	65.99	58.37	46.74	37.80	29.18	20.94	11.23	8.03	6.47	F
Brunswick	US17	B1	2.42	8.91	6.49	9.5	100.00	100.00	100.00	100.00	98.33	81.24	64.09	54.83	43.78	30.40	12.06	6.39	F
Brunswick	US17	B1	2.36	2.92	6.91	9.5	100.00	100.00	100.00	99.61	96.27	71.39	49.74	43.29	36.12	26.34	10.64	5.92	F
Brunswick	US17	B1	2.41	7.38	5.69	19	100.00	98.66	92.07	80.92	71.14	49.80	33.19	28.84	25.22	19.86	9.18	5.07	F
Brunswick	US17	B1	2.44	7.03	5.93	25	100.00	94.87	81.99	64.30	55.05	43.50	36.23	31.77	26.34	18.44	8.00	4.24	F
Brunswick	US17	B2	2.42	10.77	6.49	9.5	100.00	100.00	100.00	100.00	98.33	81.24	64.09	54.83	43.78	30.40	12.06	6.39	F
Brunswick	US17	B2	2.36	6.77	6.91	9.5	100.00	100.00	100.00	99.61	96.27	71.39	49.74	43.29	36.12	26.34	10.64	5.92	F
Brunswick	US17	B2	2.41	7.66	5.69	19	100.00	98.66	92.07	80.92	71.14	49.80	33.19	28.84	25.22	19.86	9.18	5.07	F
Brunswick	US17	B2	2.44	5.61	5.93	25	100.00	94.87	81.99	64.30	55.05	43.50	36.23	31.77	26.34	18.44	8.00	4.24	F
Brunswick	US17	A1	2.40	8.06	6.47	9.5	100.00	100.00	99.99	99.30	96.50	78.55	62.38	53.61	42.68	29.78	12.10	6.97	F
Brunswick	US17	A1	2.37	3.60	6.96	9.5	100.00	100.00	100.00	99.70	94.57	67.22	46.89	40.16	33.54	25.23	10.65	5.61	F
Brunswick	US17	A1	2.41	5.73	5.75	19	100.00	100.00	96.50	82.04	69.10	49.30	37.20	32.01	27.79	22.26	9.73	5.54	F
Brunswick	US17	A1	2.43	7.27	5.55	25	100.00	90.11	82.75	69.80	62.10	49.27	41.13	35.13	28.08	18.84	7.53	3.93	F
Brunswick	US17	A2	2.40	8.59	6.47	9.5	100.00	100.00	99.99	99.30	96.50	78.55	62.38	53.61	42.68	29.78	12.10	6.97	F
Brunswick	US17	A2	2.37	2.30	6.96	9.5	100.00	100.00	100.00	99.70	94.57	67.22	46.89	40.16	33.54	25.23	10.65	5.61	F
Brunswick	US17	A2	2.41	4.39	5.75	19	100.00	100.00	96.50	82.04	69.10	49.30	37.20	32.01	27.79	22.26	9.73	5.54	F
Brunswick	US17	A2	2.43	7.15	5.55	25	100.00	90.11	82.75	69.80	62.10	49.27	41.13	35.13	28.08	18.84	7.53	3.93	F
Union	US601	A1	2.48	5.90	6.29	12.5	100.00	100.00	99.59	92.34	85.75	65.53	50.46	42.48	32.75	18.68	8.10	3.67	F
Union	US601	A1	2.47	5.90	6.30	12.5	100.00	100.00	100.00	96.30	86.63	64.84	49.16	39.26	27.24	14.96	7.74	4.17	F
Union	US601	A1	2.43	9.97	7.18	9.5	100.00	100.00	100.00	99.37	98.18	83.64	73.35	63.41	44.93	25.08	10.57	5.45	F
Union	US601	A1	2.52	5.50	5.33	19	100.00	100.00	99.60	84.50	64.06	46.74	43.28	38.13	24.11	11.60	4.59	1.77	F
Union	US601	B1	2.49																P
Union	US601	B1	2.47																P
Union	US601	B1	2.43																P
Union	US601	B1	2.52																P
Union	US601	B2	2.49	5.42	6.21	9.5	100.00	100.00	100.00	97.07	92.62	70.91	53.83	44.99	34.53	19.52	8.33	3.82	F
Union	US601	B2	2.47	6.14	6.51	12.5	100.00	100.00	98.14	93.14	83.19	62.93	50.43	41.59	29.58	16.51	8.33	4.35	F
Union	US601	B2	2.43	10.52	7.46	9.5	100.00	100.00	99.64	98.47	96.25	82.09	71.97	61.89	42.67	22.73	8.41	3.25	F
Union	US601	B2	2.52	8.09	5.44	19	100.00	100.00	98.67	82.37	61.05	56.57	52.52	46.26	28.54	14.10	5.68	1.90	F
New Hanover	US76	B1	2.40	8.09	6.94	9.5	100.00	100.00	100.00	99.39	94.40	73.40	52.89	44.74	36.56	22.37	9.42	3.78	F
New Hanover	US76	B1	2.42	10.51	6.37	9.5	100.00	100.00	100.00	100.00	97.97	79.14	67.43	57.37	42.34	25.41	12.50	4.43	F
New Hanover	US76	B1	2.42	11.00	5.50	9.5	100.00	100.00	98.47	96.14	91.77	66.66	48.88	40.21	27.88	16.23	9.23	4.08	F
New Hanover	US76	A1	2.41	8.57	6.78	9.5	100.00	100.00	100.00	100.00	98.21	82.90	69.13	59.63	47.57	32.60	11.94	5.33	F
New Hanover	US76	A1	2.43	11.10	5.94	9.5	100.00	100.00	100.00	100.00	98.98	74.26	50.70	41.04	32.96	24.64	15.47	6.57	F
New Hanover	US76	A1	2.43	14.63	5.38	19	100.00	100.00	95.89	88.77	82.45	58.52	42.03	34.68	26.60	18.51	9.60	4.24	F
Cumberland	NC87	A1	2.43	5.40	5.91	9.5	100.00	100.00	100.00	99.52	91.65	69.63	54.88	44.85	34.99	21.15	10.89	5.91	F
Cumberland	NC87	A1	2.42	7.04	6.28	9.5	100.00	100.00	100.00	99.50	94.60	70.07	54.63	43.31	33.20	21.17	10.79	5.77	F
Cumberland	NC87	A1	2.41	4.71	6.54	9.5	100.00	100.00	100.00	100.00	97.35	76.17	63.79	58.19	38.46	20.17	8.27	3.51	F
Cumberland	NC87	A1	2.42	7.17	6.09	12.5	100.00	100.00	100.00	91.68	82.98	61.76	49.92	45.43	36.72	19.18	6.01	1.57	F
Cumberland	NC87	A1	2.44	4.68	5.65	19	100.00	100.00	99.40	84.41	68.70	47.66	39.17	31.08	17.68	5.48	1.46	0.51	P
Cumberland	NC87	B1	2.42	6.56	6.02	9.5	100.00	100.00	100.00	99.03	93.20	69.06	54.11	44.00	33.96	20.42	10.30	5.34	F
Cumberland	NC87	B1	2.43	8.40	5.96	9.50	100.00	100.00	99.79	98.99	92.66	70.25	53.61	41.68	31.20	19.37	9.82	5.10	F
Cumberland	NC87	B1	2.41	7.94	6.53	9.50	100.00	100.00	100.00	99.86	97.98	78.17	66.76	60.34	40.19	22.05	9.65	4.26	F
Cumberland	NC87	B1	2.41	8.51	6.13	9.50	100.00	100.00	100.00	97.50	94.28	76.66	61.00	53.79	41.68	23.09	8.32	2.68	F
Cumberland	NC87	B1	2.40	4.59	6.52	19.00	100.00	100.00	99.42	88.38	74.86	58.15	50.79	40.38	30.49	6.39	1.69	0.64	F
Cumberland	NC87	A2	2.43	6.19	5.91	9.5	100.00	100.00	100.00	99.52	91.65	69.63	54.88	44.85	34.99	21.15	10.89	5.91	F
Cumberland	NC87	A2	2.42	4.09	6.28	9.50	100.00	100.00	100.00	99.50	94.60	70.07	54.63	43.31	33.20	21.17	10.79	5.77	F
Cumberland	NC87	A2	2.41	4.73	6.54	9.50	100.00	100.00	100.00	100.00	97.35	76.17	63.79	58.19	38.46	20.17	8.27	3.51	F
Cumberland	NC87	A2	2.42	6.33	6.09	12.50	100.00	100.00	100.00	91.68	82.98	61.76	49.92	45.43	36.72	19.18	6.01	1.57	F
Cumberland	NC87	A2	2.44	5.45	5.65	19.00	100.00	100.00	99.40	84.41	68.70	47.66	39.17	31.08	17.68	5.48	1.46	0.51	P
Cumberland	NC87	B2	2.42	8.17	6.02	9.5	100.00	100.00	100.00	99.03	93.20	69.06	54.11	44.00	33.96	20.42	10.30	5.34	F
Cumberland	NC87	B2	2.43	5.84	5.96	9.50	100.00	100.00	99.79	98.99	92.66	70.25	53.61	41.68	31.20	19.37	9.82	5.10	F
Cumberland	NC87	B2	2.41	3.00	6.53	9.50	100.00	100.00	100.00	99.86	97.98	78.17	66.76	60.34	40.19	22.05	9.65	4.26	F
Cumberland	NC87	B2	2.41	6.26	6.13	9.50	100.00	100.00	100.00	97.50	94.28	76.66	61.00	53.79	41.68	23.09	8.32	2.68	F
Cumberland	NC87	B2	2.40	4.13	6.52	19.00	100.00	100.00	99.42	88.38	74.86	58.15	50.79	40.38	30.49	6.39	1.69	0.64	F
Swain	US74	B1	2.53	4.28	6.44	9.5	100.00	100.00	100.00	99.70	95.26	83.15	62.64	47.88	37.01	26.98	16.88	7.57	F
Swain	US74	B1	2.60	4.84	5.28	19.00	100.00	100.00	98.53	75.04	61.19	48.90	39.54	31.66	25.14	18.57	11.74	5.77	F
Swain	US74	B1	2.52	10.74	5.44	19.00	100.00	100.00	98.55	81.25	70.45	54.57	48.24	42.37	30.30	18.47	10.43	4.94	F
Swain	US74	A1	2.54	3.49	5.89	9.5	100.00	100.00	100.00	99.67	96.15	82.65	60.40	45.54	34.72	24.68	14.76	7.03	F
Swain	US74	A1	2.61	3.93	4.91	19.00	100.00	100.00	96.63	75.75	61.52	51.82	40.53	31.51	24.67	18.28	11.78	5.85	F
Swain	US74	A1	2.51	8.01	5.98	19.00	100.00	100.00	98.66	82.57	68.35	51.47	45.98	40.60	29.07	17.76	9.99	4.82	F
Haywood	NC209	A1	2.52	7.31	7.01	9.5	100.00	100.00	100.00	100.00	97.25	75.47	61.23	44.32	31.99	21.85	13.56	6.63	F
Haywood	NC209	A1	2.50	7.39	6.49	9.50	100.00	100.00	100.00	99.83	96.84	75.14	57.40	41.86	30.22	20.95	12.44	5.96	F
Haywood	NC209	A1	2.62	8.31	4.68	19.00	100.00	100.00	94.26	75.01	64.41	44.06	33.43	25.26	19.31	14.28	9.09	4.84	P
Haywood	NC209	B1	2.52	5.04	7.01	9.5	100.00	100.00	100.00	100.00	97.25	75.47	61.23	44.32	31.99	21.85	13.56	6.63	F
Haywood	NC209	B1	2.50	6.84	6.49	9.50	100.00	100.00	100.00	99.83	96.84	75.14	57.40	41.86	30.22	20.95	12.44	5.96	F
Haywood	NC209	B1	2.62	6.23	4.68	19.00	100.00	100.00	94.26	75.01	64.41	44.06	33.43	25.26	19.31	14.28	9.09	4.84	P

Table A.7 Master Database part 4 of test level 2

		Field	Mixture info.																	
						Gradation (% Passing)														
County	Route	Loc ID	Gmm	%AV	%AC	NMSA	1.5in (37.5mm)	1" (25mm)	3/4 (19mm)	1/2 (12.5mm)	3/8 (9.5mm)	#4 (4.75mm)	#8 (2.36mm)	#16 (1.18mm)	#30 (0.6mm)	#50 (0.3mm)	#100 (0.15mm)	#200 (0.075mm)		
Martin	US13	A1	2.47	4.72	5.60	12.5	100.00	100.00	100.00	96.18	88.94	62.32	48.24	38.14	28.35	16.70	9.36	5.28	F	
Martin	US13	A1	2.49	6.52	5.27	9.50	100.00	100.00	99.43	96.75	90.34	61.56	41.62	32.78	25.11	14.47	7.89	4.33	P	
Martin	US13	A1	2.49	7.58	4.22	19.00	100.00	100.00	97.75	77.49	69.46	43.11	31.06	24.67	19.11	11.01	6.04	3.44	P	
Martin	US13	B1	2.48	6.14	5.13	12.5	100.00	100.00	99.18	94.50	88.84	69.15	55.90	45.40	34.52	19.04	10.22	5.63	F	
Martin	US13	B1	2.49	7.08	4.43	12.50	100.00	100.00	100.00	93.36	86.67	58.91	44.58	35.11	26.29	15.74	9.03	5.10	F	
Martin	US13	B1	2.51	8.24	4.19	12.50	100.00	100.00	100.00	90.65	81.73	64.34	52.10	40.09	27.51	17.29	10.64	6.22	F	
Martin	US13	B2	2.48	7.73	5.13	12.5	100.00	100.00	99.18	94.50	88.84	69.15	55.90	45.40	34.52	19.04	10.22	5.63	F	
Martin	US13	B2	2.49	6.30	4.43	12.50	100.00	100.00	100.00	93.36	86.67	58.91	44.58	35.11	26.29	15.74	9.03	5.10	F	
Martin	US13	B2	2.51	7.51	4.19	12.50	100.00	100.00	100.00	90.65	81.73	64.34	52.10	40.09	27.51	17.29	10.64	6.22	F	
Martin	US13	A2	2.47	6.09	5.60	12.5	100.00	100.00	100.00	96.18	88.94	62.32	48.24	38.14	28.35	16.70	9.36	5.28	F	
Martin	US13	A2	2.49	6.69	5.27	9.50	100.00	100.00	99.43	96.75	90.34	61.56	41.62	32.78	25.11	14.47	7.89	4.33	P	
Martin	US13	A2	2.49	7.27	4.22	19.00	100.00	100.00	97.75	77.49	69.46	43.11	31.06	24.67	19.11	11.01	6.04	3.44	P	
Richmond	NC177	B1	2.49	9.48	5.65	9.5	100.00	100.00	100.00	100.00	94.55	72.58	55.59	44.66	33.06	19.52	10.07	5.15	F	
Richmond	NC177	B1	2.35	8.80	7.42	9.50	100.00	100.00	100.00	100.00	95.75	81.70	69.30	58.33	43.22	24.29	10.88	4.87	F	
Richmond	NC177	A1	2.50	8.17	5.68	9.5	100.00	100.00	100.00	99.60	92.59	68.64	53.80	44.40	33.27	19.35	9.58	4.80	F	
Richmond	NC177	A1	2.38	7.69	8.27	9.50	100.00	100.00	100.00	99.67	95.87	80.36	65.95	54.39	40.01	22.46	10.15	4.61	F	
Richmond	NC177	A2	2.50	7.90	5.68	9.5	100.00	100.00	100.00	99.60	92.59	68.64	53.80	44.40	33.27	19.35	9.58	4.80	F	
Richmond	NC177	A2	2.38	6.55	8.27	9.50	100.00	100.00	100.00	99.67	95.87	80.36	65.95	54.39	40.01	22.46	10.15	4.61	F	
Richmond	NC177	B2	2.49	8.88	5.65	9.5	100.00	100.00	100.00	100.00	94.55	72.58	55.59	44.66	33.06	19.52	10.07	5.15	F	
Richmond	NC177	B2	2.35	8.16	7.42	9.50	100.00	100.00	100.00	100.00	95.75	81.70	69.30	58.33	43.22	24.29	10.88	4.87	F	
Montgomery	US220	B1	2.45	9.09	5.93	9.5	100.00	100.00	100.00	99.41	90.30	66.10	54.02	45.33	33.12	17.50	6.59	3.32	F	
Montgomery	US220	B1	2.48	6.21	6.19	9.50	100.00	100.00	100.00	100.00	97.93	75.04	59.71	47.35	35.00	20.86	12.21	7.02	F	
Montgomery	US220	B1	2.43	8.52	6.54	9.50	100.00	100.00	100.00	100.00	99.83	90.84	70.20	59.65	44.38	23.61	9.50	3.06	F	
Montgomery	US220	A1	2.44	9.21	5.96	9.5	100.00	100.00	100.00	99.08	91.91	67.46	54.79	46.00	33.72	17.44	6.92	3.75	F	
Montgomery	US220	A1	2.47	6.80	6.49	9.50	100.00	100.00	100.00	100.00	98.92	78.54	62.91	50.01	37.14	21.89	11.76	7.66	F	
Montgomery	US220	A1	2.41	6.68	7.11	9.50	100.00	100.00	100.00	100.00	98.38	85.96	68.89	54.23	38.90	21.55	10.11	4.70	F	
Davidson	NC47	B1	2.52	11.35	4.77	9.5	100.00	100.00	100.00	99.48	96.92	51.89	32.02	24.55	18.97	13.61	8.68	4.71	C	
Davidson	NC47	B1	2.44	11.67	6.06	9.50	100.00	100.00	100.00	99.57	95.26	68.81	52.50	39.39	27.77	17.62	10.29	5.24	F	
Davidson	NC47	B1	2.40	9.64	8.34	9.50	100.00	100.00	100.00	96.84	91.83	67.67	48.96	36.90	25.87	15.56	9.18	4.17	P	
Davidson	NC47	A1	2.47	8.30	5.18	9.5	100.00	100.00	100.00	99.82	96.69	58.41	35.74	26.45	19.66	13.89	8.86	4.83	C	
Davidson	NC47	A1	2.44	11.22	5.97	9.50	100.00	100.00	100.00	100.00	95.75	72.37	53.93	40.04	28.20	18.24	11.11	6.09	F	
Davidson	NC47	B2	2.52	12.08	4.77	9.5	100.00	100.00	100.00	99.48	96.92	51.89	32.02	24.55	18.97	13.61	8.68	4.71	C	
Davidson	NC47	B2	2.44	8.78	6.06	9.50	100.00	100.00	100.00	99.57	95.26	68.81	52.50	39.39	27.77	17.62	10.29	5.24	F	
Davidson	NC47	B2	2.40	10.53	8.34	9.50	100.00	100.00	100.00	96.84	91.83	67.67	48.96	36.90	25.87	15.56	9.18	4.17	P	
Cumberland	NC82	B1	2.38	8.39	7.36	9.5	100.00	100.00	100.00	100.00	96.93	78.38	63.21	53.48	42.28	23.43	10.37	5.27	F	
Cumberland	NC82	B1	2.41	12.86	6.83	9.50	100.00	100.00	100.00	100.00	96.99	79.33	68.77	63.23	42.60	23.74	12.10	4.09	F	
Cumberland	NC82	B1	2.45	10.41	5.45	12.50	100.00	100.00	100.00	94.36	82.36	57.37	43.50	34.69	24.02	12.07	6.13	3.02	F	
Cumberland	NC82	A1	2.38	8.47	7.56	9.5	100.00	100.00	100.00	100.00	96.95	77.15	61.57	51.98	41.14	23.15	10.38	5.38	F	
Cumberland	NC82	A1	2.41	10.78	6.55	9.50	100.00	100.00	100.00	99.82	95.41	76.18	65.67	59.11	41.64	24.73	10.14	3.47	F	
Cumberland	NC82	A1	2.42	10.26	6.80	9.50	100.00	100.00	100.00	100.00	99.52	86.83	76.42	68.24	44.76	21.89	9.39	3.87	F	
Cumberland	NC82	A1	2.42	13.36	6.04	9.50	100.00	100.00	100.00	99.66	97.54	88.40	72.85	59.77	37.68	15.54	6.18	2.02	F	
Cumberland	US401	A1	2.47	7.01	5.24	9.5	100.00	100.00	100.00	100.00	94.74	58.82	40.31	29.92	18.41	10.37	6.73	4.41	C	
Cumberland	US401	A1	2.43	7.96	5.94	9.50	100.00	100.00	100.00	99.63	90.10	62.46	50.62	43.49	34.86	20.36	9.19	4.73	F	
Cumberland	US401	A1	2.43	8.45	6.16	9.50	100.00	100.00	100.00	99.57	96.89	80.58	69.70	63.19	37.74	19.63	10.59	4.02	F	
Cumberland	US401	A1	2.42	11.23	6.46	9.50	100.00	100.00	100.00	99.45	94.56	59.57	35.37	27.39	19.67	11.96	7.97	4.00	C	
Cumberland	US401	A1	2.38	10.15	6.94	9.50	100.00	100.00	100.00	98.78	95.02	80.33	69.71	56.52	39.51	19.21	9.10	3.09	F	
Cumberland	US401	B1	2.47	9.86	5.34	9.5	100.00	100.00	100.00	99.72	95.13	60.61	42.33	32.54	19.64	9.99	5.80	3.46	P	
Cumberland	US401	B1	2.43	12.81	5.92	9.50	100.00	100.00	100.00	99.62	90.74	64.54	52.50	45.78	37.24	21.00	8.68	4.38	F	
Cumberland	US401	B1	2.42	8.29	6.23	9.50	100.00	100.00	100.00	99.59	96.11	81.14	71.64	64.67	39.65	21.36	10.76	3.47	F	
Cumberland	US401	B1	2.38	8.47	7.78	9.50	100.00	100.00	100.00	100.00	98.36	73.21	56.36	49.23	36.39	21.30	11.64	3.91	F	
Cumberland	US401	B1	2.41	8.48	6.71	9.50	100.00	100.00	100.00	98.70	95.83	83.04	74.10	62.04	43.86	21.43	8.62	2.45	F	
Harnett	NC55	A1	2.39	7.28	6.72	9.5	100.00	100.00	100.00	100.00	92.95	85.81	66.70	57.82	43.89	21.60	8.27	4.15	F	
Harnett	NC55	A1	2.45	11.60	6.03	9.50	100.00	100.00	100.00	100.00	100.00	84.99	73.39	62.91	44.99	24.77	11.01	5.54	F	
Harnett	NC55	A1	2.44	2.23	5.91	12.50	100.00	100.00	100.00	97.59	87.52	61.27	46.26	40.54	30.62	17.20	7.95	3.82	F	
Harnett	NC55	A1	2.44	3.23	4.82	19.00	100.00	100.00	99.43	89.13	80.56	28.40	21.10	18.11	14.44	8.55	3.54	1.35	C	
Harnett	NC55	B1	2.46	10.55	6.58	9.5	100.00	100.00	100.00	99.82	95.46	71.72	57.62	50.27	37.92	18.48	8.33	3.62	F	
Harnett	NC55	B1	2.39	8.72	6.66	9.50	100.00	100.00	100.00	100.00	99.54	50.06	42.46	36.07	25.24	12.38	5.38	2.91	P	
Harnett	NC55	B1	2.44	4.08	5.90	12.50	100.00	100.00	100.00	98.88	89.06	63.53	48.67	42.84	32.23	18.17	10.35	4.41	F	
Harnett	NC55	B1	2.41	1.99	4.93	19.00	100.00	100.00	99.32	82.67	69.88	49.88	38.28	33.54	25.36	13.84	5.24	1.84	F	
Brunswick	NC179	A1	2.37	5.16	7.69	9.5	100.00	100.00	100.00	99.80	98.04	82.21	67.75	58.90	46.89	29.00	9.20	5.21	F	
Brunswick	NC179	A1	2.39	6.58	6.20	9.50	100.00	100.00	100.00	100.00	95.23	68.70	52.41	44.25	32.74	20.49	10.41	5.51	F	
Brunswick	NC179	A1	2.41	10.55	6.42	9.50	100.00	100.00	100.00	99.19	93.82	74.21	64.04	61.58	56.96	38.42	9.29	0.92	F	
Brunswick	NC179	B1	2.37	5.67	7.31	9.5	100.00	100.00	100.00	98.70	96.11	80.22	65.43	57.21	46.55	30.50	10.46	6.14	F	
Brunswick	NC179	B1	2.42	6.75	7.52	9.50	100.00	100.00	100.00	99.28	93.05	73.98	58.90	49.68	38.46	24.80	10.77	5.69	F	
Brunswick	NC179	B1	2.37	9.12	6.25	9.50	100.00	100.00	100.00	99.46	94.86	75.79	65.66	63.27	58.05	38.27	8.93	0.75	F	
Avery	NC194	B1	2.50	9.63	6.07	9.5	100.00	100.00	100.00	100.00	97.33	76.54	50.78	34.98	25.08	17.48	11.14	4.46	P	
Avery	NC194	B1	2.44	6.39	6.67	9.50	100.00	100.00	100.00	100.00	95.81	65.34	47.99	35.27	25.62	16.67	10.39	7.04	P	
Avery	NC194	B1	2.51	8.92	7.15	9.50	100.00	100.00	100.00	100.00	99.70	89.37	69.04	50.39	35.42	22.14	13.57	5.88	F	
Avery	NC194	B1	2.51	9.82	6.42	9.50	100.00	100.00	100.00	99.63	98.01	65.69	30.46	14.90	9.17	6.59	4.89	3.38	C	
Avery	NC194	A1	2.50	10.37	6.07	9.5	100.00	100.00	100.00	100.00	97.45	76.26	48.59	32.70	23.51	15.63	9.67	3.67	P	
Avery	NC194	A1	2.44	5.60	6.82	9.50	100.00	100.00	100.00	100.00	96.58	66.96	46.79	34.33	24.55	16.44	11.27	6.99	P	
Avery	NC194	A1	2.43	4.35	8.30	9.50	100.00	100.00	100.00	100.00	97.71	75.62	57.77	43.42	32.85	22.48	14.35	6.82	F	
Avery	NC194	A1	2.53	4.91	7.02	9.50	100.00	100.00	100.00	99.98	99.03	78.81	46.56	29.46	20.09	14.28	11.87	5.87	C	
Avery	NC194	A1	2.49	3.78	6.25	9.50	100.00	100.00	100.00	99.99	98.28	76.99	52.95	37.42	27.36	18.95	13.29	6.41	P	
Avery	NC194	A2																	P	
Avery	NC194	A2																	P	
Avery	NC194	A2																	P	
Avery	NC194	A2																	P	
Avery	NC194	A2																	P	
Avery	NC194	B2																	P	
Avery	NC194	B2																	P	
Avery	NC194	B2																	P	
Avery	NC194	B2																	P	
Alamance	SR1530	B1	2.44	2.28	6.42	9.5	100.00	100.00	100.00	99.24	96.79	75.46	54.58	43.51	32.46	18.49	10.52	5.57	F	
Alamance	SR1530	B1	2.52	4.39	6.58	9.50	100.00	100.00	100.00	98.34	95.25	76.67	60.67	50.37	36.12	18.37	11.86	4.95	F	
Alamance	SR1530	B1	2.56	7.10	6.33	9.50	100.00	100.00	100.00	100.00	98.21	77.26	53.38	39.10	28.68	17.43	10.47	6.32	F	
Alamance	SR1530	B1	2.47	14.25	6.79	9.50	100.00	100.00	100.00	100.00	99.47	79.39	62.37	48.99	31.65	14.88	7.47	4.22	F	
Alamance	SR1530	B2																	P	
Alamance	SR1530	B2																	P	
Alamance	SR1530	B2																	P	
Alamance	SR1530	B2																	P	
Alamance	SR1530	G1	2.54	6.91	6.32	9.5	100.00	100.00	100.00	99.80	97.05	76.45	64.05	58.87	42.34	21.77	11.34	5.43	F	
Alamance	SR1530	G1	2.60	2.19	5.46	9.50	100.00	100.00	99.06	94.16	92.58	60.49	41.20	33.20	23.57	13.42	11.15	4.77	P	
Alamance	SR1530	G1	2.58	4.76	5.69	12.50	100.00	100.00	100.00	96.09	87.73	51.35	36.70	33.11	24.12	14.49	8.66	4.48	F	
Alamance	SR1530	G1	2.51	7.88	6.82	9.50	100.00	100.00	100.00	99.31	98.56	79.25	62.39	51.18	25.79	13.48	11.96	4.52	P	
Alamance	SR1530	G1	2.51	10.23	8.04	9.50	0.00	100.00	100.00	97.36	92.00	62.34	46.82	40.23	24.78	14.09	9.96	4.49	P	

Table A.8 Master Database part 5 of test level 1

		Field Observ	Sub-Structure																	
County	Route	Loc ID	Base Type	DCP			Soil Calssification													
				Base thick	Ebase	Esubgrade	Soil Type (1st)	Thickness (in.)	Esoil (psi)	Soil Type (2st)	Thickness (in.)	Esoil (psi)	Soil Type (3st)	Thickness (in.)	Esoil (psi)	Soil Type (4th)	Thickness (in.)	Esoil (psi)	SA	AFT
Wake	I-540	B1	CTABC	200	1,500,000	11835	A-4	7.09	13,875	A-4	3.94	13,875	A-7-6	38.98	7,635				26.9	8.4
Wake	I-540	B1	CTABC	200	1,500,000	11835	A-4	7.09	13,875	A-4	14	13,875	A-7-6	38.98	7,635				19.9	12.4
Wake	I-540	B1	CTABC	200	1,500,000	11835	A-4	7.09	13,875	A-4	14	13,875	A-7-6	38.98	7,635				20.9	10.8
Wake	I-540	B1	CTABC	200	1,500,000	11835	A-4	7.09	13,875	A-4	14	13,875	A-7-6	38.98	7,635				17.1	13.2
Wake	I-540	A1	CTABC	200	1,500,000	14,259	A-4	7.09	13,875	A-4	14	13,875	A-7-6	38.98	7,635				26.9	9.4
Wake	I-540	A1	CTABC	200	1,500,000	14,259	A-4	7.09	13,875	A-4	14	13,875	A-7-6	38.98	7,635				18.7	13.2
Wake	I-540	A1	CTABC	200	1,500,000	14,259	A-4	7.09	13,875	A-4	14	13,875	A-7-6	38.98	7,635				19.6	10.9
Wake	I-540	A1	CTABC	200	1,500,000	14,259	A-4	7.09	13,875	A-4	14	13,875	A-7-6	38.98	7,635				21.3	10.6
Wake	I-540	B2	CTABC	200	1,500,000	15,649	A-4	7.09	13,875	A-4	14	13,875	A-7-6	38.98	7,635				26.9	8.4
Wake	I-540	B2	CTABC	200	1,500,000	15,649	A-4	7.09	13,875	A-4	14	13,875	A-7-6	38.98	7,635				19.9	12.4
Wake	I-540	B2	CTABC	200	1,500,000	15,649	A-4	7.09	13,875	A-4	14	13,875	A-7-6	38.98	7,635				20.9	10.8
Wake	I-540	B2	CTABC	200	1,500,000	15,649	A-4	7.09	13,875	A-4	14	13,875	A-7-6	38.98	7,635				17.1	13.2
Wake	I-540	A2	CTABC	200	1,500,000	19,268	A-4	7.09	13,875	A-4	14	13,875	A-7-6	38.98	7,635				26.9	9.4
Wake	I-540	A2	CTABC	200	1,500,000	19,268	A-4	7.09	13,875	A-4	14	13,875	A-7-6	38.98	7,635				18.7	13.2
Wake	I-540	A2	CTABC	200	1,500,000	19,268	A-4	7.09	13,875	A-4	14	13,875	A-7-6	38.98	7,635				19.6	10.9
Wake	I-540	A2	CTABC	200	1,500,000	19,268	A-4	7.09	13,875	A-4	14	13,875	A-7-6	38.98	7,635				21.3	10.6
Mecklenburg	NC24	B1	SABC	230	54,635	16242	A-4	5.91	12,271	A-7-6	36.22	6,206							27.5	8.4
Mecklenburg	NC24	B1	SABC	230	54,635	16242	A-4	5.91	12,271	A-7-6	36.22	6,206							25.7	10
Mecklenburg	NC24	B1	SABC	230	54,635	16242	A-4	5.91	12,271	A-7-6	36.22	6,206							18.5	12.7
Mecklenburg	NC24	A1	SABC	380	58,884	12851	A-4	5.91	12,271	A-7-6	36.22	6,206							29.7	7.4
Mecklenburg	NC24	A1	SABC	380	58,884	12851	A-4	5.91	12,271	A-7-6	36.22	6,206							24.4	10.8
Mecklenburg	NC24	A1	SABC	380	58,884	12851	A-4	5.91	12,271	A-7-6	36.22	6,206							20.2	11.7
Mecklenburg	NC24	B2	SABC	180	31,559	17164	A-4	5.91	12,271	A-7-6	36.22	6,206							27.5	8.4
Mecklenburg	NC24	B2	SABC	180	31,559	17164	A-4	5.91	12,271	A-7-6	36.22	6,206							25.7	10
Mecklenburg	NC24	B2	SABC	180	31,559	17164	A-4	5.91	12,271	A-7-6	36.22	6,206							18.5	12.7
Johnston	US-70	B1	ABC	227	119,925	43,486	A-2-4	14.17	16,861	A-4	24.02	16,125	A-6	31.89	12,461				29.2	8.4
Johnston	US-70	B1	ABC	227	119,925	43,486	A-2-4	14.17	16,861	A-4	24.02	16,125	A-6	31.89	12,461				26.5	8.9
Johnston	US-70	B1	ABC	227	119,925	43,486	A-2-4	14.17	16,861	A-4	24.02	16,125	A-6	31.89	12,461				28.1	9.7
Johnston	US-70	B1	ABC	227	119,925	43,486	A-2-4	14.17	16,861	A-4	24.02	16,125	A-6	31.89	12,461				24.5	8.3
Johnston	US-70	B2	ABC	238	54,294	21,834	A-2-4	14.17	16,861	A-4	24.02	16,125	A-6	31.89	12,461				29.2	8.4
Johnston	US-70	B2	ABC	238	54,294	21,834	A-2-4	14.17	16,861	A-4	24.02	16,125	A-6	31.89	12,461				26.5	8.9
Johnston	US-70	B2	ABC	238	54,294	21,834	A-2-4	14.17	16,861	A-4	24.02	16,125	A-6	31.89	12,461				28.1	9.7
Johnston	US-70	B2	ABC	238	54,294	21,834	A-2-4	14.17	16,861	A-4	24.02	16,125	A-6	31.89	12,461				24.5	8.3
Johnston	US-70	A1	ABC	243	60,092	15,215	A-2-4	14.17	16,861	A-4	24.02	16,125	A-6	31.89	12,461				29.5	8.5
Johnston	US-70	A1	ABC	243	60,092	15,215	A-2-4	14.17	16,861	A-4	24.02	16,125	A-6	31.89	12,461				30.7	7.9
Johnston	US-70	A1	ABC	243	60,092	15,215	A-2-4	14.17	16,861	A-4	24.02	16,125	A-6	31.89	12,461				27.9	10
Johnston	US-70	A1	ABC	243	60,092	15,215	A-2-4	14.17	16,861	A-4	24.02	16,125	A-6	31.89	12,461				28.2	7
Johnston	US-70	A2	ABC	239	74,186	26,792	A-2-4	14.17	16,861	A-4	24.02	16,125	A-6	31.89	12,461				29.5	8.5
Johnston	US-70	A2	ABC	239	74,186	26,792	A-2-4	14.17	16,861	A-4	24.02	16,125	A-6	31.89	12,461				30.7	7.9
Johnston	US-70	A2	ABC	239	74,186	26,792	A-2-4	14.17	16,861	A-4	24.02	16,125	A-6	31.89	12,461				27.9	10
Johnston	US-70	A2	ABC	239	74,186	26,792	A-2-4	14.17	16,861	A-4	24.02	16,125	A-6	31.89	12,461				28.2	7
Brunswick	US17	B1	ABC	203	25,971	26,259	A-2	25.98	16,881	A-3	14.96	35,186	A-3	16.93	16,881	A-2-4	27.17	24,061	43.2	7.4
Brunswick	US17	B1	ABC	203	25,971	26,259	A-2	25.98	16,881	A-3	14.96	35,186	A-3	16.93	16,881	A-2-4	27.17	24,061	37.7	9
Brunswick	US17	B1	ABC	203	25,971	26,259	A-2	25.98	16,881	A-3	14.96	35,186	A-3	16.93	16,881	A-2-4	27.17	24,061	29.7	9.2
Brunswick	US17	B1	ABC	203	25,971	26,259	A-2	25.98	16,881	A-3	14.96	35,186	A-3	16.93	16,881	A-2-4	27.17	24,061	27.4	10.4
Brunswick	US17	B2	ABC	203	23,851	22,916	A-2	25.98	16,881	A-3	14.96	35,186	A-3	16.93	16,881	A-2-4	27.17	24,061	43.2	7.4
Brunswick	US17	B2	ABC	203	23,851	22,916	A-2	25.98	16,881	A-3	14.96	35,186	A-3	16.93	16,881	A-2-4	27.17	24,061	37.7	9
Brunswick	US17	B2	ABC	203	23,851	22,916	A-2	25.98	16,881	A-3	14.96	35,186	A-3	16.93	16,881	A-2-4	27.17	24,061	29.7	9.2
Brunswick	US17	B2	ABC	203	23,851	22,916	A-2	25.98	16,881	A-3	14.96	35,186	A-3	16.93	16,881	A-2-4	27.17	24,061	27.4	10.4
Brunswick	US17	A1	ABC	203	17,171	21,861	A-2	25.98	16,881	A-3	14.96	35,186	A-3	16.93	16,881	A-2-4	27.17	24,061	43.8	7.3
Brunswick	US17	A1	ABC	203	17,171	21,861	A-2	25.98	16,881	A-3	14.96	35,186	A-3	16.93	16,881	A-2-4	27.17	24,061	36.2	9.5
Brunswick	US17	A1	ABC	203	17,171	21,861	A-2	25.98	16,881	A-3	14.96	35,186	A-3	16.93	16,881	A-2-4	27.17	24,061	32.3	8.6
Brunswick	US17	A1	ABC	203	17,171	21,861	A-2	25.98	16,881	A-3	14.96	35,186	A-3	16.93	16,881	A-2-4	27.17	24,061	28.1	9.4
Brunswick	US17	A2	ABC	203	12,868	26,114	A-2	25.98	16,881	A-3	14.96	35,186	A-3	16.93	16,881	A-2-4	27.17	24,061	43.8	7.3
Brunswick	US17	A2	ABC	203	12,868	26,114	A-2	25.98	16,881	A-3	14.96	35,186	A-3	16.93	16,881	A-2-4	27.17	24,061	36.2	9.5
Brunswick	US17	A2	ABC	203	12,868	26,114	A-2	25.98	16,881	A-3	14.96	35,186	A-3	16.93	16,881	A-2-4	27.17	24,061	32.3	8.6
Brunswick	US17	A2	ABC	203	12,868	26,114	A-2	25.98	16,881	A-3	14.96	35,186	A-3	16.93	16,881	A-2-4	27.17	24,061	28.1	9.4
Union	US601	A1	ABC	289	59,660	17,521	A-4	5.91	12,271	A-7-6	36.22	6,206							29.7	10.5
Union	US601	A1	ABC	289	59,660	17,521	A-4	5.91	12,271	A-7-6	36.22	6,206							28.2	11.1
Union	US601	A1	ABC	289	59,660	17,521	A-4	5.91	12,271	A-7-6	36.22	6,206							40.7	8.8
Union	US601	A1	ABC	289	59,660	17,521	A-4	5.91	12,271	A-7-6	36.22	6,206							20.5	12.3
Union	US601	B1	ABC	234	85,741	18,951	A-4	5.91	12,271	A-7-6	36.22	6,206								
Union	US601	B1	ABC	234	85,741	18,951	A-4	5.91	12,271	A-7-6	36.22	6,206								
Union	US601	B1	ABC	234	85,741	18,951	A-4	5.91	12,271	A-7-6	36.22	6,206								
Union	US601	B1	ABC	234	85,741	18,951	A-4	5.91	12,271	A-7-6	36.22	6,206								
Union	US601	B2	ABC	244	88,074	13,662	A-4	5.91	12,271	A-7-6	36.22	6,206							31	9.7
Union	US601	B2	ABC	244	88,074	13,662	A-4	5.91	12,271	A-7-6	36.22	6,206							29.6	10.9
Union	US601	B2	ABC	244	88,074	13,662	A-4	5.91	12,271	A-7-6	36.22	6,206							34.3	10.9
Union	US601	B2	ABC	244	88,074	13,662	A-4	5.91	12,271	A-7-6	36.22	6,206							23.8	11
New Hanover	US76	B1	ABC	240	73,730	28,668	A-3	3.15	16,374	A-3	11.81	16,374	A-3	14.96	16,282	A-3	50.00	16,374	32.4	10.5
New Hanover	US76	B1	ABC	240	73,730	28,668	A-3	3.15	16,374	A-3	11.81	16,374	A-3	14.96	16,282	A-3	50.00	16,374	39	8
New Hanover	US76	B1	ABC	240	73,730	28,668	A-3	3.15	16,374	A-3	11.81	16,374	A-3	14.96	16,282	A-3	50.00	16,374	29.2	9
New Hanover	US76	A1	ABC	290	32,897	28,370	A-3	3.15	16,374	A-3	11.81	16,374	A-3	14.96	16,282	A-3	50.00	16,374	43.5	7.7
New Hanover	US76	A1	ABC	290	32,897	28,370	A-3	3.15	16,374	A-3	11.81	16,374	A-3	14.96	16,282	A-3	50.00	16,374	40.5	7
New Hanover	US76	A1	ABC	290	32,897	28,370	A-3	3.15	16,374	A-3	11.81	16,374	A-3	14.96	16,282	A-3	50.00	16,374	29.9	8.6
Cumberland	NC87	A1	Soil	349	27,354	29,685	A-3	24.02	17,073	A-2	18.11	17,074	A-3	37.80	17,755					
Cumberland	NC87	A1	Soil	349	27,354	29,685	A-3	24.02	17,073	A-2	18.11	17,074	A-3	37.80	17,755					
Cumberland	NC87	A1	Soil	349	27,354	29,685	A-3	24.02	17,073	A-2	18.11	17,074	A-3	37.80	17,755					
Cumberland	NC87	A1	Soil	349	27,354	29,685	A-3	24.02	17,073	A-2	18.11	17,074	A-3	37.80	17,755					
Cumberland	NC87	A1	Soil	349	27,354	29,685	A-3	24.02	17,073	A-2	18.11	17,074	A-3	37.80	17,755					
Cumberland	NC87	B1	Soil	228	25,849	6,254	A-3	24.02	17,073	A-2	18.11	17,074	A-3	37.80	17,755				34.3	8.5
Cumberland	NC87	B1	Soil	228	25,849	6,254	A-3	24.02	17,073	A-2	18.11	17,074	A-3	37.80	17,755				33.1	8.8
Cumberland	NC87	B1	Soil	228	25,849	6,254	A-3	24.02	17,073	A-2	18.11	17,074	A-3	37.80	17,755				36.1	8.8
Cumberland	NC87	B1	Soil	228	25,849	6,254	A-3	24.02	17,073	A-2	18.11	17,074	A-3	37.80	17,755				32.2	9.2
Cumberland	NC87	B1	Soil	228	25,849	6,254	A-3	24.02	17,073	A-2	18.11	17,074	A-3	37.80	17,755				16.6	19.1
Cumberland	NC87	A2	Soil	288	29,786	17,359	A-3	24.02	17,073	A-2	18.11	17,074	A-3	37.80	17,755				36.4	7.8
Cumberland	NC87	A2	Soil	288	29,786	17,359	A-3	24.02	17,073	A-2	18.11	17,074	A-3	37.80	17,755				35.8	8.6
Cumberland	NC87	A2	Soil	288	29,786	17,359	A-3	24.02	17,073	A-2	18.11	17,074	A-3	37.80	17,755				32.4	9.8
Cumberland	NC87	A2	Soil	288	29,786	17,359	A-3	24.02	17,073	A-2	18.11	17,074	A-3	37.80	17,755				25.9	11.6
Cumberland	NC87	A2	Soil	288	29,786	17,359	A-3	24.02	17,073	A-2	18.11	17,074	A-3	37.80	17,755				12.4	22.1
Cumberland	NC87	B2	Soil	378	31,895	14,060	A-3	24.02	17,073	A-2	18.11	17,074	A-3	37.80	17,755					
Cumberland	NC87	B2	Soil	378	31,895	14,060	A-3	24.02	17,073	A-2	18.11	17,074	A-3	37.80	17,755					
Cumberland	NC87	B2	Soil	378	31,895	14,060	A-3	24.02	17,073	A-2	18.11	17,074	A-3	37.80	17,755					
Cumberland	NC87	B2	Soil	378	31,895	14,060	A-3	24.02	17,073	A-2	18.11	17,074	A-3	37.80	17,755					
Cumberland	NC87	B2	Soil	378	31,895	14,060	A-3	24.02	17,073	A-2	18.11	17,074	A-3	37.80	17,755					
Swain	US74	B1	Coarse ABC	260	88,331	20,638	A-5	11.02	19,370	A-6	9.84	11,479	A-4	5.12	19,513				45.7	6.8
Swain	US74	B1	Coarse ABC	260	88,331	20,638	A-5	11.02	19,370	A-6	9.84	11,479	A-4	5.12	19,513				32.8	7.7
Swain	US74	B1	Coarse ABC	260	88,331	20,638	A-5	11.02	19,370	A-6	9.84	11,479	A-4	5.12	19,513				31.8	8.3
Swain	US74	A1	Coarse ABC	300	89,583	25,258	A-5	11.02	19,370	A-6	9.84	11,479	A-4	5.12	19,513				42.3	6.7
Swain	US74	A1	Coarse ABC	300	89,583	25,258	A-5	11.02	19,370	A-6	9.84	11,479	A-4	5.12	19,513				32.8	7
Swain	US74	A1	Coarse ABC	300	89,583	25,258	A-5	11.02	19,370	A-6	9.84	11,479	A-4	5.12	19,513				31.3	9.3
Haywood	NC209	A1	ABC	260	52,701	20,001	A-4	5.12	21,300	A-7-6	33.07	8,125	A-7-6	9.84	10,528	A-4	11.81	19,735	39.5	8.7
Haywood	NC209	A1	ABC	260	52,701	20,001	A-4	5.12	21,300	A-7-6	33.07	8,125	A-7-6	9.84	10,528	A-4	11.81	19,735	36.4	8.7
Haywood	NC209	A1	ABC	260	52,701	20,001	A-4	5.12	21,300	A-7-6	33.07	8,125	A-7-6	9.84	10,528	A-4	11.81	19,735	26.1	8.4
Haywood	NC209	B1	ABC	280	50,199	16,256	A-4	5.12	21,300	A-7-6	33.07	8,125	A-7-6	9.84	10,528	A-4	11.81	19,735	39.5	8.7
Haywood	NC209	B1	ABC	280	50,199	16,256	A-4	5.12	21,300	A-7-6	33.07	8,125	A-7-6	9.84	10,528	A-4	11.81	19,735	36.4	8.7
Haywood	NC209	B1	ABC	280	50,199	16,256	A-4	5.12	21,300	A-7-6	33.07	8,125	A-7-6	9.84	10,528	A-4	11.81	19,735	26.1	8.4

Table A.9 Master Database part 5 of test level 2

		Field Obser…		Sub-Structure																
County	Route	Loc ID	Base Type	DCP			Soil Calssification													
				Base thick	Ebase	Esubgrade	Soil Type (1st)	Thickness (in.)	Esoil (psi)	Soil Type (2st)	Thickness (in.)	Esoil (psi)	Soil Type (3st)	Thickness (in.)	Esoil (psi)	Soil Type (4th)	Thickness (in.)	Esoil (psi)	SA	AFT
Martin	US13	A1	ABC	262	62,619	27,759	A-2	25.98	16,881	A-2-4	14.96	35,186	A-3	16.93	16,881	A-2-4	27.17	24,061	31.1	8.8
Martin	US13	A1	ABC	262	62,619	27,759	A-2	25.98	16,881	A-2-4	14.96	35,186	A-3	16.93	16,881	A-2-4	27.17	24,061	26.9	9.4
Martin	US13	A1	ABC	262	62,619	27,759	A-2	25.98	16,881	A-2-4	14.96	35,186	A-3	16.93	16,881	A-2-4	27.17	24,061	21.1	9.2
Martin	US13	B1	ABC	234	84,411	28,162	A-2	25.98	16,881	A-2-4	14.96	35,186	A-3	16.93	16,881	A-2-4	27.17	24,061	34.8	7.1
Martin	US13	B1	ABC	234	84,411	28,162	A-2	25.98	16,881	A-2-4	14.96	35,186	A-3	16.93	16,881	A-2-4	27.17	24,061	29.8	7
Martin	US13	B1	ABC	234	84,411	28,162	A-2	25.98	16,881	A-2-4	14.96	35,186	A-3	16.93	16,881	A-2-4	27.17	24,061	34.1	5.8
Martin	US13	B2	ABC	382	57,986	38,928	A-2	25.98	16,881	A-2-4	14.96	35,186	A-3	16.93	16,881	A-2-4	27.17	24,061	34.8	7.1
Martin	US13	B2	ABC	382	57,986	38,928	A-2	25.98	16,881	A-2-4	14.96	35,186	A-3	16.93	16,881	A-2-4	27.17	24,061	29.8	7
Martin	US13	B2	ABC	382	57,986	38,928	A-2	25.98	16,881	A-2-4	14.96	35,186	A-3	16.93	16,881	A-2-4	27.17	24,061	34.1	5.8
Martin	US13	A2	ABC	259	30,603	19,174	A-2	25.98	16,881	A-2-4	14.96	35,186	A-3	16.93	16,881	A-2-4	27.17	24,061	31.1	8.8
Martin	US13	A2	ABC	259	30,603	19,174	A-2	25.98	16,881	A-2-4	14.96	35,186	A-3	16.93	16,881	A-2-4	27.17	24,061	26.9	9.4
Martin	US13	A2	ABC	259	30,603	19,174	A-2	25.98	16,881	A-2-4	14.96	35,186	A-3	16.93	16,881	A-2-4	27.17	24,061	21.1	9.2
Richmond	NC177	B1	Soil	362	14,507	9,507	A-2	20.87	17,038	A-2-4	12.99	16,721	A-2	22.05	17,038	A-6	16.14	15,766	34.2	8
Richmond	NC177	B1	Soil	362	14,507	9,507	A-2	20.87	17,038	A-2-4	12.99	16,721	A-2	22.05	17,038	A-6	16.14	15,766	38.7	9.5
Richmond	NC177	A1	Soil	297	21,804	13,332	A-2	20.87	17,038	A-2-4	12.99	16,721	A-2	22.05	17,038	A-6	16.14	15,766	33.1	8.3
Richmond	NC177	A1	Soil	297	21,804	13,332	A-2	20.87	17,038	A-2-4	12.99	16,721	A-2	22.05	17,038	A-6	16.14	15,766	36.1	11.6
Richmond	NC177	A2	Soil	234	31,259	18,908	A-2	20.87	17,038	A-2-4	12.99	16,721	A-2	22.05	17,038	A-6	16.14	15,766	33.1	8.3
Richmond	NC177	A2	Soil	234	31,259	18,908	A-2	20.87	17,038	A-2-4	12.99	16,721	A-2	22.05	17,038	A-6	16.14	15,766	36.1	11.6
Richmond	NC177	B2	Soil	332	12,317	6,769	A-2	20.87	17,038	A-2-4	12.99	16,721	A-2	22.05	17,038	A-6	16.14	15,766	34.2	8
Richmond	NC177	B2	Soil	332	12,317	6,769	A-2	20.87	17,038	A-2-4	12.99	16,721	A-2	22.05	17,038	A-6	16.14	15,766	38.7	9.5
Montgomery	US220	B1	JCP				A-4	9.06	15,980	A-7-6	38.98	6,556	A-7-6	20.08	7,860				28.3	10.1
Montgomery	US220	B1	JCP				A-4	9.06	15,980	A-7-6	38.98	6,556	A-7-6	20.08	7,860				39.3	7.7
Montgomery	US220	B1	JCP				A-4	9.06	15,980	A-7-6	38.98	6,556	A-7-6	20.08	7,860				35.1	9.1
Montgomery	US220	A1	JCP				A-4	9.06	15,980	A-7-6	38.98	6,556	A-7-6	20.08	7,860				29.2	9.9
Montgomery	US220	A1	JCP				A-4	9.06	15,980	A-7-6	38.98	6,556	A-7-6	20.08	7,860				41.4	7.7
Montgomery	US220	A1	JCP				A-4	9.06	15,980	A-7-6	38.98	6,556	A-7-6	20.08	7,860				36.4	9.6
Davidson	NC47	B1	ABC	267	26,524	11,174	A-4	7.09	13,875	A-4	3.94	13,875	A-7-6	38.98	7,635				26.1	8.6
Davidson	NC47	B1	ABC	267	26,524	11,174	A-4	7.09	13,875	A-4	3.94	13,875	A-7-6	38.98	7,635				32.2	9.2
Davidson	NC47	B1	ABC	267	26,524	11,174	A-4	7.09	13,875	A-4	3.94	13,875	A-7-6	38.98	7,635				28.8	14.8
Davidson	NC47	A1	ABC	211	30,683	9,872	A-4	7.09	13,875	A-4	3.94	13,875	A-7-6	38.98	7,635				26.8	9.2
Davidson	NC47	A1	ABC	211	30,683	9,872	A-4	7.09	13,875	A-4	3.94	13,875	A-7-6	38.98	7,635				34.5	8.4
Davidson	NC47	B2	ABC	186	30,308	8,943	A-4	7.09	13,875	A-4	3.94	13,875	A-7-6	38.98	7,635				26.1	8.6
Davidson	NC47	B2	ABC	186	30,308	8,943	A-4	7.09	13,875	A-4	3.94	13,875	A-7-6	38.98	7,635				32.2	9.2
Davidson	NC47	B2	ABC	186	30,308	8,943	A-4	7.09	13,875	A-4	3.94	13,875	A-7-6	38.98	7,635				28.8	14.8
Cumberland	NC82	B1	ABC	309	33,775	6,393	A-4	5.12	20,438	A-6	17.72	9,868	A-6	42.13	8,850				37.6	9.8
Cumberland	NC82	B1	ABC	309	33,775	6,393	A-4	5.12	20,438	A-6	17.72	9,868	A-6	42.13	8,850				38.4	8.7
Cumberland	NC82	B1	ABC	309	33,775	6,393	A-4	5.12	20,438	A-6	17.72	9,868	A-6	42.13	8,850				23	11.4
Cumberland	NC82	A1	ABC	340	18,284	4,964	A-4	5.12	20,438	A-6	17.72	9,868	A-6	42.13	8,850				37.5	10.1
Cumberland	NC82	A1	ABC	340	18,284	4,964	A-4	5.12	20,438	A-6	17.72	9,868	A-6	42.13	8,850				35.9	9
Cumberland	NC82	A1	ABC	340	18,284	4,964	A-4	5.12	20,438	A-6	17.72	9,868	A-6	42.13	8,850				36.8	9.1
Cumberland	NC82	A1	ABC	340	18,284	4,964	A-4	5.12	20,438	A-6	17.72	9,868	A-6	42.13	8,850				28.4	10.2
Cumberland	US401	A1	ABC	310	36,800	21,896	A-2	20.87	17,038	A-2-4	12.99	16,721	A-2	22.05	17,038	A-6	16.14	15,766	23.9	10.3
Cumberland	US401	A1	ABC	310	36,800	21,896	A-2	20.87	17,038	A-2-4	12.99	16,721	A-2	22.05	17,038	A-6	16.14	15,766	32.5	8.8
Cumberland	US401	A1	ABC	310	36,800	21,896	A-2	20.87	17,038	A-2-4	12.99	16,721	A-2	22.05	17,038	A-6	16.14	15,766	35.8	8.4
Cumberland	US401	A1	ABC	310	36,800	21,896	A-2	20.87	17,038	A-2-4	12.99	16,721	A-2	22.05	17,038	A-6	16.14	15,766	24.4	13
Cumberland	US401	A1	ABC	310	36,800	21,896	A-2	20.87	17,038	A-2-4	12.99	16,721	A-2	22.05	17,038	A-6	16.14	15,766	32.6	10.6
Cumberland	US401	B1	ABC	313	23,207	12,869	A-2	20.87	17,038	A-2-4	12.99	16,721	A-2	22.05	17,038	A-6	16.14	15,766	22.5	11.2
Cumberland	US401	B1	ABC	313	23,207	12,869	A-2	20.87	17,038	A-2-4	12.99	16,721	A-2	22.05	17,038	A-6	16.14	15,766	33	8.6
Cumberland	US401	B1	ABC	313	23,207	12,869	A-2	20.87	17,038	A-2-4	12.99	16,721	A-2	22.05	17,038	A-6	16.14	15,766	35.8	8.4
Cumberland	US401	B1	ABC	313	23,207	12,869	A-2	20.87	17,038	A-2-4	12.99	16,721	A-2	22.05	17,038	A-6	16.14	15,766	34.4	11.4
Cumberland	US401	B1	ABC	313	23,207	12,869	A-2	20.87	17,038	A-2-4	12.99	16,721	A-2	22.05	17,038	A-6	16.14	15,766	33.3	9.9
Harnett	NC55	A1	ABC	256	28,597	12,170	A-2	20.87	17,038	A-2-4	12.99	16,721	A-2	22.05	17,038	A-6	16.14	15,766	35.3	9.3
Harnett	NC55	A1	ABC	256	28,597	12,170	A-2	20.87	17,038	A-2-4	12.99	16,721	A-2	22.05	17,038	A-6	16.14	15,766	40.9	7.1
Harnett	NC55	A1	ABC	256	28,597	12,170	A-2	20.87	17,038	A-2-4	12.99	16,721	A-2	22.05	17,038	A-6	16.14	15,766	28.7	10.1
Harnett	NC55	A1	ABC	256	28,597	12,170	A-2	20.87	17,038	A-2-4	12.99	16,721	A-2	22.05	17,038	A-6	16.14	15,766	14.1	16
Harnett	NC55	B1	ABC	274	25,196	9,056	A-2	20.87	17,038	A-2-4	12.99	16,721	A-2	22.05	17,038	A-6	16.14	15,766	31	10.4
Harnett	NC55	B1	ABC	274	25,196	9,056	A-2	20.87	17,038	A-2-4	12.99	16,721	A-2	22.05	17,038	A-6	16.14	15,766	22.3	14.7
Harnett	NC55	B1	ABC	274	25,196	9,056	A-2	20.87	17,038	A-2-4	12.99	16,721	A-2	22.05	17,038	A-6	16.14	15,766	31.6	9.2
Harnett	NC55	B1	ABC	274	25,196	9,056	A-2	20.87	17,038	A-2-4	12.99	16,721	A-2	22.05	17,038	A-6	16.14	15,766	20.8	11.1
Brunswick	NC179	A1	Soil	310	59,651	22,997	A-3	3.15	16,374	A-3	11.81	16,374	A-3	14.96	16,282	A-3	50.00	16,374	40.1	9.6
Brunswick	NC179	A1	Soil	310	59,651	22,997	A-3	3.15	16,374	A-3	11.81	16,374	A-3	14.96	16,282	A-3	50.00	16,374	34.4	8.8
Brunswick	NC179	A1	Soil	310	59,651	22,997	A-3	3.15	16,374	A-3	11.81	16,374	A-3	14.96	16,282	A-3	50.00	16,374	37.2	8.4
Brunswick	NC179	B1	Soil	320	45,674	13,876	A-3	3.15	16,374	A-3	11.81	16,374	A-3	14.96	16,282	A-3	50.00	16,374	42.4	8.5
Brunswick	NC179	B1	Soil	320	45,674	13,876	A-3	3.15	16,374	A-3	11.81	16,374	A-3	14.96	16,282	A-3	50.00	16,374	38.4	9.7
Brunswick	NC179	B1	Soil	320	45,674	13,876	A-3	3.15	16,374	A-3	11.81	16,374	A-3	14.96	16,282	A-3	50.00	16,374	37.2	8.2
Avery	NC194	B1	SABC	210	20,106	5,785	A-5	7.09	24,024	A-4	22.83	21,032	A-4	29.92	23,117				30.8	9.6
Avery	NC194	B1	SABC	210	20,106	5,785	A-5	7.09	24,024	A-4	22.83	21,032	A-4	29.92	23,117				34	9.7
Avery	NC194	B1	SABC	210	20,106	5,785	A-5	7.09	24,024	A-4	22.83	21,032	A-4	29.92	23,117				39.9	8.9
Avery	NC194	B1	SABC	210	20,106	5,785	A-5	7.09	24,024	A-4	22.83	21,032	A-4	29.92	23,117				17.5	17.8
Avery	NC194	A1	Coarse_ABC	415	16,936	37,945	A-5	7.09	24,024	A-4	22.83	21,032	A-4	29.92	23,117				28.2	10.5
Avery	NC194	A1	Coarse_ABC	415	16,936	37,945	A-5	7.09	24,024	A-4	22.83	21,032	A-4	29.92	23,117				34	9.8
Avery	NC194	A1	Coarse_ABC	415	16,936	37,945	A-5	7.09	24,024	A-4	22.83	21,032	A-4	29.92	23,117				39.8	10.5
Avery	NC194	A1	Coarse_ABC	415	16,936	37,945	A-5	7.09	24,024	A-4	22.83	21,032	A-4	29.92	23,117				31.4	11
Avery	NC194	A1	Coarse_ABC	415	16,936	37,945	A-5	7.09	24,024	A-4	22.83	21,032	A-4	29.92	23,117				36.1	8.5
Avery	NC194	A2	Coarse_ABC	270	32,347	101,041	A-5	7.09	24,024	A-4	22.83	21,032	A-4	29.92	23,117					
Avery	NC194	A2	Coarse_ABC	270	32,347	101,041	A-5	7.09	24,024	A-4	22.83	21,032	A-4	29.92	23,117					
Avery	NC194	A2	Coarse_ABC	270	32,347	101,041	A-5	7.09	24,024	A-4	22.83	21,032	A-4	29.92	23,117					
Avery	NC194	A2	Coarse_ABC	270	32,347	101,041	A-5	7.09	24,024	A-4	22.83	21,032	A-4	29.92	23,117					
Avery	NC194	A2	Coarse_ABC	270	32,347	101,041	A-5	7.09	24,024	A-4	22.83	21,032	A-4	29.92	23,117					
Avery	NC194	B2	Coarse_ABC	243	27,064	33,419	A-5	7.09	24,024	A-4	22.83	21,032	A-4	29.92	23,117					
Avery	NC194	B2	Coarse_ABC	243	27,064	33,419	A-5	7.09	24,024	A-4	22.83	21,032	A-4	29.92	23,117					
Avery	NC194	B2	Coarse_ABC	243	27,064	33,419	A-5	7.09	24,024	A-4	22.83	21,032	A-4	29.92	23,117					
Avery	NC194	B2	Coarse_ABC	243	27,064	33,419	A-5	7.09	24,024	A-4	22.83	21,032	A-4	29.92	23,117					
Alamance	SR1530	B1	ABC	162	30,735	10,327	A-2-4	9.06	29,542	A-7-6	25.98	8,377	A-6	11.02	11,369				34.7	9
Alamance	SR1530	B1	ABC	162	30,735	10,327	A-2-4	9.06	29,542	A-7-6	25.98	8,377	A-6	11.02	11,369				35.5	9.1
Alamance	SR1530	B1	ABC	162	30,735	10,327	A-2-4	9.06	29,542	A-7-6	25.98	8,377	A-6	11.02	11,369				34	9
Alamance	SR1530	B1	ABC	162	30,735	10,327	A-2-4	9.06	29,542	A-7-6	25.98	8,377	A-6	11.02	11,369				29.9	11.2
Alamance	SR1530	B2	Soil	201	40,946	10,041	A-2-4	9.06	29,542	A-7-6	25.98	8,377	A-6	11.02	11,369					
Alamance	SR1530	B2	Soil	201	40,946	10,041	A-2-4	9.06	29,542	A-7-6	25.98	8,377	A-6	11.02	11,369					
Alamance	SR1530	B2	Soil	201	40,946	10,041	A-2-4	9.06	29,542	A-7-6	25.98	8,377	A-6	11.02	11,369					
Alamance	SR1530	B2	Soil	201	40,946	10,041	A-2-4	9.06	29,542	A-7-6	25.98	8,377	A-6	11.02	11,369					
Alamance	SR1530	G1	Soil	60	8,944	7,999	A-2-4	9.06	29,542	A-7-6	25.98	8,377	A-6	11.02	11,369				38.5	8
Alamance	SR1530	G1	Soil	60	8,944	7,999	A-2-4	9.06	29,542	A-7-6	25.98	8,377	A-6	11.02	11,369				29	9.1
Alamance	SR1530	G1	Soil	60	8,944	7,999	A-2-4	9.06	29,542	A-7-6	25.98	8,377	A-6	11.02	11,369				27.3	10.2
Alamance	SR1530	G1	Soil	60	8,944	7,999	A-2-4	9.06	29,542	A-7-6	25.98	8,377	A-6	11.02	11,369				32.1	10.4
Alamance	SR1530	G1	Soil	60	8,944	7,999	A-2-4	9.06	29,542	A-7-6	25.98	8,377	A-6	11.02	11,369				29.2	14

Appendix B: Field Observation and Record

1. Interstate Highway 540 (Wake County)

On June 22, 2011, NCDOT personnel and the research team took falling weight deflectometer (FWD) and dynamic cone penetrometer (DCP) measurements and extracted 26 cores from I-540 eastbound (EB) in Raleigh in Wake County. According to the NCDOT construction history and profile database, this section was constructed or resurfaced in 2002 using S12.5D, I19.0B, and B25.0B mixes and a cement treated aggregate base (CTAB). The thicknesses of each layer are $2^{3}/_{4}$, 3, and $4^{1}/_{4}$ inches, respectively. The Pavement Condition Rating of this section is marked as 84.2 in the 2010 condition survey. The field test level of this section is Level 1, and the condition of this section falls in the category of *Young and Poor* roadways. Of the 26 cores extracted from this section, 15 cores, including cores with smooth delamination, were in sound condition such that horizontal coring for lab testing could be completed. Figure B.1 shows representative cracking patterns in the section investigated.

Figure B.1 Photographs of cracking in 'bad' condition region of I-540, Raleigh, Wake County

Two summaries of the pavement core data are given in Table B.1 and, and photographs of the cores are shown in Figure B.2. As shown in Table B.1 and Figure B.1, the field-extracted cores comprise 4 asphalt layers on top of about 8 inches of CTAB. The average thicknesses of each layer are $1^{1}/_{2}$, $2^{1}/_{8}$, $3^{3}/_{8}$, and $4^{13}/_{16}$ inches, respectively. The sum of the average thicknesses of the 2nd, 3rd and 4th layers of an extracted core is $10^{3}/_{8}$ inches, which is similar to the overall

thickness of the asphalt layer of this section that is found in the construction history database. However, the construction history database indicates that this section has only 3 asphalt layers. Thus, it is probable that the top layer has been resurfaced. Most of the vertical cracks exist in the top layer, which also indicates a high possibility of top-down cracking. Because it took fairly long time to core through the CTAB layer, only four holes were made for the DCP testing. Although the total length of this section is slightly longer than 2 miles, 0.4 mile (1500 feet) was selected for investigation due to safety issues caused by the relatively high speed limit on this section of roadway.

Table B.1 Summary of core data for I-540, Raleigh, Wake County

ID	Layer Thickness (inch)				Condition
	1st	2nd	3rd	4th	
B1-CL1	1 1/2	2 1/4	3 3/4	4 7/8	Cracked
B1-CL2	1 3/4	2 1/4	3 3/4	5	Delamination/Intact
B1-CL3	1 3/4	2	3 3/4	4 1/2	Cracked
B1-WP1	1 3/8	2 1/4	3 5/8	5 1/4	Cracked
B1-WP2	1 1/4	2 1/4	3 1/2	5	Cracked
B1-WP3	1 1/4	2 1/8	3 1/2	4 3/4	Intact
B1-WP4	1 3/8	2	3 1/4	5	Cracked
B1-WP5	1 3/8	2 1/8	3 1/8	4 1/4	Intact
A1-WP1	1 1/2	2 1/8	3 1/2	4 1/4	Intact
A1-WP2	1 1/2	2 3/8	3 1/4	5	Intact
A1-WP3	1 3/8	2 1/4	3	5	Delamination/Intact
A1-CL1	1 3/8	2 1/2	3 1/4	4 5/8	Intact
A1-CL2	1 1/2	2 3/8	3 3/8	4 5/8	Delamination/Intact
B2-W1	1 1/2	2 1/4	3 1/8	4 3/4	Delamination/Cracked
B2-W2	1 1/2	2 1/4	3 5/8	5 1/8	Delamination/Cracked
B2-W3	1 1/2	2 1/4	3 1/4	5	Delamination/Intact
B2-W4	1 3/8	2	3 3/8	5 1/8	Cracked
B2-W5	1 1/2	2	3 1/5	5 1/4	Intact
B2-CL1	1 5/8	2 1/4	3 3/8	4 1/2	Cracked
B2-CL2	1 1/2	2	3	5	Delamination/Cracked
B2-CL3	1 1/2	1 7/8	3	5	Delamination/Intact
B2-CL4	1 5/8	2	3 1/4	4	Delamination/Intact
A2-CL1	1 1/2	2 1/8	3 1/2	4 3/4	Cracked
A2-CL2	1 1/2	1 7/8	3 1/2	4 1/2	Intact
A2-W1	1 1/2	2 1/8	3 3/4	4 7/8	Delamination/Intact
A2-W2	1 3/8	2	3 5/8	5	Delamination/Intact

Table B.2 Additional summary of core data for I-540, Raleigh, Wake County

ID	Note
B1-CL1	Crack on top surface connected to vertical cracking in 1st and 2nd layers
B1-CL2	Delamination between 1st & 2nd layers, no cracks, sound condition
B1-CL3	Crack on top surface connected to 2 vertical cracks in 1st layer
B1-WP1	Crack on top surface connected to vertical crack in 1st layer
B1-WP2	Crack on top surface connected to 3 vertical cracks in 1st layer
B1-WP3	Sound condition
B1-WP4	Crack on top surface connected to vertical crack in 1st layer
B1-WP5	Sound condition
A1-WP1	Sound condition
A1-WP2	Sound condition
A1-WP3	Delamination between 3rd & 4th layers, no cracks, sound condition
A1-CL1	Sound condition
A1-CL2	Delamination between 1st & 2nd layers, no crack, sound condition
B2-W1	Delamination between 2nd & 3rd layers, cracks on top surface connected to vertical crack in 1st layer, not smooth delamination
B2-W2	Delamination between 2nd & 3rd layers, delamination connected to vertical crack in 1st layer, not smooth delamination
B2-W3	Delamination between 3rd & 4th layers, no crack, sound condition
B2-W4	Fatigue cracking on surface of top layer
B2-W5	Sound condition
B2-CL1	Crack on top surface connected to vertical crack in 1st layer
B2-CL2	Delamination between 1st & 2nd layers, macrocracks on top surface connected to vertical crack in 1st layer, severe crack and delamination in 1st layer but not broken in pieces
B2-CL3	Delamination between 1st & 2nd layers, no cracks, sound condition
B2-CL4	Delamination between 1st & 2nd layers, not smooth delamination, no crack, sound condition
A2-CL1	Horizontal crack at bottom of 2nd layer
A2-CL2	Sound condition
A2-W1	Delamination between 1st & 2nd layers, no cracks, sound condition
A2-W2	Delamination between 2nd & 3rd layers, not smooth delamination, no cracks, sound condition


B1-CL1
B1-CL2
B1-CL3
B1-WP1
B1-WP2
B1-WP3
B1-WP4
B1-WP5
A1-CL1
A1-CL2
A1-WP1
A1-WP2
A1-WP3
B2-CL1
B2-CL2
B2-CL3
B2-CL4
B2-WP1
B2-WP2
B2-WP3
B2-W4
B2-W5
A2-CL1
A2-CL2
A2-WP1

A2-WP2

Figure B.2 Cores taken from I-540, Raleigh, Wake County

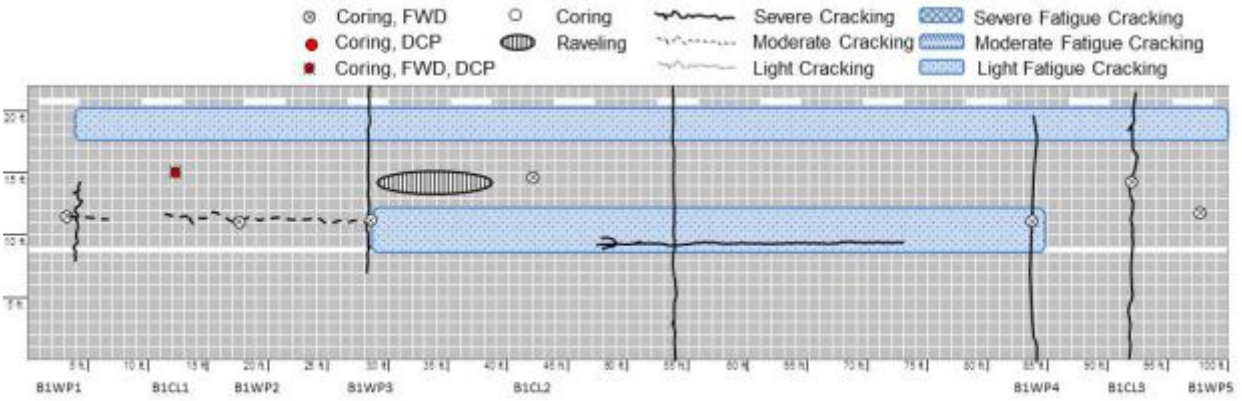

Figure B.3 Crack condition survey mapping of B1 region in I-540

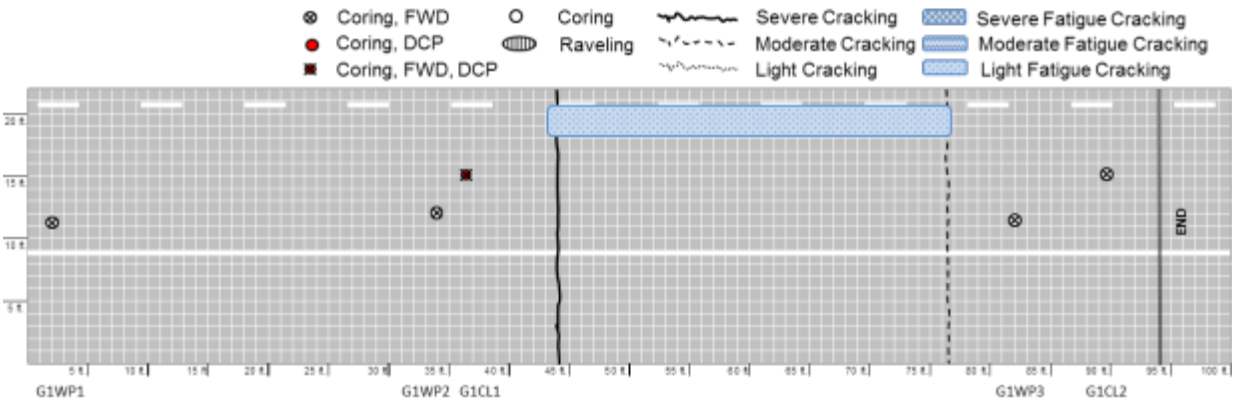

Figure B.4 Crack condition survey mapping of A1 region in I-540

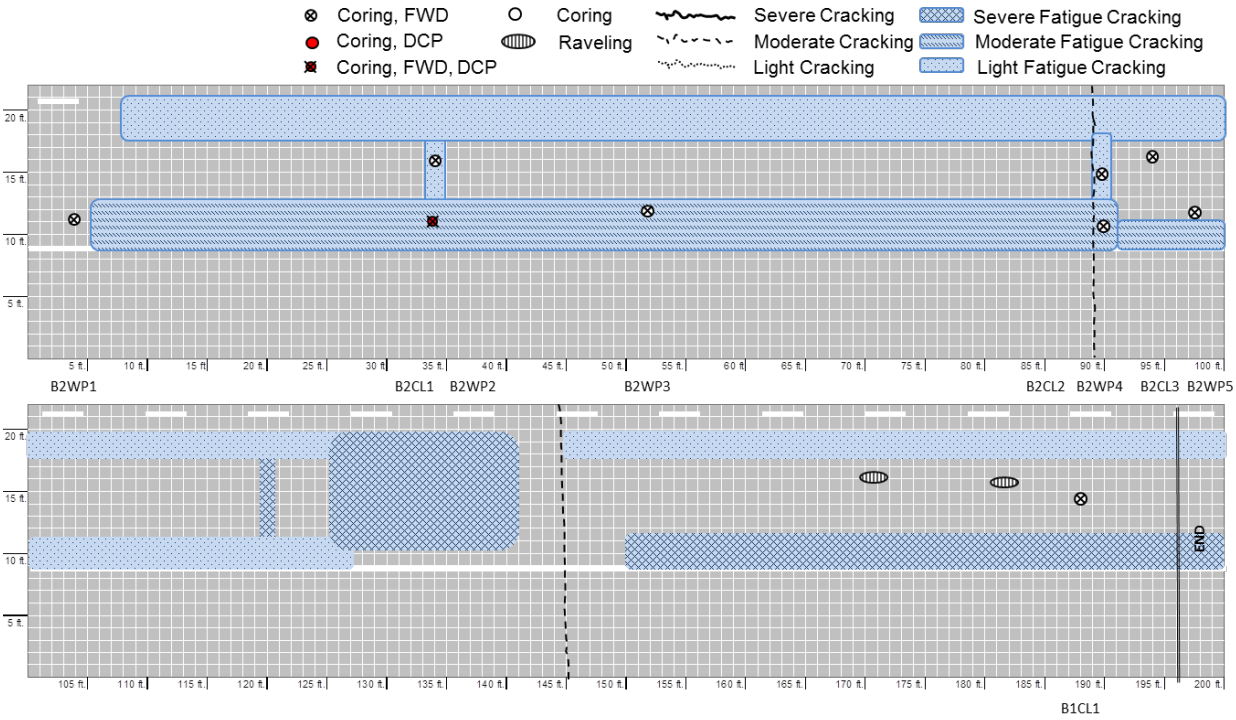

Figure B.5 Crack condition survey mapping of B2 region in I-540

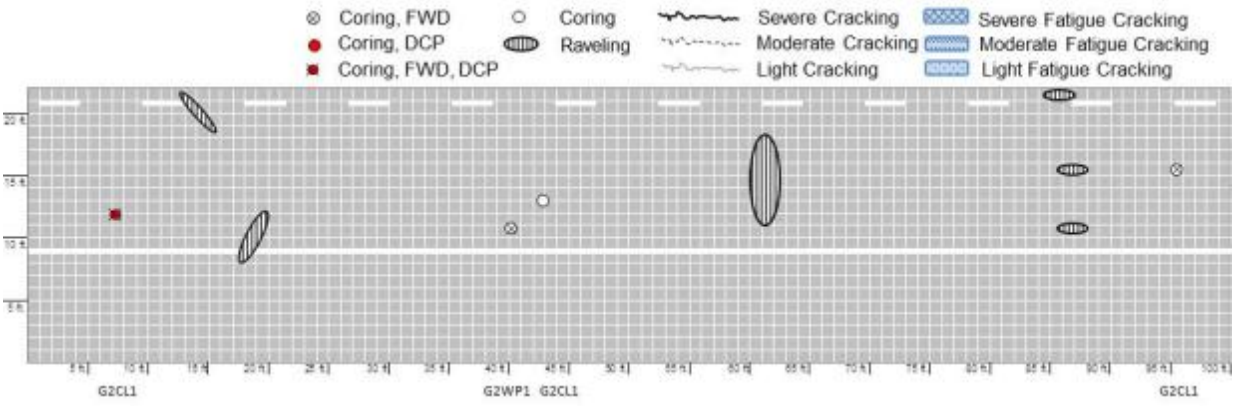

Figure B.6 Crack condition survey mapping of A2 region in I-540

2. NC Route 24 (Mecklenburg County)

On August 10, 2011, NCDOT personnel and the research team took FWD and DCP measurements and extracted 19 cores from NC-24 eastbound (EB) near Charlotte in Mecklenburg County. According to the NCDOT construction history and profile database, the section was constructed in 2001 using S12.5C and I19.0C mixes. The section is 2 lanes per direction of divided highway. The field test level of this section is Level 1, and this section is in the group of *Young and Poor* condition roadways. Of the 19 cores extracted from the field, 12 cores were obtained in sound condition so that horizontal coring for lab testing could be completed. This section had not been resurfaced after initial construction.

Although the entire section has the same construction history, and the condition survey targeted 1.4 miles in length, only a 0.6-mile segment was selected due to safety issues. This section is on one side only of a signal light. The overall cracking condition of the section is 'moderate to severe', but severe fatigue cracking was evident in a region of curved road. Fatigue cracking was found in both the inner and outer wheel paths, but was more prevalent in the outer wheel path. Figure B.7 shows fatigue cracking patterns in the 'bad' condition region.

Figure B.7 Photographs of cracking patterns in the 'bad' condition region of NC-24

Some of the delamination found in other sections may be caused by the shear force caused by the movement of the core drill bit. However, the delamination in this section clearly shows that delamination was present prior to coring. Figure B.8 shows delamination lines in the material of the extraction holes. The photograph on the left-hand side of the figure shows the

delaminated areas of the hole, and the photograph on the right-hand side shows water that has leaked from a delamination line in the hole. Water leaked for quite a long time after coring, which indicates that the delaminated area near the hole was extensive.

Figure B.8 Photographs of delamination in 'bad' condition region of NC-24

A summary of all the pavement core data is given in Table B.3, and photographs of the cores are shown in Figure B.9. According to the construction database, the pavement in this section is composed of a 2½-inch thick surface layer and 3½-inch thick intermediate layer on top of an 8-inch thick aggregate base course. The average thicknesses of the 1st, 2nd, and 3rd layers presented in the summary table are 1¾ inches, 1¼ inches, and 4 inches, respectively. The sums of the average thicknesses of the 1st and 2nd layers and the average thickness of the 3rd layer are about ½ inch thicker than the thicknesses shown in the construction database. Therefore, the 1st and 2nd layers in the summary table should be regarded as sublayers of the surface layer.

Table B.3 Summary of core data for NC-24, Charlotte, Mecklenburg County

ID	Layer Thickness (inch)			Condition	Note
	1st	2nd	3rd		
B1M1	1 1/4	1 1/8	4 1/8	Intact	Sound condition
B1M2	1 3/4	1 3/8	3 1/2	Cracked	Delamination between 1st & 2nd layers, vertical crack on 1st layer, crack connected to macrocrack in top surface
B1M3	1 3/4	1 1/4	3 7/8	Intact	Sound condition
B1M4	2	1 1/2	3 3/4	Delamination/Intact	Delamination between 1st & 2nd layers
B1W1	1 1/2	1 1/2	4	Broken	Delamination between 1st & 2nd layers and 2nd & 3rd layers
B1W2	2	1 1/4	3 1/2	Delamination/Intact	Delamination between 1st & 2nd layers
B1W3	2	1 3/8	3 1/2	Delamination/Intact	Delamination between 1st & 2nd layers
A1M1	1 7/8	1 1/8	4	Intact	Sound condition
A1M2	1 1/2	1 3/8	4 1/2	Intact	Sound condition
A1M3	1 3/4	1 3/8	4 3/4	Intact	Sound condition
A1W1	1 5/8	1 1/4	4	Cracked	Cracks on surface connected to 1 vertical crack on 1st layer
A1W2	1 1/2	1 1/4	5	Delamination/Intact	Delamination between 1st & 2nd layers
A1W3	1 3/4	1 1/4	4 1/4	Intact	Sound condition
B2M1	1 1/4	1 3/8	3 1/4	Cracked/	Cracks on top surface connected to 1 vertical crack on 1st layer
B2M2	1 5/8	1 3/8	4	Delamination/Intact	Delamination between 1st & 2nd layers
B2M3	1 1/2	1 3/4	4 1/4	Delamination/Intact	Delamination between 1st & 2nd layers
B2M4	1 5/8	1 3/8	4 1/2	Cracked	Cracks on surface connected to 1 vertical crack on 1st layer
B2W1	1 3/8	1 1/4	3 3/8	Cracked	Delamination and horizontal crack at/near bottom of top layer (1st layer)
B2W2	1 3/8	1 3/8	4	Cracked	Cracks on surface connected to 1 vertical crack on 1st layer

Figure B.9 Cores taken from NC-24, Charlotte, Mecklenburg County

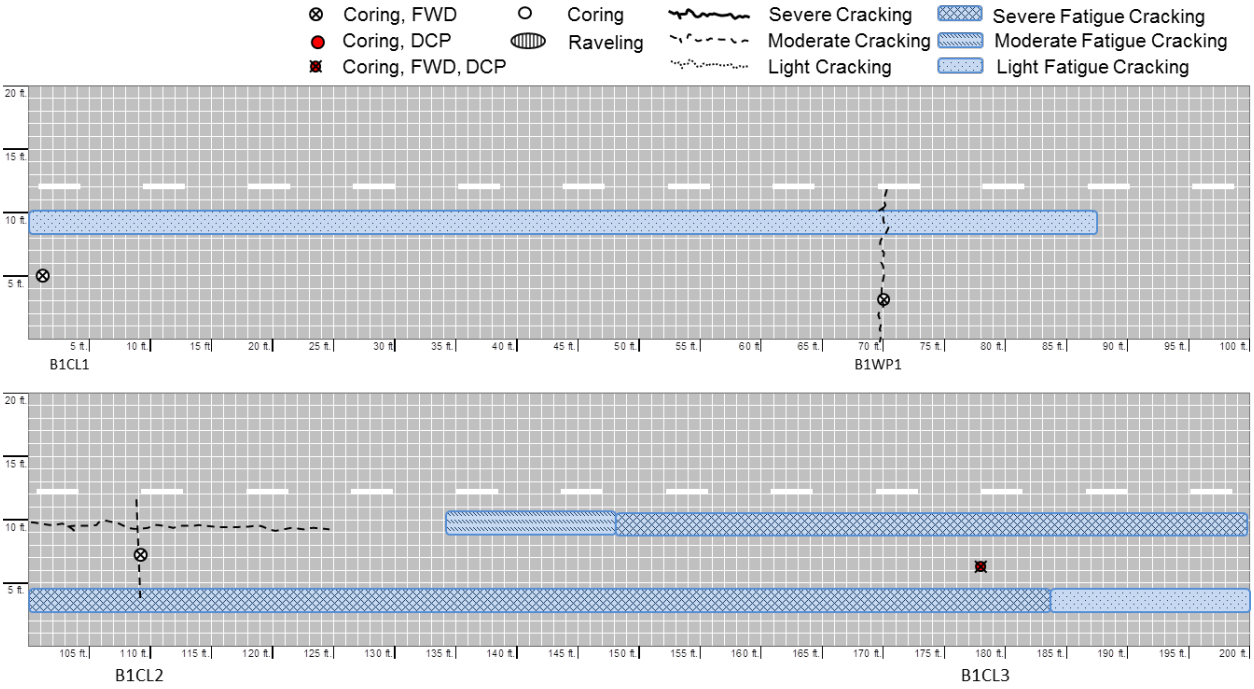

Figure B.10 Crack condition survey mapping of B1 region in NC-24

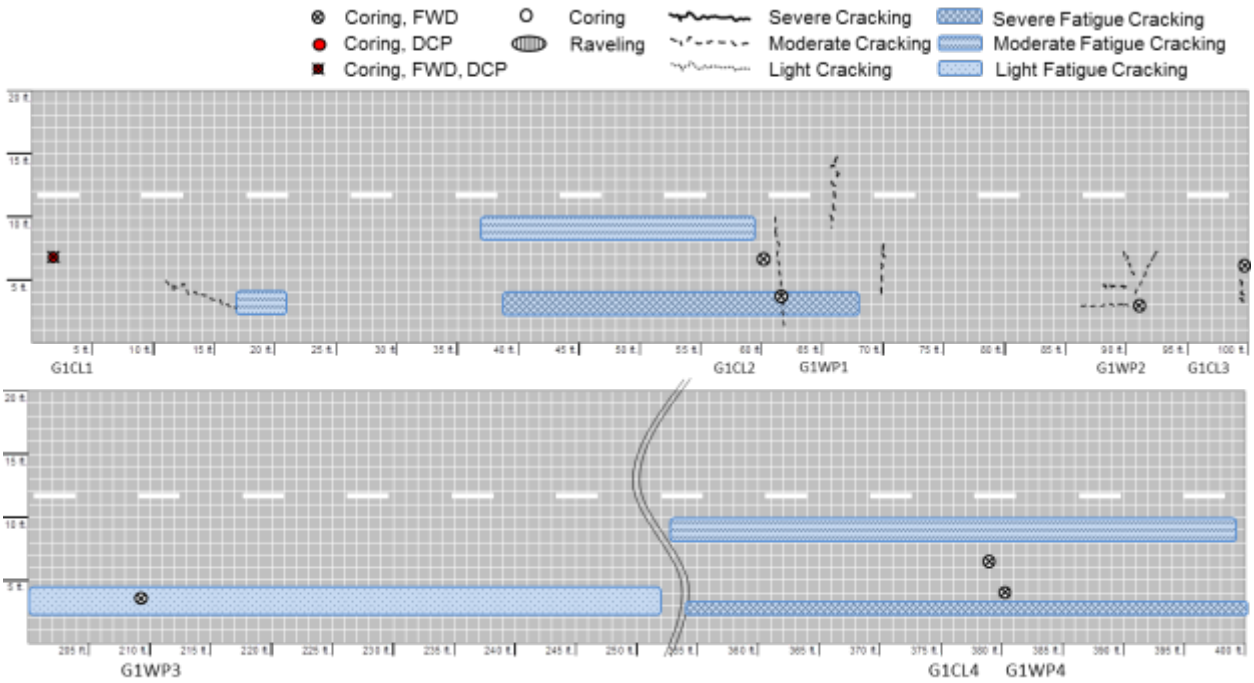

Figure B.11 Crack condition survey mapping of A1 region in NC-24

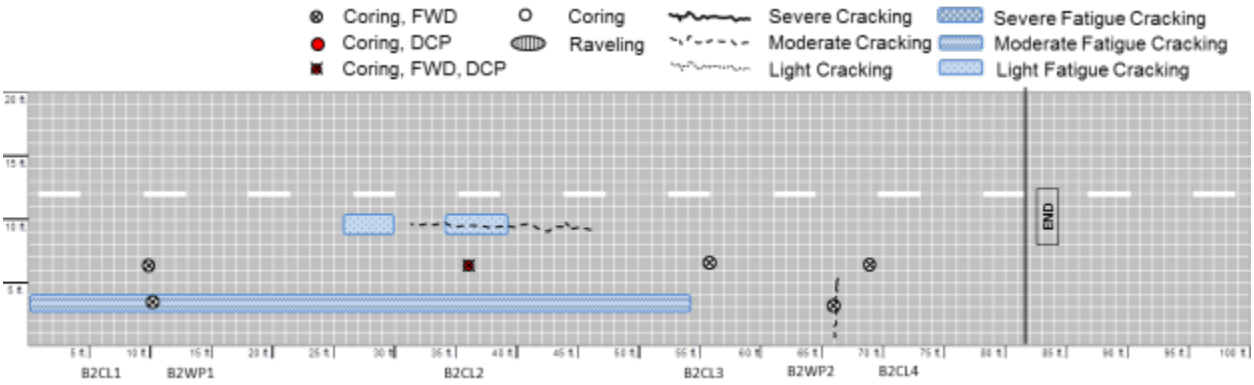

Figure B.12 Crack condition survey mapping of B2 region in NC-24

3. US Route 17 (Brunswick County)

On June 15, 2011, NCDOT personnel and the research team took FWD and DCP measurements and extracted 25 cores from US-17 (Ocean Highway) Northbound (NB) in Supply, Brunswick County. This section was categorized as an *Old and Good* condition roadway. Therefore, the overall condition of the section is good.

Four regions (two good condition regions and two bad condition regions) of the outer lane of the pavement section were selected and marked on the side of each region prior to the test date. However, on the test date, part of the median in the section was under construction for new traffic signals and to pave the left turn lane for left turn traffic. Therefore, the left lane (inner lane) of the four-lane divided highway was closed due to construction. Although the total length of the section was about 1.8 mile, the available test section was only 0.4 mile beyond the construction site due to safety concerns. Division maintenance and traffic control engineers only allowed traffic cones on the inner lane to prevent confusion for drivers. Therefore, four test regions were selected once again on the test date, and only the inner lane was selected. Because the section was designated as an *Old and Good* condition roadway, the main purpose of lab testing field samples from this section was not to find the cause of cracking but rather to compare results with samples from *Young and Poor* condition roadways. Accordingly, the research team decided to use the inner lane for field testing, unlike for the other sections.

Of the 25 cores extracted from the field, 23 cores were obtained in sound condition so that horizontal coring for lab testing could be completed. Portions of the two cores with vertical cracking on the top or on both the top and second layers also could be used for horizontal coring. A summary of all the pavement cores is given in Table B.4, and photographs of those cores are shown in Figure B.13.

Table B.4 Summary of cores for US-17 (Ocean Highway) NB, Supply, Brunswick County

ID	Layer Thickness (inch)					Condition	Note
	1st	2nd	3rd	4th	Total		
B1-WP1	1 1/4	1 3/4	2 1/2	4	9 1/2	Intact	
B1-WP2	1	1 1/4	2 3/8	4	8 5/8	Cracking	Crack on top surface connected to vertical cracking (Top layer only: possibility of top-down cracking)
B1-WP3	1	1 1/4	2 1/2	4	8 3/4	Intact	
B1-CL1	1 3/8	1 1/2	2 5/8	3 7/8	9 3/8	Cracking	Crack on top surface connected to vertical cracking (Top layer only: possibility of top-down cracking)
B1-CL2	1 3/8	1 1/2	2 1/4	4	9 1/8	Intact	
B1-CL3	1 1/4	1 1/2	1 3/4	4 1/2	9	Intact	
B1-CL4	1	1 3/8	2 1/4	4	8 5/8	Intact	
B2-WP1	1 3/8	1 1/2	1 7/8	4 3/4	9 1/2	Intact	
B2-WP2	1 1/8	1 1/4	2 3/8	4 1/4	9	Intact	
B2-WP3	1	1 3/8	1 7/8	4 5/8	8 7/8	Intact	
B2-CL1	1 1/4	1 5/8	2	4 7/8	9 3/4	Intact	
B2-CL2	7/8	1 5/8	2	4	8 1/2	Intact	
B2-CL3	1	1 3/4	2	4 3/4	9 1/2	Intact	
A1-WP1	1 1/8	1 1/2	3	4	9 5/8	Intact	
A1-WP2	1 1/8	1 1/2	3	4 1/8	9 3/4	Intact	
A1-WP3	1 1/8	1 1/2	2 1/2	4 1/4	9 3/8	Intact	
A1-WP4	1 1/8	1 3/4	2 3/4	4 3/4	10 3/8	Intact	
A1-CL1	1 1/4	1 1/2	2 1/4	4	9	Intact	
A1-CL2	1 1/8	1 7/8	2 1/4	4 1/8	9 3/8	Intact	
A2-WP1	1 3/4	1 7/8	2 5/8	4	10 1/4	Intact	
A2-WP2	1 1/2	1 5/8	1 1/2	5	9 5/8	Intact	
A2-WP3	1 3/8	1 3/8	3	4 1/8	9 7/8	Intact	
A2-CL1	1 3/8	1 3/4	2 3/4	4	9 7/8	Intact	
A2-CL2	1 1/2	1 1/4	3	4 1/4	10	Intact	
A2-CL3	1 3/4	1 3/4	2 1/2	5	11	Intact	

Figure B.13 Cores taken from US-17 (Ocean Highway) NB, Supply, Brunswick County

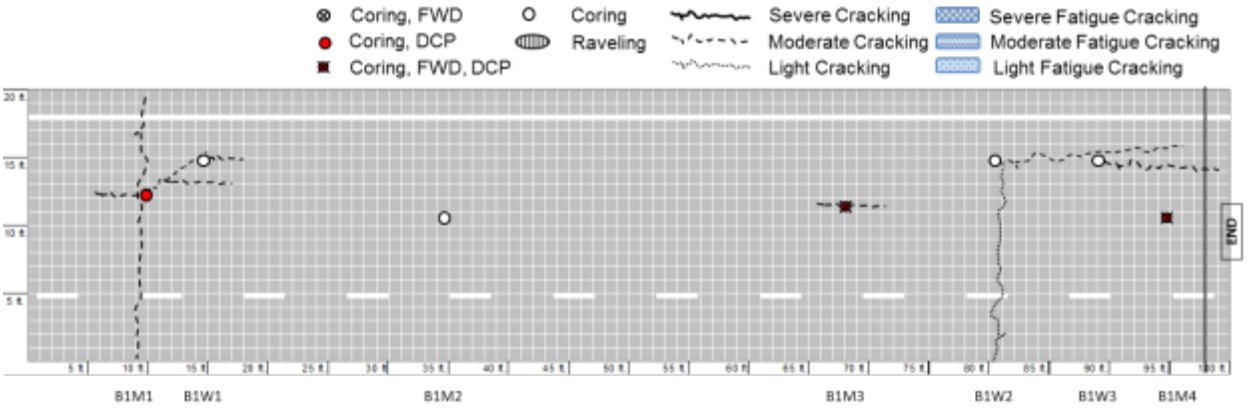

Figure B.14 Crack condition survey mapping of B1 region in US-17

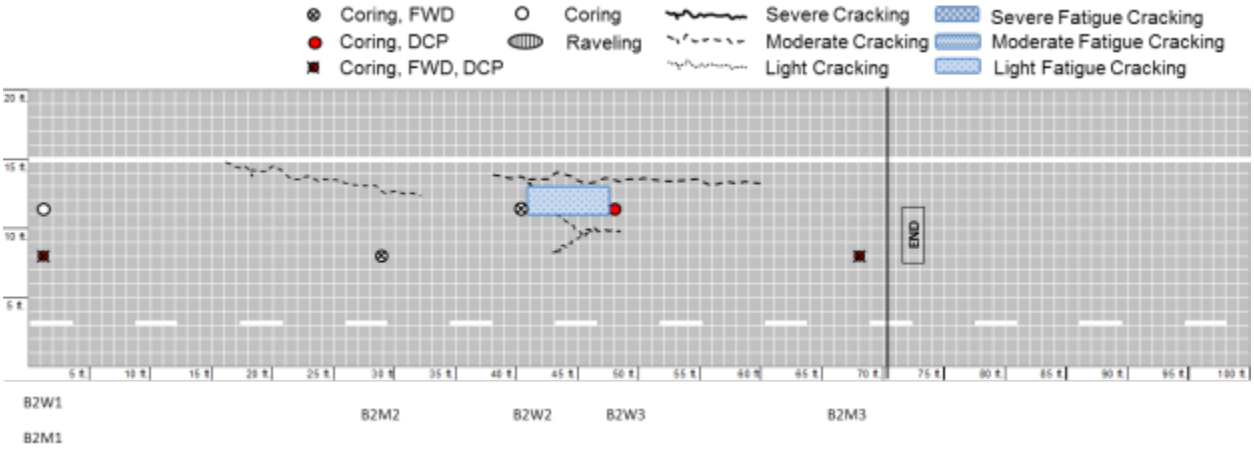

Figure B.15 Crack condition survey mapping of B2 region in US-17

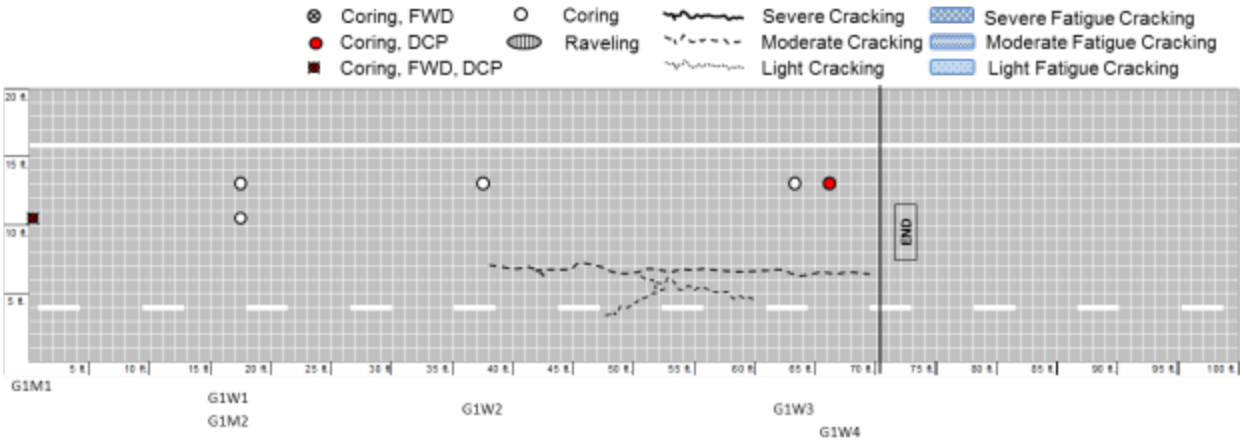

Figure B.16 Crack condition survey mapping of A1 region in US-17

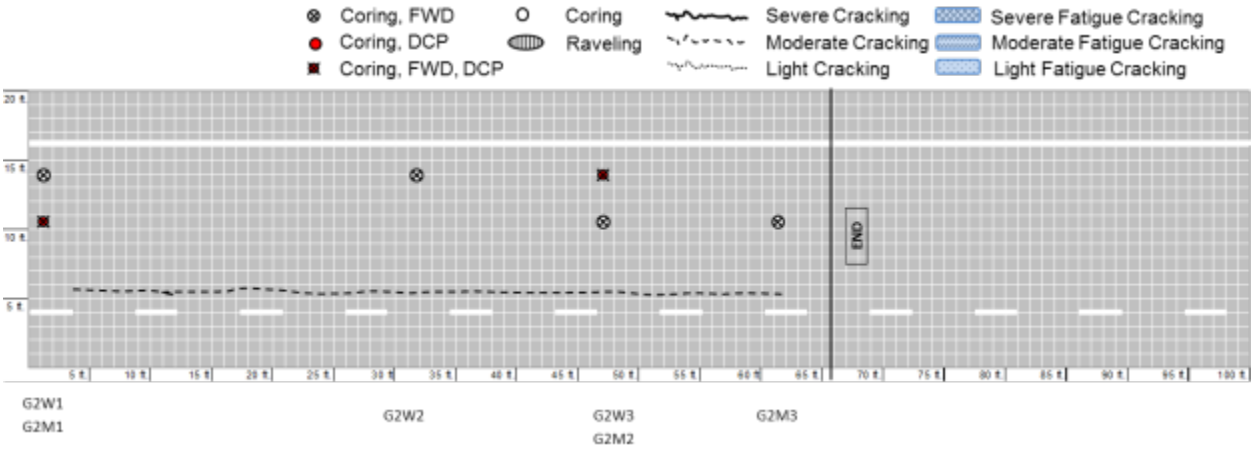

Figure B.17 Crack condition survey mapping of A2 region in US-17

4. NC Route 87 (Cumberland County)

On May 26, 2011, NCDOT personnel and the research team took falling weight deflectometer (FWD) and dynamic cone penetrometer (DCP) measurements and extracted 26 cores from NC-87 southbound (SB) near Fayetteville in Cumberland County. According to the NCDOT construction history and profile database, this section was resurfaced in 2003 with a heavy duty surface (HDS) asphalt course and a heavy duty binder (HDB) course. This section is marked as 85.1 in a 2010 pavement condition survey. The field test level of this section is Level 1, and this section is in the group of *Young and Poor* condition roadways. Of the 26 cores extracted from the field, 12 cores were obtained in sound condition so that horizontal coring for lab testing could be completed.

This section also is divided into two good regions and two bad regions like the other sections. In the second bad region of the section, severe longitudinal cracking and pavement drops were observed on the outer wheel-path. However, the overall longitudinal cracking on the wheel-path in this section was neither severe, as found in this particular location, nor is there a pavement drop. This cracking is only 218 feet long out of 0.98 mile. Such localized cracking appears to be caused by structural failures that, in turn, are caused by widening the roadway, because the thickness of the cores (B2-WP1, B2-WP3, and B2-WP3) from the adjacent areas is thinner than for the other cores. Further detailed investigation of this phenomenon will be needed in the upcoming quarter. Figure B.18 shows part of the severe longitudinal cracking on the outer wheel-path and the pavement drop.

Figure B.18 Photographs of cracking and pavement drop in second bad region in the section (same location but difference in detail)

A summary of all the pavement cores is given in Table B.7 and Table B.6, and photographs of the cores are shown in Figure B.24. Cores with partial or full depth vertical cracking are of primary interest because these cores show vertical cracks connected to cracks on top of the core. These cores can be regarded as exhibiting either top-down cracking or a trace of bottom-up cracking that has spread diagonally through the pavement thickness. Photographs and crack mapping data will be used to try to clarify whether the observed cracking is in fact top-down cracking or a reflection of nearby bottom-up cracking.

Cores from the first bad region and the second good region in the section have a bituminous surface treatment (BST) layer, but cores in the remaining two regions do not have BST layers. Also, some cores extracted at the lane center from the second good region and both of the bad regions have a sand mix layer at the bottom of the cores, but all the cores from the outer wheel-path do not have a sand mix layer. It is not clear if the NCDOT used sand mix during the initial construction phase for the pavement structure. These two cases need to be discussed with the Materials and Tests Unit (MTU).

Table B.5 Summary of cores for NC-87 SB, Fayetteville, Cumberland County

ID	Layer Thickness (inch)											Condition
	1st	2nd	3rd	4th	5th	6th	7th	8th	9th	10th	11th	
A1-WP1	1 1/2	1 1/8	2 1/8	1 5/8	4 7/8							Intact
A1-WP2	1 3/8	1 1/2	1 7/8	1 3/4	5							Intact
A1-WP3	1 1/2	1 1/4	2	2 1/2	5							Intact
A1-CL1	1 1/4	1 1/4	2 1/8	2	4 3/8							Intact
A1-CL2	1 3/8	1 1/4	2	1 3/4	5							Intact
B1-WP1	1 1/8	1 1/4	1 3/8	3/4	1	3/4	1 3/4	1 1/2	3			Intact
B1-WP2	1 1/8	1 1/8	1 3/8	1	1 1/4	1 1/2	1 1/2	3 1/4				Vertical cracking
B1-CL1	1 1/2	1 1/4	1 1/4	3/4	1	7/8	7/8	1/2	1 1/2	2	2	Delamination, Vertical cracking
B1-WP3	1	1 1/4	1 1/2	3/4	1 1/8	3/4	1	2 1/8	3 1/2			Vertical cracking
B1-WP4	1	1 1/4	1 1/2	3/4	1	2 5/8	1 1/2	3				Intact
B1-CL2	1 1/8	1 1/4	1 1/4	5/8	1	2 3/4	3/4	1 3/4				Full depth cracking
B1-WP5	1 1/8	1 1/4	1 1/2	5/8	1	3/4	1/2	1	1 1/2	3		Full depth cracking
A2-WP1	1 5/8	1 1/8	1	3/4	1 5/16	15/16	1 1/8	7/8	1 1/4	4		Intact
A2-WP2	1 3/8	1 1/8	1 1/8	3/4	3/4	1	1	3/4	1 3/4	2 3/8	2	Intact
A2-CL1	1 3/8	1 1/4	1 1/8	3/4	1	1	3/4	1	1 1/2	2 3/4	1	Intact
A2-WP3	1 1/4	1 1/8	1 1/8	3/4	1 3/4	1	1 1/2	3 3/4				Full depth cracking
B2-WP1	1 1/4	1 3/4	1 3/8	2 3/4								Delamination, Vertical cracking
B2-WP2	1 1/8	1	1	2	1 1/2	1	1 1/2	4				Delamination, Vertical cracking
B2-CL1	2	1 1/4	2	1 1/2	2	2 1/2	1 1/4					Full depth cracking
B2-WP(A)	1 1/4	7/8	1 1/4	1	3 1/2	1 3/8	3 1/2	7/8				Delamination
B2-CL(A)	1 3/8	3/4	1	3/4	1	1 1/2	2 1/8	2 1/4	2			Intact
B2-WP3	1	1	1 1/4	3								Delamination
B2-CL2	1 1/8	3/4	1	1	3	1 1/2	3	1 1/2				Delamination, Full depth cracking
B2-WP4	1 3/4	1 1/4	3/4	7/8	2	2	2 3/4	1				Intact
B2-CL3	2 1/8	2	1 1/8	7/8	2							Delamination, Vertical cracking
B2-WP5	1 1/4	1/2	1	7/8	2 3/4							Delamination

Table B.6 Additional summary of cores for NC-87 SB, Fayetteville, Cumberland County

ID	Note
A1-WP1	No macro cracking
A1-WP2	No macro cracking
A1-WP3	No macro cracking
A1-CL1	No macro cracking
A1-CL2	No macro cracking
B1-WP1	No macro cracking, BST layer
B1-WP2	Delamination and diagonal cracking are connected, excessive tack coat, BST layer
B1-CL1	Sand mix layer at the bottom, BST layer in the middle core sample, vertical cracking from the top layer to delamination, excessive tack coat layer
B1-WP3	Vertical cracking in one layer (on the upper layer of BST layer)
B1-WP4	BST layer
B1-CL2	Sand mix layer at the bottom, full depth cracking connected to the crack on the surface of top layer, BST layer
B1-WP5	Delamination, BST layer, full depth cracking connected to the crack on the surface of top layer
A2-WP1	BST layer in the middle core sample
A2-WP2	BST layer in the middle core sample
A2-CL1	Sand mix layer at the bottom, BST layer in the middle core sample
A2-WP3	BST layer in the middle core sample, full depth cracking connected to the crack on the surface of top layer
B2-WP1	Delamination, vertical cracking below delamination line, lane marking paint on delamination line, thinner than other cores (looks like widening construction done)
B2-WP2	2 delaminations, full depth cracking, lane marking paint layer between third and fourth main mix layer, thinner than other cores (looks like widening construction done)
B2-CL1	Crack on top layer, full depth cracking, sand mix layer at the bottom, looks like five main mixture layers
B2-WP(A)	Delamination, FWD test was not conducted on this coring spot (cored for obtaining sound condition core)
B2-CL(A)	Sand mix layer at the bottom, FWD test was not conducted on this coring spot (cored for obtaining sound condition core)
B2-WP3	Delamination, lane marking paint on the delamination surface, thinner than other cores (looks like widening construction done)
B2-CL2	Delamination, cracking on top surface, sand mix layer at the bottom
B2-WP4	From inner wheel path, No macro cracking
B2-CL3	Delamination, vertical cracking from the bottom (looks like bottom-up cracking), two lane marking paint layer between third and fourth and fourth and fifth layers.
B2-WP5	Delamination, thinner than other cores (looks like widening construction done)


A1-WP1


A1-WP2


A1-WP3


A1-CL1


A1-CL2


B1-WP1


B1-WP2


B1-WP3


B1-WP4


B1-WP5


B1-CL1


B1-CL2


A2-WP1


A2-WP2


A2-WP3


A2-CL1


B2-WP1


B2-WP2


B2-WP3


B2-WP4


B2-WP5


B2-CL1


B2-CL2


B2-CL3


B2-WP(A)

B2-CL(A)

Figure B.19 Cores for NC-87 SB, Fayetteville, Cumberland County

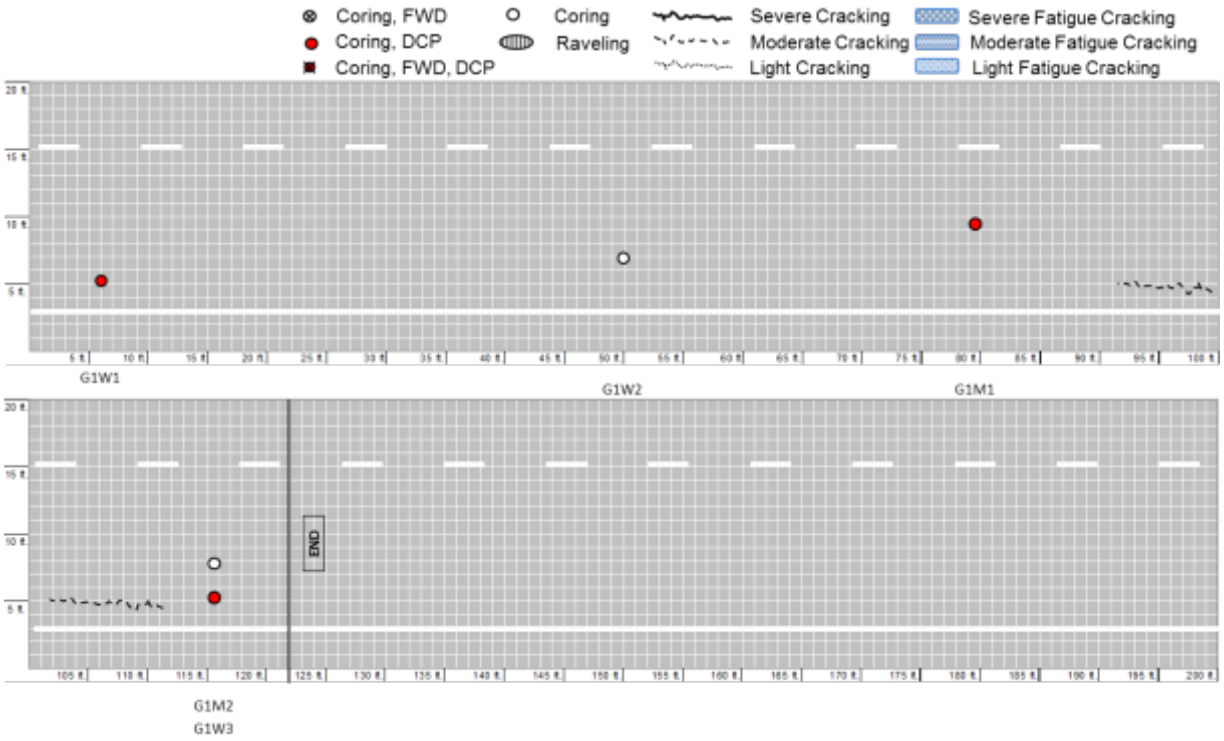

Figure B.20 Crack condition survey mapping of A1 region in NC-87

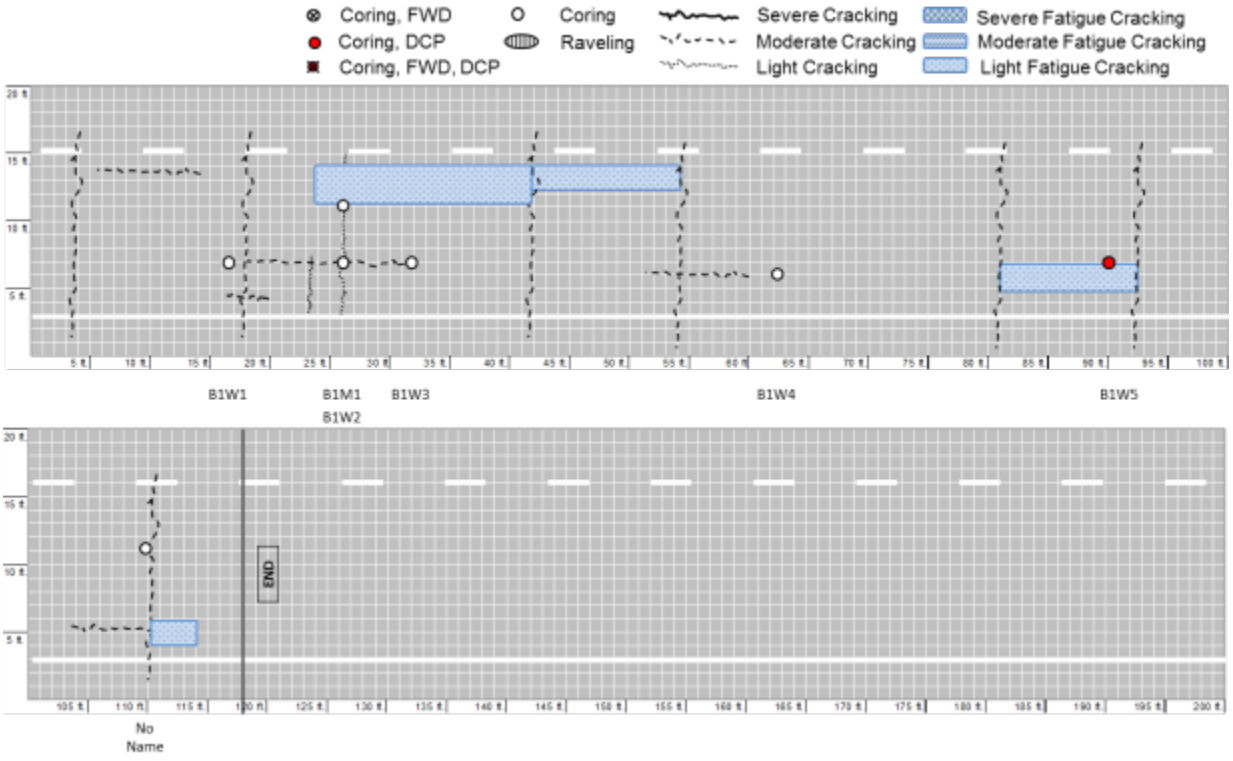

Figure B.21 Crack condition survey mapping of B1 region in NC-87

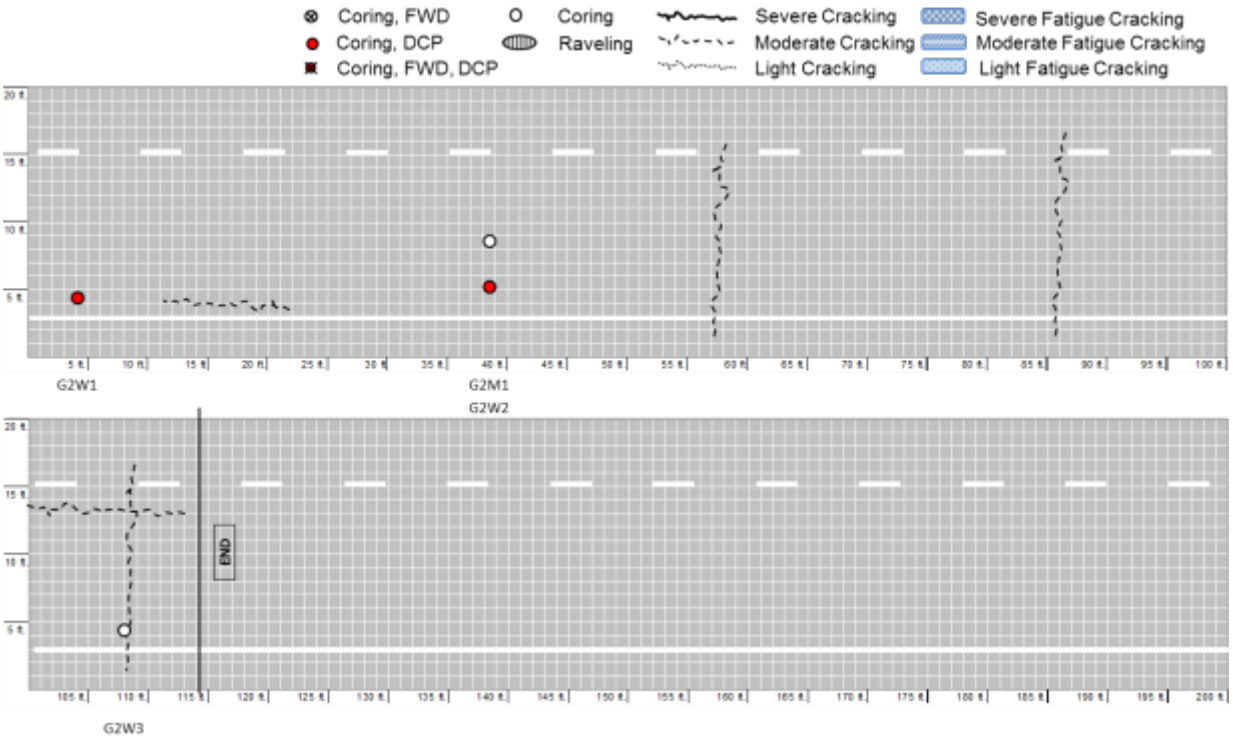

Figure B.22 Crack condition survey mapping of A2 region in NC-87

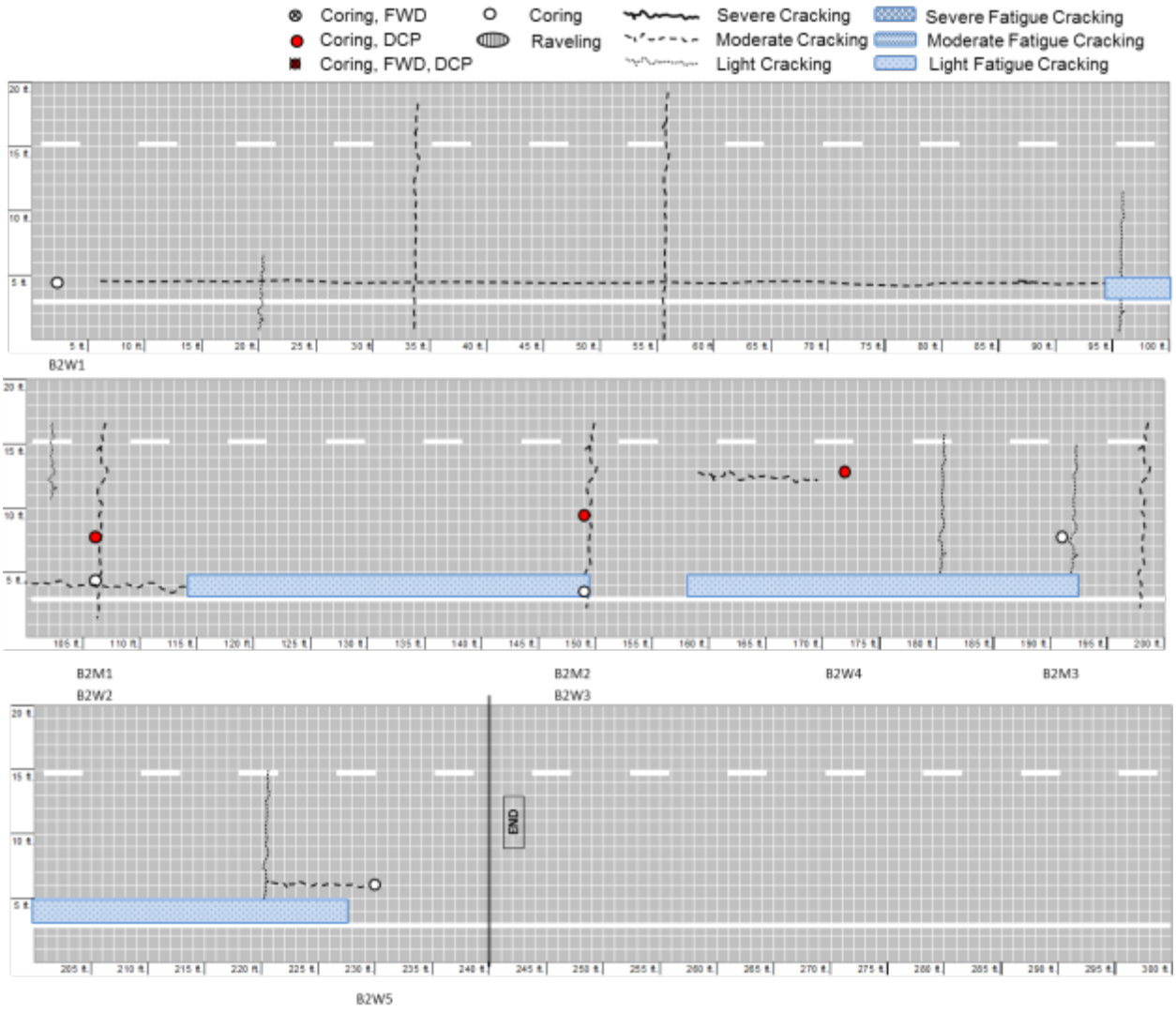

Figure B.23 Crack condition survey mapping of B2 region in NC-87

5. US Route 70 (Johnston County)

On March 3, 2011, NCDOT personnel and the research team took FWD and DCP measurements and extracted 18 cores from US 70 eastbound (EB) near Selma in Johnston County. The section identification (ID) of this section in the priority list is COGH-2, which means this section belongs in both the 'old' and 'good' pavement section categories. The field test level of this section is Level 1. According to the PMU's database, the asphalt layer thickness of this section is 4.5 in., but the thickness of actual field-extracted cores was twice that in the database. Of the 18 cores, 5 cores were obtained in sound condition so that horizontal coring for lab testing could be completed; 10 out of 11 cores with delamination were possible for horizontal coring; and 4 out of 18 cores had vertical cracks. Further detailed investigation will be needed in the upcoming quarter.

Photographs of all the pavement cores are shown in Figure B.24, and a summary of each is given is Table B.7. B2-IWP1 (1st inner wheel path in 2nd bad region in the section), B2-IWP2 and B2-WP3 (3rd outer wheel paths in 2nd bad region in the section) are of primary interest because these cores show vertical cracks connected to cracks on top of the core. These cores can be regarded as exhibiting either top-down cracking or a trace of bottom-up cracking that has spread diagonally through the pavement thickness. Photographs and crack mapping data will be used to try to clarify whether the observed cracking is in fact top-down cracking or a reflection of nearby bottom-up cracking.

Figure B.24 Cored field samples taken from US-70 EB near Selma, Johnston County

Table B.7 Summary of cored field samples for US-70 EB, Selma, Johnston County

ID	Layer Thickness (inch)						Condition	Note
	1st	2nd	3rd	4th	5th	6th		
B1-WP1	2	1	1 3/4	3	3 <		Intact	
B1-WP2	2	1 1/8	?	?	3 1/2		Delamination and Cracks	Severe horizontal cracking near delamination area
B1-CL1	1 7/8	1 1/8	1 3/8	2 3/4	3		Delamination	
B1-CL2	1 3/4	1 1/4	1 3/8	3	2 3/4 <		Delamination	
B2-CL1	1 1/2	1 1/8	1 1/8	1 1/2	1 5/8	3 1/2	Intact	Appears that 4th & 5th layers were constructed during the same period
B2-CL2	1 1/2	1 1/4	1 3/8	3 1/8	3 1/2		Delamination	
B2-IWP1	1 3/4	1 1/8	1 1/4	2 5/8	3 7/8		Cracks	Possible top-down cracking, 2 vertical cracks connected to macro cracks on top of the core
B2-CL3	1 1/2	1 1/4	1 1/2	3	3 1/2<		Intact	
B2-IWP2	1 1/2	1 1/4	1 1/2	3	4		Cracks	Possible top-down cracking, 2 vertical cracks connected to macro cracks on top of the core
B2-WP3	1 3/4	1	1 1/4	3 1/8	3 1/2		Cracks	High possibility of top-down cracking, 2 vertical cracks connected to macro cracks on top of the core
A1-WP1	2	1 1/4	1 3/8	3 1/8	3<		Delamination	
A1-WP2	1 7/8	1 1/4	1 3/8	3 1/8	3 <		Delamination	
A1-CL1	1 7/8	1 1/8	1 1/2	2 7/8	3<		Delamination	
A1-CL2	1 7/8	1	1 3/8	3	3<		Delamination	
A2-WP1	1 1/4	1 1/2	1 1/4	1 3/8	3 1/8	3 1/4<	Delamination	
A2-WP2	1 5/16	1 1/2	1 1/8	1 1/4	3	4<	Intact	
A2-CL1	1 3/8	1 3/4	1	1 1/2	2 3/4	3 3/4	Delamination	
A2-CL2	1 3/8	1 5/8	1	1 1/4	2 3/4	3 3/4	Intact	

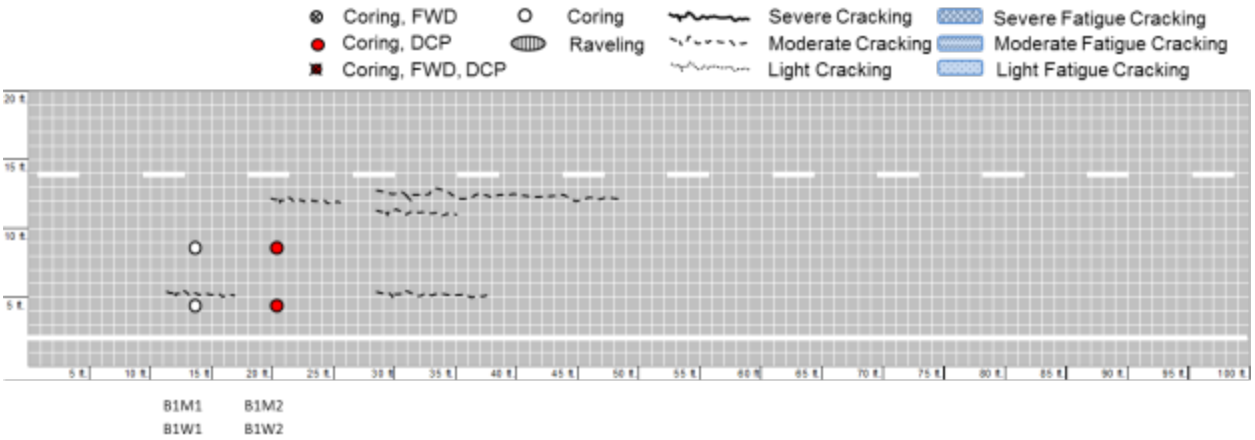

Figure B.25 Crack condition survey mapping of B1 region in US-70

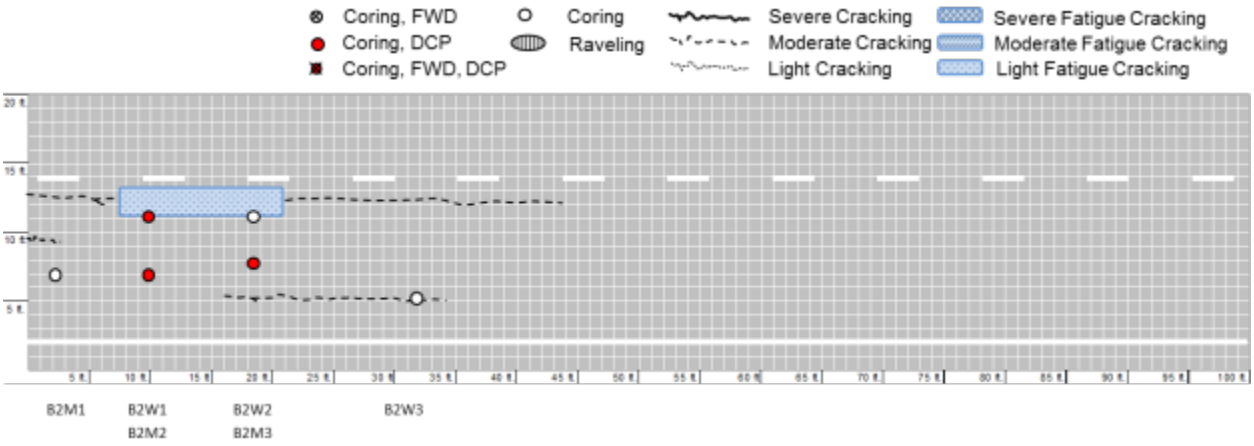

Figure B.26 Crack condition survey mapping of B2 region in US-70

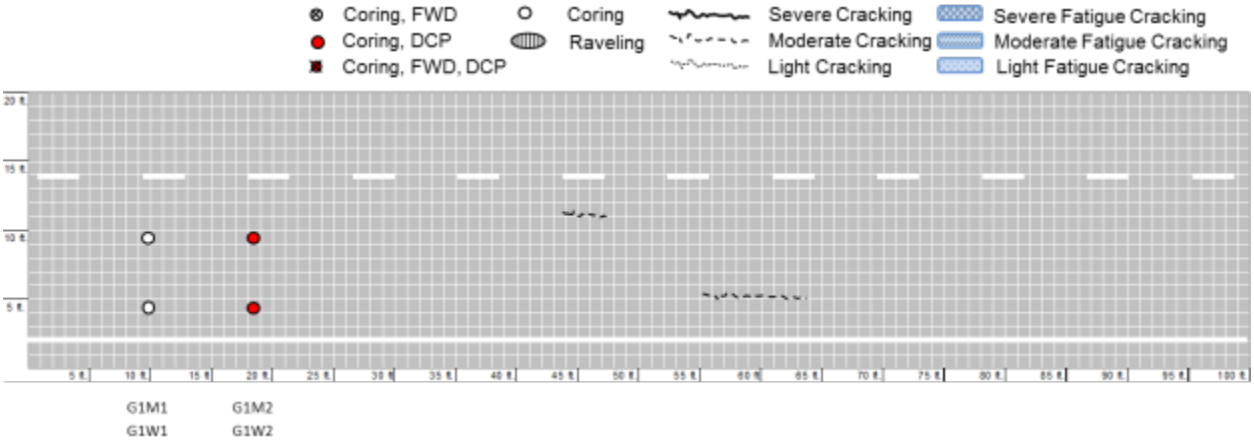

Figure B.27 Crack condition survey mapping of A1 region in US-70

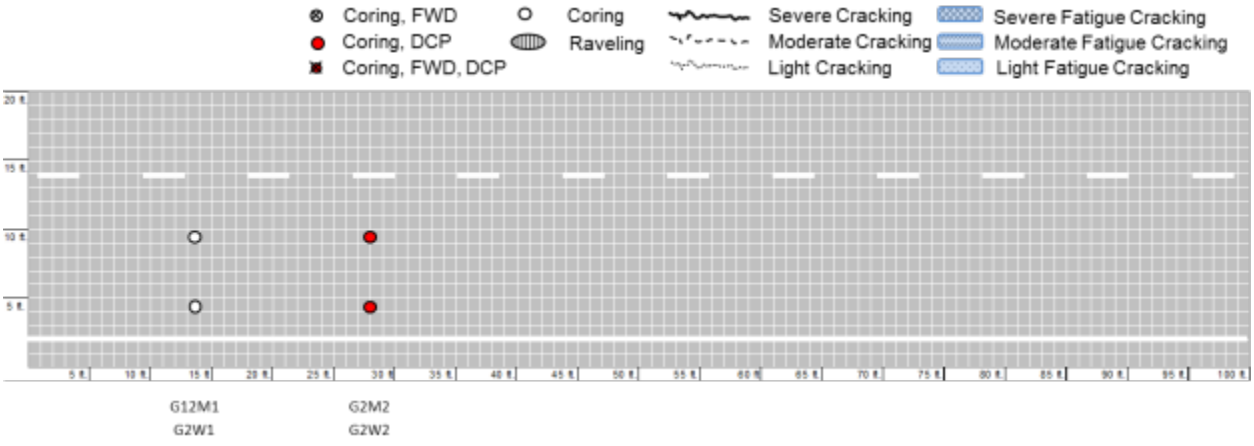

Figure B.28 Crack condition survey mapping of A2 region in US-70

6. US Route 74 (Swain County)

On November 17, 2011, NCDOT personnel and the research team took FWD measurements and extracted 15 cores from US-74 westbound in Bryson City, Swain County. This section is a 2-lane divided highway in the Smoky Mountains. The total length of the section that was constructed at the same time is 2.23 miles. A 12,000 foot segment on relatively straight and flat ground was selected for testing because the safety of field personnel is compromised on extremely winding and steep roadways in the Smoky Mountains. According to the NCDOT construction history and profile database, previous surface treatments include: 1½ inches of S9.5B mixture, 1 inch of I-2 mixture, 2 inches of BCSC mixture, and 2 inches of bituminous concrete binder (BCBIN) that were constructed in 2002, 1988, 1976 and 1976, respectively. The field test level of this section is Level 1, and the condition of this section falls in the category of *Young and Poor* roadways. The overall condition of this section is *Poor*, and distinguishing between *good* condition locations and *bad* condition locations was difficult. Therefore, the test results from the *good* and *bad* locations are not expected to differ significantly. Representative cracking patterns in a *bad* location (a) and a *good* location (b) are shown in Figure B.29.

(a) (b)

Figure B.29 Photographs of representative cracking patterns on US-74, Bryson City, Swain County: (a) *bad* location, and (b) *good* location

The initial testing for this section was planned for November 16, 2011, but testing was postponed due to inclement weather and roadway conditions. As an alternative plan, the research team and NCDOT personnel decided to test this section in the morning of the following day and consented to reduce the number of cores and FWD tests in order to test another section, scheduled on the next date, in the afternoon. Of the 15 cores extracted from this section, 10 cores were in sound condition, so horizontal coring for the lab testing could be completed. A summary of the pavement core data is given in Table B.8, and photographs of the cores are shown in Figure B.30.

Table B.8 Summary of Core Data for US-74, Bryson City, Swain County

ID	Layer Thickness (inch)				Condition	Note
	1st	2nd	3rd	4th		
B1-CL1	1 5/8	3 1/2	1 3/4		Intact	Sound condition
B1-CL2	1 3/8	3 1/2	1 7/8		Intact	Sound condition
B1-WP1	1 3/4	3	2		Cracked	Horizontal cracks in the upper end of 4th layer connected to 3 vertical cracks that propagate to the bottom of core
B1-WP2	1 1/2	3 7/8	1		Intact	Sound condition
B1-WP3	1 3/4	3 1/4	1 3/4		Intact	Sound condition
B1-WP4	1 3/8	3 1/2	1 1/2		Intact	Sound condition
B1-WP5	1 5/8	2 1/2	1 1/8	1 3/4	Cracked	2 vertical macrocracks from top to bottom; wide vertical cracks in 4th layer filled with dust, and those cracks connected to vertical cracks that propagated to the top of core
B1-WP6	1 1/2	3 1/2	2 1/4		Cracked	3 vertical macrocracks from top to bottom; horizontal crack in the middle of 3rd layer; wide vertical cracks in 4th layer filled with dust, and those cracks connected to vertical cracks that propagated to the top of core
A1-CL1	1 1/2	2 2/3	1 1/8	2 1/2	Broken	2 vertical macrocracks from top to bottom; partial delamination in the surface of sublayers in 4th layer
A1-CL2	1 7/8	2 3/8	1 1/4	1 3/4	Intact	Sound condition
A1-CL3	1 1/2	2 1/4	1 1/4	1 7/8	Intact	Sound condition
A1-CL4	1 3/8	2 3/8	1 1/4	1 1/4	Intact	Sound condition, but hairline crack on top surface
A1-WP1	1 3/4	3 3/8	1	2	Intact	Sound condition
A1-WP2	1 3/4	2 1/2	7/8	2	Intact	Sound condition
A1-WP3	1 1/2	2 3/8	1	1 3/8	Cracked	3 vertical macrocracks from top to bottom; horizontal crack in 4th layer

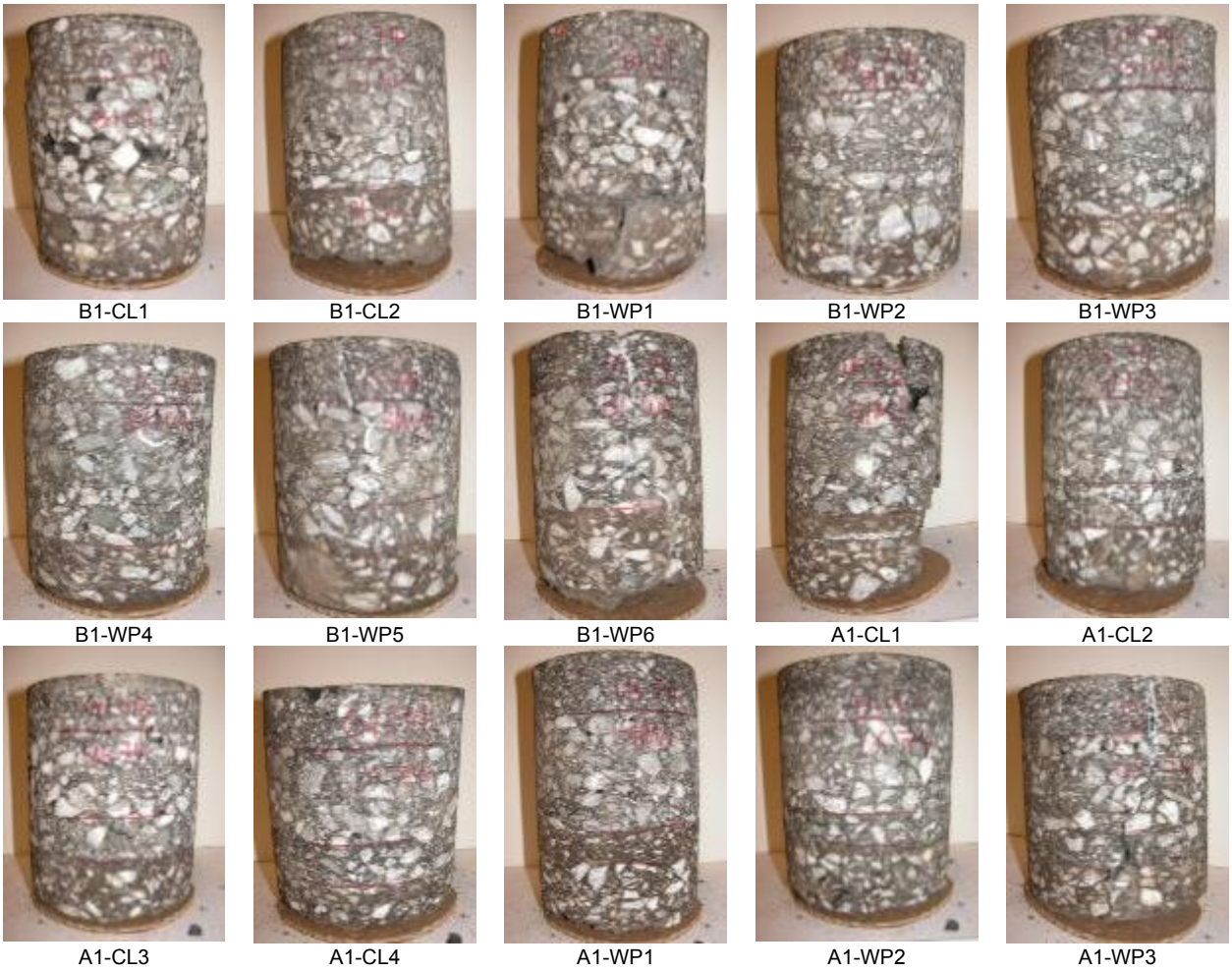

Figure B.30 Cores taken from US-74, Bryson City, Swain County

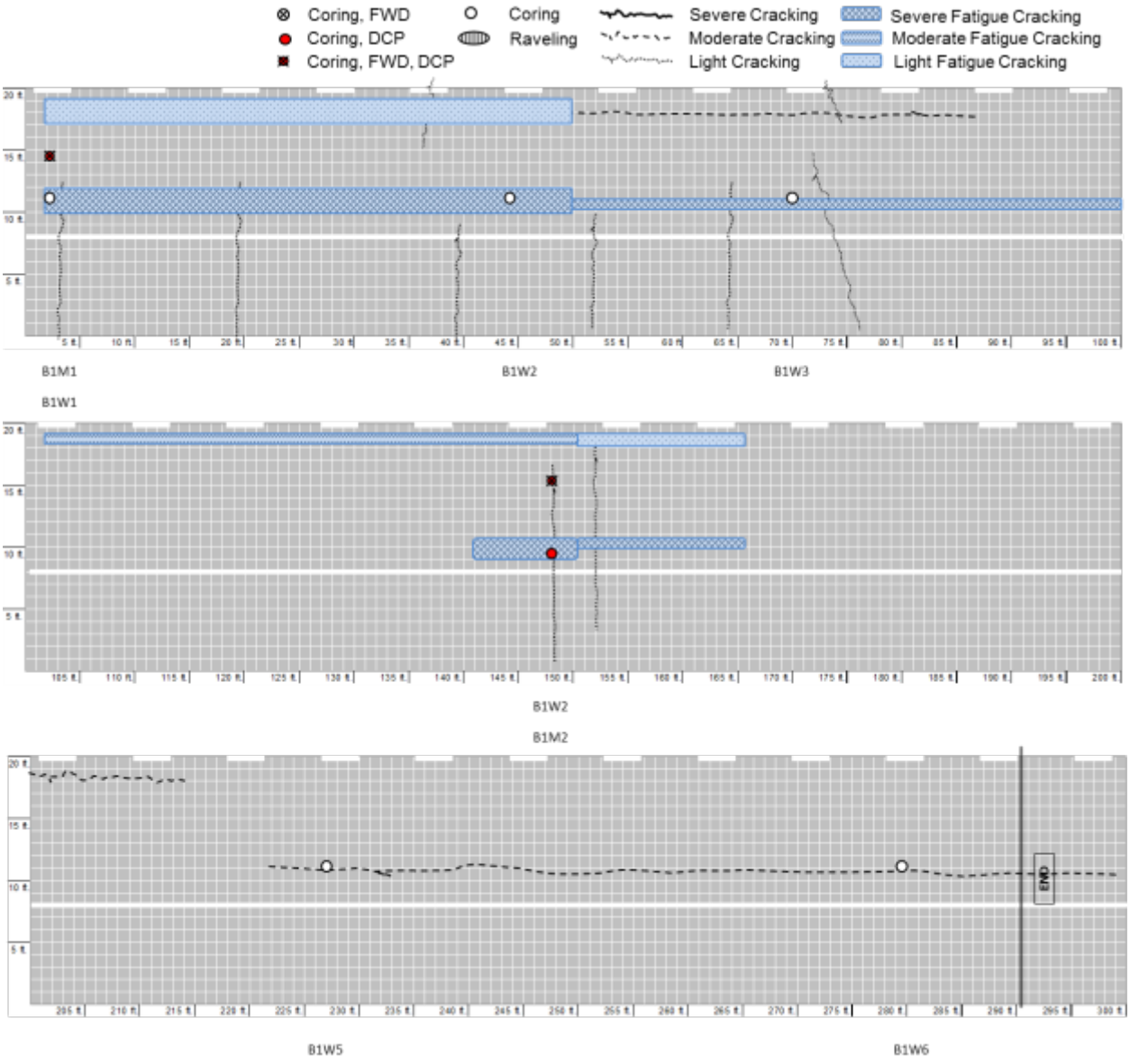

Figure B.31 Crack condition survey mapping of B1 region in US-74

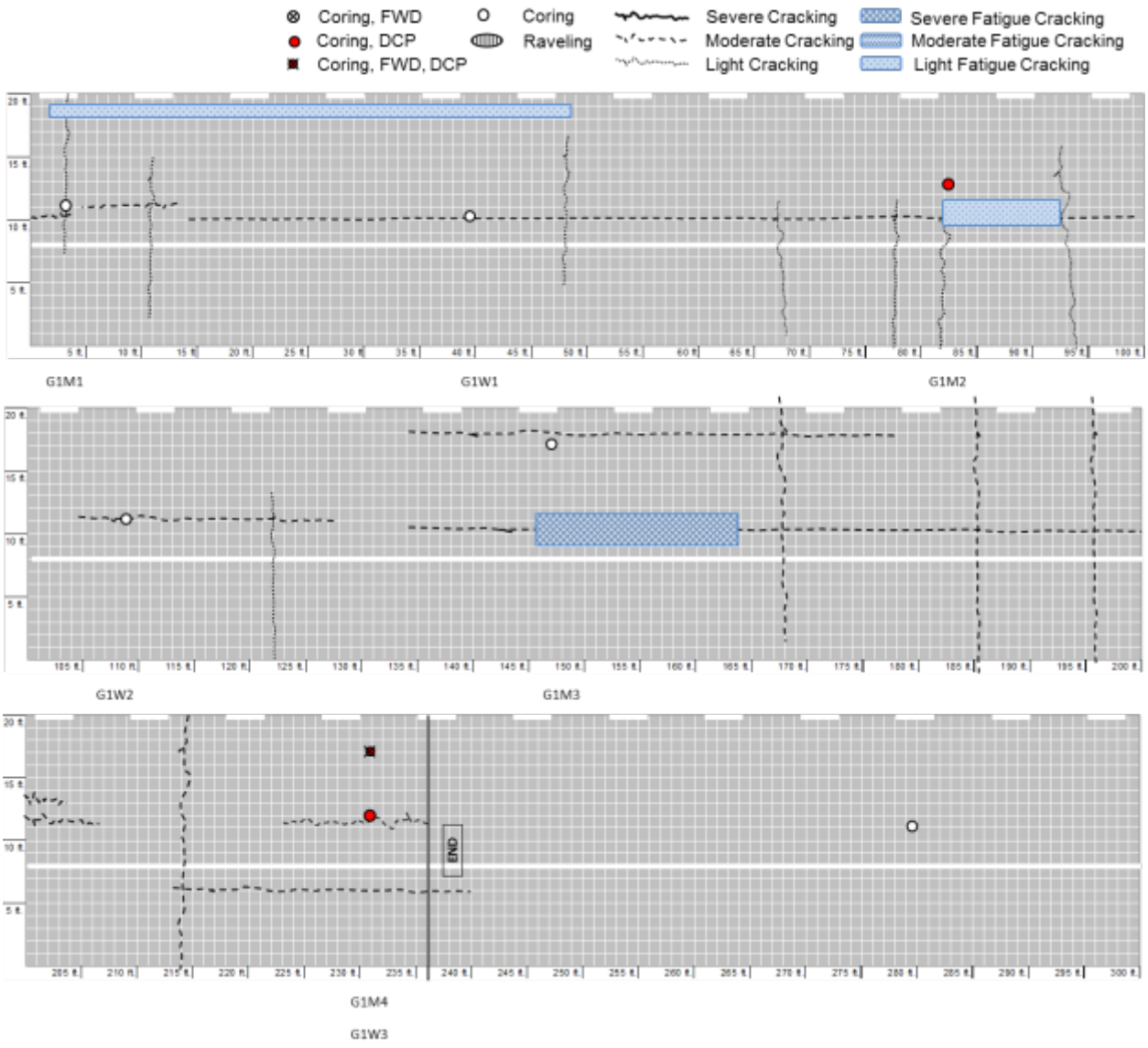

Figure B.32 Crack condition survey mapping of A1 region in US-74

7. US Route 601 (Union County)

On August 11, 2011, NCDOT personnel and the research team took FWD and DCP measurements and extracted 20 cores from US-601 northbound (NB) near Monroe in Union County. According to the NCDOT construction history and profile database, the section was resurfaced in 2001with heavy-duty asphalt. Although the section is 1 lane per direction, the roadway nonetheless has quite a high volume of heavy truck traffic. The field test level of this section is Level 1, and this section is in the group of *Young and Poor* condition roadways. Of the 20 cores extracted from the field, 13 cores were obtained in sound condition so that horizontal coring for lab testing could be completed.

Figure B.33 shows cracking patterns in the section. Longitudinal cracking and irregular interval transversal cracking are distributed throughout the entire section. Permanent deformation on the outer wheel path is more severe than for the other sections. This distress may be caused by the high volume of truck traffic and the low speed limit.

Figure B.33 Photographs of cracking patterns on US-601

Summaries of all the pavement core data are given in Table B.9 and Table B.9, and photographs of those cores are shown in Figure B.35. Three cores have wide soil-filled cracks at the bottom of the cores. It is not clear when the soil filled these cracks, but there is a high possibility that the soil-filled cracks were not milled or cleaned prior to the overlay construction. That is, most of the soil-filled cracks are not connected to the vertical cracks that begin from the

top surface of the cores. Figure B.34 shows the cracks and delamination line filled with soil or dust.

Table B.9 Summary of core data for US-601, Monroe, Union County

ID	Layer thickness (inch)							Condition
	1st		2nd		3rd		4th	
A1-CL1	1 3/4		1 3/4		1 5/8		1 3/4	Intact
A1-CL2	1	3/4	1 1/2		2		1 5/8	Cracked
A1-CL3	1 1/2		1 3/4		7/8	1 1/4	1 5/8	Intact
A1-CL4	2		2 1/2		7/8	1 1/4	1 3/4	Intact
A1-WP1	1		1 1/2	1/2	1 1/4		1 1/2	Cracked
A1-WP2	1/2	1/2	2		1 5/8		1 5/8	Intact
A1-WP3	1 3/4		2		1 1/2		1 3/4	Intact
A1-WP4	1 5/8		2		1 5/8		2	Intact
B1-CL1	1 1/2		1 1/4		2		1 1/4	Delamination/Broken
B1-CL2	1 3/8		1 1/8		3/4	1	1 1/2	Intact
B1-WP1	1 1/2		1 3/8		1/2	1	1 7/8	Intact
B1-WP2	1 1/8		1 1/4		1 1/2		2 1/8	Delamination/Cracked
B1-WP3	1 3/8		1 3/8		3/4	1 1/4	1 3/4	Cracked
B1-WP4	1 1/4		1 7/8		2		2	Cracked
B2-CL1	1 3/8		1 1/2		2		1 7/8	Intact
B2-CL2	1 3/8		1 3/8		1 5/8		2	Intact
B2-CL3	1 1/2		1 3/8		1	1 1/4	1 1/4	Intact
B2-WP1	?							Broken
B2-WP2	1 1/4		1 1/2		1 7/8		2 1/8	Intact
B2-WP3	1 1/4		1 1/2		7/8	1 1/8	1 7/8	Intact

Table B.10 Additional summary of core data for US-601, Monroe, Union County

ID	Note
A1-CL1	Sound condition, looks like 2nd layer has 2 sublayers, but those 2 sublayers have different binder contents
A1-CL2	Vertical cracks in 1st layer connected to minor cracks on top surface, soil-filled vertical crack connected from horizontal crack in between sublayer of 2nd layer to bottom of core
A1-CL3	Sound condition
A1-CL4	Sound condition
A1-WP1	Vertical cracks in 1st layer connected to cracks on top surface, sound condition except for 1st layer.
A1-WP2	Sound condition
A1-WP3	Sound condition
A1-WP4	Sound condition
B1-CL1	Entire core broken into 2 major pieces, not smooth delamination at top of 3rd layer
B1-CL2	Sound condition
B1-WP1	Sound condition, wide soil-filled crack in 4th layer
B1-WP2	Not smooth delamination in between 2nd & 3rd layers, wide soil-filled cracks in 4th layer and cracks connected from delamination surface to those wide cracks
B1-WP3	Vertical cracks connected to cracks on top surface, wide soil-filled cracks in 3rd & 4th layers, many vertical cracks not connected to cracks on top surface
B1-WP4	Horizontal crack in middle of 2nd layer, 2 vertical cracks connected to cracks on top surface
B2-CL1	Sound condition
B2-CL2	Sound condition
B2-CL3	Sound condition
B2-WP1	Totally broken, thickness of broken layer could not be measured
B2-CL2	Sound condition
B2-WP3	Sound condition

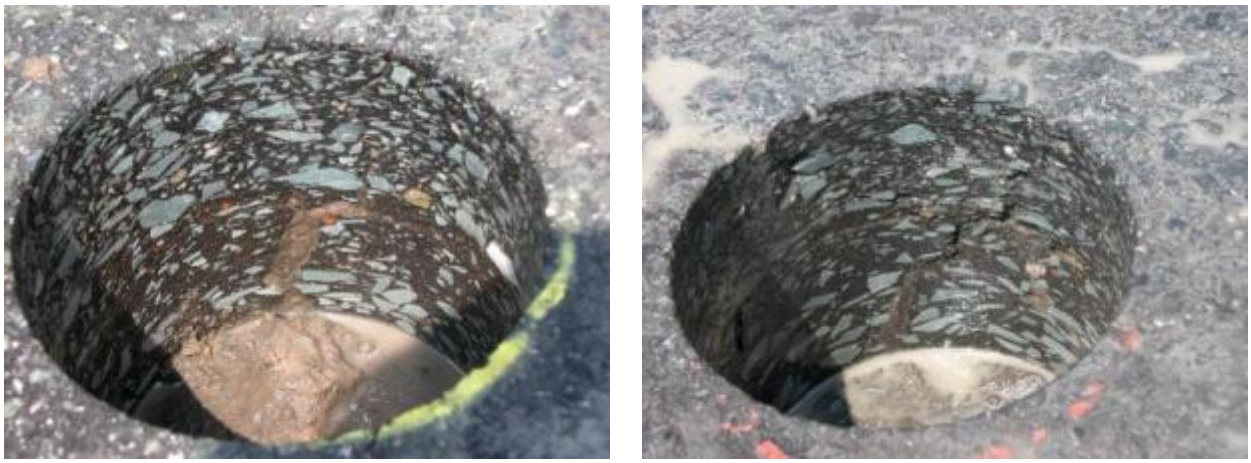

Figure B.34 Photographs of delamination and cracks filled with soil on US-601

Figure B.35 Cores taken from US-601, Monroe, Union County

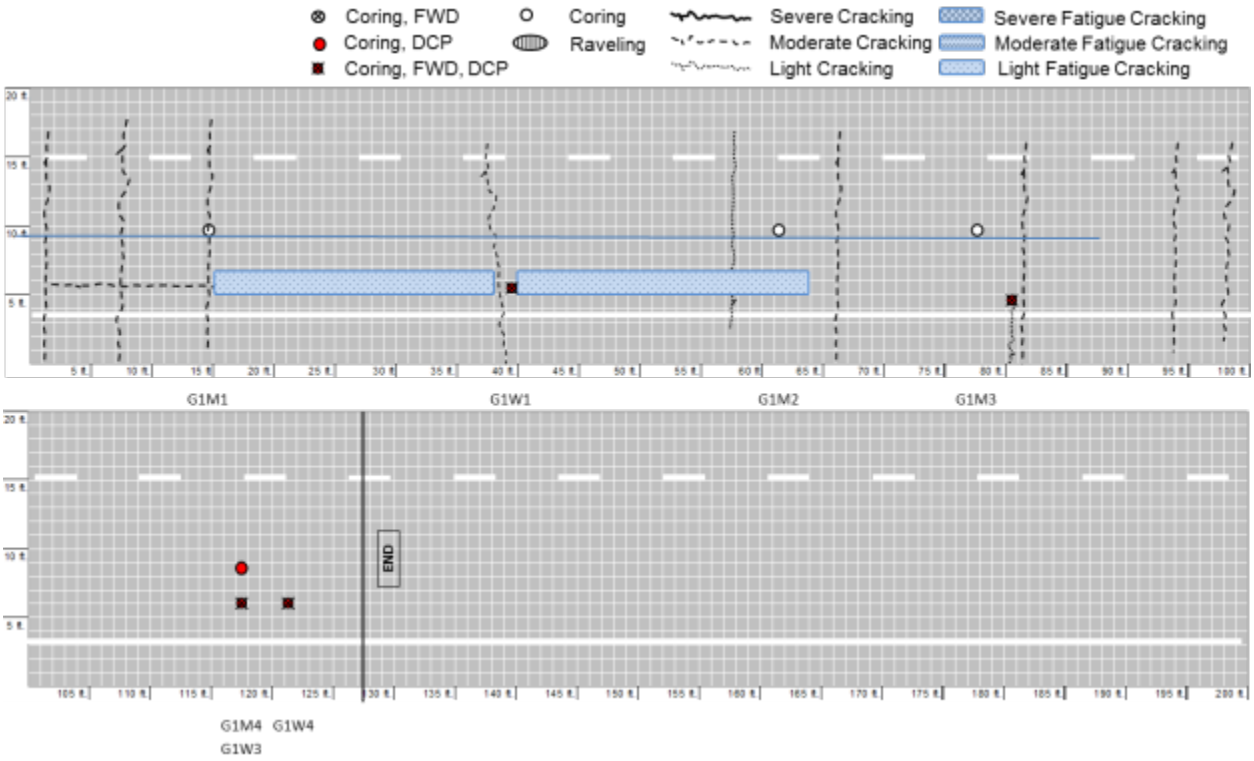

Figure B.36 Crack condition survey mapping of A1 region in US-601

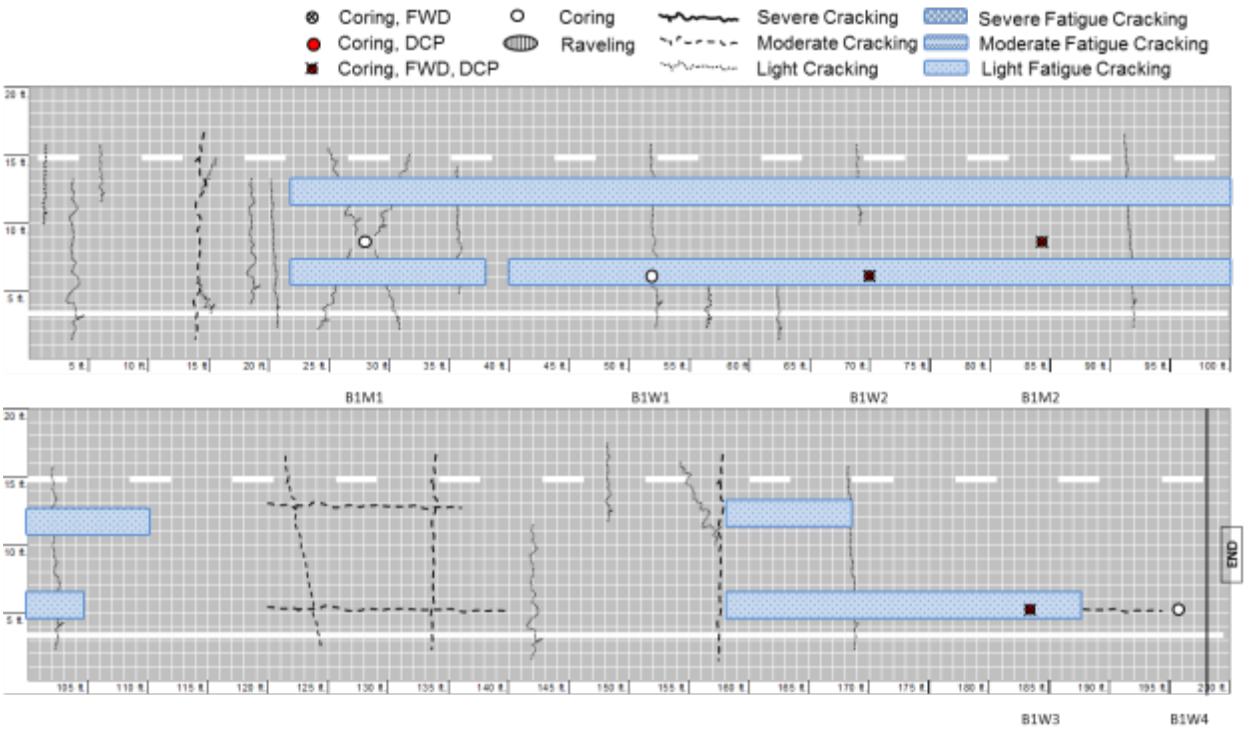

Figure B.37 Crack condition survey mapping of B1 region in US-601

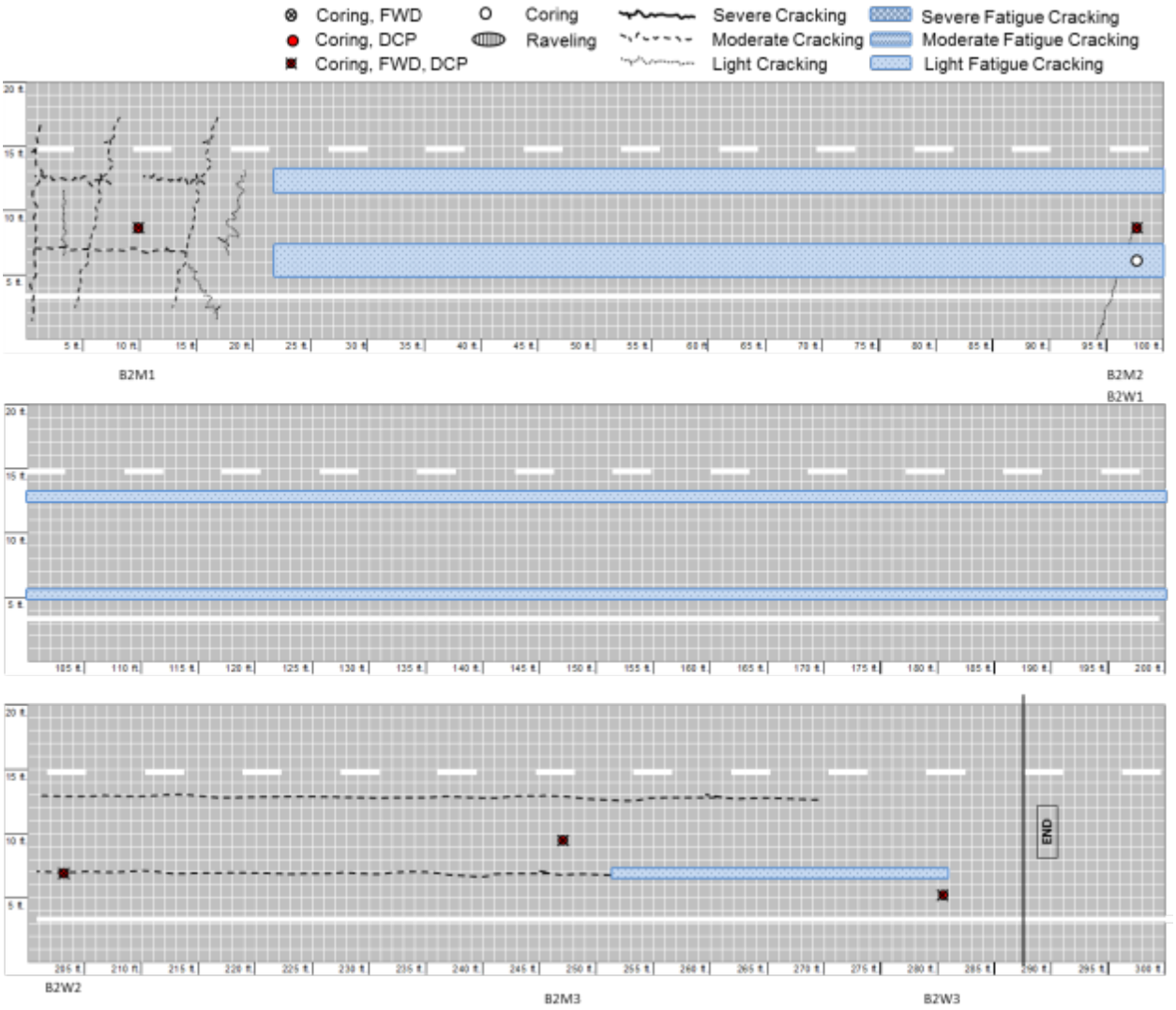

Figure B.38 Crack condition survey mapping of B2 region in US-601

8. NC Route 209 (Haywood County)

On November 17, 2011, NCDOT personnel and the research team took FWD and DCP measurements from 16 cores extracted from NC-209 northbound in Clyde, Haywood County. This section is a one lane per direction rural roadway. According to the NCDOT construction history and profile database, this section was constructed in 1994 using a Marshall mix I surface course (I-1), Marshall mix asphalt binder course (H), and aggregate base course (ABC). The thickness of each layer is 2, 2, and 8 inches, respectively. The pavement condition rating of this section is marked as 95 in the 2010 condition survey. The field test level of this section is Level 1, and the condition of this section falls in the category of *Old and Good* roadways.

Of the 16 cores extracted from this section, all 16 cores were in sound condition, so horizontal coring for lab testing could be completed. The noticeable characteristic of this section is that, although it was constructed in 1994, it contained no cracks at all, according to observations made by the research team. Therefore, the research team contacted the Division maintenance engineer to query the NCDOT database record; the Division maintenance engineer replied that no resurfacing had been conducted after initial construction. Therefore, distinguishing between *good* condition locations and *bad* locations in this section was based on surface smoothness rather than cracking conditions. Similar test results from the two different condition locations were expected. The photographs in Figure B.39 show a *good* condition location (a) and a *bad* condition location (b). A summary of all pavement core data is given in Table B.11, and photographs of the cores are shown in Figure B.40.

(a) (b)

Figure B.39 Photographs of cracking patterns on NC-209, Clyde, Haywood County: (a) *good* condition location, and (b) *bad* condition location

Table B.11 Summary of core data for NC-209, Clyde, Haywood County

ID	Layer Thickness (inch)				Condition
	Layer 1			Layer 2	
	Sub 1	Sub 2	Sub 3		
A1-CL1	1	1	1 1/4	1 5/8	Sound condition
A1-CL2	7/8	1	1/4	2	Sound condition
A1-WP1	3/4	7/8	1 1/4	1 7/8	Sound condition
A1-WP2	3/4	7/8	1 1/16	1 5/8	Sound condition
A1-WP3	3/4	7/8	1 1/4	2	Sound condition
A1-WP4	3/4	1	1 3/8	2	Sound condition
B1-CL1	3/4	1 1/8	1	1 5/8	Sound condition
B1-CL2	1	1 1/16	1 1/8	1 3/4	Sound condition
B1-WP1	3/4	1	1 1/4	2	Sound condition
B1-WP2	1 7/8	1	1 1/4	2	Sound condition
B1-WP3	3/4	1	1 1/8	1 3/4	Sound condition
B1-WP4	3/4	7/8	1 1/8	1 5/8	Sound condition
A2-CL1	1	1	1 3/8	1 3/4	Sound condition
A2-WP1	7/8	1 1/8	1 1/4	2 1/4	Sound condition
A2-WP2	15/16	7/8	1 1/2	2 1/4	Sound condition
A2-WP3	3/4	1	1 5/8	2 1/4	Sound condition

Figure B.40 cores taken from NC-209, Clyde, Haywood County

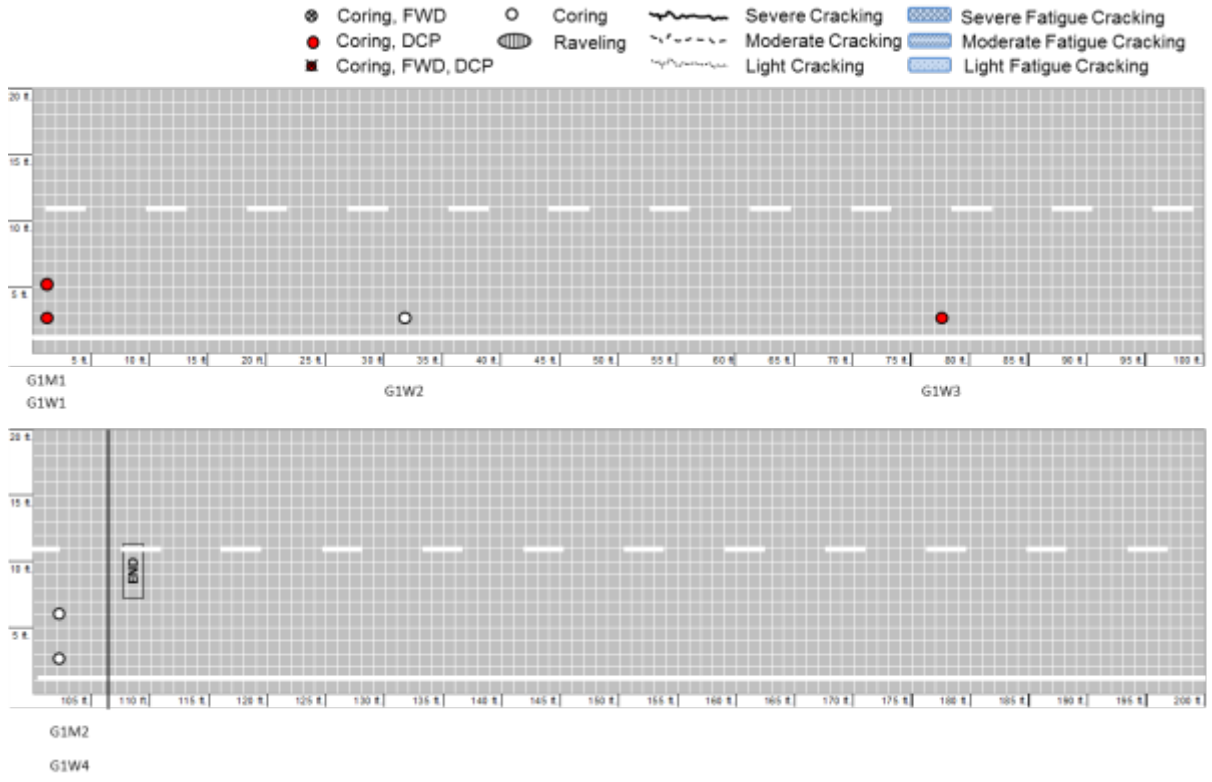

Figure B.41 Crack condition survey mapping of A1 region in NC-209

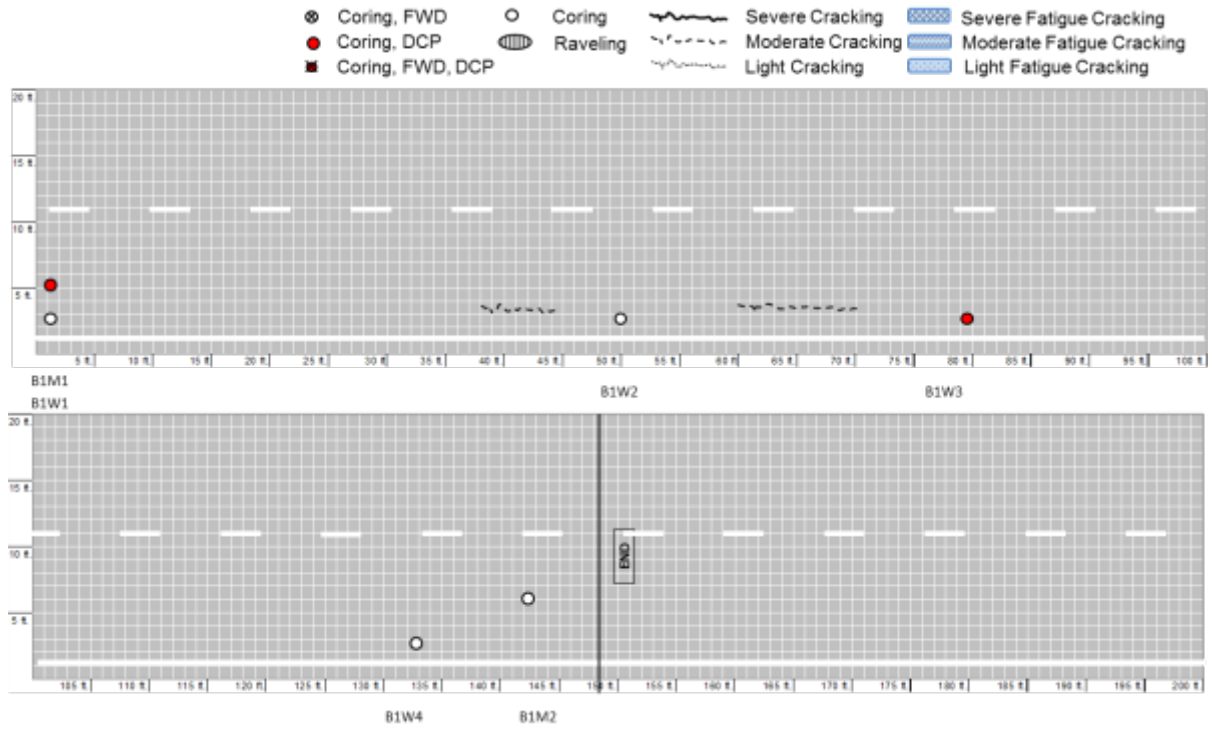

Figure B.42 Crack condition survey mapping of B1 region in NC-209

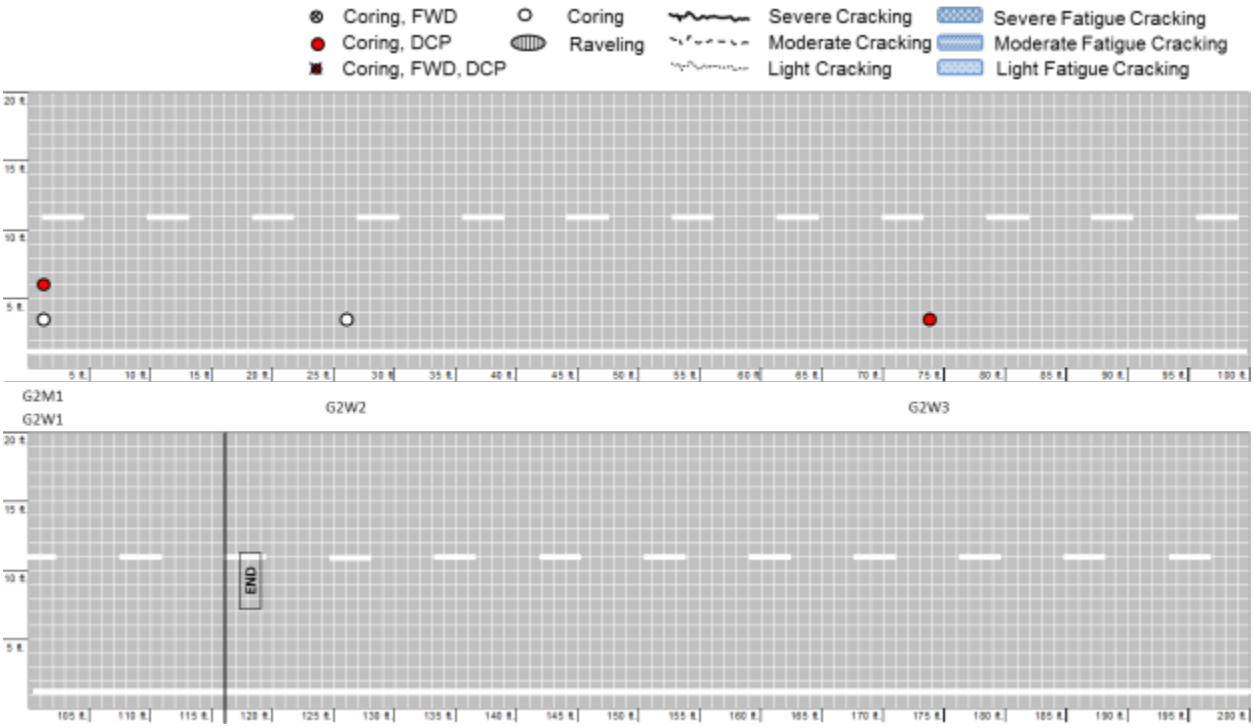

Figure B.43 Crack condition survey mapping of A2 region in NC-209

9. US Route 76 (New Hanover County)

On July 17, 2012, NCDOT personnel and the research team took DCP measurements and extracted fourteen cores from US 76 eastbound in Wilmington, New Hanover County. According to the NCDOT construction history and profile database, the latest (2001) resurfacing work used a heavy-duty asphalt surface course material with an overlay thickness recorded as $2^1/_2$ inches. Prior to this most recent resurfacing effort, treatment methods included: $1^1/_2$ inches of I-2 material in 1983, 1 inch of a BCSC in 1970, and HMS in 1952 without a thickness record. This site does not have a paved shoulder, and the outer lane is curved and directly contacts a pedestrian path. The field test level for this site was planned for Level 2 but shifted to Level 1 because extracted cores from the bad condition region clearly showed a top-down cracking pattern. The condition of this site falls in the category of *Young and Poor* roadways.

Figure B.44 (a) and (b) show severe fatigue cracking in the bad condition region, and the good condition region shows a dramatically better surface condition and a different cracking pattern from that seen in the bad region. Also, cores taken from the good condition region have more layers than the cores extracted from the bad condition region. This pavement structural difference may be the cause of the dramatically different cracking patterns seen on the surface. It is not clear to judge from a visual inspection, but it appears that the construction history data match the cores from the good condition region better than those from the bad condition region. Once the gradation analysis is complete, this hypothesis can be confirmed or denied. The BW1 core shown in Figure B.45 clearly exhibits top-down cracking.

(a) (b)

Figure B.44 Photographs of representative cracking patterns on US-76, Wilmington, New Hanover County: (a) *bad* location and (b) *good* location

Table B.12 Summary of Core Data for US-76, Wilmington, New Hanover County

ID	Layer Thickness (inch)					Condition
	1st	2nd	3rd	4th	5th	
BM1	1 1/8	1	2 3/8			Sound
BM2	1 4/8	7/8	2 5/8			Sound
BM3	1 4/8	6/8	2 4/8			Sound
BW1	1 1/8	1 4/8	2 4/8			Cracks on surface connected to vertical crack through the middle of 2nd layer
BM4	1 1/8	6/8	2			Sound
BM5	7/8	1	2 5/8			Sound
BM6	7/8	1 2/8	2			Sound
BM7	1 1/8	7/8	1 7/8			Sound
GM1	1	2 3/8	1 1/8	1	3 2/8	Sound
GM2	1 3/8	2 6/8	1 1/8	1 1/8	2 4/8	Sound
GM3	1 4/8	1	1 1/8	1	6/8	Cracks on surface connected to vertical crack through the middle of 1st layer
GW1	1 5/8	7/8	7/8	1 1/8	1 5/8	Cracks on surface but no vertical cracks
GM4	1 1/8	1	1 5/8	7/8	3 2/8	Sound
GW2	1 1/8	7/8	1 7/8			Full-depth vertical crack


BM1


BM2


BM3


BW1


BM4


BM5


BM6


BM7


GM1


GM2


GM3


GW1


GM4


GW2

Figure B.45 Photographs of cores taken from US-76, Wilmington, New Hanover County

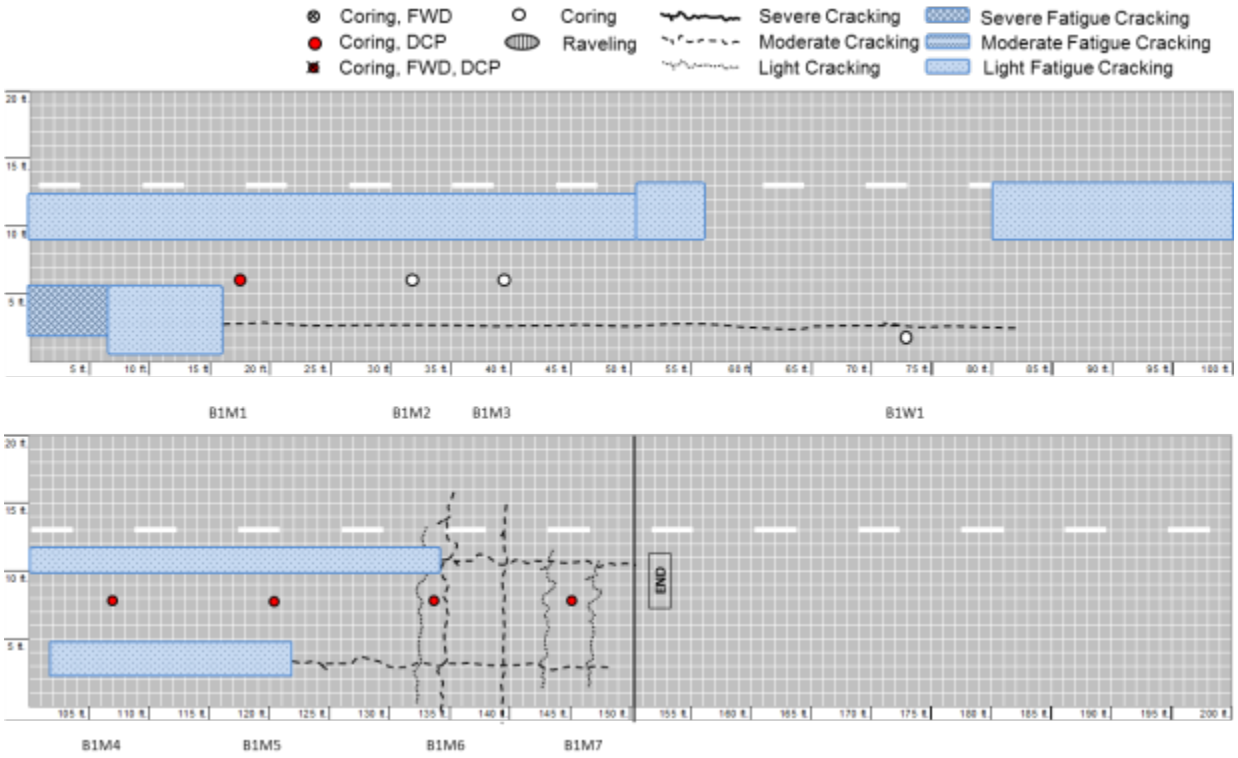

Figure B.46 Crack condition survey mapping of B1 region in US-76

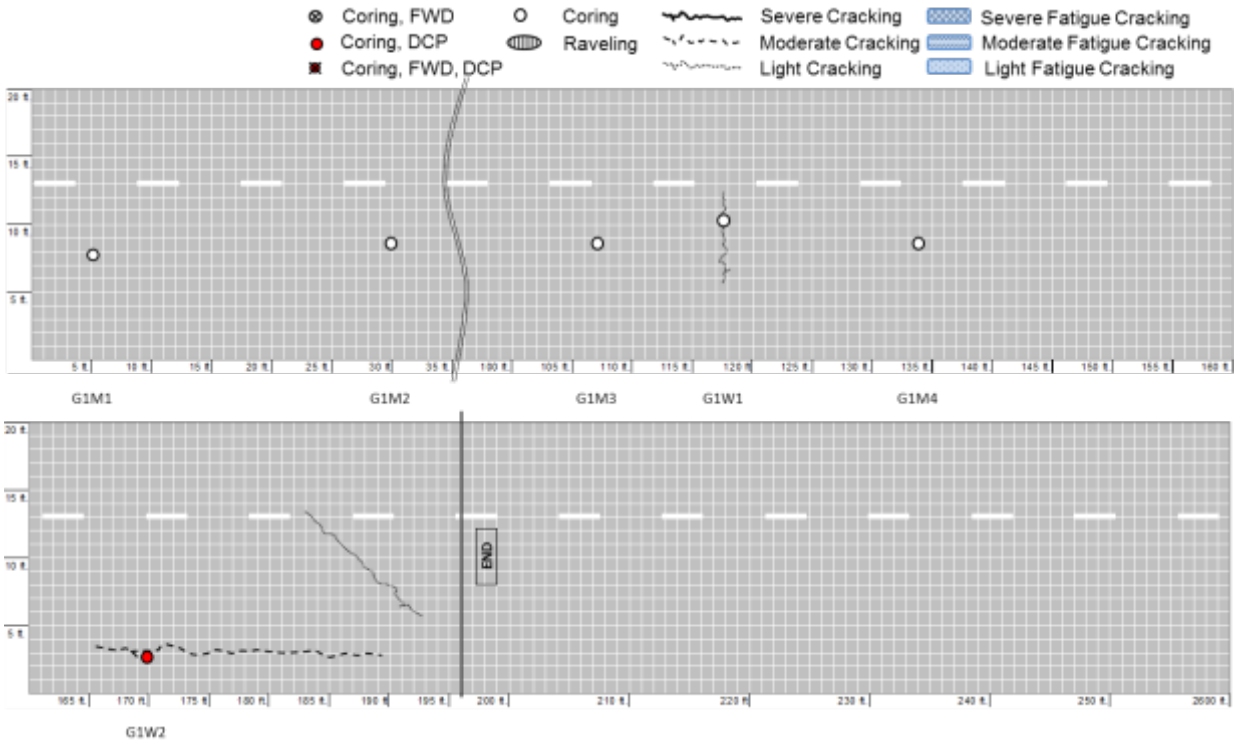

Figure B.47 Crack condition survey mapping of A1 region in US-76

10. NC Route 194 (Avery County)

On July 28, 2011, NCDOT personnel and the research team took FWD and DCP measurements and extracted 21 cores from NC-194 eastbound (EB) in Banner Elk in Avery County. Because the half of the entire section passes through the downtown of Banner Elk, it was difficult to control turning traffic at every intersection; therefore, the other half of the section was selected for field investigation. According to the NCDOT construction history and profile database, the section was resurfaced in 2001 using S9.5B mix. The field test level for this section is Level 1, and this section is in the group of *Young and Poor* condition roadways. Of the 21 cores extracted from the field, 8 cores were obtained in sound condition so that horizontal coring for lab testing could be completed.

Although this section was divided into two 'bad' regions and two 'good' regions, most of the section exhibited severe longitudinal cracking, transversal cracking with pavement drop, and localized severe fatigue cracking. Representative cracking patterns are shown in Figure B.48. A notable observation is the pavement drop near the transverse cracking. Therefore, careful attention to the pavement structure is needed.

Figure B.48 Photographs of cracking patterns on NC-194, Banner Elk, Avery County

Summaries of all the pavement core data are given in Table B.13 and Table B.14, and photographs of the cores are shown in Figure B.49. In the summary tables and photographs, S identifies a core taken from the shoulder, which was extracted to try to determine any possibility of roadway expansion. Because 2 out of 21 cores were totally broken, it was not possible to measure the thickness of each layer. According to the construction database, this section has 6 asphalt layers; however, 14 out of 21 cores had fewer than 6 asphalt layers.

Table B.13 Summary of core data for NC-194 EB, Banner Elk, Avery County

ID	Layer Thickness (inch)						Condition
	1st	2nd	3rd	4th	5th	6th	
B1-CL1	1 1/4	1 3/4	2 1/4	1/4	3		Intact
B1-CL2	1 1/8	1 3/4	2 1/4	3 1/2			Intact
B1-W1	1 1/4	1 1/2	1 5/8	1 1/4	2 3/4		Delamination/Cracked
B1-WP2	1 1/2	1 5/8	3/4	?	5/8	2 1/4	Delamination/Cracked
B1-WP3	1 1/4	2 1/8	7/8	3/4	3/4		Delamination/Intact
B1-WP4	?						Broken
A1-CL1	1 5/8	1 5/8	7/8	1/2	1/4	1 3/8	Intact
A1-WP1	1 1/2	1 1/4	1	7/8	1 3/8	1 1/2	Intact
A1-WP2	1 5/8	1 1/2	1 1/2	1/2	1		Cracked
A1-WP3	1	1 3/8	1 1/8	1/2	7/8	1 3/8	Delamination
A2-CL1	1 1/8	1 7/8	1	3/4	3/4		Delamination
A2-WP1	1 1/4	1 1/2	1	1 1/4	1	2	Delamination
A2-WP2	1 1/8	2	1	1/2	5/8	1	Intact
A2-WP3	1 1/8	1 3/4	1	1	1 7/8		Intact
B2-CL1	1 1/8	3/4	7/8	1 1/2			Delamination
B2-CL2	1 1/8	3/4	3/4	5/8	1 1/2		Delamination
B2-WP1	1 3/4	1 5/8	1 1/4	1 1/8			Intact
B2-WP2	1 1/8	1 5/8	5/8	3/4	1		Delamination
B2-WP3	1 1/8	1 1/8	1 1/8	1 5/8			Cracked
B2-WP4	1 3/4	?					Delamination/Broken
B2-S1	1 3/4	1	3				Cracked

Table B.14 Additional summary of core data for NC-194 EB, Banner Elk, Avery County

ID	Note
B1-CL1	Sound condition
B1-CL2	Sound condition
B1-W1	Delamination between 3rd &4th layers, marking paint on delamination surface, vertical crack from surface to delamination line
B1-WP2	Thickness of 4th layer not measured due to loose mixture condition material, cracks on top surface but no vertical crack, delamination between 3rd &4th layers
B1-WP3	Delamination between 3rd & 4th layers, cracks on top surface but no vertical cracks
B1-WP4	Totally broken in pieces, no thickness measurement possible
A1-CL1	Sound condition
A1-WP1	Sound condition
A1-WP2	Vertical cracks begin from surface to top of 3rd layer, resembles top-down cracking, crack on surface
A1-WP3	Delamination between 3rd & 4th layers, looks like 3rd & 4th layers are same mixture and/or construction period
A2-CL1	Delamination between 1st & 2nd layers, vertical crack in 1st layer connected to cracks on surface
A2-WP1	Delamination between 1st & 2nd layers
A2-WP2	Sound condition
A2-WP3	Cracks on top surface but no vertical cracks
B2-CL1	Partial delamination between 1st & 2nd layers, vertical crack in 1st layer connected to cracks on surface
B2-CL2	Delamination between 1st & 2nd layers and 2nd & 3rd layers, vertical crack in 2nd layer, no cracks on surface.
B2-WP1	Cracks on top surface but no vertical cracks
B2-WP2	Delamination between 1st & 2nd layers and 2nd & 3rd layers, cracks on top surface connected to 2 vertical cracks in 1st layer
B2-WP3	Macrocrack on top surface but no vertical cracks
B2-WP4	Delamination between 1st & 2nd layers and 2nd & 3rd layers, totally broken except for top layer
B2-S1	Horizontal crack in middle of 3rd layer, thickness of 3rd layer could not be measured, marking paint on surface, vertical crack in 4th layer

Figure B.49 Cores taken from NC-194 EB, Banner Elk, Avery County

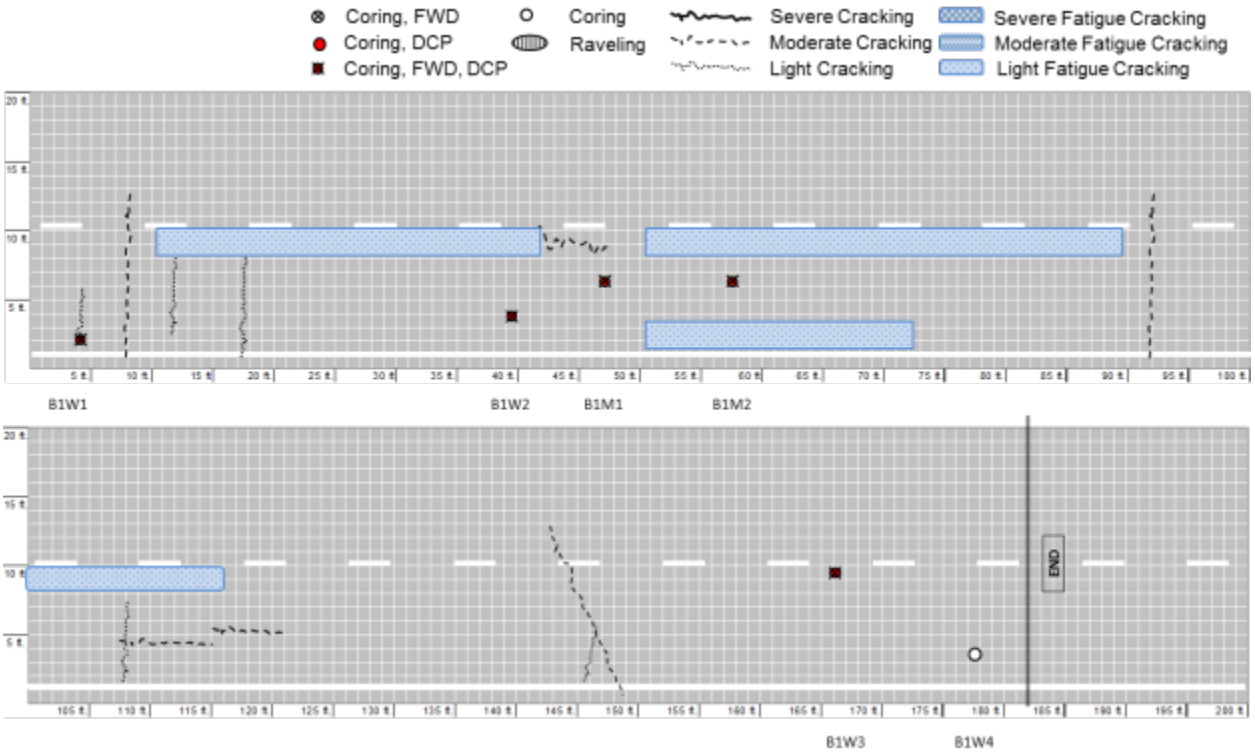

Figure B.50 Crack condition survey mapping of B1 region in NC-194

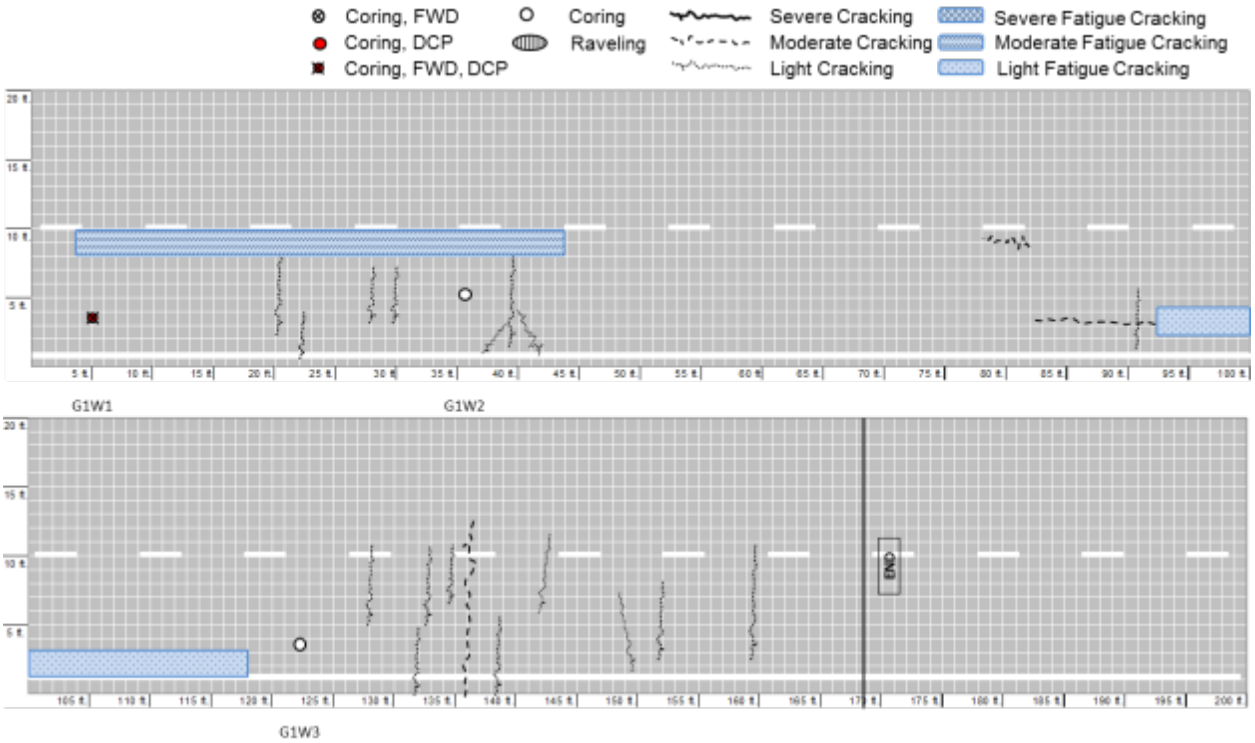

Figure B.51 Crack condition survey mapping of A1 region in NC-194

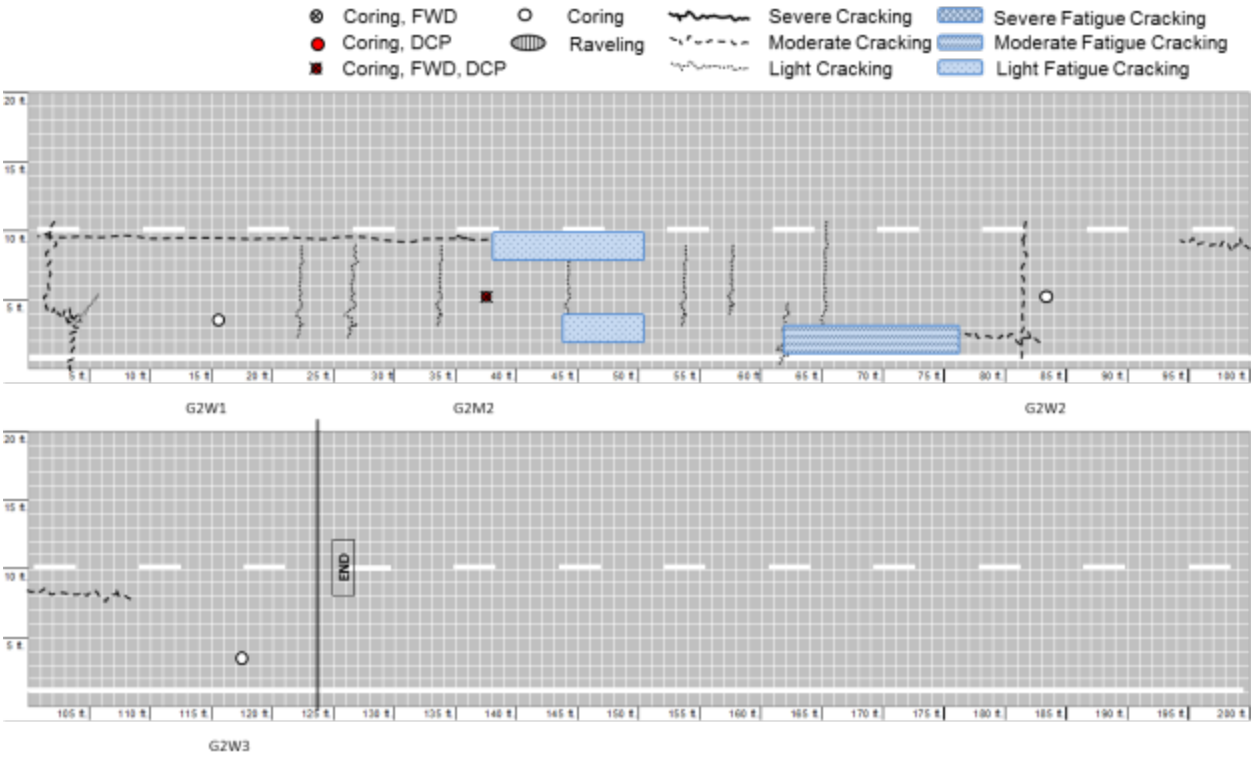

Figure B.52 Crack condition survey mapping of A2 region in NC-194

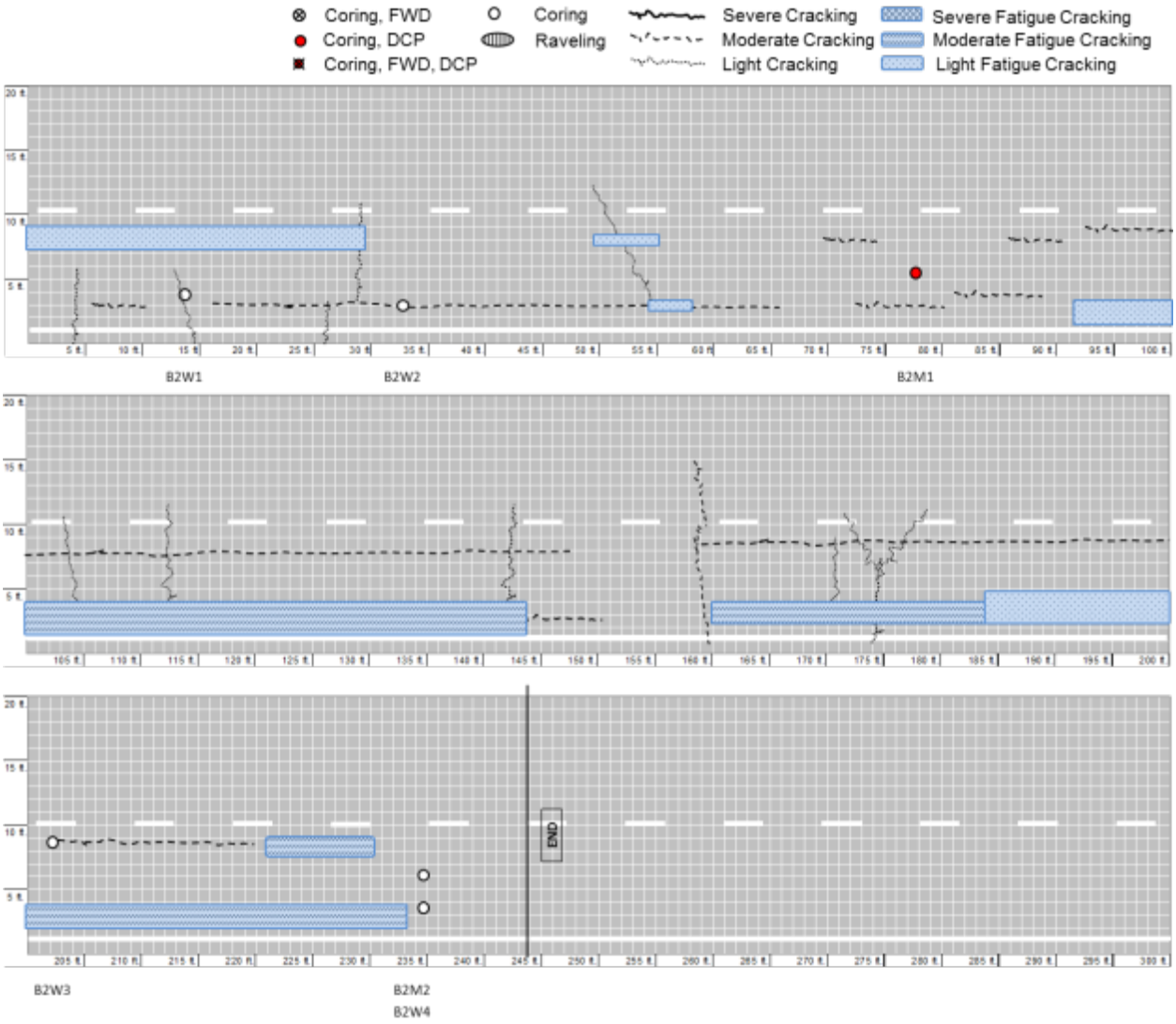

Figure B.53 Crack condition survey mapping of B2 region in NC-194

11. US Route 13 (Martin County)

On June 9, 2010, PMU personnel and the research team took FWD and DCP measurements and extracted 19 field cores from US-13 westbound (WB) near Williamston in Martin County. The research team also conducted crack mapping of the sections where the cores were extracted. This test section is estimated to be seven years old and was showing significant wheel path cracking, as shown in

Figure B.54. The asphalt concrete layers were approximately 5.5 inches thick (3 inches of surface mix and 2.5 inches of intermediate mix) and were atop an aggregate base layer.

Figure B.54 Example of fatigue cracking along the US-13 Williamston test section.

Of the 19 cores taken, 14 were obtained in sound condition so that horizontal coring for lab testing could be completed. The remaining 5 cores were taken from cracked areas to examine issues of top-down versus bottom-up cracking and to check for delamination. Most of the cores clearly showed that a tack coat had been applied between the layers. However, the four cores that were observed to have delamination did not show the presence of a tack coat between the layers. In North Carolina, a tack coat is not required if the upper layer is placed immediately after the lower layer. It is unclear if the application or non-application of a tack coat will be a reoccurring trend in study sections that show delamination; nonetheless, this finding does suggest that it may be necessary to obtain detailed construction records for this project. Delamination also may be caused by a structural collapse near the cored location that is caused by an insufficient sub-base layer or sub-grade support. Insufficient support may be the result of a drainage problem,

localized structural weakness, or bottom-up cracking. Additional and detailed investigation will be needed in the upcoming quarter.

Images of all of the pavement cores are shown in Figure B.55, and a summary of each is given in Table B.15. Core 5 is one of primary interest because it shows a crack in the surface layer and the upper part of the intermediate layer. This core can be regarded as either top-down cracking or a trace of bottom-up cracking that has spread diagonally through the pavement thickness. Photographs and crack mapping data will be used to try to clarify whether the observed cracking is in fact top-down cracking or a reflection of nearby bottom-up cracking. None of the other 19 cores show evidence of top-down cracking, but several of the cores show clear evidence that cracking had spread through the thickness (cores 7, 10, and 11). It is also worth noting that, although core 12 shows delamination between the top and second lifts, it is not clear if this delamination occurred while in service or through the coring operation.

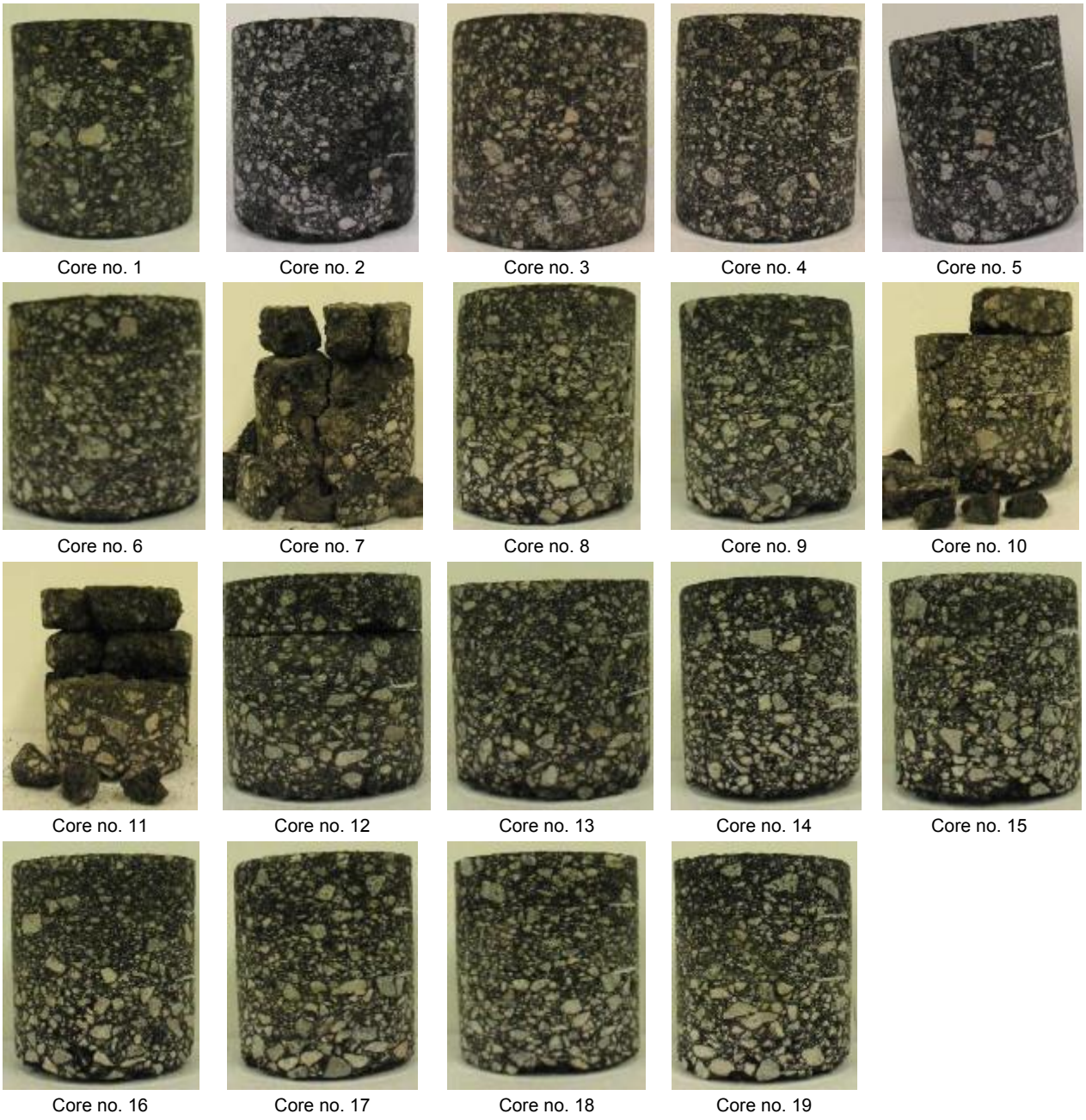

Figure B.55 Cored field samples taken from US-13 West bound, Williamston, Martin County, North Carolina.

Table B.15 Summary of Cored Field Samples for US-13 WB, Williamston, Martin County

Core No.	Thickness			Location in Lane	Condition	Note
	1st Layer	2nd Layer	3rd Layer			
1	1"	2 1/2"	2 1/2"	In between wheel path	Intact	
2	1 1/2"	2 1/4"	2 1/4"	In between wheel path	Intact	
3	1 1/2"	2 1/8"	2 3/4"	In between wheel path	Intact	Fill section
4	1 6/16"	2 7/8"	2 1/2"	In between wheel path	Intact	
5	1 5/16"	1 3/4"	2 3/4"	Under wheel path	Cracks in top and intermediate layers	Fill section
6	1 3/4"	1 3/4"	2 1/2"	In between wheel path	Intact	Fill section
7	1 1/2"	1 3/8"	3"	In between wheel path	Delamination and full-depth crack	
8	1 5/8"	2"	2 3/4"	In between wheel path	Intact	
9	1 1/2"	1 3/4"	3 1/4"	In between wheel path	Intact	
10	1 1/2"	1 7/8"	2 3/4"	Under wheel path	Delamination and full-depth crack	
11	1 1/2"	1 1/2"	2 3/4"	In between wheel path	Delamination and full-depth crack	
12	1 1/2"	1 1/2"	2 3/4"	Under wheel path	Delamnation	Fill section
13	1 1/2"	1 1/2"	2 1/2"	Under wheel path	Intact	Fill section
14	11/2"	2 1/4"	2 1/4"	In between wheel path	Intact	Fill section
15	1 5/8"	2"	2 1/2"	In between wheel path	Intact	Fill section
16	1 9/16"	2"	2 1/2"	In between wheel path	Intact	
17	1 5/8"	1 7/8"	2 3/4"	In between wheel path	Intact	
18	1 1/2"	1 3/4"	2 3/4"	In between wheel path	Intact	
19	1 3/4"	1 7/8"	2 3/4"	In between wheel path	Intact	

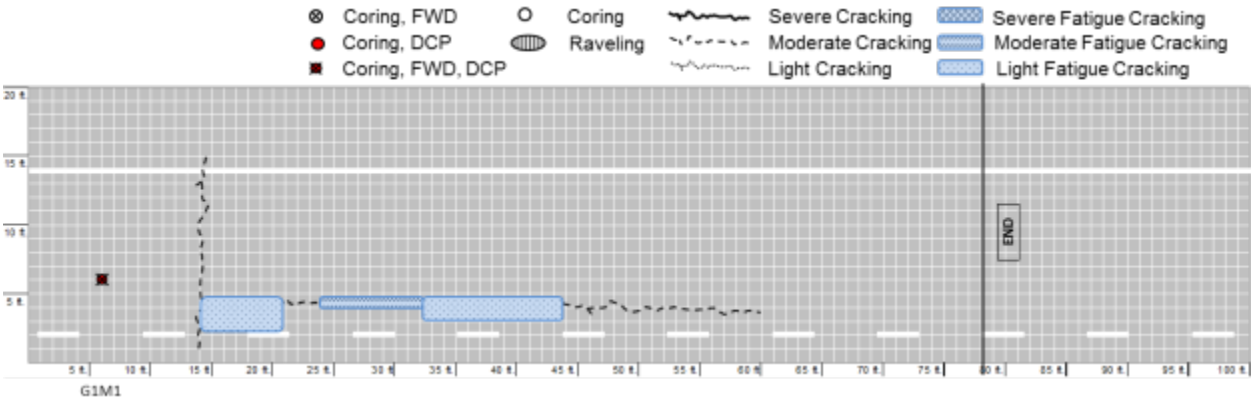

Figure B.56 Crack condition survey mapping of A1 region in US-13

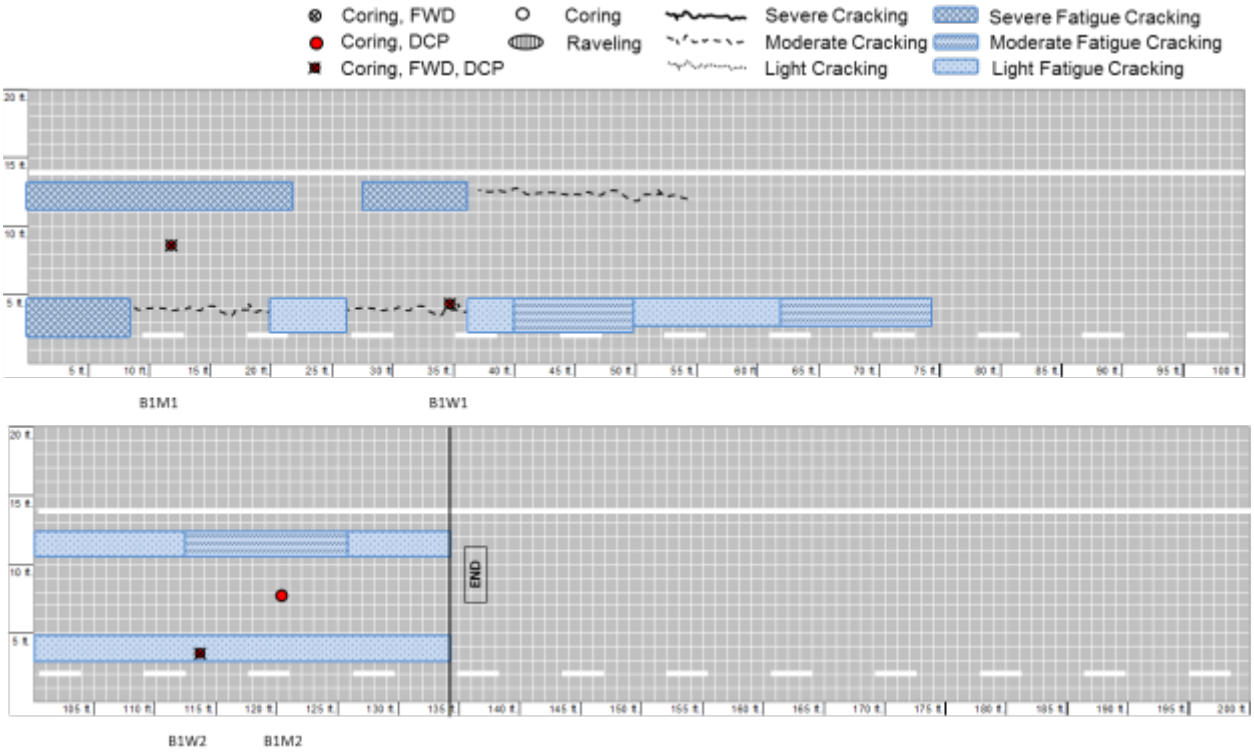

Figure B.57 Crack condition survey mapping of B1 region in US-13

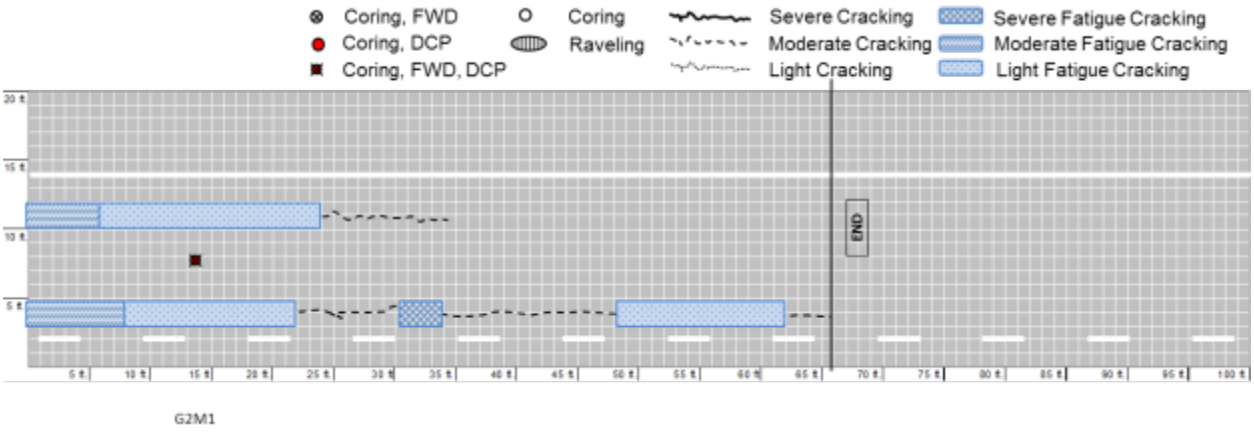

Figure B.58 Crack condition survey mapping of B2 region in US-13

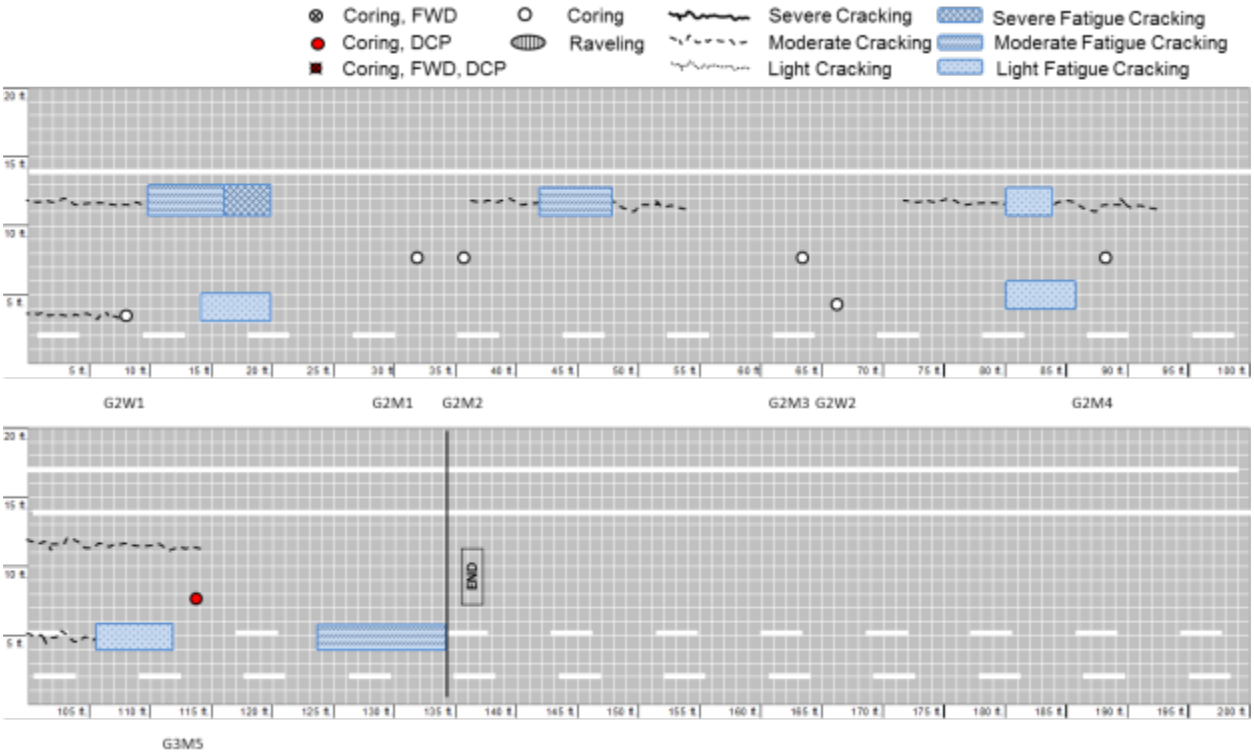

Figure B.59 Crack condition survey mapping of A2 region in US-13

12. NC Route 177 (Richmond County)

On November 3, 2011, NCDOT personnel and research team took falling weight deflectometer (FWD) and dynamic cone penetrometer (DCP) measurements and extracted 24 cores from NC-177 northbound in Hamlet in Richmond County. According to the NCDOT construction history and profile database, the latest (2004) resurfacing work used S9.5C material with an overlay thickness recorded as $1^1/_2$ inches. Prior to this most recent resurfacing effort, treatment methods included: 1 inch of bituminous concrete surface course (BCSC) in 1988, 1 inch of I-2 in 1985, 1 inch of BSBC in 1982, 1 inch of sand mix in 1969, 1 inch of sand mix in 1962, 1 inch of sand mix in 1946, ¾ inch of bituminous surface treatment (BST) in 1944, and ½ inch of BST in 1929. The pavement condition rating of this section is given as 52.4 in the 2010 condition survey. The field test level of this section is Level 1, and the condition of this section falls in the category of *Young and Poor* roadways.

Figure B.60 shows crack sealing that was conducted several years ago. (Note: the research team asked the Division maintenance engineer for exact dates for this project, but written records of the project date could not be found.) A noticeable characteristic of this section is the pavement color, which is lighter than other sections that were constructed during approximately the same period. This color differential indicates that excessive oxidization may have caused the fatigue cracking that is evident in this section. Therefore, the research team was very interested in testing the binder in this section. Also, as shown in Figure B.61, this section has about 5 mm of natural gravel (6^{th} layer) that exhibits a weak bond. Of the 24 cores extracted, 23 cores have a broken layer in the middle of the 6^{th} layer due to the shear force caused by the core drill bit during the coring procedure. The yellow circles in each of the photographs presented in Figure B.61 show the material used for the 6^{th} layer.

Many sections selected for field investigation contain a sand mix layer, and usually, this sand mix layer has a petroleum smell. The year of the most recent construction of the sand mix layer, according to the NCDOT construction history and profile database, is 1969. It is not clear why the sand mix layer still has a strong petroleum smell after over 40 years, and whether the smell is related to the performance of the pavement. Therefore, further investigation is needed.

Figure B.60 Photographs of crack seal section

Figure B.61 Photographs of material used for 6th layer of the cores: (a) broken 6th layer in B2-WP4 core, (b) 6th layer in a coring hole, (c) broken surface of 6th layer stuck in a coring hole, and (d) broken material found in 6th layer

Of the 24 cores extracted from this section, 14 cores, including cores with broken 6th layers, were in sound condition, which allowed horizontal coring or cutting for lab testing to be completed. Two summaries of the pavement core data are given in Table B.16 and Table B.17, and photographs of the cores are shown in Figure B.62.

Table B.16 Summary of Core Data for NC-177, Hamlet, Richmond County

ID	Layer Thickness (inch)									Condition
	1st	2nd	3rd	4th	5th	6th	7th	8th	9th	
B1-WP1	1 5/8	1/2	7/8	7/8	7/8	?				Broken
B1-WP2	1 3/4	3/4	5/8	>1 1/4						Broken
B1-WP3	1 3/4	1/8	7/8	3/4	3/4	3/4	3/4	1 1/4		Intact
B1-CL1	1 5/8	1/4	3/4	7/8	5/8	> 7/8	1 1/8	?		Cracked
B1-CL2	1 1/2	1/8	3/4	3/4	3/4	> 3/4	3/4	1 1/4		Intact
A1-CL1	1 5/8	1/8	5/8	1/2	> 5/8	?	> 7/8	1		Cracked
A1-CL2	1 5/8	1/8	3/4	5/8	3/4	> 1 1/2	1 1/2	3/4		Intact
A1-CL3	1 5/8	1/8	7/8	1	1/2	> 1	1 7/8	1		Intact
A1-WP1	2	1/8	7/8	3/4	3/4	?	1 1/2	> 1 1/4		Cracked
A1-WP2	2	1/8	5/8	1 1/8	5/8	?				Intact
A1-A1	1 3/4	1/4	7/8	1 1/4	1/2	> 1	1 3/8	7/8		Intact
A2-CL1	1 1/2	1/8	7/8	1 1/4	5/8	> 1 1/2	1 3/4	7/8		Intact
A2-CL2	1 1/2	1/8	3/4	1 1/8	5/8	> 3/4	1 1/2	1		Cracked
A2-CL3	2	1/8	1 1/8	1 1/2	3/4	> 1				Intact
A2-WP1	1 7/8	1/8	7/8	1	1/2	> 2 1/8	1 5/8	7/8		Intact
A2-WP2	2 1/8	1/8	1 1/8	1 5/8	7/8	> 1 1/2	3/4	1 1/8		Intact
B2-CL1	1 1/4	1/8	3/4	1 1/8	3/4	> 7/8	1 1/4	1		Intact
B2-CL2	1	1/8	7/8	1 1/8	3/4	> 1	1 3/8	3/4		Intact
B2-WP1	1 3/8	1/8	1	7/8	1	> 1 1/4	1 3/4	7/8	3/4	Cracked
B2-WP2	1 3/4	1/4	7/8	1	1	> 1/2	2	3/4		Broken
B2-WP3	1 5/8	1/4	7/8	3/4	7/8	> 3/4	1 5/8	1	1/2	Cracked
B2-WP4	1 3/8	1/8	7/8	3/4	3/4	> 1	1 1/2	1		Cracked
B2-WP5	1 1/2	1/8	7/8	3/4	3/4	> 1	1 5/8	7/8	1/2	Intact
B2-A1	1 1/8	1/8	7/8	1	1	> 1	1 3/4	7/8		Intact

Table B.17 Additional Core Data for NC-177, Hamlet, Richmond County

ID	Note
B1-WP1	Macrocrack on top surface connected to 3 vertical cracks; layers below 6th layer were stuck in the coring hole; horizontal crack in 3rd layer
B1-WP2	Crack sealer on entire top surface; 3 vertical full-depth cracks
B1-WP3	Sound condition, except for 6th layer
B1-CL1	Horizontal crack in 3rd layer connected to vertical crack in 4th & 5th layers; cracks on top surface
B1-CL2	Sound condition
A1-CL1	Partial chip out on 3rd and 4th layers; 6th layer disappeared due to shear force during coring
A1-CL2	Intact, except for 6th layer
A1-CL3	Partial vertical cracks in 7th and 8th layers
A1-WP1	Vertical crack in 4th and 5th layers
A1-WP2	Part of sample (below 6th layer) was stuck in the coring hole
A1-A1	Vertical crack in 7th and 8th layers; sound condition down to 5th layer
A2-CL1	Sound condition, except for 6th layer
A2-CL2	Crack on top surface connected to vertical cracks in 1st layer
A2-CL3	Part of sample (below 6th layer) was stuck in the coring hole
A2-WP1	Sound condition down to 5th layer, but vertical crack in 7th and 8th layers filled with dust
A2-WP2	Sound condition down to 5th layer, but vertical crack in 7th and 8th layers filled with material used for 7th layer
B2-CL1	Sound condition, except for 6th layer
B2-CL2	Sound condition, except for 6th layer
B2-WP1	Vertical cracks from 6th layer to the bottom of core; a crack on top surface connected to 2 vertical cracks that begin from 1st layer and extend to the top of 6th layer; sand mix layer (9th layer) at the bottom of core
B2-WP2	Macrocrack on top surface connected to 3 vertical cracks in 4th and 5th layers
B2-WP3	Partially broken sand mix layers (4th and 5th layers); horizontal crack begins from the middle of 3rd layer and extends to 5th layer; material used for 6th layer fills vertical cracks in 7th and 8th layers; sand mix layer at the bottom of core
B2-WP4	Vertical cracks from 2nd layer down to the middle of 8th layer; wide vertical crack in 7th and 8th layers filled with dust (may be 6th layer material)
B2-WP5	Sound condition, except for 6th layer
B2-A1	Sound condition, except for 6th layer

Figure B.62 Cores taken from NC-177, Hamlet, Richmond County

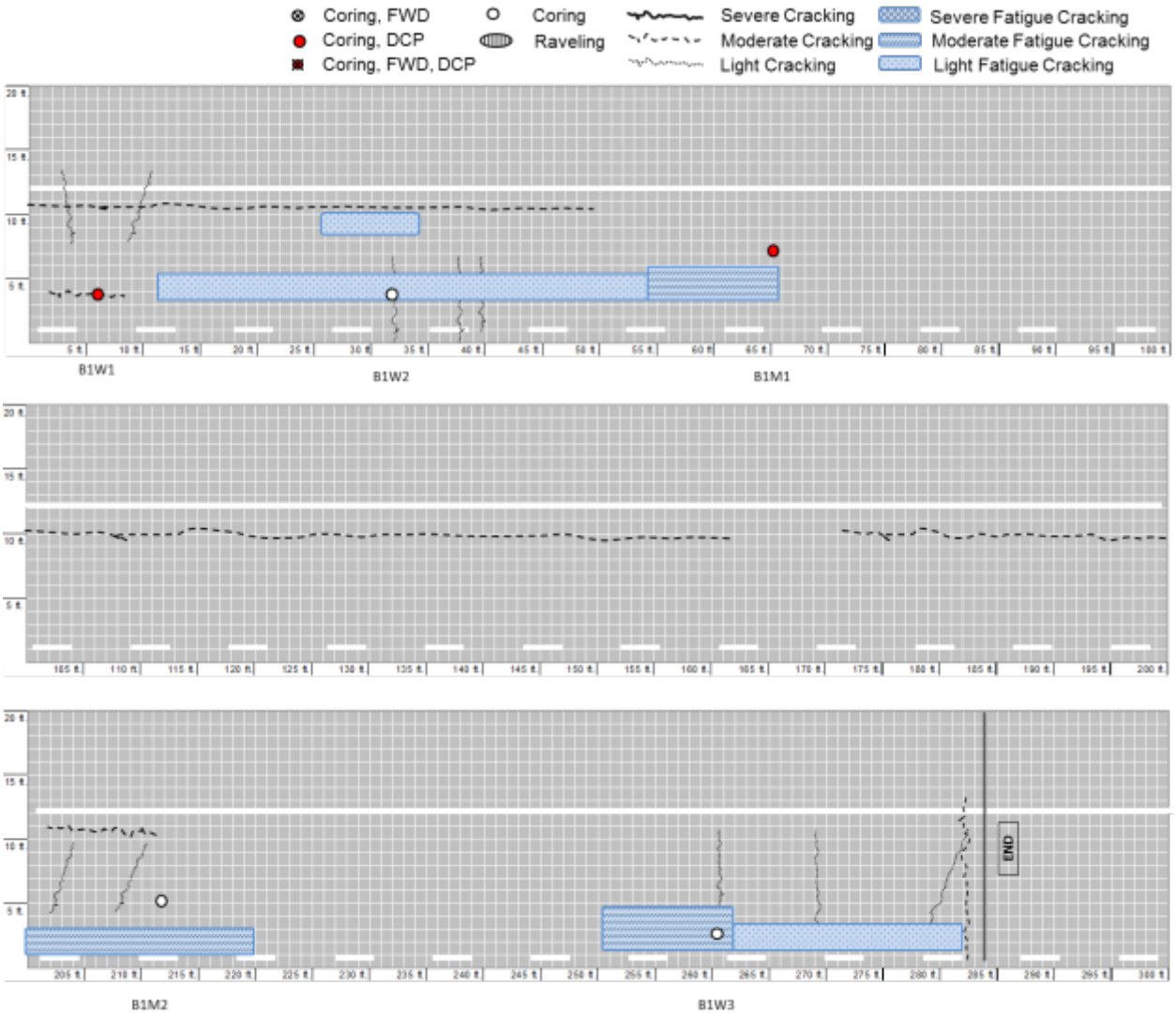

Figure B.63 Crack condition survey mapping of B1 region in NC-177

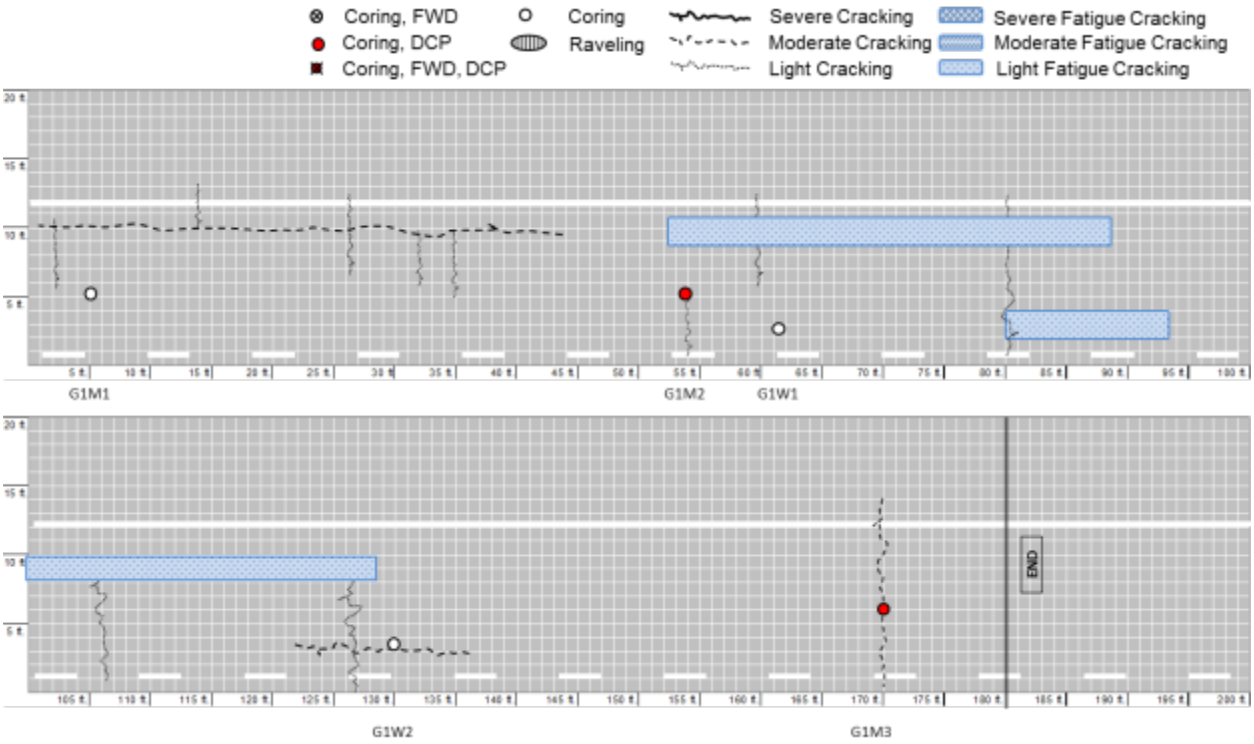

Figure B.64 Crack condition survey mapping of A1 region in NC-177

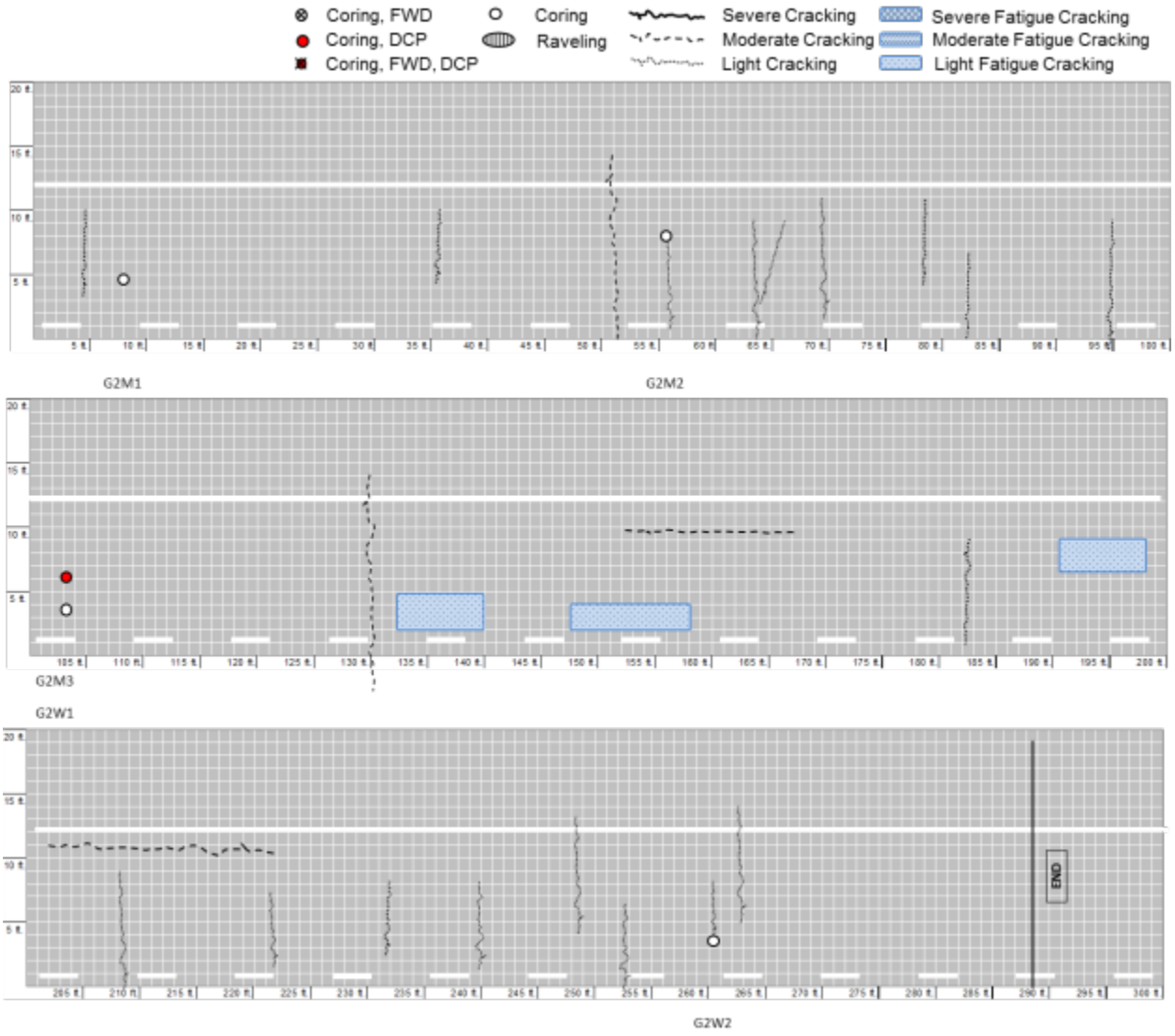

Figure B.65 Crack condition survey mapping of A2 region in NC-177

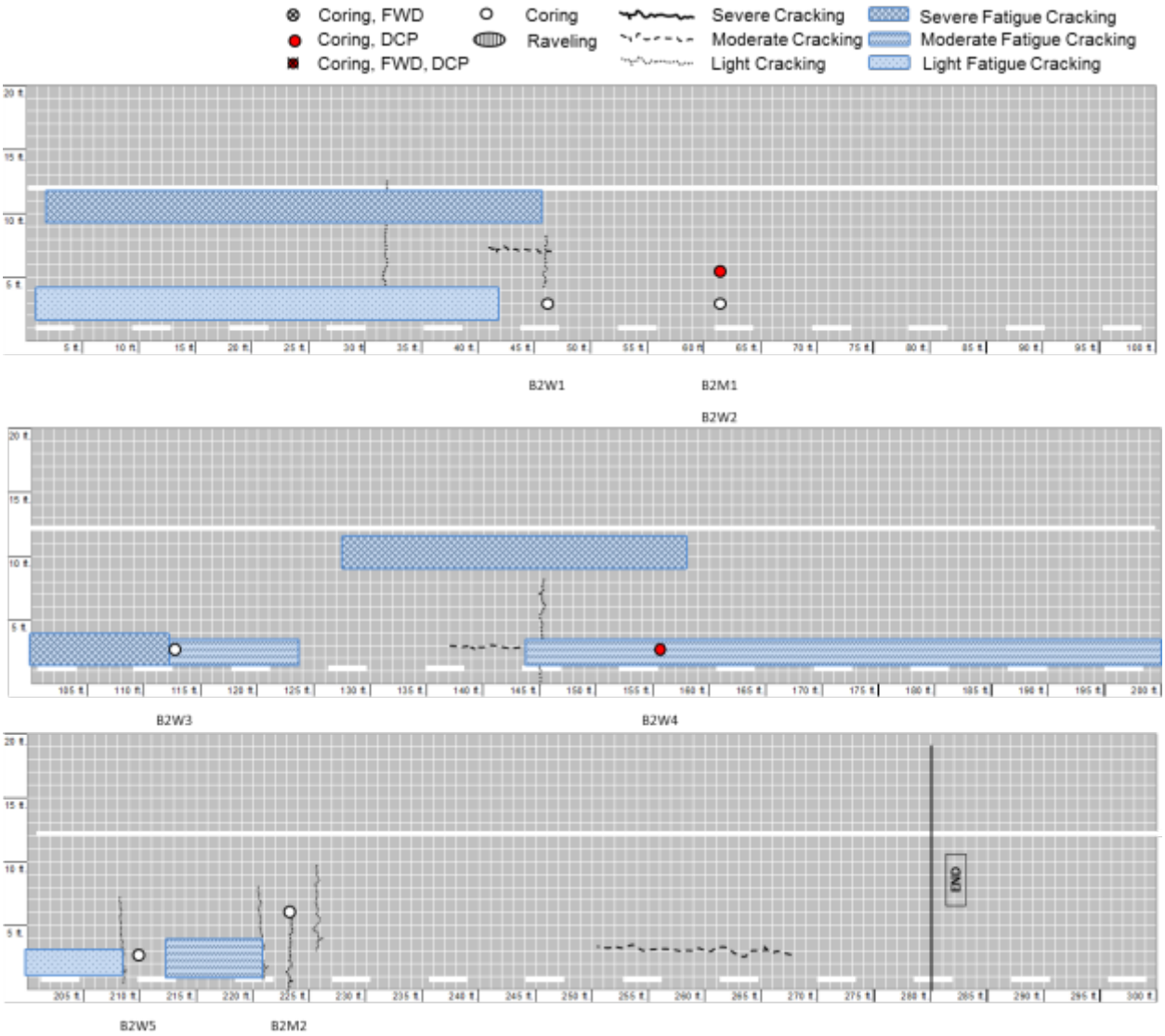

Figure B.66 Crack condition survey mapping of B2 region in NC-177

13. State Route 1530 (Alamance County)

On March 16, 2011, NCDOT personnel and the research team took FWD and DCP measurements and extracted 30 cores from SR 1530 (Burch Bridge Rd) northbound (NB) in Burlington in Alamance County. The section ID of this section in the priority list is PYPM-2. The priority list indicates that this section is Level 2, but Level 1 field work was conducted because an agreement was made between the research team and the steering committee that the first two field sections would be tested at Level 1. According to the PMU database, the thickness of this pavement section was 11.5 in., but the actual average thickness of the section was thicker than 11.5 in.

According to the Division maintenance engineer and PMU personnel, this section was part of a bridge project; therefore, in order to match the new bridge elevation with the existing pavement elevation, the final pavement thickness was actually thicker than the thickness found in the database. Furthermore, this section had to be widened in order to match the width of bridge; therefore, the northbound section contained longitudinal cracks between the centerline of the lane and the outer wheel path. For this reason, cores were taken from the inner wheel path that was not located on the bridge itself (B1 section). At the north end of this pavement section, severe fatigue cracks were observed; therefore, four additional cores were taken for comparison purposes. Nine DCP tests were conducted. FWD testing was conducted at each cored location and at 100 ft intervals of the whole section. Of the 26 cores, 17 cores were obtained in sound condition so that the horizontal coring for lab testing could be completed. Three out of 26 cores have delamination, but two layers were possible for horizontal coring.

Photographs of all of the pavement cores are shown in Figure B.67, and a summary of each is given is Table B.18. B2-IWP1 (1st inner wheel path in 2nd bad region in the section), B2-IWP2 and B2-WP3 (3rd outer wheel path in 2nd bad region in the section) are of primary interest because these cores show vertical cracks connected to cracks on top of the core. These cores exhibit either top-down cracking or a trace of bottom-up cracking that has spread diagonally through the pavement thickness.

Table B.18 Summary of cored field samples for SR 1530 (Burch Bridge Rd) NB, Burlington, Alamance County

ID	Layer Thickness (inch)								Condition	Note
	1st	2nd	3rd	4th	5th	6th	7th	8h		
B1-CL1	1 1/4	1 1/4	1 7/8	2	2<					
B1-CL2	1 1/4	1 1/4	1 7/8	1 5/8	2 1/2<					
B1-CL3	1	2	1 1/4	3/4	1 3/4	2<				
B1-CL4	1 1/8	2 1/4	1 3/4	1	1 3/4	2<			Crack	Looks like 2nd and 3rd layers are constructed during the same period, but tack coat line is visible
B1-WP1	1 1/4	1 1/8	1	1 5/8	2 1/2<				Crack	Cracks on top of core and 2 vertical cracks
B1-WP2	1 1/4	2 7/8	1 1/4	2 1/2<					Delamination	Delamination in 4th layer, and lower layer of 4th layer is broken in pieces
B1-WP3	1 1/4	4 7/8	1 3/4	2 3/4<					Delamination	4th layer broken after coring, so it is not a good example of bottom-up cracking, but vertical cracking begins from the bottom of 3rd layer
B2-CL1	1 1/4	1 7/8	2 5/8	5 1/2						
B2-CL2	1 1/4	1	3 1/4	5 1/4						
B2-CL3	1	1 1/4	3 1/4	5 1/4						
B2-CL4	1	1 1/4	3 1/4	5						
B2-WP1	3/4	1 1/4	3	5					Crack	Inner wheel path, 1 macro crack on top of core but no vertical crack connected to top, smooth bottom
B2-WP2	1	1 1/4	3	4 7/8					Crack	3 macro cracks on top of core and 1 vertical crack connected to the top, high possibility of top-down cracking, smooth bottom
B2-WP3	1	1	2 3/4	5 1/4						Bottom of core is very smooth, direct soil contact (B2-WP1~3)
B2-WP4	1 1/4	1 1/2	2 1/4	5 1/2						
A1-CL1	1 1/4	2	1 1/4	1 3/4	2 1/2	1 3/8	2 1/8	1/2		There is 9th layer and it is thicker than 2 in.
A1-CL2	1 1/4	1	1 1/2	1	1 7/8	3	7/8	1 5/8	Crack	Very smooth surface of bottom of core, horizontal crack near 1st and 2nd layers
A1-CL3	1	1	7/8	2 1/4	1 1/4	5 1/2<				Smooth surface at the bottom of core, looks like soil contacted asphalt directly
A1-CL4	1 1/2	1 1/8	2 1/8	1	6<					Same as for A1-CL4
A1-WP1	1 1/2	1 3/4	1	1 7/8	2 1/2	1	1 3/8	2<	Delamination	Bottom of core (8th layer) is smooth
A1-WP2	2	1 3/8	5/8	2 3/8	3 3/8	2 3/4				Bottom of core (6th layer) is smooth
A2-CL1	1 1/4	1 1/8	1 1/2	2 3/8	2 3/4	3 7/8				
A2-CL2	3/4	1 5/8	3 3/8	2 1/2	2	1 3/4				
A2-CL3	1	2 1/4	2	4 1/2	1 1/4	1 1/4	1			
A2-WP1	1 1/4	2 3/4	3 7/8	5 1/4					Crack	3 macro cracks on top of core but no vertical cracking
A2-WP2	2	3 1/8	2	1 1/2	1/2					
A1	1	6<								6 cracks on top of core but no vertical cracking
A2	7/8	7/8	1/4	1/4	1/2	1 1/2				Looks like BST
A3	1	7							Crack	Hairline cracks on top of core
A4	1	1 1/4	1/2	1/2	1/2	1<				


B1-CL1
B1-CL2
B1-CL3
B1-CL4
B1-WP1
B1-WP2
B1-WP3
B2-CL1
B2-CL2
B2-CL3
B2-CL4
B2-WP1
B2-WP2
B2-WP3
B2-WP4
A1-CL1
A1-CL2
A1-CL3
A1-CL4
A1-WP1
A1-WP2
A2-CL1
A2-CL2
A2-CL3
A2-WP1

Figure B.67 Cored field samples taken from SR 1530 (Burch Bridge Rd) NB, Burlington, Alamance County

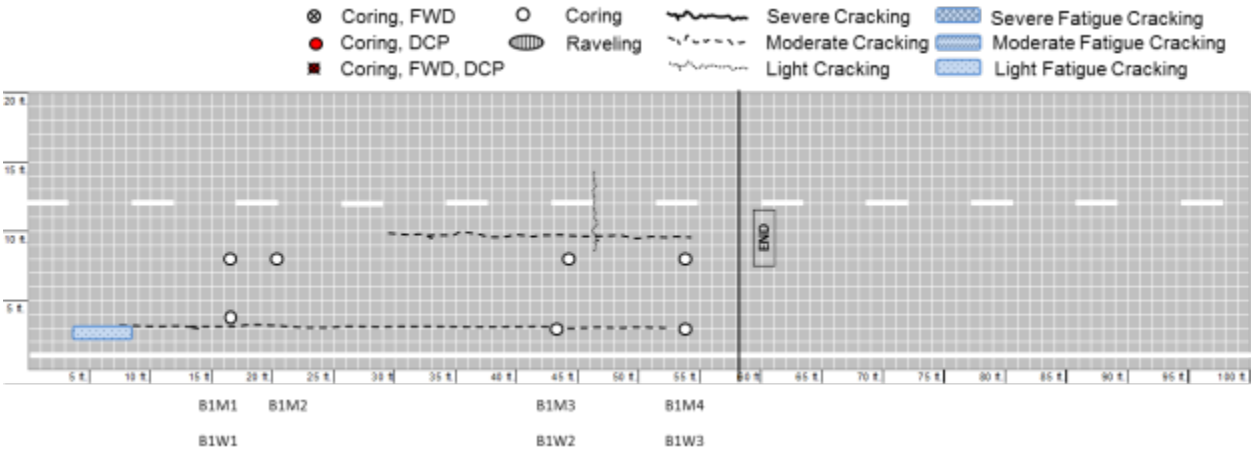

Figure B.68 Crack condition survey mapping of B1 region in SR-1530

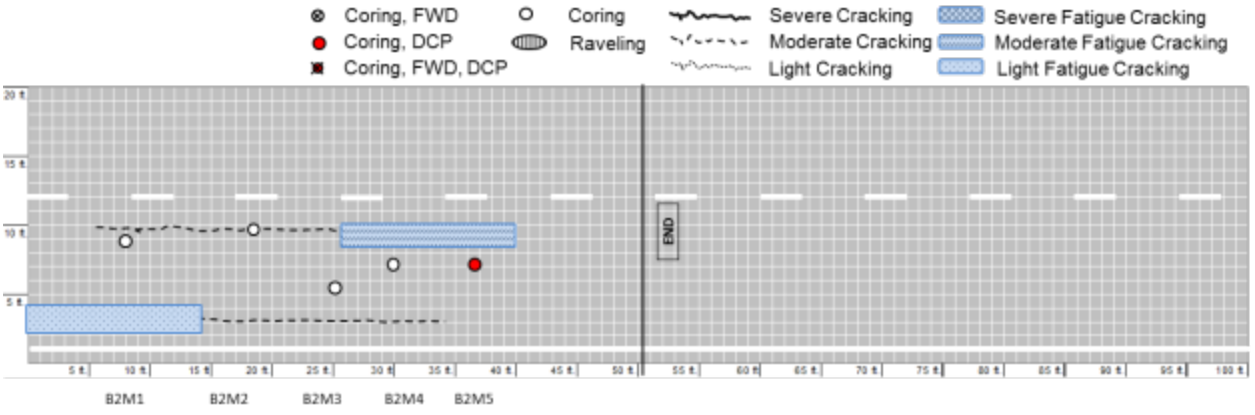

Figure B.69 Crack condition survey mapping of B2 region in SR-1530

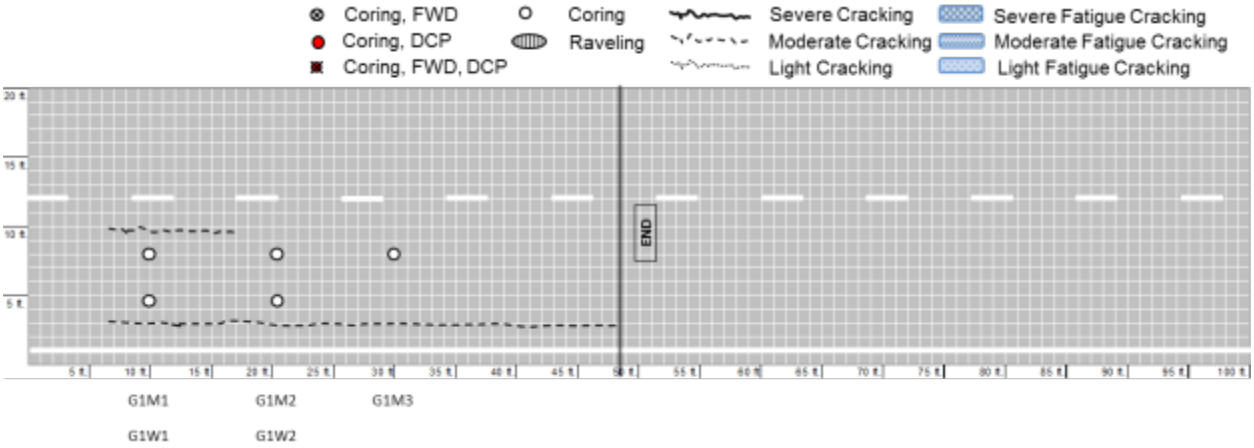

Figure B.70 Crack condition survey mapping of A1 region in SR-1530

14. NC Route 47 (Davidson County)

On August 9, 2011, NCDOT personnel and the research team took FWD and DCP measurements and extracted 20 cores from NC-47 eastbound (EB) near Lexington in Davidson County. According to the NCDOT construction history and profile database, the section was resurfaced in 2002 using S9.5B mix. The field test level of this section is Level 1, and this section is in the group of *Young and Poor* condition roadways. Of the 20 cores extracted from the field, 6 cores were obtained in sound condition so that horizontal coring for lab testing could be completed.

Although the entire section length was from the same construction period, and the condition survey was compiled for 1.3 miles, only 0.23 mile (1200 feet) was selected for investigation because the section is part of a rural highway with 1 lane per direction with numerous curves and a relatively high volume of traffic. As shown in Figure B.71, the entire section exhibits severe fatigue cracking; therefore, the section was divided into 2 ‘bad’ regions and 1 ‘good’ region. Summaries of all the pavement core data are given in Table B.19 and

Table B.20, and photographs of the cores are shown in Figure B.72. As shown in the summary tables and photographs, because the number of sound condition cores is less than for the other sections, it is highly possible that the cores contain some minor cracking. Therefore, special care must be taken for horizontal coring and lab testing.

Figure B.71 Photographs of cracking patterns on NC-47, Lexington, Davidson County

Table B.19 Summary of core data for NC-47, Lexington, Davidson County

ID	Layer thickness (inch)									Condition
	1st	2nd	3rd	4th	5th	6th	7th	8th	9th	
B1-CL1	1 3/4	1 3/8	3/4	3/8	5/8	1/2	3/4			Delamination/Intact
B1-CL2	2	1/8	?							Broken
B1-WP1	1 3/4	1 3/8	1	1/4	3/8	5/8	3/4			Cracked
B1-WP2	1 7/8	1 3/4	1 1/8	3/8	3/8	3/8	1/2			Broken
B1-WP3	2	1 7/8	?	?						Broken/Delamination
B1-WP4	1 3/4	1 1/2	3/8	1	1					Broken
A1-CL1	1 7/8	1 1/8	7/8	1/2	5/8	1/4	3/4			Intact
A1-CL2	1 1/2	1 1/8	5/8	5/8	1/2	1/4	3/4			Intact
A1-CL3	1 7/8	1 1/4	1 1/8	1/4	1/4	3/8	7/8			Delamination/Intact
A1-WP1	2	1 7/8	1 1/4	5/8	1					Delamination/Cracked
A1-WP2	2 1/2	1 1/8	3/4							Cracked
A1-WP3	2 1/4	2	1 1/4	1						Cracked
A1-WP4	2 1/8	1 1/8	3/4	1 1/4	1/2	1/4	1/2			Cracked
B2-CL1	1 5/8	1 3/4	1 1/8	1/4	3/8	1/2	1/4	1		Delamination/Cracked
B2-CL2	1 3/4	1 5/8	1	1/2	5/8	1/2	1/4	7/8		Delamination/Intact
B2-CL3	1 3/4	2 1/4	1 3/4	1/4	3/4	3/8	3/8	1/4	1	Cracked
B2-WP1	1/2	?								Broken
B2-WP2	2									Broken
B2-WP3	1 3/4	1 1/2	1/4	3/4	1/2	1 1/8	2			Delamination/Cracked
B2-WP4	2	1 7/8	7/8	1 1/4						Intact

Table B.20 Additional summary of core data for NC-47, Lexington, Davidson County

ID	Note
B1-CL1	Delamination between 1st & 2nd layers and 2nd & 3rd layers
B1-CL2	1 vertical crack connected to cracks on top surface, broken into 2 major pieces from 2nd layer to the bottom of core, marking paint at bottom of 2nd layer, thickness of broken layer could not be measured
B1-WP1	Vertical crack from bottom to horizontal crack in middle of 3rd layer, no cracks on top surface
B1-WP2	2 vertical cracks in 1st layer connected to cracks on top surface, totally broken from horizontal crack in middle of 2nd layer to bottom of core
B1-WP3	Totally broken into 2 major pieces from horizontal crack at bottom of 1st layer to bottom of core, vertical macrocracks in bottom of core filled with soil, delamination between 1st & 2nd, 2nd & 3rd, and 3rd & 4th layers, thickness of broken layer could not be measured
B1-WP4	1 macrocrack on top surface connected to 2 vertical cracks in 1st layer, broken into 2 major pieces from horizontal crack at bottom of 2nd layer to bottom of core, marking paint between 2nd & 3rd layers
A1-CL1	Sound condition
A1-CL2	Overall sound condition but looks like beginning phase of delamination between 2nd & 3rd layers
A1-CL3	Not smooth delamination between 2nd & 3rd layers
A1-WP1	1 vertical crack connected to cracks on top surface, partial delamination and horizontal crack at bottom of 2nd layer, looks like 2nd and 3rd layers constructed in same period due to visually same mixture, marking paint between 3rd & 4th layers, soil-filled wide cracks from bottom of core to middle of 3rd layer
A1-WP2	2 Soil-filled wide cracks from 2nd layer to bottom of core, no cracks on top surface
A1-WP3	Vertical crack in middle of 2nd layer, horizontal crack in middle of 3rd layer, marking paint between 2nd & 3rd layers
A1-WP4	2 vertical cracks on top surface connected to cracks on top surface, horizontal crack near bottom of 1st layer, vertical cracks begin from horizontal crack and end at soil-filled wide crack at bottom of core
B2-CL1	1st layer broken into 2 pieces, not smooth delamination between 1st & 2nd layers and 2nd & 3rd layers, vertical cracks from bottom of core to delamination surface of 3rd layer
B2-CL2	Delamination in middle of 3rd layer
B2-CL3	Vertical cracks from middle of 2nd layer to bottom, soil-filled wide cracks from bottom of core to 6th layer
B2-WP1	Totally broken except for 1st layer, marking paint between 2nd & 3rd layers, thickness of broken layer could not be measured
B2-WP2	Totally broken, thickness of broken layer could not be measured
B2-WP3	Delamination between 1st & 2nd layers, vertical crack from middle of 3rd layer to bottom of core, marking paint between 4th & 6th layers
B2-WP4	Macrocrack on top surface but no vertical crack, vertical roadway expansion trace from 2nd layer to bottom (exceptional case)

Figure B.72 Cores taken from NC-47, Lexington, Davidson County

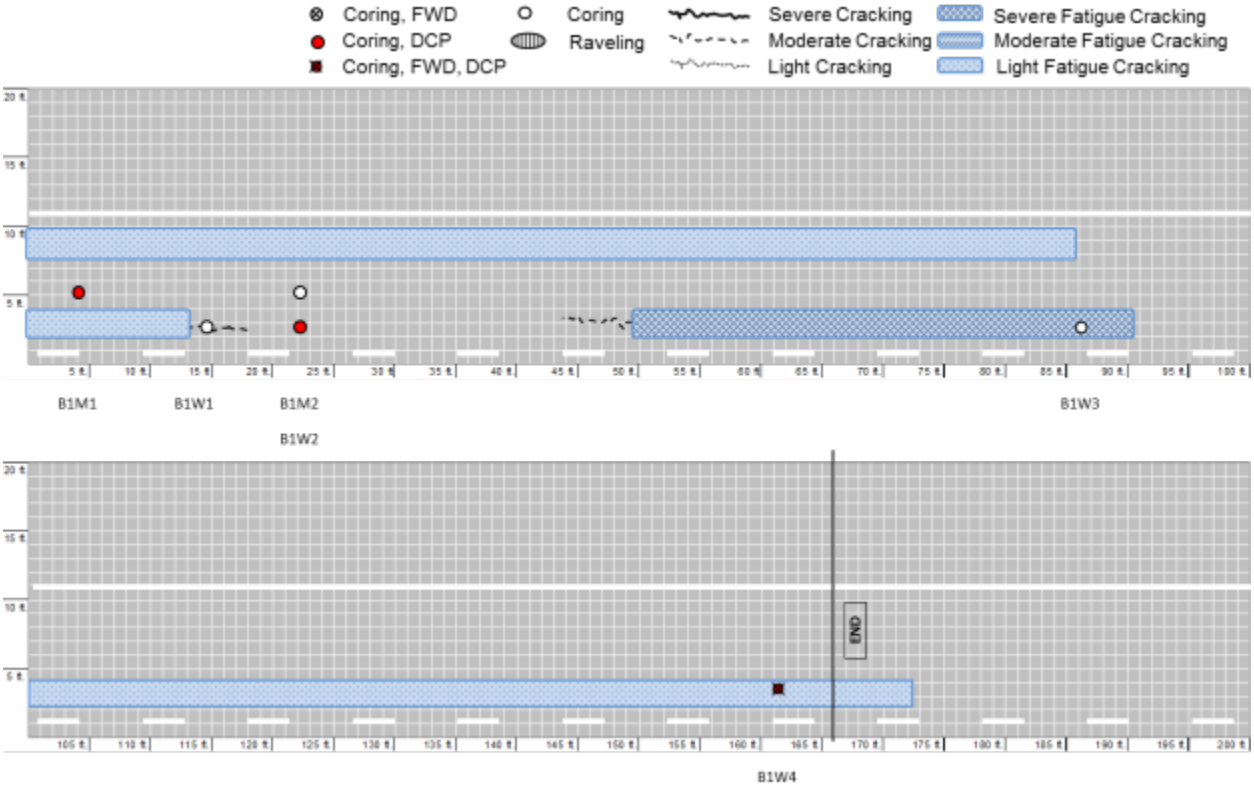

Figure B.73 Crack condition survey mapping of B1 region in NC-47

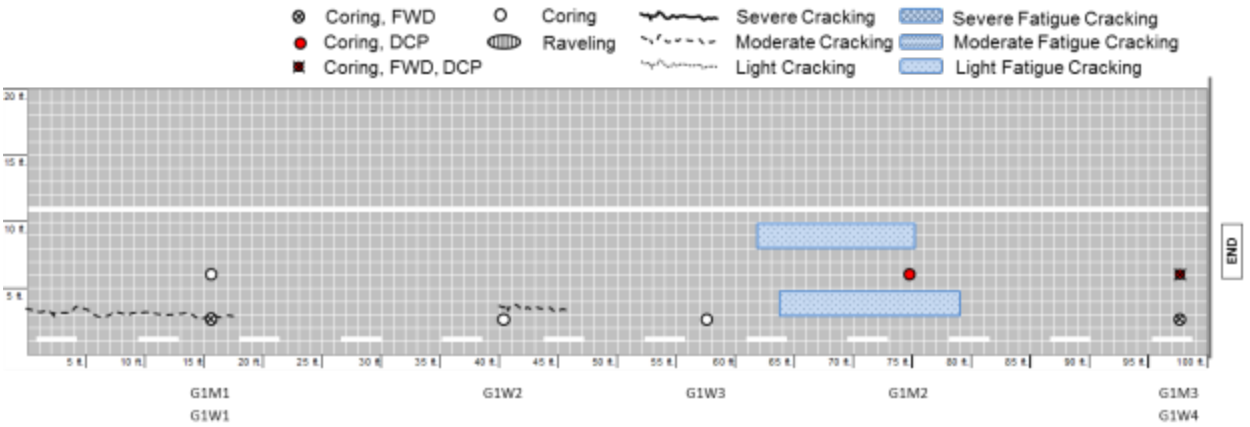

Figure B.74 Crack condition survey mapping of A1 region in NC-47

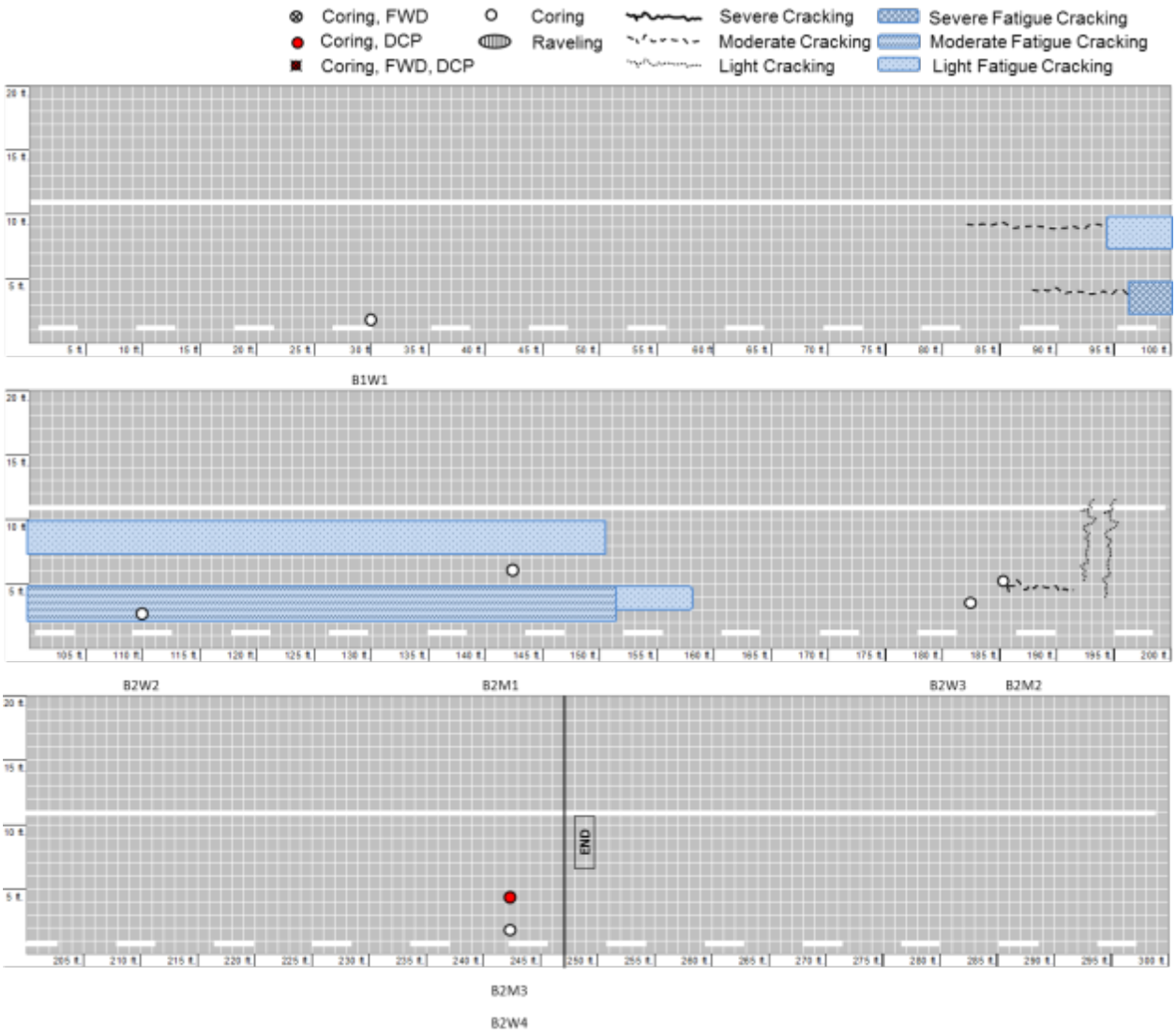

Figure B.75 Crack condition survey mapping of B2 region in NC-47

15. US Route 220 (Montgomery County)

On July 13, 2011, NCDOT personnel and the research team took FWD measurements and extracted 9 cores from US-220 Alternate (Martin St.) northbound (NB) in Star, Montgomery County. This section is categorized as a *Young and Poor* condition roadway. This section was scheduled for resurfacing in late July, 2011. Eight cores were taken from the middle of the wheel path, and all of the cores were in sound condition so that lab testing could be completed.

The NCDOT's construction history and profile database showed debug errors after changing contractors, and because this section was scheduled for resurfacing in late July 2011, the research team selected and scheduled this section for Level 1 investigation. As shown in Figure B.76, most of the macrocracks in the section were sealed, but some were not sealed. It is not clear when the Montgomery County maintenance engineers conducted the crack sealing, nor whether the cracks that were not sealed appeared after sealing or whether the contractor simply missed some of the cracks. The cracking pattern shows transversal cracking at regular intervals and shows also that most of the longitudinal cracking is located in the outer wheel path. Because this cracking pattern is similar to reflective cracking caused by joint concrete pavement (JCP), the NCDOT personnel and the research team decided to core the outer wheel path for verification. The photographs in Figure B.77 show the coring location and extracted core. The location of the longitudinal crack on top of the sample core was exactly the same as that at the edge of the concrete pavement layer. Therefore, the research team decided to change the test level of the section from Level 1 to Level 2. After repairing the debug error in the database, it was found that the section has a JCP layer constructed in 1941.

Figure B.76 Photographs of cracking pattern on US-220 Alt. NB, Star, Montgomery County

Figure B.77 Photographs of Sample Core Taken for the Verification of Roadway Expansion

According to the construction history and profile database, the section was resurfaced 4 times on top of the JCP layer in 2004, 1991, 1980, and 1972. In 1972, the section was rehabilitated with 4-inch asphalt base course and 1-inch surface course. In the other three times, the surface course was used to resurface the existing pavement. Photographs in Figure B.77 indicate that the section was expanded during the rehabilitation in 1972.The thicknesses of each layer shown in the database are similar to those of the field cores; however, the thickness of the 1st layer of all the field cores is thicker than that indicated in the database (1 inch). Most of the 3rd layers of the field-extracted cores are thinner than those in the database. These differences may be caused by the partial milling for the construction of the 2nd layer. According to the database, a 4-inch thick bituminous concrete base course (BCBC), which is the 5th layer from the top layer, was constructed on top of the JCP layer in 1972. Although it is not clear how and why the NCDOT used sand mix for the BCBC, all of the field cores have a sand mix layer for the 5th layer. A summary of all the pavement core data is given in Table B.21, and photographs of the cores are shown in Figure B.78.

Table B.21 Summary of core data for US-220 Alt. NB, Star, Montgomery County

ID	Layer Thickness (inch)					Condition	Note
	1st	2nd	3rd	4th	sand mix layer		
B-CL1	1 3/4	7/8	5/8	1	7/8	Intact	Sound condition, no crack
B-CL2	1 7/8	1	3/8	1 1/4	7/8	Delamination/ Intact	Delamination between 1st and 2nd layers, no crack
B-CL3	1 7/8	1	1/4	1	1 5/8	Intact	Sound condition, no crack
B-CL4	1 3/4	7/8	5/8	1	1 1/4	Intact	Sound condition, no crack
A-CL1	1 3/4	7/8	7/8	1	1/2	Intact	Sound condition, no crack
A-CL2	1 5/6	7/8	1 1/2	1 1/2	1	Intact	Sound condition, no crack
A-CL3	1 5/8	7/8	3/4	1	1 1/8	Intact	Sound condition, no crack
A-CL4	1 3/4	3/4	7/8	7/8	3/8	Intact	Sound condition, no crack

Figure B.78 Cores taken from US-220 Alt. NB, Star, Montgomery County

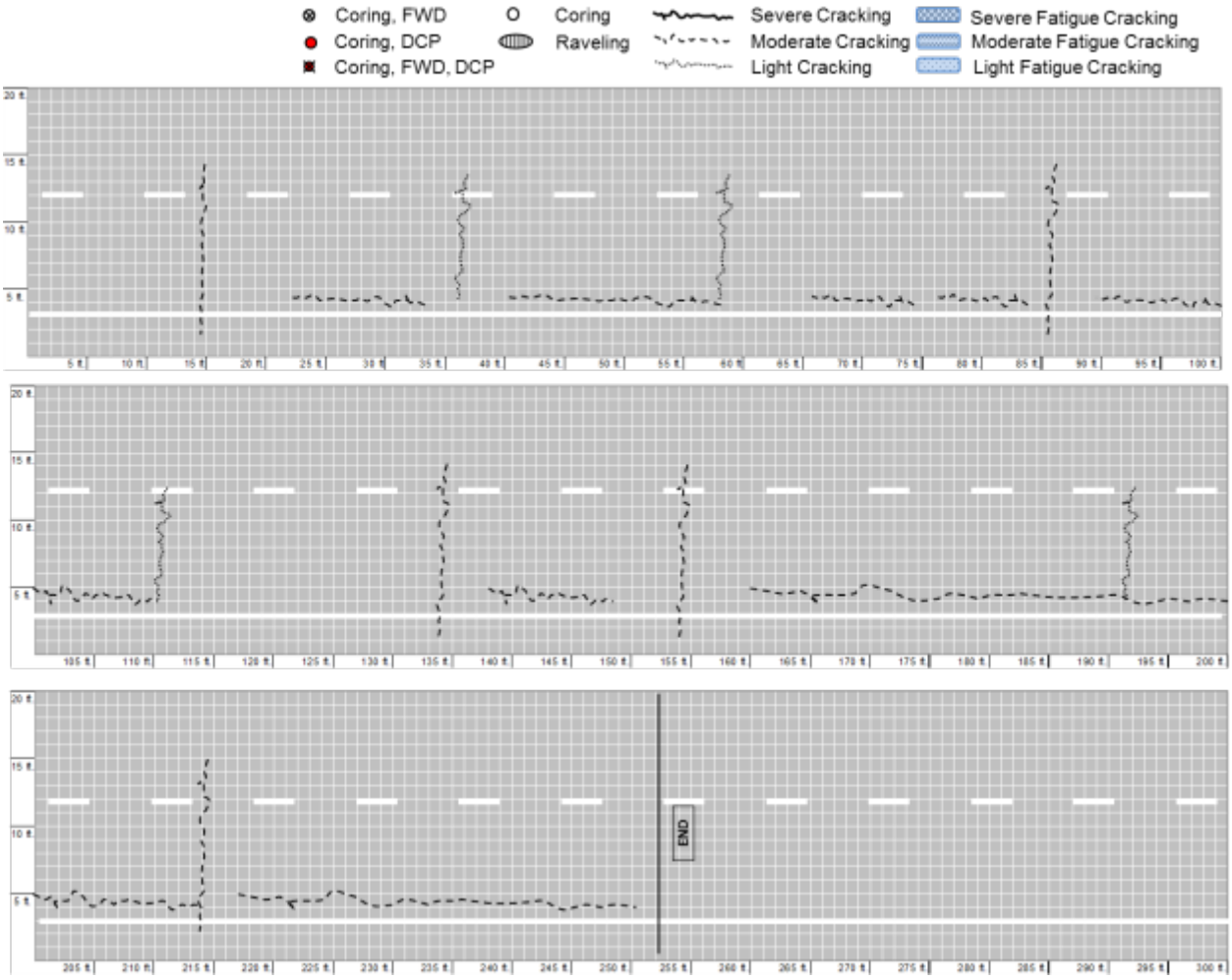

Figure B.79 Crack condition survey mapping of B1 region in US-220

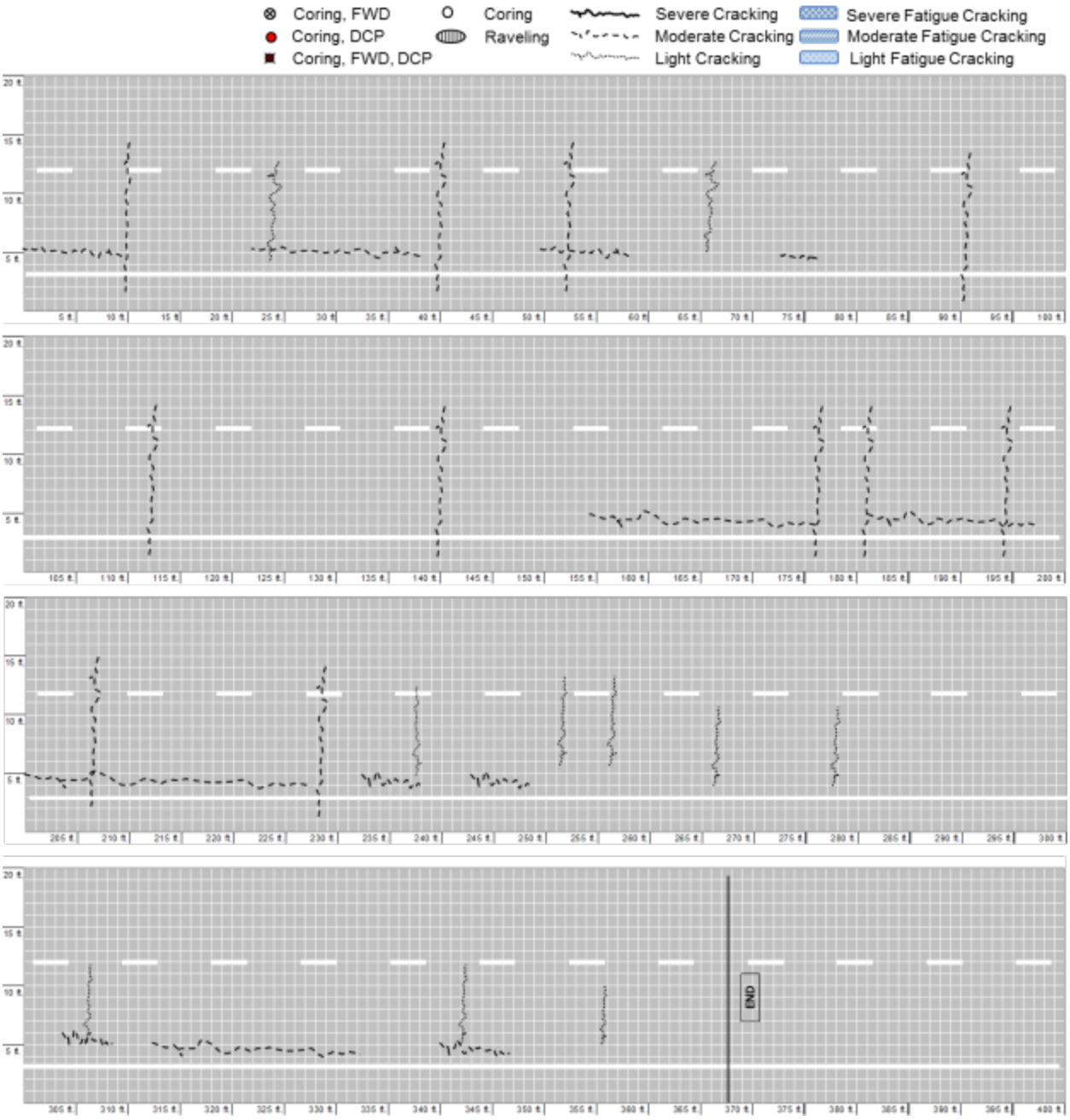

Figure B.80 Crack condition survey mapping of A1 region in US-220

16. NC Route 55 (Harnett County)

On June 19, 2012, NCDOT personnel and the research team took dynamic cone penetrometer (DCP) measurements and extracted ten cores from NC 55 northbound in Angier in Harnett County. According to the NCDOT construction history and profile database, the latest (2001) resurfacing work used I-1 (Marshall Mix I-Type surface course) material with an overlay thickness recorded as $1^{1}/_{2}$ inches. Prior to this most recent resurfacing effort, treatment methods included: 1 inch of I-2 material in 1984, 1 inch of a bituminous concrete surface course (BCSC) in 1973, 2 inches of a BCSC in 1955, and a half inch of bituminous surface treatment (BST) in 1929. This site does not have a paved shoulder. The field test level for this site is Level 2, and the condition of this site falls in the category of *Young and Poor* roadways.

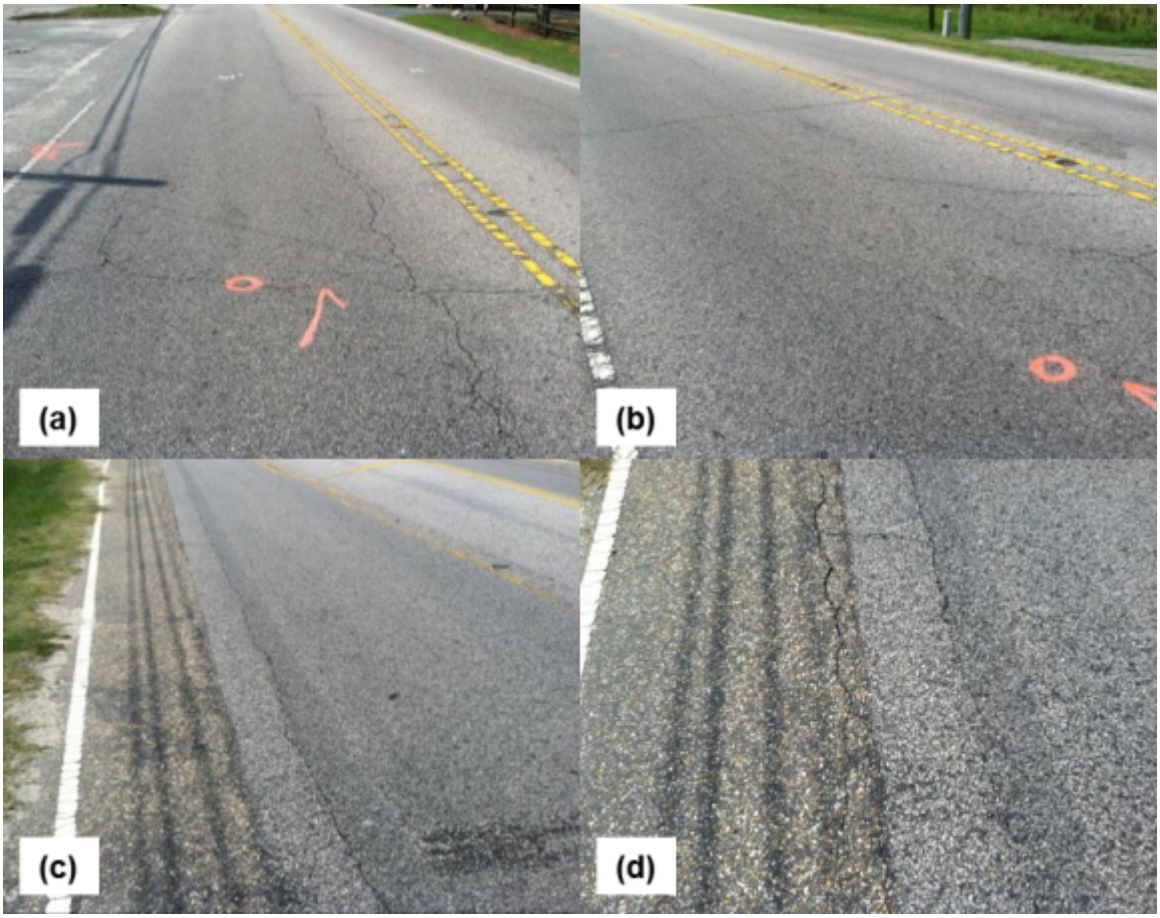

Figure B.81(a) and (b) show major longitudinal cracking in the inner wheel-path area for both of the two different condition regions (*bad and good*). The southbound lane (opposite direction

lane) also has major longitudinal cracking in the inner wheel-path area. The photographs shown in

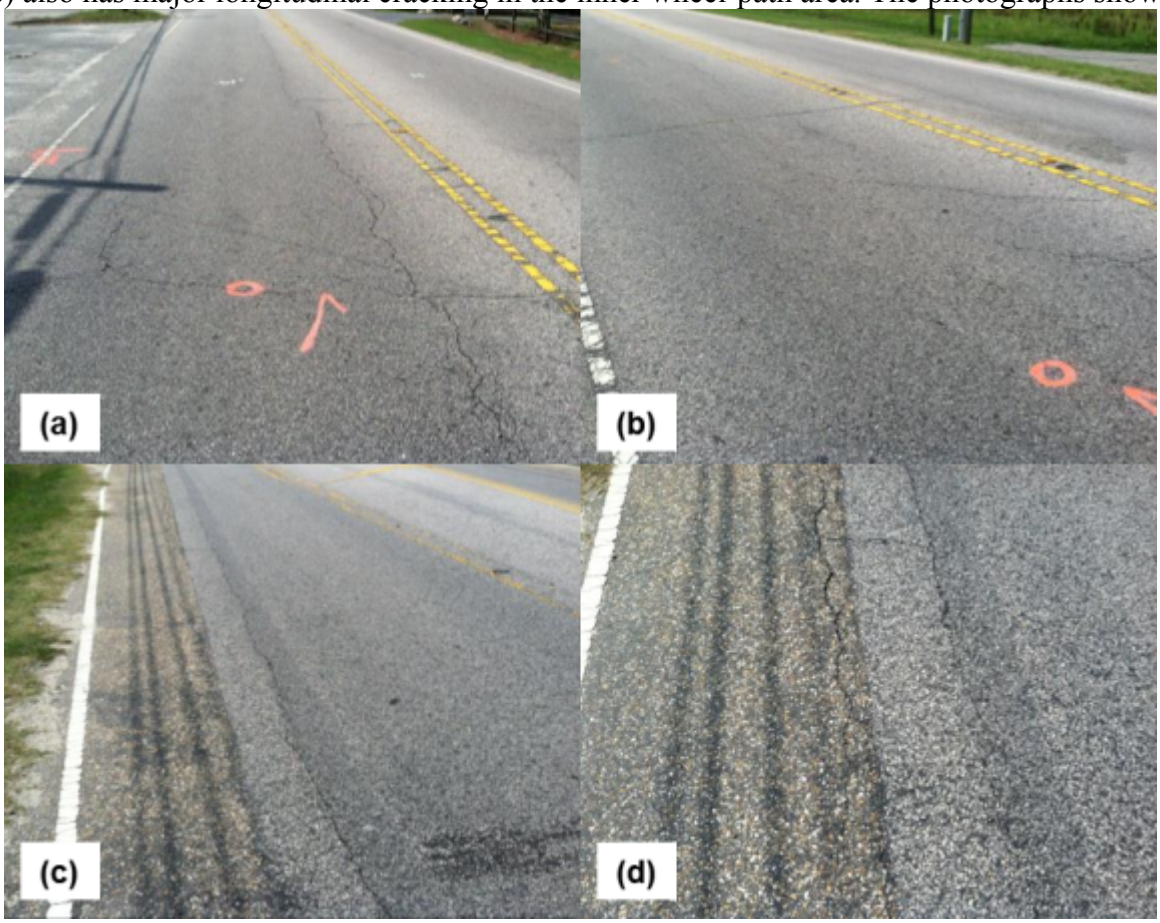

Figure B.81(c) and (d) were taken where the good condition region begins. In the good condition region, longitudinal cracking can be observed in both the inner and outer wheel-path areas, but no outer longitudinal cracking is observed in the bad condition region. Usually, longitudinal cracking is observed more in the outer wheel-path area; but, this site is not representative of a commonly observed case.

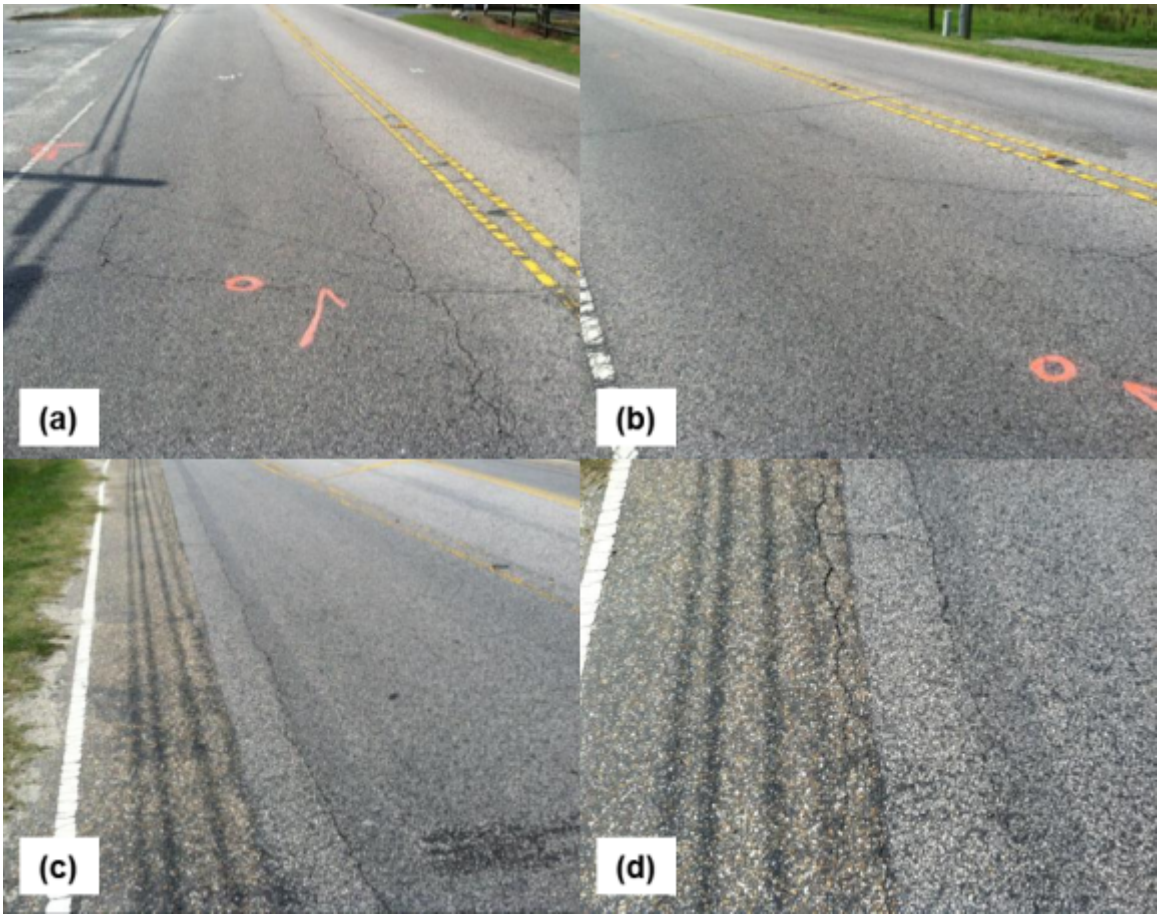

Figure B.81 Photographs of representative cracking patterns on NC-55, Angier, Harnett County: (a) *bad* condition location, (b) *good* condition location, (c) at the beginning of the *good* condition region, and (d) magnified view of photograph of (c)

Photographs of all of the pavement cores are shown in Figure B.82, and a summary of each is given in Table B.22. Because this site is one of the sites in the Level 2 investigation, all of the cores were taken from the middle of the lane, i.e., between the wheel-paths. A sand mix layer was observed in the middle of each core, and two different mixtures were observed both above and below the sand mix layer.

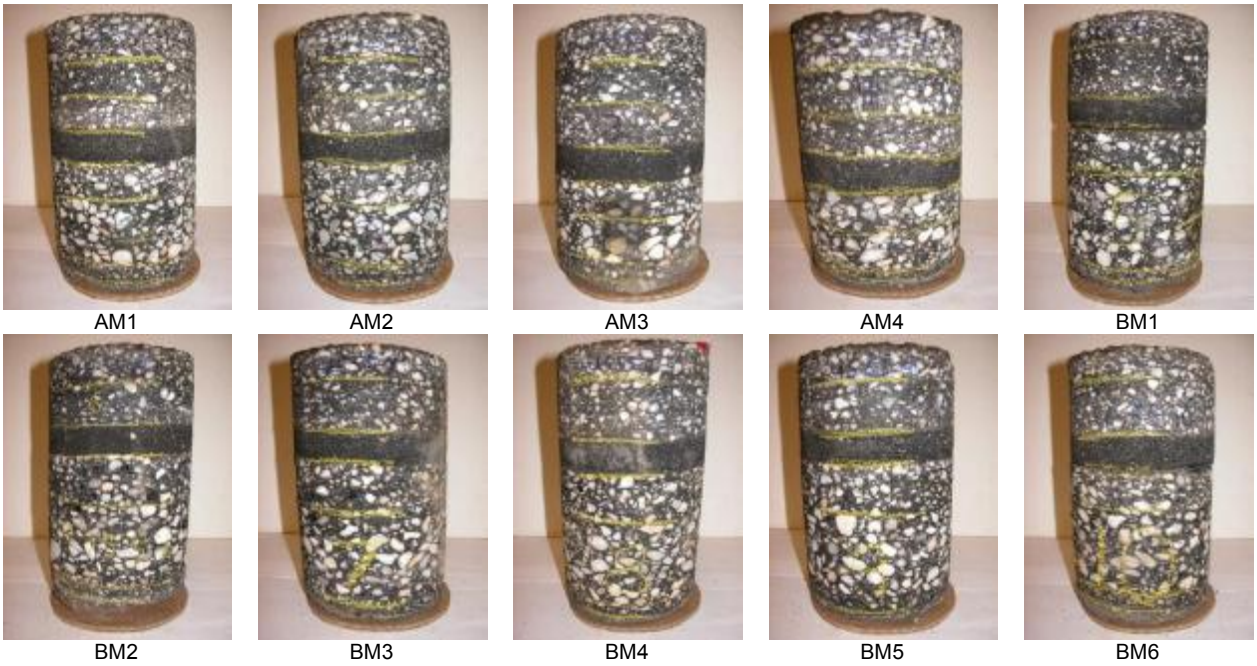

Figure B.82 Photographs of cores taken from NC-55, Angier, Harnett County

Table B.22 Summary of core data for NC-55, Angier, Harnett County

ID	Layer Thickness (inch)						Condition
	1st	2nd	3rd	4th	5th	6th	
AM1	1 4/8	2 1/8	1	1 1/8	2 2/8	5/8	Sound
AM2	1 2/8	2 1/8	7/8	1 2/8	1 7/8	5/8	Sound
AM3	1 3/8	2 4/8	1 1/8	1 1/8	1 3/8	6/8	Sound
AM4	1 4/8	2 2/8	1	1 1/8	1 3/8	4/8	Sound
BM1	1 1/8	1 5/8	1	1 4/8	3 2/8	5/8	Debonding between 3rd and 4th layers; vertical crack from 1st through 3rd layers
BM2	1 2/8	1 2/8	1	1 4/8	2 6/8	4/8	Sound
BM3	1	1 3/8	1	1 4/8	3 1/8	3/8	Sound
BM4	1 2/8	1 6/8	1	1 5/8	3 1/8	4/8	Sound
BM5	1	1 3/8	7/8	1 5/8	2 7/8	3/8	Sound
BM6	1 1/8	1 5/8	1	1 1/8	3	5/8	Debonding between 3rd and 4th layers

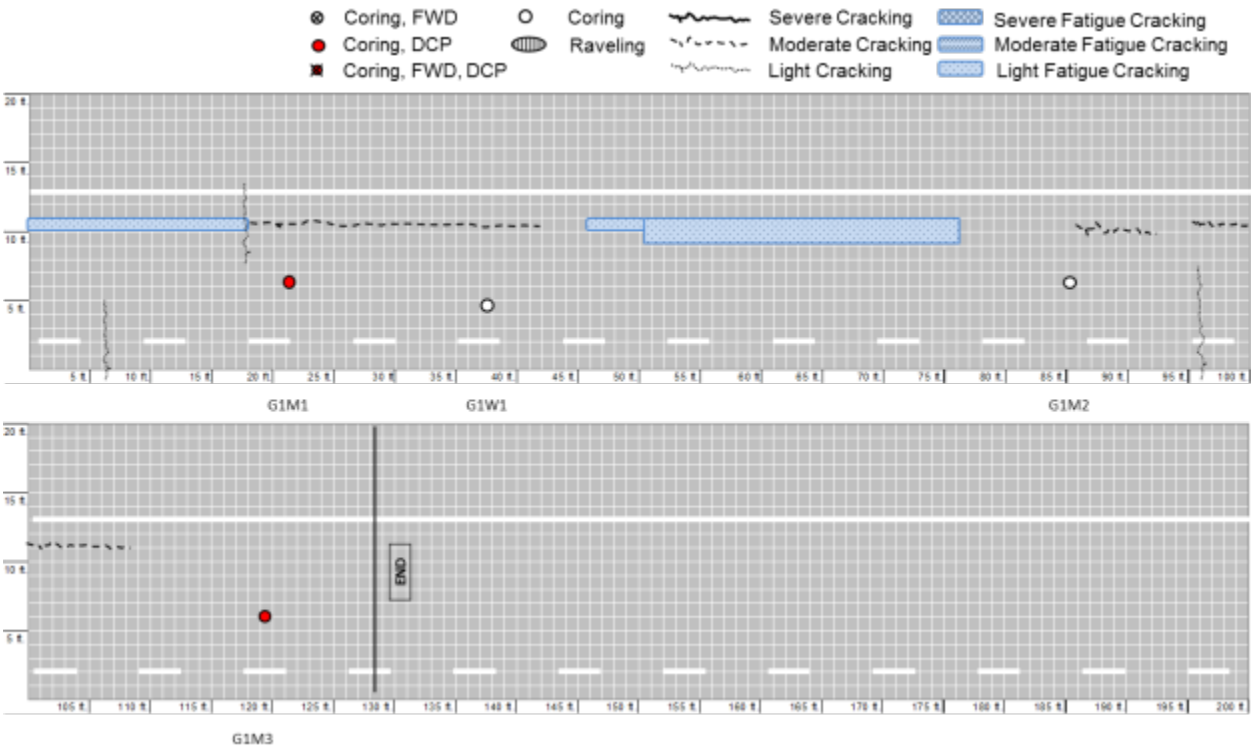

Figure B.83 Crack condition survey mapping of A1 region in NC-55

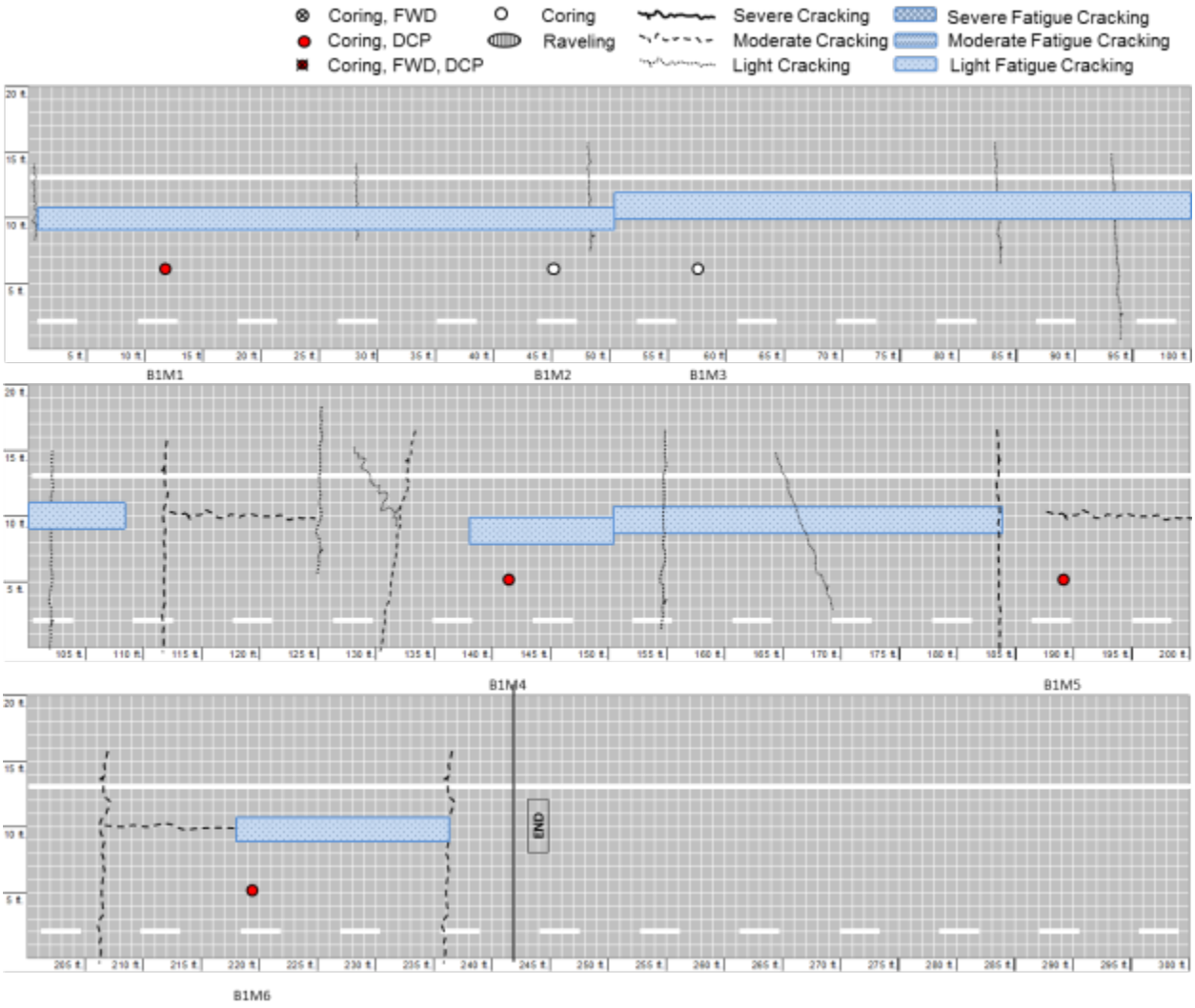

Figure B.84 Crack condition survey mapping of B1 region in NC-55

17. NC Route 179 (Brunswick County)

On July 17, 2012, NCDOT personnel and the research team took DCP measurements and extracted fourteen cores from NC 179 northbound in Ocean Isle Beach in Brunswick County. According to the NCDOT construction history and profile database, this site was reconstructed in 2009 with 1½ inches of S9.5B mixture, 2½ inches of I19.0B mixture, and 4½ inches of B25.0B mixture. Prior to this most recent reconstruction effort, treatment methods included: 1½ inches of I-2 material in 1995, ¾ inch of a BST and 1½ inches of I-2 material in 1995. This site does not have a paved shoulder. The field test level for this site is Level 2, and the condition of this site falls in the category of *Young and Poor* roadways.

According to the Division engineer's comments, partial patching was done at the site in 2011. Figure 5 shows this partial patching condition. Because patching was done at the site, cores were taken from an unpatched area with and without surface cracks. Most of the patching is located on the outer wheel-path and between the wheel-path areas. The BA core taken from the outside of the lane has a different pavement layer structure from the other cores that were taken from the middle or inner wheel-path area. Therefore, it is expected that reflective cracking caused by road widening has resulted in the longitudinal cracking seen in the outer wheel-path area. This recurrence of longitudinal cracking in the outer wheel-path may have required resurfacing with patching after reconstruction in 2009; or it may reflect that the NCDOT database contains the 2009 construction record only for the road widening effort and not the patching effort.

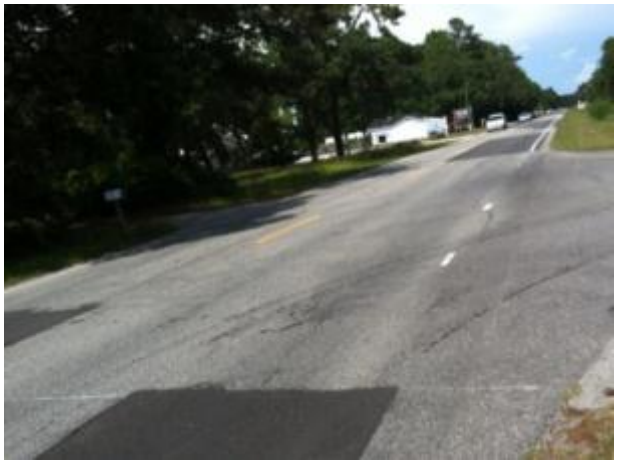

Figure B.85 Photographs of NC 179, Ocean Isle Beach, Brunswick County

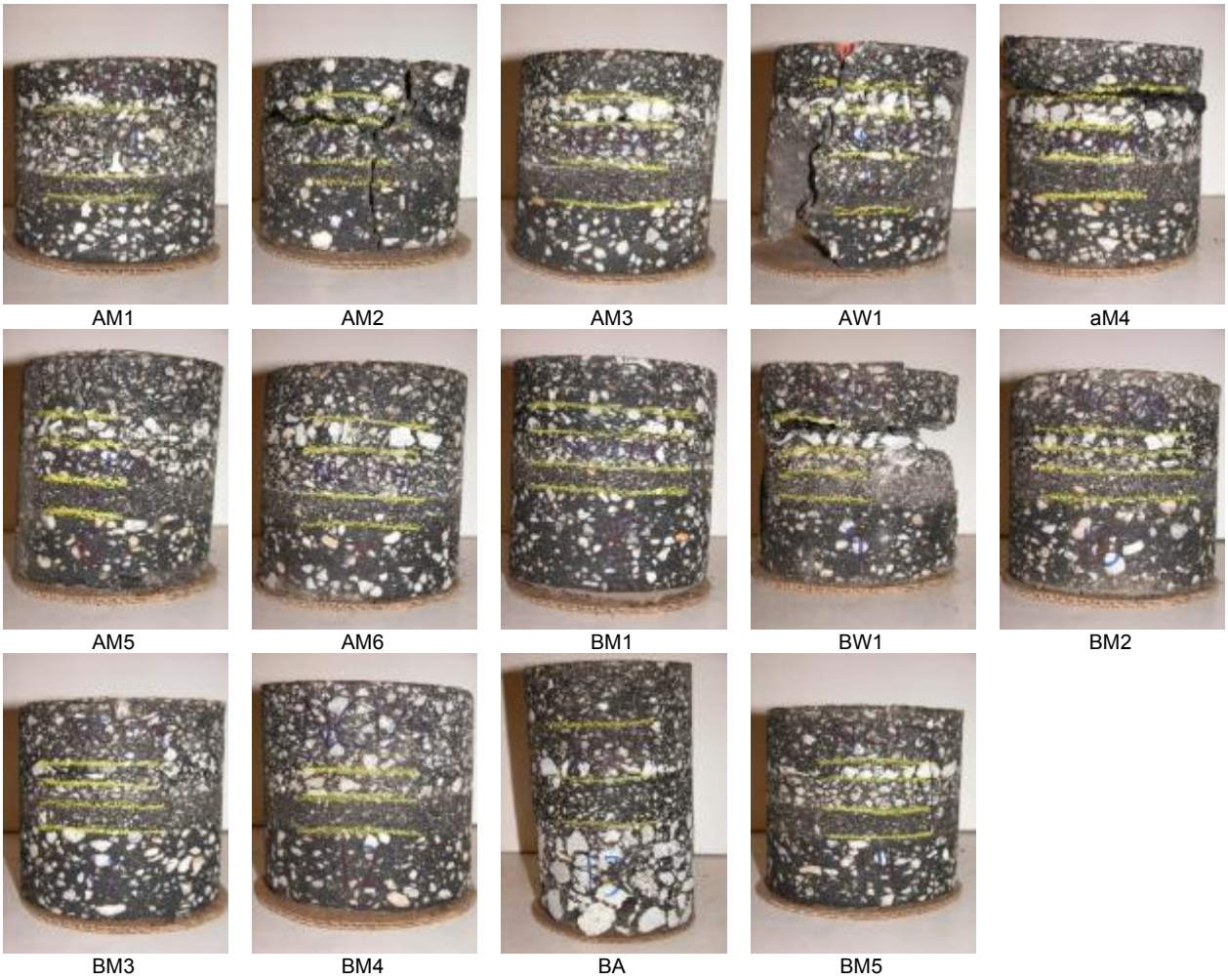

Figure B.86 Photographs of cores taken from NC 179, Ocean Isle Beach, Brunswick County

Table B.23 Summary of core data for NC 179, Ocean Isle Beach, Brunswick County

ID	Layer Thickness (inch)				Condition
	1st	2nd	3rd	4th	
GM1	1 1/8	1 5/8	3/8	1 4/8	Sound
GM2	7/8	4/8	3/8	1 5/8	Full-depth vertical cracking; debonding between 2nd and 3rd layers
GM3	1 1/8	5/8	6/8	1 6/8	Sound
GW1	1 1/8	5/8	1 2/8	1 4/8	Full-depth vertical cracking
GM4	1 1/8	6/8	7/8	1 6/8	Debonding between 1st and 2nd layers
GM5	1 4/8	4/8	6/8	1 6/8	Cracks of surface connected to vertical crack through 2nd layer
GM6	1 2/8	5/8	5/8	1 6/8	Sound
BM1	1 1/8	4/8	4/8	2 3/8	Sound
BW1	1 2/8	5/8	5/8	2	Full-depth vertical cracking; debonding between 2nd and 3rd layers
BM2	1 3/8	4/8	5/8	2 1/8	Sound
BM3	1 3/8	5/8	5/8	2 1/8	Sound
BM4	2	6/8	1 6/8		Sound
BA	1 7/8	1 4/8	3 6/8		Sound; extracted from shoulder
BM5	1 2/8	6/8	5/8	1 6/8	Sound

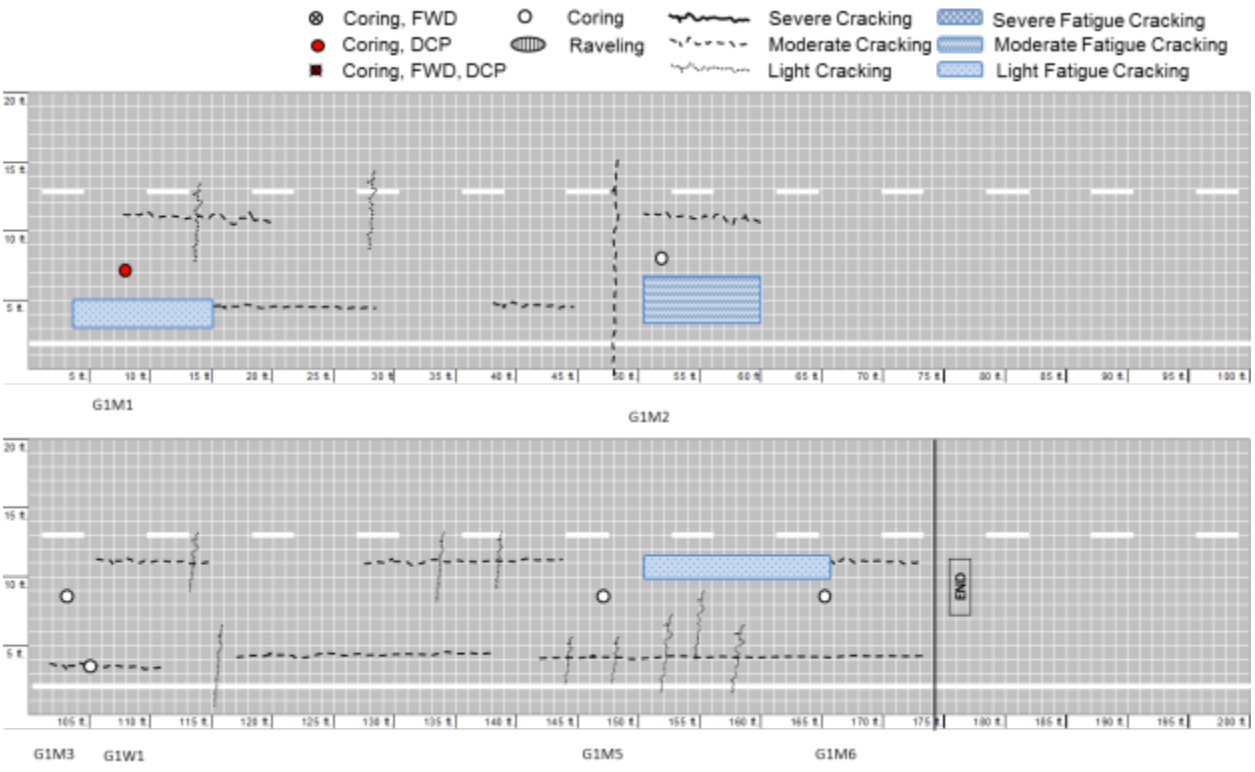

Figure B.87 Crack condition survey mapping of G1 region in NC-179

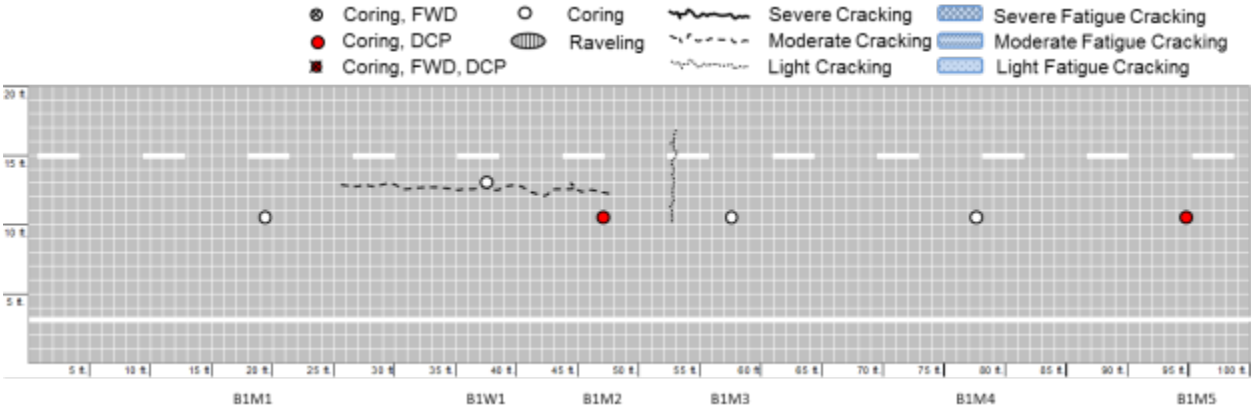

Figure B.88 Crack condition survey mapping of B1 region in NC-179

18. US Route 401 (Cumberland County)

On May 22, 2012, NCDOT personnel and the research team took dynamic cone penetrometer (DCP) measurements and extracted eight cores from US 401 southbound in Linden in Cumberland County. According to the NCDOT construction history and profile database, the latest (2002) resurfacing work used S9.5C material with an overlay thickness recorded as $1^1/_2$ inches. Prior to this most recent resurfacing effort, treatment methods included: $1^1/_2$ inches of a heavy-duty surface (HDS) asphalt course in 1995, 1 inch of I-2 in 1986, 1 inch of a bituminous concrete surface course (BCSC) in 1979, 1 inch of sand mix in 1965, and a half inch of bituminous surface treatment (BST) in 1929. No records exist regarding the thickness of the BCSC and sand treatment methods conducted in 1950 and 1939, respectively. The field test level for this section is Level 2, and the condition of this section falls in the category of *Young and Poor* roadways.

(a) (b)

Figure B.89 Photographs of representative cracking patterns on US-401, Linden, Cumberland County: (a) *bad* location and (b) *good* location

A marking paint layer lies between the 2nd and 3rd layers of the 3rd core extracted from the middle of the *bad* condition region. A school zone marking was located near the coring location in the middle of the traffic lane. Therefore, the marking paint does not indicate roadway widening. The pavement condition of the southbound lane of the site was worse than that of the northbound lane, even though the site is a one lane per direction rural roadway with an unpaved shoulder.

Table B.24 Summary of core data for US-401, Linden, Cumberland County

ID	Layer Thickness (inch)							Condition
	1st	2nd	3rd	4th	5th	6th	7th	
B-M1	1.26	1.65	2.17	0.71	0.71	1.10	3.54	Sound
B-M2	1.34	1.69	1.93	0.55	0.67	0.94	3.74	Sound
B-M3	1.42	1.57	1.97	0.71	0.71	0.98	3.54	Sound
B-M4	1.38	1.61	2.05	0.59	0.63	0.98	3.23	Sound
A-M1	1.18	1.65	1.89	0.87	0.75	0.98	3.54	Partial delamination in between 2nd and 3rd layers
A-M2	1.22	1.97	2.05	0.79	0.63	1.18	3.54	Sound
A-M3	1.10	2.05	1.77	0.91	0.79	1.14	3.46	Sound
A-W1	1.22	1.97	2.05	0.79	0.63	1.18	3.54	Horizontal crack in 5th layer

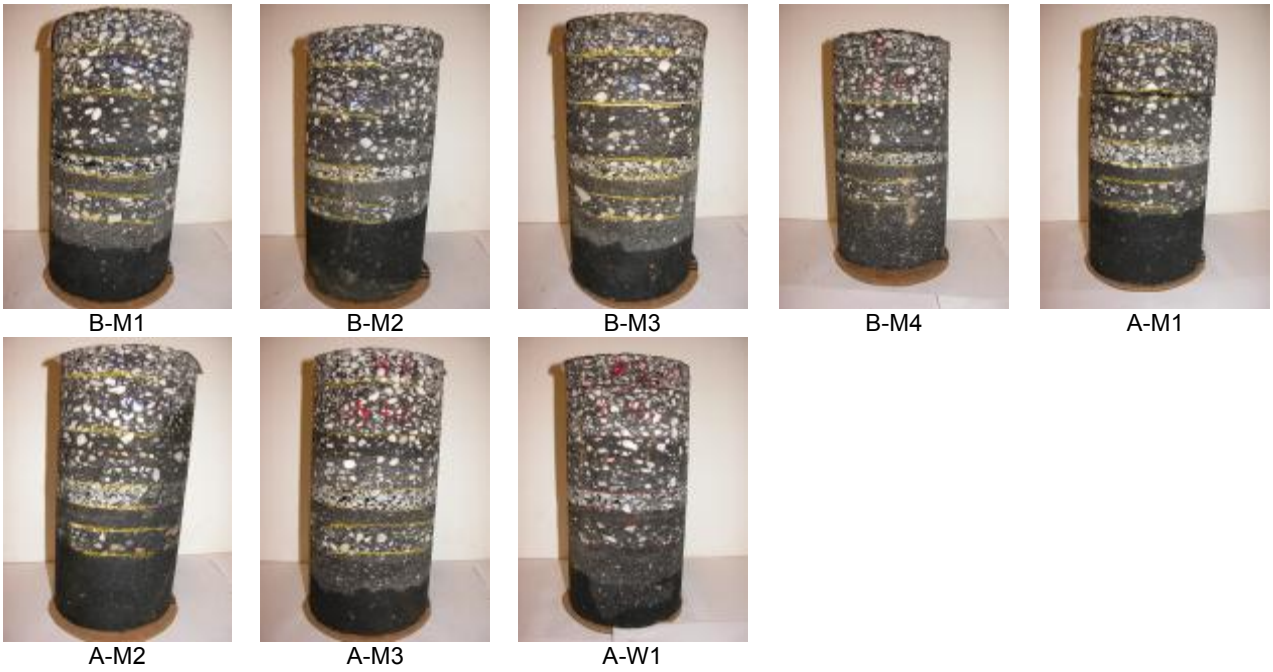

Figure B.90 Photographs of cores taken from US-401, Linden, Cumberland County

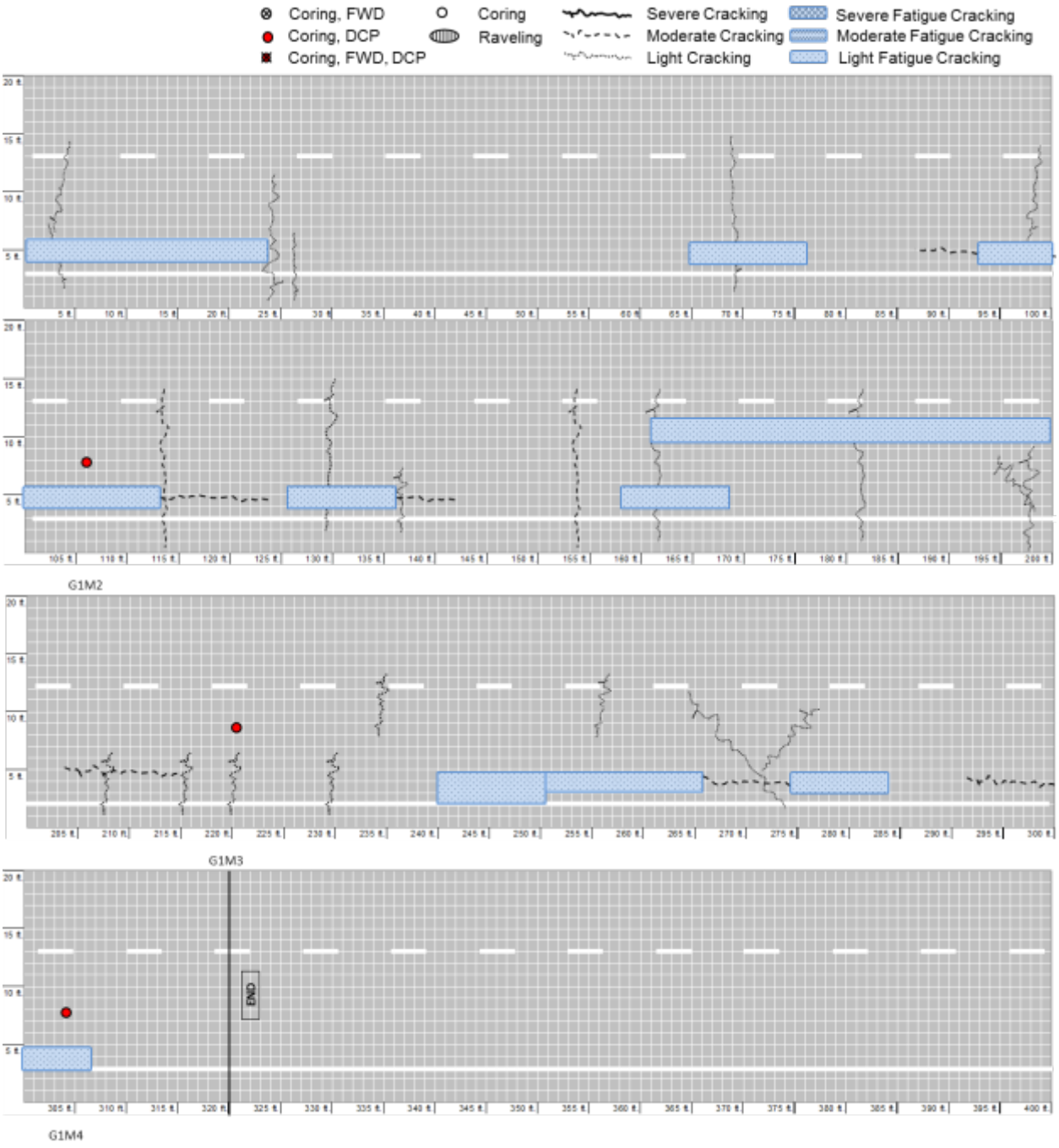

Figure B.91 Crack condition survey mapping of A1 region in US-401

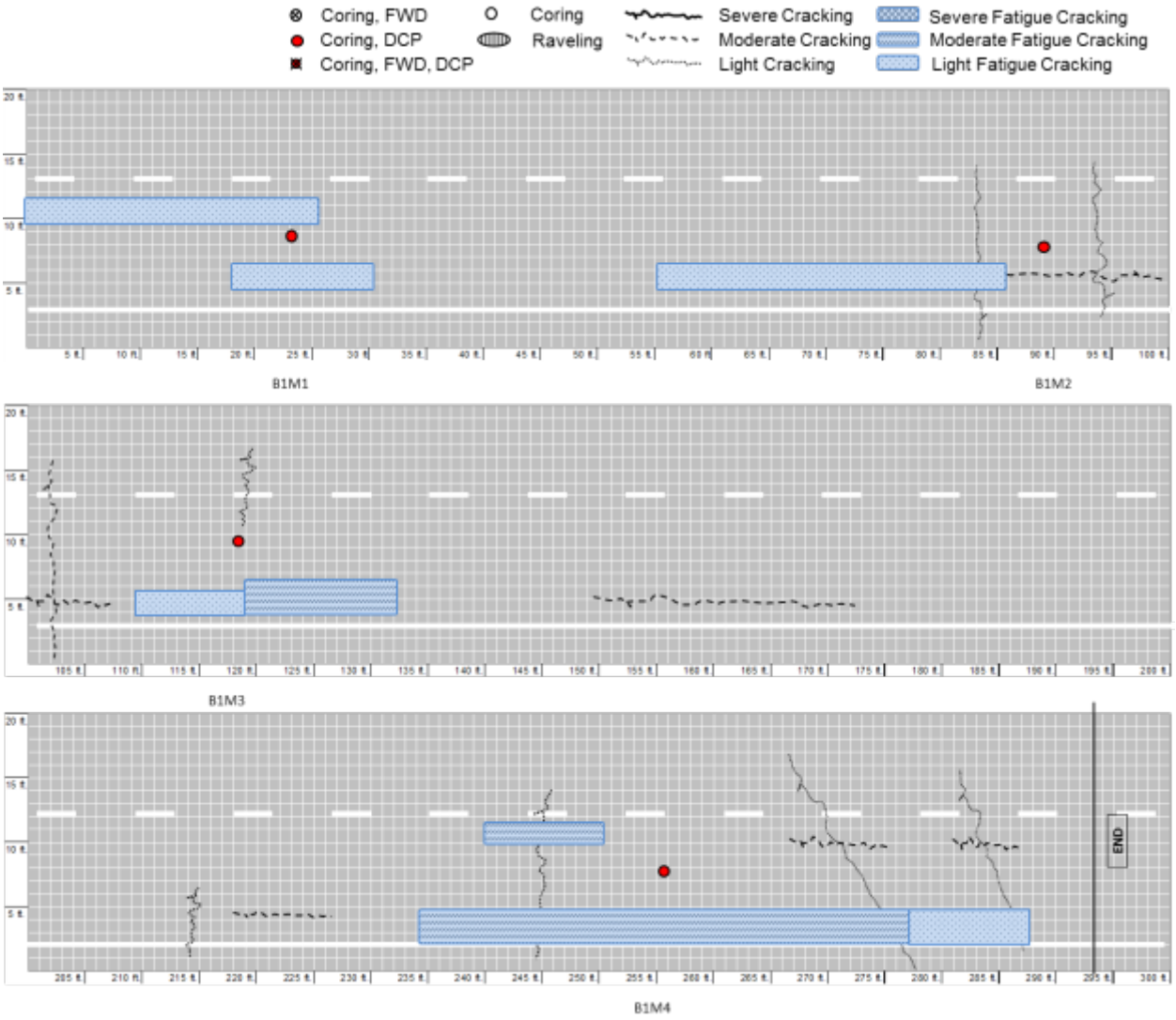

Figure B.92 Crack condition survey mapping of B1 region in US-401

19. NC Route 82 (Cumberland County)

On May 22, 2012, NCDOT personnel and the research team took dynamic cone penetrometer (DCP) measurements and extracted eight cores from NC 82 westbound in Linden in Cumberland County. According to the NCDOT construction history and profile database, the latest (2006) resurfacing work used S9.5A material with an overlay thickness recorded as 1 inch. Prior to this most recent resurfacing effort, treatment methods included: $1^{1}/_{2}$ inches of BCSC in 1988, 2 inches of I-2 in 1985, 1 inch of BCSC in 1982, 1 inch of BCSC in 1969, and 1 inch of HDS in 1951. The field test level of this section is Level 2, and the condition of this section falls in the category of *Young and Poor* roadways. As shown in Figure B.93, most of the major cracks at the site had been sealed. The site does not have a paved shoulder and is located in the middle of a small town (Godwin). On the testing date, the traffic volume was very light.

Figure B.93 Photograph of representative cracking patterns on NC 82, Godwin, Cumberland County

Table B.25 Summary of Core Data for NC 82, Godwin, Cumberland County

ID	Layer Thickness (inch)					Condition
	1st	2nd	3rd	4th	5th	
B-M1	1.42	0.71	1.18	1.57	1.77	Sound
B-M2	1.34	0.59	0.98	0.98	2.36	Sound
B-M3	1.42	0.63	0.98	1.42	2.17	Sound
B-M4	1.26	0.71	0.98	1.65	2.05	Sound
G-M1	1.38	0.59	0.98	1.57	0.55	Sound
G-M2	1.38	0.94	0.94	1.38	0.55	Sound; school marking paint in between 3rd and 4th layers
G-M3	1.10	0.63	1.06	1.18	0.39	Sound
G-M4	1.18	0.79	1.26	1.10	0.59	Delamination in between 3rd and 4th layers

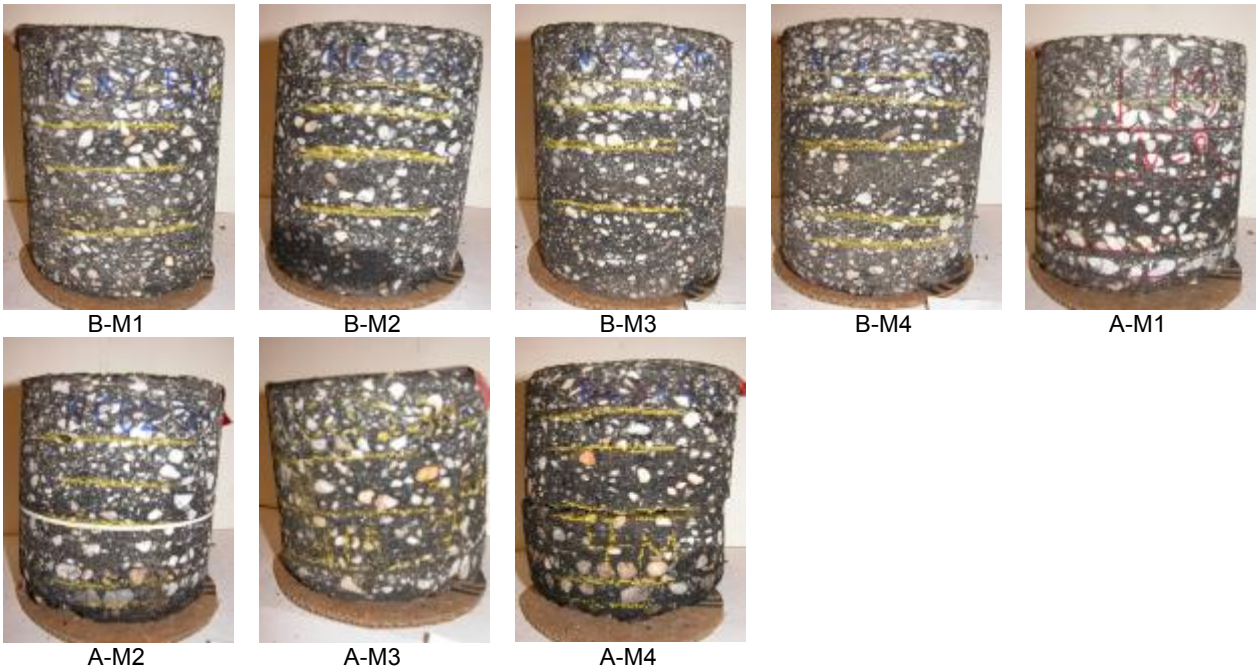

Figure B.94 Photographs of cores taken from NC 82, Godwin, Cumberland County

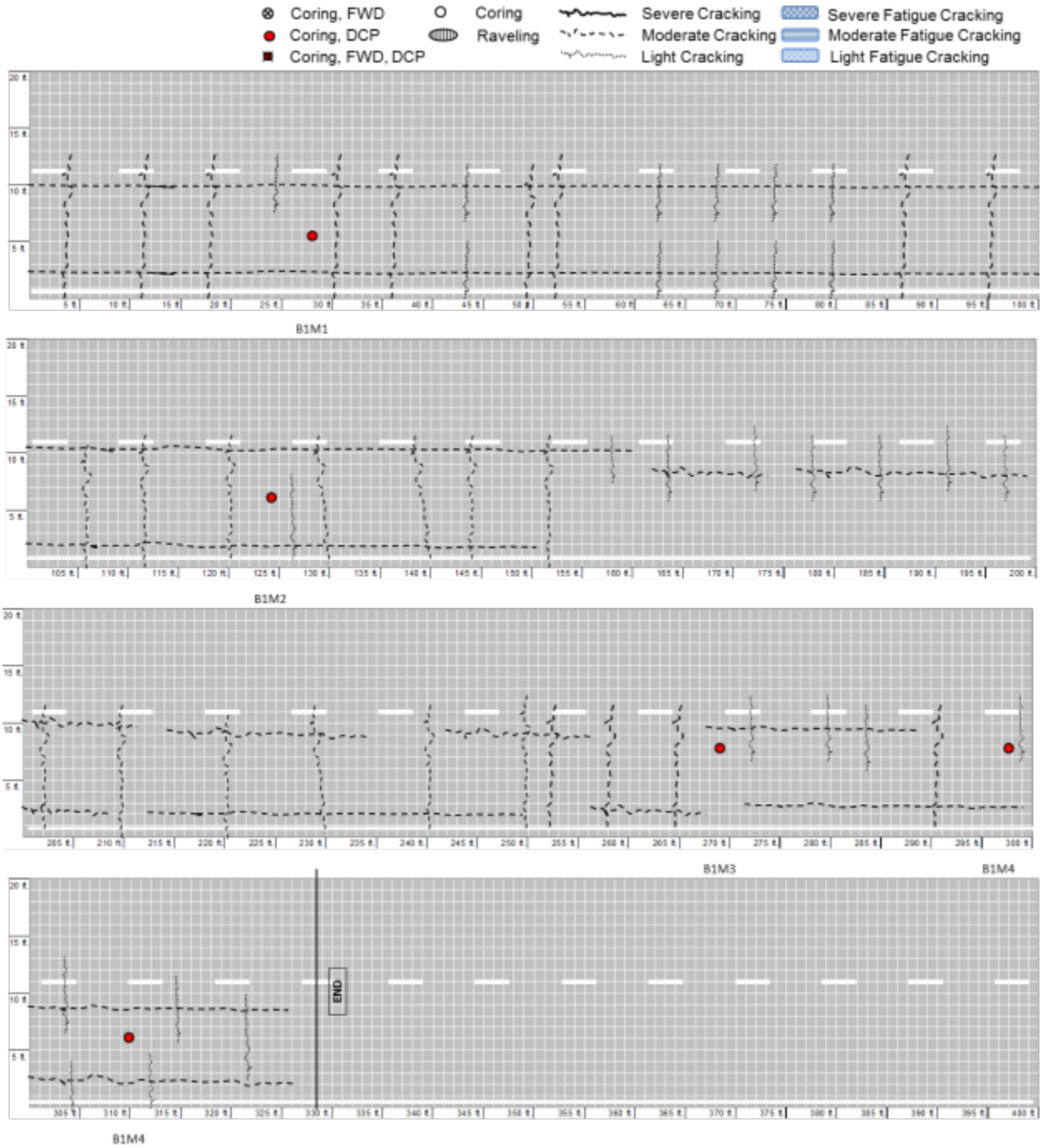

Figure B.95 Crack condition survey mapping of B1 region in NC-82

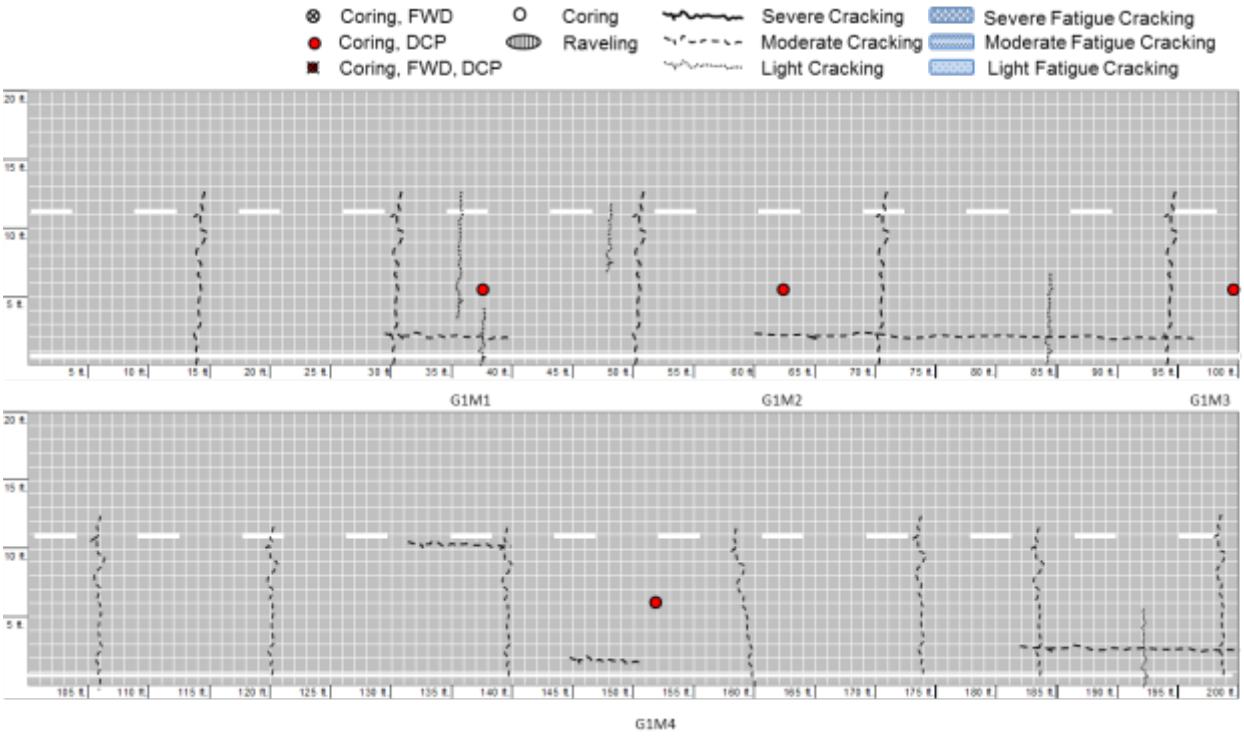

Figure B.96 Crack condition survey mapping of A1 region in US-82

Appendix C: Field Extracted Material Test Results

1. Interstate Highway 540 (Wake County)

Table C.1 Summary of field data and field core test result for I-540

Cond Region	TDC?	BUC?	ACI	TCI	Base Thick (mm)	Base Modulus (psi)	Subgrade Modulus (psi)	Layer	Air void (%)	Asphalt content (%)	NMSA (mm)
B1	Yes	No	55.3	98.6	200	15,000 K	11,835	1st	7.47	4.78	12.5
								2nd	8.58	5.17	9.5
								3rd	11.96	4.76	19.0
								4th	5.56	4.84	25.0
A1	No	No	91.4	100.0	200	15,000 K	14,259	1st	7.52	5.19	12.5
								2nd	6.30	5.09	12.5
								3rd	12.37	4.60	19.0
								4th	5.21	4.84	25.0
B2	Yes	No	32.6	100.0	200	15,000 K	15,649	1st	7.42	4.78	12.5
								2nd	7.56	5.17	9.5
								3rd	11.30	4.76	19.0
								4th	5.49	4.84	25.0
A2	No	No	97.6	100.0	200	15,000 K	19,268	1st	6.20	5.19	12.5
								2nd	9.99	5.09	12.5
								3rd	4.77	4.60	19.0
								4th	3.43	4.84	25.0

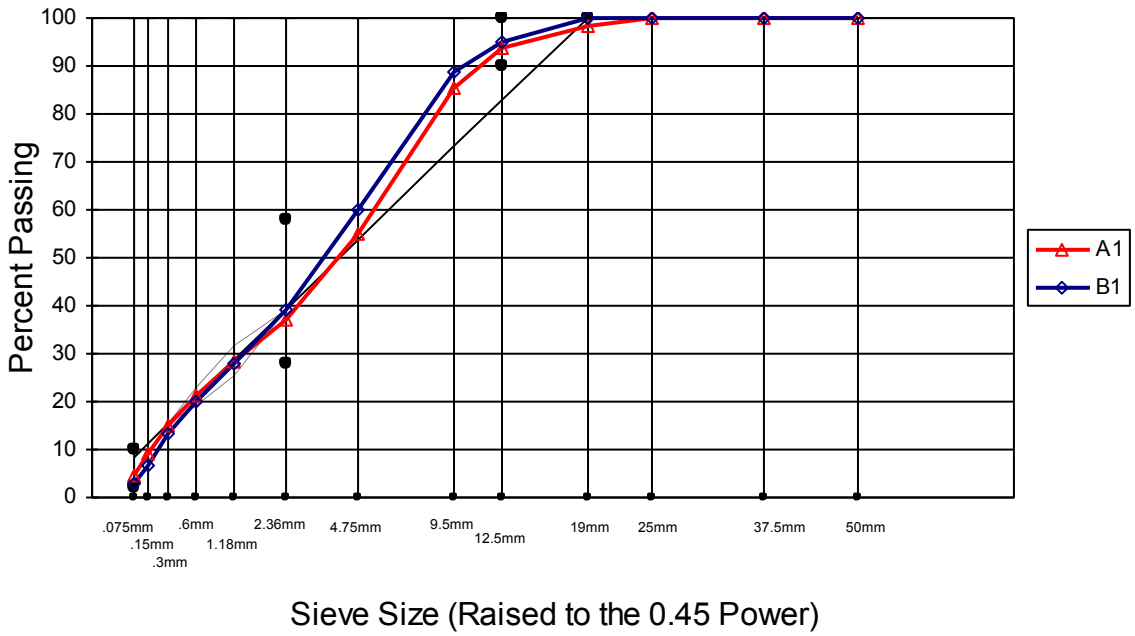

Figure C.1 Sieve analysis result from 1st layer of I 540

Figure C.2 Sieve analysis result from 2nd layer of I 540

Figure C.3 Sieve analysis result from 3rd layer of I 540

Figure C.4 Sieve analysis result from 4th layer of I 540

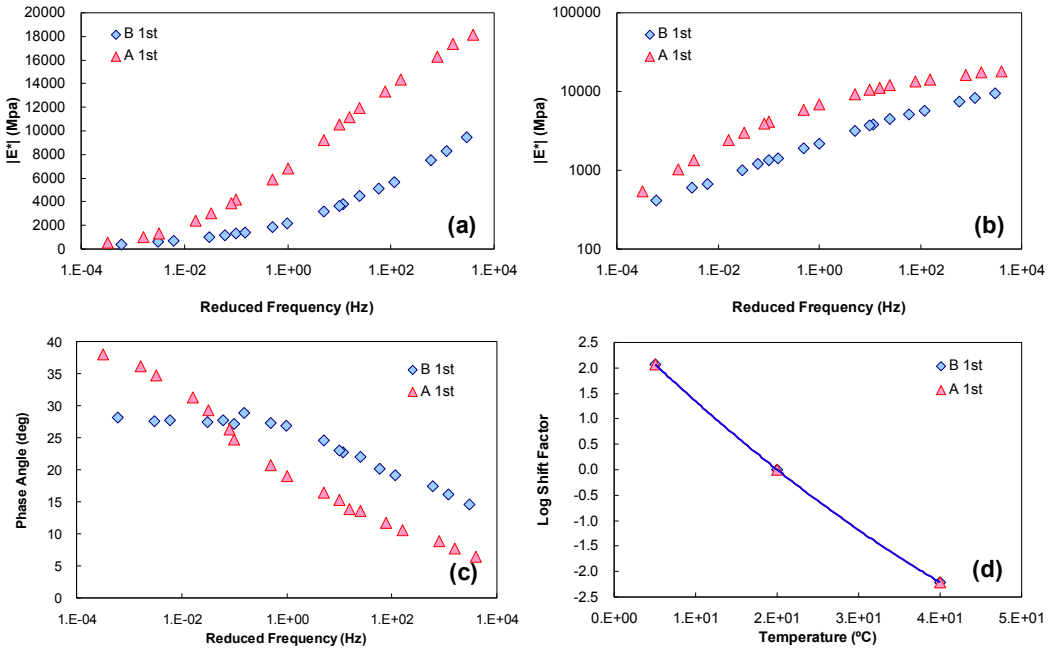

Figure C.5 Linear viscoelastic characteristics from 1st layer of field samples from I-540: (a) dynamic modulus in semi-log space, (b) dynamic modulus in log-log space, (c) phase angle and (d) shift factors

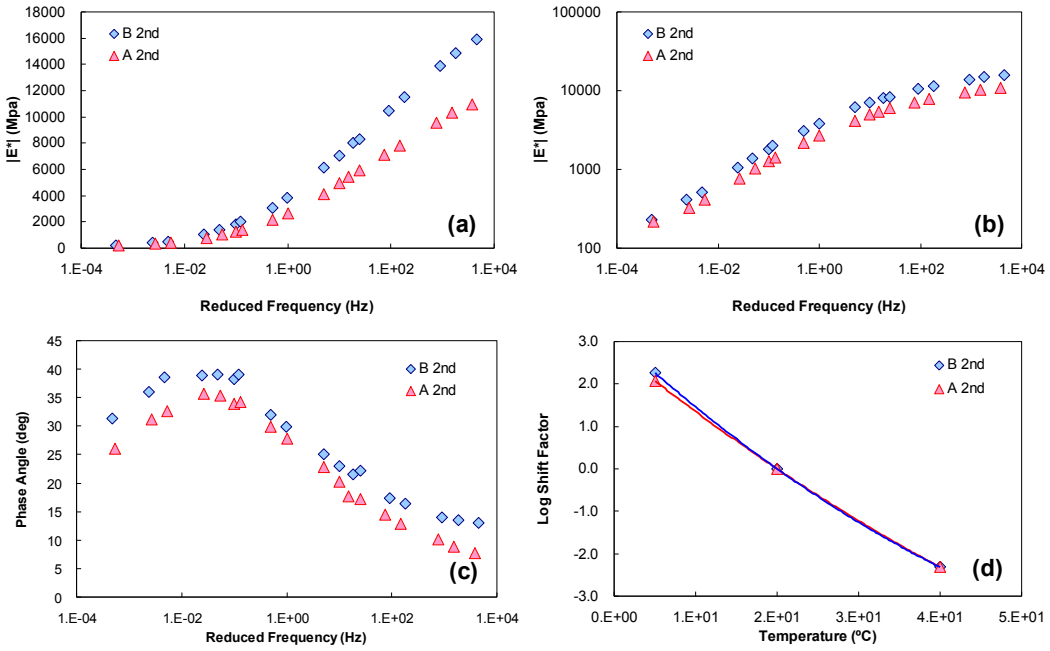

Figure C.6 Linear viscoelastic characteristics from 2nd layer of field samples from I-540: (a) dynamic modulus in semi-log space, (b) dynamic modulus in log-log space, (c) phase angle and (d) shift factors

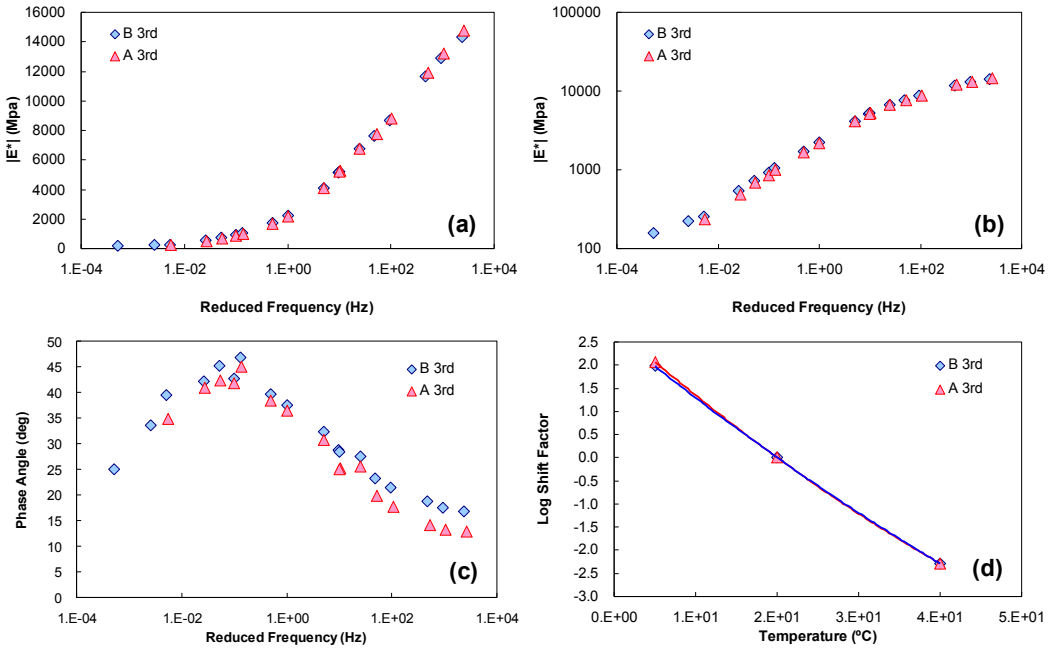

Figure C.7 Linear viscoelastic characteristics from 3rd layer of field samples from I-540: (a) dynamic modulus in semi-log space, (b) dynamic modulus in log-log space, (c) phase angle and (d) shift factors

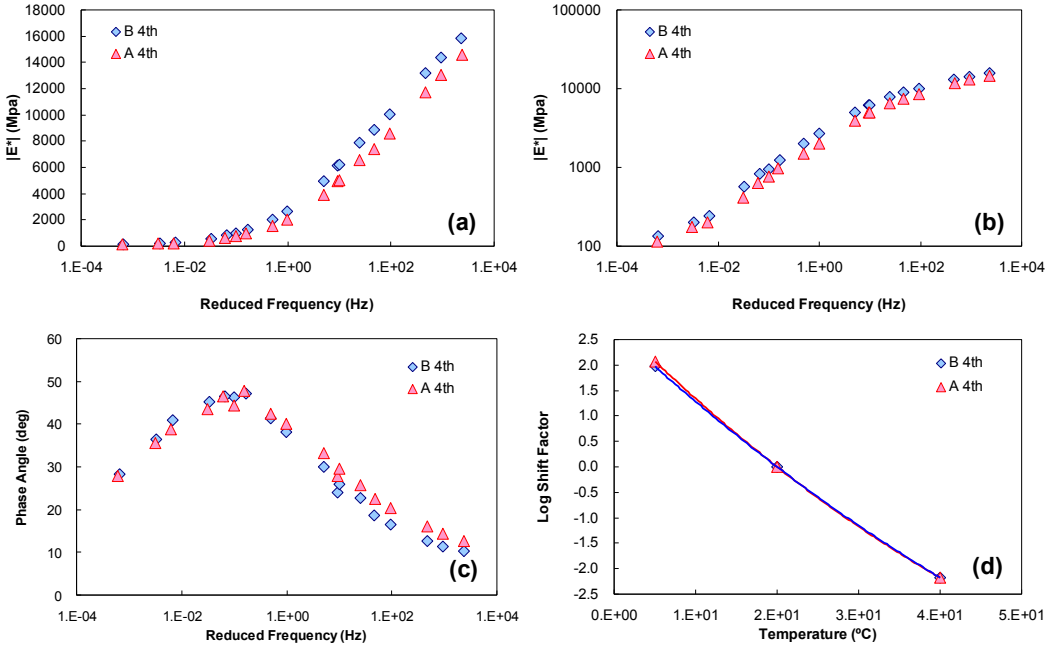

Figure C. 8 Linear viscoelastic characteristics from 4th layer of field samples from I-540: (a) dynamic modulus in semi-log space, (b) dynamic modulus in log-log space, (c) phase angle and (d) shift factors

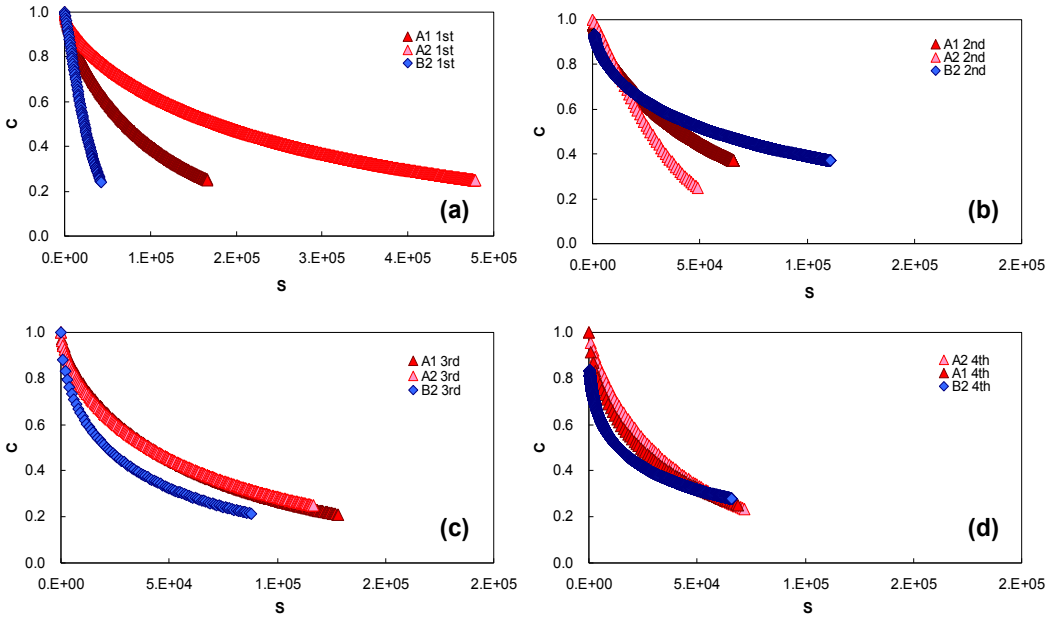

Figure C.9 Mixture damage characteristic curves for I-540 pavement: (a) 1st layer, (b) 2nd layer, (c) 3rd layer, and (d) 4th layer

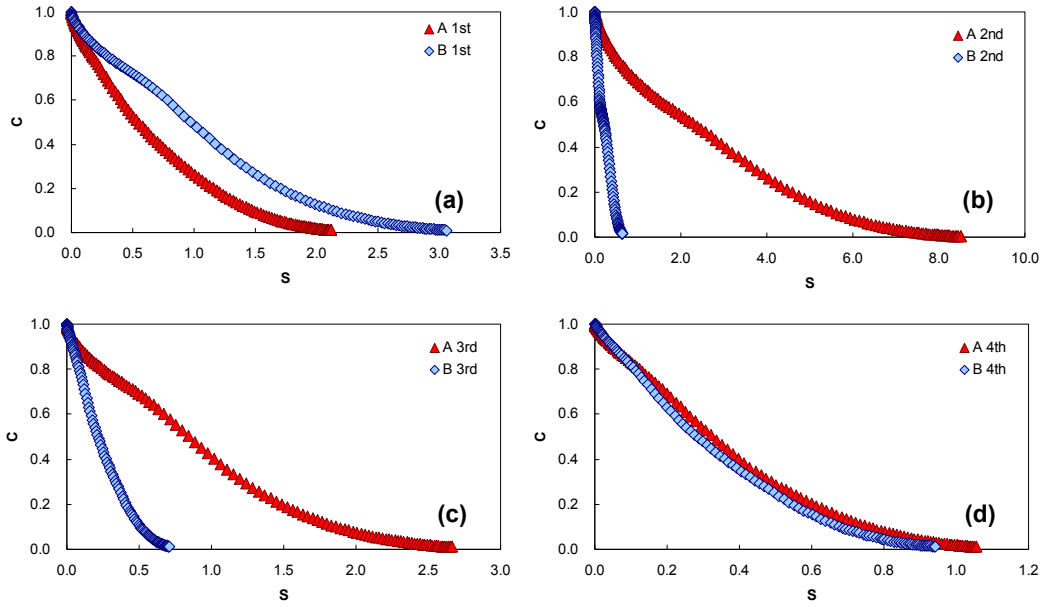

Figure C.10 Binder damage characteristic curves for I-540 pavement: (a) 1st layer, (b) 2nd layer, (c) 3rd layer, and (d) 4th layer

2. NC Route 24 (Mecklenburg County)

Table C.2 Summary of field data and field core test result for NC-24

Cond. Region	TDC?	BUC?	ACI	TCI	Base Thick (mm)	Base Modulus (psi)	Subgrade Modulus (psi)	Layer	Air void (%)	Asphalt content (%)	NMSA (mm)
B1	Yes	No	62.9	100.0	230	65,635	16,242	1st	9.54	4.87	9.5
								2nd	7.49	5.40	9.5
								3rd	6.31	4.98	19
A1	Yes	No	71.6	90.6	380	58,884	12,851	1st	7.40	4.74	9.5
								2nd	6.39	5.47	9.5
								3rd	7.50	4.96	19
B2	Yes	No	82.1	100.0	180	31,559	17,164	1st	11.50	4.87	9.5
								2nd	7.40	5.40	9.5
								3rd	7.55	4.98	19

Figure C.11 Sieve analysis result from 1st layer of NC-24

Figure C.12 Sieve analysis result from 2nd layer of NC-24

Figure C.13 Sieve analysis result from 3rd layer of NC-24

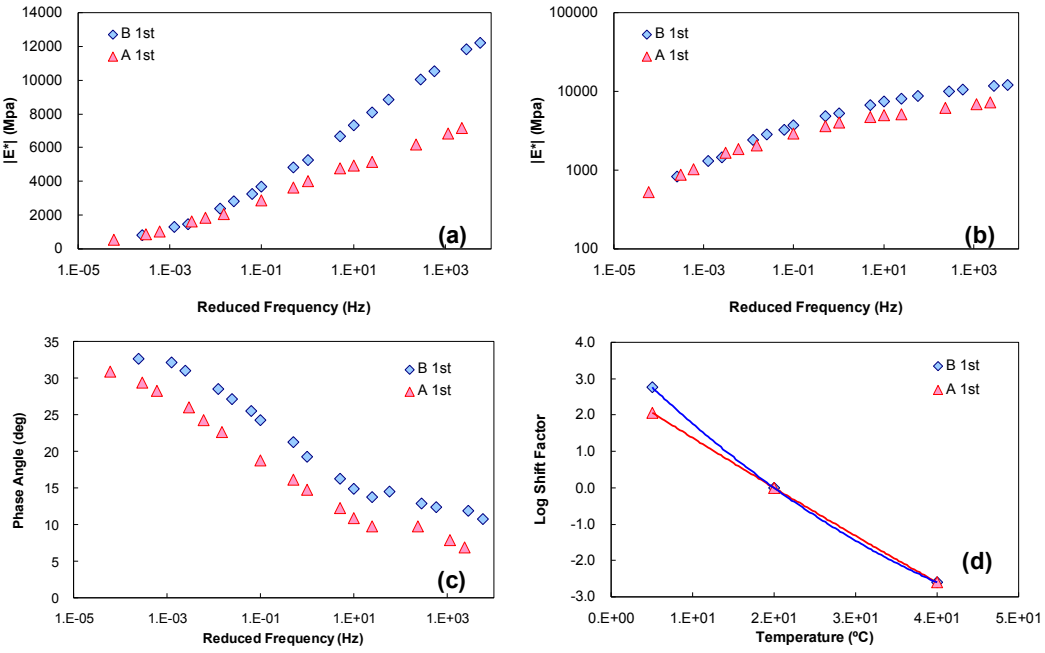

Figure C.14 Linear viscoelastic characteristics from 1st layer of field samples from NC-24: (a) dynamic modulus in semi-log space, (b) dynamic modulus in log-log space, (c) phase angle and (d) shift factors

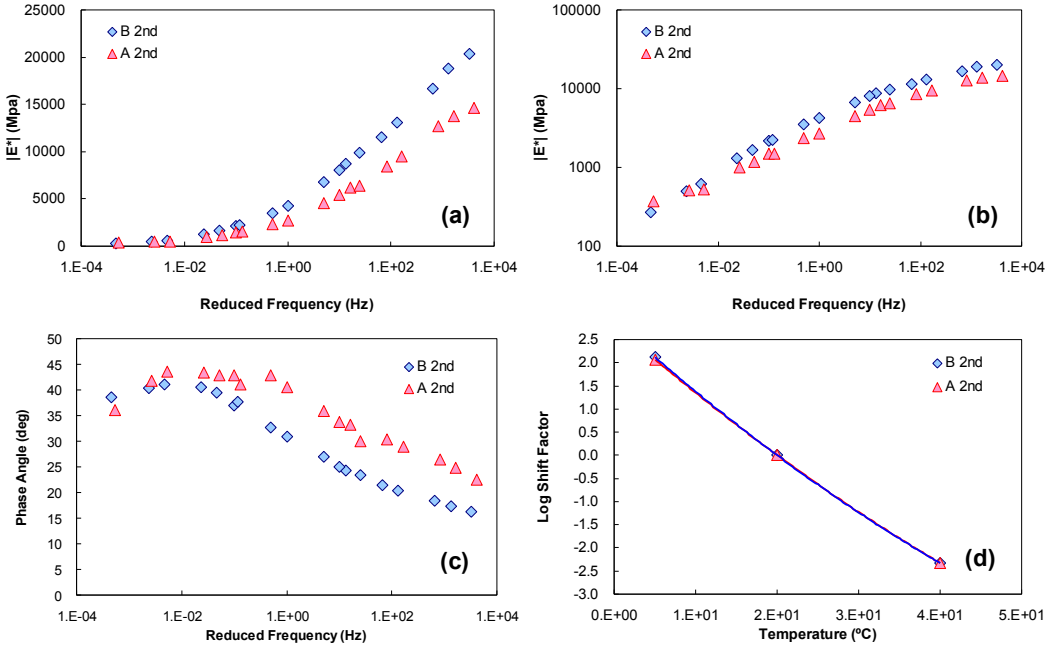

Figure C.15 Linear viscoelastic characteristics from 2nd layer of field samples from NC-24: (a) dynamic modulus in semi-log space, (b) dynamic modulus in log-log space, (c) phase angle and (d) shift factors

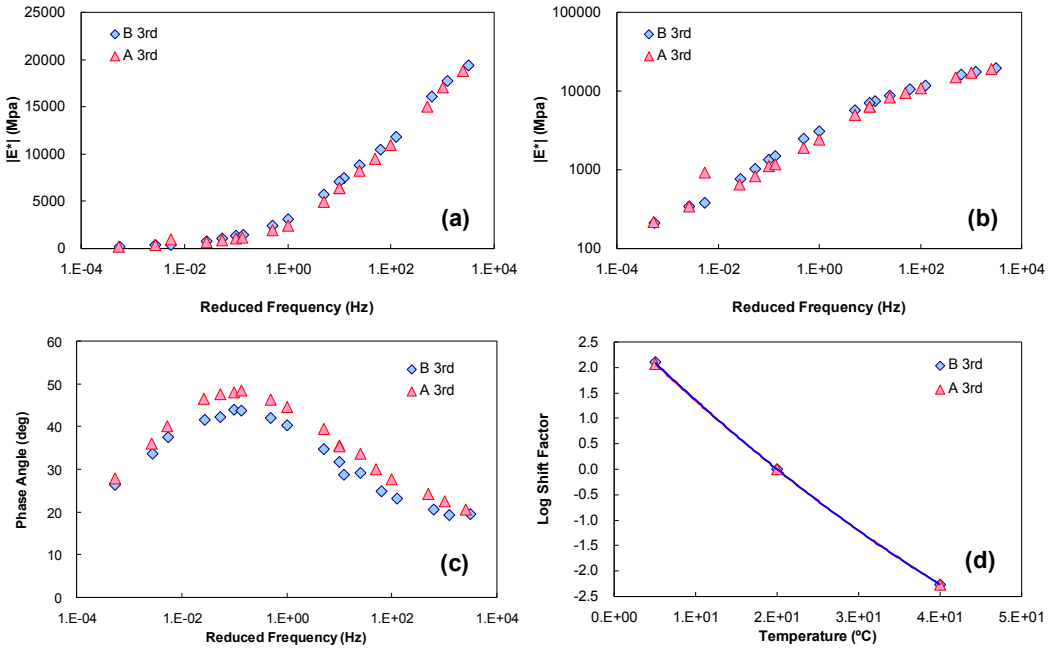

Figure C.16 Linear viscoelastic characteristics from 3rd layer of field samples from NC-24: (a) dynamic modulus in semi-log space, (b) dynamic modulus in log-log space, (c) phase angle and (d) shift factors

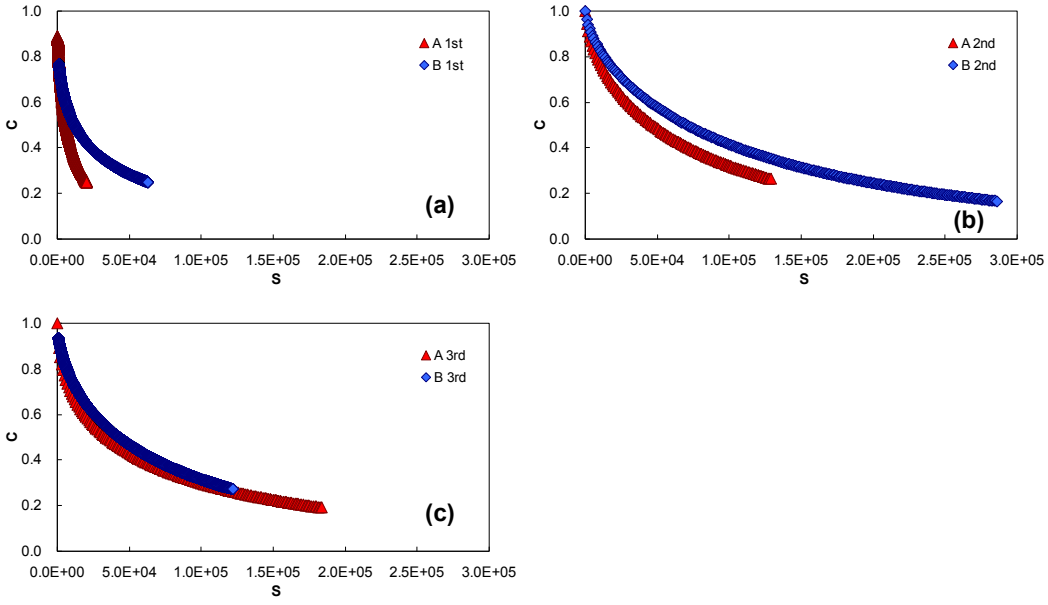

Figure C.17 Mixture damage characteristic curves for NC-24 pavement: (a) 1st layer, (b) 2nd layer, and (c) 3rd layer

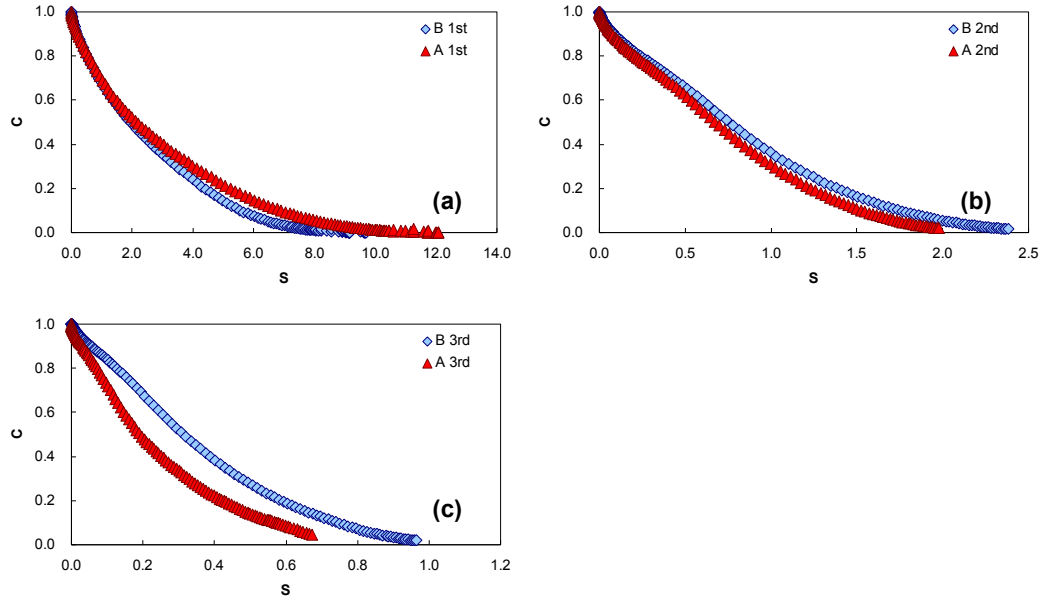

Figure C.18 Binder damage characteristic curves for NC-24 pavement: (a) 1st layer, (b) 2nd layer, and (c) 3rd layer

3. US Route 17 (Brunswick County)

Table C.3 Summary of field data and field core test result for US-17

Cond. Region	TDC?	BUC?	ACI	TCI	Base Thick (mm)	Base Modulus (psi)	Subgrade Modulus (psi)	Layer	Air void (%)	Asphalt content (%)	NMSA (mm)
B1	Yes	No	91.8	100	203	25,971	26,259	1st	8.91	6.49	9.5
								2nd	2.92	6.91	9.5
								3rd	7.38	5.69	19
								4th	7.03	5.93	25
B2	Yes	No	91.7	100	203	23,851	22,916	1st	10.77	6.49	9.5
								2nd	6.77	6.91	9.5
								3rd	7.66	5.69	19
								4th	5.61	5.93	25
A1	No	No	92.0	100	203	17,171	21,861	1st	8.06	6.47	9.5
								2nd	3.60	6.96	9.5
								3rd	5.73	5.75	19
								4th	7.27	5.55	25
A2	No	No	90.5	100	203	12,868	26,114	1st	8.59	6.47	9.5
								2nd	2.30	6.96	9.5
								3rd	4.39	5.75	19
								4th	7.15	5.55	25

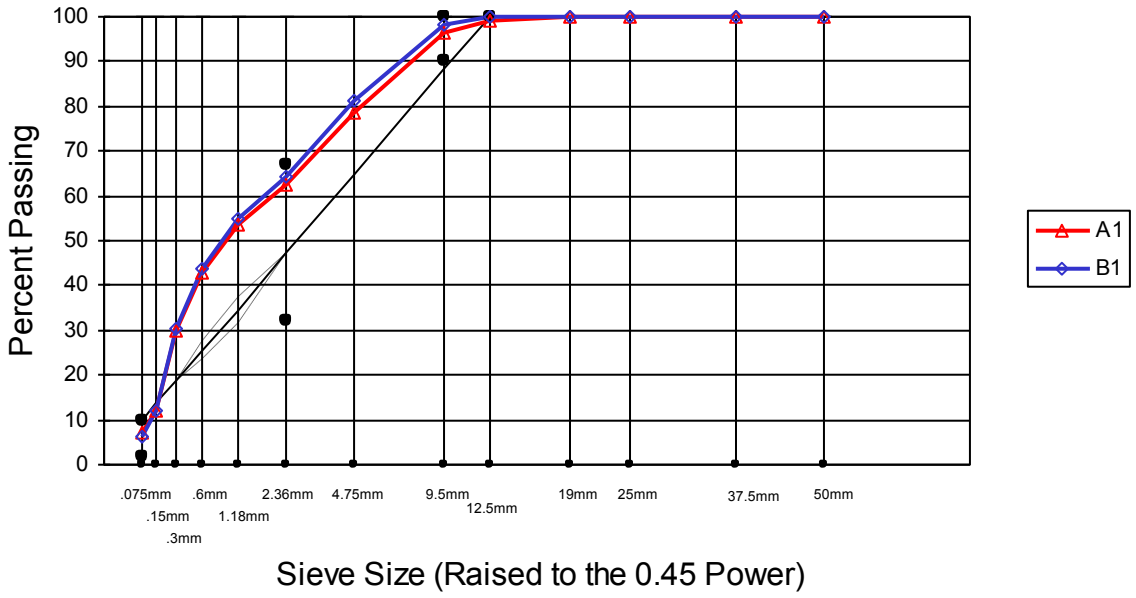

Figure C.19 Sieve analysis result from the 1st layer of US-17

Figure C.20 Sieve analysis result from the 2nd layer of US-17

Figure C.21 Sieve analysis result from the 4th layer of US-17

Figure C.22 Sieve analysis result from the 4th layer of US-17

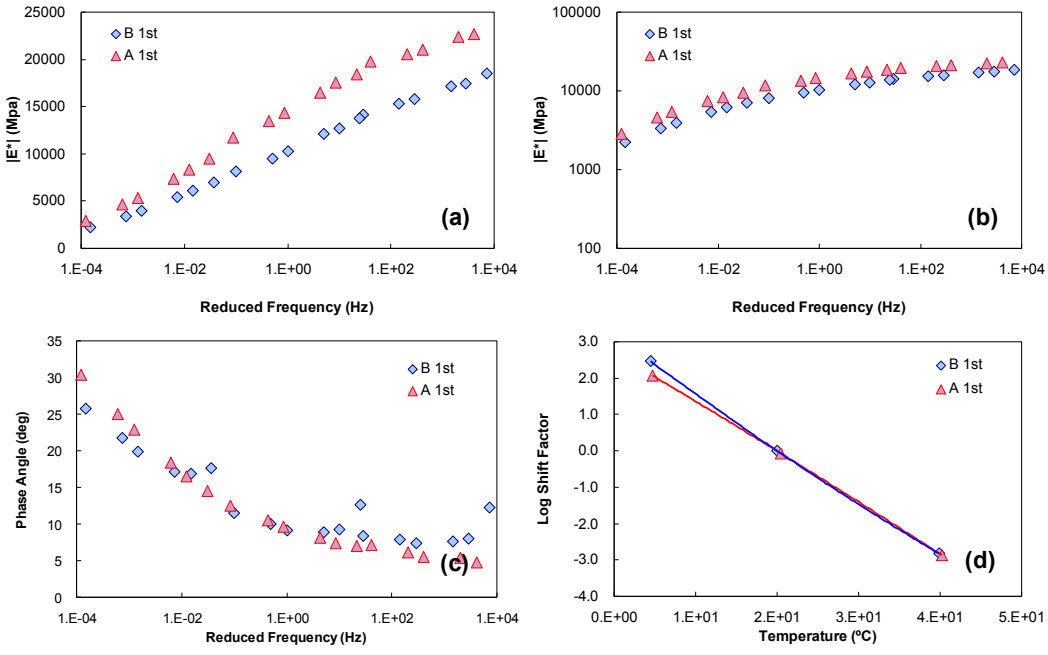

Figure C.23 Linear viscoelastic characteristics from 1st layer of field samples from NC-17: (a) dynamic modulus in semi-log space, (b) dynamic modulus in log-log space, (c) phase angle and (d) shift factors

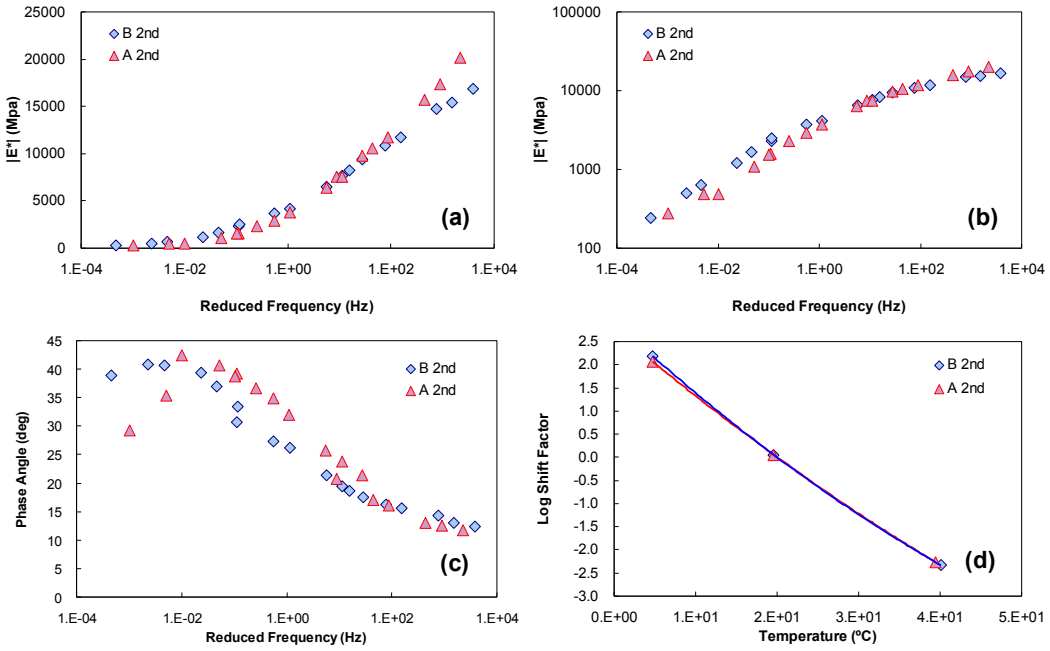

Figure C.24 Linear viscoelastic characteristics from 2nd layer of field samples from NC-17: (a) dynamic modulus in semi-log space, (b) dynamic modulus in log-log space, (c) phase angle and (d) shift factors

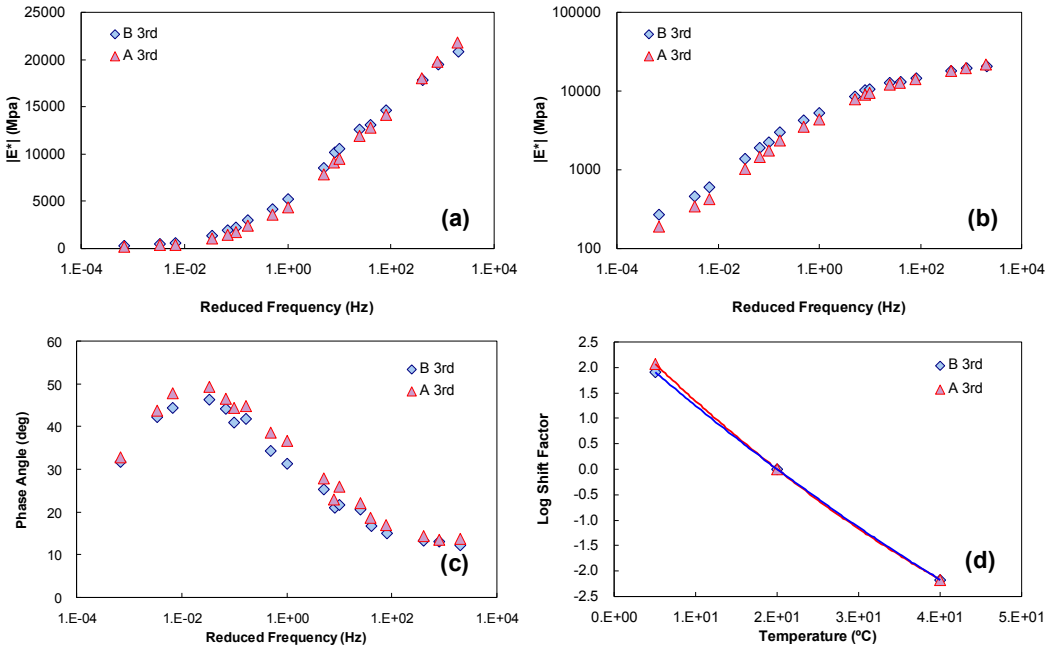

Figure C.25 Linear viscoelastic characteristics from 3rd layer of field samples from NC-17: (a) dynamic modulus in semi-log space, (b) dynamic modulus in log-log space, (c) phase angle and (d) shift factors

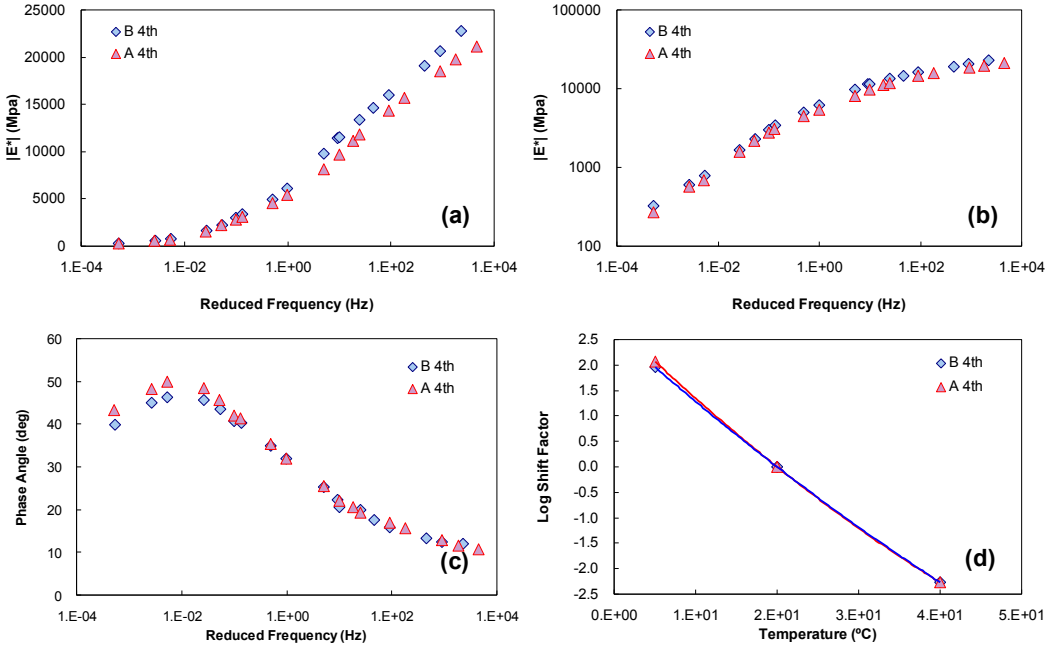

Figure C.26 Linear viscoelastic characteristics from 4th layer of field samples from NC-17: (a) dynamic modulus in semi-log space, (b) dynamic modulus in log-log space, (c) phase angle and (d) shift factors

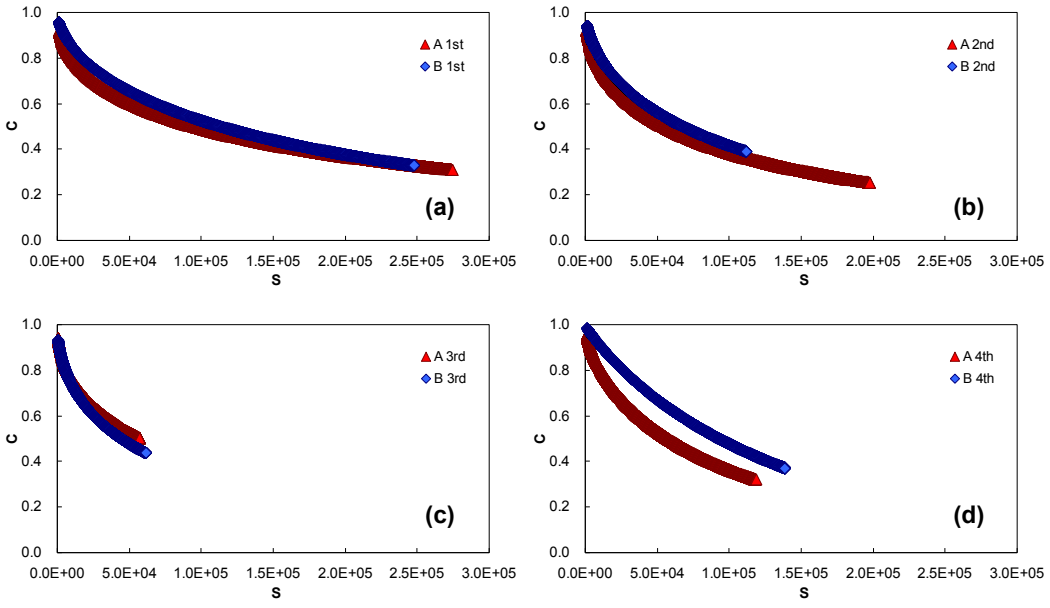

Figure C.27 Mixture damage characteristic curves for NC-17 pavement: (a) 1st layer, (b) 2nd layer, (c) 3rd layer, and (d) 4th layer

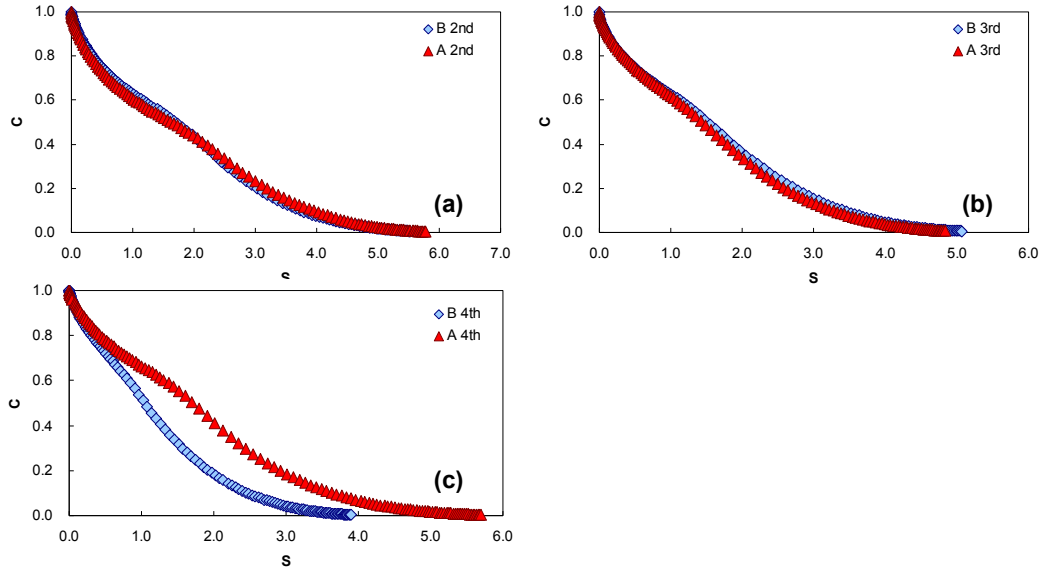

Figure C.28 Binder damage characteristic curves for NC-17 pavement: (a) 2nd layer, (b) 3rd layer, and (c) 4th layer

3. NC Route 87 (Cumberland County)

Table C.4 Summary of field data and field core test result for NC-87

Cond. Region	TDC?	BUC?	ACI	TCI	Base Thick (mm)	Base Modulus (psi)	Subgrade Modulus (psi)	Layer	Air void (%)	Asphalt content (%)	NMSA (mm)
A1	No	No	96.3	100.0	349	27,354	39,685	1st	5.40	5.91	9.5
								2nd	7.04	6.28	9.5
								3rd	4.71	6.54	9.5
								4th	7.17	6.09	12.5
								5th	4.68	5.65	19.0
B1	Yes	No	88.6	83.1	228	25,849	6,254	1st	6.56	6.02	9.5
								2nd	8.40	5.96	9.5
								3rd	7.94	6.53	9.5
								4th	8.51	6.13	9.5
								5th	4.59	6.52	19.0
A2	No	Yes	95.5	100.0	288	29,786	17,359	1st	6.19	5.91	9.5
								2nd	4.09	6.28	9.5
								3rd	4.73	6.54	9.5
								4th	6.33	6.09	12.5
								5th	5.45	5.65	19.0
B2	Yes	Yes	87.9	95.7	378	31,895	14,060	1st	8.17	6.02	9.5
								2nd	5.84	5.96	9.5
								3rd	3.00	6.53	9.5
								4th	6.26	6.13	9.5
								5th	4.13	6.52	19.0

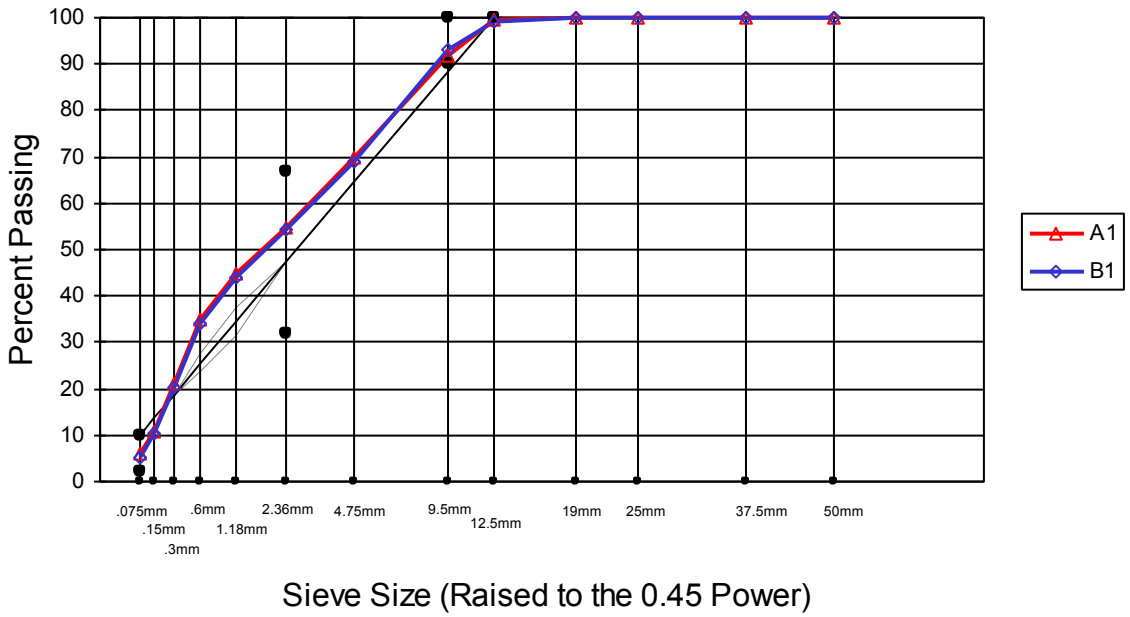

Figure C.29 Sieve analysis result from the 1st layer of NC-87

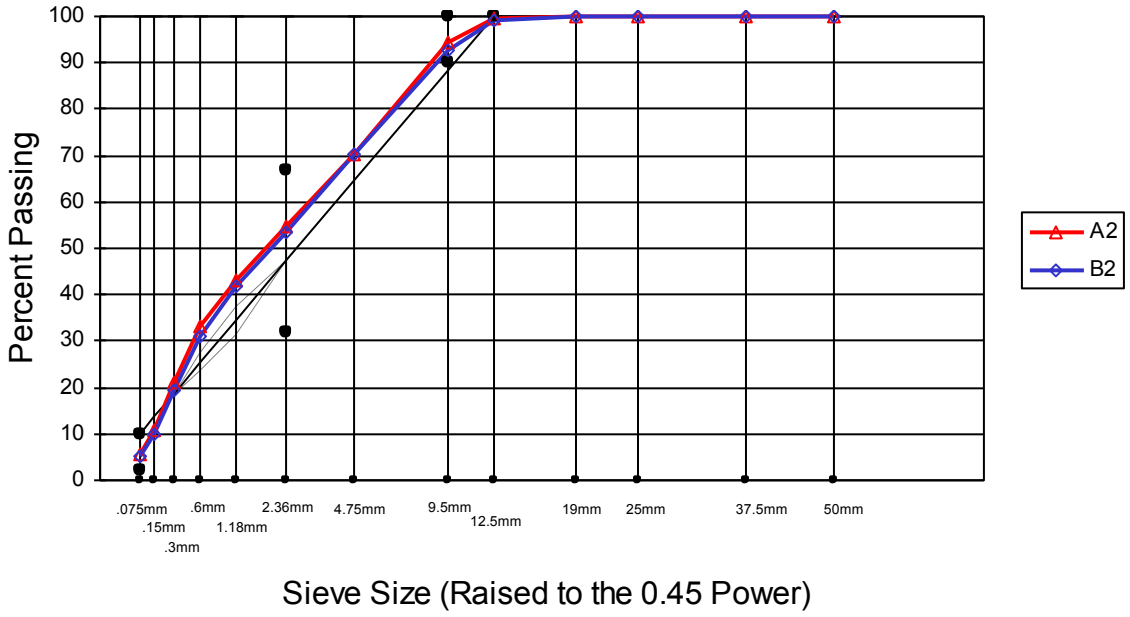

Figure C.30 Sieve analysis result from the 2nd layer of NC-87

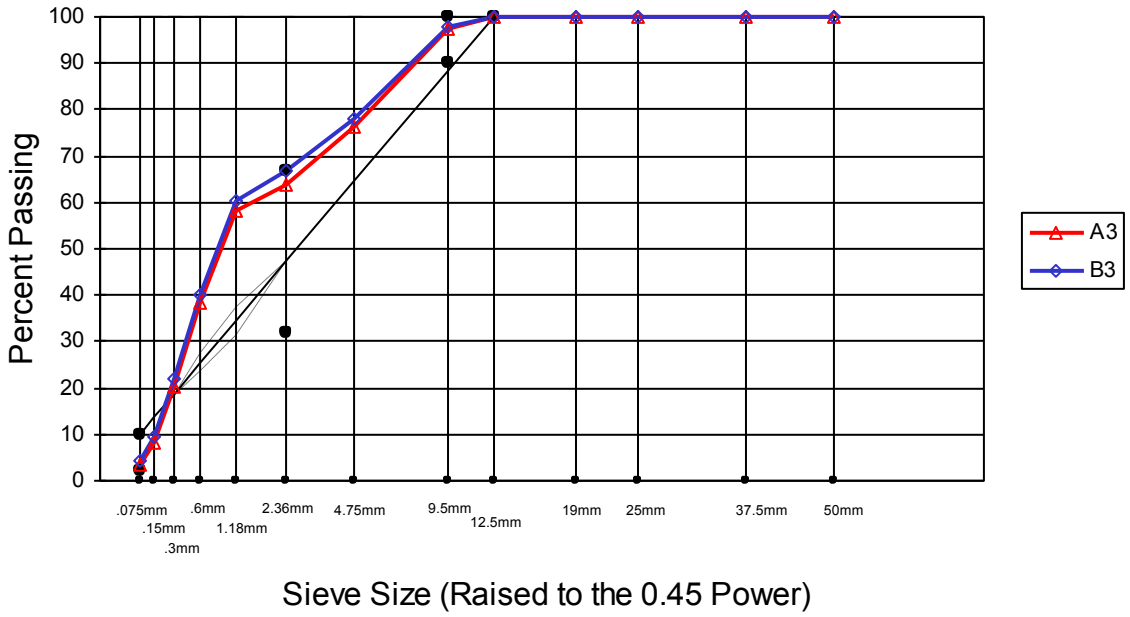

Figure C.31 Sieve analysis result from the 3rd layer of NC-87

Figure C.32 Sieve analysis result from the 4th layer of NC-87

Figure C.33 Sieve analysis result from the 5th layer of NC-87

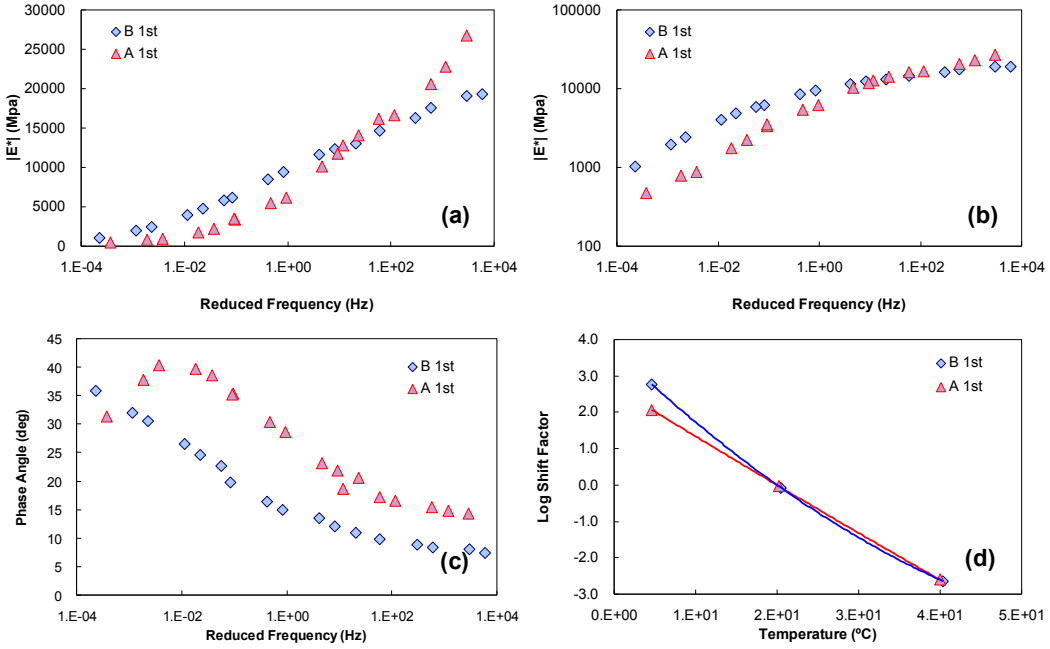

Figure C.34 Linear viscoelastic characteristics from 1st layer of field samples from NC-87: (a) dynamic modulus in semi-log space, (b) dynamic modulus in log-log space, (c) phase angle and (d) shift factors

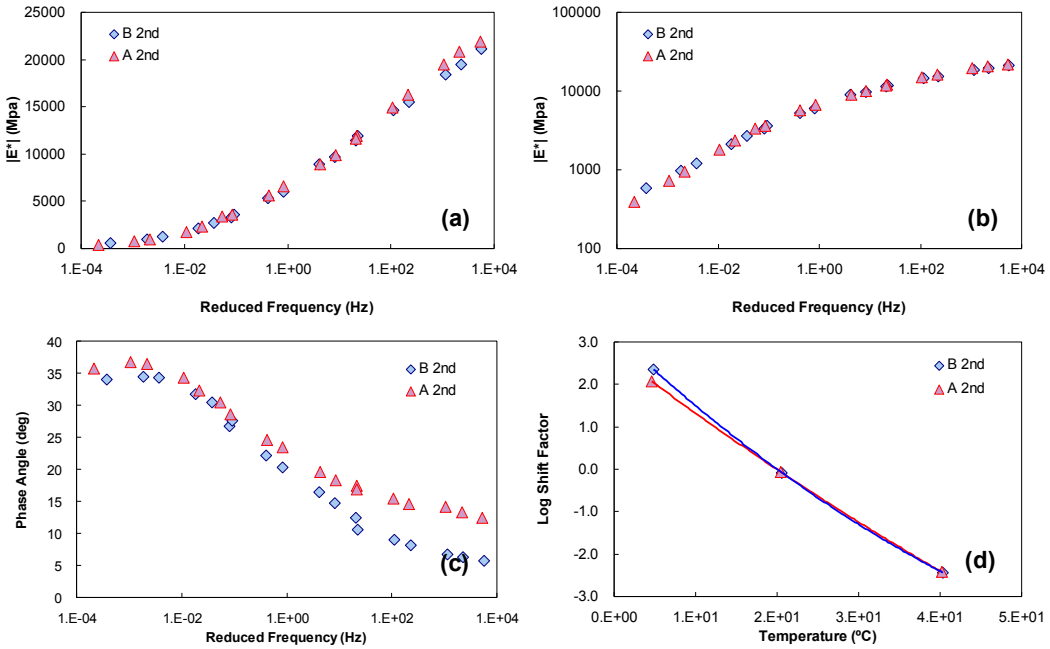

Figure C.35 Linear viscoelastic characteristics from 2nd layer of field samples from NC-87: (a) dynamic modulus in semi-log space, (b) dynamic modulus in log-log space, (c) phase angle and (d) shift factors

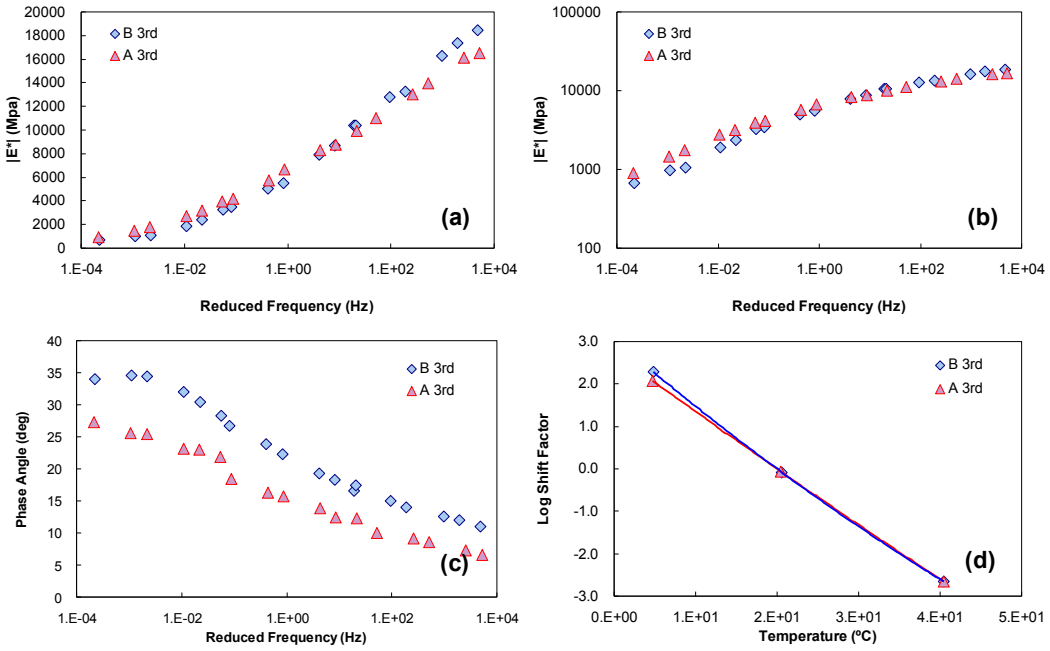

Figure C.36 Linear viscoelastic characteristics from 3rd layer of field samples from NC-87: (a) dynamic modulus in semi-log space, (b) dynamic modulus in log-log space, (c) phase angle and (d) shift factors

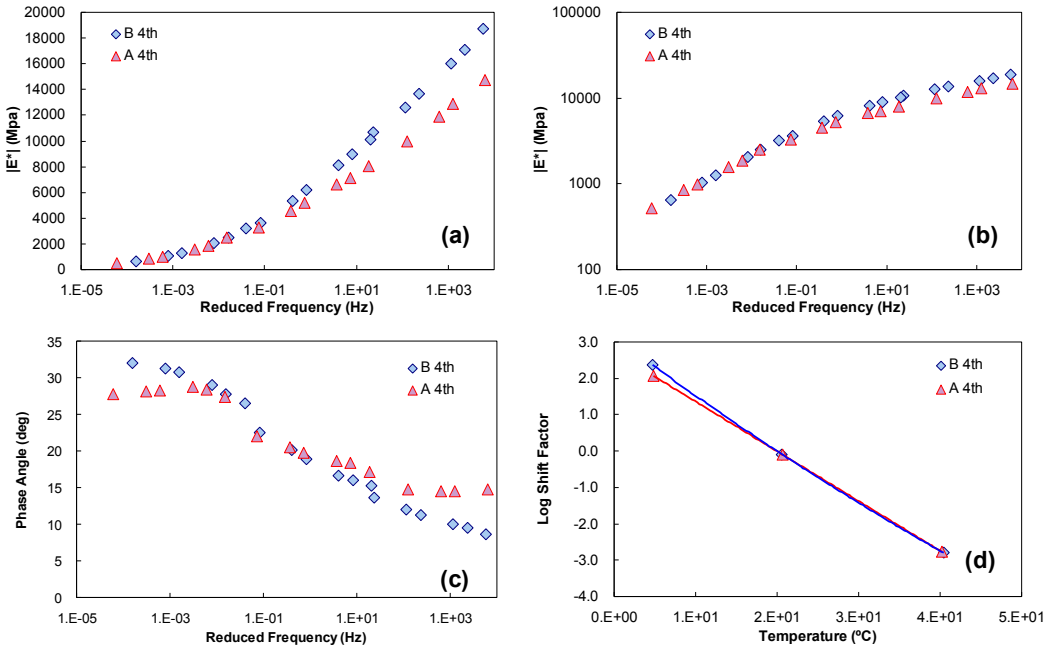

Figure C.37 Linear viscoelastic characteristics from 4th layer of field samples from NC-87: (a) dynamic modulus in semi-log space, (b) dynamic modulus in log-log space, (c) phase angle and (d) shift factors

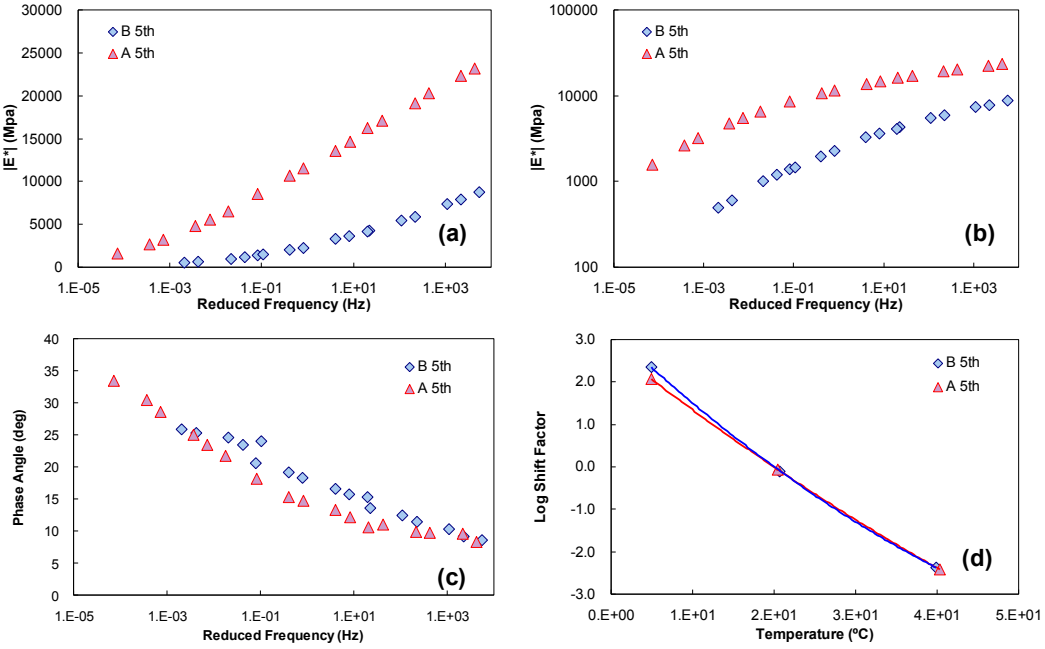

Figure C.38 Linear viscoelastic characteristics from 5th layer of field samples from NC-87: (a) dynamic modulus in semi-log space, (b) dynamic modulus in log-log space, (c) phase angle and (d) shift factors

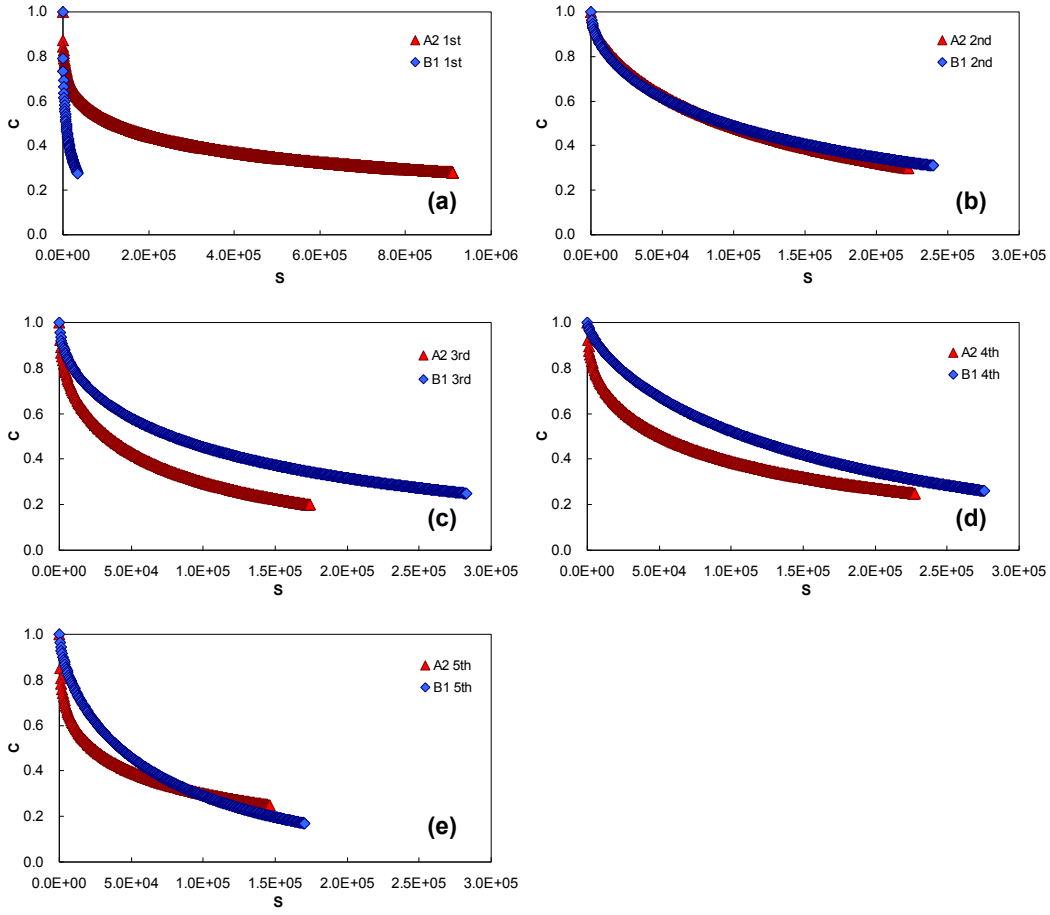

Figure C.39 Mixture damage characteristic curves for NC-87 pavement: (a) 1st layer, (b) 2nd layer, (c) 3rd layer, (d) 4th layer, and 5th layer (e)

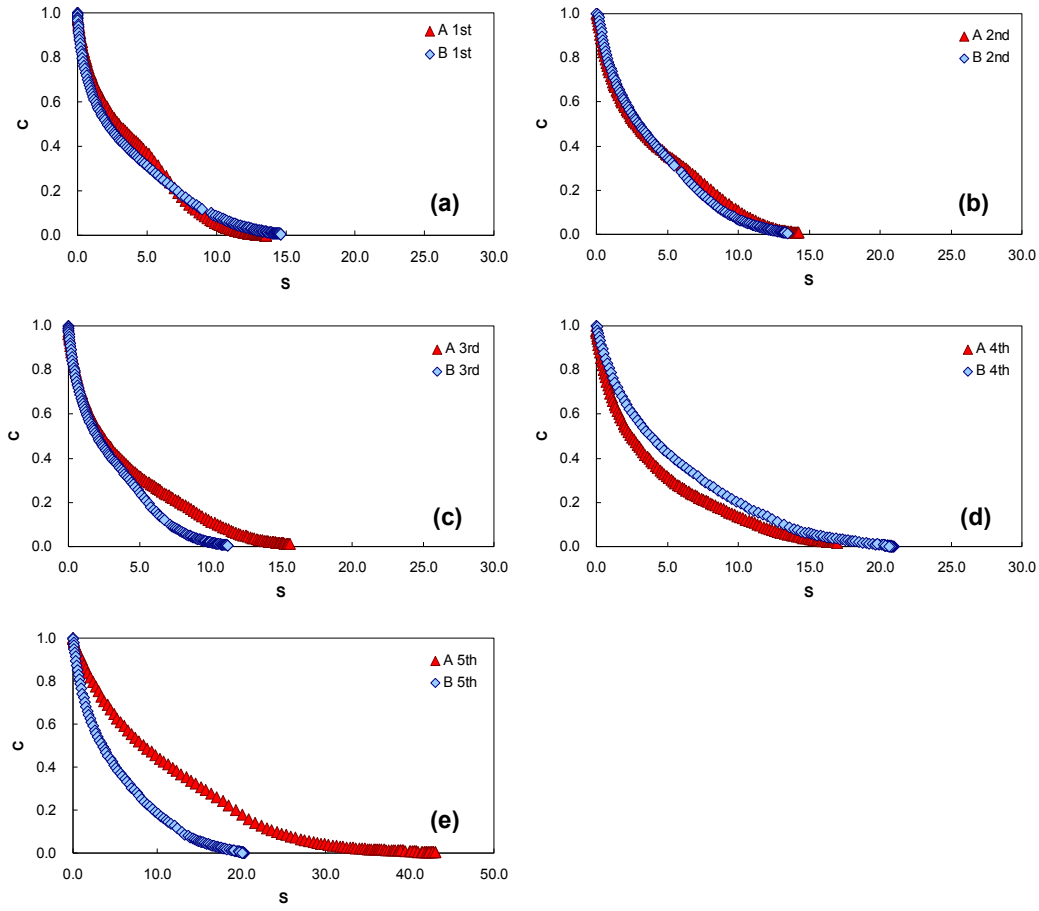

Figure C.40 Binder damage characteristic curves for NC-87 pavement: (a) 1st layer, (b) 2nd layer, (c) 3rd layer, (d) 4th layer, and 5th layer (e)

3. US Route 70 (Johnston County)

Table C.5 Summary of field data and field core test result for US-70

Cond. Region	TDC?	BUC?	ACI	TCI	Base Thick (mm)	Base Modulus (psi)	Subgrade Modulus (psi)	Layer	Air void (%)	Asphalt content (%)	NMSA (mm)
B1	No	No	92.9	100.0	227	119,925	43,486	1st	-	5.17	9.5
								2nd	-	5.01	9.5
								3rd	-	5.66	9.5
								4th	-	4.39	25.0
B2	Yes	No	90.9	100.0	238	54,294	21,834	1st	10.07	5.17	9.5
								2nd	12.06	5.01	9.5
								3rd	7.58	5.66	9.5
								4th	4.53	4.39	25.0
A1	No	No	96.7	100.0	243	60,092	15,215	1st	8.57	5.28	9.5
								2nd	11.43	5.09	9.5
								3rd	3.83	5.77	9.5
								4th	5.42	4.33	25.0
A2	No	No	100.0	100.0	239	74,186	26,792	1st	10.34	5.28	9.5
								2nd	9.11	5.09	9.5
								3rd	3.53	5.77	9.5
								4th	6.57	4.33	25.0

Figure C.41 Sieve analysis result from the 1st layer of US-70

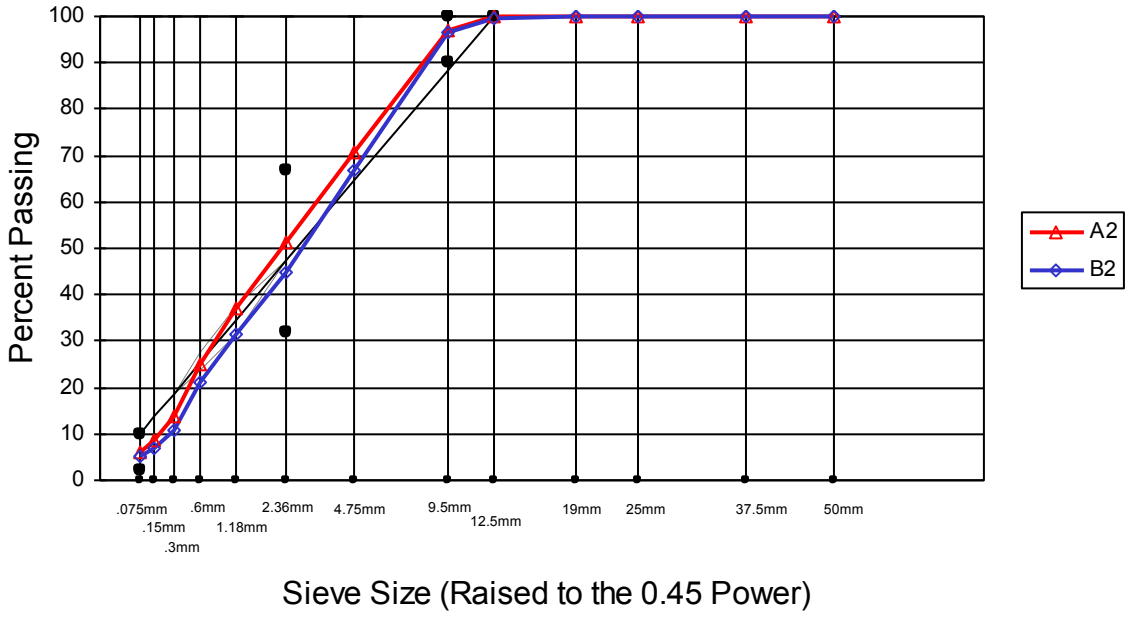

Figure C.42 Sieve analysis result from the 2nd layer of US-70

Figure C.43 Sieve analysis result from the 3rd layer of US-70

Figure C.44 Sieve analysis result from the 4th layer of US-70

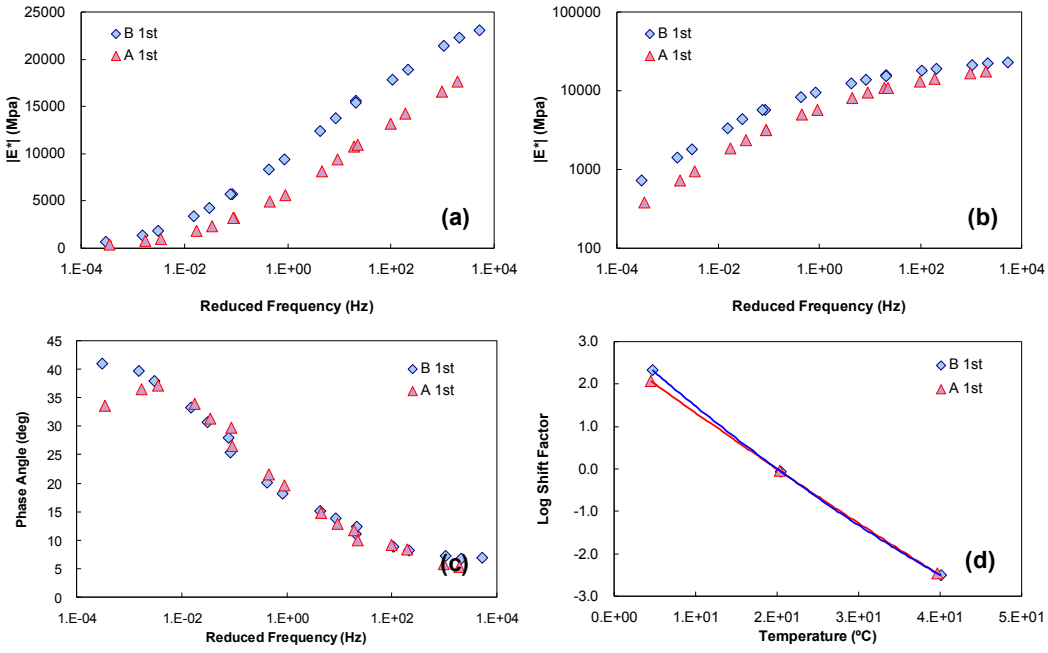

Figure C.45 Linear viscoelastic characteristics from 1st layer of field samples from US-70: (a) dynamic modulus in semi-log space, (b) dynamic modulus in log-log space, (c) phase angle and (d) shift factors

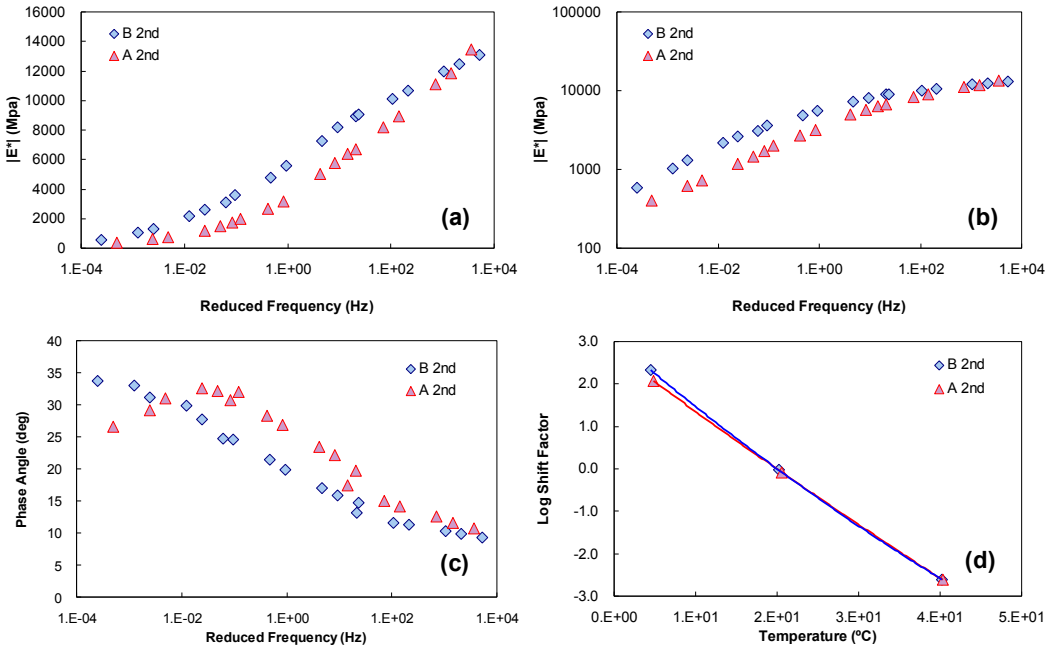

Figure C.46 Linear viscoelastic characteristics from 2nd layer of field samples from US-70: (a) dynamic modulus in semi-log space, (b) dynamic modulus in log-log space, (c) phase angle and (d) shift factors

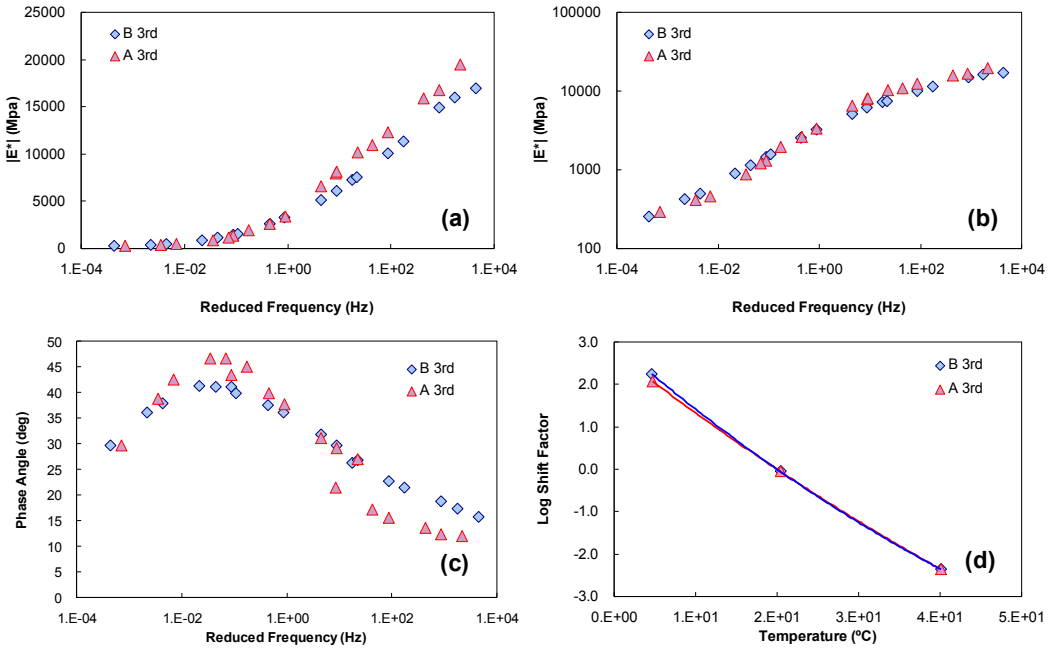

Figure C.47 Linear viscoelastic characteristics from 3rd layer of field samples from US-70: (a) dynamic modulus in semi-log space, (b) dynamic modulus in log-log space, (c) phase angle and (d) shift factors

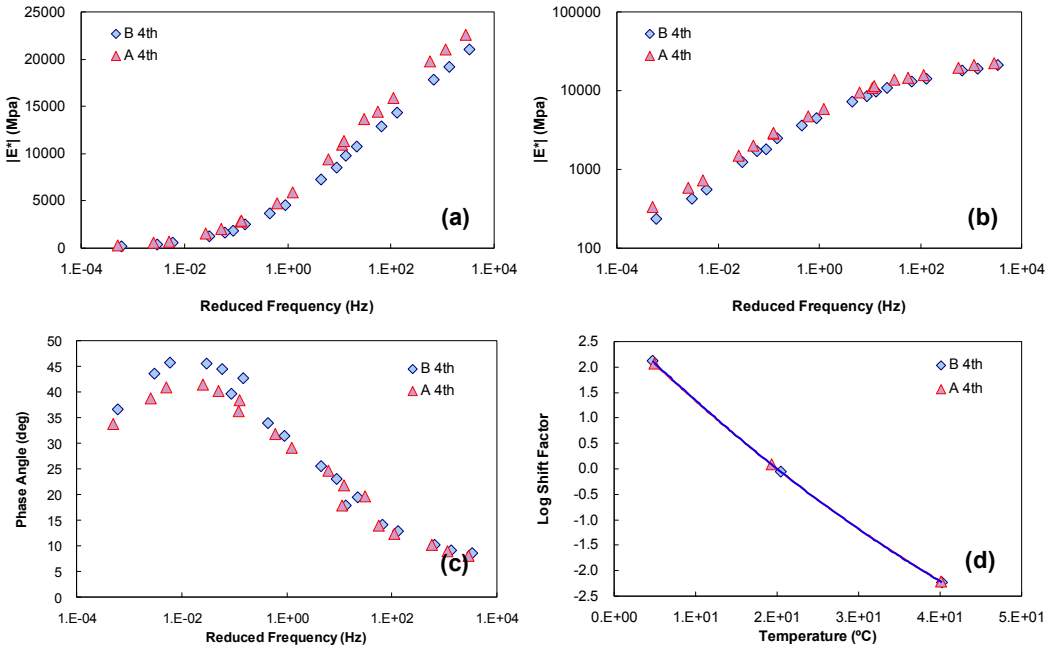

Figure C.48 Linear viscoelastic characteristics from 4th layer of field samples from US-70: (a) dynamic modulus in semi-log space, (b) dynamic modulus in log-log space, (c) phase angle and (d) shift factors

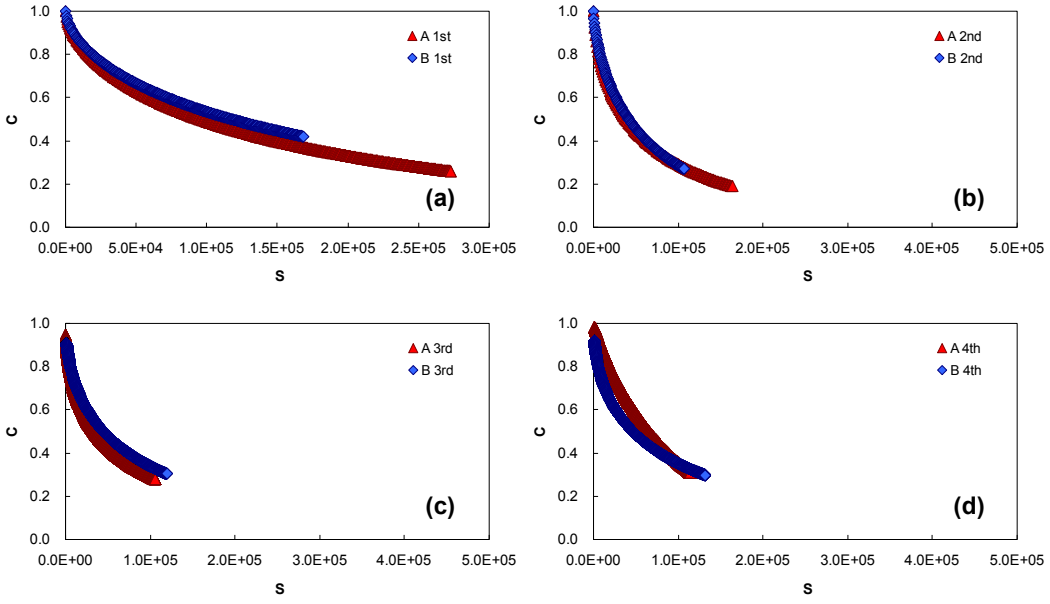

Figure C.49 Mixture damage characteristic curves for US-70 pavement: (a) 1st layer, (b) 2nd layer, (c) 3rd layer, and (d) 4th layer

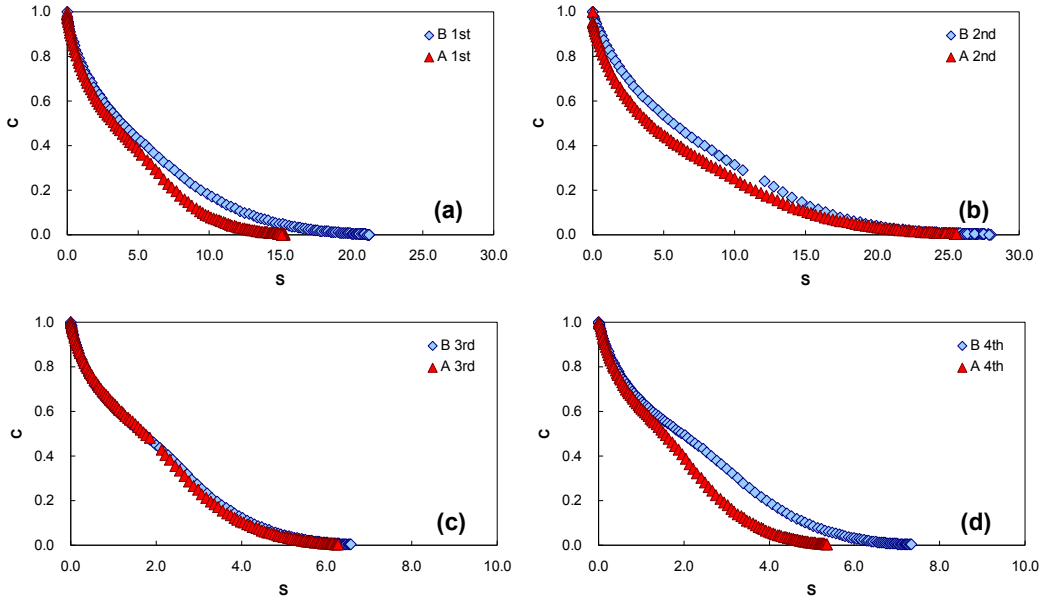

Figure C.50 Binder damage characteristic curves for US-70 pavement: (a) 1st layer, (b) 2nd layer, (c) 3rd layer, and (d) 4th layer

6. US Route 74 (Swain County)

Table C.6 Summary of field data and field core test result for US-76

Cond. Region	TDC?	BUC?	ACI	TCI	Base Thick (mm)	Base Modulus (psi)	Subgrade Modulus (psi)	Layer	Air void (%)	Asphalt content (%)	NMSA (mm)
B1	No	Yes	68.7	93.7	260.00	88,331	20,638	1st	4.28	6.44	9.5
								2nd	4.84	5.28	19.0
								3rd	10.74	5.44	19.0
A1	No	Yes	81.1	94.2	300.00	89,583	25,258	1st	3.49	5.89	9.5
								2nd	3.93	4.91	19.0
								3rd	8.01	5.98	19.0

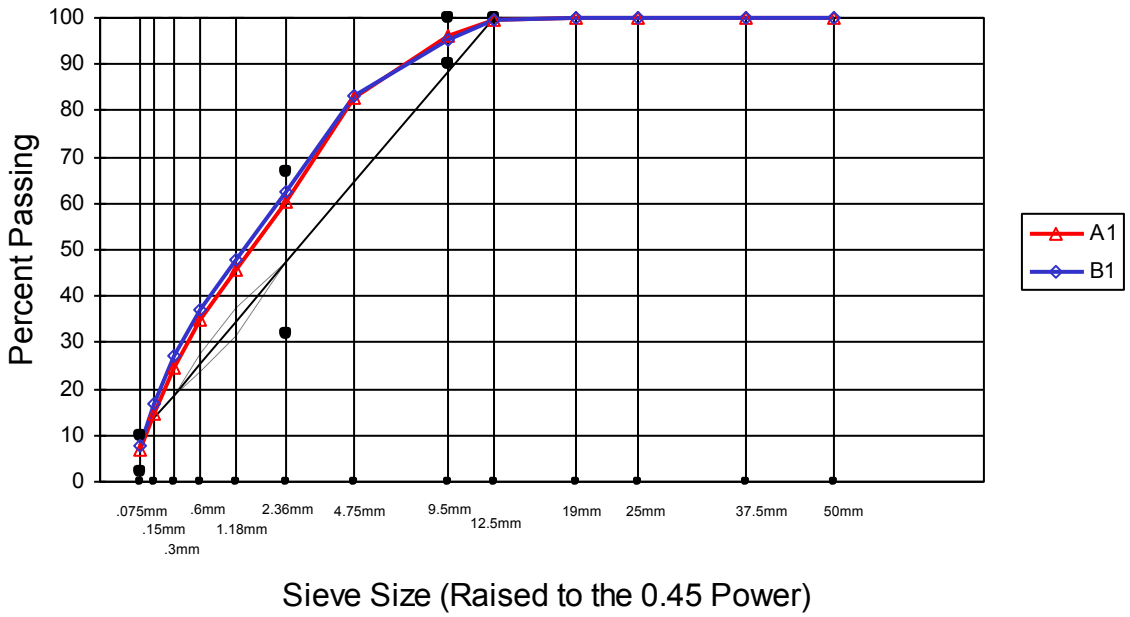

Figure C.51 Sieve analysis result from the 1st layer of US-74

Figure C.52 Sieve analysis result from the 2nd layer of US-74

Figure C.53 Sieve analysis result from the 3rd layer of US-74

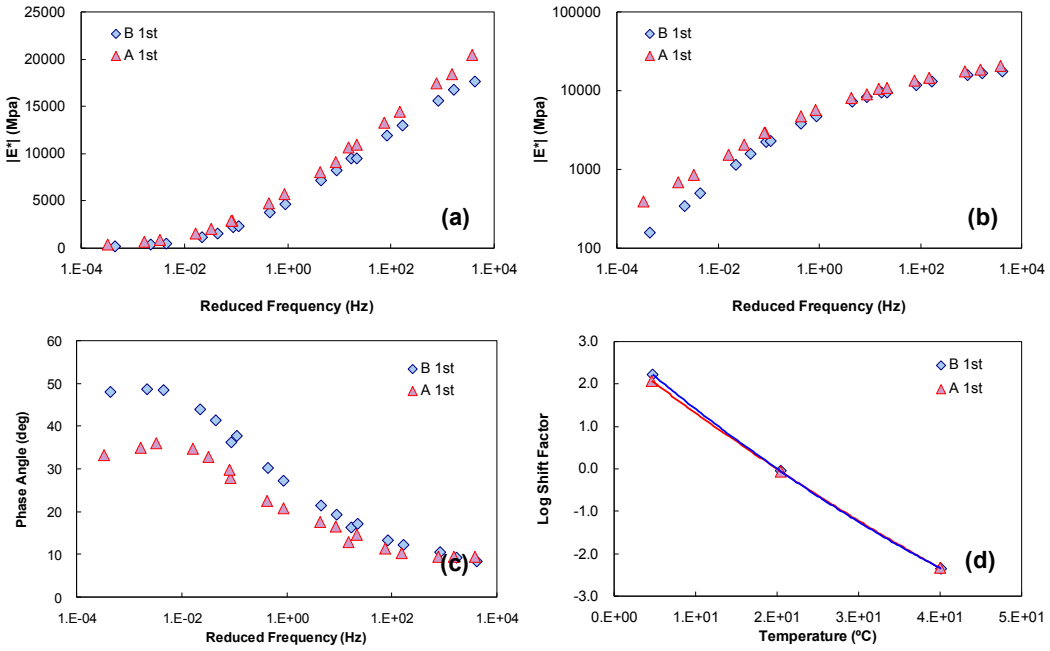

Figure C.54 Linear viscoelastic characteristics from 1st layer of field samples from US-74: (a) dynamic modulus in semi-log space, (b) dynamic modulus in log-log space, (c) phase angle and (d) shift factors

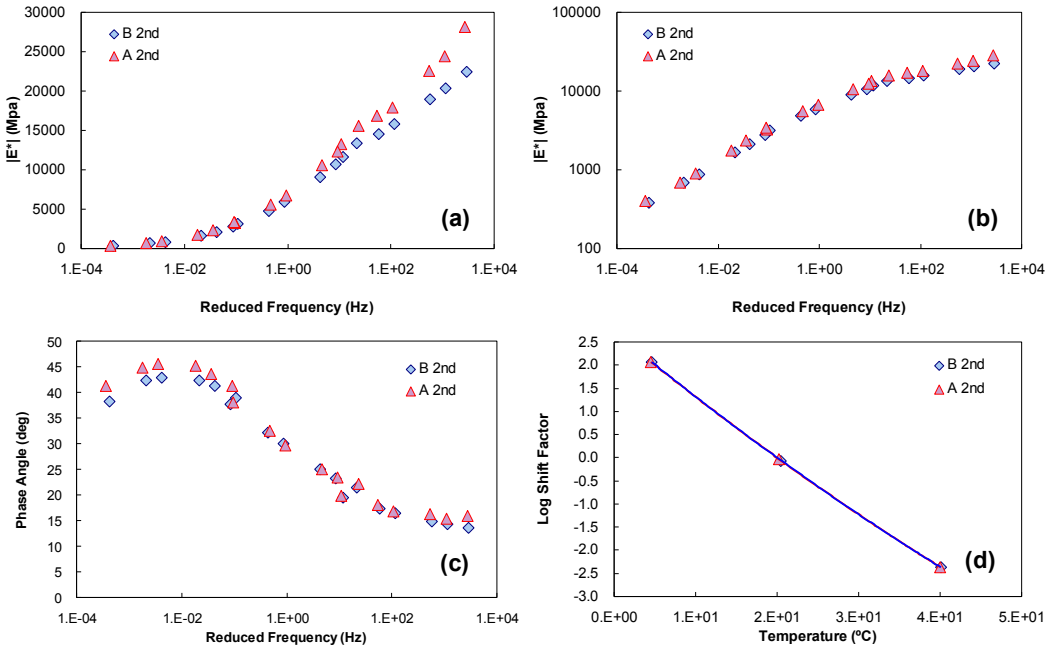

Figure C.55 Linear viscoelastic characteristics from 2nd layer of field samples from US-74: (a) dynamic modulus in semi-log space, (b) dynamic modulus in log-log space, (c) phase angle and (d) shift factors

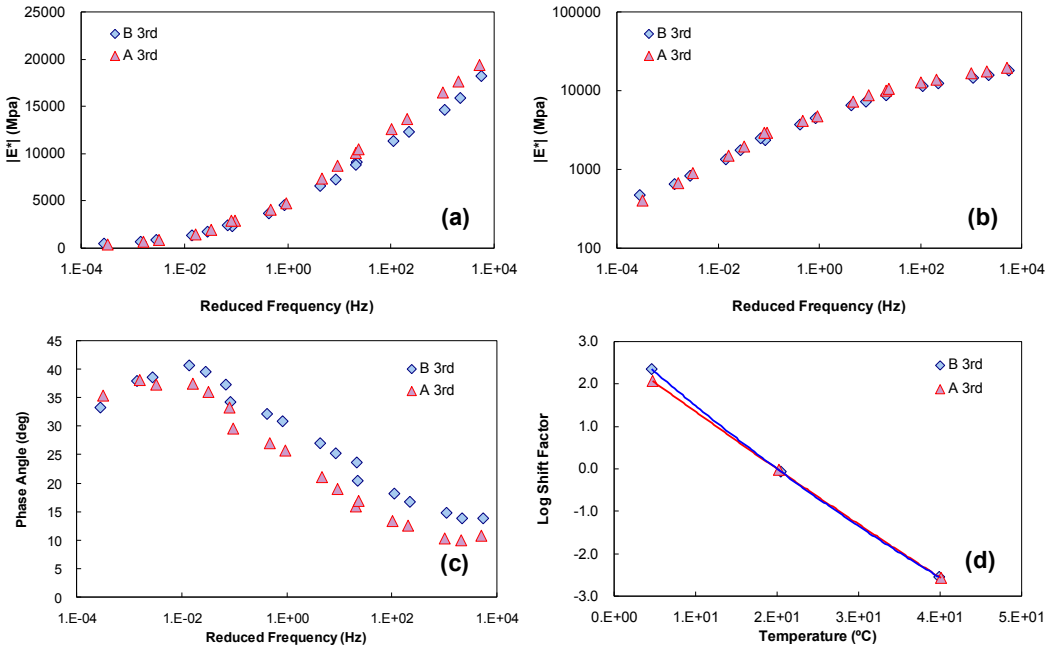

Figure C.56 Linear viscoelastic characteristics from 3rd layer of field samples from US-74: (a) dynamic modulus in semi-log space, (b) dynamic modulus in log-log space, (c) phase angle and (d) shift factors

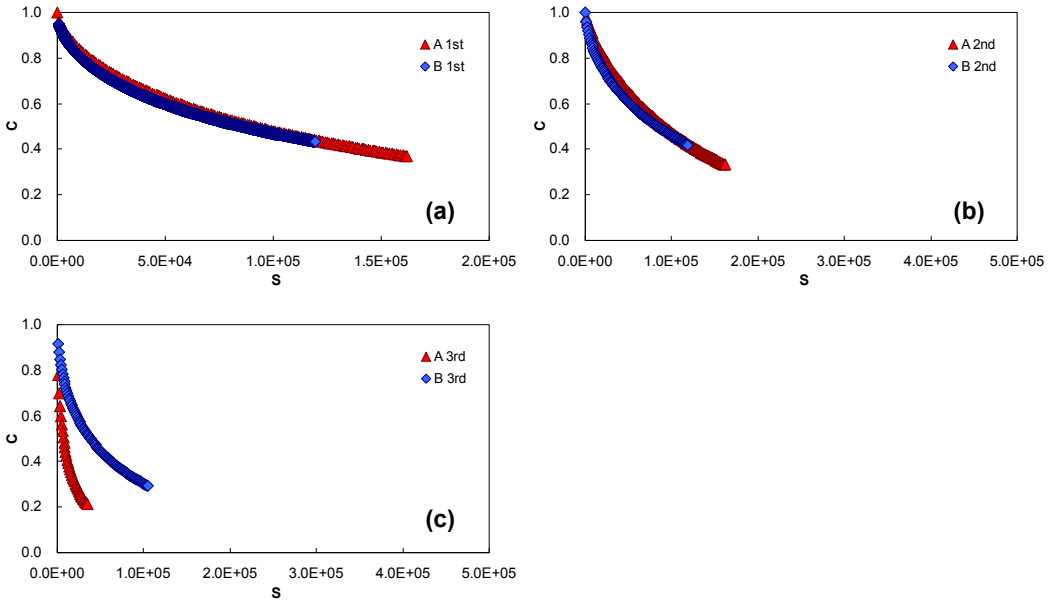

Figure C.57 Mixture damage characteristic curves for US-74pavement: (a) 1st layer, (b) 2nd layer, and (c) 3rd layer

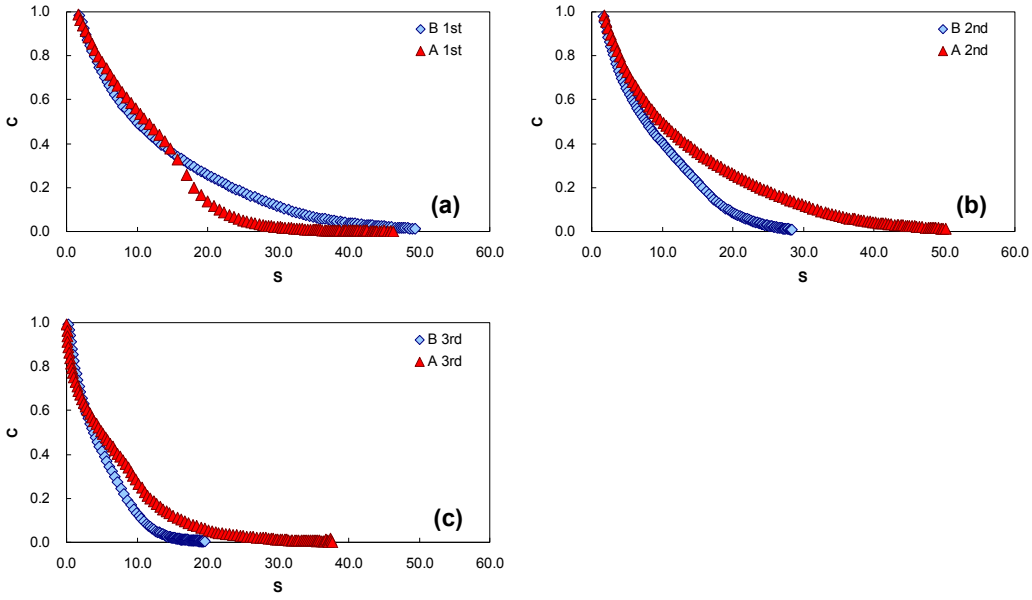

Figure C.58 Binder damage characteristic curves for US-74pavement: (a) 1st layer, (b) 2nd layer, and (c) 3rd layer

7. US Route 601 (Union County)

Table C.7 Summary of field data and field core test result for US-601

Cond. Region	TDC?	BUC?	ACI	TCI	Base Thick (mm)	Base Modulus (psi)	Subgrade Modulus (psi)	Layer	Air void (%)	Asphalt content (%)	NMSA (mm)
A1	Yes	Yes	92.9	100.0	227	119,925	43,486	1st	5.90	6.29	12.5
								2nd	5.90	6.30	12.5
								3rd	9.97	7.18	9.5
								4th	5.50	5.33	19.0
B1	Yes	Yes	90.9	100.0	238	54,294	21,834	1st	-	-	-
								2nd	-	-	-
								3rd	-	-	-
								4th	-	-	-
B2	No	Yes	96.7	100.0	243	60,092	15,215	1st	5.42	6.21	9.5
								2nd	6.14	6.51	12.5
								3rd	10.52	7.46	9.5
								4th	8.09	5.44	19.0

Figure C.59 Sieve analysis result from the 1st layer of US-601

Figure C.60 Sieve analysis result from the 2nd layer of US-601

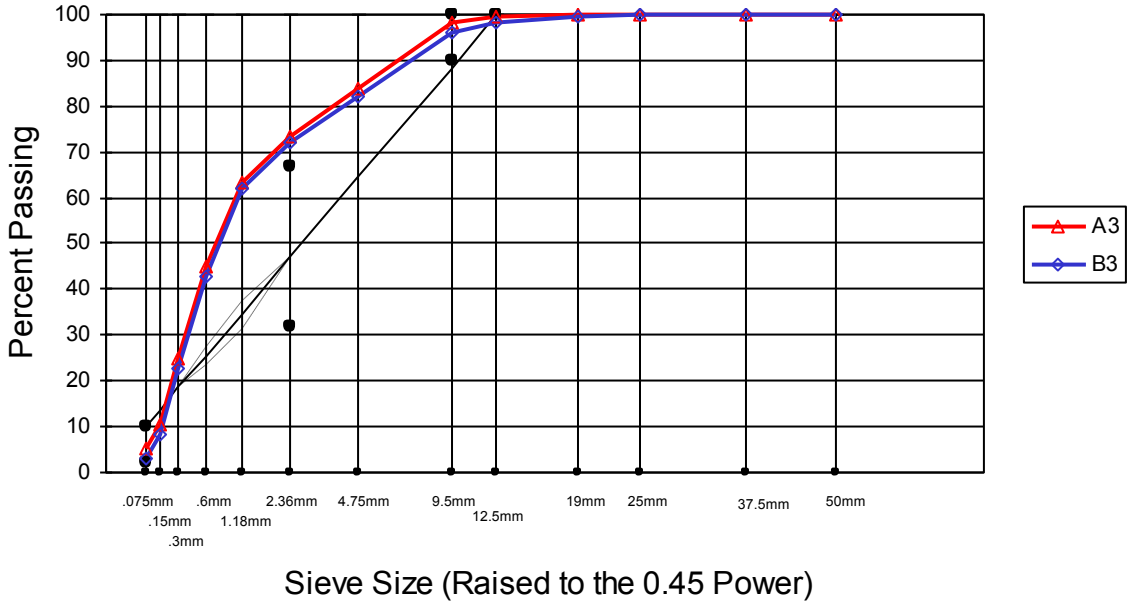

Figure C.61 Sieve analysis result from the 3rd layer of US-601

Figure C.62 Sieve analysis result from the 4th layer of US-601

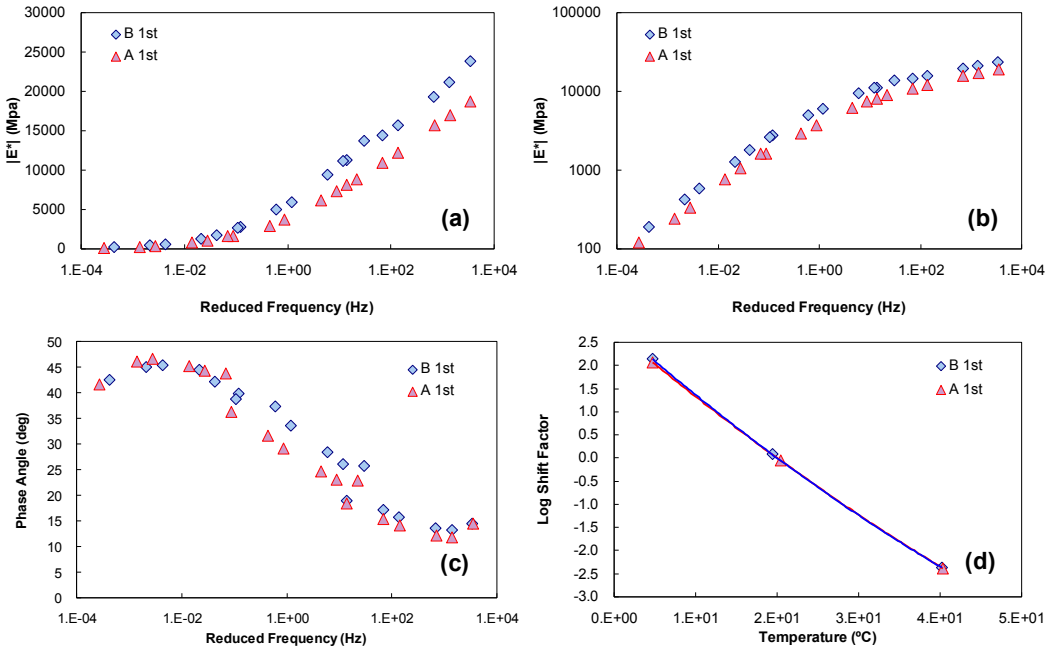

Figure C.63 Linear viscoelastic characteristics from 1st layer of field samples from US-601: (a) dynamic modulus in semi-log space, (b) dynamic modulus in log-log space, (c) phase angle and (d) shift factors

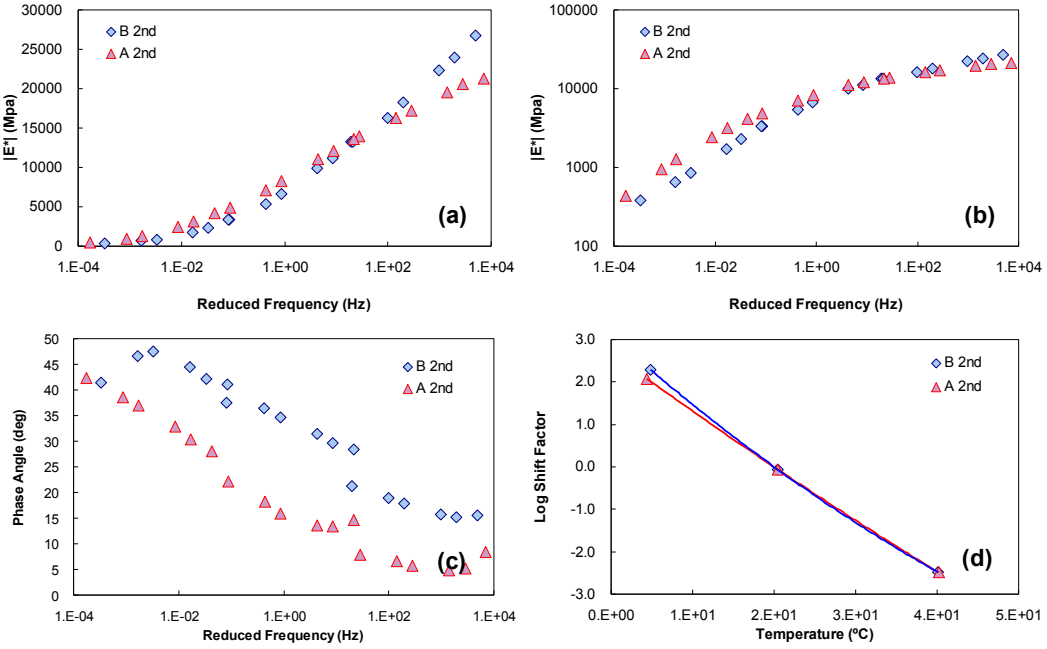

Figure C.64 Linear viscoelastic characteristics from 2nd layer of field samples from US-601: (a) dynamic modulus in semi-log space, (b) dynamic modulus in log-log space, (c) phase angle and (d) shift factors

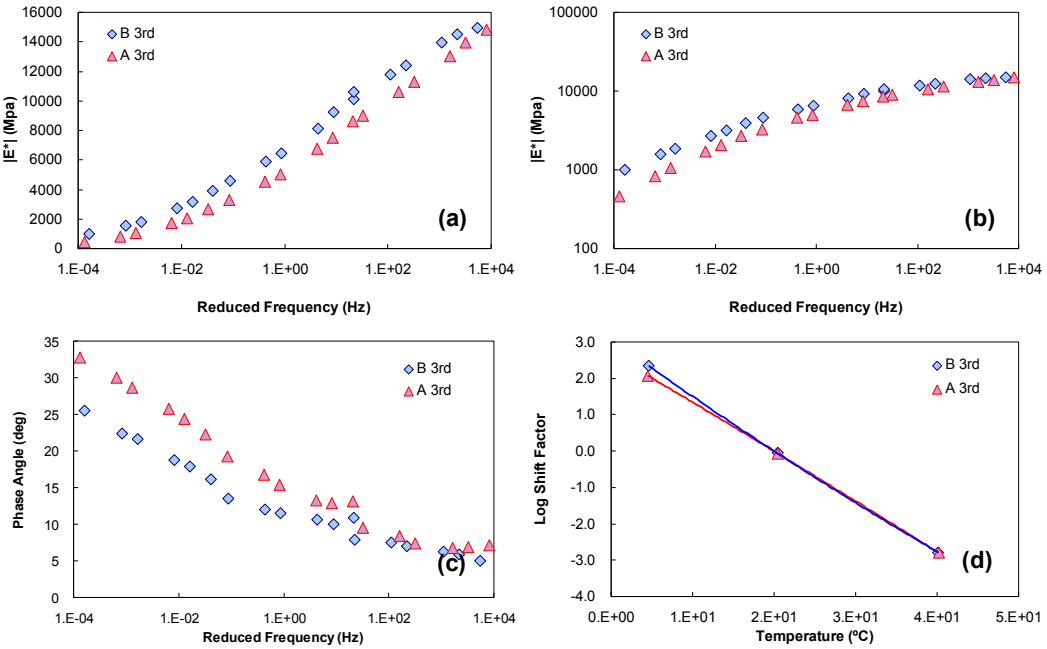

Figure C.65 Linear viscoelastic characteristics from 3rd layer of field samples from US-601: (a) dynamic modulus in semi-log space, (b) dynamic modulus in log-log space, (c) phase angle and (d) shift factors

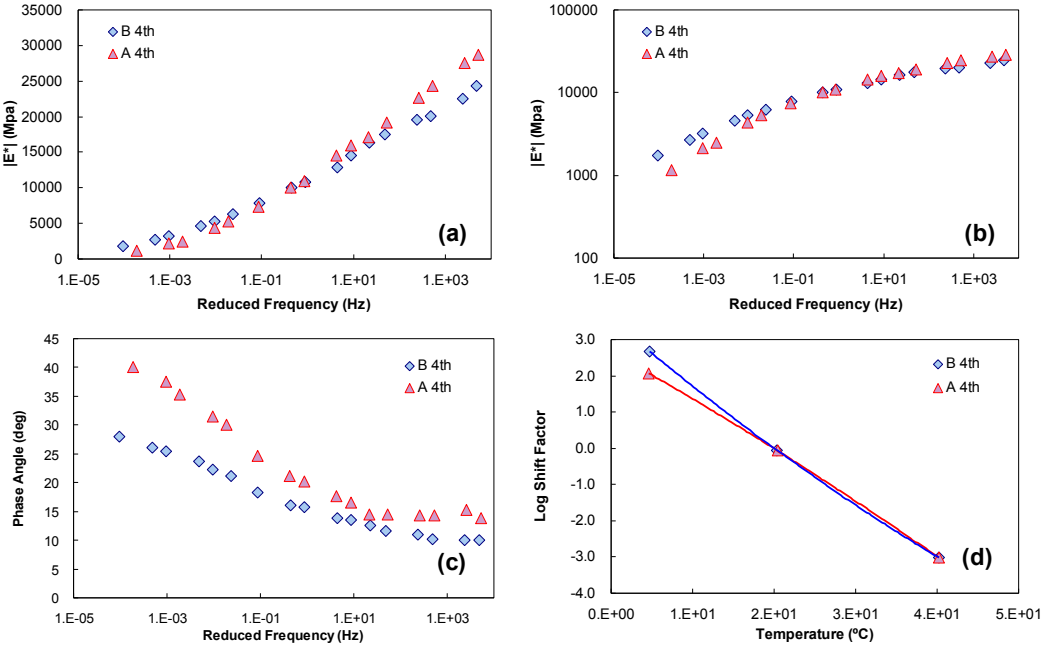

Figure C.66 Linear viscoelastic characteristics from 4th layer of field samples from US-601: (a) dynamic modulus in semi-log space, (b) dynamic modulus in log-log space, (c) phase angle and (d) shift factors

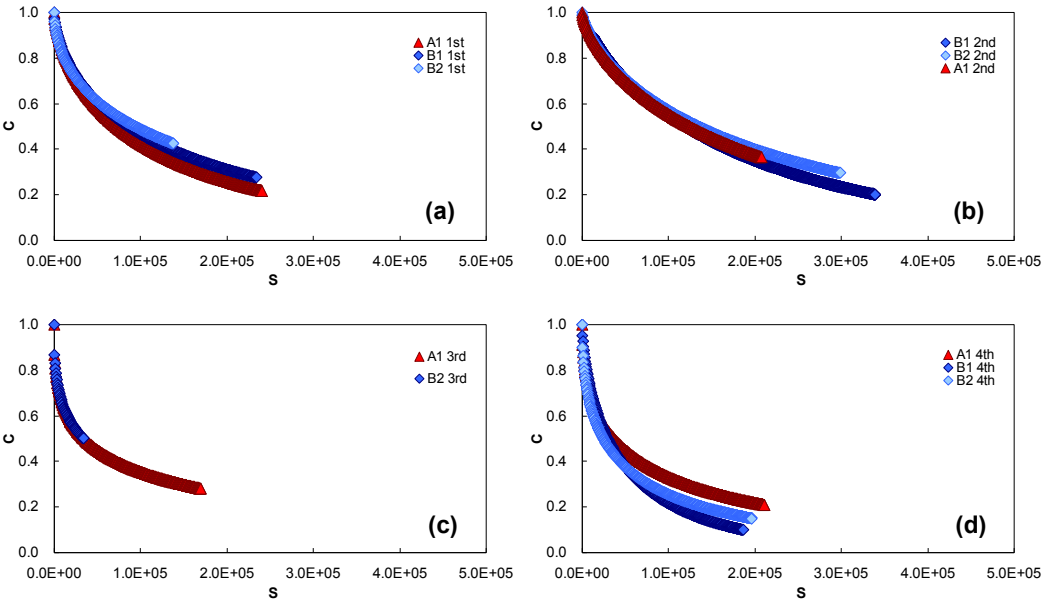

Figure C.67 Mixture damage characteristic curves for US-601pavement: (a) 1st layer, (b) 2nd layer, (c) 3rd layer, and (d) 4th layer

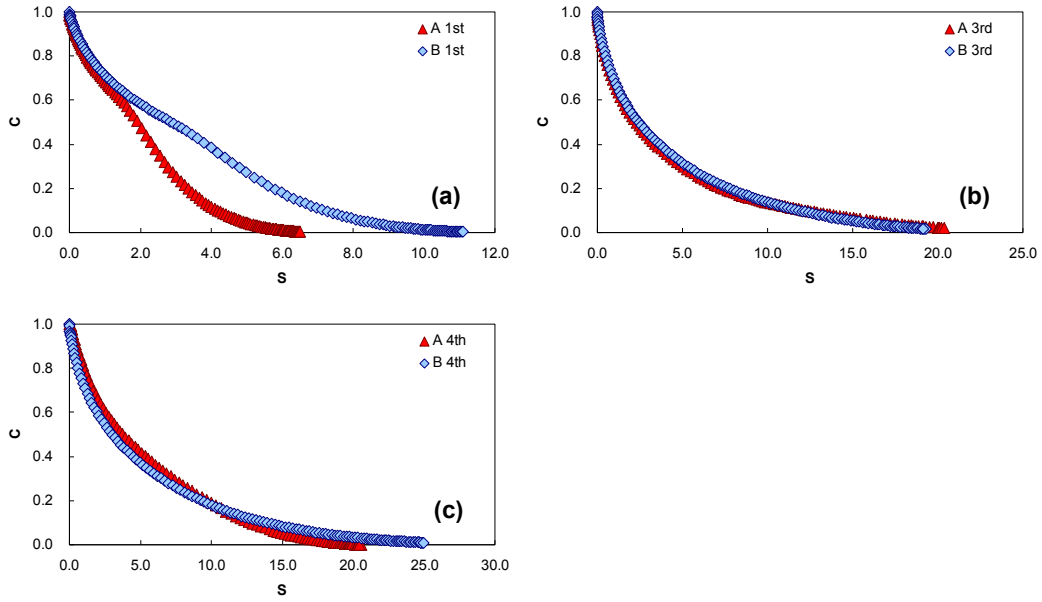

Figure C.68 Binder damage characteristic curves for US-601pavement: (a) 1st layer, (b) 3rd layer, and (c) 4th layer

8. NC Route 209 (Swain County)

Table C.8 Summary of field data and field core test result for NC-209

Cond. Region	TDC?	BUC?	ACI	TCI	Base Thick (mm)	Base Modulus (psi)	Subgrade Modulus (psi)	Layer	Air void (%)	Asphalt content (%)	NMSA (mm)
A1	No	No	100.0	100.0	260	88,331	20,638	1st	7.31	7.01	9.50
								2nd	7.39	6.49	9.50
								3rd	8.31	4.68	19.00
B1	No	No	95.9	100.0	280	89,583	25,258	1st	5.04	7.01	9.50
								2nd	6.84	6.49	9.50
								3rd	6.23	4.68	19.00

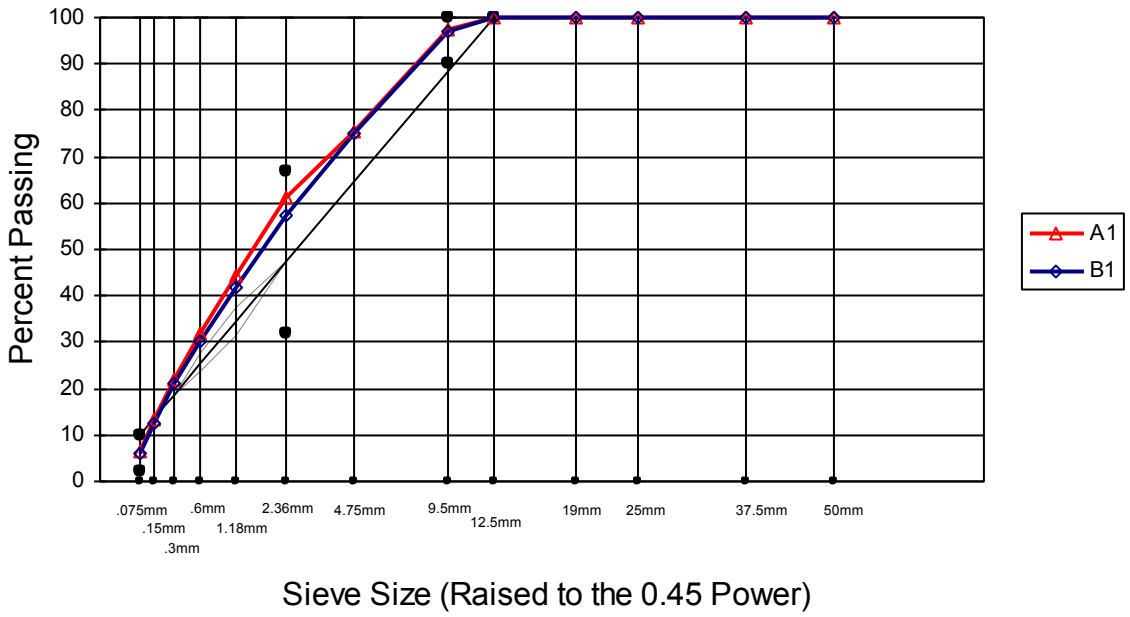

Figure C.69 Sieve analysis result from the 1st layer of NC-209

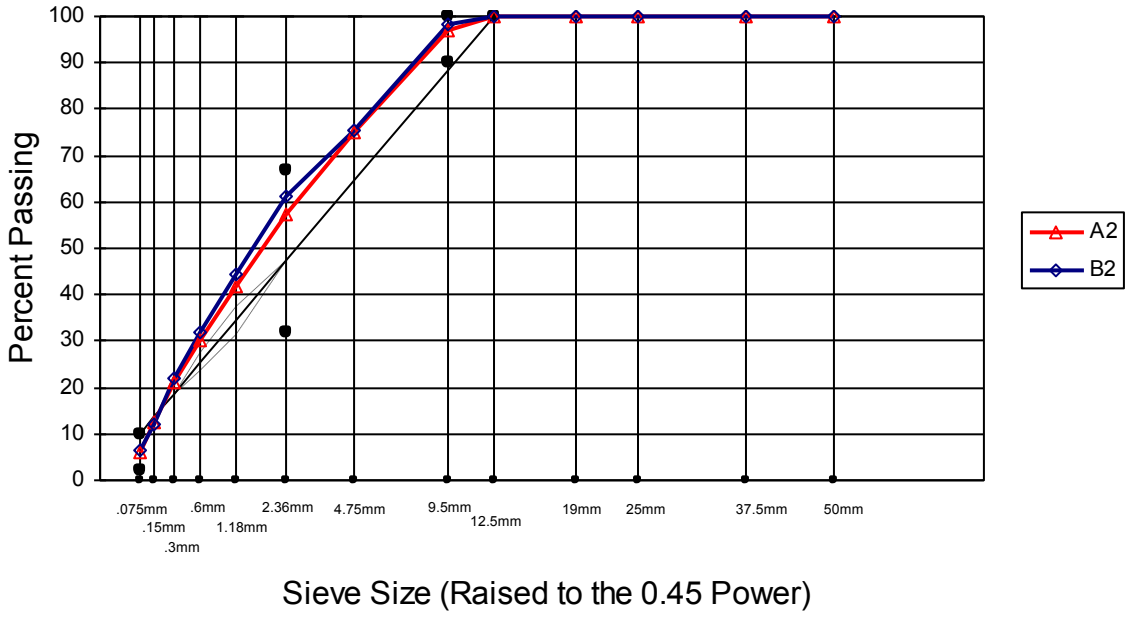

Figure C.70 Sieve analysis result from the 2nd layer of NC-209

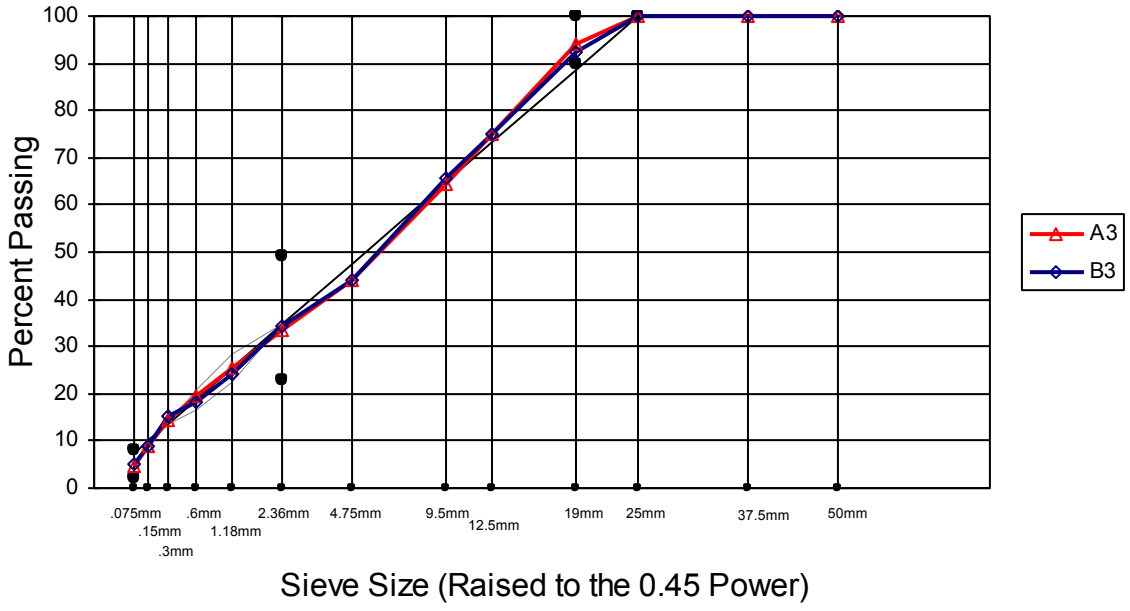

Figure C.71 Sieve analysis result from the 3rd layer of NC-209

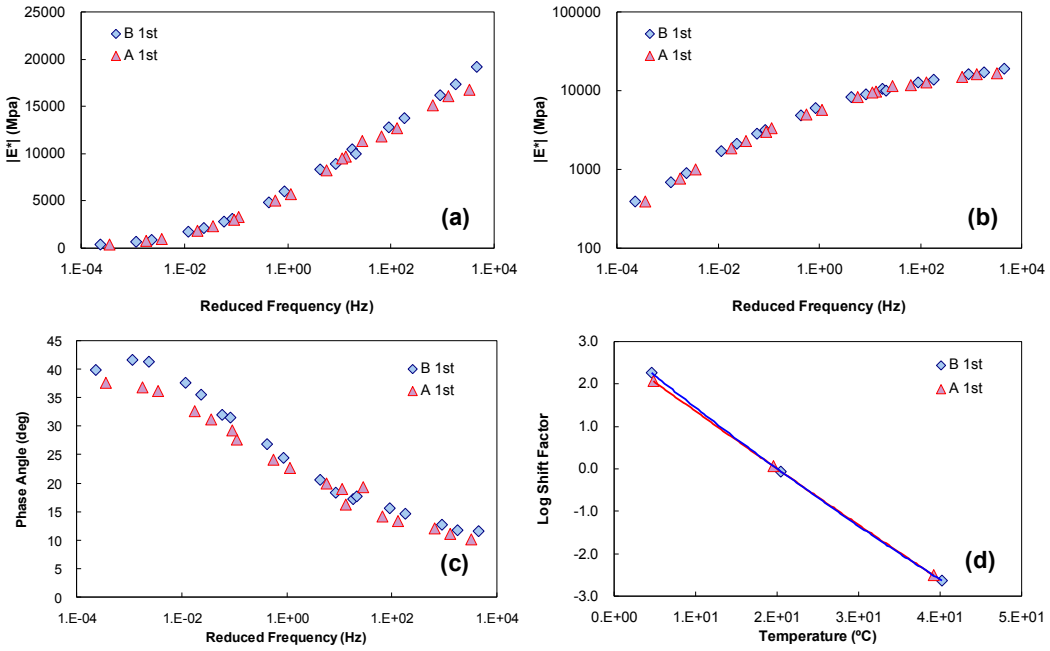

Figure C.72 Linear viscoelastic characteristics from 1st layer of field samples from NC-209: (a) dynamic modulus in semi-log space, (b) dynamic modulus in log-log space, (c) phase angle and (d) shift factors

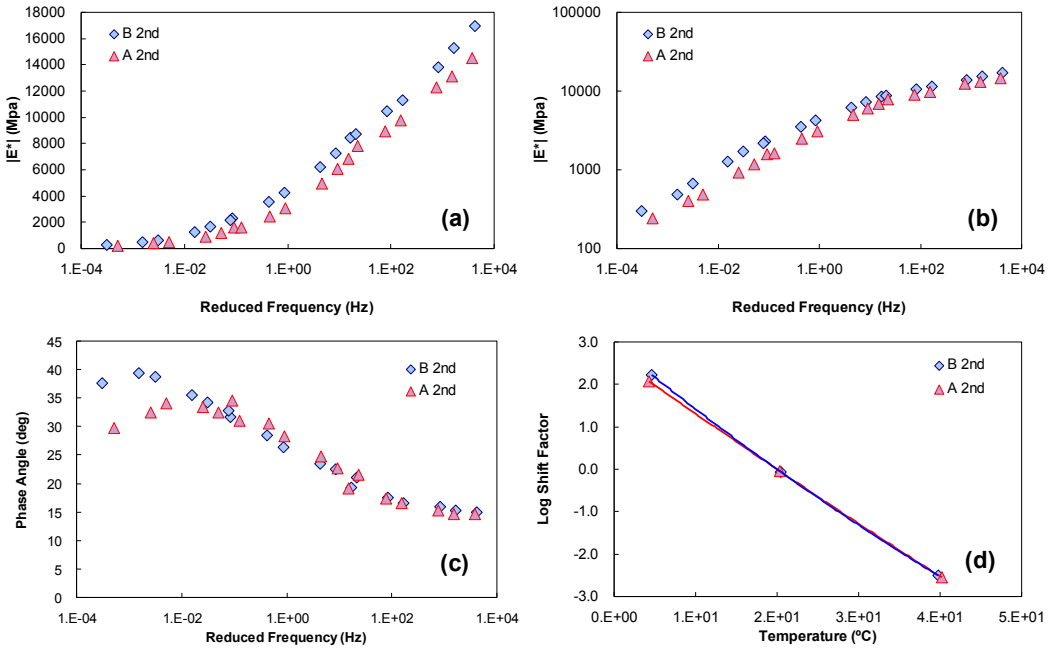

Figure C.73 Linear viscoelastic characteristics from 2nd layer of field samples from NC-209: (a) dynamic modulus in semi-log space, (b) dynamic modulus in log-log space, (c) phase angle and (d) shift factors

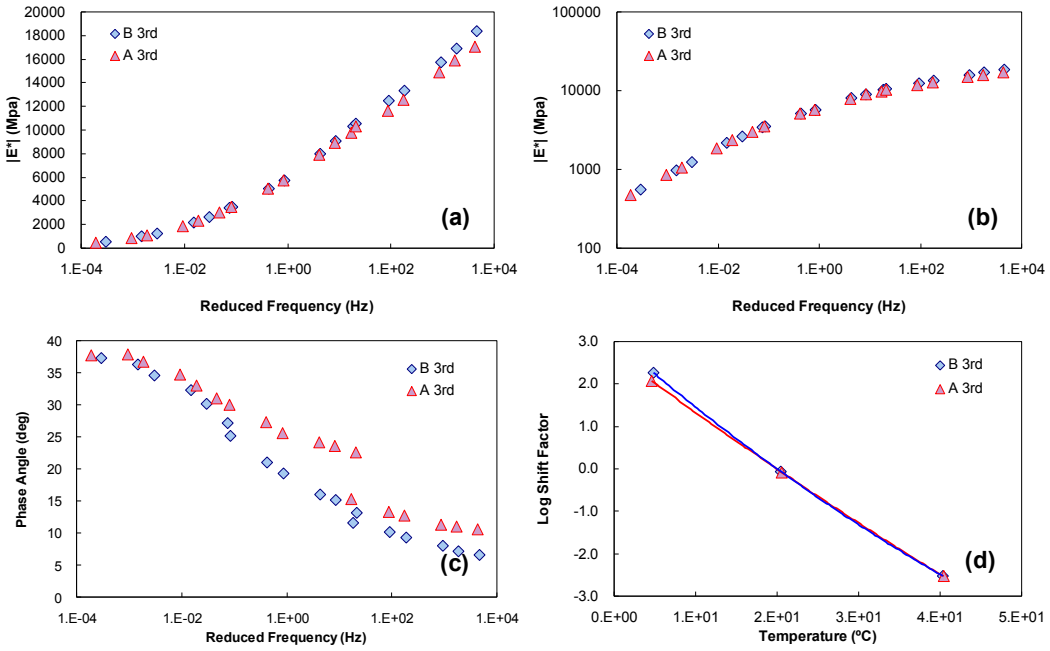

Figure C.74 Linear viscoelastic characteristics from 3rd layer of field samples from NC-209: (a) dynamic modulus in semi-log space, (b) dynamic modulus in log-log space, (c) phase angle and (d) shift factors

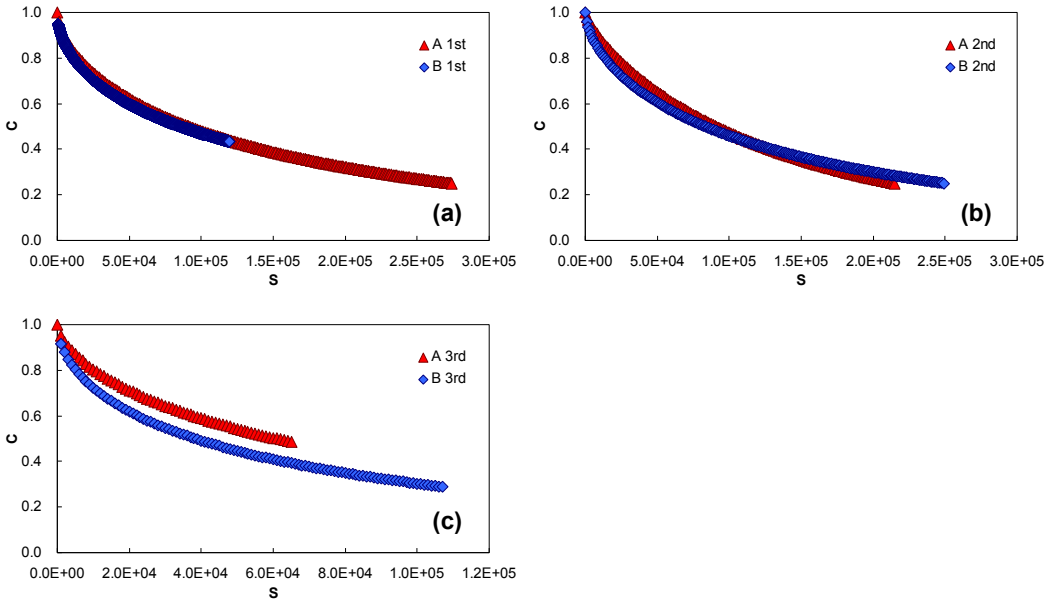

Figure C.75 Mixture damage characteristic curves for NC-209 pavement: (a) 1st layer, (b) 2nd layer, and (c) 3rd layer

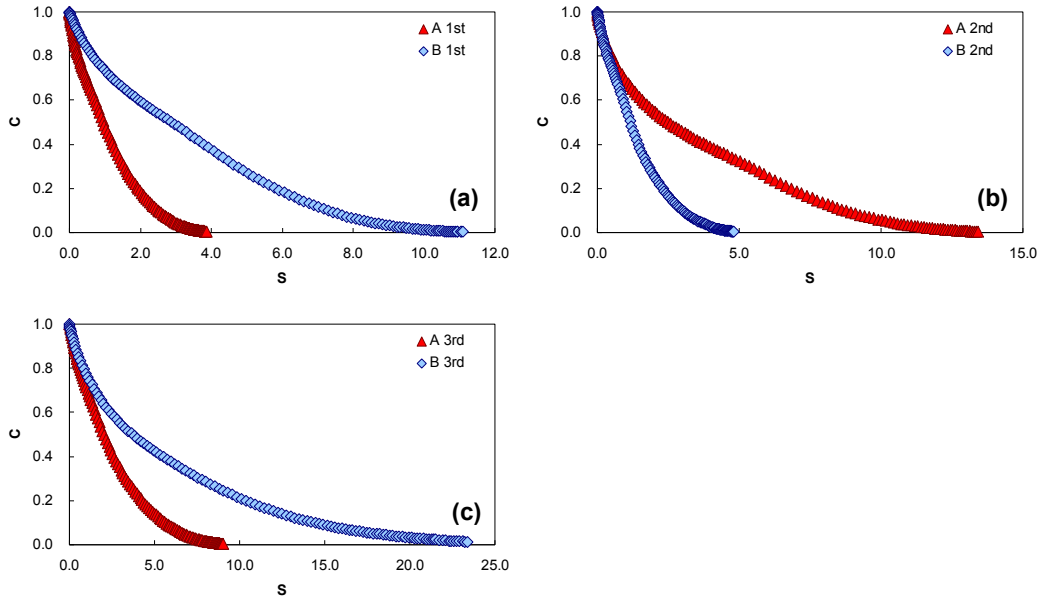

Figure C.76 Binder damage characteristic curves for NC-209 pavement: (a) 1st layer, (b) 2nd layer, and (c) 3rd layer

9. US Route 76 (New Hanover County)

Table C.9 Summary of field data and field core test result for US-76

Cond. Region	TDC?	BUC?	ACI	TCI	Base Thick (mm)	Base Modulus (psi)	Subgrade Modulus (psi)	Layer	Air void (%)	Asphalt content (%)	NMSA (mm)
B1	Yes	No	75.2	96.0	240.00	73,730	28,668	1st	8.09	6.94	9.5
								2nd	10.51	6.37	9.5
								3rd	11.00	5.50	9.5
A1	Yes	Yes	96.7	100.0	290.00	32,897	28,370	1st	8.57	6.78	9.5
								2nd	11.10	5.94	9.5
								3rd	14.63	5.38	19.0

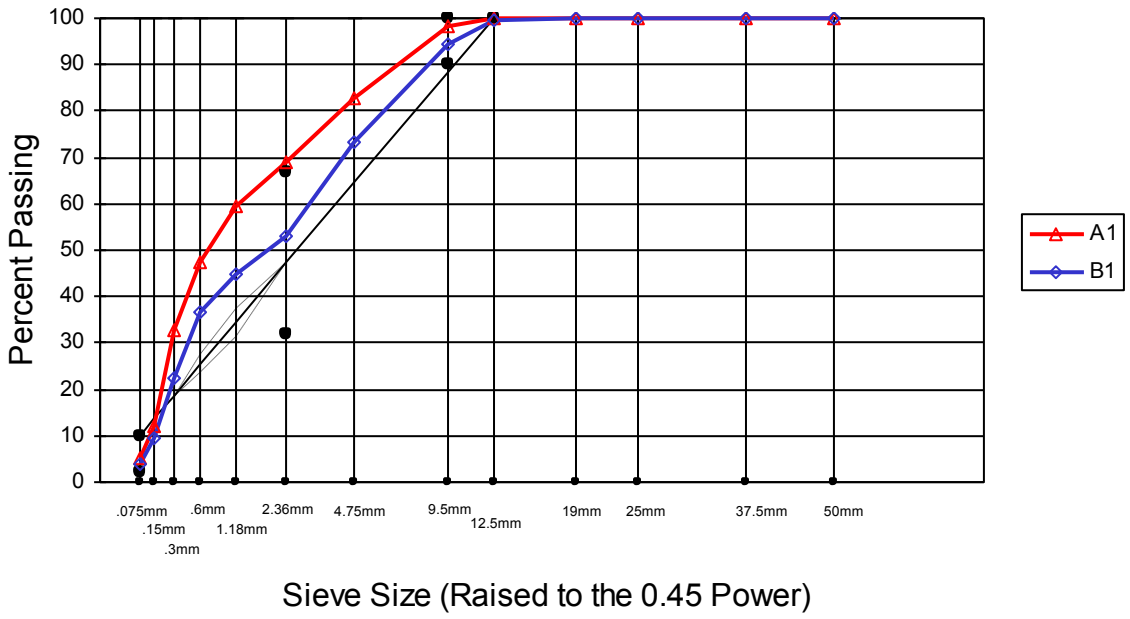

Figure C.77 Sieve analysis result from the 1st layer of US-76

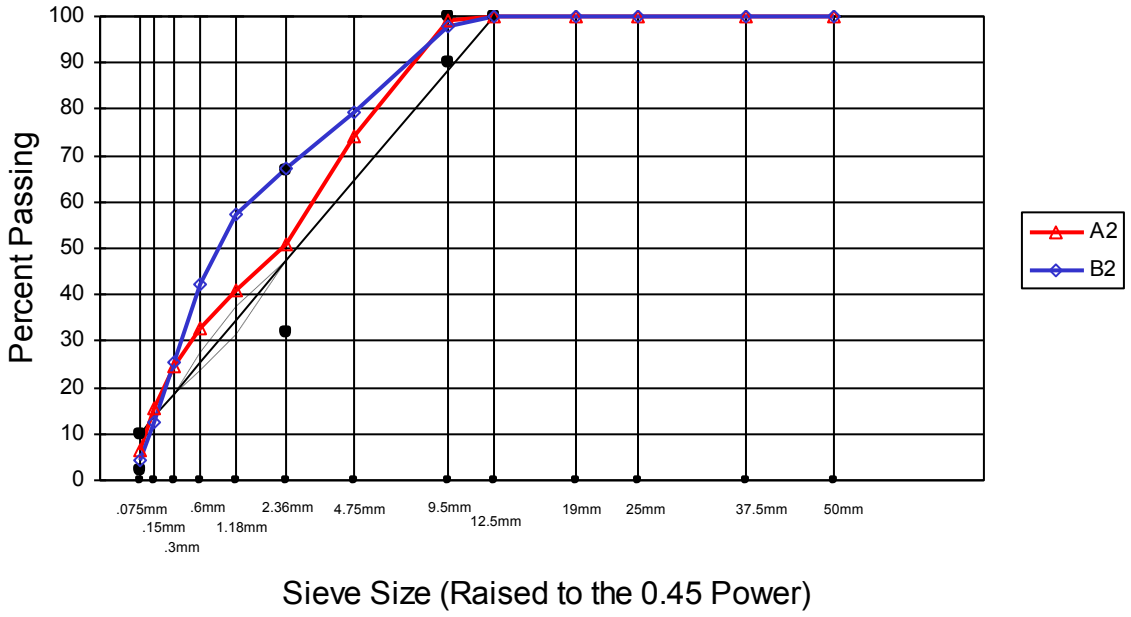

Figure C.78 Sieve analysis result from the 2nd layer of US-76

Figure C.79 Sieve analysis result from the 3rd layer of US-76

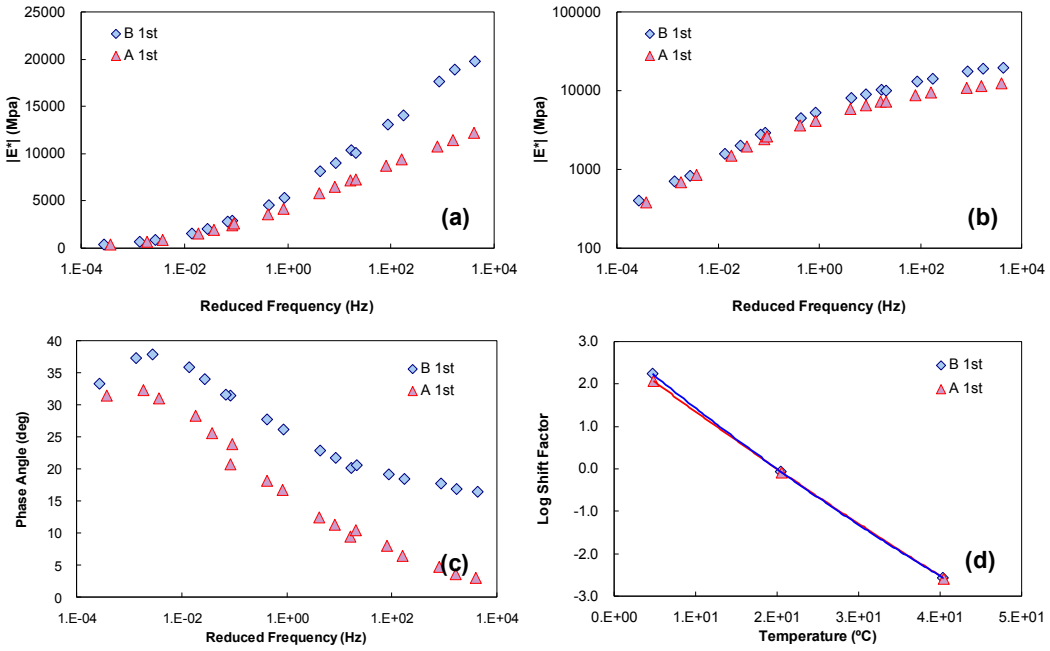

Figure C.80 Linear viscoelastic characteristics from 1st layer of field samples from US-76: (a) dynamic modulus in semi-log space, (b) dynamic modulus in log-log space, (c) phase angle and (d) shift factors

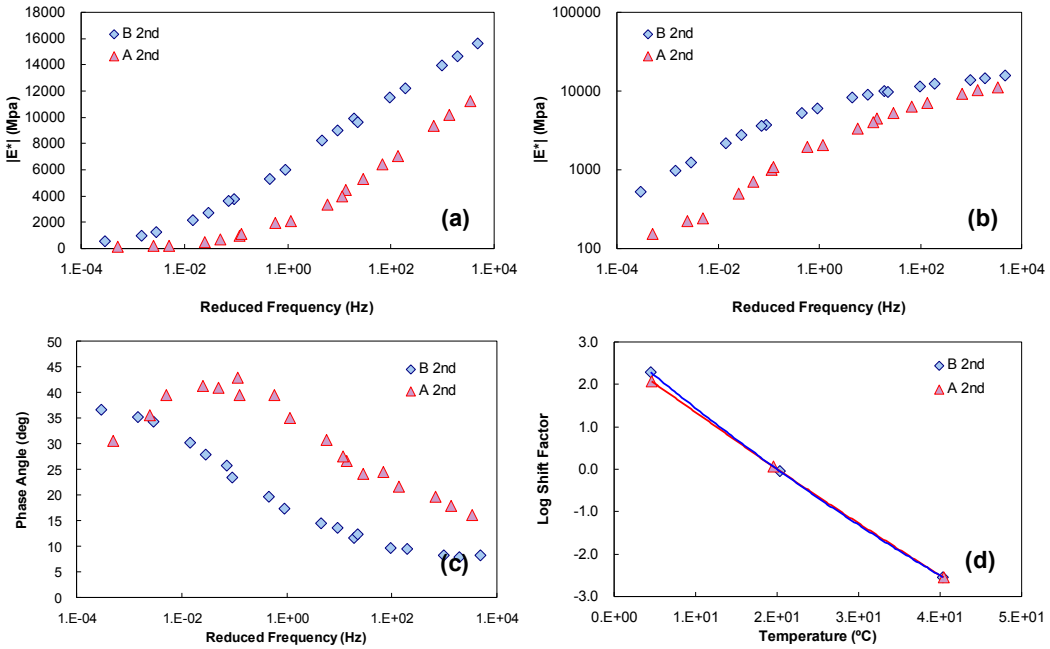

Figure C.81 Linear viscoelastic characteristics from 2nd layer of field samples from US-76: (a) dynamic modulus in semi-log space, (b) dynamic modulus in log-log space, (c) phase angle and (d) shift factors

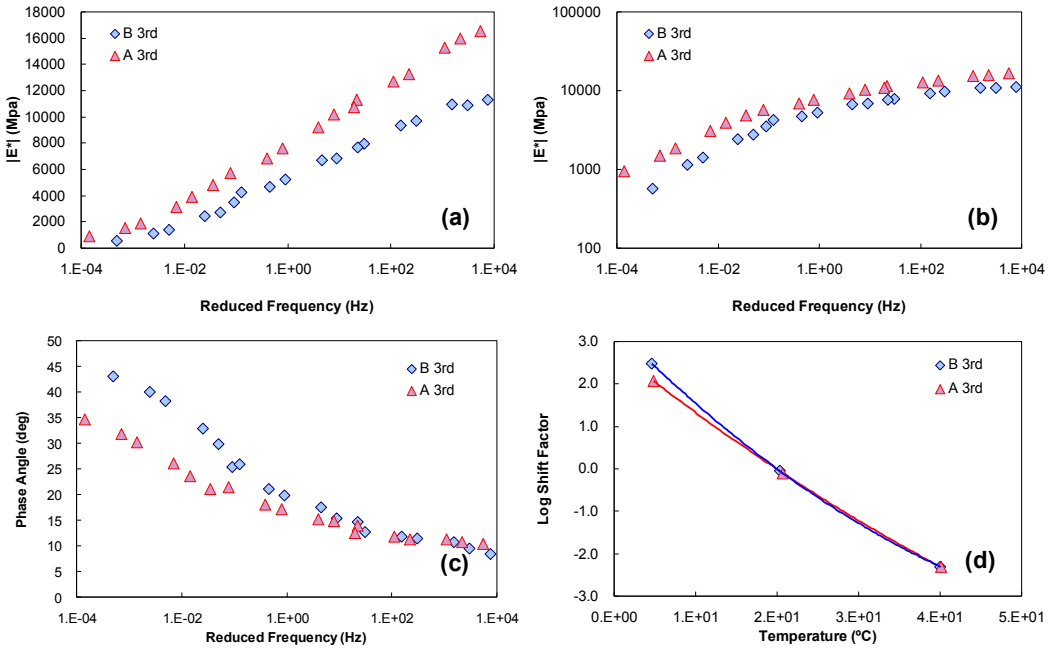

Figure C.82 Linear viscoelastic characteristics from 3rd layer of field samples from US-76: (a) dynamic modulus in semi-log space, (b) dynamic modulus in log-log space, (c) phase angle and (d) shift factors

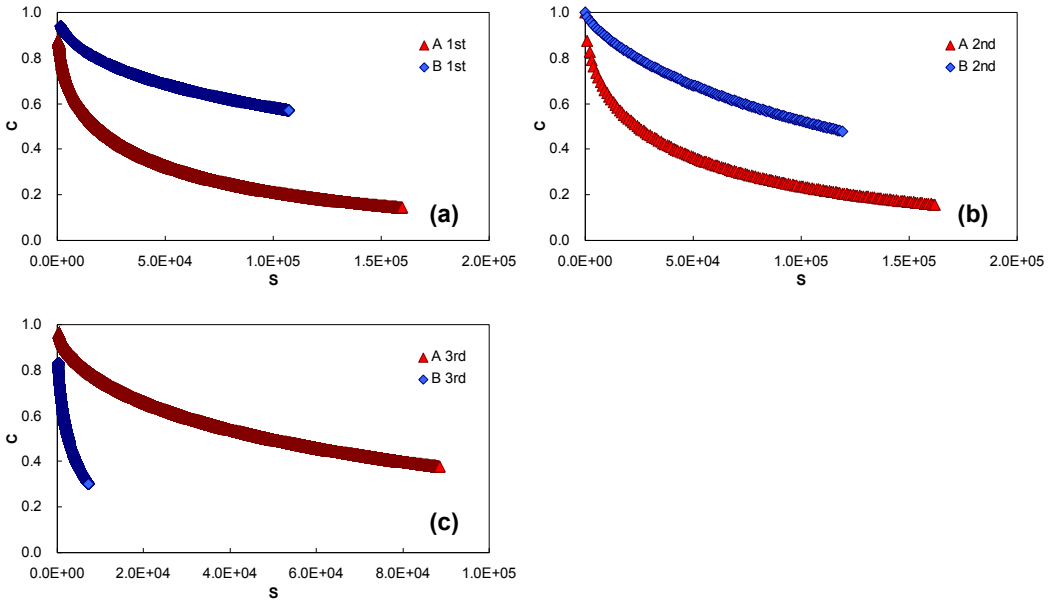

Figure C.83 Mixture damage characteristic curves for US-76 pavement: (a) 1st layer, (b) 2nd layer, and (c) 3rd layer

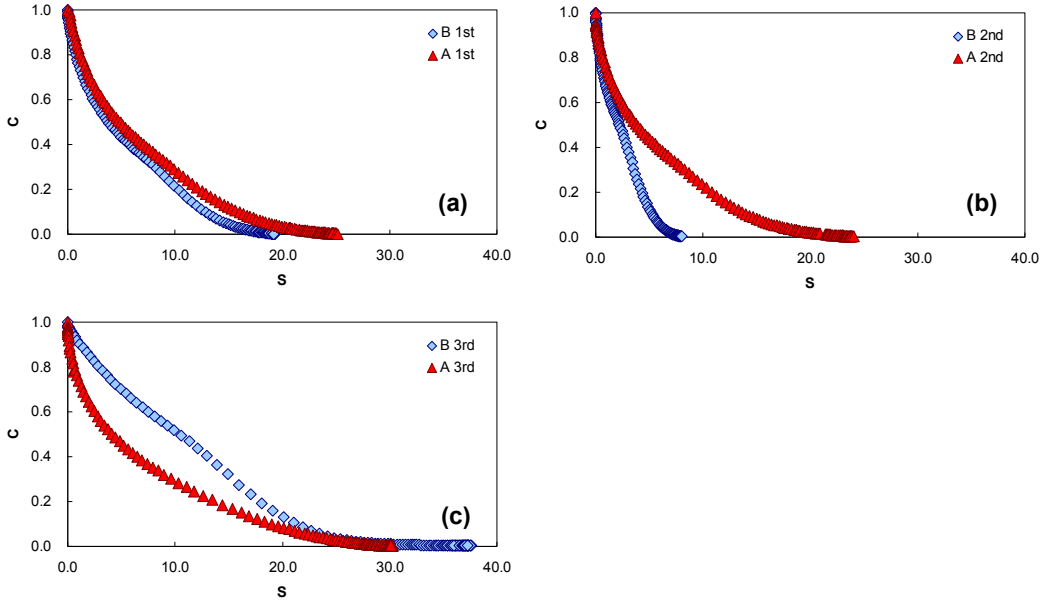

Figure C.84 Binder damage characteristic curves for US-76 pavement: (a) 1st layer, (b) 2nd layer, and (c) 3rd layer

10. NC Route 194 (Avery County)

Figure C.85 Sieve analysis result from the 1st layer of NC-194

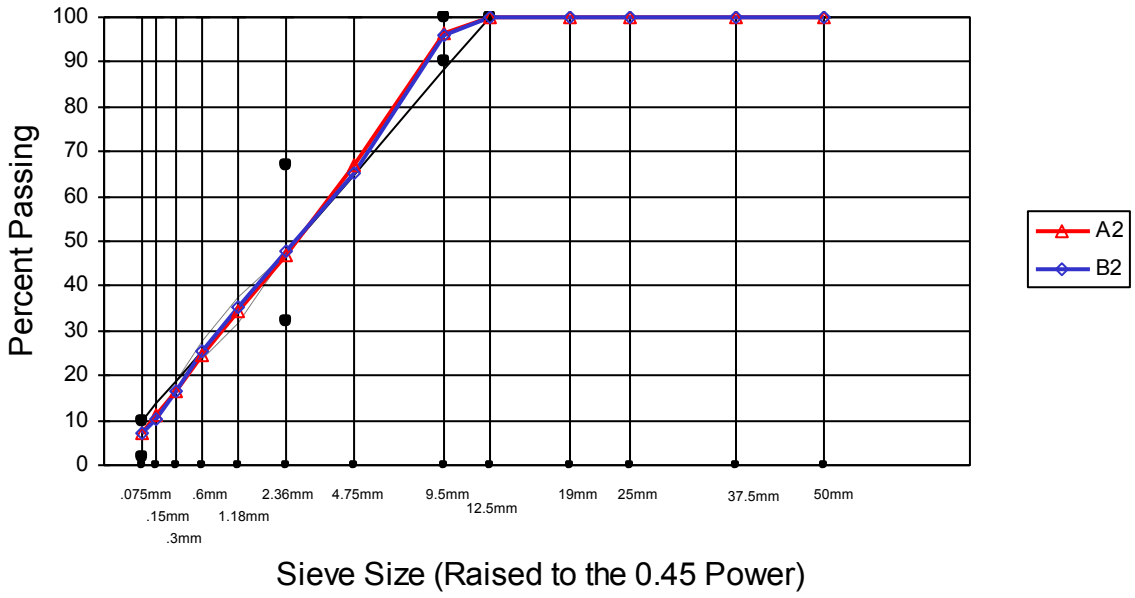

Figure C.86 Sieve analysis result from the 2nd layer of NC-194

Figure C.87 Sieve analysis result from the 3rd layer of NC-194

Figure C.88 Sieve analysis result from the 4th layer of NC-194

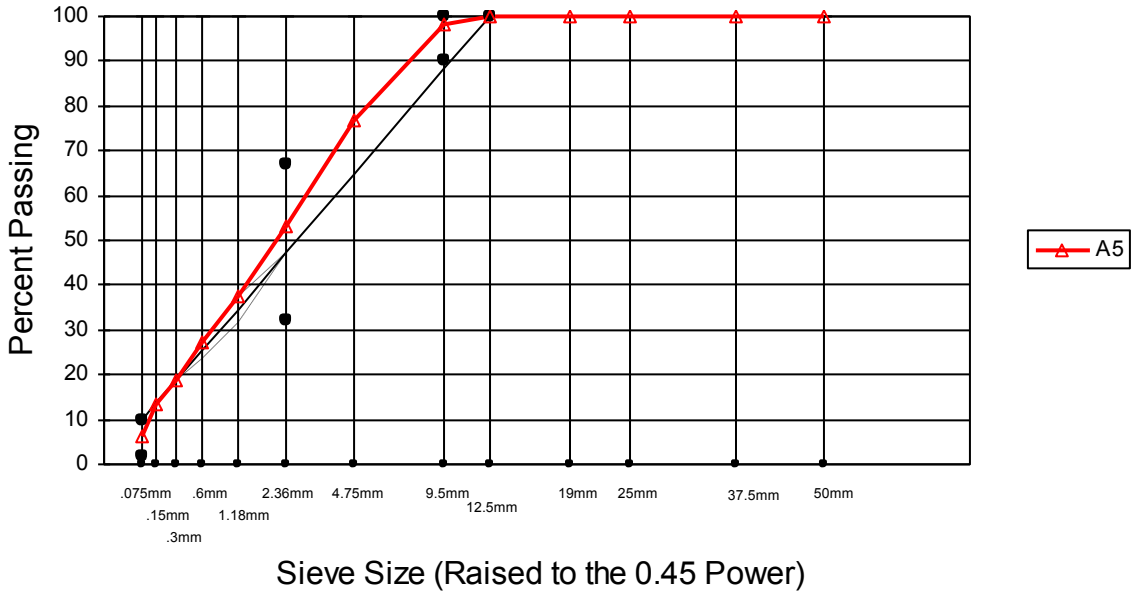

Figure C.89 Sieve analysis result from the 5th layer of NC-194

11. US Route 13 (Martin County)

Figure C.90 Sieve analysis result from the 1st layer of US-13

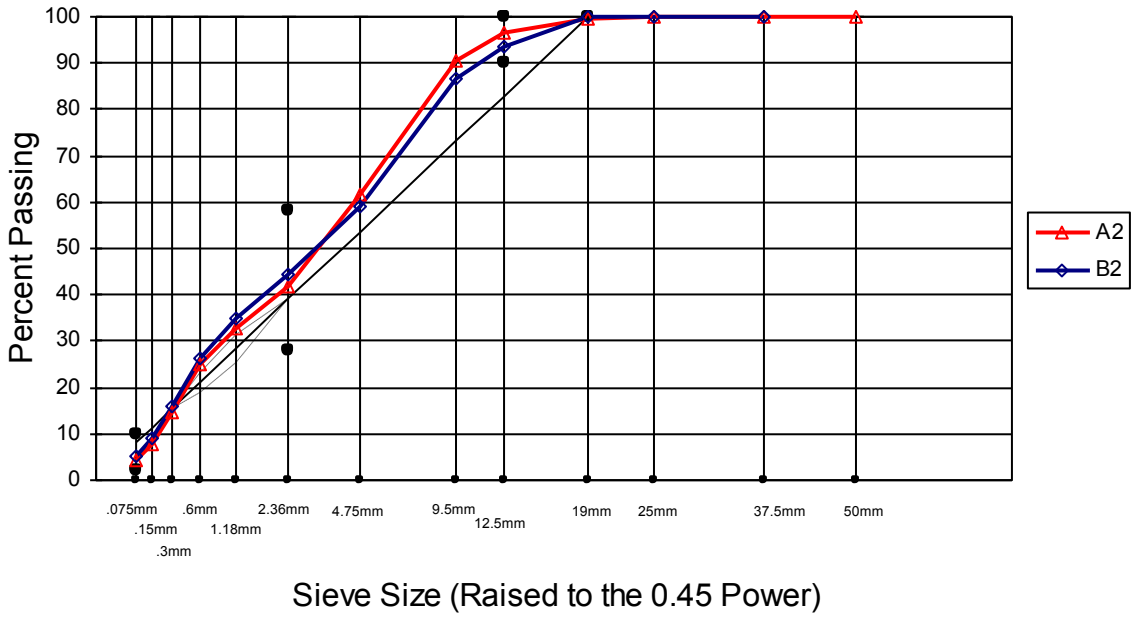

Figure C.91 Sieve analysis result from the 2nd layer of US-13

Figure C.92 Sieve analysis result from the 3rd layer of US-13

12. NC Route 177 (Richmond County)

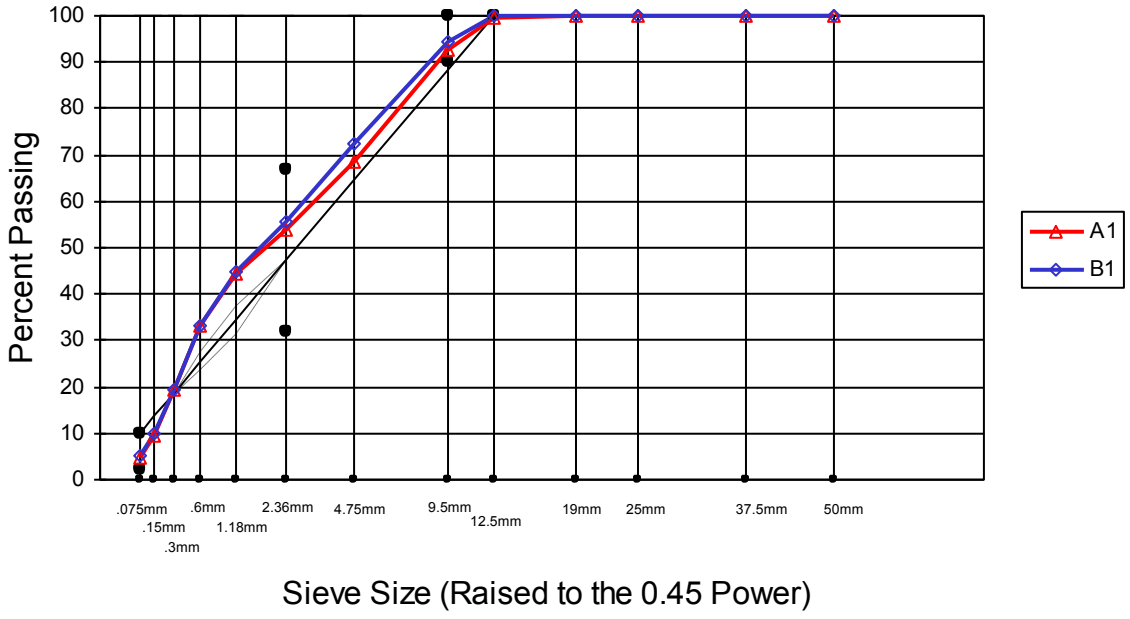

Figure C.93 Sieve analysis result from the 1st layer of NC-177

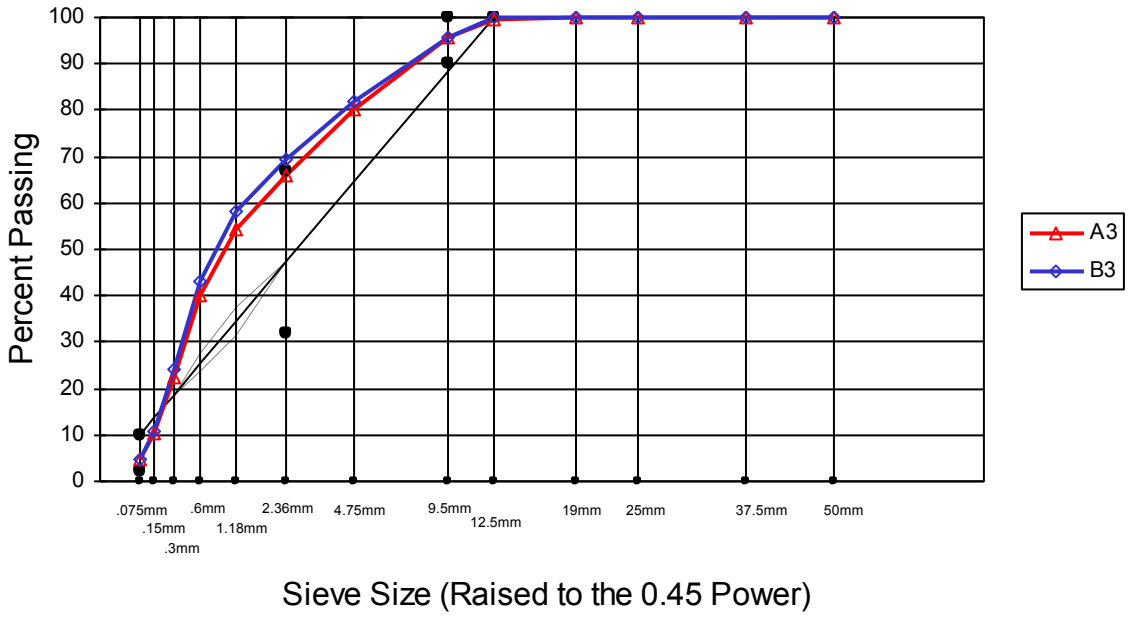

Figure C.94 Sieve analysis result from the 3rd layer of NC-177

12. State Route 1530 (Alamance County)

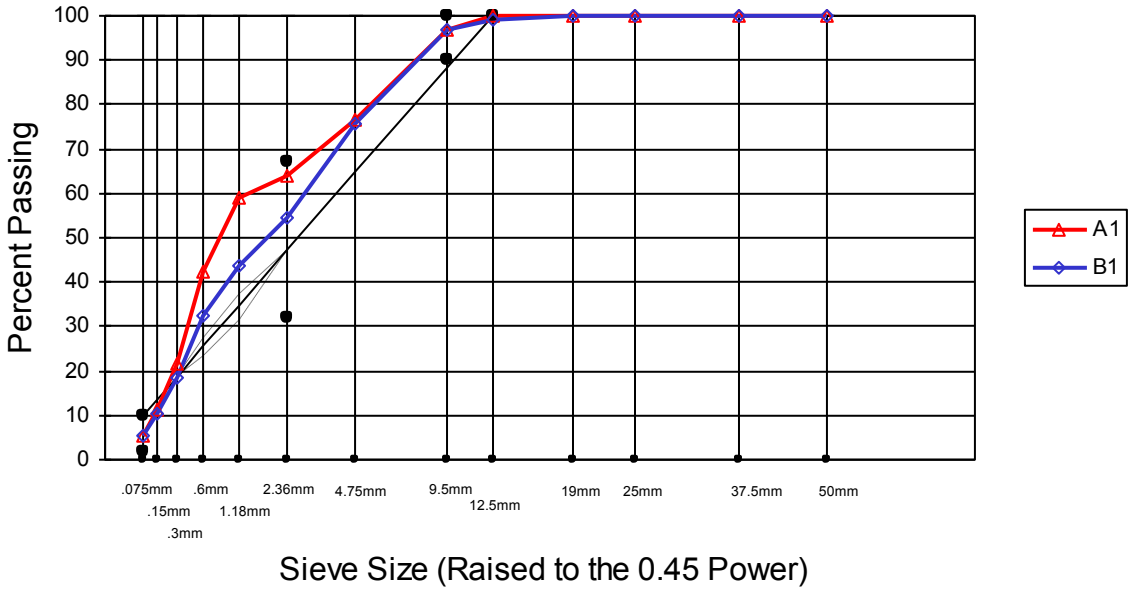

Figure C.95 Sieve analysis result from the 1st layer of SR-1530

Figure C.96 Sieve analysis result from the 2nd layer of SR-1530

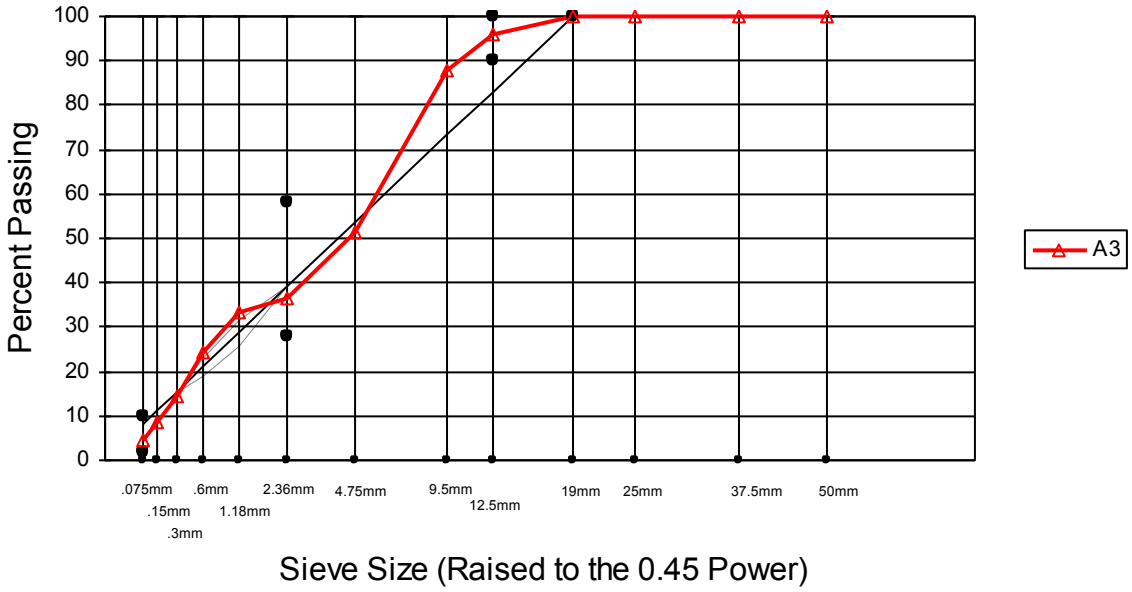

Figure C.97 Sieve analysis result from the 3rd layer of SR-1530

Figure C.98 Sieve analysis result from the 4th layer of SR-1530

Figure C.99 Sieve analysis result from the 5th layer of SR-1530

14. NC Route 47 (Davidson County)

Figure C.100 Sieve analysis result from the 1st layer of NC-47

Figure C.101 Sieve analysis result from the 2nd layer of NC-47

Figure C.102 Sieve analysis result from the 3rd layer of NC-47

15. US Route 220 (Montgomery County)

Figure C.103 Sieve analysis result from the 1st layer of US-220

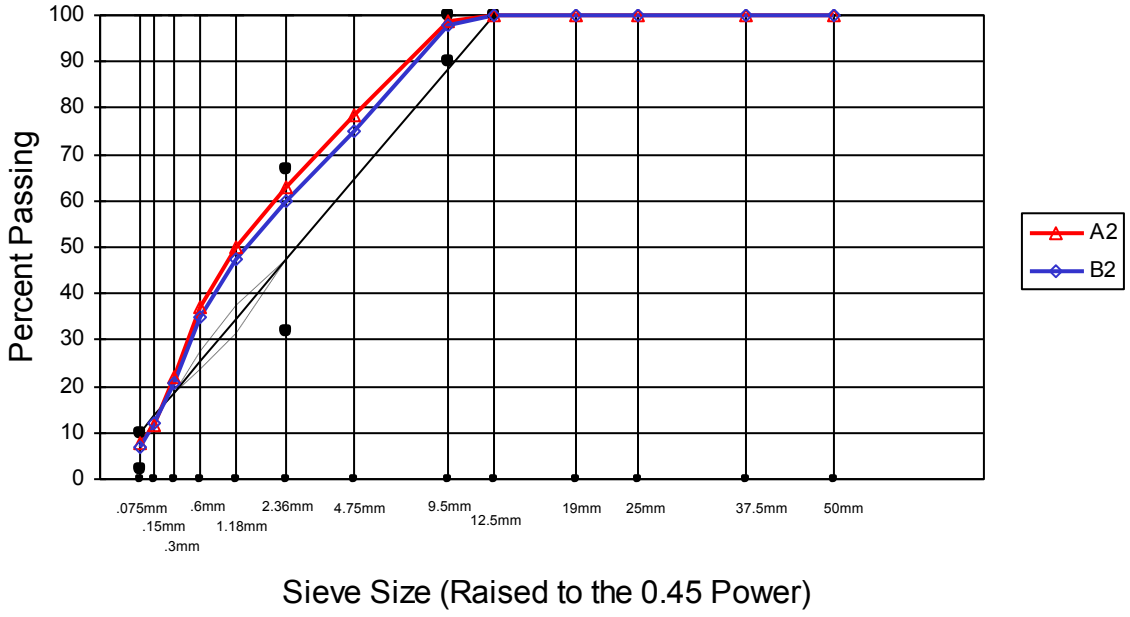

Figure C.104 Sieve analysis result from the 2nd layer of US-220

Figure C.105 Sieve analysis result from the 3rd layer of US-220

15. NC Route 55 (Harnett County)

Figure C.106 Sieve analysis result from the 1st layer of NC-55

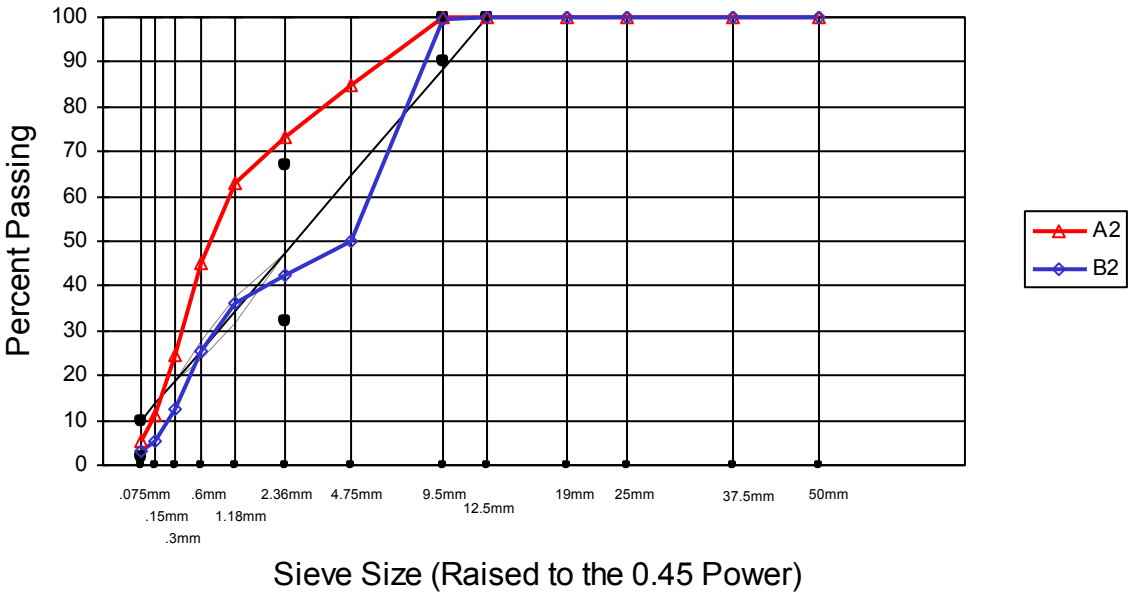

Figure C.107 Sieve analysis result from the 2nd layer of NC-55

Figure C.108 Sieve analysis result from the 3rd layer of NC-55

Figure C.109 Sieve analysis result from the 4th layer of NC-55

17. NC Route 179 (Brunswick County)

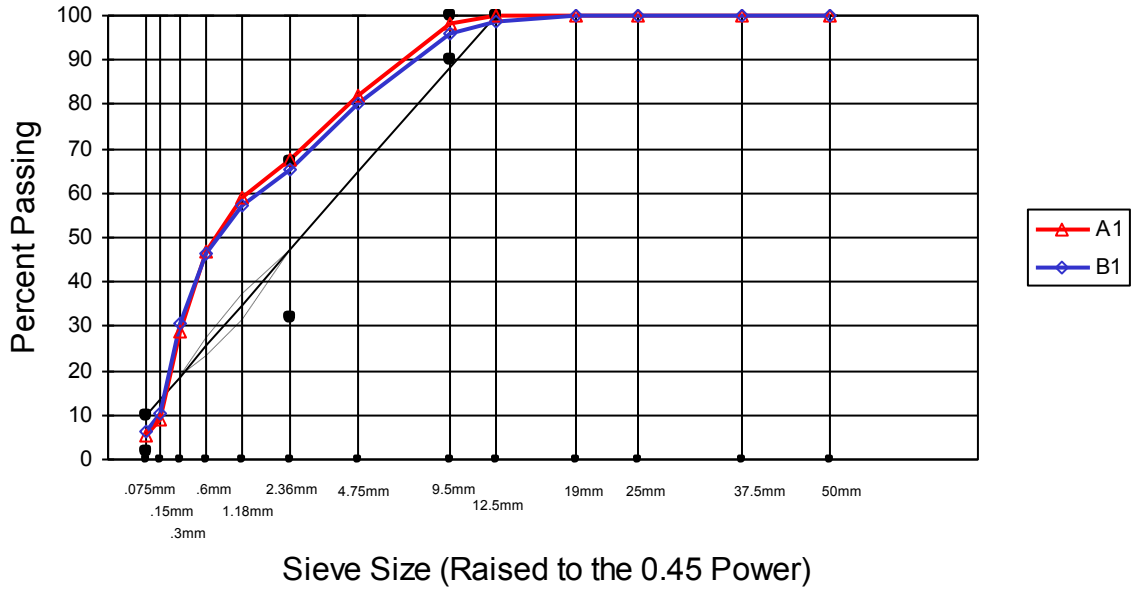

Figure C.110 Sieve analysis result from the 1st layer of NC-179

Figure C.111 Sieve analysis result from the 2nd layer of NC-179

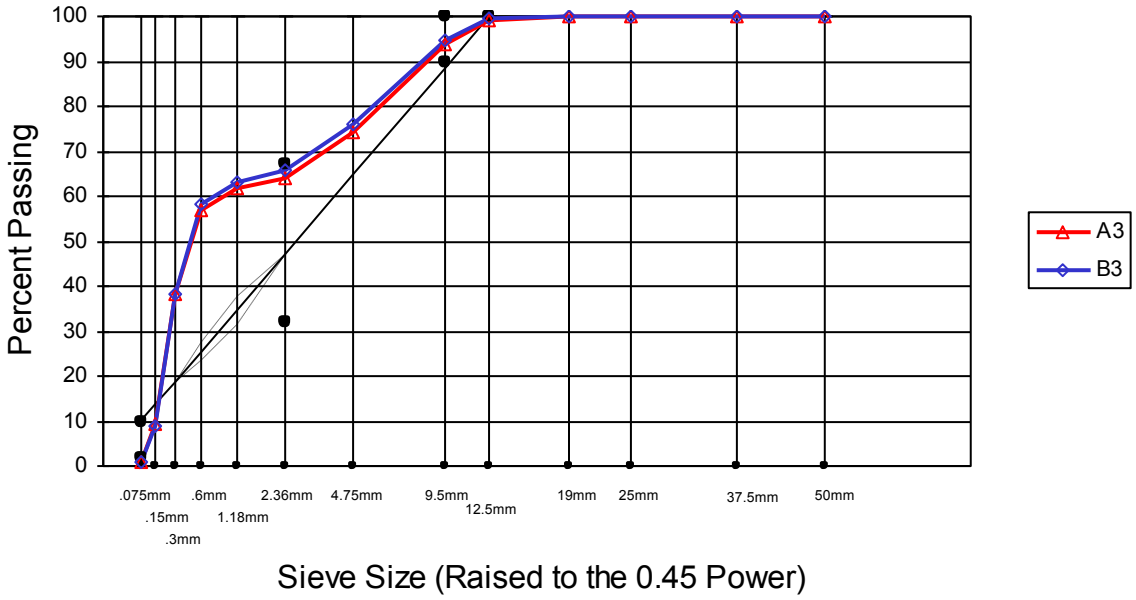

Figure C.112 Sieve analysis result from the 3rd layer of NC-179

18. US Route 401 (Cumberland County)

Figure C.113 Sieve analysis result from the 1st layer of US-401

Figure C.114 Sieve analysis result from the 2nd layer of US-401

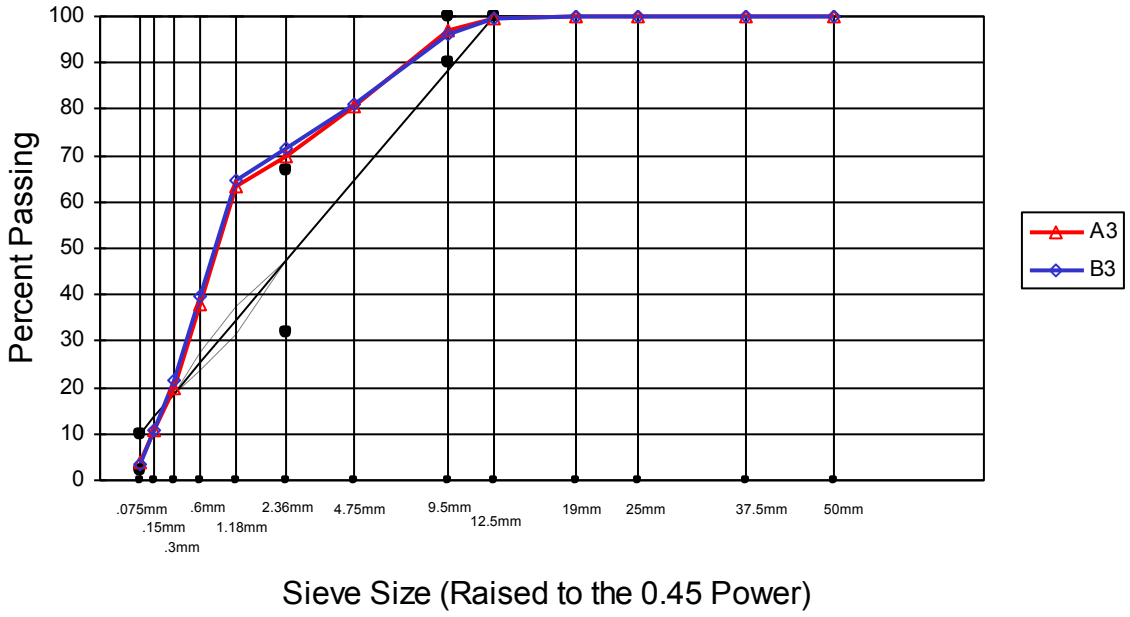

Figure C.115 Sieve analysis result from the 3rd layer of US-401

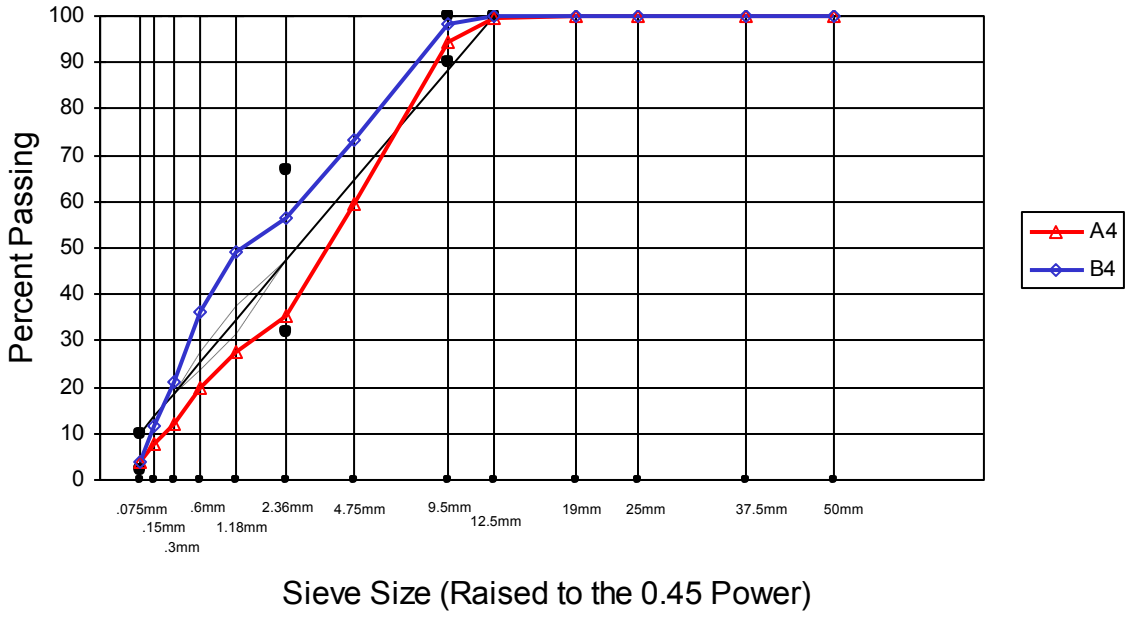

Figure C.116 Sieve analysis result from the 4th layer of US-401

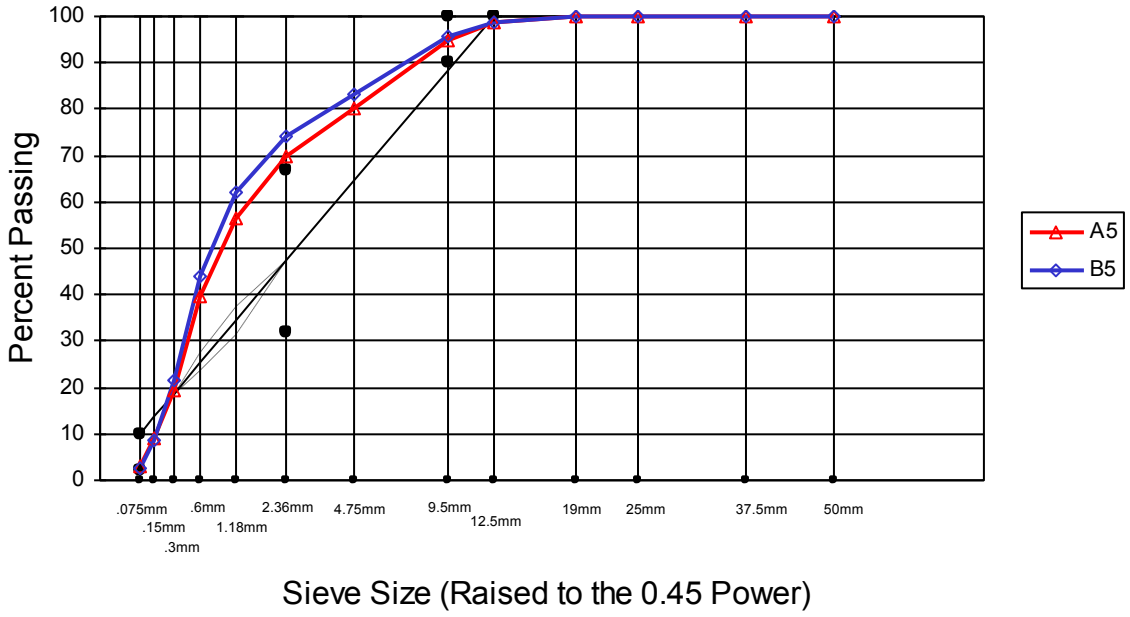

Figure C.117 Sieve analysis result from the 5th layer of US-401

19. NC Route 82 (Cumberland County)

Figure C.118 Sieve analysis result from the 1st layer of NC-82

Figure C.119 Sieve analysis result from the 2nd layer of NC-82

Figure C.120 Sieve analysis result from the 3rd layer of NC-82

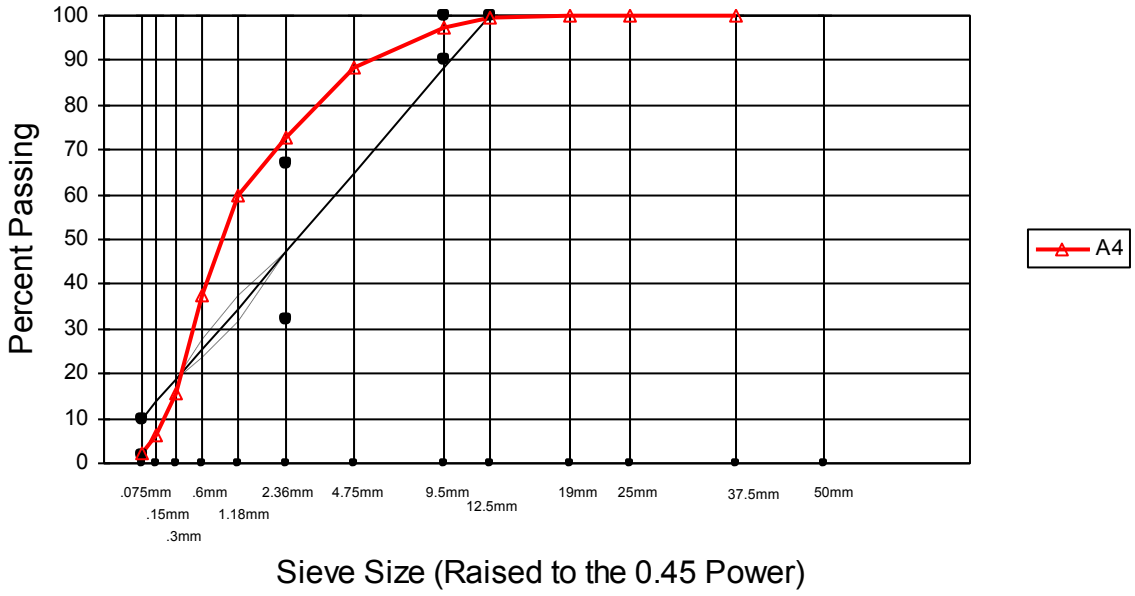

Figure C.121 Sieve analysis result from the 4th layer of NC-82